universität bonn igg

Institut für
Geodäsie und Geoinformation

Schriftenreihe

30

Lecture Notes from the Summer School of DFG SPP1257 Global Water Cycle

September 12-16, 2011

Ed. by A. Eicker, J. Kusche

Summer School of DFG SPP1257 Global Water Cycle • Lecture Notes

universitätbonn igg

Institut für Geodäsie und Geoinformation

Schriftenreihe

30

Lecture Notes from the Summer School of DFG SPP1257 Global Water Cycle

September 12-16, 2011

Ed. by A. Eicker, J. Kusche

Diese Veröffentlichung erscheint anlässlich der
Summer School of DFG SPP1257 – Global Water Cycle,
die vom 12. - 16. September 2011 in Mayschoss/Ahr stattfand.

Schriftenreihe des Instituts für Geodäsie und Geoinformation
der Rheinischen Friedrich-Wilhelms-Universität Bonn

Herausgeber: Prof. Dr.-Ing. Wolfgang Förstner
Prof. Dr.-Ing. Theo Kötter
Prof. Dr.-Ing. Heiner Kuhlmann
Prof. Dr.-Ing. Jürgen Kusche
Prof. Dr. Lutz Plümer
Prof. Dr. techn. Wolf-Dieter Schuh

Die Aufnahme dieser Arbeit in die Schriftenreihe wurde von den
Herausgebern der Reihe einstimmig beschlossen.

Bonn 2013 ISSN 1864-1113

Summerschool 'Global Hydrological Cycle' of the DFG-SPP1257

Mayschoss/Ahr, September 12-16, 2011

In 2006, the German Research Association DFG had established the coordinated Priority Program *SPP1257 Mass distribution and Mass Transport in the Earth System*. According to DFG's philosophy, SPP's are meant to enable broad-scale research in new, emerging fields. The objective of the SPP1257 was to facilitate integrated analysis of novel-type data collected from dedicated gravity field and radar altimetry satellite missions, to improve our knowledge about mass distribution and mass transport processes within the Earth system such as melting of continental ice sheets and glaciers, changes in ocean circulation pattern and in sea level, variations of surface and ground water levels and river discharge, glacial-isostatic adjustment, mantle convection and tectonics, and to investigate interactions between these processes. During six years, many Ph.D. students and postdocs from more than 30 institutions worked together in collaborative projects.

These lecture notes were compiled on the occasion of the summer school *Global Hydrological Cycle*, organized by the SPP1257 at September 12-16, 2011 in Mayschoss/Ahr, in which about 70 Ph.D. students, postdoc researchers and master students participated.The challenge imposed on thelecturers wasto familiarize students with widely differentbackground (geodesy, hydrology, oceanography, geophysics, mathematics) with

- concepts of observation systems and data processing, such as analysis of data from the Gravity Recovery and Climate Experiment (GRACE) gravity mission, and from radar altimetric satellite missions, associated problems such as noise, spatio-temporal sampling and aliasing, data post-processing techniques such as spherical harmonic synthesis and analysis, gridding, smoothing, covariance analysis, EOF analysis, and

- concepts of modelling and interpretation in hydrology and hydro-meteorology, oceanography and sea level, tides, ice sheet modelling, climate dynamics, and solid-Earth geodynamics.

The focus of the summer school wason concepts, and technical proofs were avoided. Lectures were accompanied by exercises, practicals and group work. Last not least, exciting discussions could be continued during barbecue, walks on the *Rotweinwanderweg*, and in the cellar of the *Winzergenossenschaft*.

Thanks go to all participants and, in particular, to the lecturers of the summer school, who decided to make almost all lecture material, data sets and codes freely available.

Jürgen Kusche and Annette Eicker

Bonn, February 11, 2013

Lecture Notes

from the

Summer School of DFG SPP1257 Global Water Cycle

September 12-16, 2011
Mayschoss/Ahr
Germany

Content

Mass transport and mass distribution in the system Earth

DFG

SPP 1257

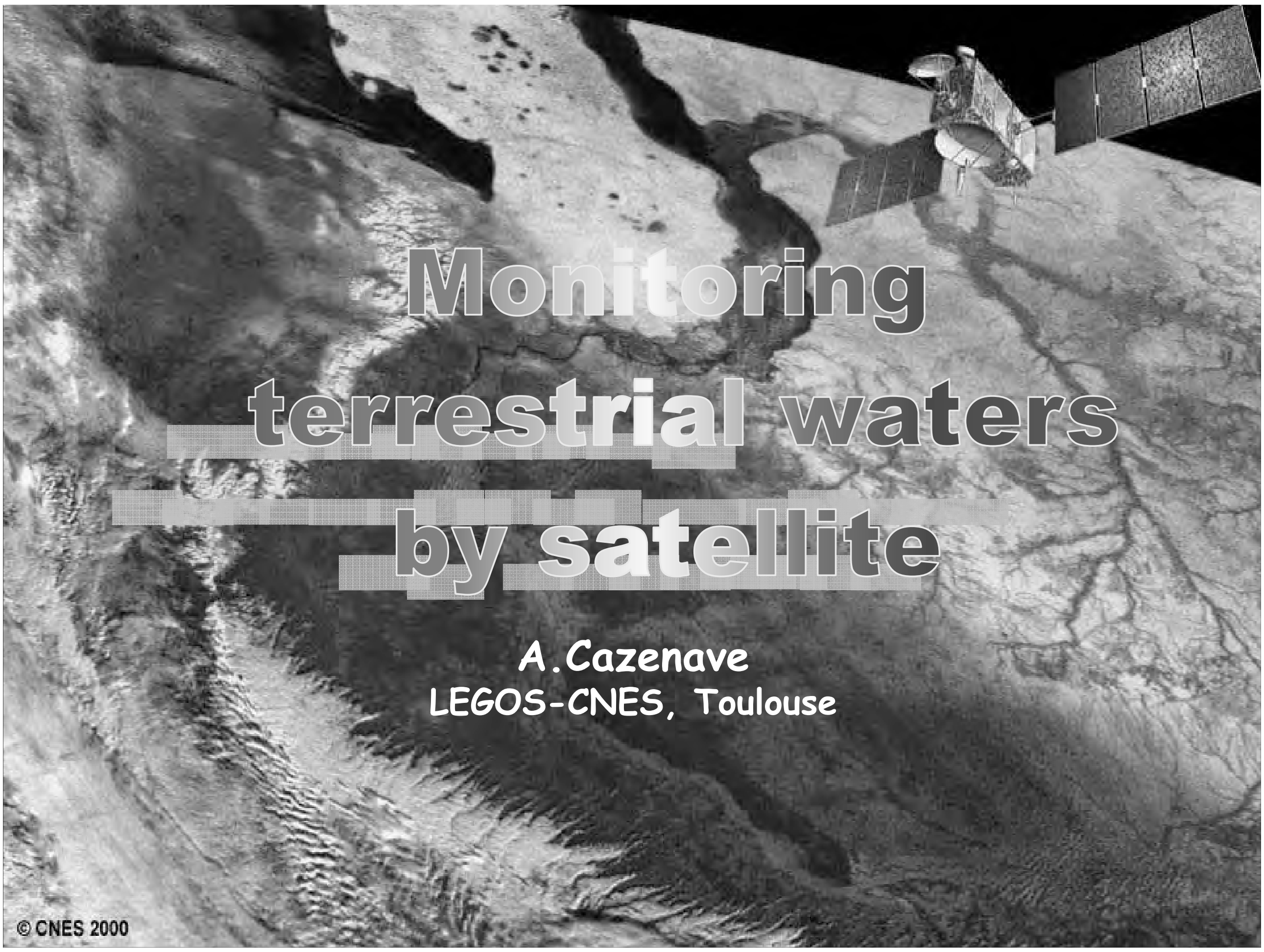

Outline

- Brief overview on the continental water cycle
- In situ data
- Global land surface models
- Satellite data for hydrology
- Monitoring surface waters by radar altimetry
- Altimetry-derived water level data bases
- Validation; derived products
- Soil moisture from space
- Space gravimetry (GRACE)
- problems with current missions
- Future prospects

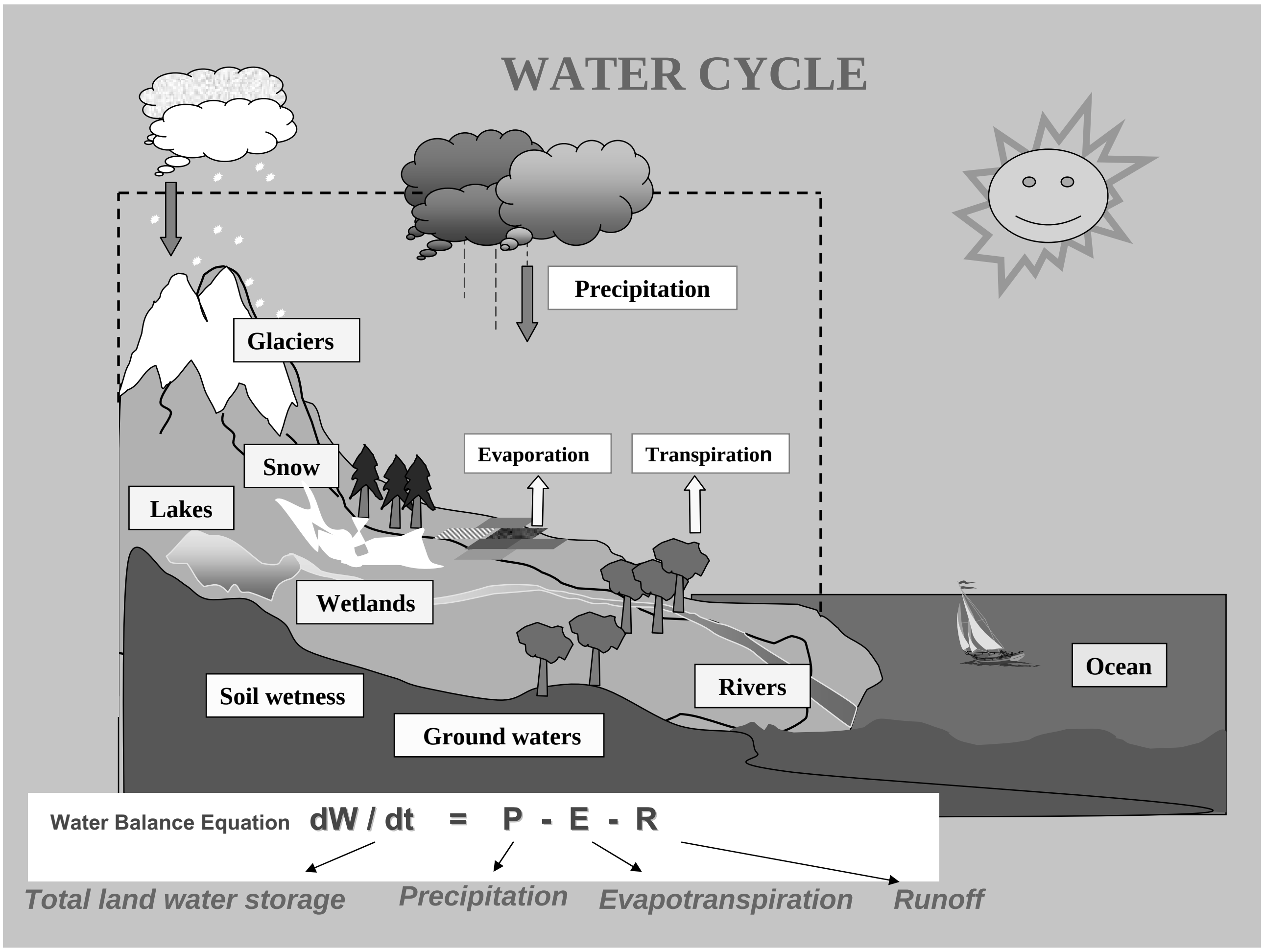

Causes of spatio-temporal change of the continental water cycle

- Climate variability (natural and anthropogenic)

- Direct human effects:

  - groundwater mining
  - irrigation
  - dam building
  - urbanization
  - deforestation
  - change in land use

Continental Water Cycle

Water flux exchanges between reservoirs

- Water mass exchanges?
- Time scales of exchanges?
- Water holding capacity of reservoirs?
- Rates of water renewal inside reservoirs

Mechanisms

- Mass and energy transfert between land surface and lower atmosphere
- Lower atmosphere dynamics
- Biogeochemical processes
- etc.

Applications

- Weather forecast
- Climate modelling
- Water resources management
- Natural Hazards:
- floods, droughts
- Agriculture (irrigation)
- Hydro-electric energy production
- Fluvial navigation
- Land use and management
- Carbon cycle
- Sediment transport
- Sea level change
- Etc.

Water balance at river basin scale

$$dW/dt = P - E - R$$

Total storage Precipitation Evapotranspiration Runoff

Importance of each parameter

- Precipitation:

! Main forcing term
! Controls water storage and runoff

-Evaporation; Vegetation transpiration :

! Drives mass and energy exchange between lower atmosphere and surface
! Dépends on solar radiation, lower atmospheric state, soil wetness, type of vegetation
! Direct link with air temperature

-Runoff:

! Linked to basin-scale water budget

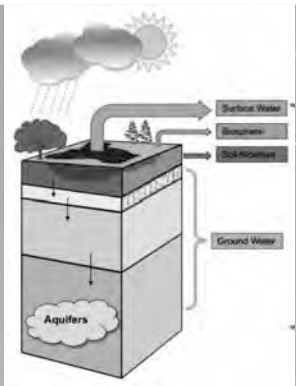

Water balance at river basin scale

$$dW/dt = P - E - R$$

Total storage Precipitation Evapotranspiration Runoff

Total water storage:
importance of each component:

- Surface waters:
! Direct response to precipitation
! Flood plains → control ecosystem dynamics and CO_2 exchanges with the atmosphere

- Soil moisture:
! Drives evapotranspiration and vegetation growth (→ carbon cycle)
! Important parameter for weather forecast and climate modelling

- Snow pack :
! Influence planet albedo, hence total radiative budget

- Ground waters :
! Main water resource in semi arid regions

Water Balance Equation (river basin scale)

Water mass balance : $dW/dt = P - E - R$

W: Land water mass (surface and underground waters; snowpack)

P : Precipitation

E : Evapotranspiration

R: Runoff

Approach

Observations: in situ and remote sensing

Modelling → Data assimilation

Water level and discharge data available in the GRDC data base (status in March 2011)

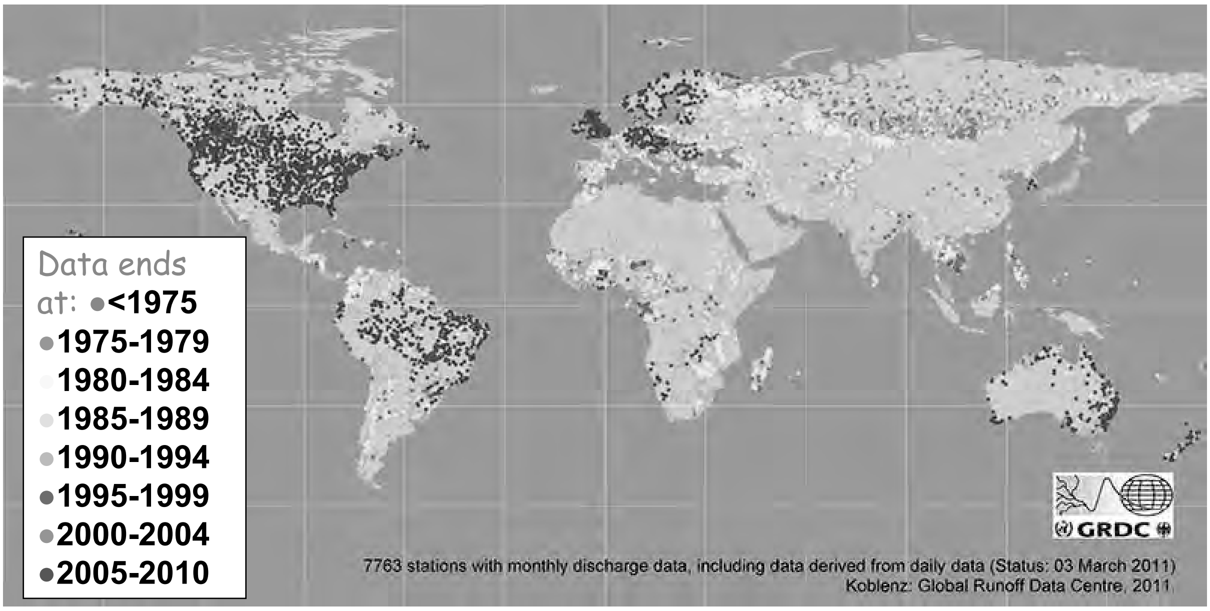

Global Runoff Data Center

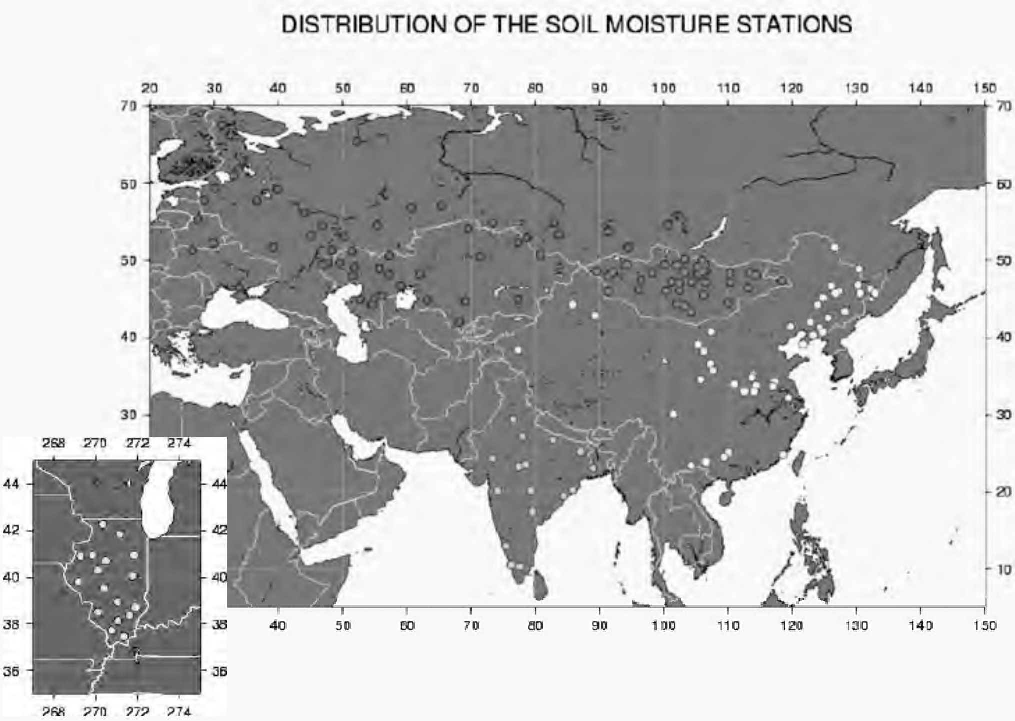

Global Soil Moisture Data Bank

Land Surface Models

- Compute mass and energy budget at the atmosphere-soil interface + water storage in the different reservoirs + runoff

- Input parameters : low atmospheric state (T, H, wind speed) + mass and energy fluxes (precipitation and radiation)

Modelling Land Surface Processes

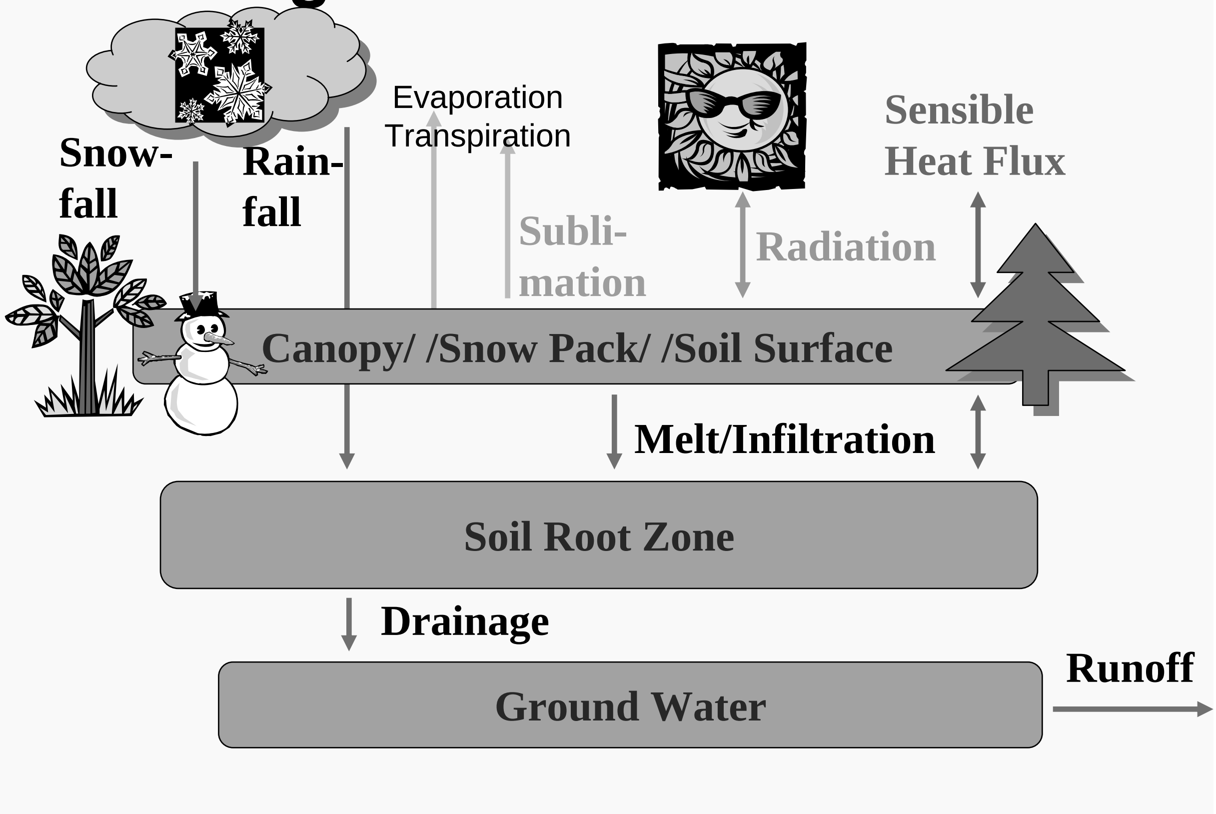

Remote sensing technique	Soil moisture	Ground waters	Snow pack	Surface waters (extent, level, volume, discharge)
Visible Imagery	Extent		Extent	Extent
Passive and ative microwaves (Radiometry)	Extent Volume		Extent Thickness	Extent
Altimetry				Water Level
Space Gravimetry (GRACE)		Total water mass		

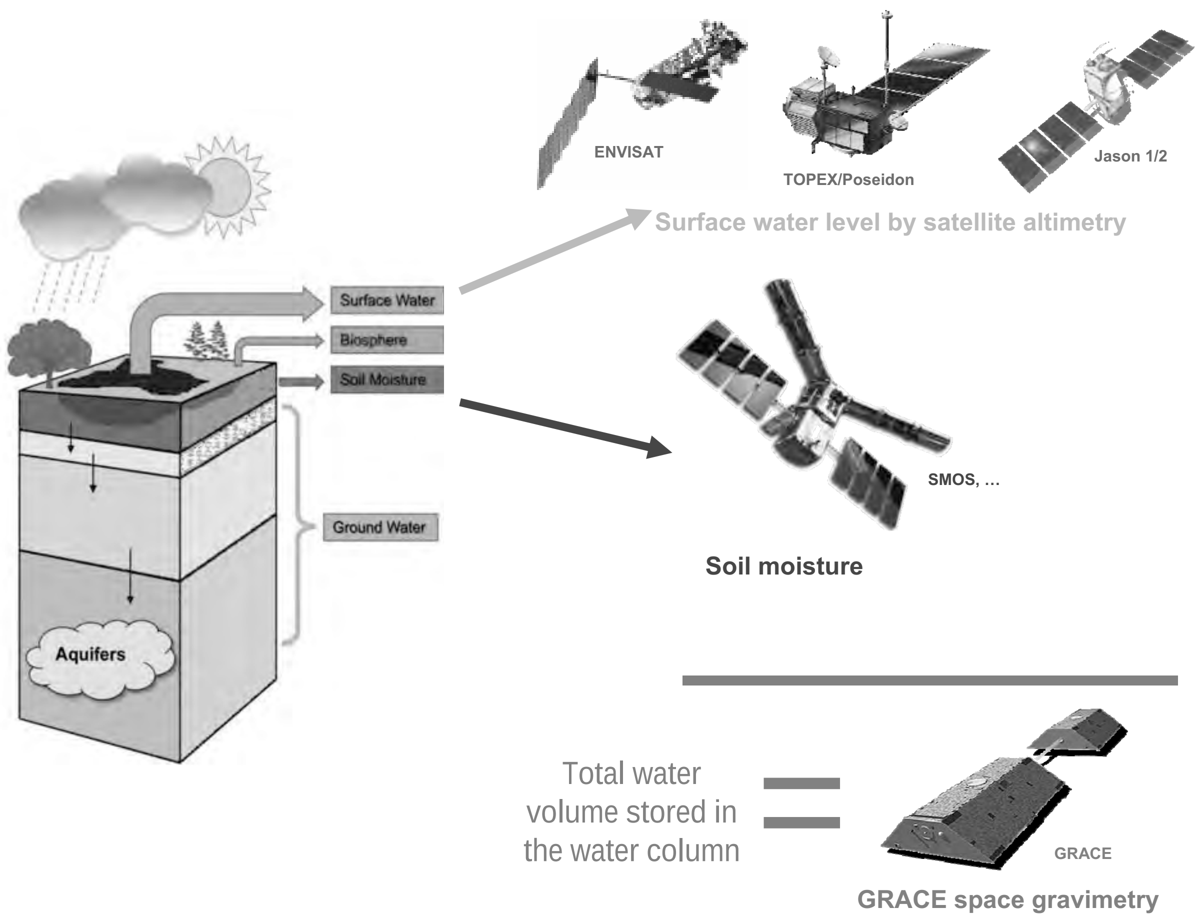

Primary and derived hydrological products
(by combining obs. from different remote sensing techniques)

- **Soil moisture** : microwaves + SMOS
- **Water levels** : altimetry Topex/Poseidon, Jason-1/2, ERS, Envisat
- **Snow pack** : microwaves, GRACE
- **Land water storage**: GRACE
- **Surface water volume: imagery + altimetry**
- **River discharge**: altimetry + modelling (Manning equation)
- **Ground waters**: GRACE + altimetry + imagery +SMOS
- **Evapotranspiration (basin-scale)** : GRACE + runoff + precipitation

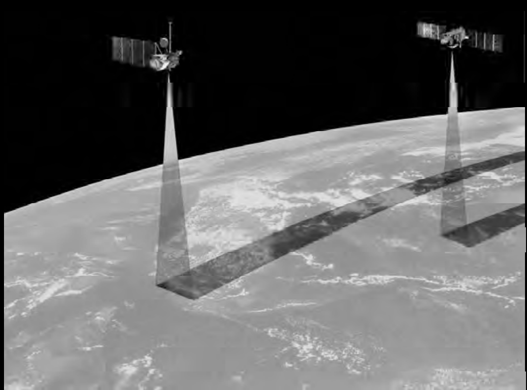

Satellite altimetry

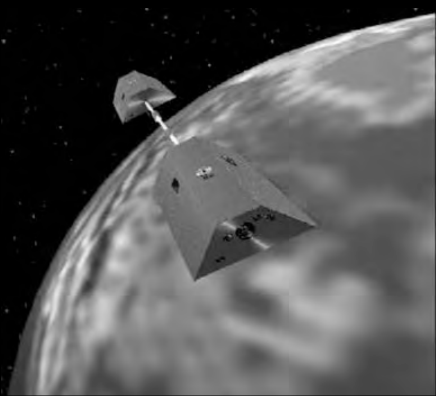

Space gravimetry

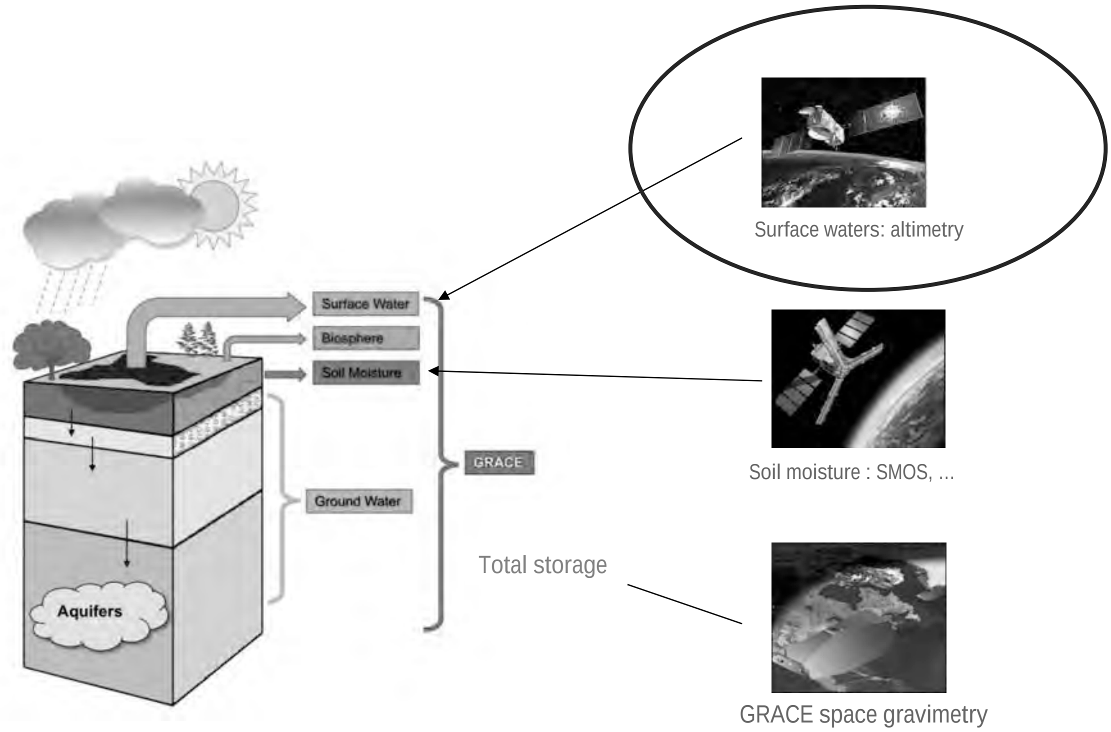
Surface waters: altimetry
Surface Water
Biosphere
Soil Moisture
GRACE
Ground Water
Aquifers
Total storage
Soil moisture : SMOS, ...
GRACE space gravimetry

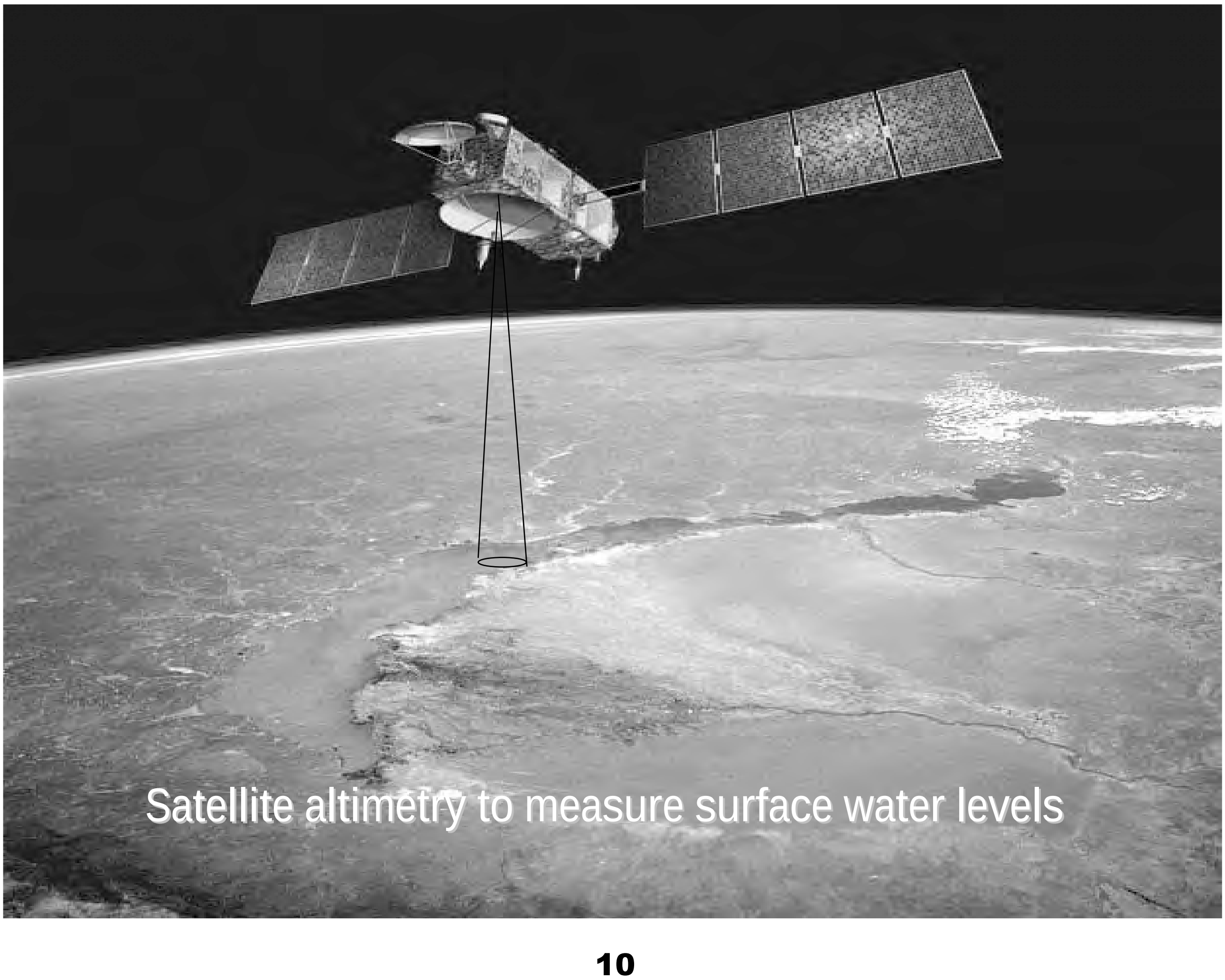
Satellite altimetry to measure surface water levels

Satellite altimetry

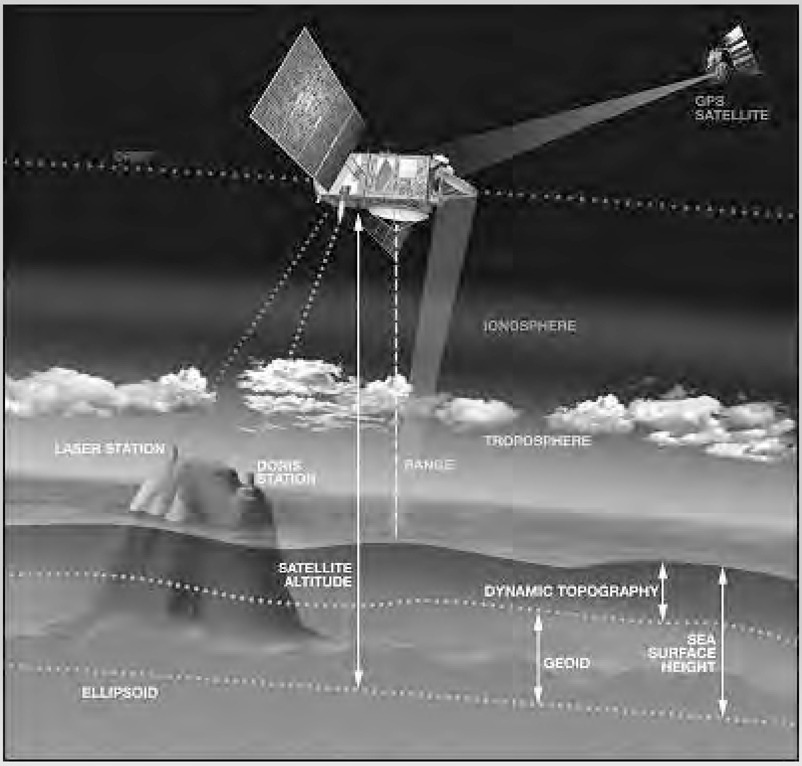

Global Earth coverage in a few days

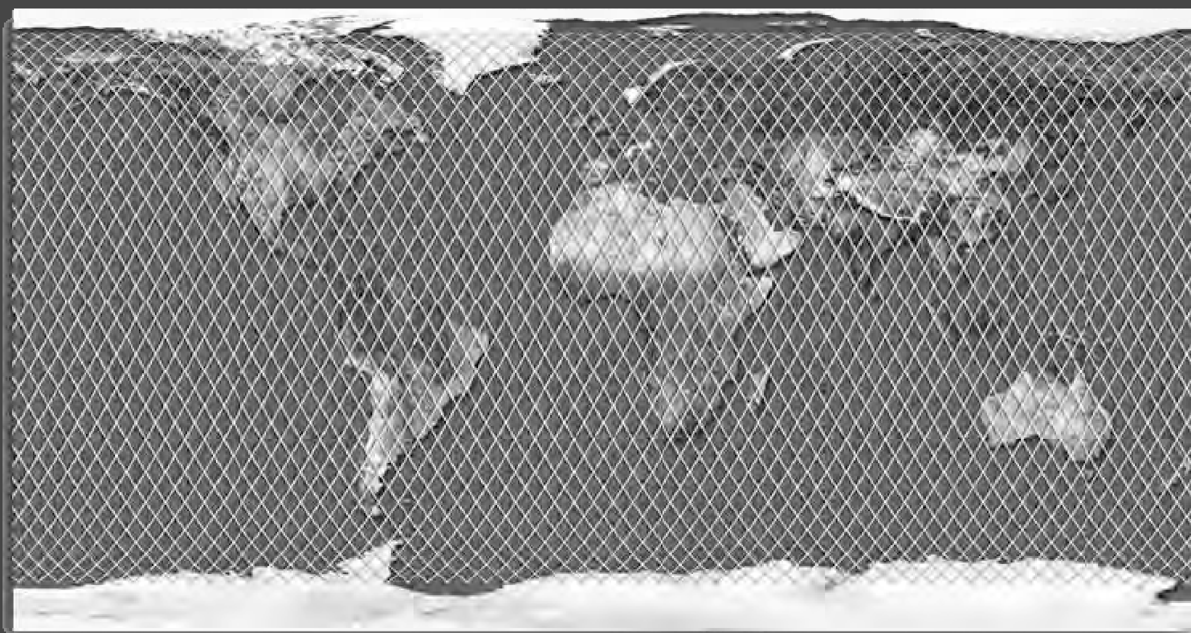

Sea level measurements by satellite altimetry

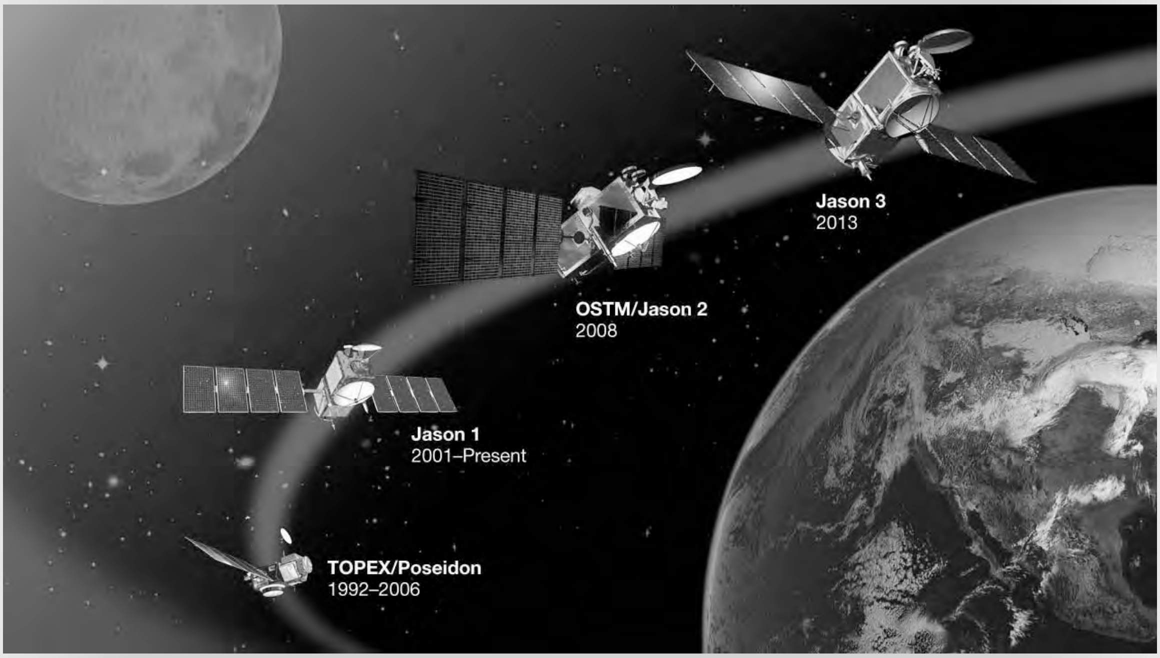

Satellite Altimetry :

Topex/Poseidon (1992-2006)
ERS-1 (1992-1996)
ERS-2 (1995- 2007)
Jason-1 (2001-)
ENVISAT (2002-)
GFO (2000-)
Jason-2 (2008-)

Important achievements in oceanography with high-precision satellite altimetry

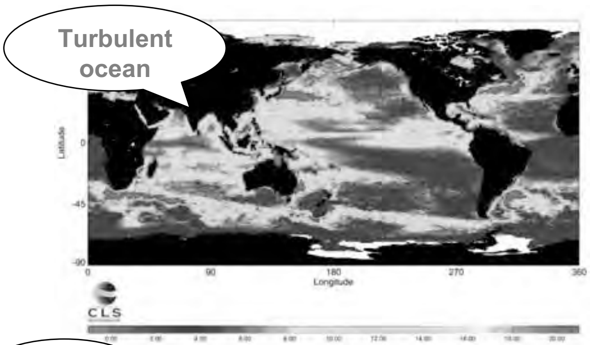

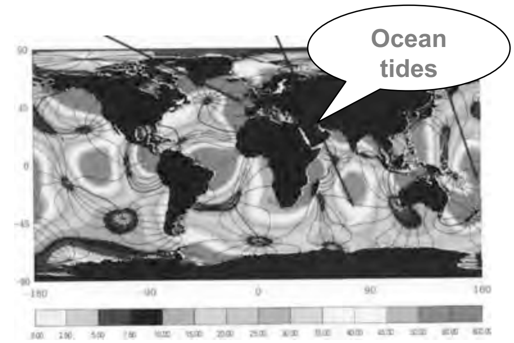

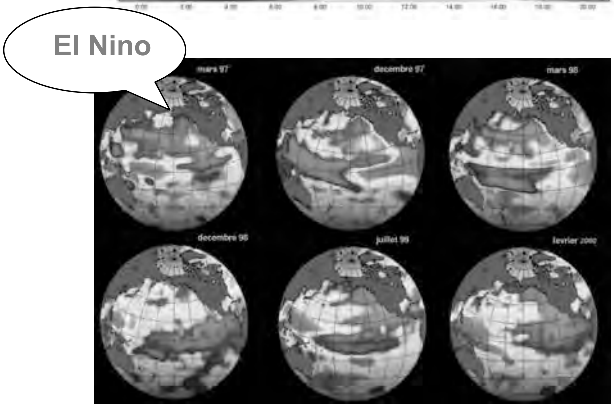

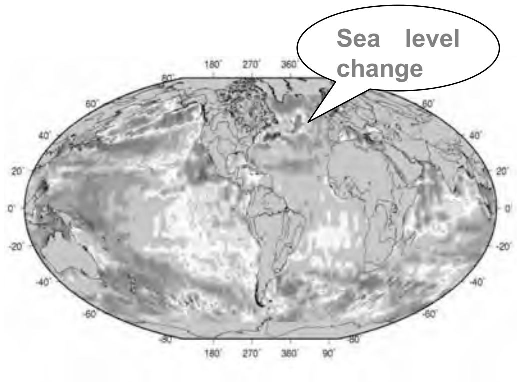

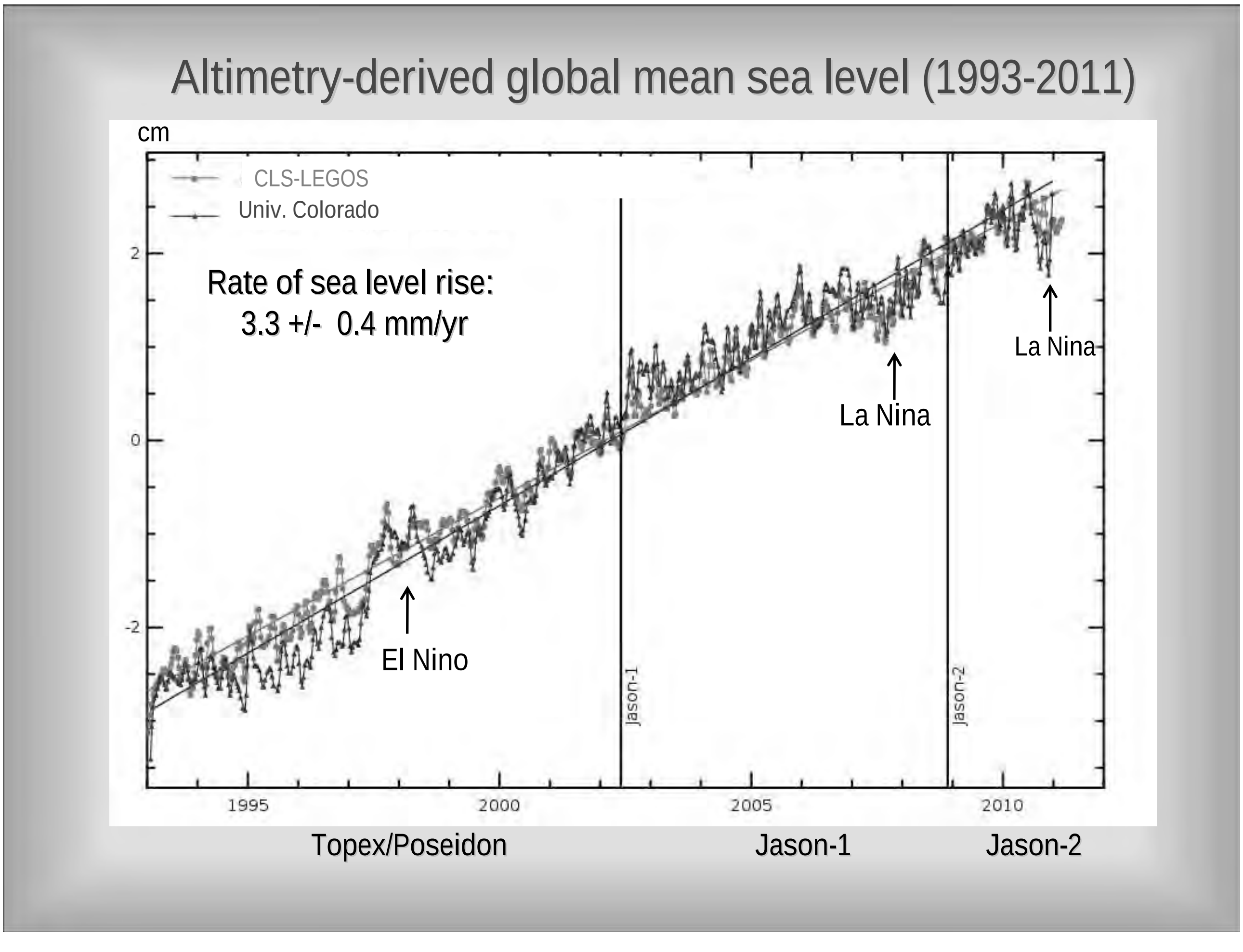

Examples of altimetric coverage over lakes

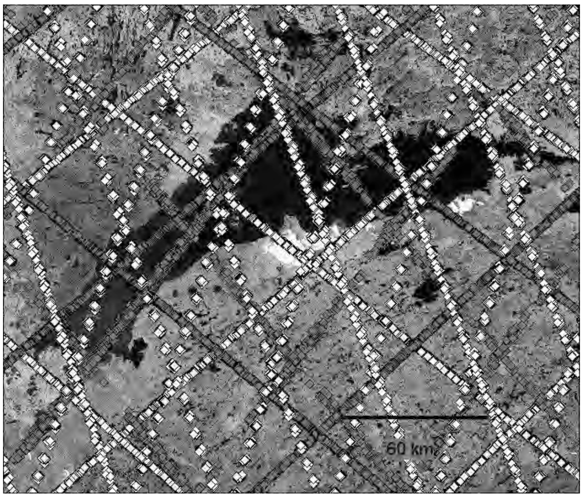

Athabasca Lake

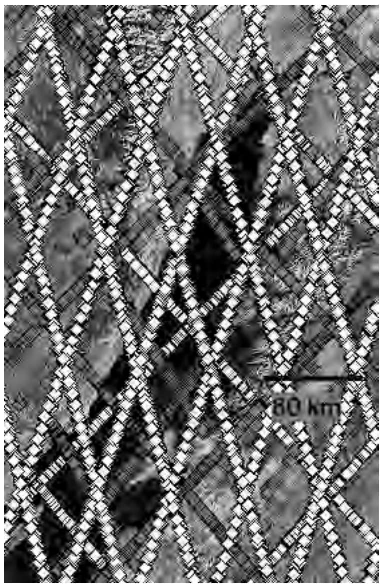

Baikal Lake

Lake Victoria (Afrique de l'Est)

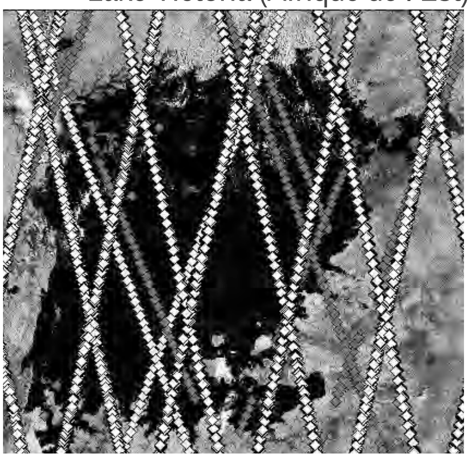

Water level variations

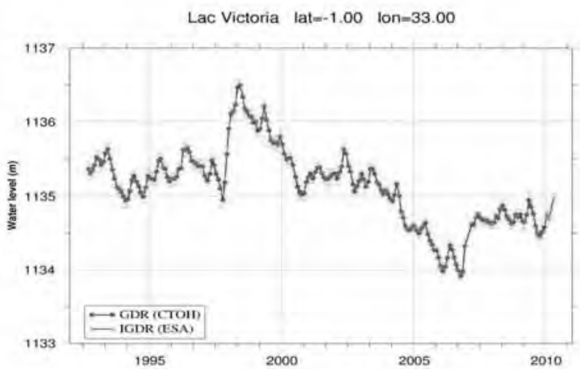

Lake Tharthar (Irak)

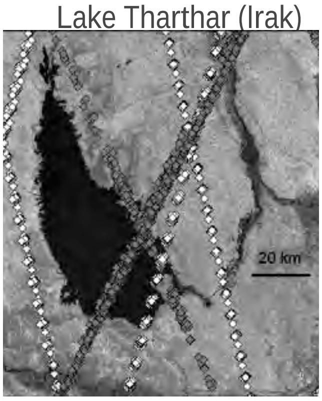

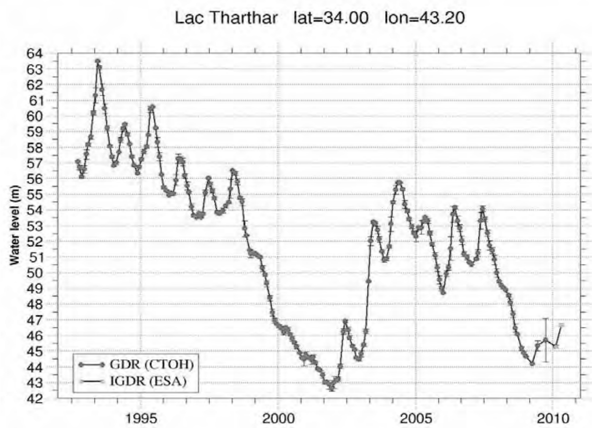

Hydroweb (Legos)

LakeVictoria

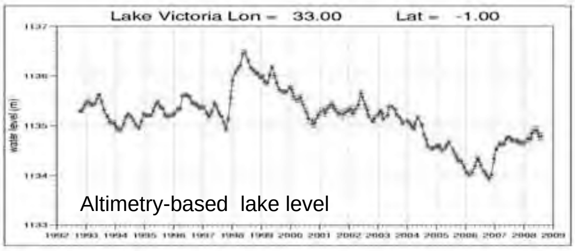

1992 2009

Lake Tanganika

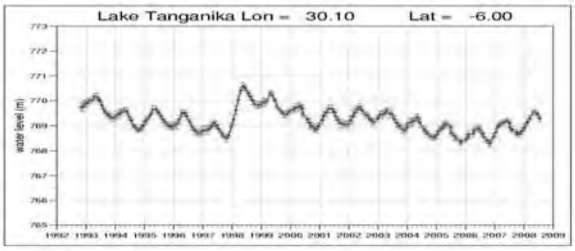

Lake Malawi

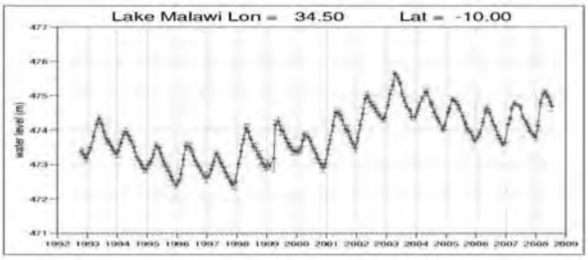

East African Lakes

Legos

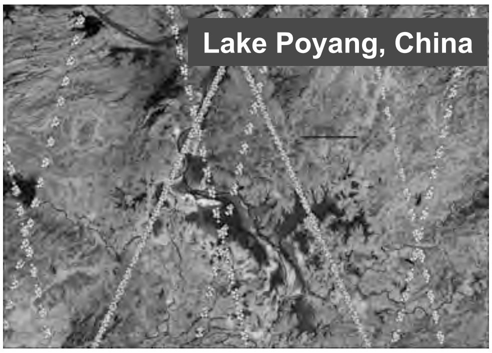

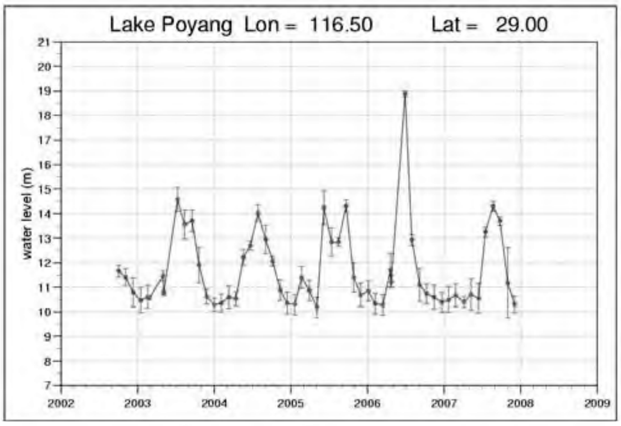

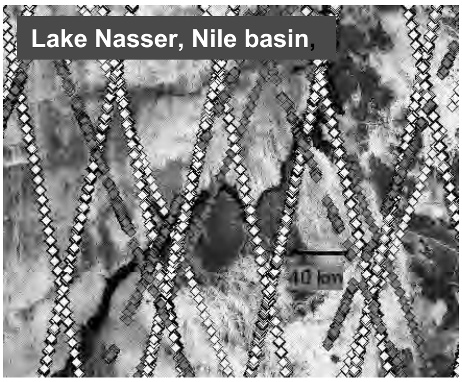

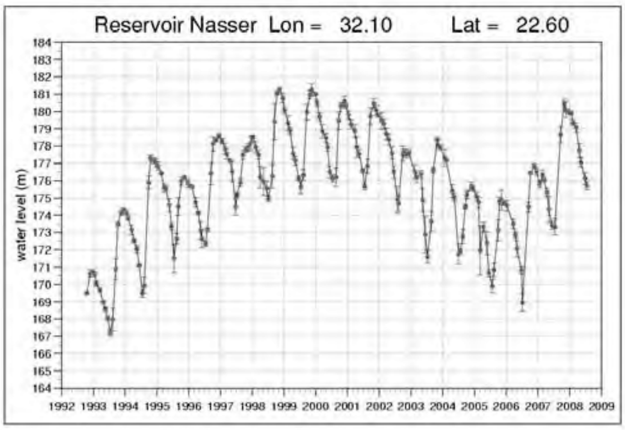

HYDROWEB, Legos

Example of 'virtual' station

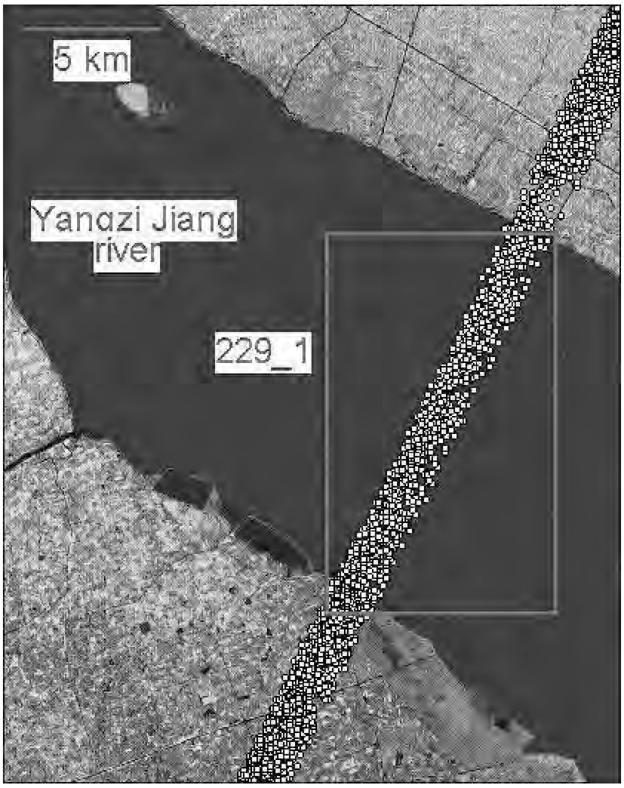

Example of altimetric coverage over rivers

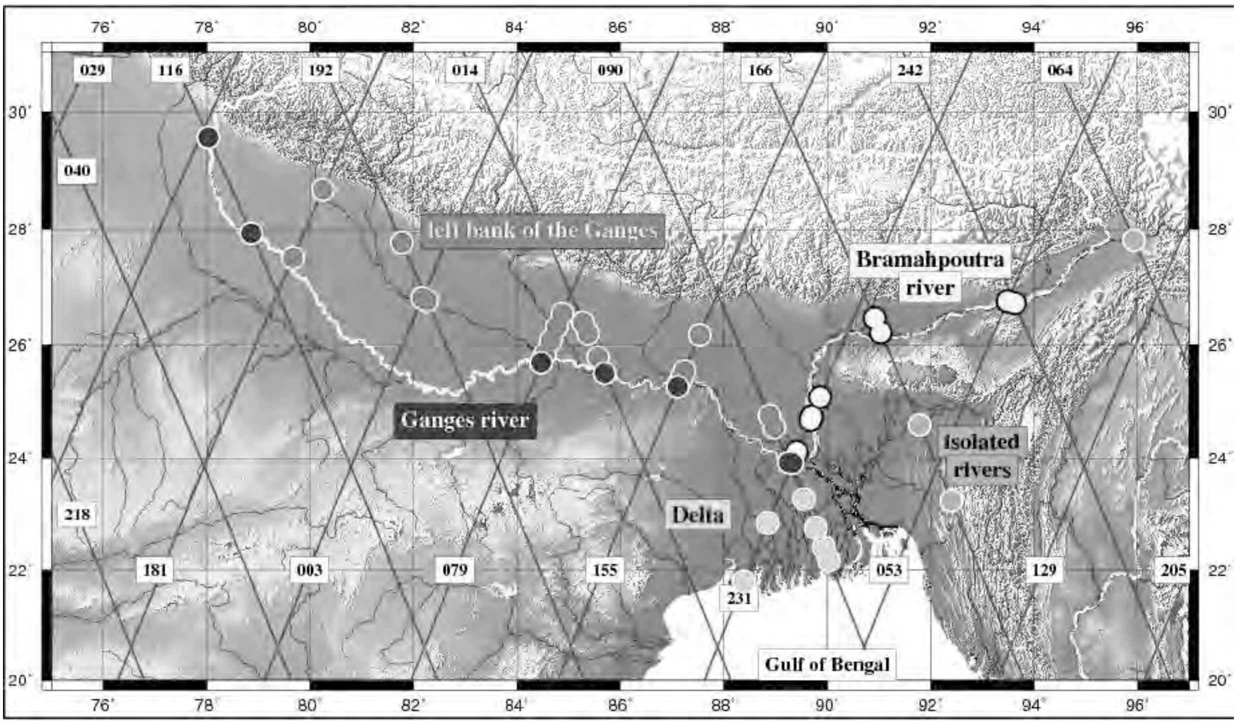

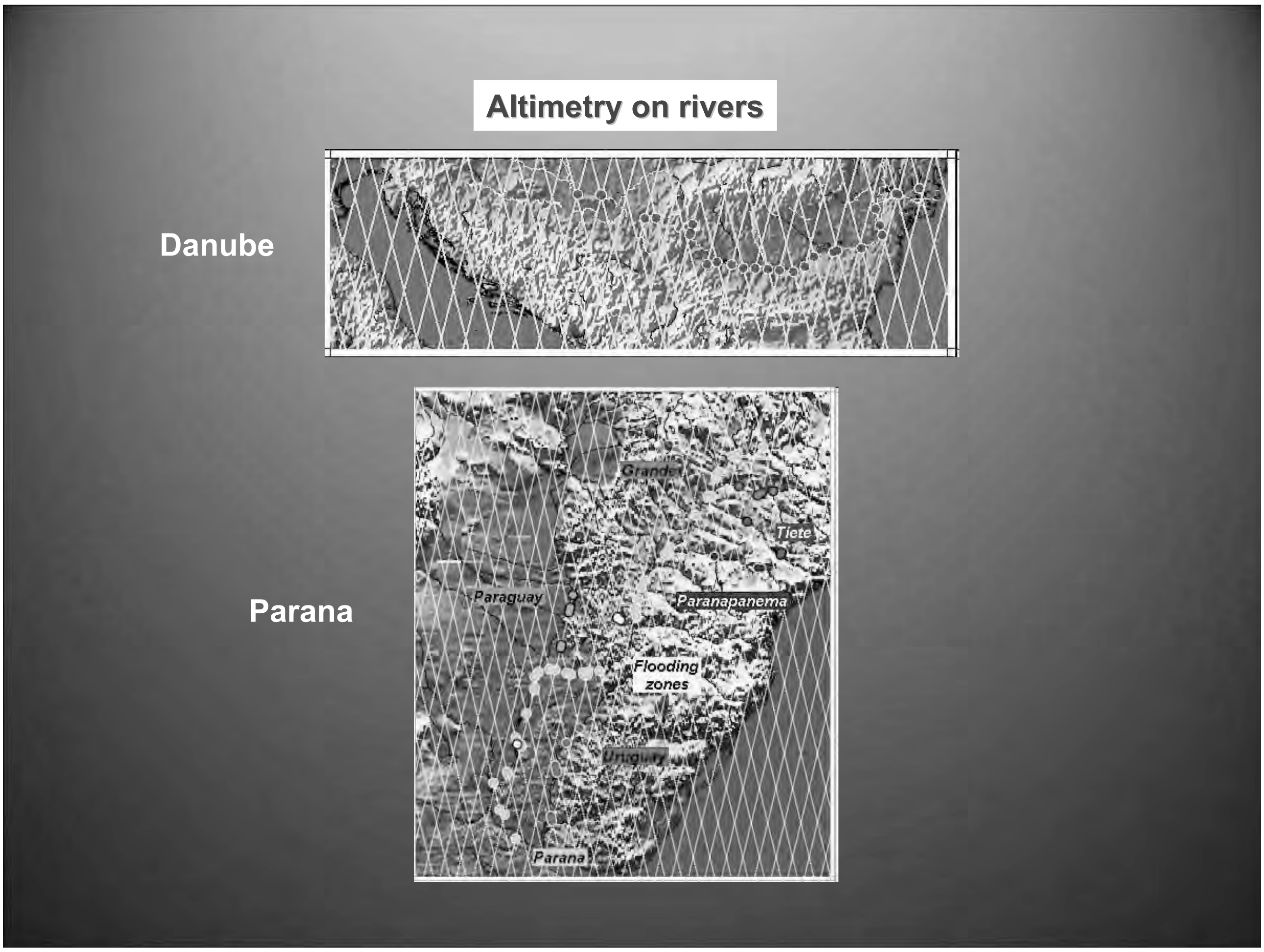
Altimetry on rivers
Danube
Parana
Grande
Tiete
Paraguay
Paranapanema
Flooding zones
Uruguay
Parana

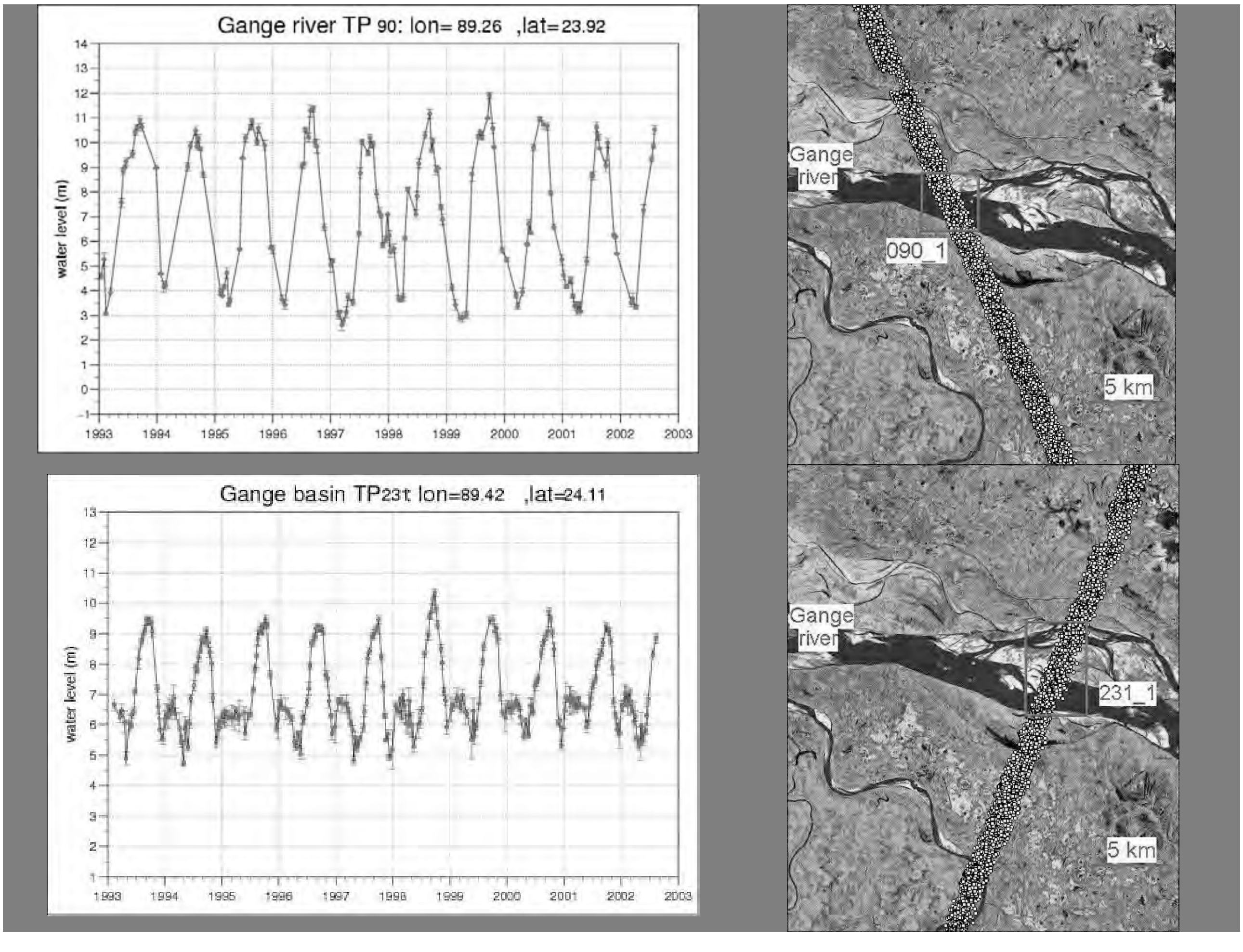
Gange river TP 90: lon= 89.26 ,lat=23.92
water level (m)
Gange basin TP231: lon=89.42 ,lat=24.11
water level (m)
Gange river
090_1
5 km
Gange river
231_1
5 km

ENVISAT satellite coverage

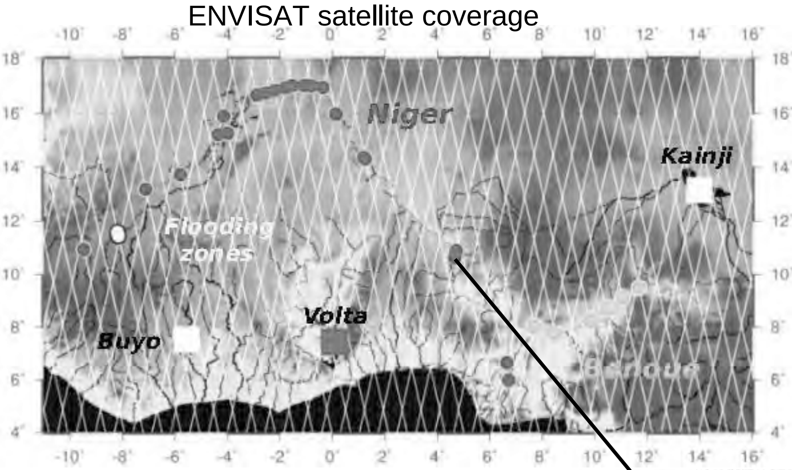

Niger Basin

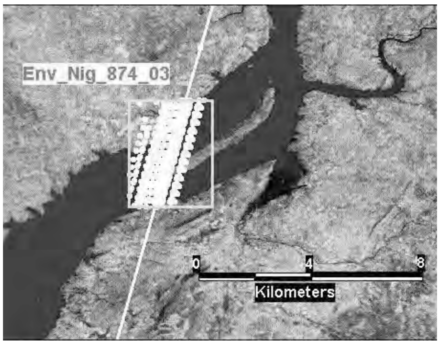

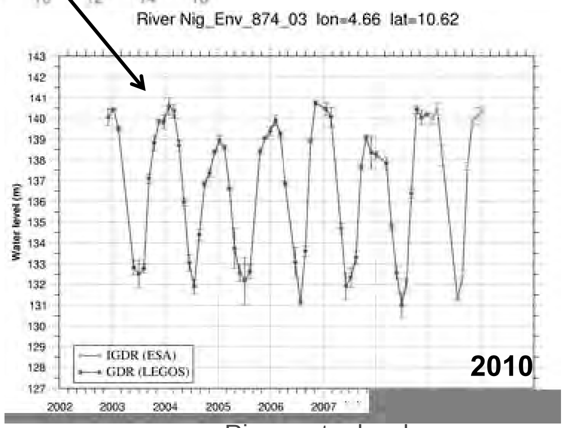

River water level

HYDROWEB, Legos

Water level on rivers

Envisat satellite coverage

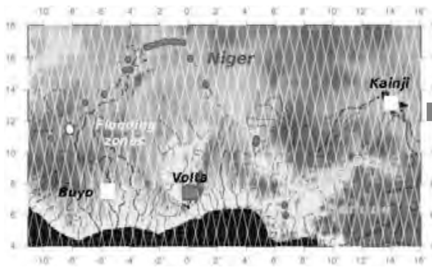

Niger

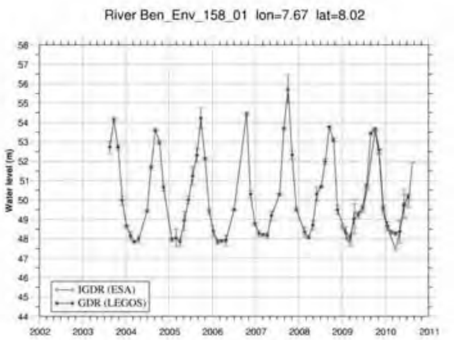

2002 2011

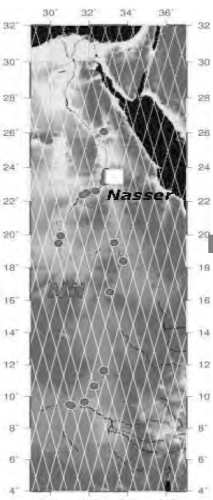

Nil

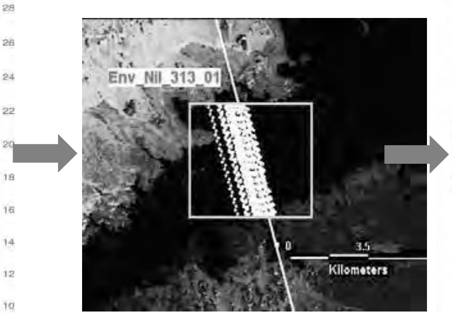

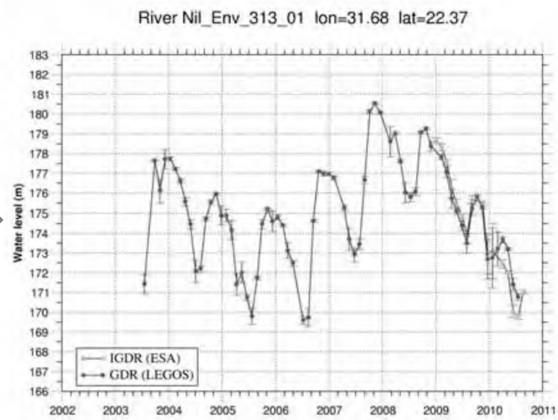

HYDROWEB (LEGOS)

'Altimetry' virtual stations supplementary of in situ gauges

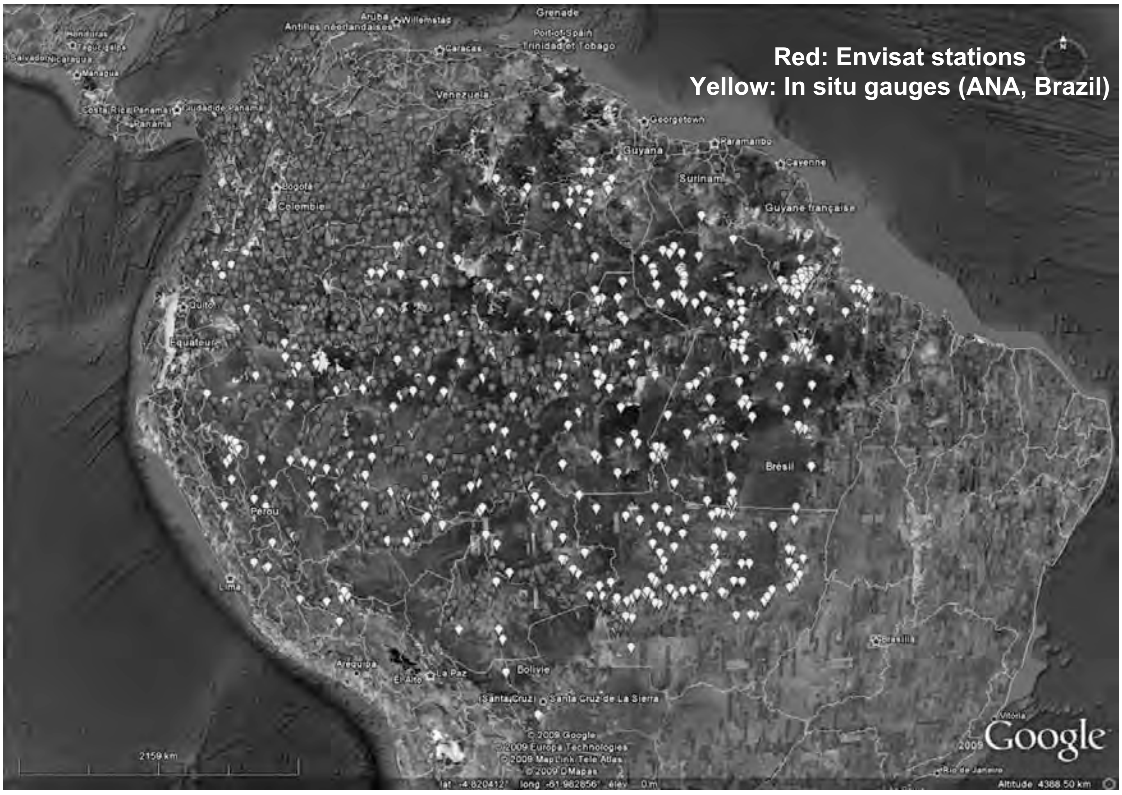

LEGOS/LMTG

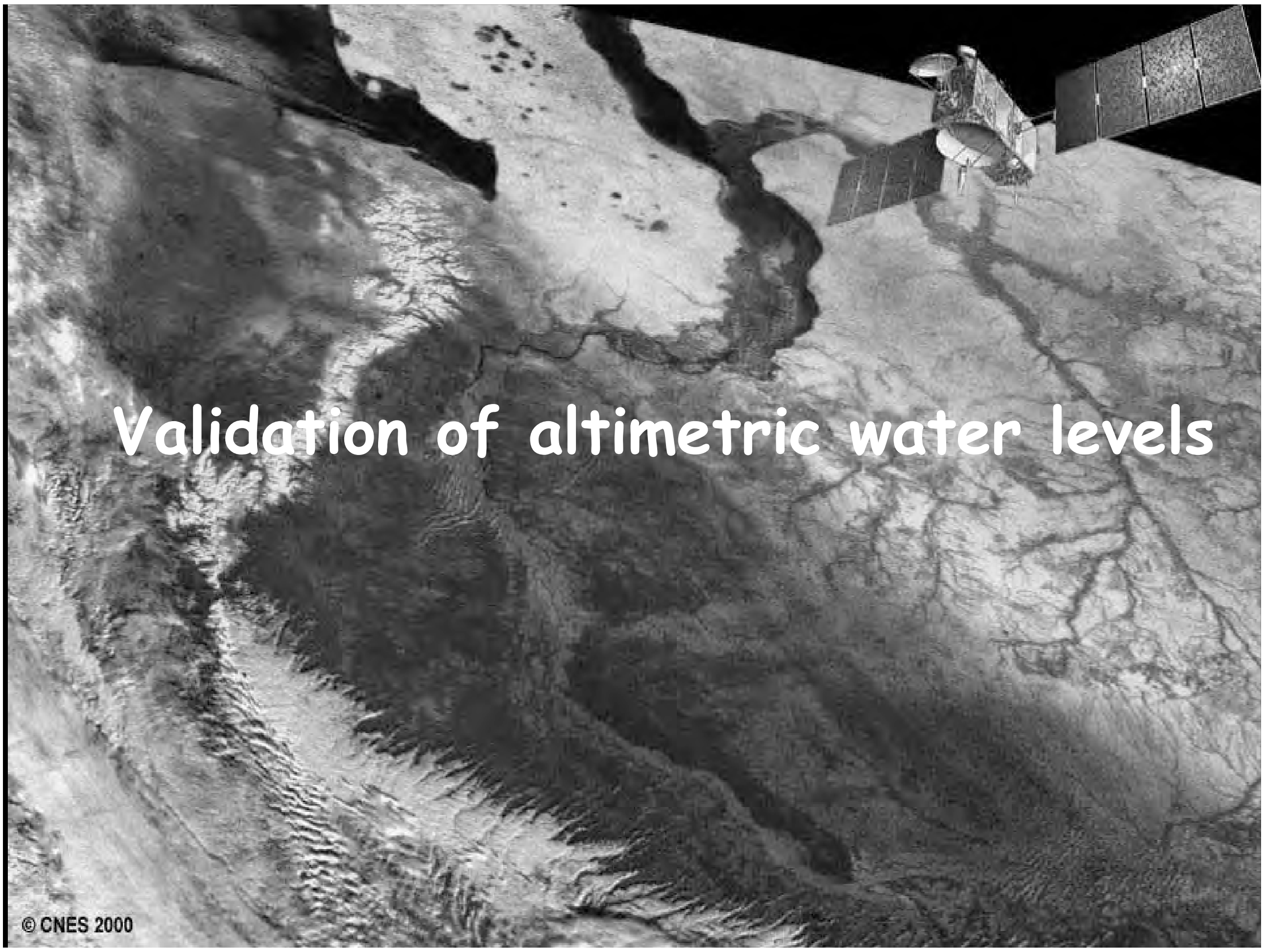

Comparison of altimetry and in situ water levels

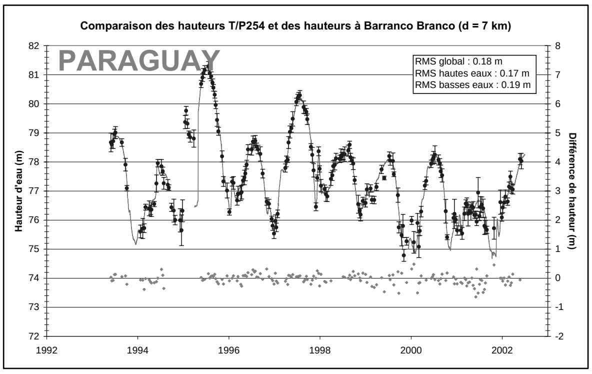

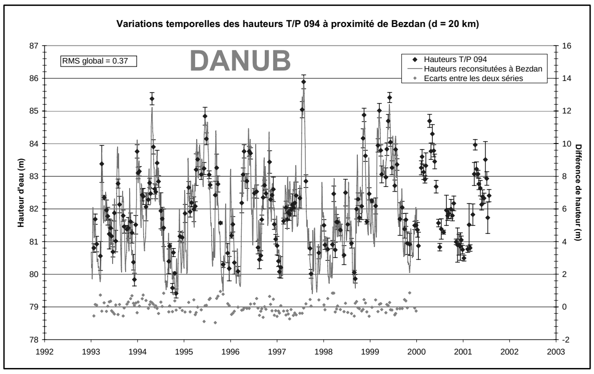

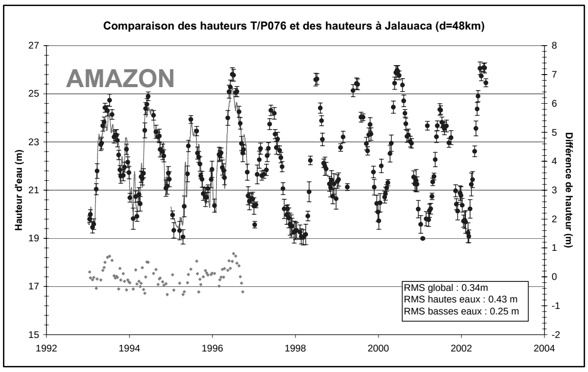

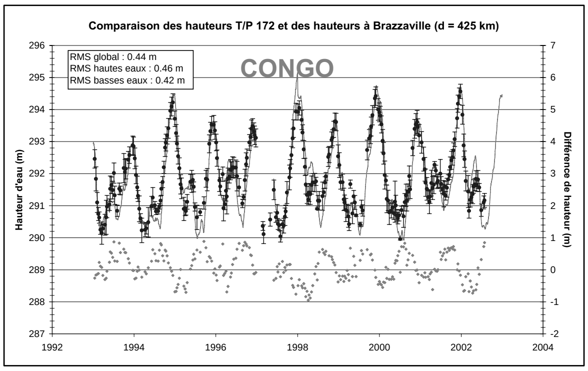

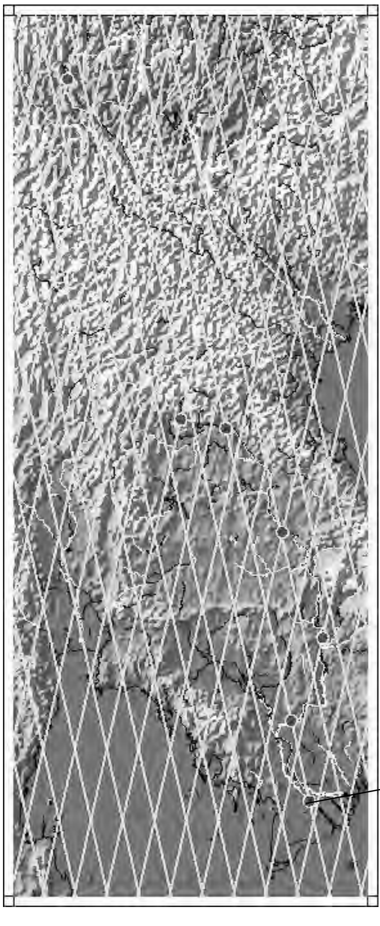

MEKONG RIVER

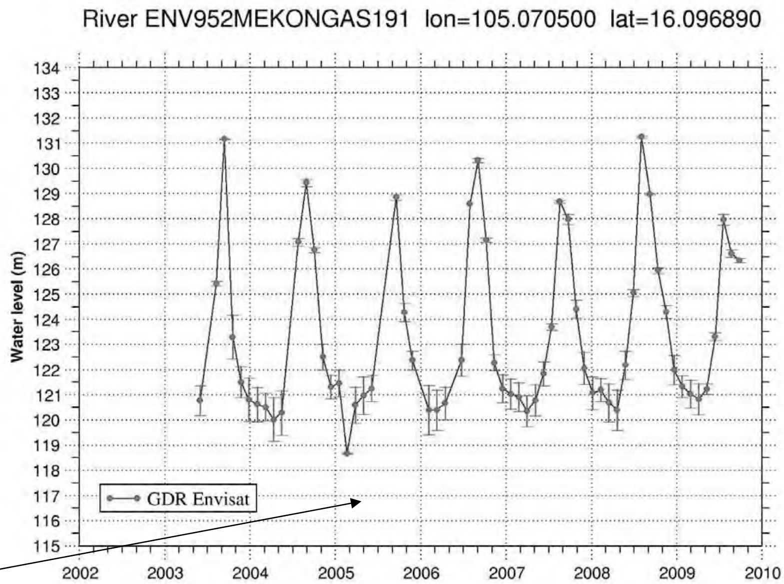

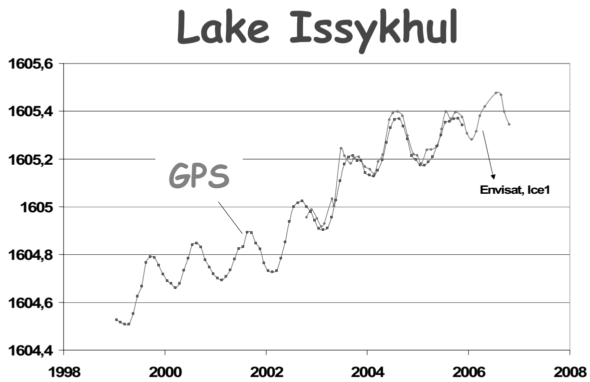

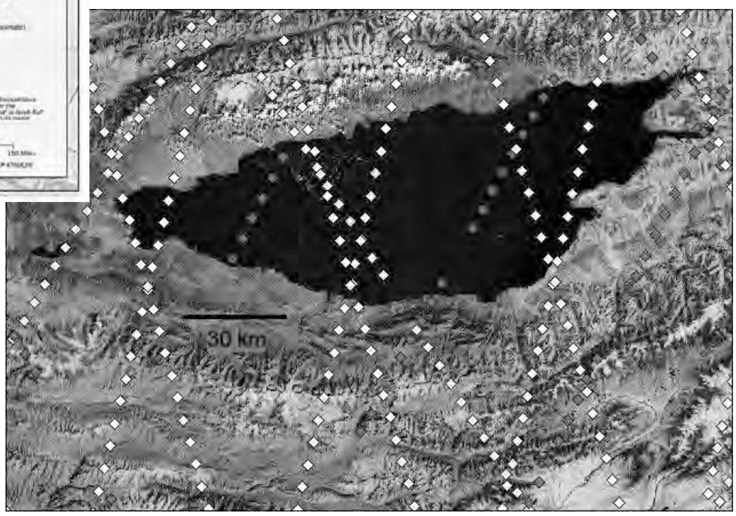

white: Envisat
yellow: Topex (2002-2005)
red: Jason, Topex 1993-2005
green: GFO

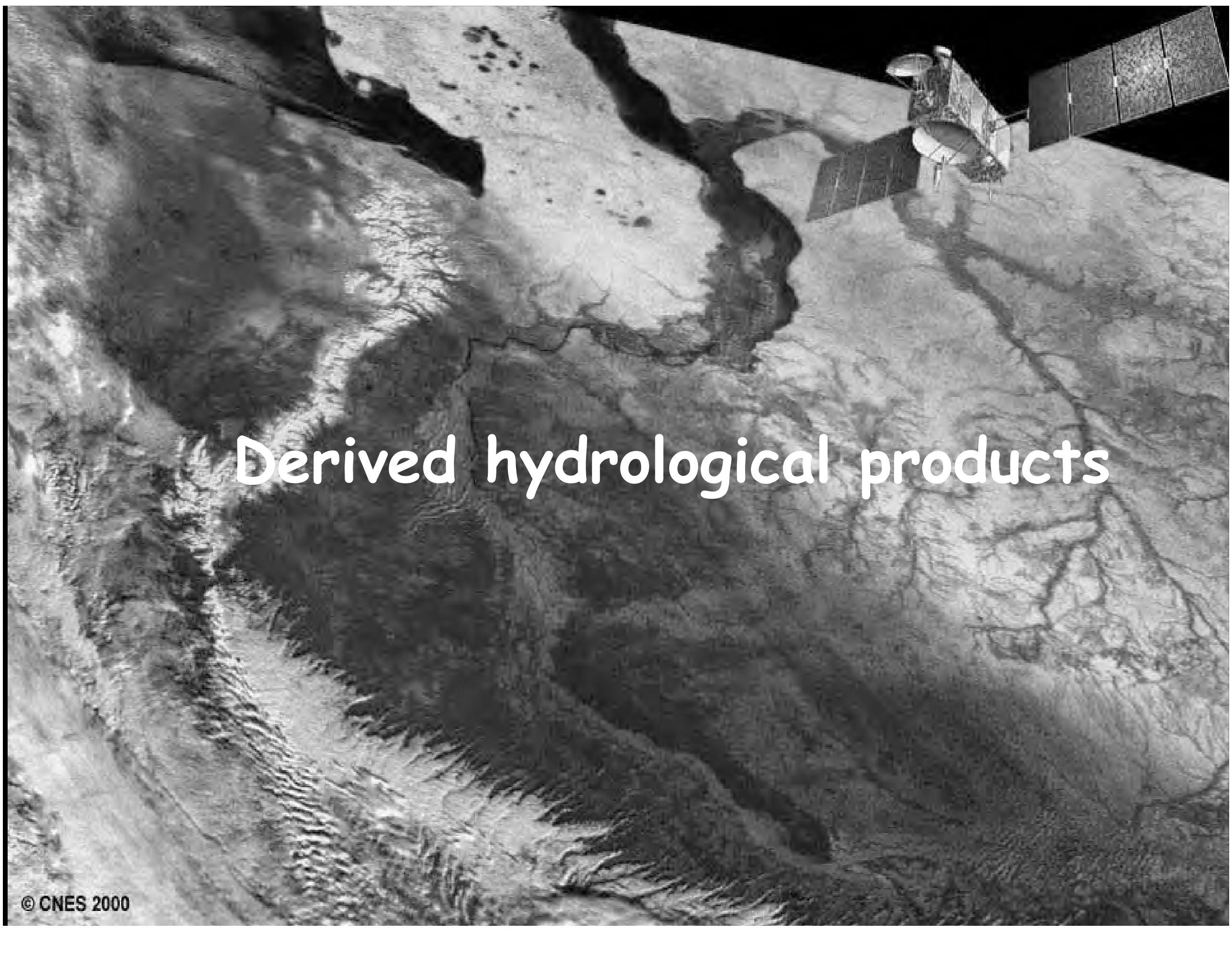

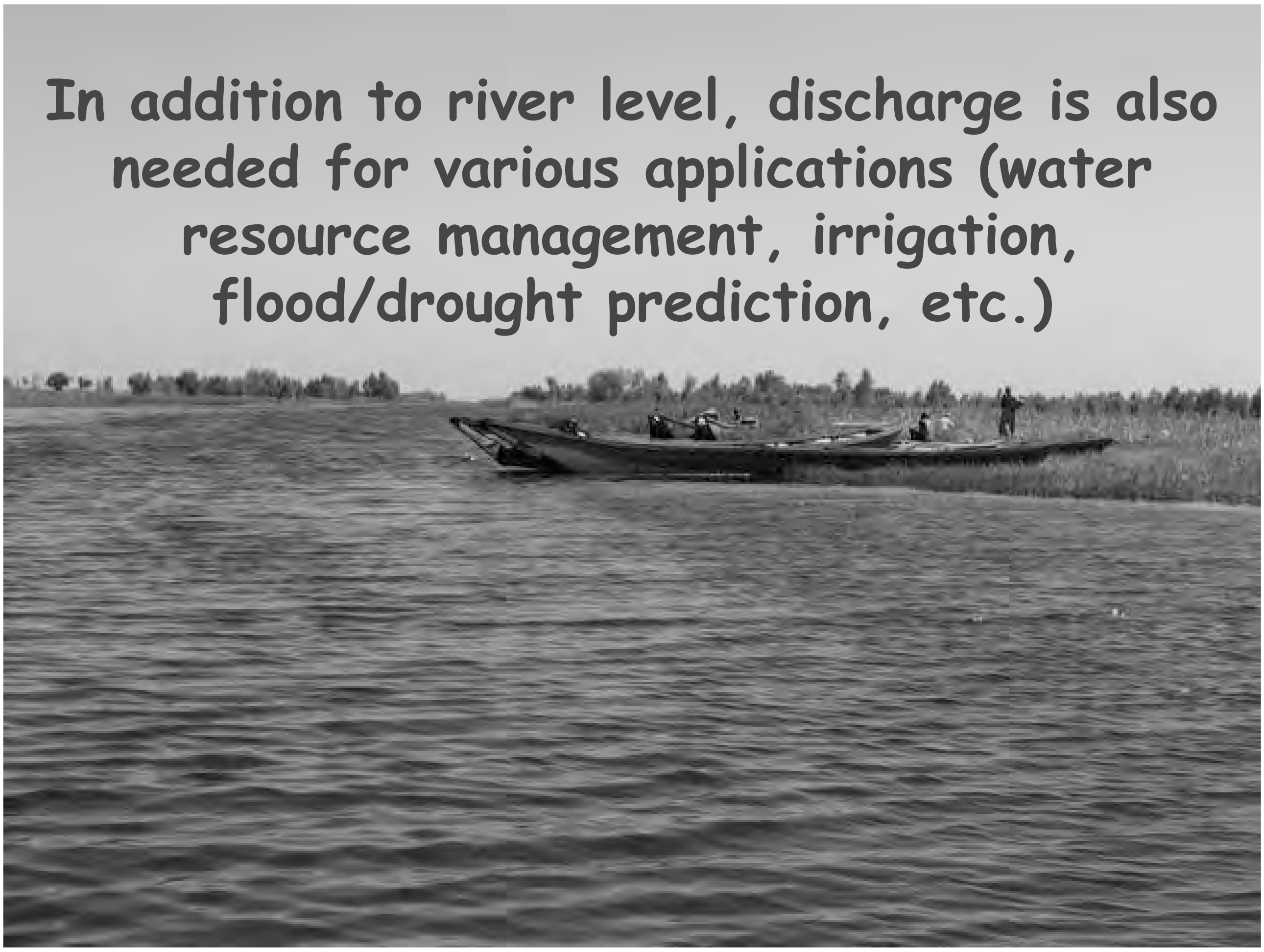
In addition to river level, discharge is also needed for various applications (water resource management, irrigation, flood/drought prediction, etc.)

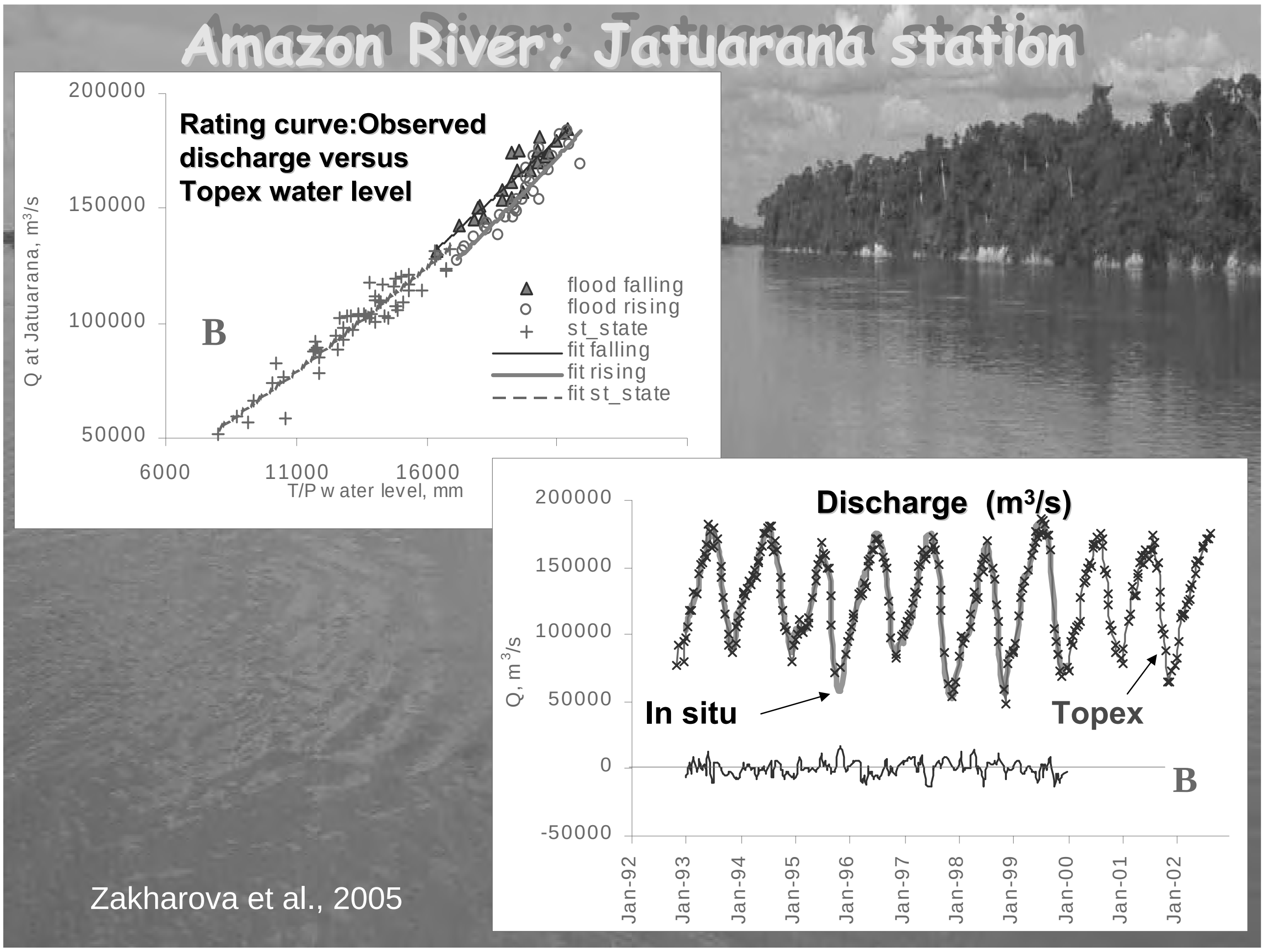
Amazon River: Jatuarana station
Rating curve:Observed discharge versus Topex water level
Q at Jatuarana, m3/s
200000
150000
100000
50000
6000
11000
16000
T/P w ater level, mm
flood falling
flood rising
st_state
fit falling
fit rising
fit st_state
B
Discharge (m3/s)
Q, m3/s
200000
150000
100000
50000
0
-50000
In situ
Topex
B
Jan-92
Jan-93
Jan-94
Jan-95
Jan-96
Jan-97
Jan-98
Jan-99
Jan-00
Jan-01
Jan-02
Zakharova et al., 2005

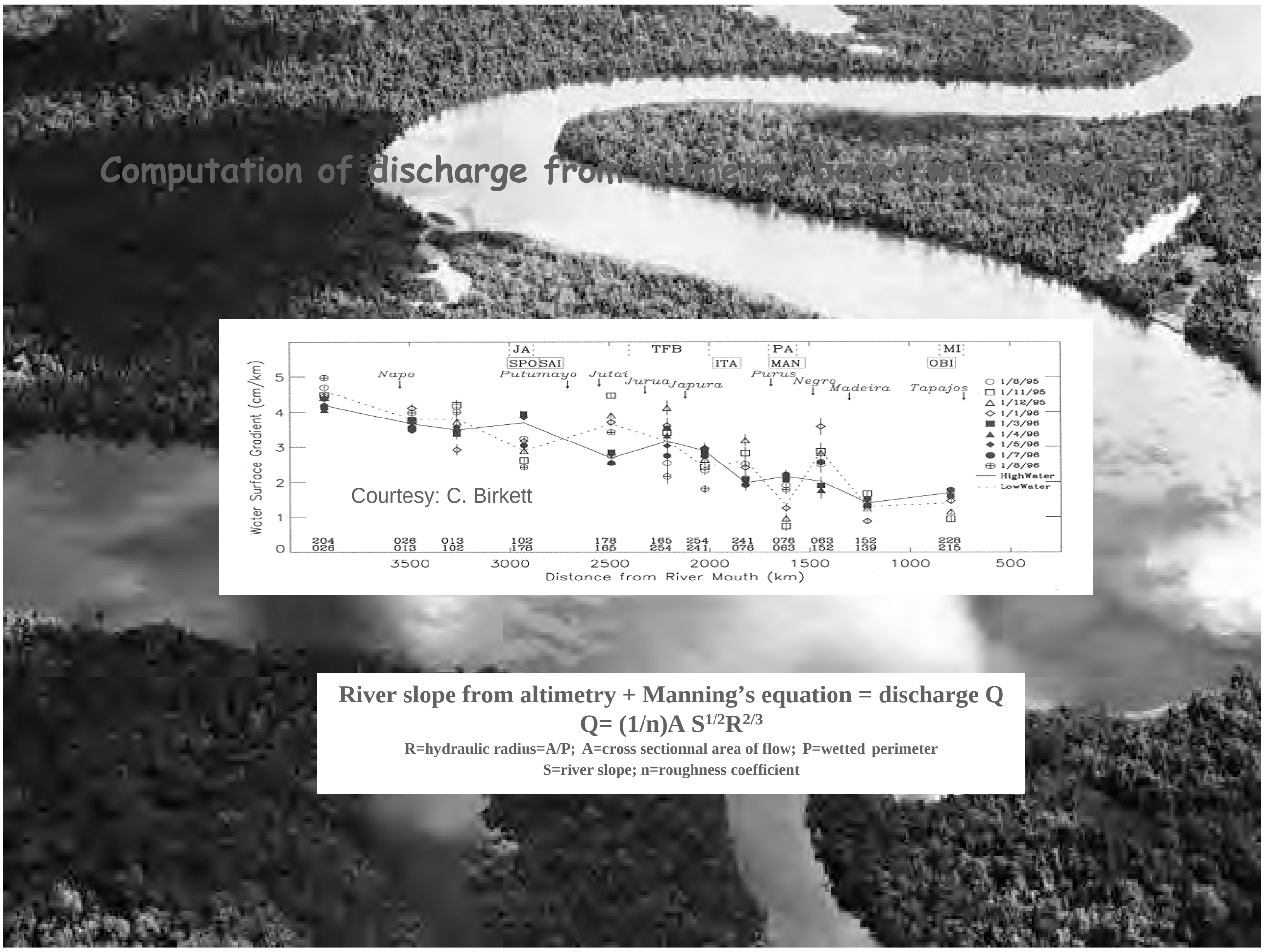
Computation of discharge from
Water Surface Gradient (cm/km)
Distance from River Mouth (km)
JA
SPOSAI
TFB
ITA
PA
MAN
MI
OBI
Napo
Putumayo
Jutai
Jurua
Japura
Purus
Negro
Madeira
Tapajos
1/8/95
1/11/95
1/12/95
1/1/96
1/3/96
1/4/96
1/5/96
1/7/96
1/8/96
HighWater
LowWater
Courtesy: C. Birkett
River slope from altimetry + Manning's equation = discharge Q
Q= (1/n)A S^1/2R^2/3
R=hydraulic radius=A/P; A=cross sectionnal area of flow; P=wetted perimeter
S=river slope; n=roughness coefficient

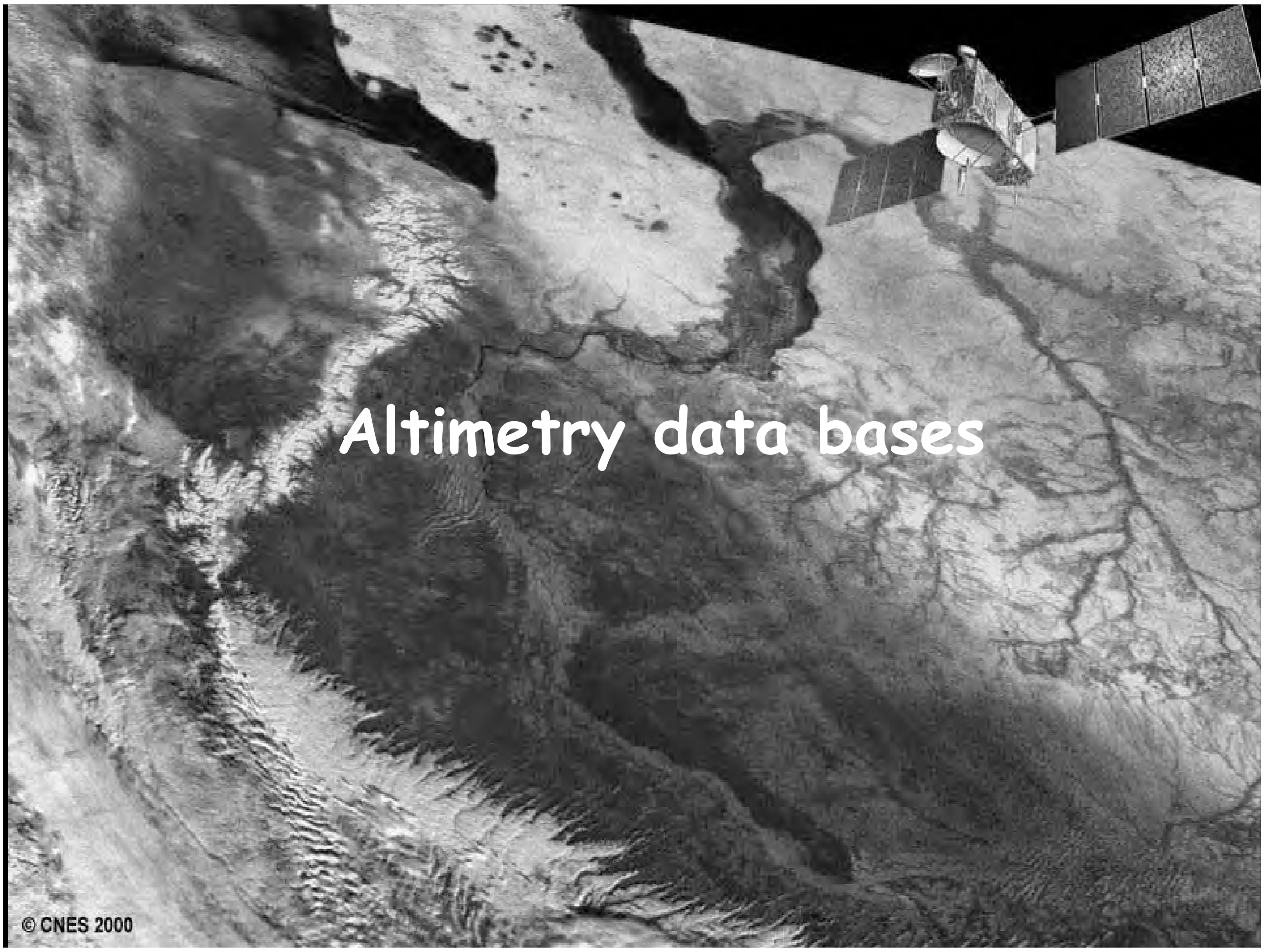
Altimetry data bases
© CNES 2000

Global Reservoirs and Lakes Data Base

http://www.pecad.fas.usda.gov/cropexplorer/global_reservoirs

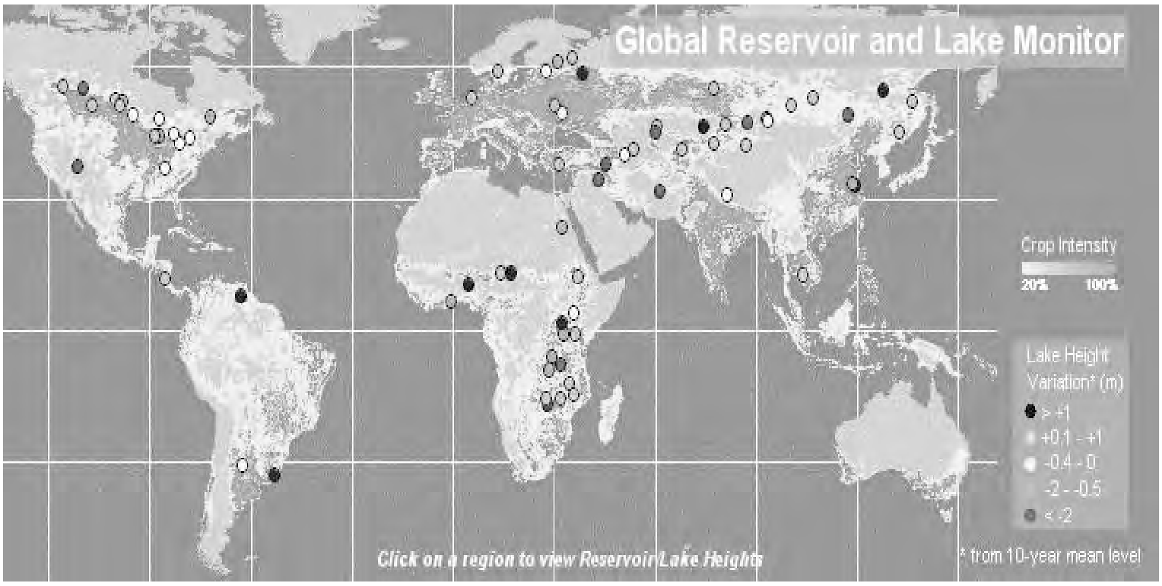

Delayed and near real time water level products ***C. Birkett (GSFC/NASA)***

PECAD data base (GSFC/NASA)

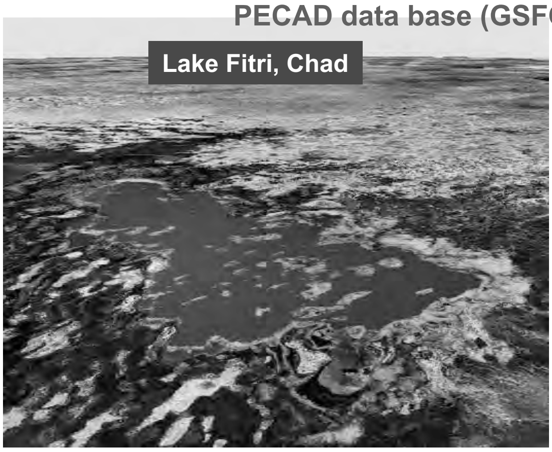

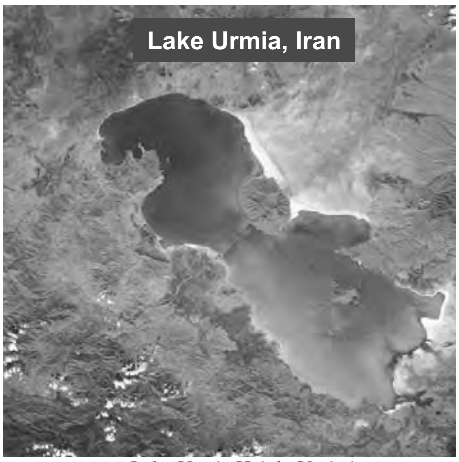

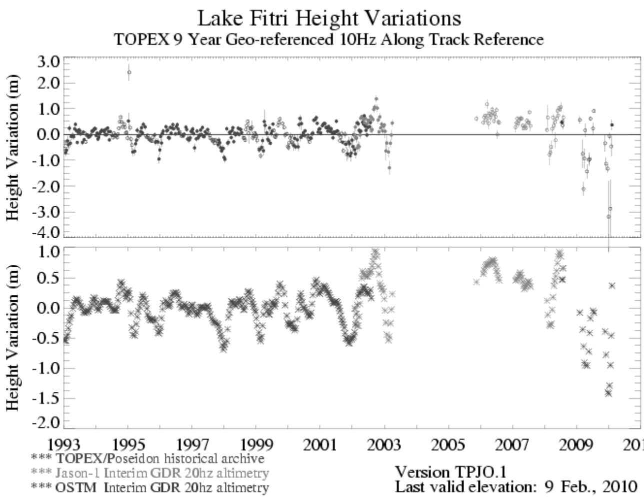

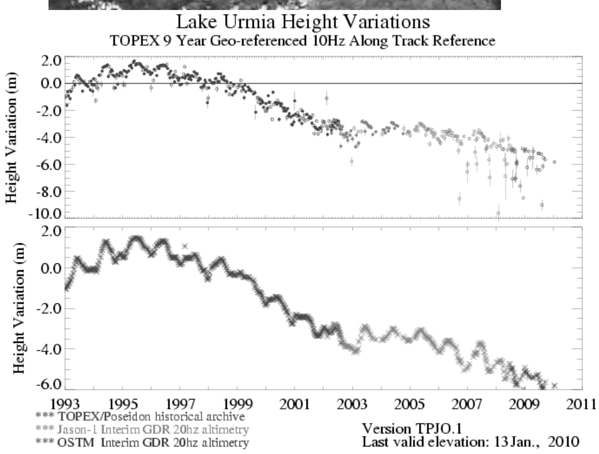

Rivers and Lakes ESA Data Base (P.Berry, UK)
mainly ERS1/2 and ENVISAT

http://earth.esa.int/riverandlake

Lake Edouard (Africa)

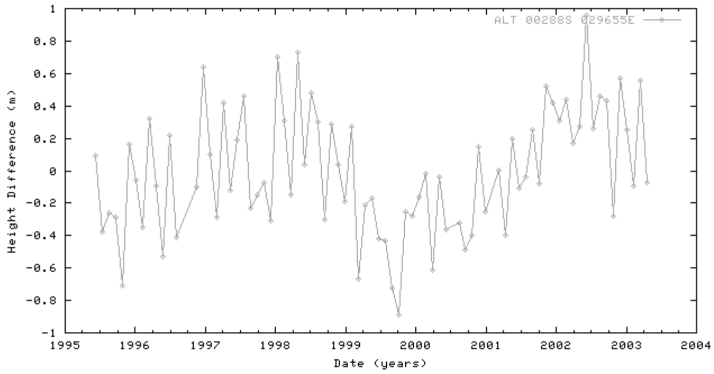

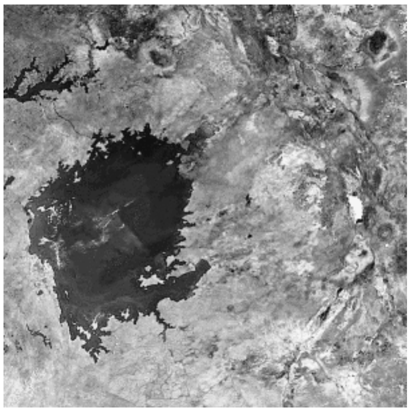

Also: near real time water levels from ENVISAT in some regions

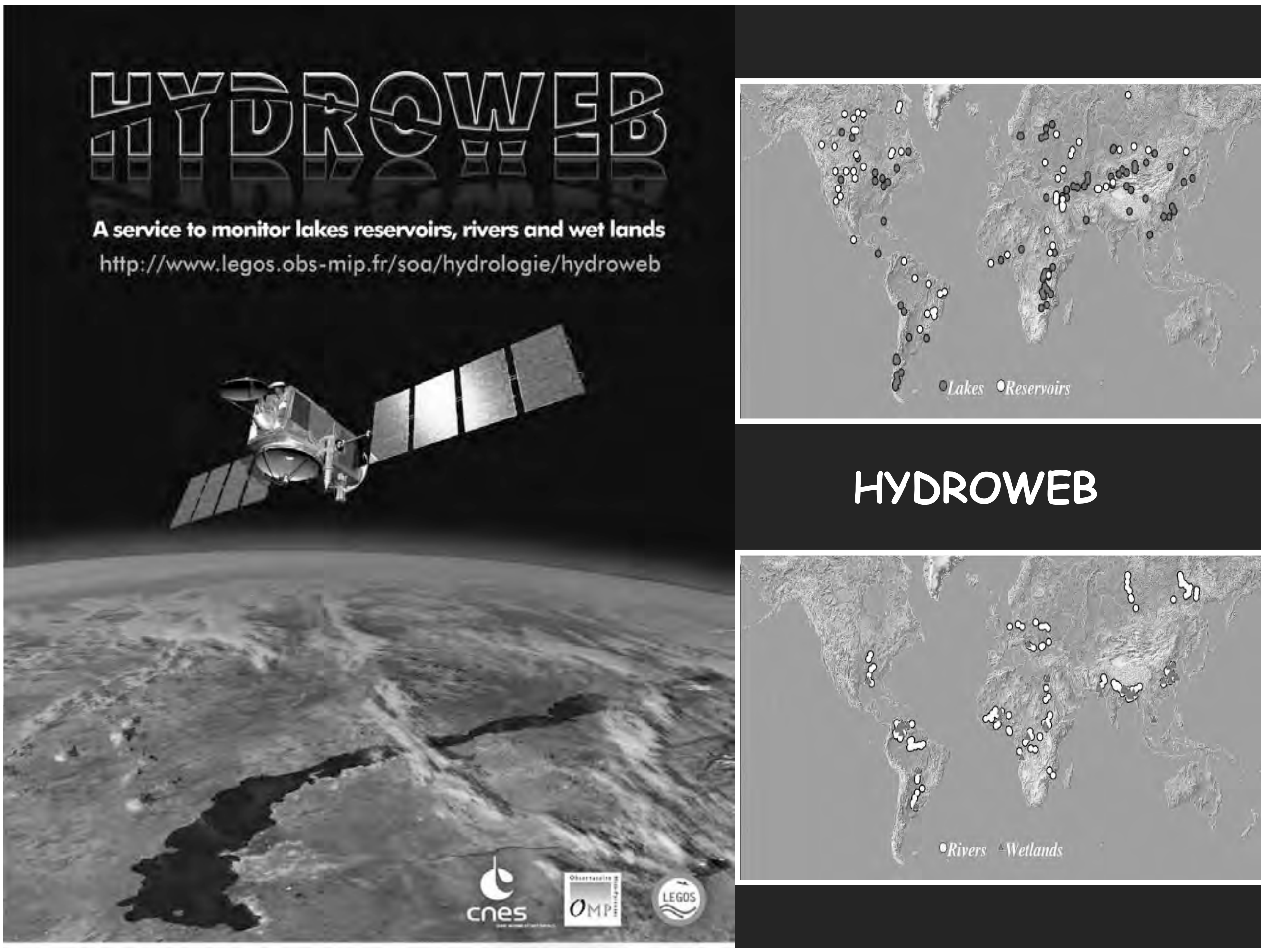

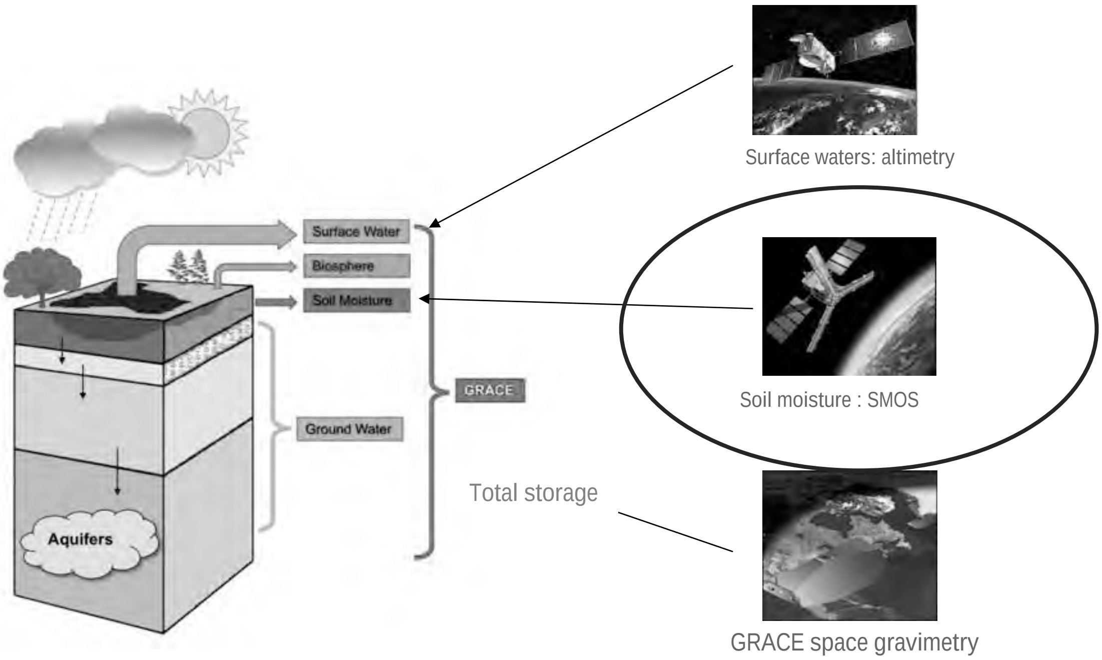
Surface waters: altimetry
Surface Water
Biosphere
Soil Moisture
GRACE
Ground Water
Aquifers
Soil moisture : SMOS
Total storage
GRACE space gravimetry


SMOS : soil moisture

Soil moisture from SMOS in western Africa during March 2010

Soil moisture values
2010/03/03 - 2010/03/23

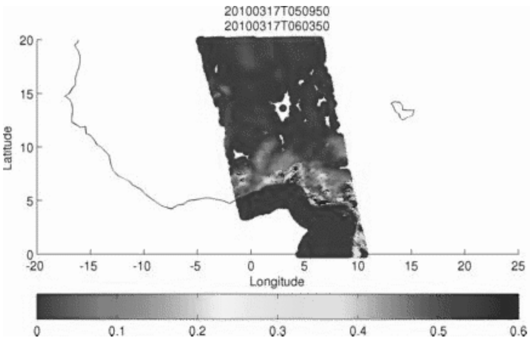

Brightness temperatures
2010/03/03 - 2010/03/23

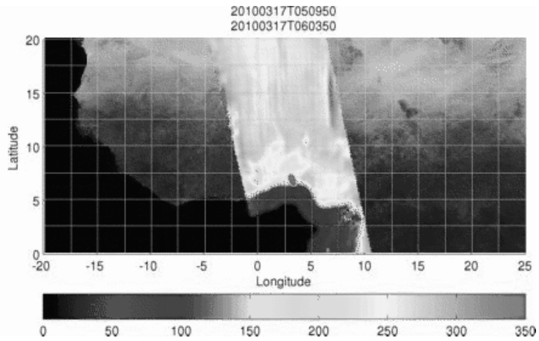

SMOS sees Pakistan floods (summer 2010)

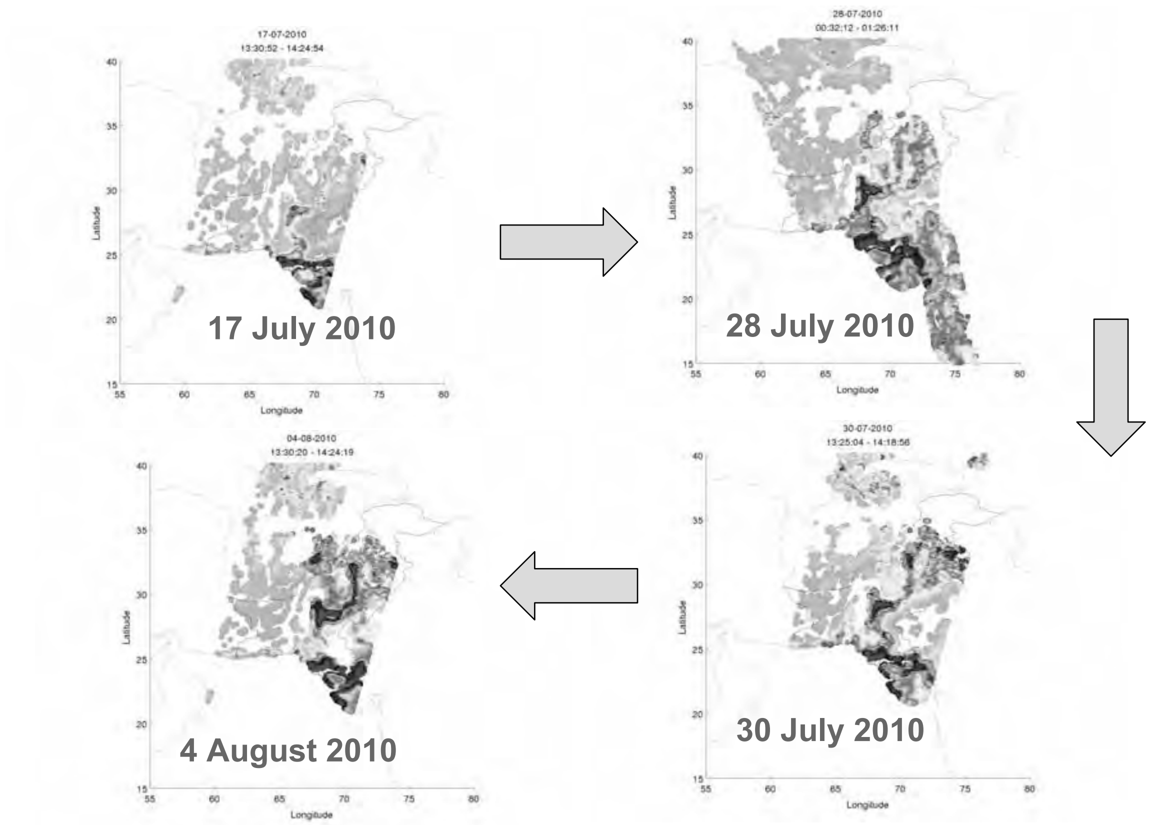

Australian floods seen by SMOS

December 2010

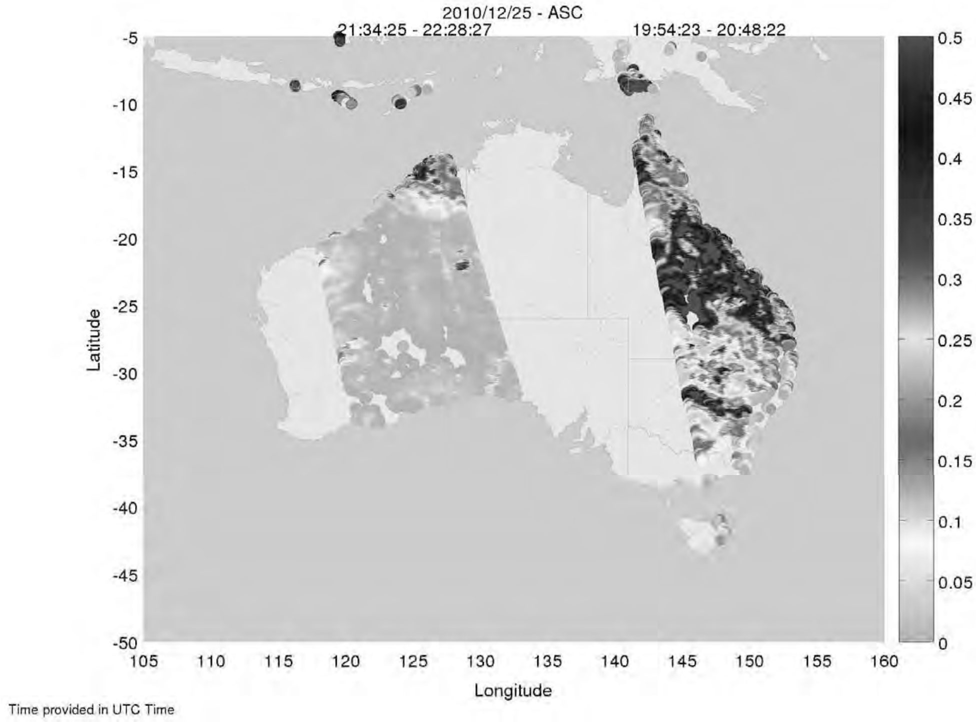

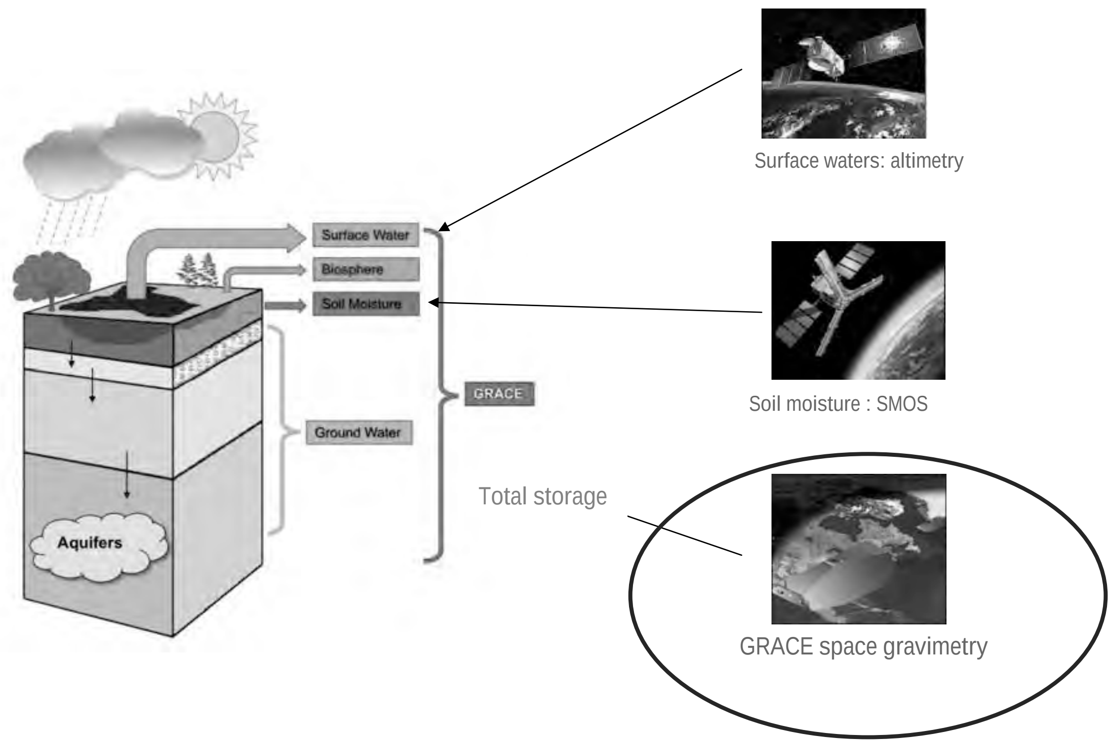

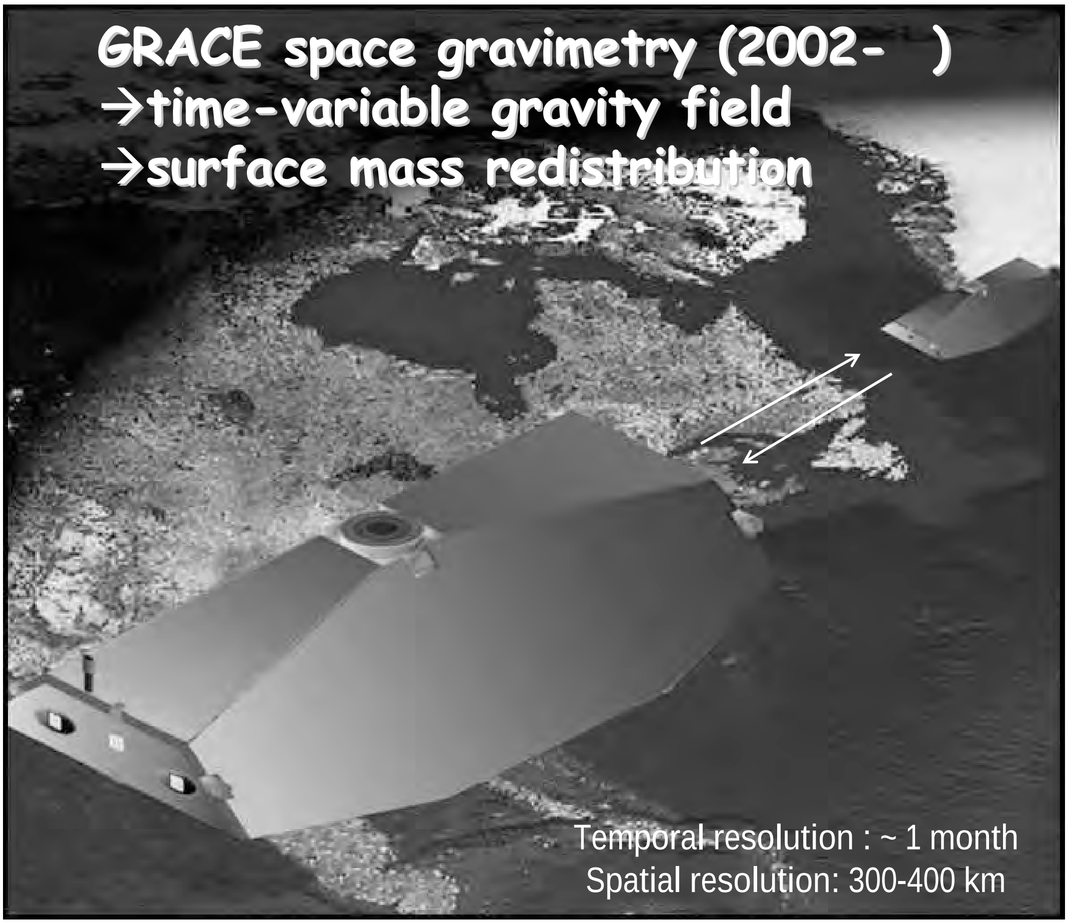
GRACE space gravimetry (2002-)
→time-variable gravity field
→surface mass redistribution
Temporal resolution : ~ 1 month
Spatial resolution: 300-400 km

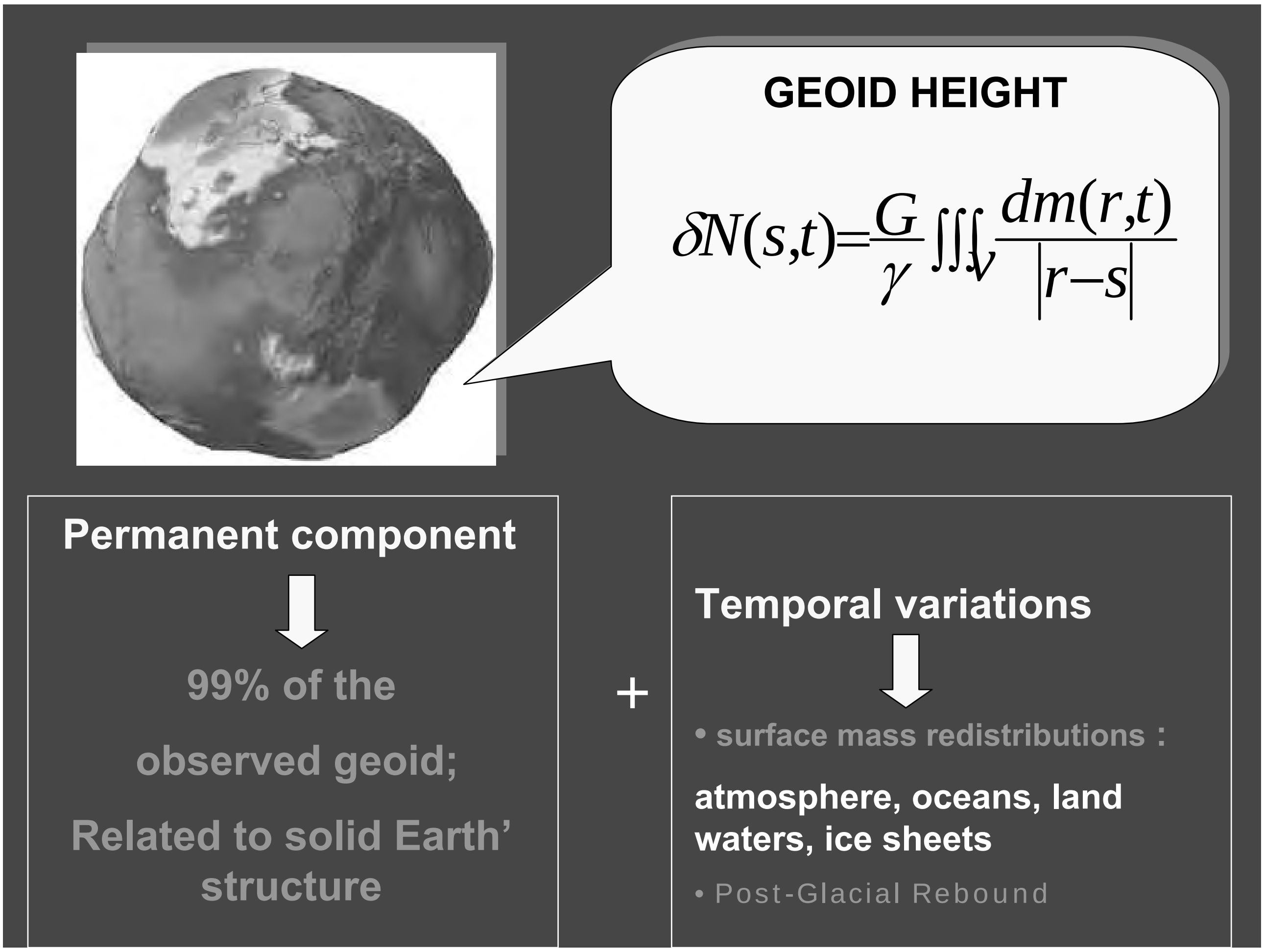
GEOID HEIGHT
$\delta N(s,t) = \frac{G}{\gamma} \iiint_V \frac{dm(r,t)}{|r-s|}$
Permanent component
99% of the
observed geoid;
Related to solid Earth' structure
+
Temporal variations
• surface mass redistributions :
atmosphere, oceans, land waters, ice sheets
• Post-Glacial Rebound

GRACE : Temporal evolution of land water storage (2002-2008)

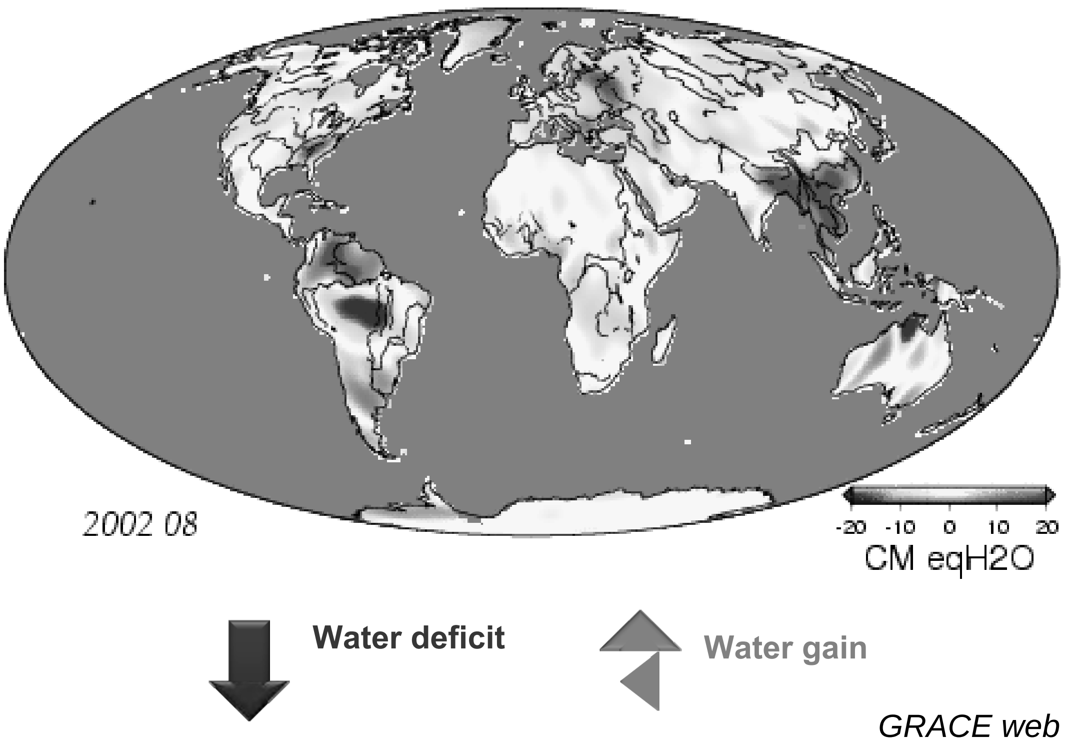

GRACE web site

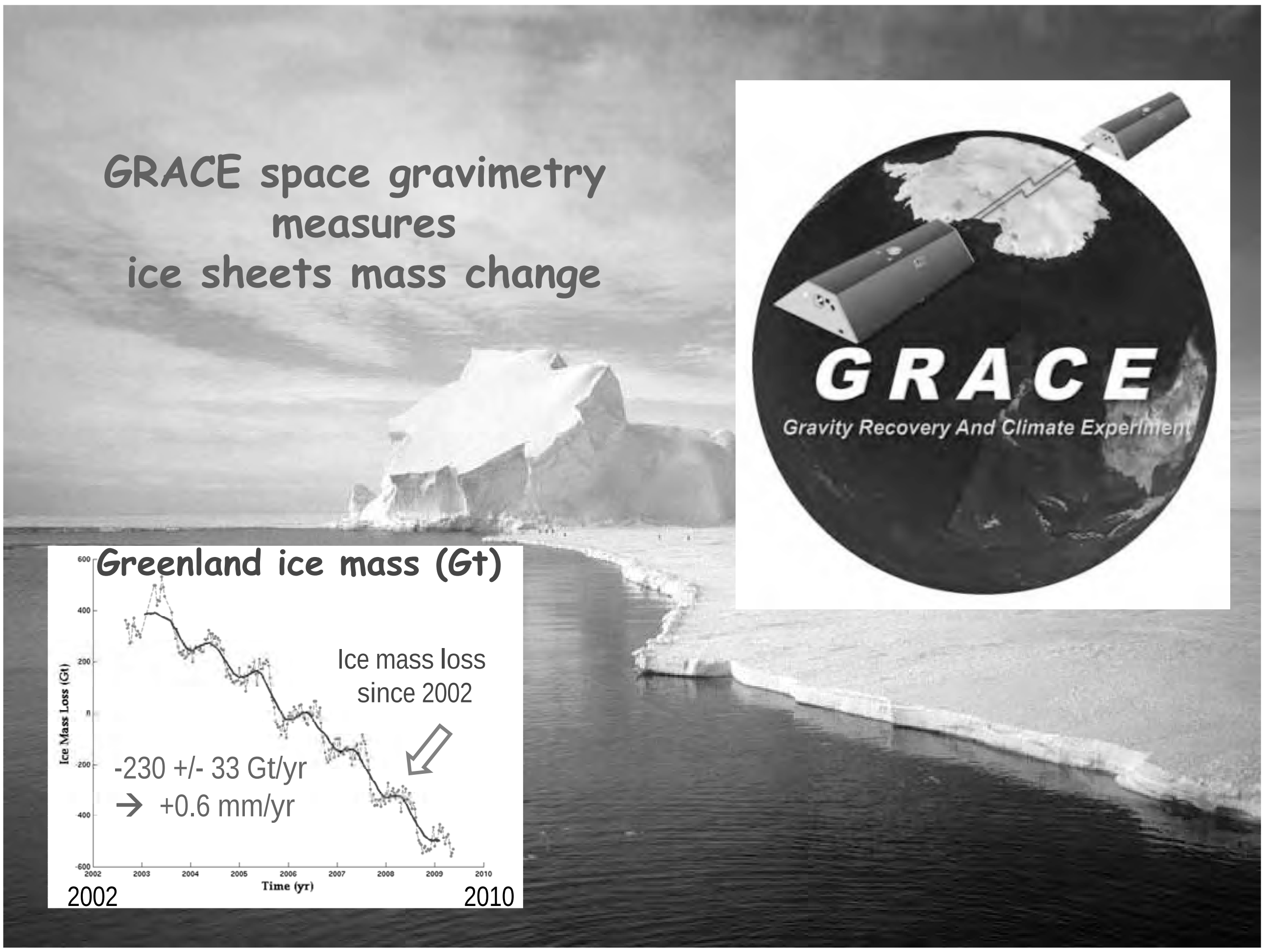

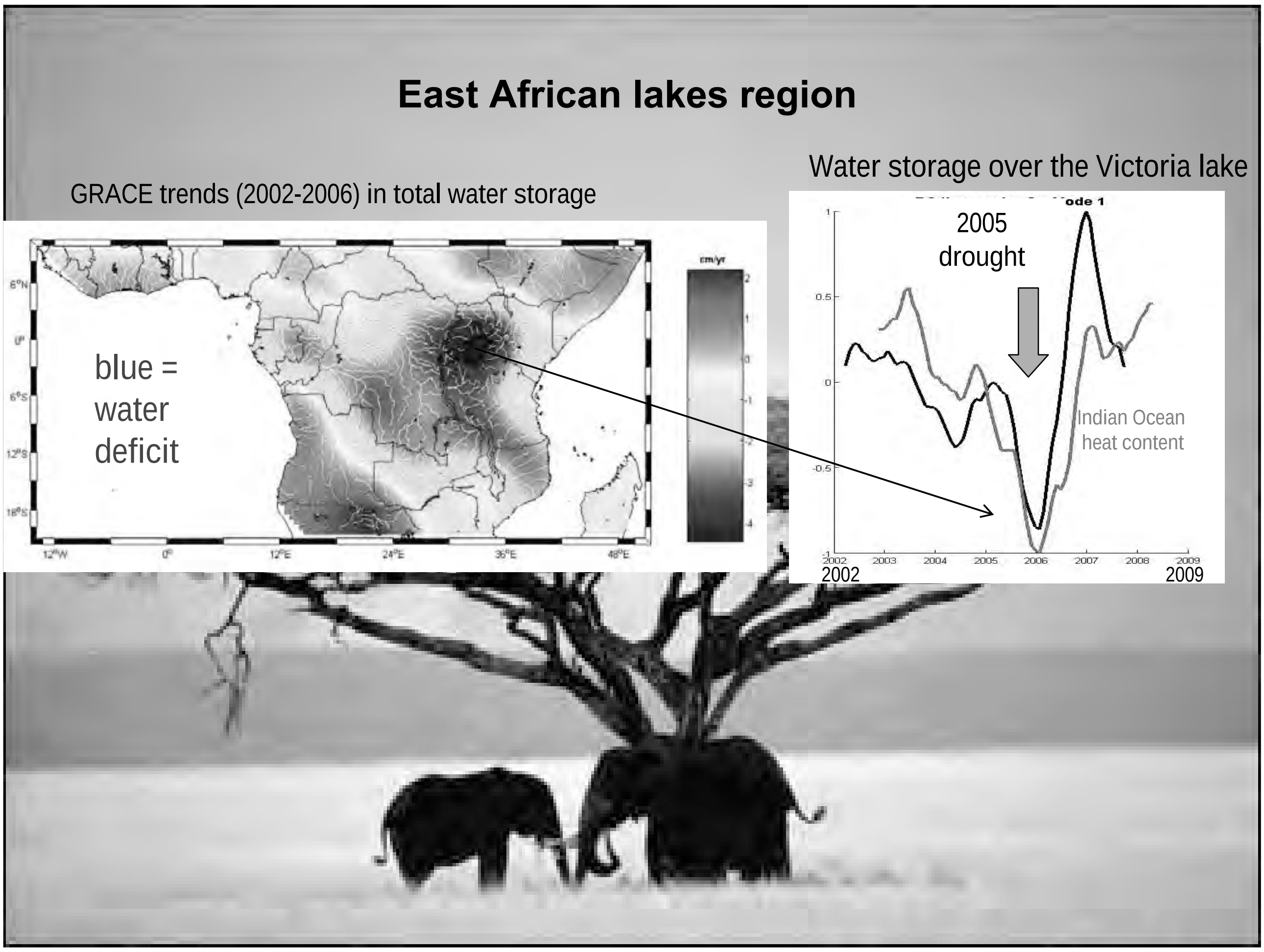

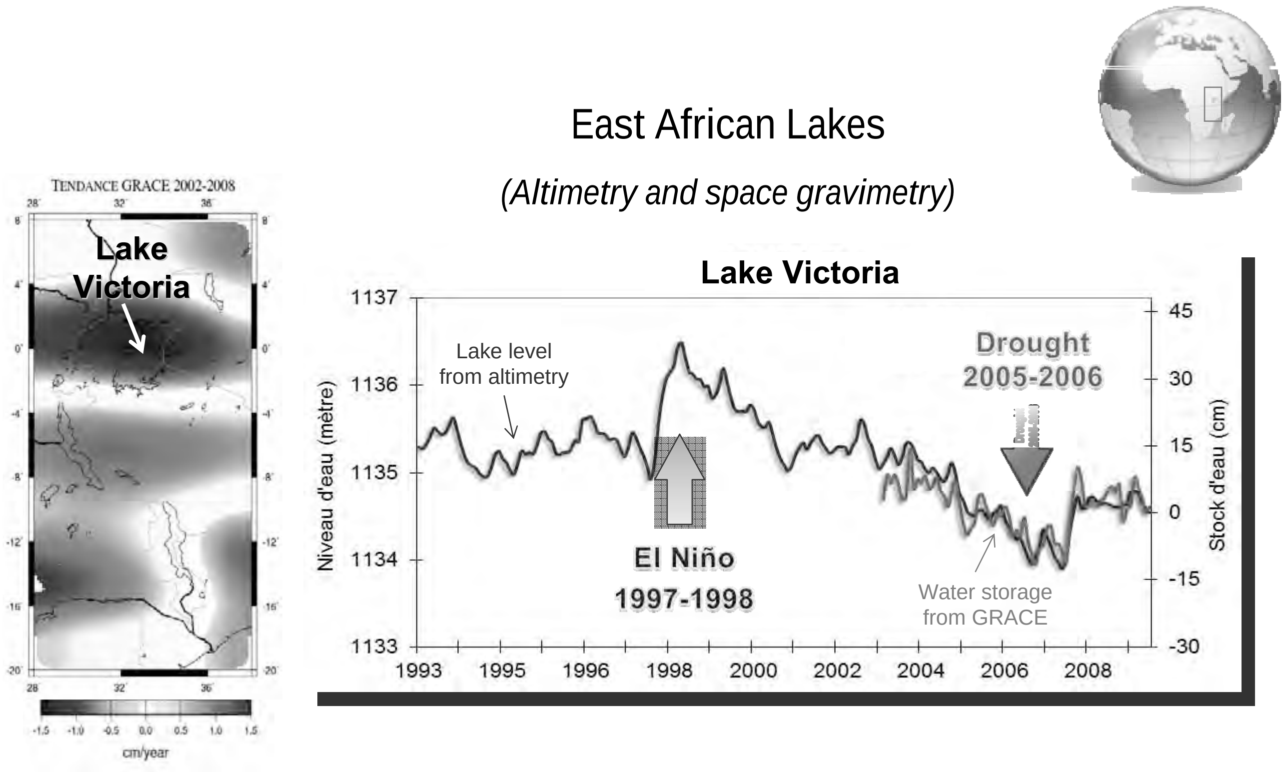

Becker et al. 2010

Amazon Basin

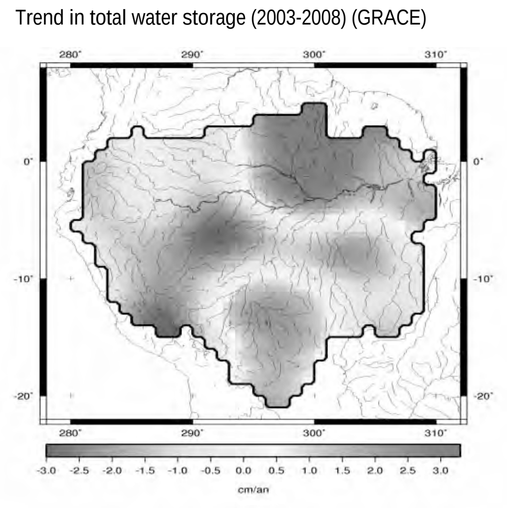

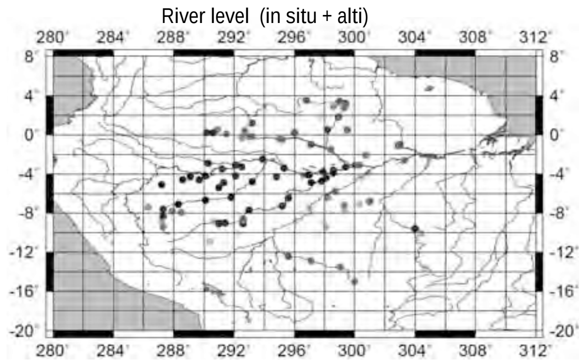

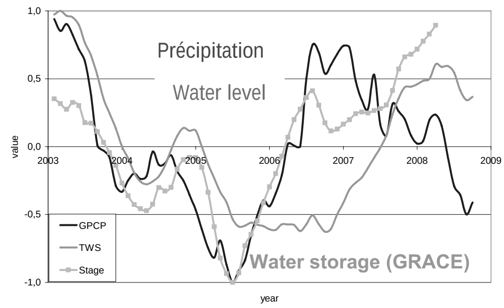

Blue = water deficit
Red = water excess

Surface water volume change from multi-satellite techniques: Combining surface water extent and altimetry-derived water height

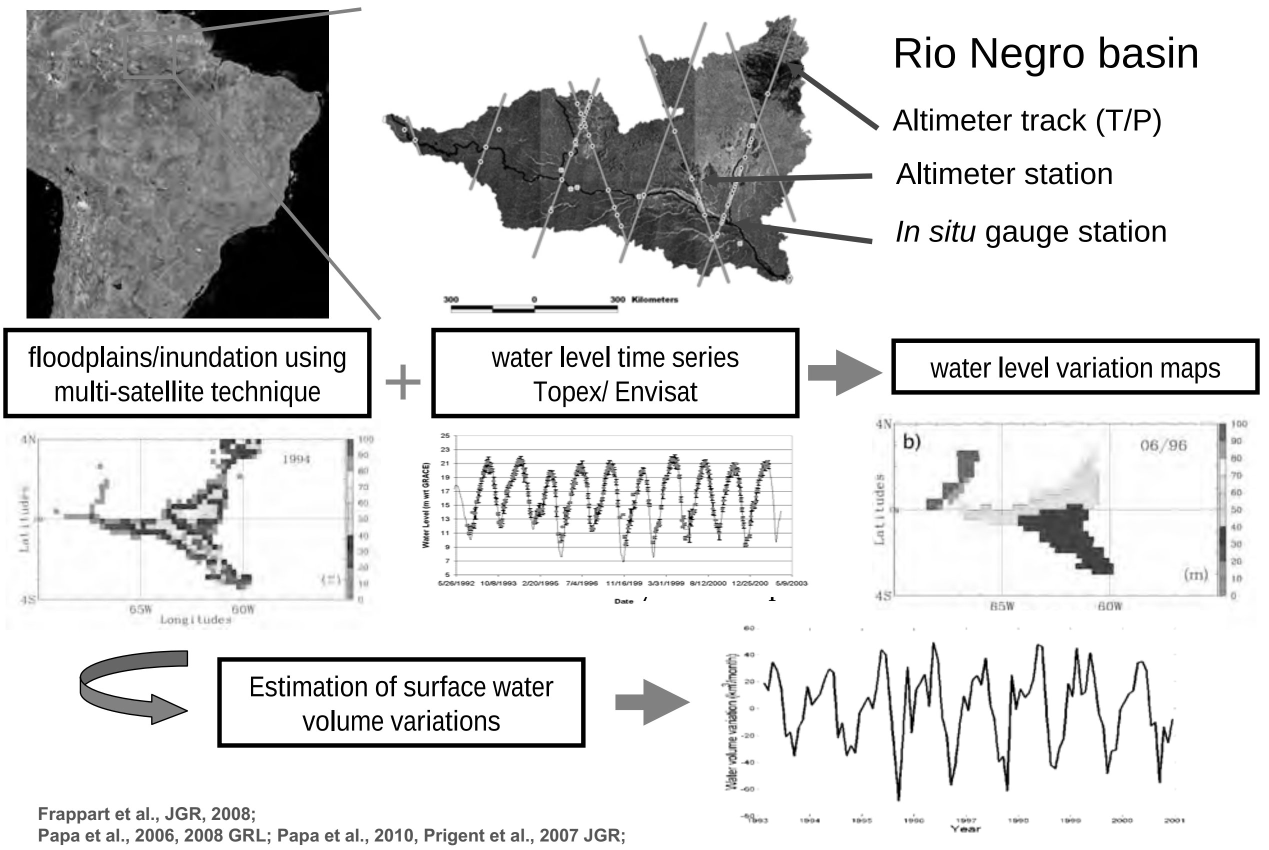

Frappart et al., JGR, 2008;
Papa et al., 2006, 2008 GRL; Papa et al., 2010, Prigent et al., 2007 JGR;

Groundwater storage variations in various large aquifers using GRACE data

- GRACE mission (2002 to present)
- Estimation of the Total Water Storage (TWS)

- Surface and near-surface layers: Land Surface Models (GLDAS, ISBA, WGHM)
- Combination of GRACE and LSM to estimate GWS variations

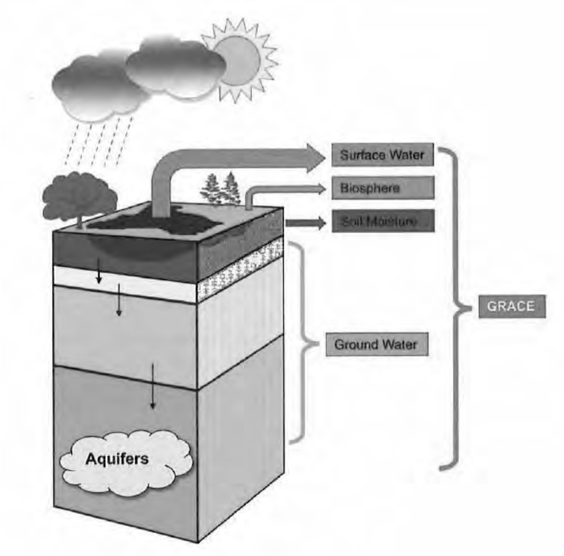

Rio Negro (Amazonia)

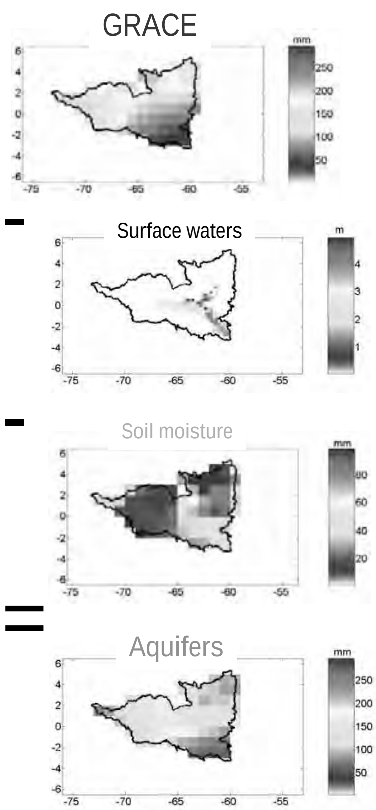

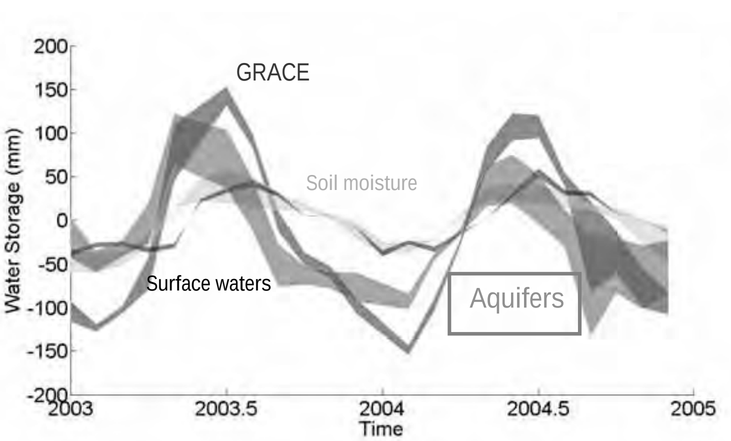

Groundwater storage variations in various large aquifers using GRACE data

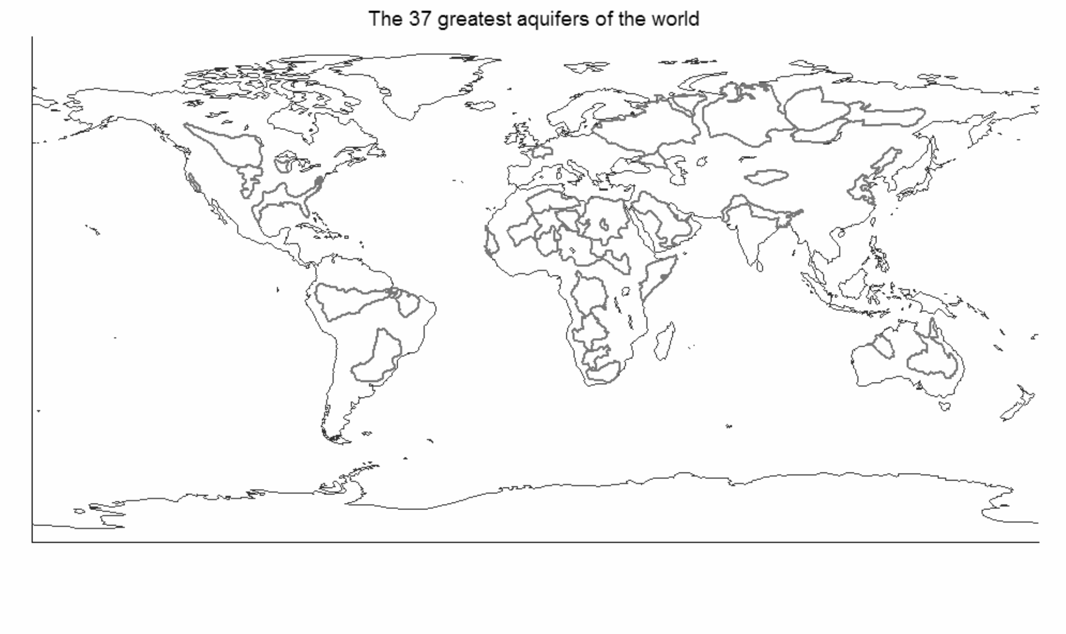

Water storage trend in the Ganges Basin

2002-2009 (cm/yr)

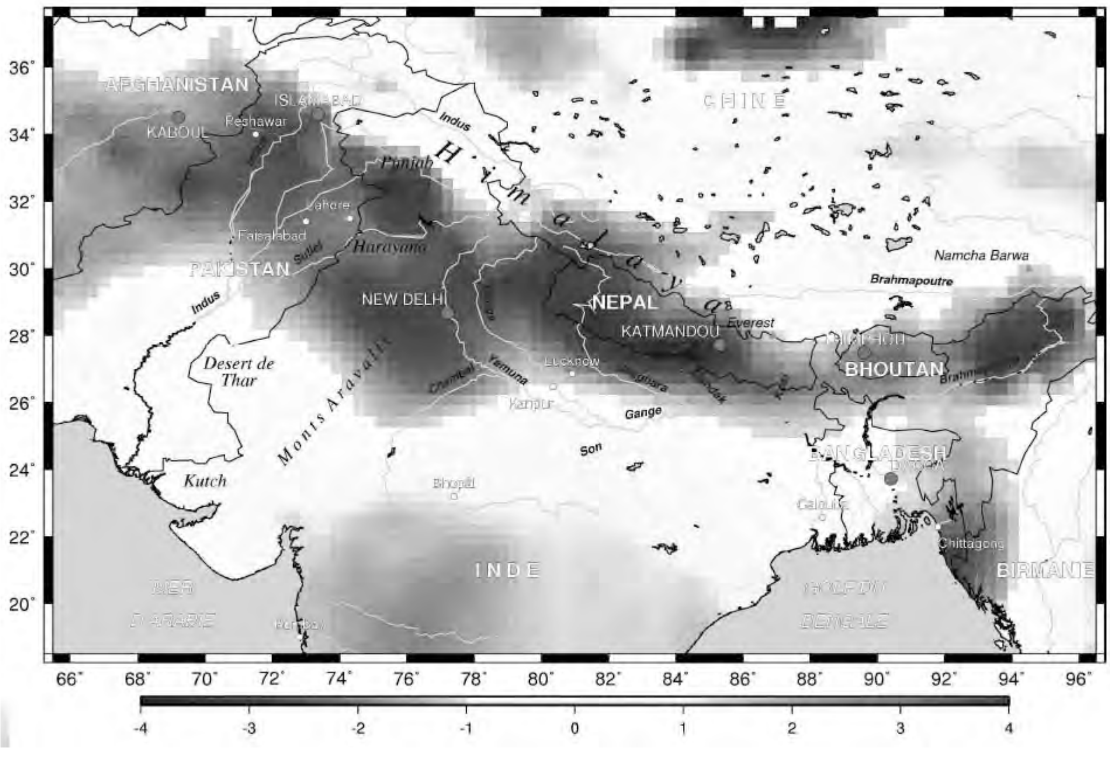

Rodell et al., 2009; Tiwari & Wahr, 2009

GRACE also sees ground water variations

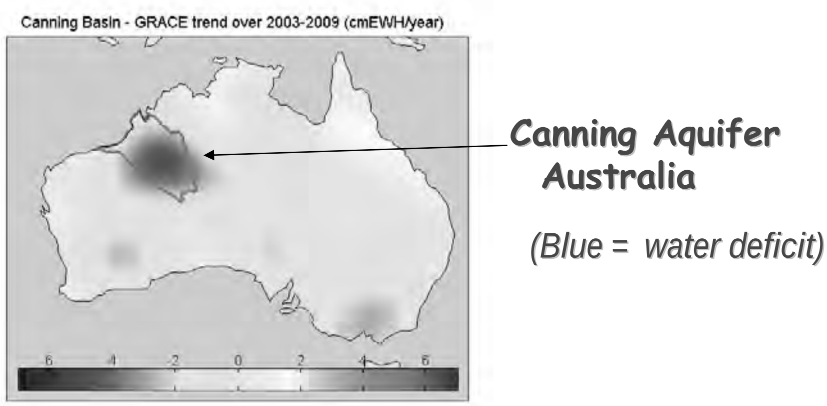

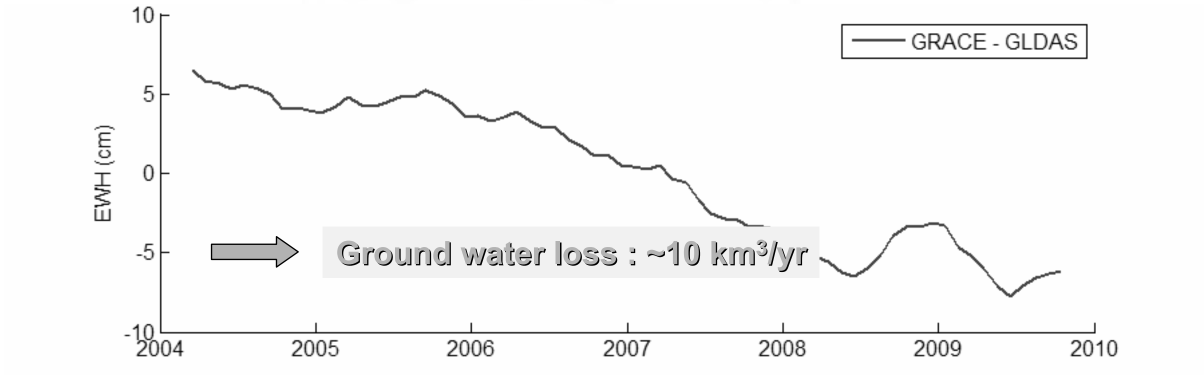

Altimetry-based global mean sea level (1993-2011)

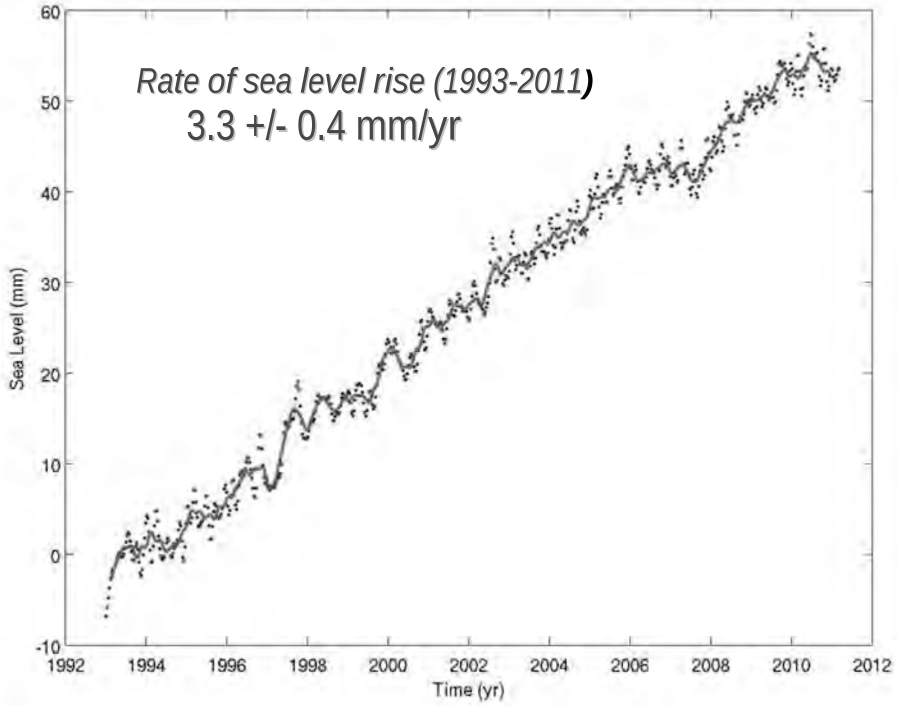

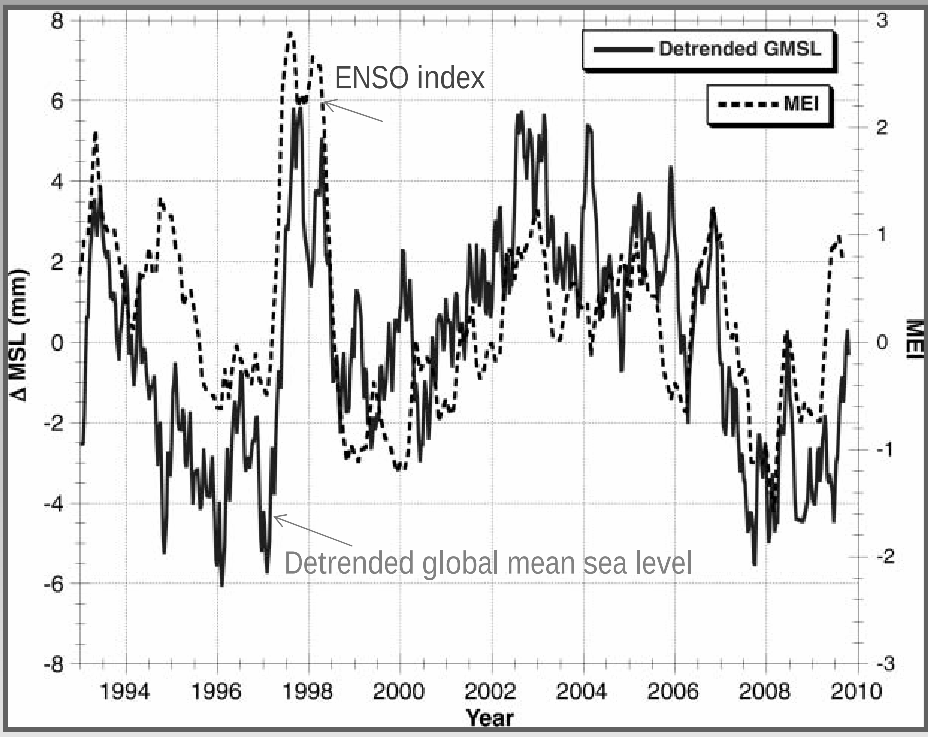

Nerem et al. (2010)

MEI: Multivariate ENSO Index

What processes control the observed correlation between interannual sea level and ENSO?:

-Ocean heat content?

-Land water storage?

Detrended global mean sea level
Land water storage from the ISBA-TRIP model

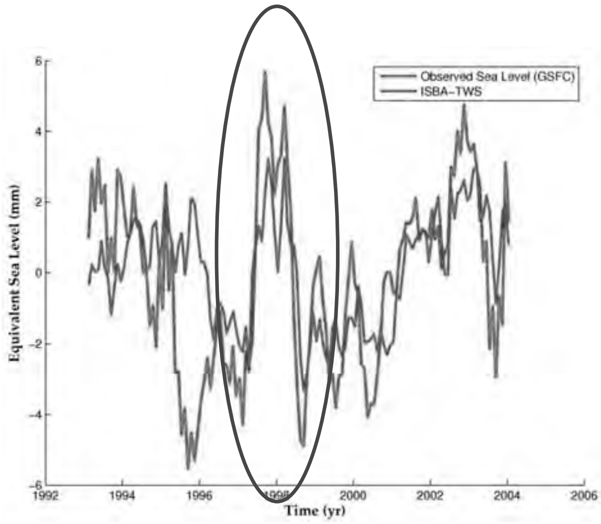

Sea level data from GSFC
(Beckley et al.)

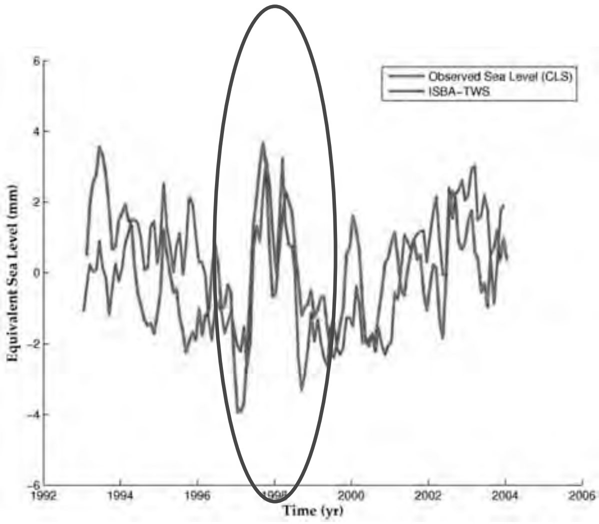

Sea level data from CLS
(Ablain et al.)

Llovel et al., 2010

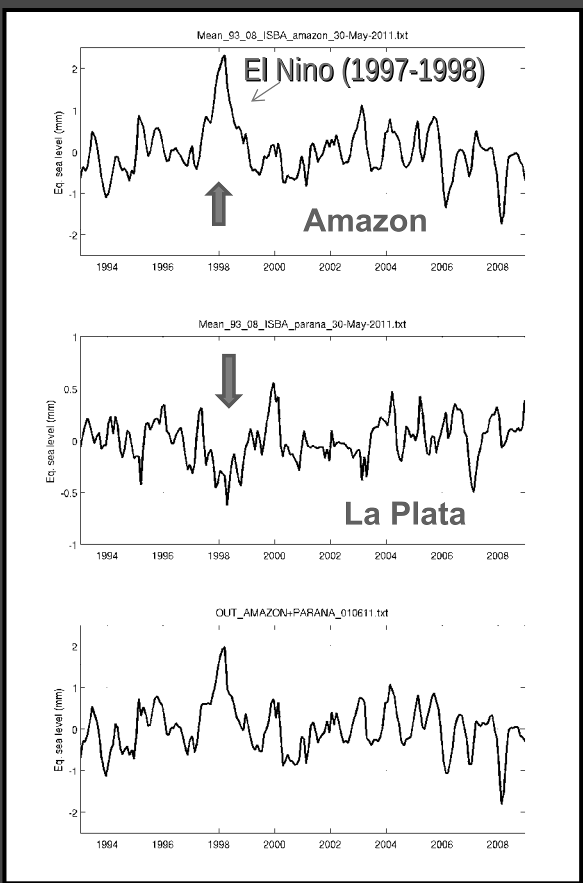

Contribution to sea leve
of total
water storage change
in the Amazon
and La Plata basins
(and sum of both)

Expressed
in equivalent sea level
(mm)

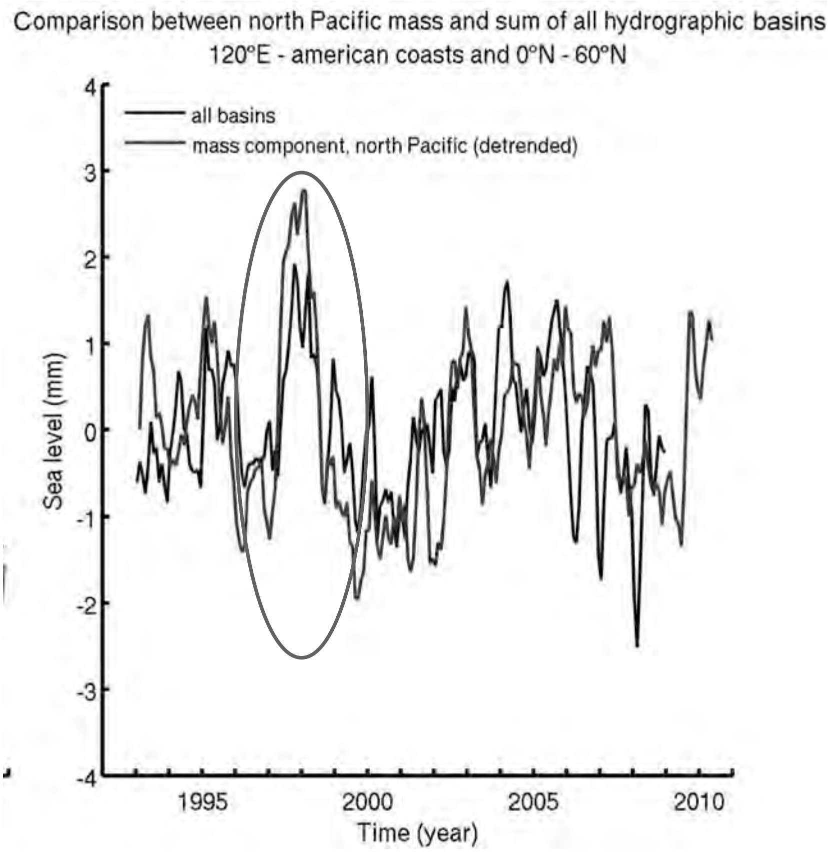

Comparison between north Pacific mass and sum of all hydrographic basins
120°E - american coasts and 0°N - 60°N
all basins
mass component, north Pacific (detrended)
Sea level (mm)
Time (year)

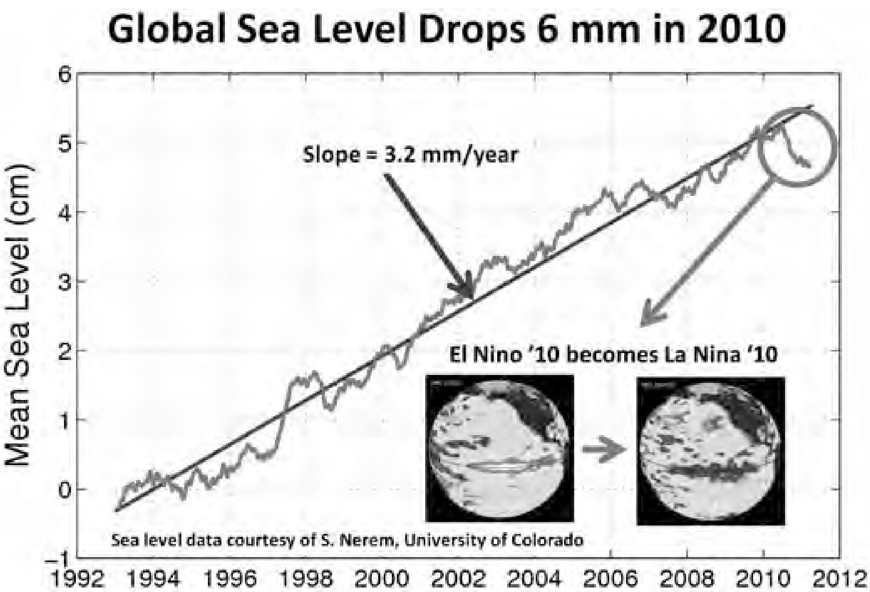

Global Sea Level Drops 6 mm in 2010
Slope = 3.2 mm/year
El Nino '10 becomes La Nina '10
Sea level data courtesy of S. Nerem, University of Colorado
Mean Sea Level (cm)

GRACE-based water storage trend 2002-2009 (km³/yr)

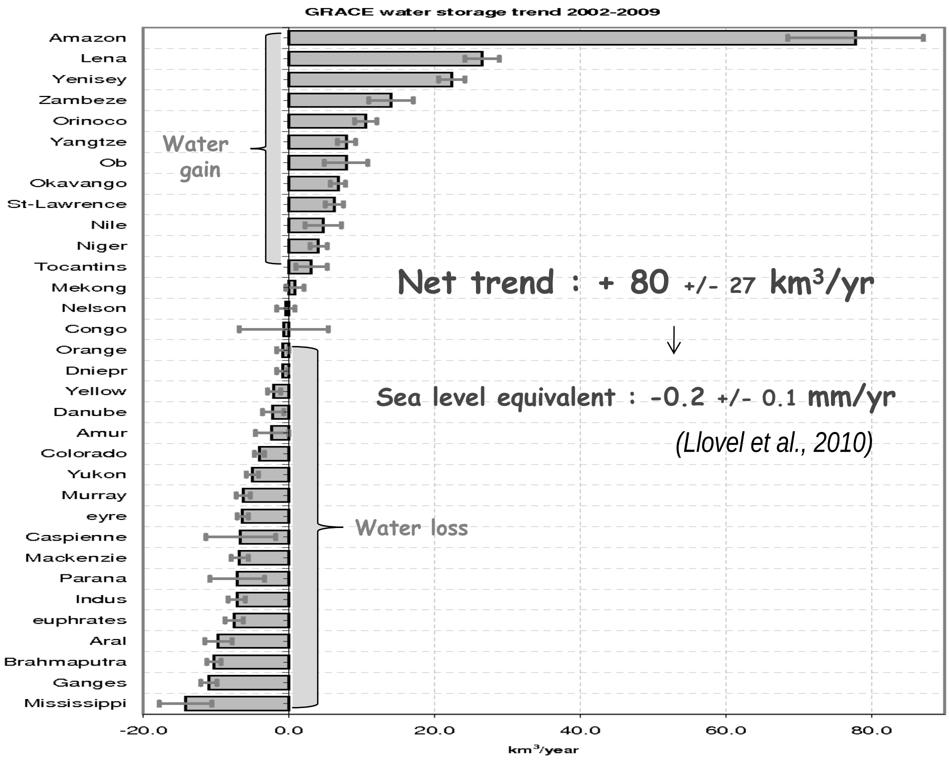

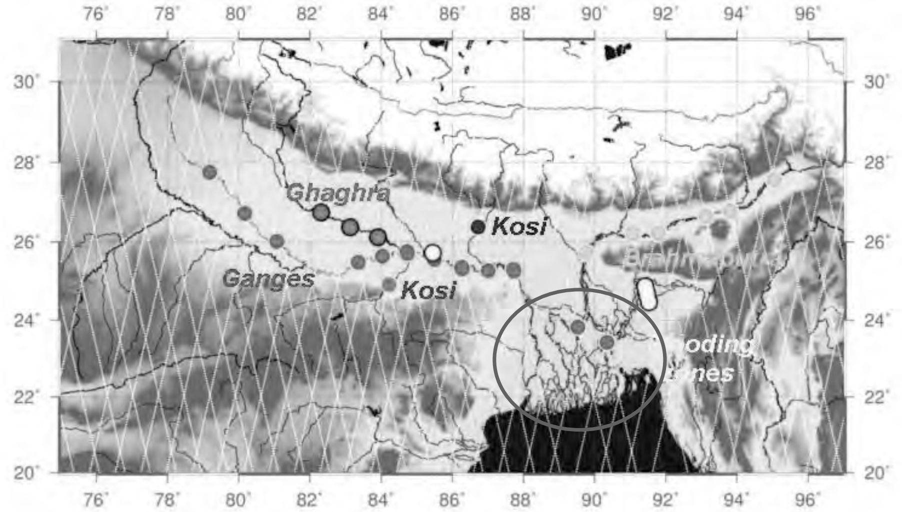

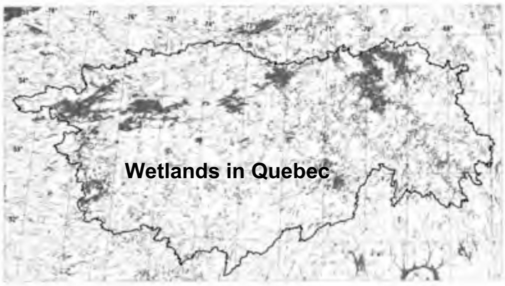

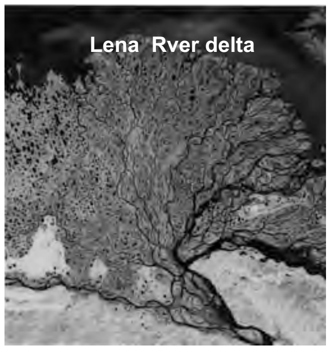

Radar waveforms

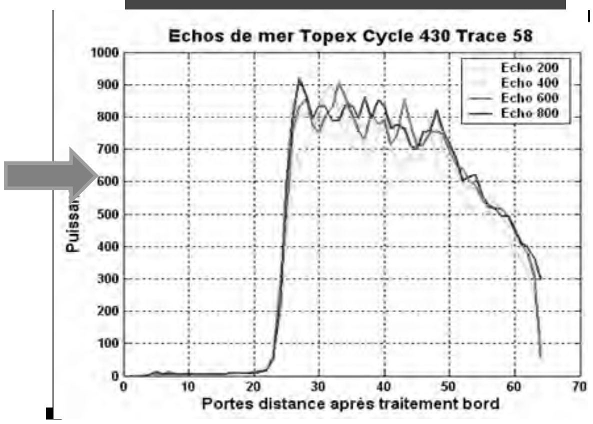

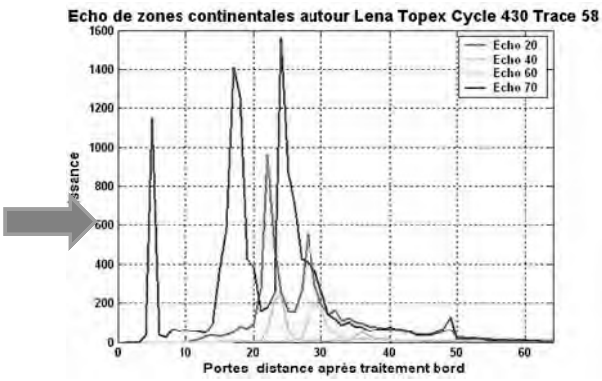

SWOT: The Surface Water and Ocean Topography

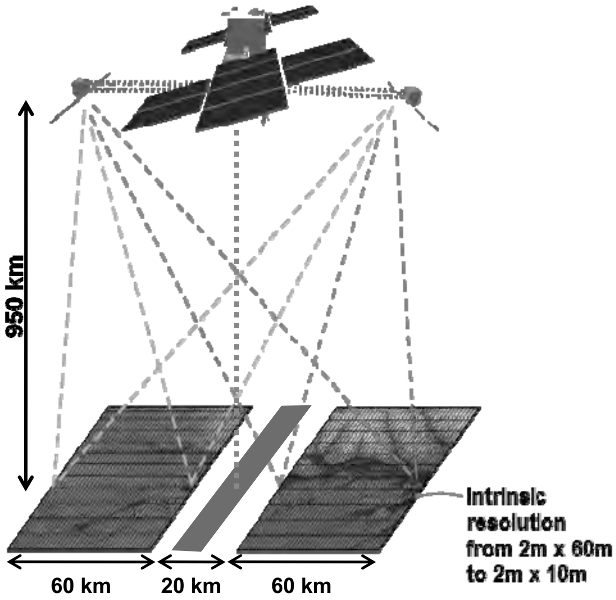

Objectives

Hydrology:

- Measurement of water levels and storage of all types of surface water bodies (lakes, rivers, wetlands) of size >100mx100m
- Revisit time : 3 days and 22 days
- Launch: 2018-2019

CNES/NASA mission

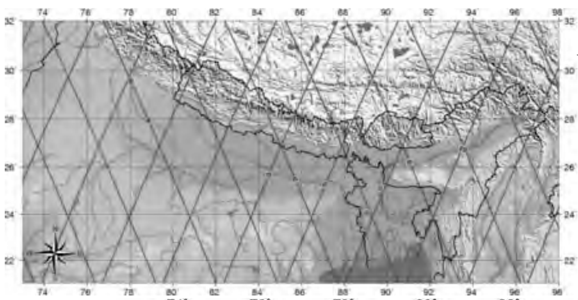

Nadir altimeter coverage

SWOT coverage

- SWOT = Water mask + water elevation (and river slope) with 2 or more observations per 22 days

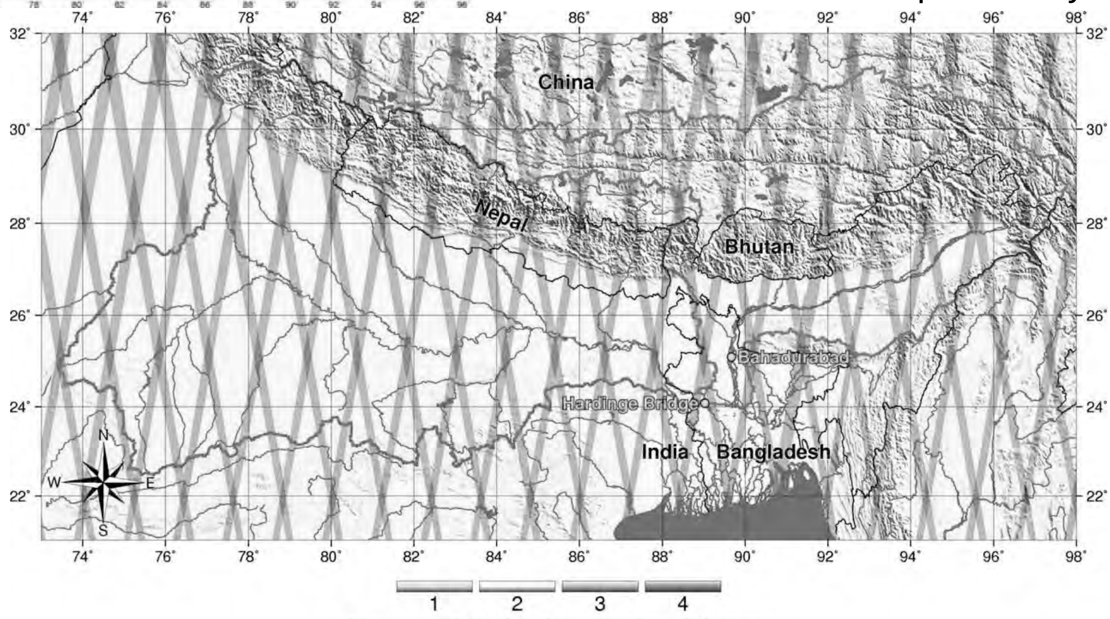

Lakes and SWOT

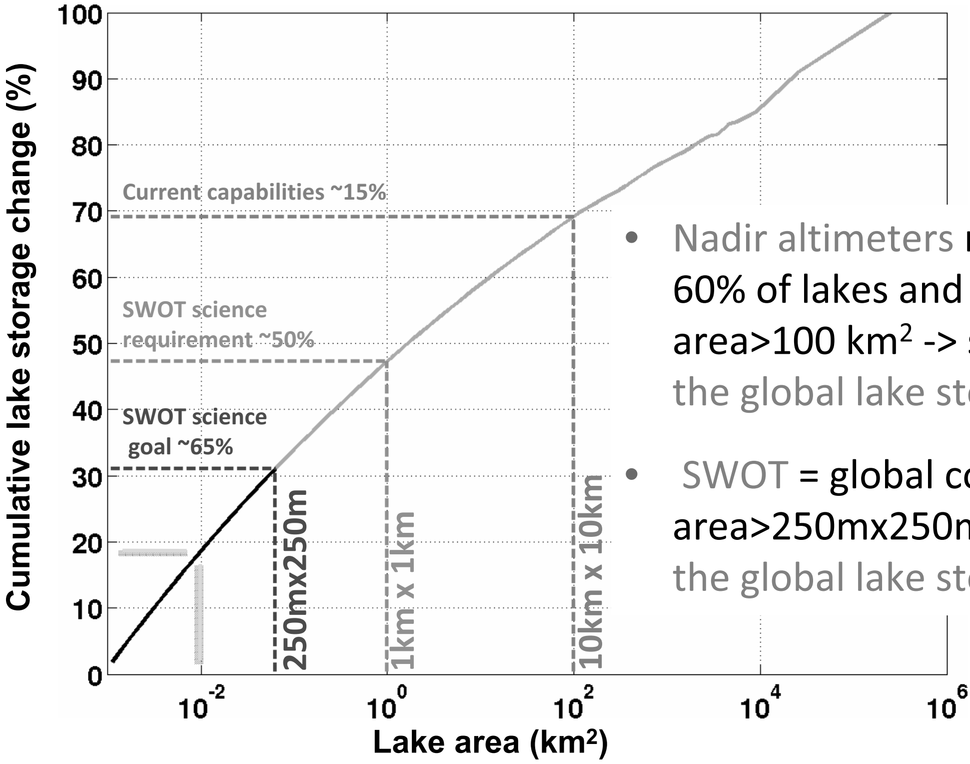

- Nadir altimeters miss more than 60% of lakes and can see area>100 km² -> see only 15% of the global lake storage change
- SWOT = global coverage and see area>250mx250m -> see 65% of the global lake storage change

Transboundary basins: Ganges

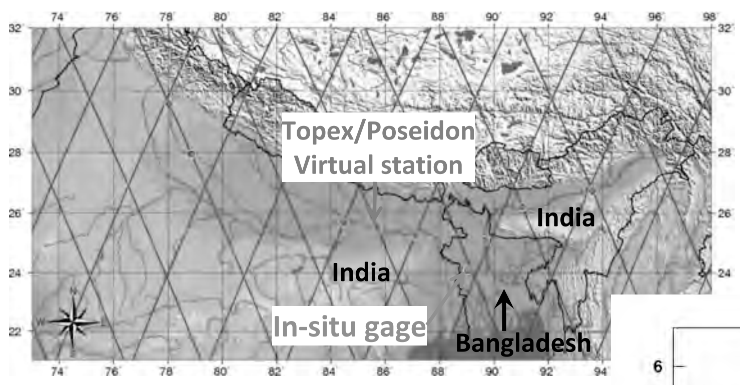

- Distance virtual station/gage=530 km
- RMSE **5-day forecast/in-situ=0.7 m**

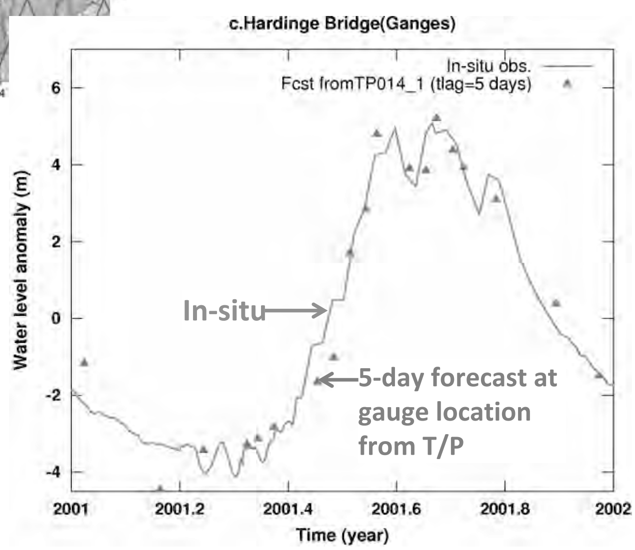

A GRACE Follow-On mission is crucially needed

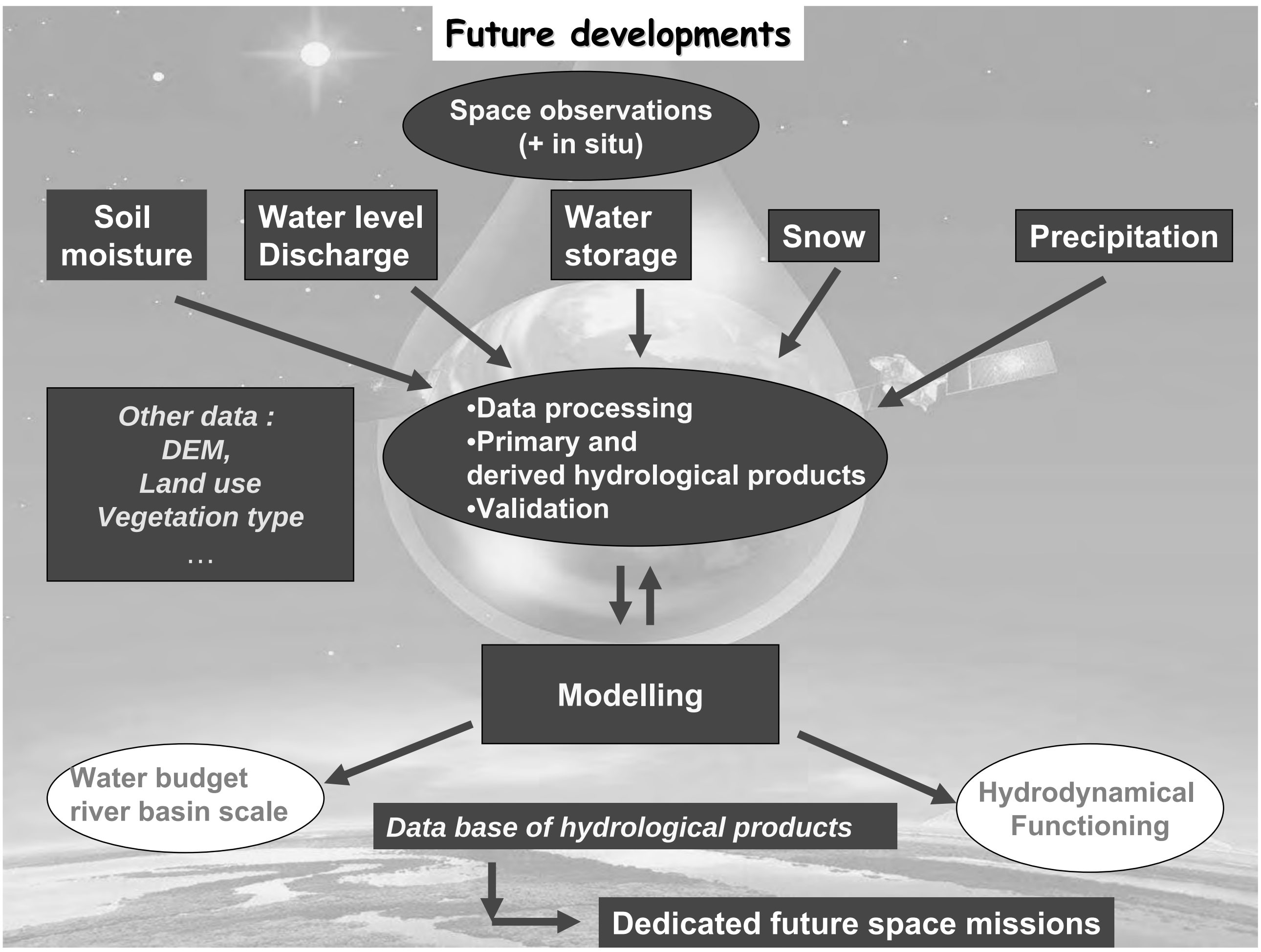


Thanks for your attention

GRACE Level-2 Products

Torsten Mayer Guerr, Frank Flechtner

Summer School „Global Water Cycle“
12.-16. September 2011
Mayschoss

1

DFG SPP 1257

Content Part 2

- GRACE Measurement Principle: Level-1B Data
- Dynamic Approach to derive Level-2 GRACE Satellite-only Models („GSM“)
- AOD1B as a „special“ Background Model
- GRACE Level-2 „Gax“ Products
- RL05 Reprocessing at GFZ (with remarks on degree 2 coefficients)
- Summary

2

DFG SPP 1257

GRACE Mission Concept

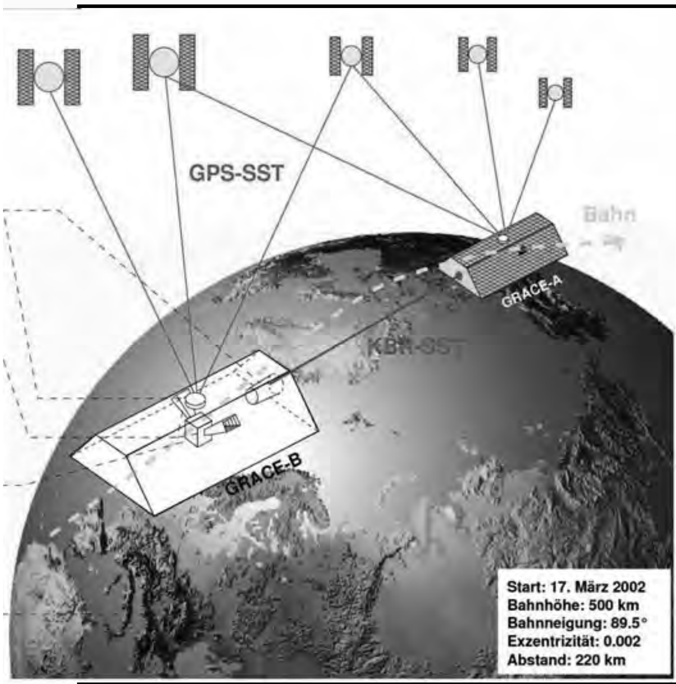

Observation of gravitationally caused orbit perturbations along the common line of sight (COM-COM) of a twin satellite pair by
high-low (GPS) + low-low (K-Band) Satellite-to Satellite Tracking (SST)

Observation of non-gravitational accelerations by 3D Accelerometer (SuperSTAR)

Observation of satellite and instrument orientation by Star Cameras

Validation of GPS-derived orbit by Satellite Laser Ranging (SLR)

GRACE Level-0 to Level-1B

Processing of Level-0 Raw Data (RDC 4/d) @ JPL

L0 Raw Data

↓

Reversible „Reformatting“

↓

L1A-Data

↓

Irreversible Transform.
- GPS time scale
- Outlier detection
- Low pass filtering (10 Hz to 1/0.2Hz)

↓

L1B-Data

Input for Level-2 gravity field determination by GRACE SDS and other centers

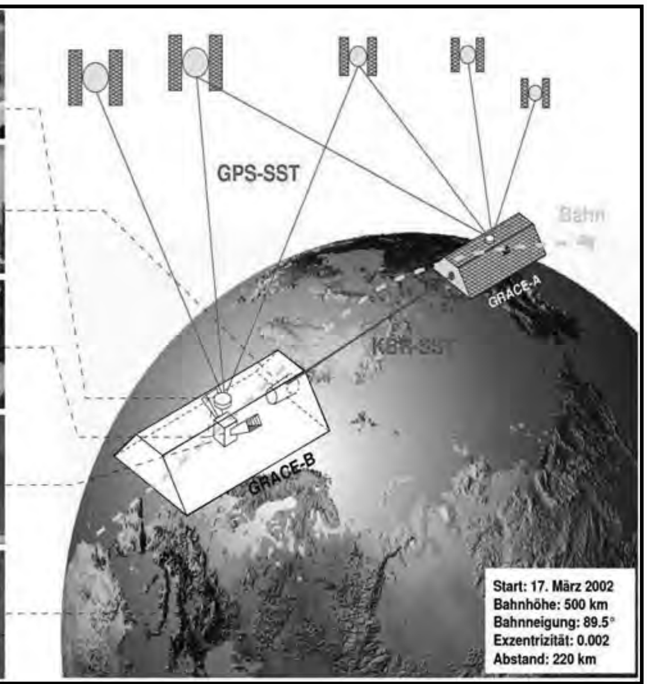

Accelerometer Level-1B (ACC1B)

- servo-driven, capacitive accelerometer (ONERA)
- 3 axis measure linear and angular accelerations
- Specification: $\sigma_{X\text{-}ACC} = 10^{-9}$ [m/s²/√Hz] , $\sigma_{Y\text{-}ACC} = \sigma_{Z\text{-}ACC} = 10^{-10}$ [m/s²/√Hz] (flight and radial direction)

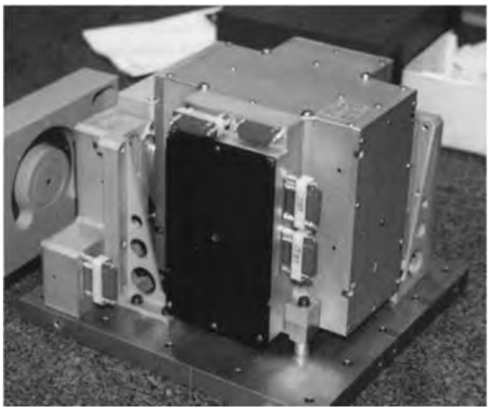

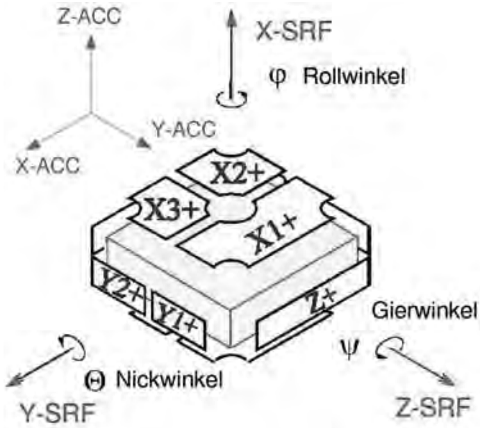

Accelerometer Level-1B (ACC1B)

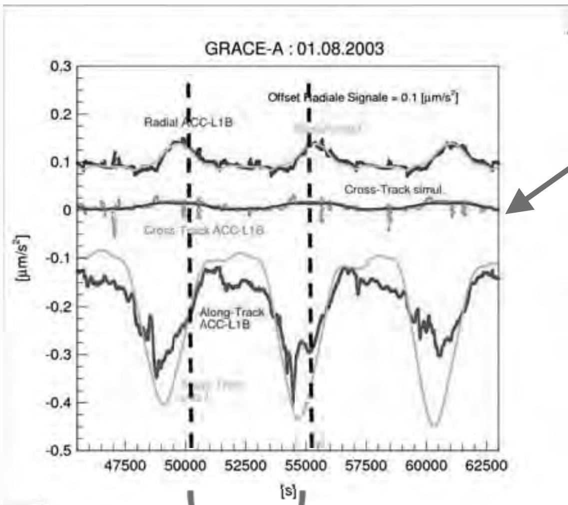

„good“ correlation with classical surface force modelling (atmospheric drag, solar radiation, albedo) …

…. linear accelerations from AOCS

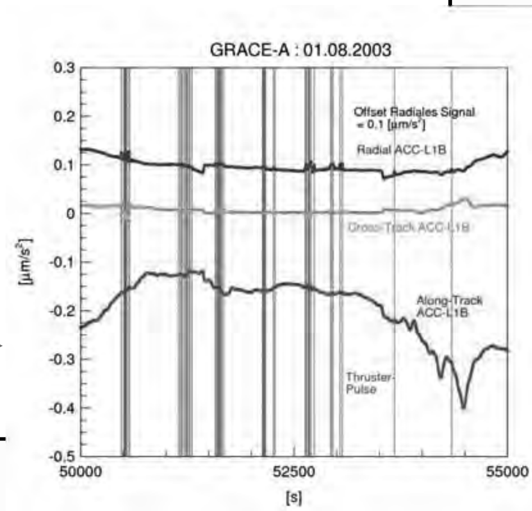

Accelerometer Level-1B (ACC1B)

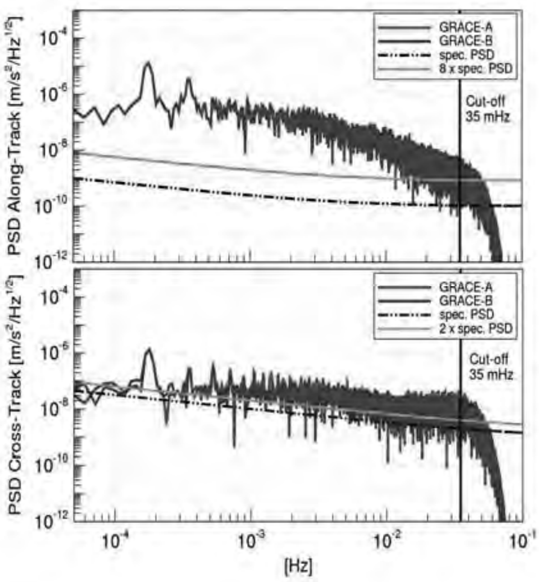

- Obviously lower accuracy than specified:
  - Radial, Along-Track ≈ 8 x Specification
  - Cross-Track ≈ 2 x Specification
- Problems/Causes:
  - intensive Attitude and Orbit Control (AOCS)
  - “Twangs” (vibrations of teflon foal at the bottom side of the satellites) due to albedo/magnetic field…
  - Unknown instrument errors
  - Combination of 2 star camera heads (accuracy to be rechecked with L1B V.02)
  - Others?

7

K-Band Level-1B (KBR1B)

- Dual one-way distance measurement based on phase measurement in K/Ka-Band
- σ_{Range} = 10 [µm] , $\sigma_{Range\text{-}Rate}$ = 1 [µm/s]

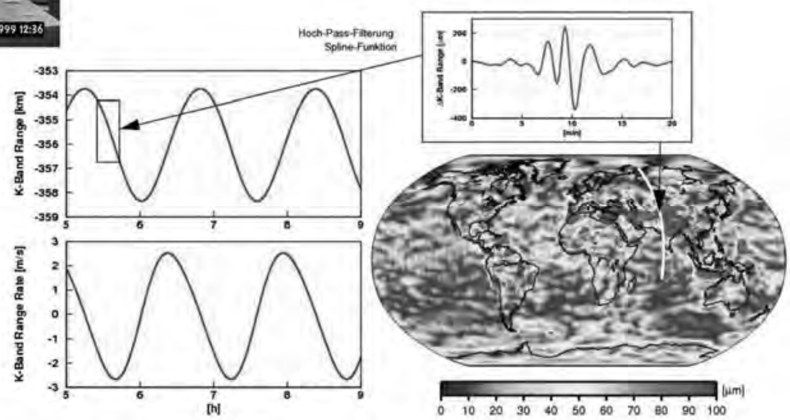

8

K-Band Level-1B (KBR1B)

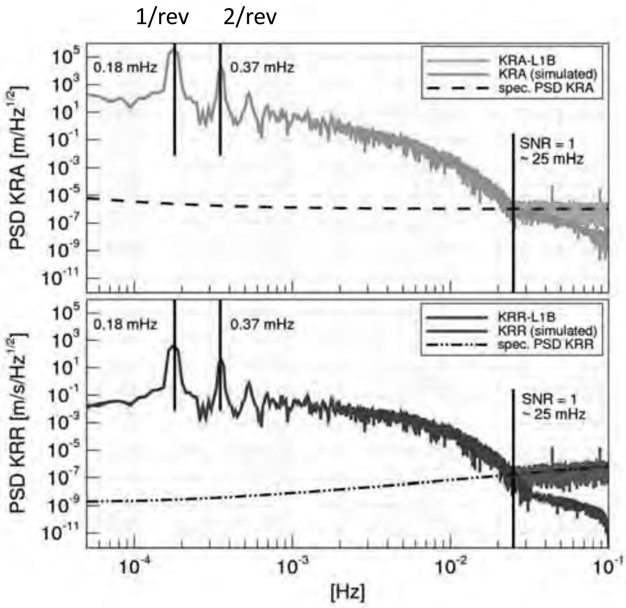

- Accuracy as expected or even better:

  - K-Band Range (KRA) ≈ 1 μm (<< specification 10 μm)

  - K-Band Range-Rate (KRR) ≈ 0.2 μm/s (<< specification = 1 μm/s)

9

DFG SPP 1257

Level-1 Instrument Data: Further Reading

Algorithm Theoretical Basis Document for GRACE Level-1B Data Processing V1.2

Sien-Chong Wu
Gerhard Kruizinga
Willy Bertiger

May 9, 2006

Jet Propulsion Laboratory
California Institute of Technology

GRACE 327-741
(JPL D-27672)

- Editing
- Correction
- Compression
- etc.

GRACE Level 1B Data Product User Handbook

Kelley Case
Gerhard Kruizinga
Sien-Chong Wu

March 24, 2010

Update with corrections for treatment of KBR1B Signal to Noise Ratio

Jet Propulsion Laboratory
California Institute of Technology

JPL D-22027

- Formats
- Interpretation of Data
- etc.

10

DFG SPP 1257

Dynamical Method: General

11

- „Classical“ method for adjustment of orbits and/or gravity models from satellite data
- Combination of
  - Numerical integration (equation of motion $\rightarrow$ orbit) plus
  - Methods of parameter adjustment („Least squares method“)
- Advantages
  - High flexibility (observation types, models…) and accuracy
  - Adjustment of observation series with gaps
  - Simultaneous adjustment of heterogeneous satellite data (integrated analysis)
- Disadvantages
  - High numerical effort (especially for gravity field determination)
  - No analytical description of functional behaviors

DFG SPP 1257

Dynamical Method: Functional Relationships

12

Functional relationship between (GPS/KBR) SST observations **b** and looked for gravity field model coefficients and other parameters **p** is not linear:

$$\mathbf{b} = \mathbf{f}(t, \mathbf{r}, \dot{\mathbf{r}}, \mathbf{p})$$

$\mathbf{p}$: Orbital parameters, Gravity field coefficients, Instrument parameters, ….

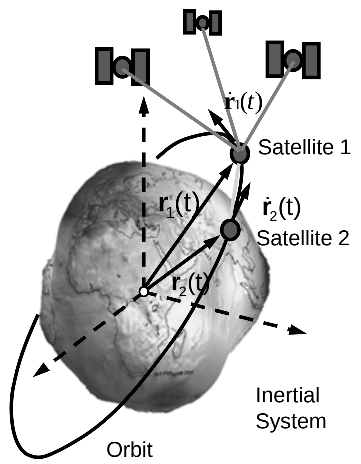

Linearized Gauß-Markoff-Model:

$$\mathbf{l} = \mathbf{A}\Delta\mathbf{p} + \mathbf{v}$$

$\mathbf{v}$: Correction of observations

$\Delta\mathbf{p}$: looked for adjustment values: $\Delta\mathbf{p} = \mathbf{p} - \mathbf{p}_0$

$\mathbf{A}$: partial derivatives $\left.\dfrac{\partial \mathbf{f}}{\partial \mathbf{p}}\right|_{\mathbf{p}_0}$

$\mathbf{l}$: Vectors of discrepancies resp. reduced observations „o-c“ $\mathbf{l} = \mathbf{b} - \mathbf{b}_0$

$\mathbf{p}_0$: Approximation of parameters (e.g. from models)

$\mathbf{b}_0$: Theoretical observations

DFG SPP 1257

Dynamical Method: Functional Relationships

Functional relationship between (GPS/KBR) SST observations **b** and looked for gravity field model coefficients and other parameters **p** is not linear:

$$\mathbf{b} = \mathbf{f}(t, \mathbf{r}, \dot{\mathbf{r}}, \mathbf{p})$$

- Orbital parameters
- Gravity field coefficients
- Instrument parameters
- ....

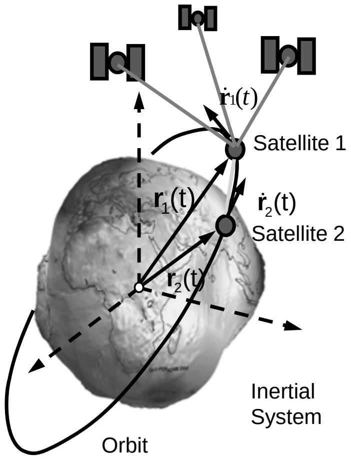

Adjustment of $\Delta\mathbf{p}$ by minimizing $\mathbf{v}^T\mathbf{P}\mathbf{v}$:

$$\Delta\mathbf{p} = (\mathbf{A}^T\mathbf{P}\mathbf{A})^{-1}\mathbf{A}^T\mathbf{P}\mathbf{l}$$

$$\mathbf{P} = \mathbf{D}(\mathbf{b})^{-1} = \sigma^2\mathbf{Q}_{\mathbf{bb}}$$

$\mathbf{p}_0$: Approximation of parameters (e.g. from models)

$\mathbf{b}_0$: Theoretical observations

13

Dynamical Method: Approximation of Observations

Get approximated/theoretical observations $\mathbf{b}_0$ by numerical integration of the equation of motion (initial value problem):

$$\ddot{\mathbf{r}} = -\frac{GM}{r^3}\mathbf{r} + \mathbf{a}_g + \mathbf{a}_{ng} + \mathbf{a}_\varepsilon$$

- Relativistic/empirical accelerations
- Non-gravitational accelerations
- Additional gravitational accelerations
- Central/KeplerTerm

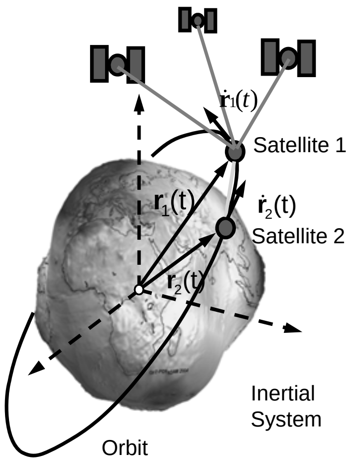

$\Rightarrow$ dynamical orbit $\mathbf{r}_0(t), \dot{\mathbf{r}}_0(t)$

$\Rightarrow$ theoretical observations $\mathbf{b}_0 = \mathbf{f}(t, \mathbf{r}_0, \dot{\mathbf{r}}_0, \mathbf{p}_0)$

14

Dynamical Method: (non)Gravitational Accelerations

15

$$\ddot{\mathbf{r}} = \underbrace{-\frac{GM}{r^3}\mathbf{r} + \mathbf{a}_g}_{} + \mathbf{a}_{ng} + \mathbf{a}_{\varepsilon}$$

<u>Non gravitational accelerations</u> from accelerometer observations:

$$\mathbf{a}_{ng} \approx \mathbf{b}_{\mathbf{AddKonst}} + \mathbf{M}_{3x3} \cdot \mathbf{a}_{\mathbf{SuperSTAR}}$$

Needs adjustment of instrument parameters (biases and scales)

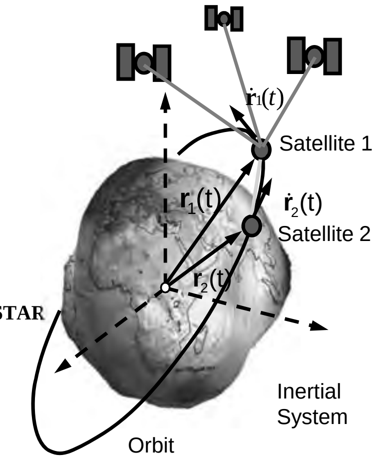

<u>Gravitational accelerations</u> as sum of gradients of *n* potential functions:

$$\mathbf{a}_g = \sum_{i=1}^{n} \nabla V_i(r, \theta, \lambda, t, \mathbf{p_0})$$

Gravity Potentials for GFZ EIGEN Solutions

16

Potential	Parameter $\mathbf{p_0}$
Static Gravity Field	$\bar{C}_{nm}, \bar{S}_{nm}$ Unknowns $\Delta\bar{C}_{nm}(t), \Delta\bar{S}_{nm}(t)$
Third Bodies	Tabled Coordinates of Planets
Earth Tides	Amplitudes + Phases $\hat{C}^{\pm}_{snm}, \hat{\varepsilon}^{\pm}_{snm}$
Ocean Tides	Amplitudes + Phases $\hat{D}^{\pm}_{snm}, \hat{\delta}^{\pm}_{snm}$
Short-term Mass Variations in Atmosphere and Oceans	6h Correction Terms $\Delta\bar{C}_{nm}(t), \Delta\bar{S}_{nm}(t)$
Atmospheric Tides	Amplitudes + Phases $\hat{A}^{\pm}_{snm}, \hat{\tau}^{\pm}_{snm}$
Pole Tides (Solid Earth, Ocean)	Pole Coordinates $x_p(t), y_p(t) \mapsto \Delta\bar{C}_{21}(t), \Delta\bar{S}_{21}(t)$
Periodic and Secular Variations e.g. in Hydrosphere or Cryosphere	Models, e.g. $\dot{\bar{C}}_{nm}, \dot{\bar{S}}_{nm}$

Summary: Level-2 Processing

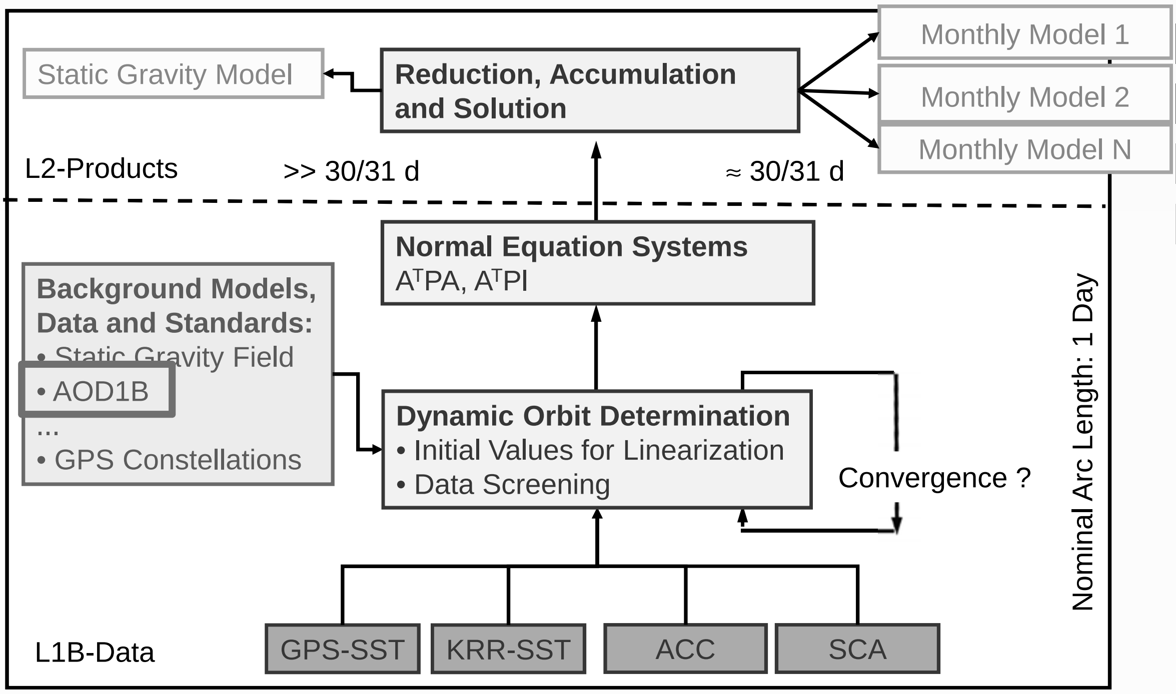

17

Sources of Gravity Variations

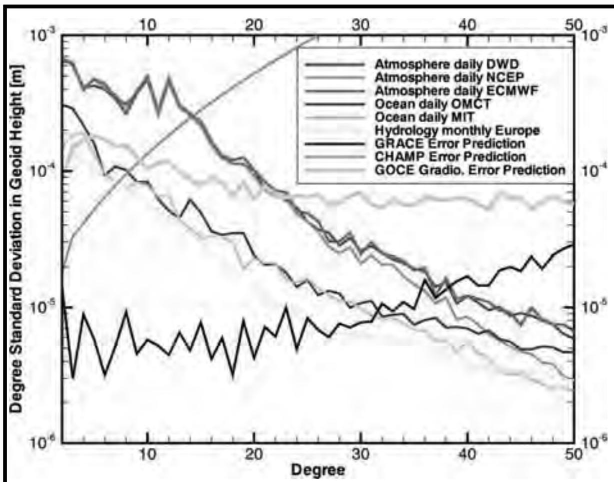

Gravity variations in terms of geoid height variations estimated from surface pressure, ocean bottom pressure and continental water heights.

High Frequency Variations (Models):

- Ocean Tides: FES2004, EOT11a…
- Atmospheric Tides: S1/S2 (Bode & Biancale, …)
- Non-tidal Atmosphere: see next
- Non-tidal Ocean: see next
- Continental Water Cycle: WGHM, … or GRACE (from multiple years or daily output)

Saisonal Variations (GRACE results)

- Continentaler Water Cycle
- Ice Mass Loss (Greenland/Antarctica)
- Surface and Deep Ocean Currents, Ocean Mass

18

AOD1B: Concept Atmosphere

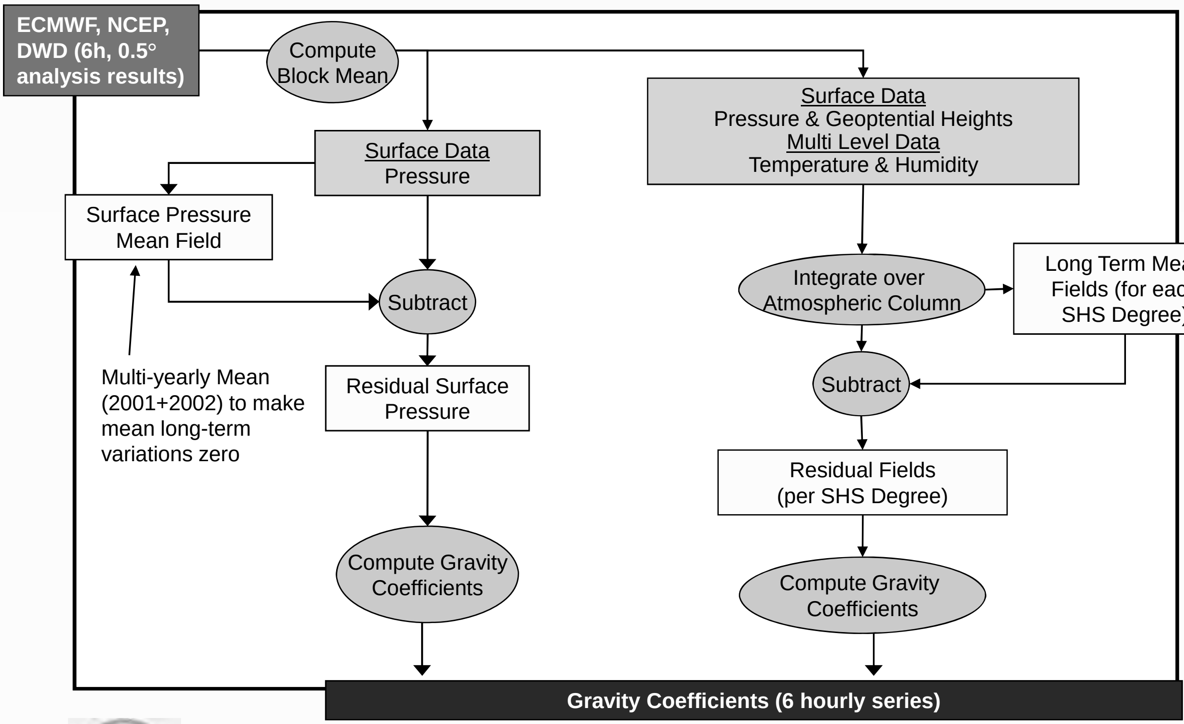

19

AOD1B: Oceanic Part (IB vs non-IB)

- Inverse barometric effect (IB) asumes that atmospheric pressure is fully compensated by the ocean: Atmospheric („SP/VI“) + oceanic mass variation = 0.
- Assumption is not sufficient for modern satellite missions: Need ocean models!

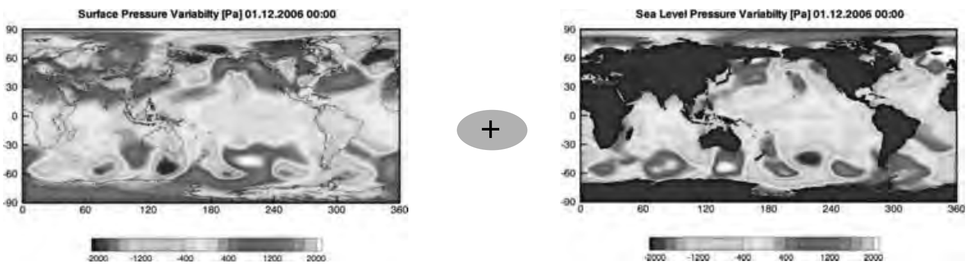

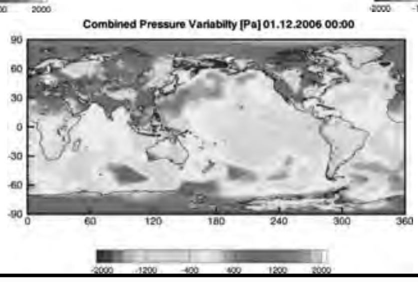

Only „Quasi-Compensation“

20

AOD1B: Concept Ocean

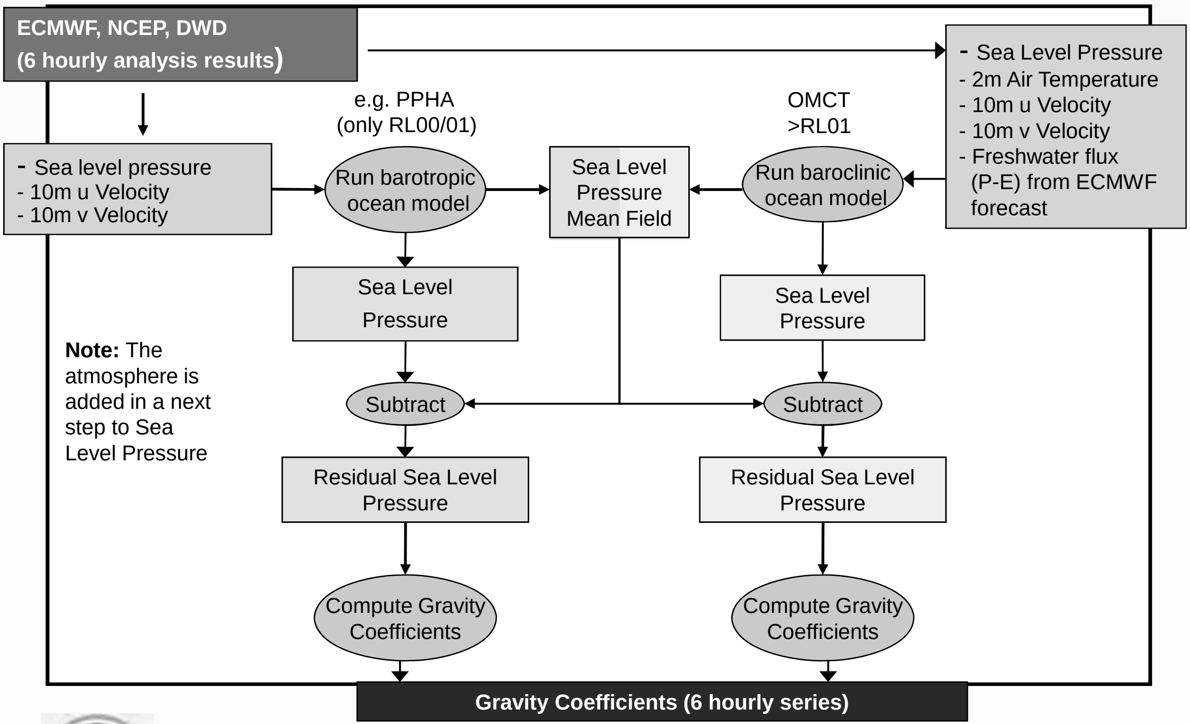

Min, Max, Mean and wRMS of **6h** RL04 for 2007-2008

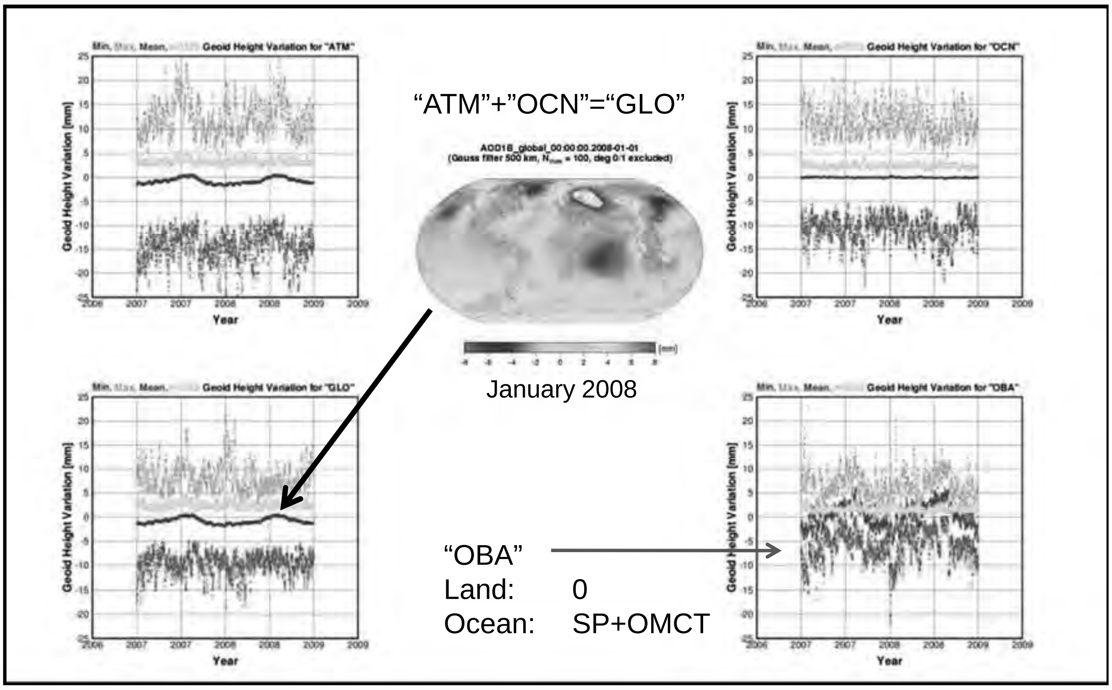

Mean GAx Products

For every (e.g. weekly/monthly) gravity field model a corresponding mean (GA = GRACE Average) for all 4 AOD1B components is provided.

Only days used within gravity field determination period are averaged.

GAA: Mean of the 6h "atm": Land: VI-Vimean Ocean: VI-Vimean
GAB: Mean of the 6h "ocn": Land: 0 Ocean: OMCT-OMCTmean
(this two products are more or less only informal)

GAC: Mean of the 6h "glo": Land: VI-Vimean Ocean: (VI-VImean)+(OMCT-OMCTmean)
(this is the mean product of 6h variations which have been subtracted during gravity field determination)

GAD: Mean of the 6h "oba": Land: 0 Ocean: (SP-SPmean)+(OMCT-OMCTmean)
(Since RL04 as should be closer to ocean bottom pressure and to decrease leakage from land)

Difference using/not using AOD1B/GAC in Gravity Field Determination

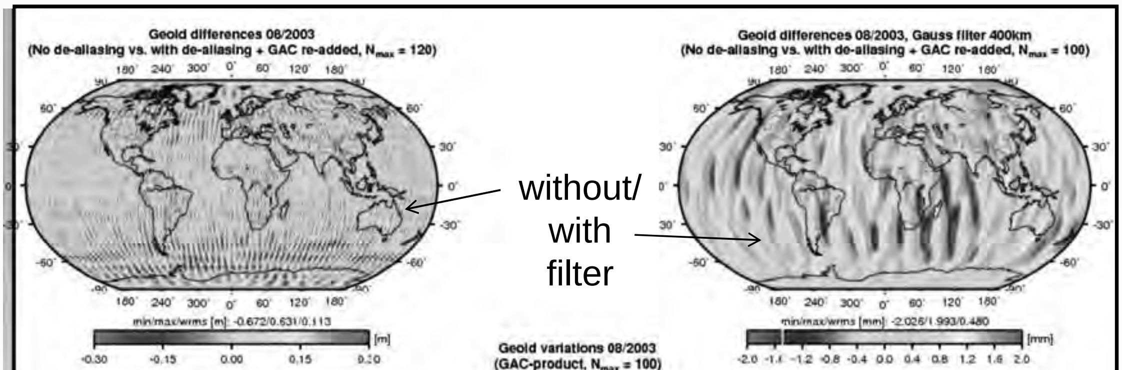

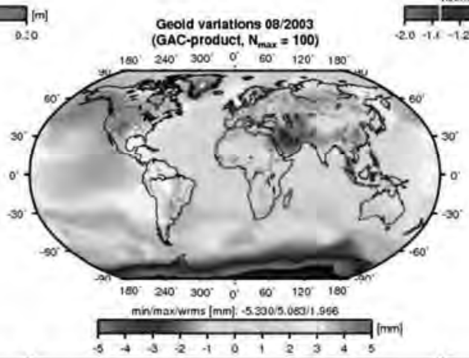

Using 6h AOD1B to derive monthly GSM and restore GAC

vs.

Not using AOD1B or GAC

Neglecting AOD1B has large impact!
- Stripes
- wRMS = 0.5 mm

AOD1B (RL05): higher temporal and spatial resolution of OMCT

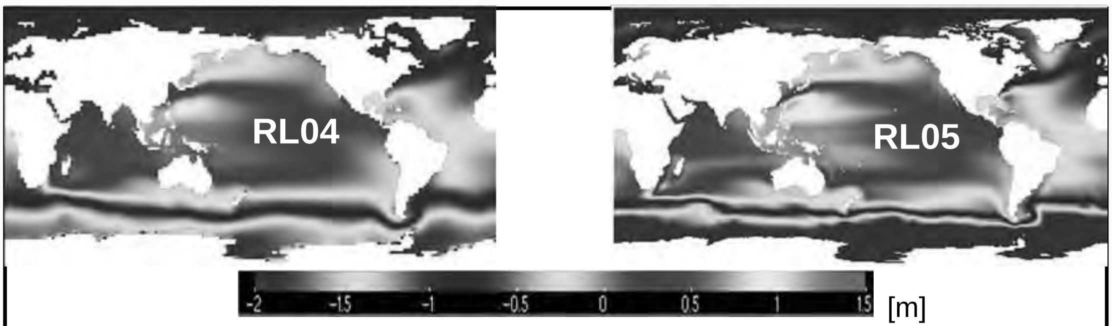

RL04 – RL05 (interpolated @ 1°)

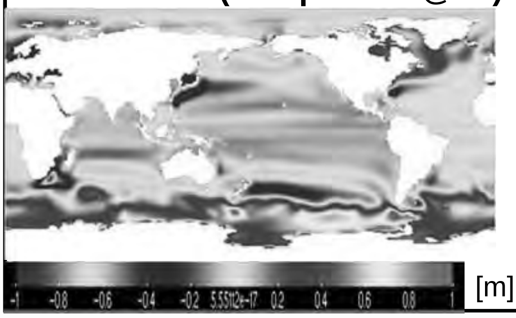

- RL05 shows enhanced gradients in most western boundary current regions (Gulf Stream, Kuroshio current)
- Subtle differences in equatorial current systems (were rather overestimated in RL04) and in the Arctic
- Strong differences in ACC region: meridional gradients are much stronger in RL05, topography apparent in the flow path

25

DFG SPP 1257

AOD1B Validation: **Daily** AOD RL04/RL05 Correlations with OBP (2008)

Corr. 2008	RL04		RL05		Improvement [%]	
	Daily GAC	Daily GAD	Daily GAC	Daily GAD	Daily GAC	Daily GAD
All	0.42	0.44	0.59	0.59	40.5	34.1
ACC	0.46	0.45	0.54	0.53	17.4	17.7
DART	0.39	0.40	0.57	0.57	46.2	42.5
FRAM	0.56	0.61	0.72	0.75	28.6	23.0

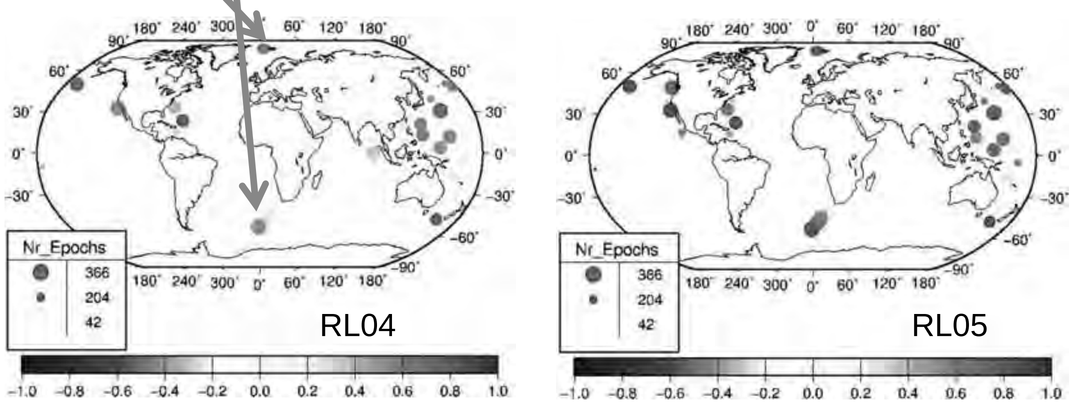

… shows large model improvements

26

DFG SPP 1257

AOD1B Validation: **Daily** AOD RL04/05/ITG Correlations with OBP (2008)

Corr. 2008	RL04		RL05		Improvement [%]	
	GAC	GAD	GAC	GAD	GAC	GAD
All	0.42	0.44	0.59	0.59	40.5	34.1
ACC	0.46	0.45	0.54	0.53	17.4	17.7
DART	0.39	0.40	0.57	0.57	46.2	42.5
FRAM	0.56	0.61	0.72	0.75	28.6	23.0

Corr. 2008	RL04		ITG2010		Improvement [%]	
	GAC	GAD	GSM+GAC	GSM+GAD	GAC	GAD
All	0.42	0.44	0.46	0.46	9.5	4,5
ACC	0.46	0.45	0.75	0.79	63.0	75.6
DART	0.39	0.40	0.37	0.37	-5.2	-7.5
FRAM	0.56	0.61	0.75	0.79	33.9	29.5

- ITG (GAC plus GRACE corrections) gives high correlations at sites with large OBP signal (ACC)
- AOD RL05 gives higher correlations at sites with small OBP signal (DART)
- Globally, AOD1B RL05 gives higher correlations (0.59 vs. 0.46)

Monthly Comparisons to Ocean Bottom Pressure for RL04 (2003-2008)

... this is what the user can compare

	DDK1 (530km) RL04				
	Stations with (OBP / GSM+GAC) SNR > 1				
	GSM	GAC (RL04)	GAD (RL04)	GSM +GAC(RL04)	GSM +GAD(RL04)
All (54)	0.02	0.47	0.47	0.62	0.61
ACC(6)	0.29	0.35	0.35	0.73	0.74
DART(7)	0.21	0.47	0.47	0.62	0.60
FRAM(6)	0.72	0.35	0.25	0.73	0.68
KESS(32)	-0.25	0.57	0.58	0.58	0.58
POL_ACCLAIM(3)	0.30	-0.03	0.05	0.40	0.46

- Geocenter motion considered for GSM+GAC product (JIGOG time series)
- Only comparisons for long time series give a clear picture (RL05 available only for 2008)

- Model (GAC/D) only gives small correlations (room for improvement, see RL05)
- GAD correlations smaller than GAD (against theory, but improved in RL05(see before))
- GRACE contributes to OBP (see daily correlations ITG2010): This is the reason why the user gets GSM <u>and</u> Gax!

AOD1B: Further Reading

All Details described in this Document ->

Also recommended:

Lecture Gummersbach 2007:
“De-aliasing von atmosphärischen und ozeanischen Kurzzeit-Massenvariationen für CHAMP, GRACE und GOCE: Stand und offene Fragen”

AOD1B quality control and status page:
http://www-app2.gfz-potsdam.de/pb1/op/grace/results/grav/g007_aod1b_rl04.html

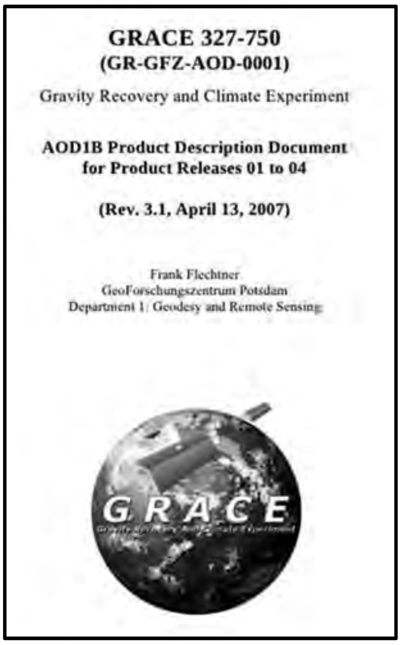

GRACE 327-750
(GR-GFZ-AOD-0001)

Gravity Recovery and Climate Experiment

AOD1B Product Description Document
for Product Releases 01 to 04

(Rev. 3.1, April 13, 2007)

Frank Flechtner
GeoForschungsZentrum Potsdam
Department 1: Geodesy and Remote Sensing

29

Level-2 Products: Further Reading

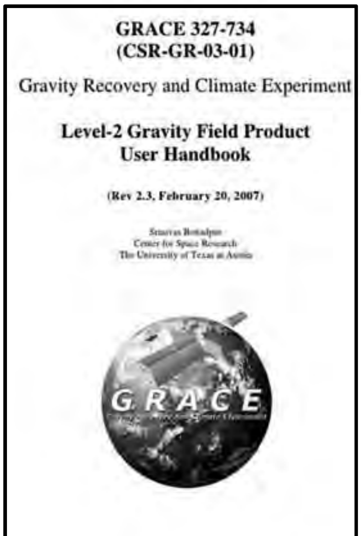

GRACE 327-734
(CSR-GR-03-01)

Gravity Recovery and Climate Experiment

Level-2 Gravity Field Product
User Handbook

(Rev 2.3, February 20, 2007)

[illegible]
Center for Space Research
The University of Texas at Austin

Provides information on GSM and Gax Level-2 data

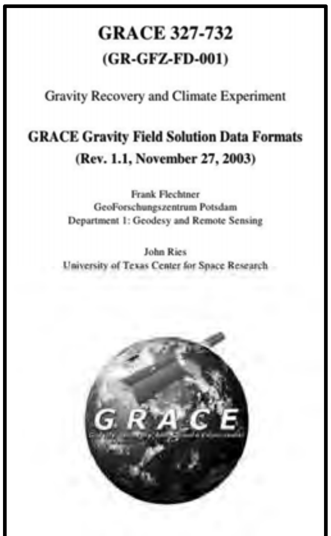

GRACE 327-732
(GR-GFZ-FD-001)

Gravity Recovery and Climate Experiment

GRACE Gravity Field Solution Data Formats
(Rev. 1.1, November 27, 2003)

Frank Flechtner
GeoForschungsZentrum Potsdam
Department 1: Geodesy and Remote Sensing

John Ries
University of Texas Center for Space Research

Format of Level-2 Products

GRACE 327-743
(GR-GFZ-STD-001)

Gravity Recovery and Climate Experiment

GFZ Level-2 Processing Standards Document

For Level-2 Product Release 0004

(Rev. 1.0, February 19, 2007)

Frank Flechtner
GeoForschungsZentrum Potsdam
Department 1: Geodesy and Remote Sensing

For each center and each release: Applied back-ground models & standards

30

RL05 Reprocessing @ GFZ: Processing Standards

- Improved L1B data & preprocessing:
  - L1B RL02 data
  - reduction of data elimination during preprocessing
- Improved GPS processing:
  - absolute antenna phase center variations, phase windup correction, GPS attitude model, IGS2008
  - GFZ derived GPS antenna maps for GRACE
- More dense accelerometer parameterization:
  - 1-hourly biases in radial, along-track and cross-track direction
  - no more scale factors
- Relative weighting of GPS-SST and KRR observations:
  - increased KRR weight (~ by a factor of 2)
  - gravity field parameters with n > 80 estimated only with KRR

31

DFG SPP 1257

RL05 Reprocessing @ GFZ: Improved Background Models

	Currently: RL04	**New: RL05**
A priori Static Gravity Field	EIGEN-GL04C	**EIGEN-6C**
Time-variable Gravity Field	none	**Trend/Annual/ Semiannual Model derived from EIGEN-6C**
Secular Rates	C_{20}, C_{30}, C_{40}, C_{21}, S_{21}	none
Ocean Tides	FES2004	**EOT11a**
Atmospheric Tides S1, S2	Bode-Biancale 2003	Bode-Biancale 2003
Atmospheric and Oceanic Non-tidal Mass Variations	AOD1B RL04	**AOD1B RL05**
Ocean Pole Tide	Desai [2002]	Desai [2002]
Solid Earth & Pole Tides	IERS2003	**IERS2010**
3rd Body Ephemerides	JPL DE403	**JPL DE421**

32

DFG SPP 1257

RL05 Reprocessing @ GFZ: Prefit Residuals 2008

33

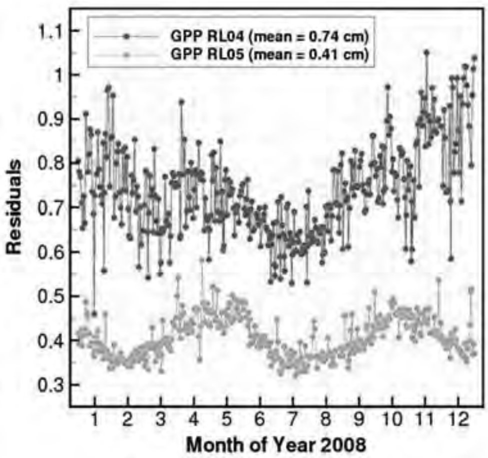

GPS phase (44%)

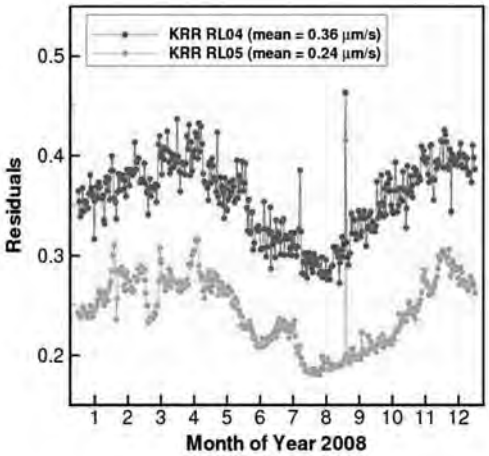

K-band range rate (33%)

RL05 Reprocessing @ GFZ: Error Characteristics 2008

34

(RL03: 17.5 x baseline)
RL04: 15 x baseline
RL05: 8 x baseline

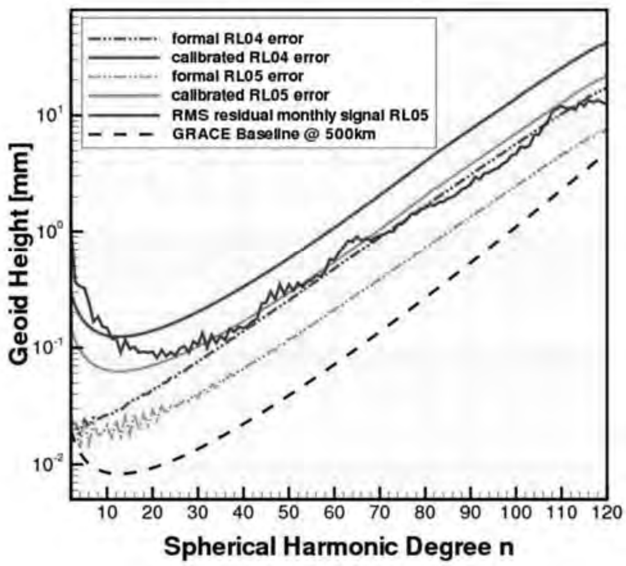

RL05 Reprocessing @ GFZ: Error Characteristics 2008

d/o 60x60: ~40-60%

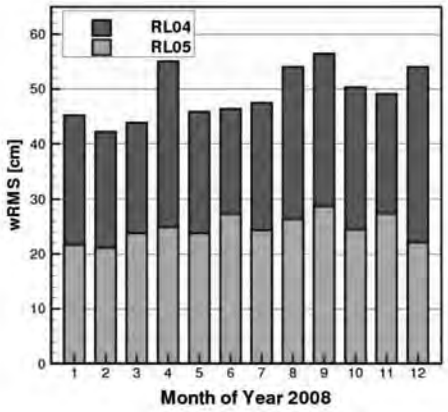

wRMS in terms of EWH [cm]
w.r.t. ITG-Grace2010s

RMS variability w.r.t. mean (EWH [cm], DDK3)

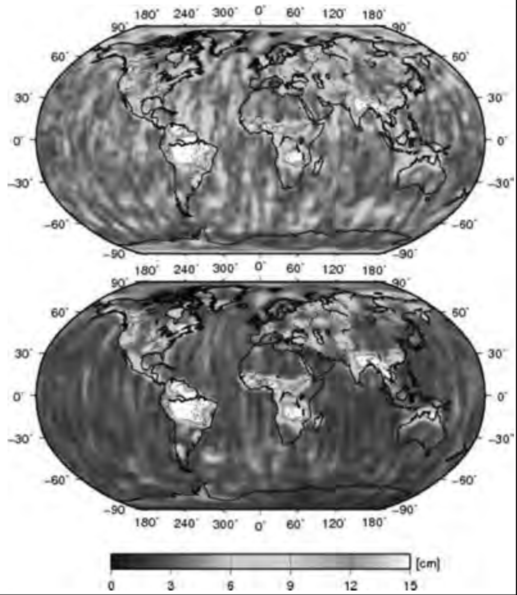

RL05 Reprocessing @ GFZ: Unresolved 161d signal in C20

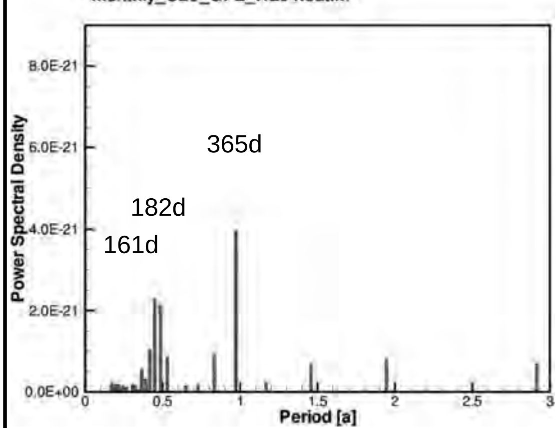

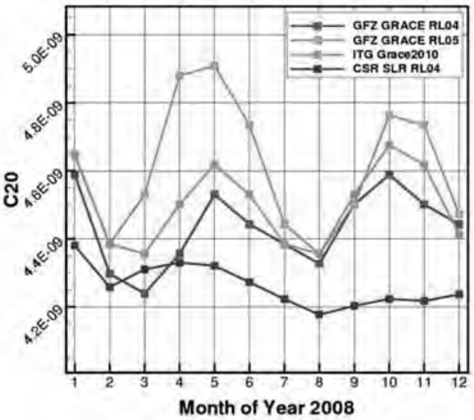

- Problem exists in all center solutions! Remains (pronounced) in GFZ RL05
- Not optimal solution for RL04: Substitute GRACE C20 coefficient by SLR derived value (see TN05)
- Plan for final RL05: Find reason or combine with SLR (GRGS approach)

RL05 Reprocessing @ GFZ: C21/S21

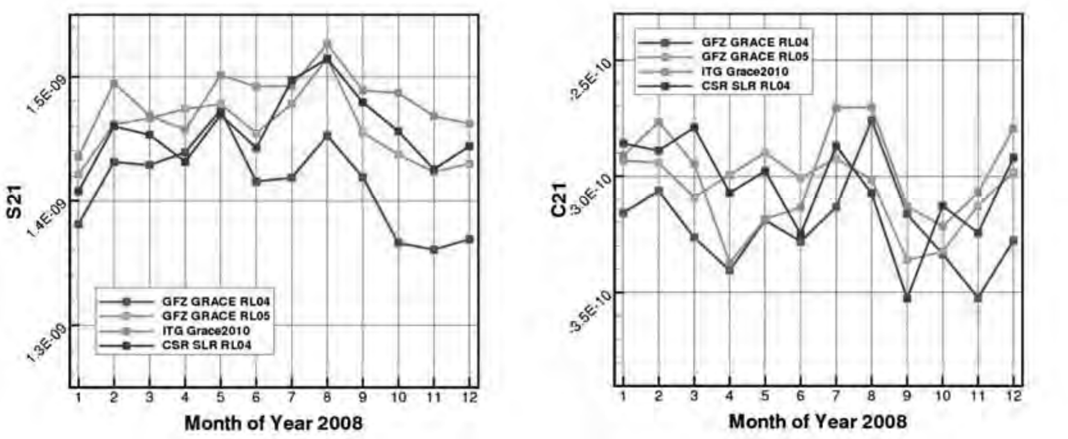

- Already much better correlations for all centers
- Notable improvement with GFZ RL05

37

DFG SPP 1257

Summary Part 2

- During GRACE Level-2 gravity field determination all “known” gravity variations (trend, sannual, semi-annual, …) are taken into account (models). Note: GIA (Global Isostatic Adjustment) model not yet used.
- Before provision to the users some (monthly mean) models are restored (e.g. hydrology, ice mass loss): impacts results mostly over land
- Over the oceans GRACE plus GAx products have to be used when comparing with in-situ OBP data! Here, also degree 1 coefficients (not provided by GRACE) have to be taken into account.
- GRACE C20 coefficient still shows spurious (unexplained) 161d signal
- A new (much improved) RL05 time series incl. a new AOD1B RL05 and reprocessed Level-1B instrument data covering the complete GRACE mission lifetime will be made available by the GRACE Science Data System on March 17, 2012 (10^{th} anniversary of GRACE)

38

DFG SPP 1257

Spherical Harmonics & Gravity field

Torsten Mayer-Gürr

Summer School „Global Water Cycle“
12.-16. September 2011
Mayschoss

Content

Part 1:
- Spherical Harmonics

- Gravity field
  - Geoid heights
  - Gravity anomalies
  - Gravity disturbances
  - Total water storage

- Degree Variances

- Upward Continuation

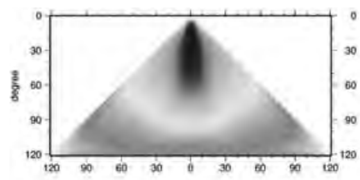

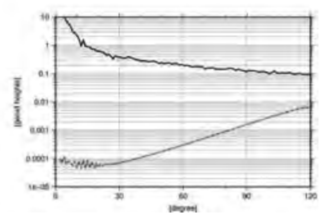

Part 2: (Frank Flechtner)
- GRACE Processing & GRACE Products

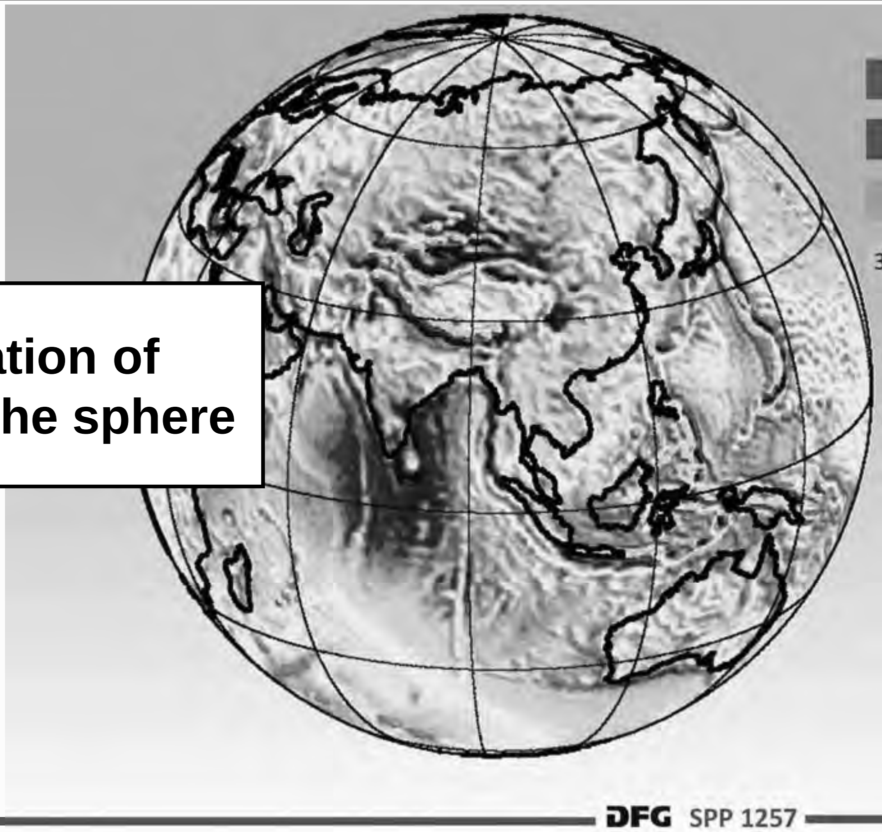

Approximation of functions on the sphere

3

Approximation

Approximation with a polynomial of degree n:

$$f(x) = a_0 p_0(x) + a_1 p_1(x) + \cdots + a_n p_n(x)$$

$$p_n(x) = x^n$$

Approximation of a periodic function with a Fourier series:

$$f(t) = c_0 + \sum_{n=1}^{\infty} c_n \cos\left(m \frac{2\pi}{T} t \right) + s_n \sin\left(m \frac{2\pi}{T} t \right)$$

Approximation of a function on the sphere with spherical harmonics:

$$f(\lambda, \vartheta) = \sum_{n=0}^{\infty} \sum_{m=-n}^{n} a_{nm} Y_{nm}(\lambda, \vartheta)$$

4

Approximation with Spherical harmonics

Spherical harmonics:

$$Y(\lambda,\vartheta)=\sum_{n=0}^{\infty}\sum_{m=-n}^{n}a_{nm}Y_{nm}(\lambda,\vartheta)$$

Approximation on the sphere:

$$\|f(\lambda,\vartheta)-Y(\lambda,\vartheta)\|^2=\iint_{\Phi}\left(f(\lambda,\vartheta)-Y(\lambda,\vartheta)\right)^2 d\Phi=\min$$

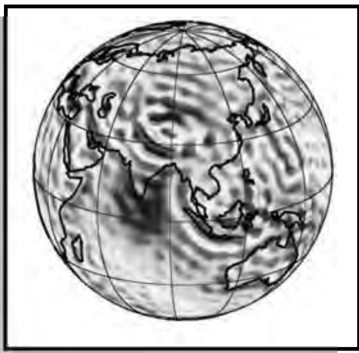

Norm and scalar product:

$$\|f\|^2=\iint_{\Phi}f^2(\lambda,\vartheta)\,d\Phi \qquad <f,g>=\iint_{\Phi}f(\lambda,\vartheta)\cdot g(\lambda,\vartheta)\,d\Phi$$

With orthogonal basis functions:

$$<Y_{nm},Y_{n'm'}>=0 \quad \text{für } n\neq n' \quad \text{oder } m\neq m'$$

The solution is simple

$$a_{nm}=\frac{1}{\|Y_{nm}\|^2}<f,Y_{nm}>$$

Approximation with Spherical harmonics

Expansion into a series of spherical harmonics:

$$f(\lambda,\vartheta)=\sum_{n=0}^{\infty}\sum_{m=-n}^{n}a_{nm}Y_{nm}(\lambda,\vartheta)$$

with the coefficients:

$$a_{nm}=\frac{1}{\|Y_{nm}\|^2}\iint_{\Phi}f(\lambda,\vartheta)\cdot Y_{nm}(\lambda,\vartheta)\,d\Phi$$

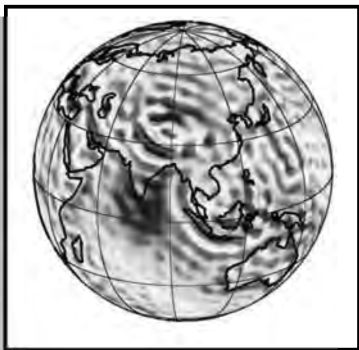

Norm of the basis functions:

$$\|Y_{nm}\|^2=\iint_{\Phi}Y_{nm}^2(\lambda,\vartheta)\,d\Phi$$

The norm is arbitrary:

Not normalized (e.g. mathematics):

$$\|Y_{nm}(\lambda,\vartheta)\|^2=\frac{4\pi}{2n+1}(2-\delta_{0m})\frac{(n+|m|)!}{(n-|m|)!}$$

Schmidt semi-normalized (e.g. magnetics)

$$\|Y_{nm}(\lambda,\vartheta)\|^2=\frac{4\pi}{2n+1}$$

Fully normalized (e.g. gravity)

$$\|Y_{nm}(\lambda,\vartheta)\|^2=4\pi$$

Coefficient triangle

Approximation of a function on the sphere

$$f(\lambda,\vartheta)=\sum_{n=0}^{\infty}\sum_{m=-n}^{n}a_{nm}Y_{nm}(\lambda,\vartheta)$$

Arrangement of coefficients in a triangle

degree n = 0: $\boxed{a_{00}}$

degree n = 1: $\boxed{a_{1,-1}}\ \boxed{a_{10}}\ \boxed{a_{11}}$

degree n = 2: $\boxed{a_{2,-2}}\ \boxed{a_{2,-1}}\ \boxed{a_{20}}\ \boxed{a_{21}}\ \boxed{a_{22}}$

degree n = 3: $\boxed{a_{3,-3}}\ \boxed{a_{3,-2}}\ \boxed{a_{3,-1}}\ \boxed{a_{30}}\ \boxed{a_{31}}\ \boxed{a_{32}}\ \boxed{a_{33}}$

degree n = 4: $\boxed{a_{4,-4}}\ \boxed{a_{4,-3}}\ \boxed{a_{4,-2}}\ \boxed{a_{4,-1}}\ \boxed{a_{40}}\ \boxed{a_{41}}\ \boxed{a_{42}}\ \boxed{a_{43}}\ \boxed{a_{44}}$

…: $\boxed{a_{5,-5}}\ \boxed{a_{5,-4}}\ \boxed{a_{5,-3}}\ \boxed{a_{5,-2}}\ \boxed{a_{5,-1}}\ \boxed{a_{50}}\ \boxed{a_{51}}\ \boxed{a_{52}}\ \boxed{a_{53}}\ \boxed{a_{54}}\ \boxed{a_{55}}$

order m →

7

DFG SPP 1257

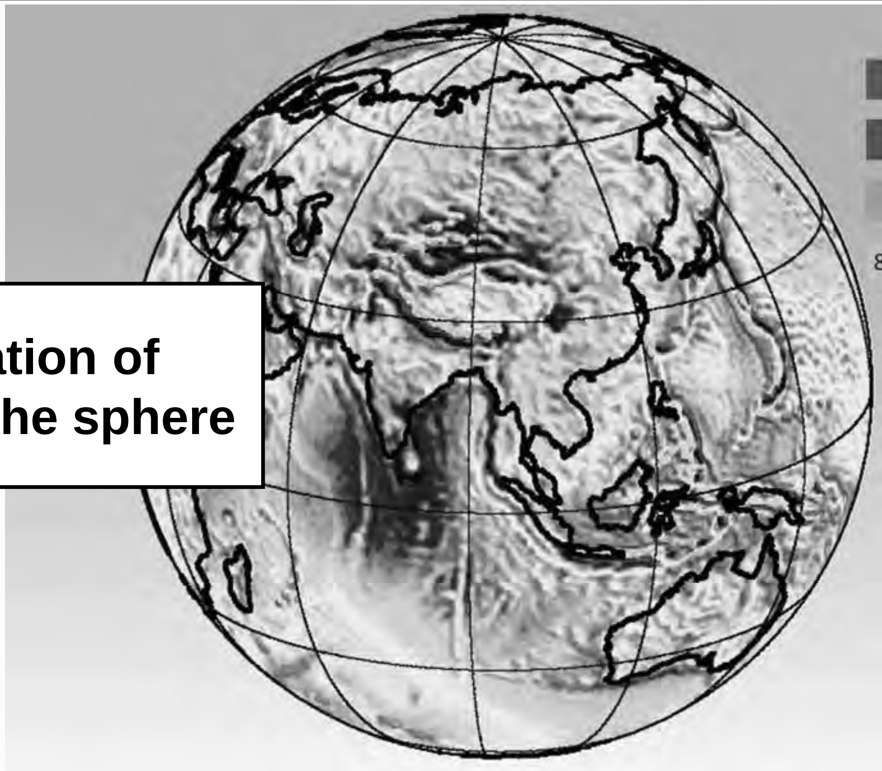

Approximation of functions on the sphere

8

DFG SPP 1257

Approx. with spherical harmonics

$$f(\lambda,\vartheta)=\sum_{n=0}^{\infty}\sum_{m=-n}^{n}a_{nm}Y_{nm}(\lambda,\vartheta)$$

Degree n	Number of coefficients
4	25
8	81
16	289
30	961
60	3721
120	14641
240	58081

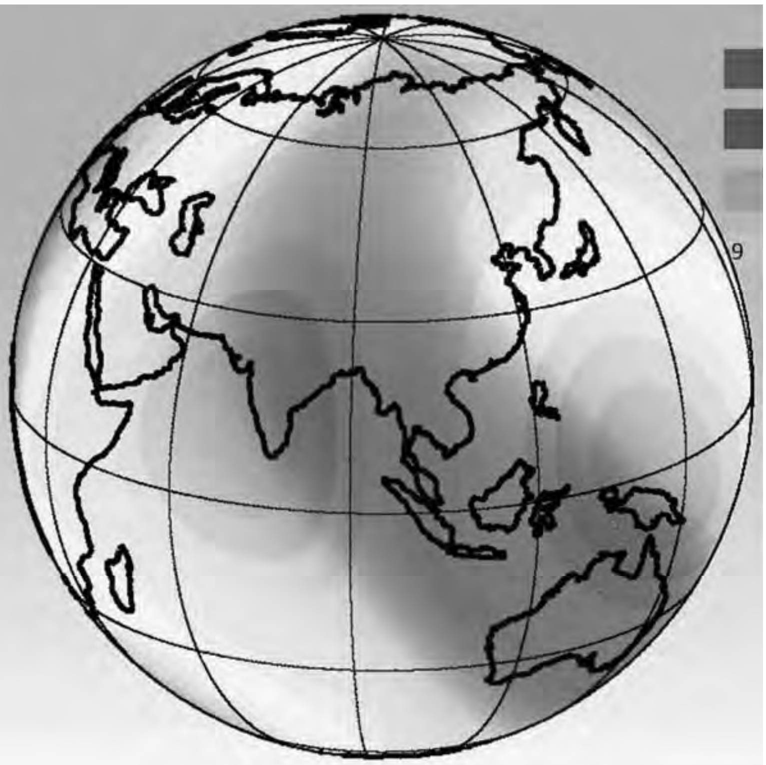

DFG SPP 1257

9

Approx. with spherical harmonics

$$f(\lambda,\vartheta)=\sum_{n=0}^{\infty}\sum_{m=-n}^{n}a_{nm}Y_{nm}(\lambda,\vartheta)$$

Degree n	Number of coefficients
4	25
8	81
16	289
30	961
60	3721
120	14641
240	58081

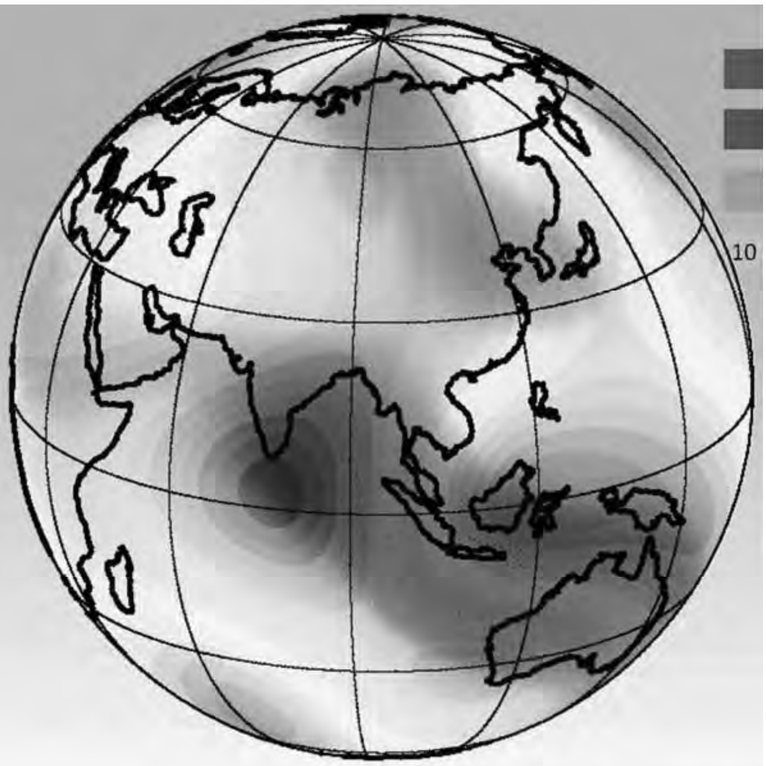

DFG SPP 1257

10

Approx. with spherical harmonics

$$f(\lambda,\vartheta)=\sum_{n=0}^{\infty}\sum_{m=-n}^{n}a_{nm}Y_{nm}(\lambda,\vartheta)$$

Degree *n*	Number of coefficients
4	25
8	81
16	289
30	961
60	3721
120	14641
240	58081

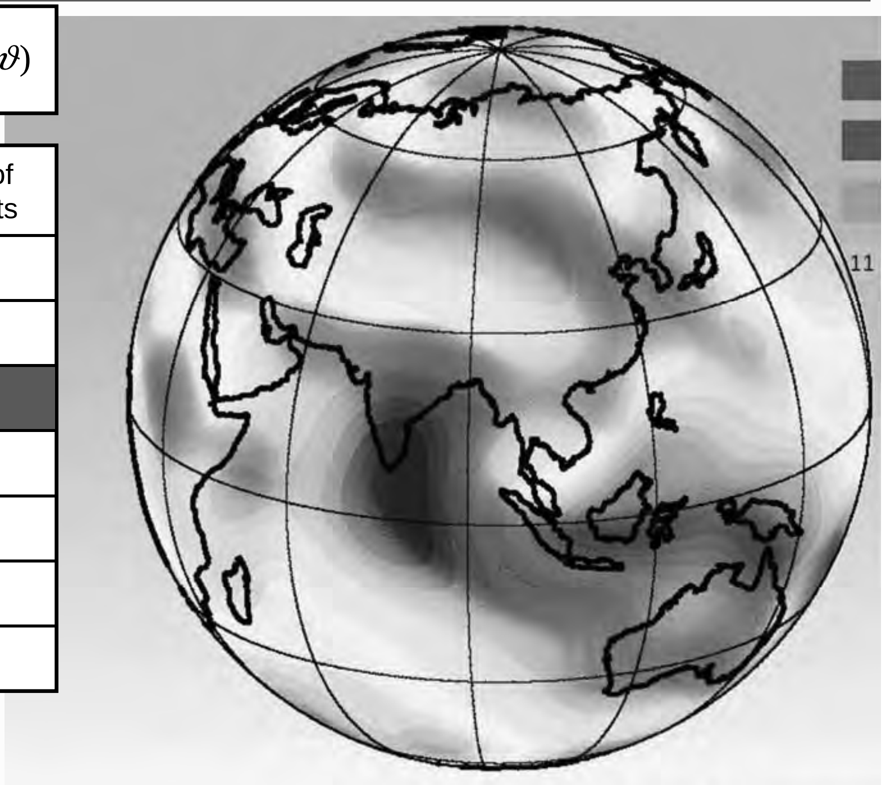

DFG SPP 1257

Approx. with spherical harmonics

$$f(\lambda,\vartheta)=\sum_{n=0}^{\infty}\sum_{m=-n}^{n}a_{nm}Y_{nm}(\lambda,\vartheta)$$

Degree *n*	Number of coefficients
4	25
8	81
16	289
30	961
60	3721
120	14641
240	58081

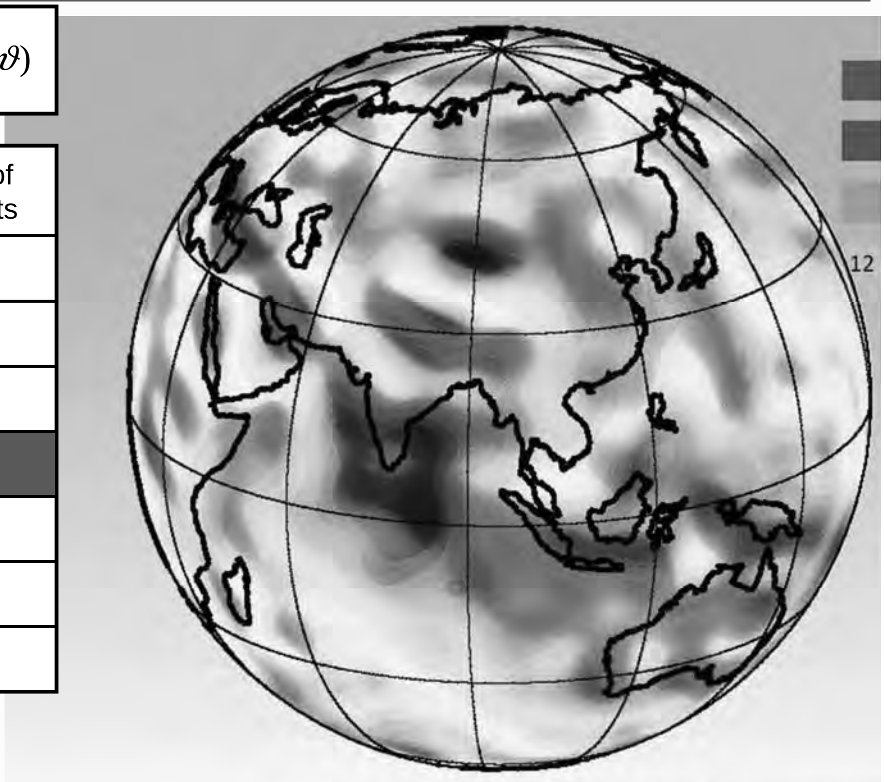

DFG SPP 1257

Approx. with spherical harmonics

$$f(\lambda,\vartheta)=\sum_{n=0}^{\infty}\sum_{m=-n}^{n}a_{nm}Y_{nm}(\lambda,\vartheta)$$

Degree n	Number of coefficients
4	25
8	81
16	289
30	961
60	3721
120	14641
240	58081

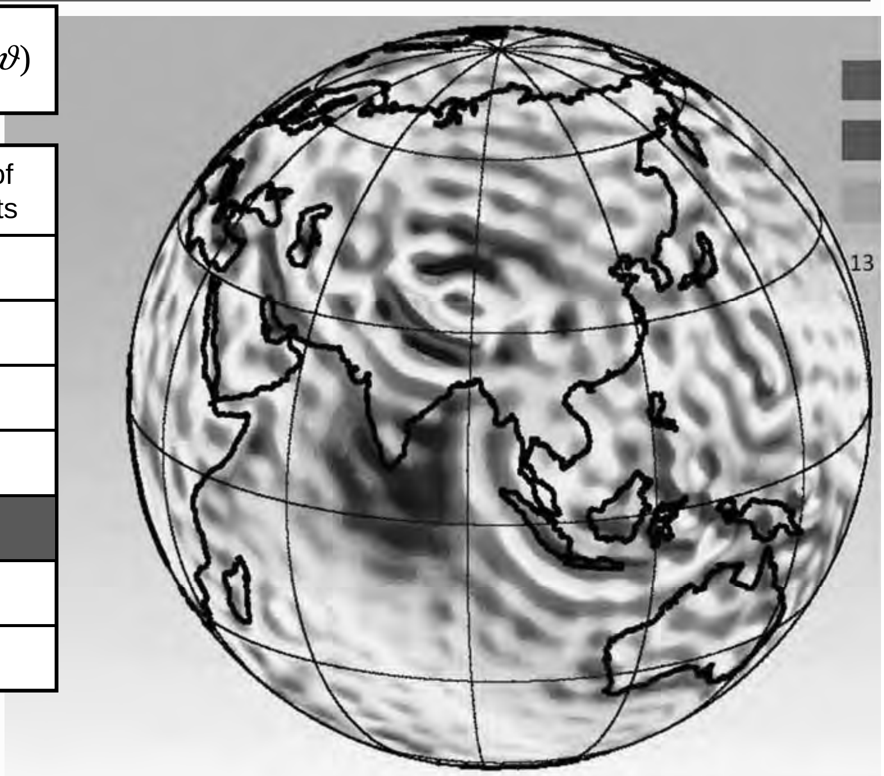

Approx. with spherical harmonics

$$f(\lambda,\vartheta)=\sum_{n=0}^{\infty}\sum_{m=-n}^{n}a_{nm}Y_{nm}(\lambda,\vartheta)$$

Degree n	Number of coefficients
4	25
8	81
16	289
30	961
60	3721
120	14641
240	58081

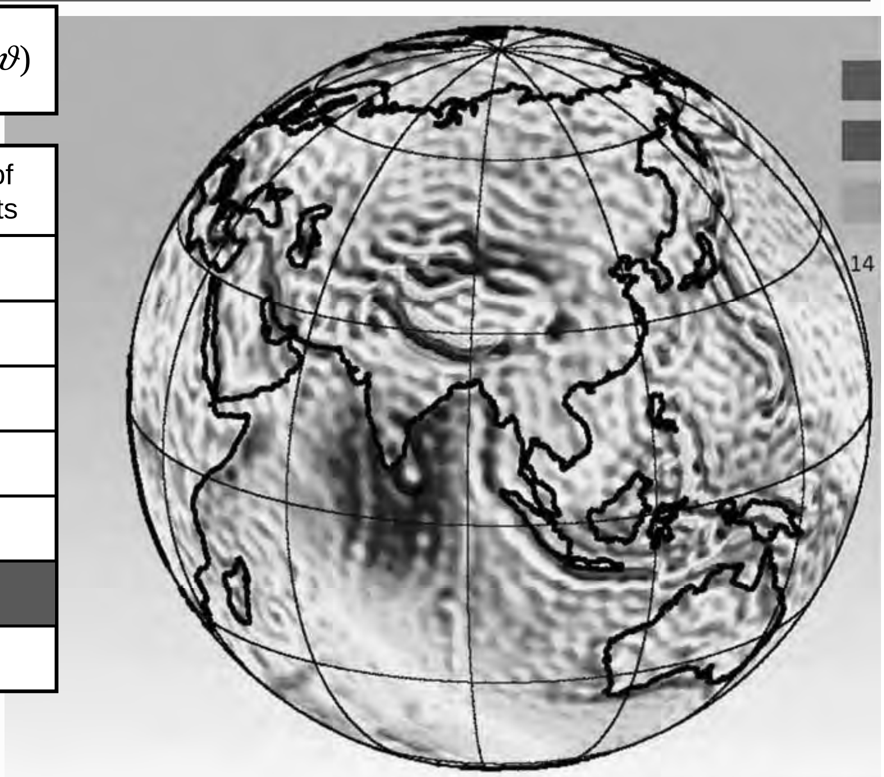

Approx. with spherical harmonics

$$f(\lambda,\vartheta)=\sum_{n=0}^{\infty}\sum_{m=-n}^{n}a_{nm}Y_{nm}(\lambda,\vartheta)$$

Degree n	Number of coefficients
4	25
8	81
16	289
30	961
60	3721
120	14641
240	58081

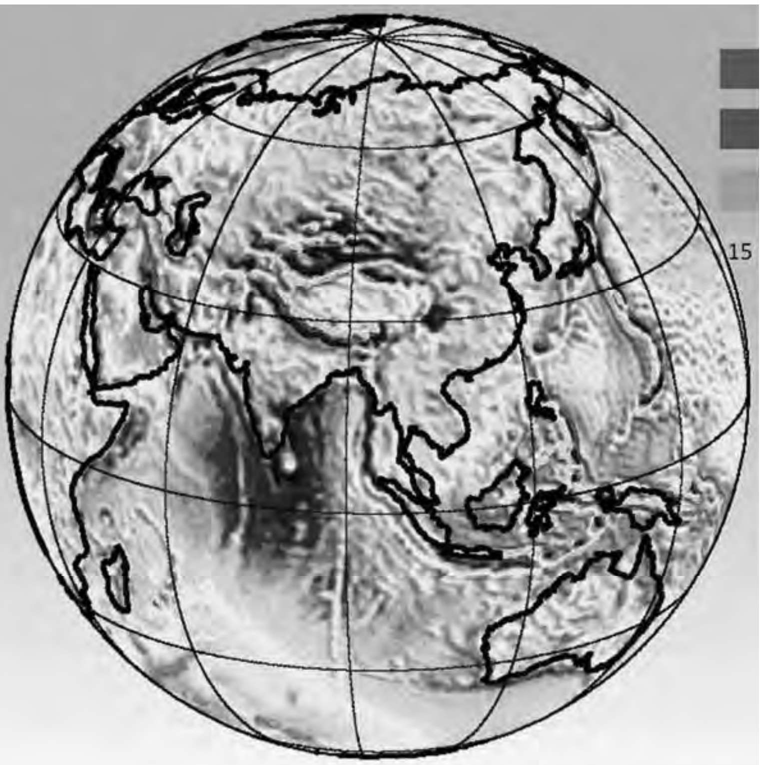

15

DFG SPP 1257

The basis functions

16

DFG SPP 1257

Approximation of a function on the sphere

$$f(\lambda,\vartheta)=\sum_{n=0}^{\infty}\sum_{m=-n}^{n} a_{nm} Y_{nm}(\lambda,\vartheta)$$

coefficients (scale) Basis functions

Basis functions

$$Y_{n,m}(\lambda,\vartheta)=\cos(m\lambda)\ P_{nm}(\cos\vartheta)$$

$$Y_{n,-m}(\lambda,\vartheta)=\sin(m\lambda)\ P_{nm}(\cos\vartheta)$$

Approximation of a function on the sphere

$$f(\lambda,\vartheta)=\sum_{n=0}^{\infty}\sum_{m=0}^{n}\big(C_{nm}\cos(m\lambda)+S_{nm}\sin(m\lambda)\big)P_{nm}(\cos\vartheta)$$

coefficients (scale)

17

DFG SPP 1257

Computation of the basis functions

$$Y_{n,m}(\lambda,\vartheta)=P_n^m(\cos\vartheta)\cos m\lambda$$

$$Y_{n,-m}(\lambda,\vartheta)=P_n^m(\cos\vartheta)\sin m\lambda$$

Legendre functions $(t=\cos\vartheta)$

$P_0^0(t)$				
$P_1^0(t)$	$P_1^1(t)$			
$P_2^0(t)$	$P_2^1(t)$	$P_2^2(t)$		
$P_3^0(t)$	$P_3^1(t)$	$P_3^2(t)$	$P_3^3(t)$	
$P_4^0(t)$	$P_4^1(t)$	$P_4^2(t)$	$P_4^3(t)$	$P_4^4(t)$

Recursion formula $(t=\cos\vartheta)$

$$P_0^0(t)=1$$

$$\longrightarrow\quad P_n^n(t)=a_n\cdot\sqrt{1-t^2}\cdot P_{n-1}^{n-1}(t)$$

$$\longrightarrow\quad P_n^{n-1}(t)=b_{n-1}^n\cdot t\cdot P_{n-1}^{n-1}(t)$$

$$\longrightarrow\quad P_n^m(t)=b_n^m\cdot t\cdot P_{n-1}^m(t)-c_n^m\cdot P_{n-2}^m(t)$$

Factors (normalized)

$$a_1=\sqrt{3}\qquad a_n=\sqrt{\frac{2n+1}{2n}}$$

$$b_n^m=\sqrt{\frac{(2n+1)(2n-1)}{(n+m)(n-m)}}$$

$$c_n^m=\sqrt{\frac{(2n+1)(n-m-1)(n+m-1)}{(2n-3)(n+m)(n-m)}}$$

8

DFG SPP 1257

Basis functions

Basis functions degree n = 4:
$C_{40}(\lambda,\vartheta) = P_4^0(\cos\vartheta)$
$C_{41}(\lambda,\vartheta) = \cos(1\lambda)\cdot P_4^1(\cos\vartheta)$
$S_{41}(\lambda,\vartheta) = \sin(1\lambda)\cdot P_4^1(\cos\vartheta)$
$C_{42}(\lambda,\vartheta) = \cos(2\lambda)\cdot P_4^2(\cos\vartheta)$
$S_{42}(\lambda,\vartheta) = \sin(2\lambda)\cdot P_4^2(\cos\vartheta)$
$C_{43}(\lambda,\vartheta) = \cos(3\lambda)\cdot P_4^3(\cos\vartheta)$
$S_{43}(\lambda,\vartheta) = \sin(3\lambda)\cdot P_4^3(\cos\vartheta)$
$C_{44}(\lambda,\vartheta) = \cos(4\lambda)\cdot P_4^4(\cos\vartheta)$
$S_{44}(\lambda,\vartheta) = \sin(4\lambda)\cdot P_4^4(\cos\vartheta)$

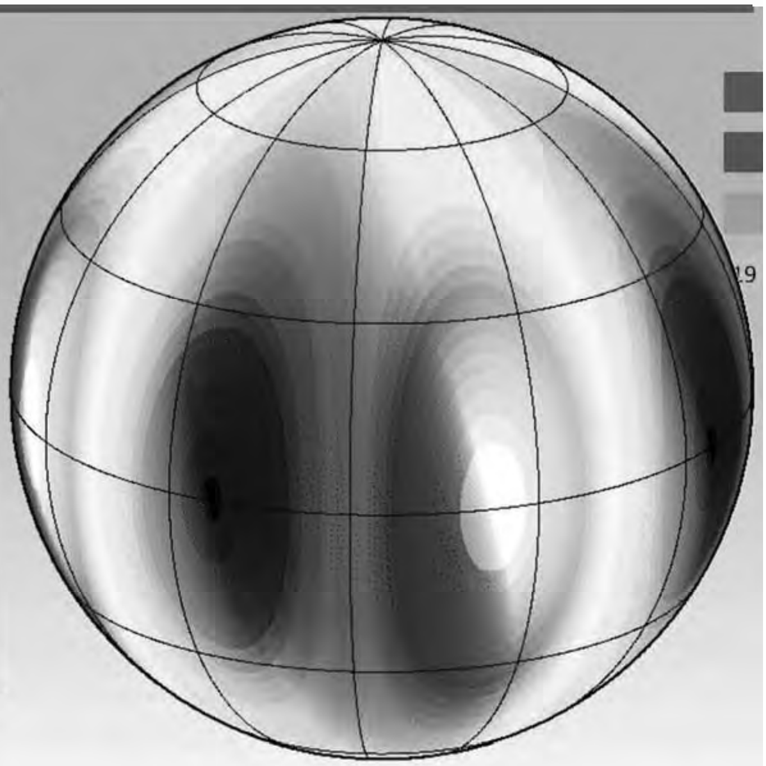

DFG SPP 1257

Basis functions

Basis functions degree n = 4:
$C_{40}(\lambda,\vartheta) = P_4^0(\cos\vartheta)$
$C_{41}(\lambda,\vartheta) = \cos(1\lambda)\cdot P_4^1(\cos\vartheta)$
$S_{41}(\lambda,\vartheta) = \sin(1\lambda)\cdot P_4^1(\cos\vartheta)$
$C_{42}(\lambda,\vartheta) = \cos(2\lambda)\cdot P_4^2(\cos\vartheta)$
$S_{42}(\lambda,\vartheta) = \sin(2\lambda)\cdot P_4^2(\cos\vartheta)$
$C_{43}(\lambda,\vartheta) = \cos(3\lambda)\cdot P_4^3(\cos\vartheta)$
$S_{43}(\lambda,\vartheta) = \sin(3\lambda)\cdot P_4^3(\cos\vartheta)$
$C_{44}(\lambda,\vartheta) = \cos(4\lambda)\cdot P_4^4(\cos\vartheta)$
$S_{44}(\lambda,\vartheta) = \sin(4\lambda)\cdot P_4^4(\cos\vartheta)$

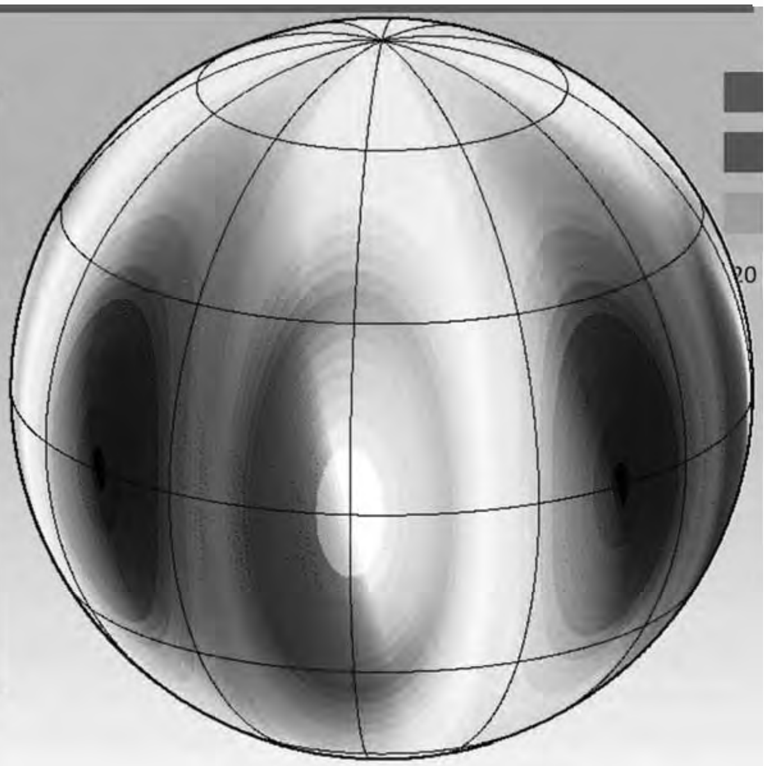

DFG SPP 1257

Basis functions

Basis functions degree n = 4:
$C_{40}(\lambda, \vartheta) = P_4^0(\cos \vartheta)$
$C_{41}(\lambda, \vartheta) = \cos(1\lambda) \cdot P_4^1(\cos \vartheta)$
$S_{41}(\lambda, \vartheta) = \sin(1\lambda) \cdot P_4^1(\cos \vartheta)$
$C_{42}(\lambda, \vartheta) = \cos(2\lambda) \cdot P_4^2(\cos \vartheta)$
$S_{42}(\lambda, \vartheta) = \sin(2\lambda) \cdot P_4^2(\cos \vartheta)$
$C_{43}(\lambda, \vartheta) = \cos(3\lambda) \cdot P_4^3(\cos \vartheta)$
$S_{43}(\lambda, \vartheta) = \sin(3\lambda) \cdot P_4^3(\cos \vartheta)$
$C_{44}(\lambda, \vartheta) = \cos(4\lambda) \cdot P_4^4(\cos \vartheta)$
$S_{44}(\lambda, \vartheta) = \sin(4\lambda) \cdot P_4^4(\cos \vartheta)$

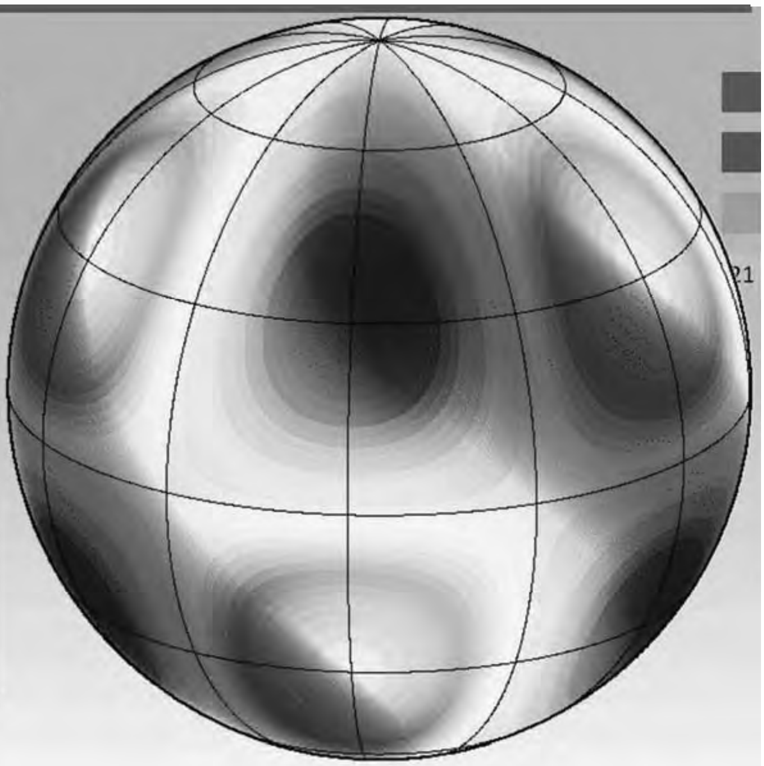

Basis functions

Basis functions degree n = 4:
$C_{40}(\lambda, \vartheta) = P_4^0(\cos \vartheta)$
$C_{41}(\lambda, \vartheta) = \cos(1\lambda) \cdot P_4^1(\cos \vartheta)$
$S_{41}(\lambda, \vartheta) = \sin(1\lambda) \cdot P_4^1(\cos \vartheta)$
$C_{42}(\lambda, \vartheta) = \cos(2\lambda) \cdot P_4^2(\cos \vartheta)$
$S_{42}(\lambda, \vartheta) = \sin(2\lambda) \cdot P_4^2(\cos \vartheta)$
$C_{43}(\lambda, \vartheta) = \cos(3\lambda) \cdot P_4^3(\cos \vartheta)$
$S_{43}(\lambda, \vartheta) = \sin(3\lambda) \cdot P_4^3(\cos \vartheta)$
$C_{44}(\lambda, \vartheta) = \cos(4\lambda) \cdot P_4^4(\cos \vartheta)$
$S_{44}(\lambda, \vartheta) = \sin(4\lambda) \cdot P_4^4(\cos \vartheta)$

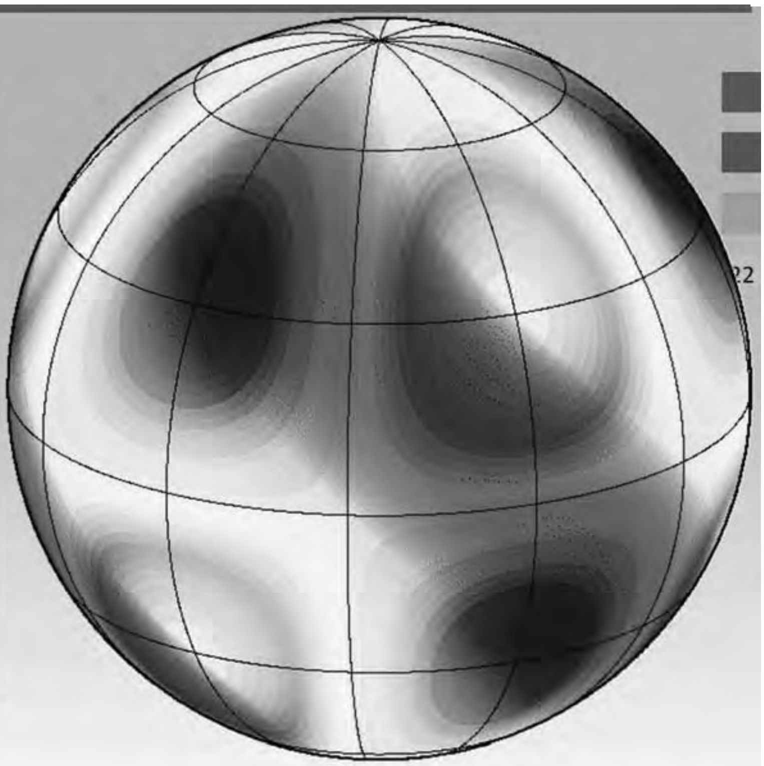

Basis functions

Basis functions degree n = 4:
$C_{40}(\lambda,\vartheta) = P_4^0(\cos\vartheta)$
$C_{41}(\lambda,\vartheta) = \cos(1\lambda)\cdot P_4^1(\cos\vartheta)$
$S_{41}(\lambda,\vartheta) = \sin(1\lambda)\cdot P_4^1(\cos\vartheta)$
$C_{42}(\lambda,\vartheta) = \cos(2\lambda)\cdot P_4^2(\cos\vartheta)$
$S_{42}(\lambda,\vartheta) = \sin(2\lambda)\cdot P_4^2(\cos\vartheta)$
$C_{43}(\lambda,\vartheta) = \cos(3\lambda)\cdot P_4^3(\cos\vartheta)$
$S_{43}(\lambda,\vartheta) = \sin(3\lambda)\cdot P_4^3(\cos\vartheta)$
$C_{44}(\lambda,\vartheta) = \cos(4\lambda)\cdot P_4^4(\cos\vartheta)$
$S_{44}(\lambda,\vartheta) = \sin(4\lambda)\cdot P_4^4(\cos\vartheta)$

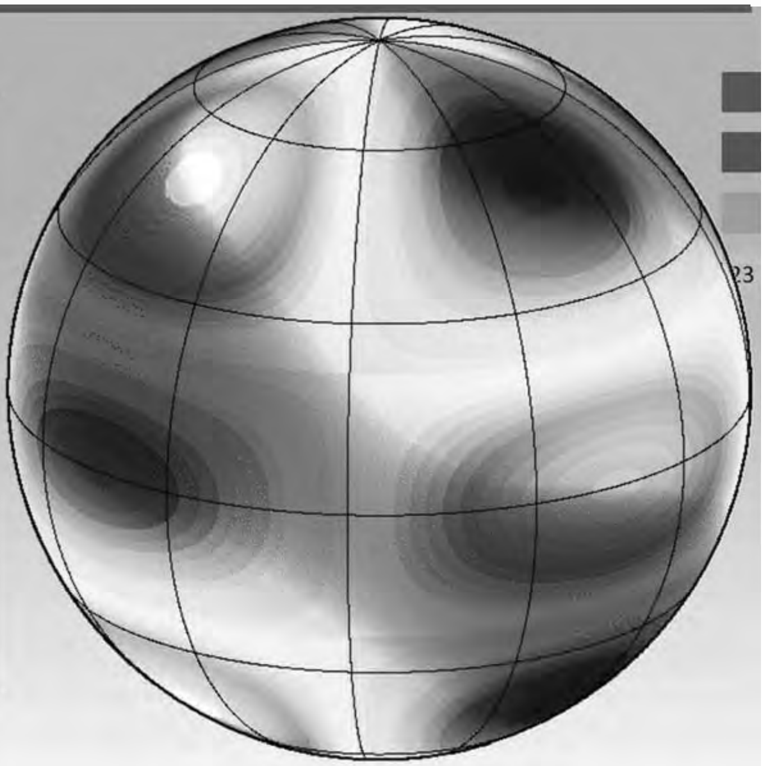

Basis functions

Basis functions degree n = 4:
$C_{40}(\lambda,\vartheta) = P_4^0(\cos\vartheta)$
$C_{41}(\lambda,\vartheta) = \cos(1\lambda)\cdot P_4^1(\cos\vartheta)$
$S_{41}(\lambda,\vartheta) = \sin(1\lambda)\cdot P_4^1(\cos\vartheta)$
$C_{42}(\lambda,\vartheta) = \cos(2\lambda)\cdot P_4^2(\cos\vartheta)$
$S_{42}(\lambda,\vartheta) = \sin(2\lambda)\cdot P_4^2(\cos\vartheta)$
$C_{43}(\lambda,\vartheta) = \cos(3\lambda)\cdot P_4^3(\cos\vartheta)$
$S_{43}(\lambda,\vartheta) = \sin(3\lambda)\cdot P_4^3(\cos\vartheta)$
$C_{44}(\lambda,\vartheta) = \cos(4\lambda)\cdot P_4^4(\cos\vartheta)$
$S_{44}(\lambda,\vartheta) = \sin(4\lambda)\cdot P_4^4(\cos\vartheta)$

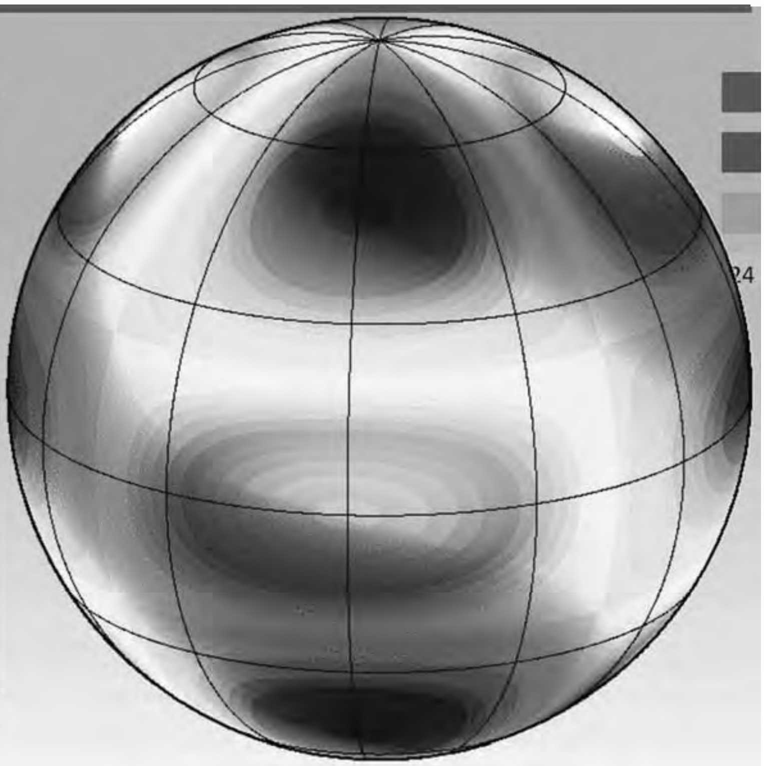

Basis functions

Basis functions degree n = 4:

$$C_{40}(\lambda,\vartheta) = P_4^0(\cos\vartheta)$$
$$C_{41}(\lambda,\vartheta) = \cos(1\lambda)\cdot P_4^1(\cos\vartheta)$$
$$S_{41}(\lambda,\vartheta) = \sin(1\lambda)\cdot P_4^1(\cos\vartheta)$$
$$C_{42}(\lambda,\vartheta) = \cos(2\lambda)\cdot P_4^2(\cos\vartheta)$$
$$S_{42}(\lambda,\vartheta) = \sin(2\lambda)\cdot P_4^2(\cos\vartheta)$$
$$C_{43}(\lambda,\vartheta) = \cos(3\lambda)\cdot P_4^3(\cos\vartheta)$$
$$S_{43}(\lambda,\vartheta) = \sin(3\lambda)\cdot P_4^3(\cos\vartheta)$$
$$C_{44}(\lambda,\vartheta) = \cos(4\lambda)\cdot P_4^4(\cos\vartheta)$$
$$S_{44}(\lambda,\vartheta) = \sin(4\lambda)\cdot P_4^4(\cos\vartheta)$$

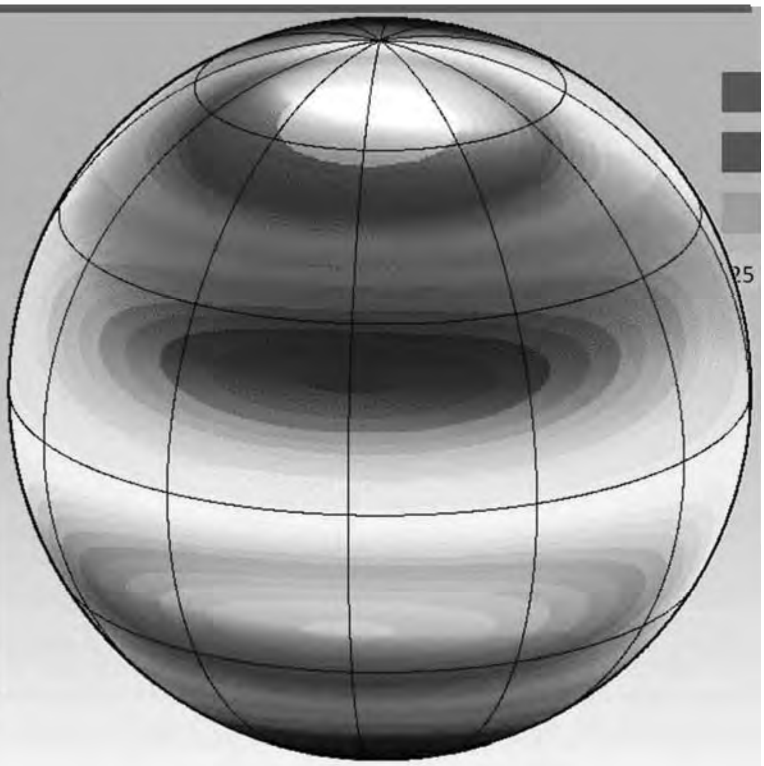

25

DFG SPP 1257

Basis functions

Basis functions degree n = 4:

$$C_{40}(\lambda,\vartheta) = P_4^0(\cos\vartheta)$$
$$C_{41}(\lambda,\vartheta) = \cos(1\lambda)\cdot P_4^1(\cos\vartheta)$$
$$S_{41}(\lambda,\vartheta) = \sin(1\lambda)\cdot P_4^1(\cos\vartheta)$$
$$C_{42}(\lambda,\vartheta) = \cos(2\lambda)\cdot P_4^2(\cos\vartheta)$$
$$S_{42}(\lambda,\vartheta) = \sin(2\lambda)\cdot P_4^2(\cos\vartheta)$$
$$C_{43}(\lambda,\vartheta) = \cos(3\lambda)\cdot P_4^3(\cos\vartheta)$$
$$S_{43}(\lambda,\vartheta) = \sin(3\lambda)\cdot P_4^3(\cos\vartheta)$$
$$C_{44}(\lambda,\vartheta) = \cos(4\lambda)\cdot P_4^4(\cos\vartheta)$$
$$S_{44}(\lambda,\vartheta) = \sin(4\lambda)\cdot P_4^4(\cos\vartheta)$$

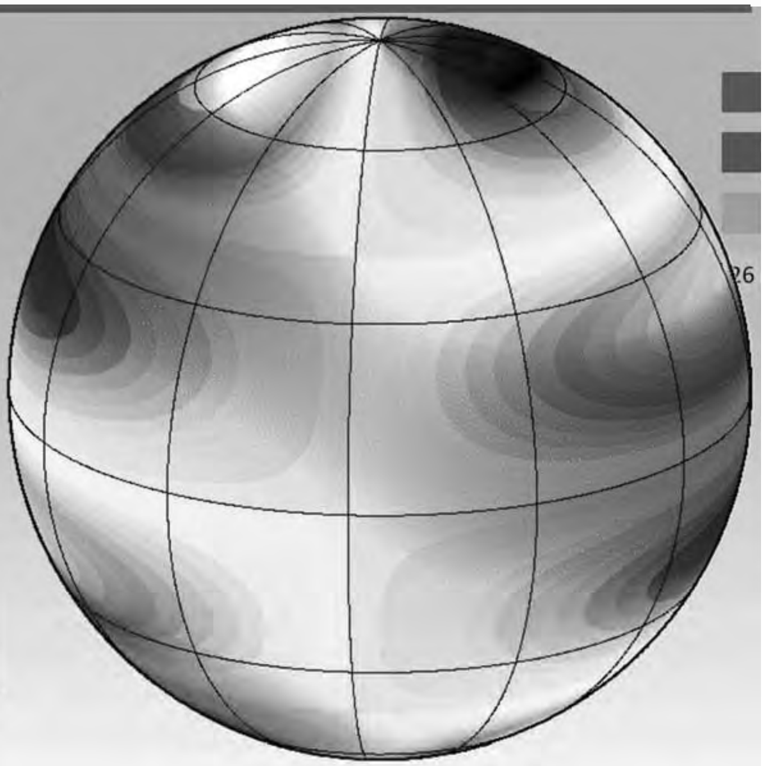

26

DFG SPP 1257

Basis functions

Basis functions degree n = 4:

$$C_{40}(\lambda,\vartheta) = P_4^0(\cos\vartheta)$$
$$C_{41}(\lambda,\vartheta) = \cos(1\lambda)\cdot P_4^1(\cos\vartheta)$$
$$S_{41}(\lambda,\vartheta) = \sin(1\lambda)\cdot P_4^1(\cos\vartheta)$$
$$C_{42}(\lambda,\vartheta) = \cos(2\lambda)\cdot P_4^2(\cos\vartheta)$$
$$S_{42}(\lambda,\vartheta) = \sin(2\lambda)\cdot P_4^2(\cos\vartheta)$$
$$C_{43}(\lambda,\vartheta) = \cos(3\lambda)\cdot P_4^3(\cos\vartheta)$$
$$S_{43}(\lambda,\vartheta) = \sin(3\lambda)\cdot P_4^3(\cos\vartheta)$$
$$C_{44}(\lambda,\vartheta) = \cos(4\lambda)\cdot P_4^4(\cos\vartheta)$$
$$S_{44}(\lambda,\vartheta) = \sin(4\lambda)\cdot P_4^4(\cos\vartheta)$$

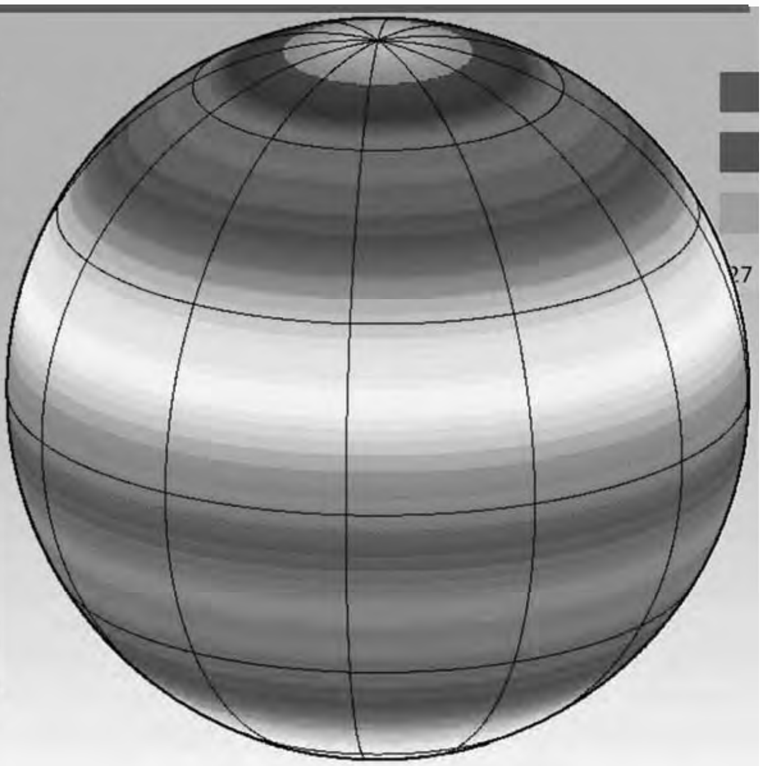

Basis functions

Basis functions degree n = 20:

$$C_{20,5}(\lambda,\vartheta) = \cos(5\lambda)\cdot P_{20}^5(\cos\vartheta)$$

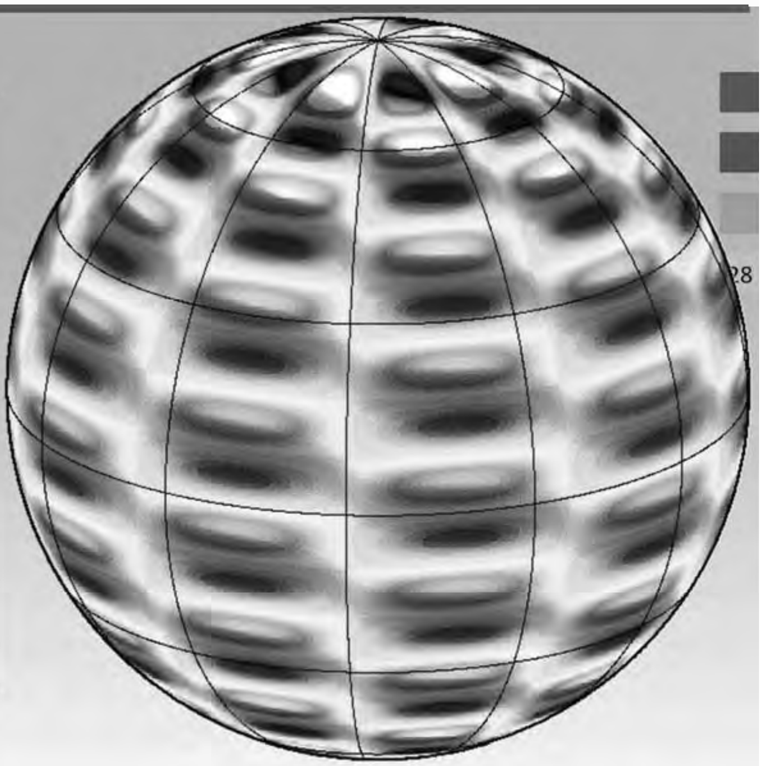

Basis functions

Basis functions degree *n* = 40:

$$C_{40,20}(\lambda,\vartheta) = \cos(20\lambda)\cdot P_{40}^{20}(\cos\vartheta)$$

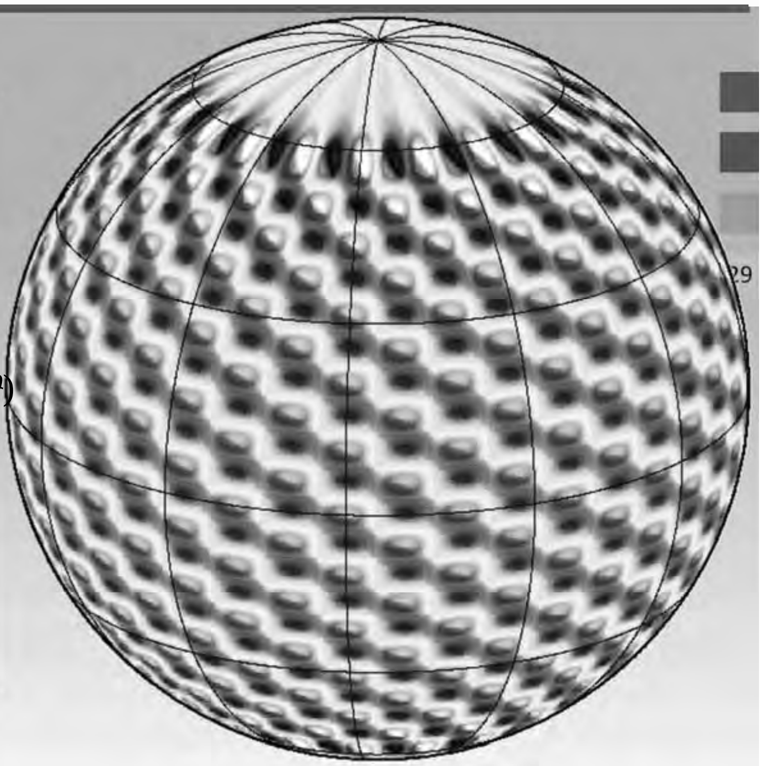

Basis functions

$$Y_{n,m}(\lambda,\vartheta) = P_n^m(\cos\vartheta)\cos m\lambda$$

$$Y_{n,-m}(\lambda,\vartheta) = P_n^m(\cos\vartheta)\sin m\lambda$$

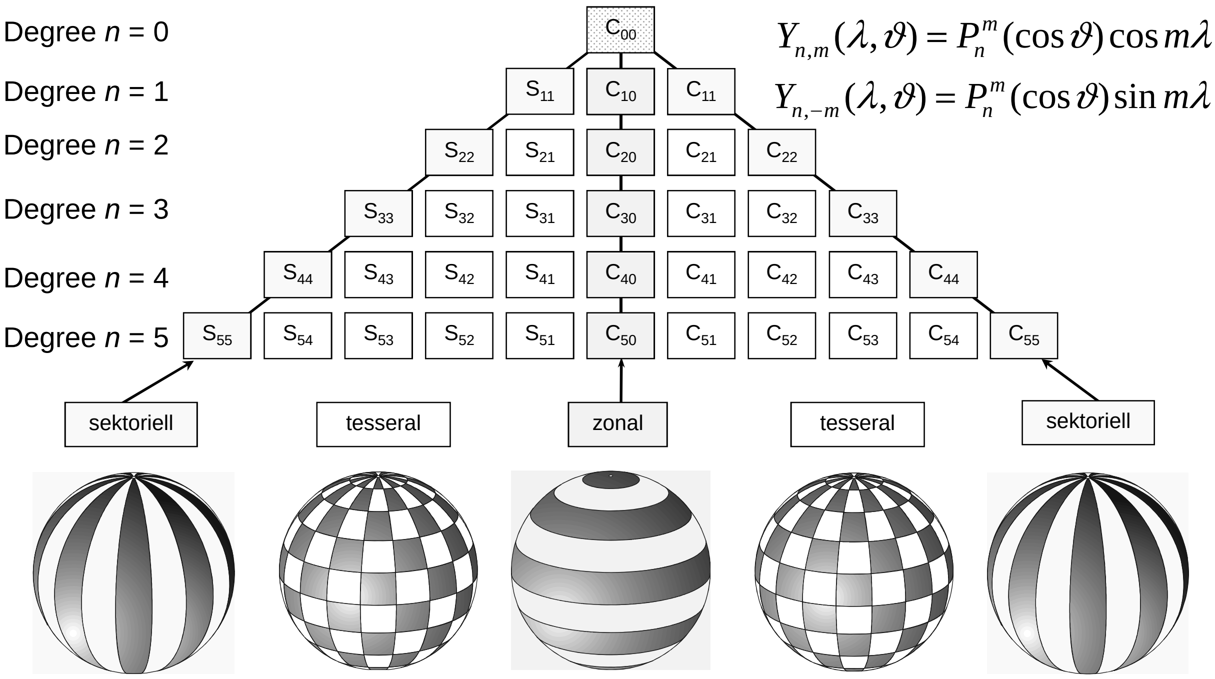

Rummel

Coefficient triangle

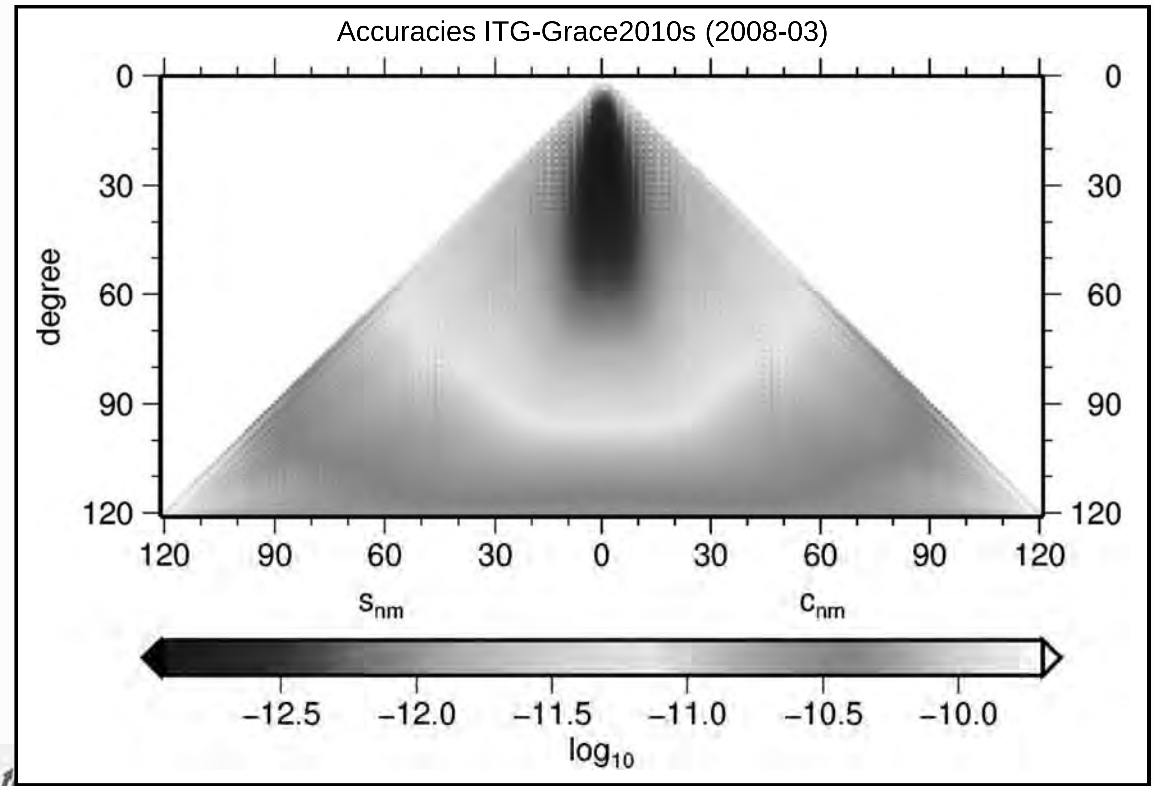

31

DFG SPP 1257

Gravity field

32

DFG SPP 1257

Feldstärke

Gravity field:

$$\mathbf{g}(\mathbf{r}) = \begin{pmatrix} g_x(\mathbf{r}) \\ g_y(\mathbf{r}) \\ g_z(\mathbf{r}) \end{pmatrix} \qquad \left[\frac{m}{s^2}\right]$$

Conservative vector field ⇔
Potential function exists:

$$\mathbf{g}(\mathbf{r}) = \nabla V(\mathbf{r}) = \begin{pmatrix} \partial V/\partial x \\ \partial V/\partial y \\ \partial V/\partial z \end{pmatrix} \qquad V(\mathbf{r})\left[\frac{m^2}{s^2}\right]$$

Source free in outer space

$$\operatorname{div}\mathbf{g} = \nabla\cdot\mathbf{g} = 0$$

Laplace equation (harmonic func.)

$$\nabla\cdot\nabla V = \Delta V = 0$$

$$\Delta V = \frac{\partial^2 V}{\partial x^2} + \frac{\partial^2 V}{\partial y^2} + \frac{\partial^2 V}{\partial z^2} = 0$$

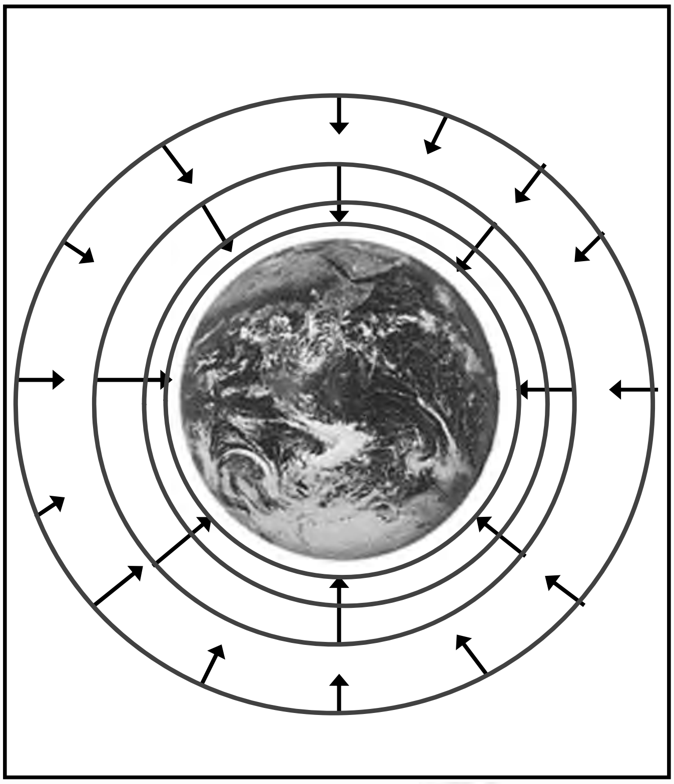

DFG SPP 1257 33

Harmonics continuation

Potential in outer space

$$V(\lambda,\vartheta,r) = \frac{R\left(R^2-r^2\right)}{4\pi}\iint_\Omega \frac{1}{l^3} V(\lambda,\vartheta)\,d\Omega$$

with $l = \sqrt{R^2 + r^2 - 2Rr\cos\psi}$

Harmonic continuation

$$\Delta V = \frac{\partial^2 V}{\partial x^2} + \frac{\partial^2 V}{\partial y^2} + \frac{\partial^2 V}{\partial z^2} = 0$$

Potential at Earth‘s surface

$$V(\lambda,\vartheta)\big|_\Omega$$

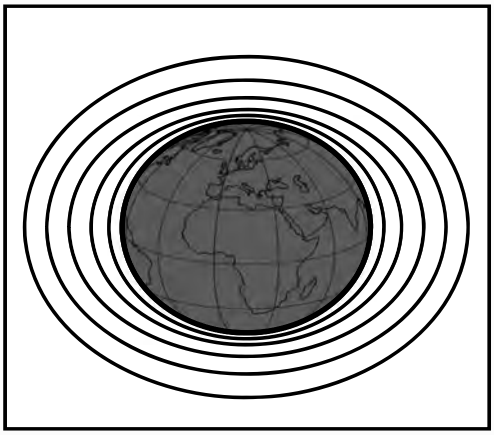

DFG SPP 1257 34

Harmonics continuation

Potential in outer space
(solid spherical harmonics)

$$V(\lambda,\vartheta,r) = \frac{GM}{R}\sum_{n=0}^{\infty}\left(\frac{R}{r}\right)^{n+1}\sum_{m=-n}^{n} a_{nm}Y_{nm}(\lambda,\vartheta)$$

Harmonic continuation

$$\Delta V = \frac{\partial^2 V}{\partial x^2} + \frac{\partial^2 V}{\partial y^2} + \frac{\partial^2 V}{\partial z^2} = 0$$

Potential at Earth's surface
(in spherical harmonics)

$$V(\lambda,\vartheta) = \frac{GM}{R}\sum_{n=0}^{\infty}\sum_{m=-n}^{n} a_{nm}Y_{nm}(\lambda,\vartheta)$$

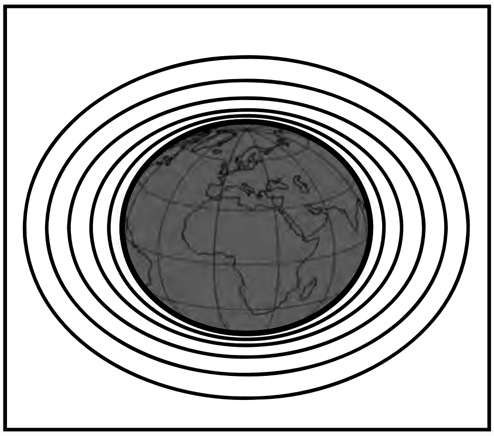

Gravity

Gravity acceleration
at Earth's surface

$$g = 9{,}78\frac{m}{s^2}\ldots 9{,}83\frac{m}{s^2}$$

$$\pm\, 0{,}0004\frac{m}{s^2}$$

Gravity disturbances

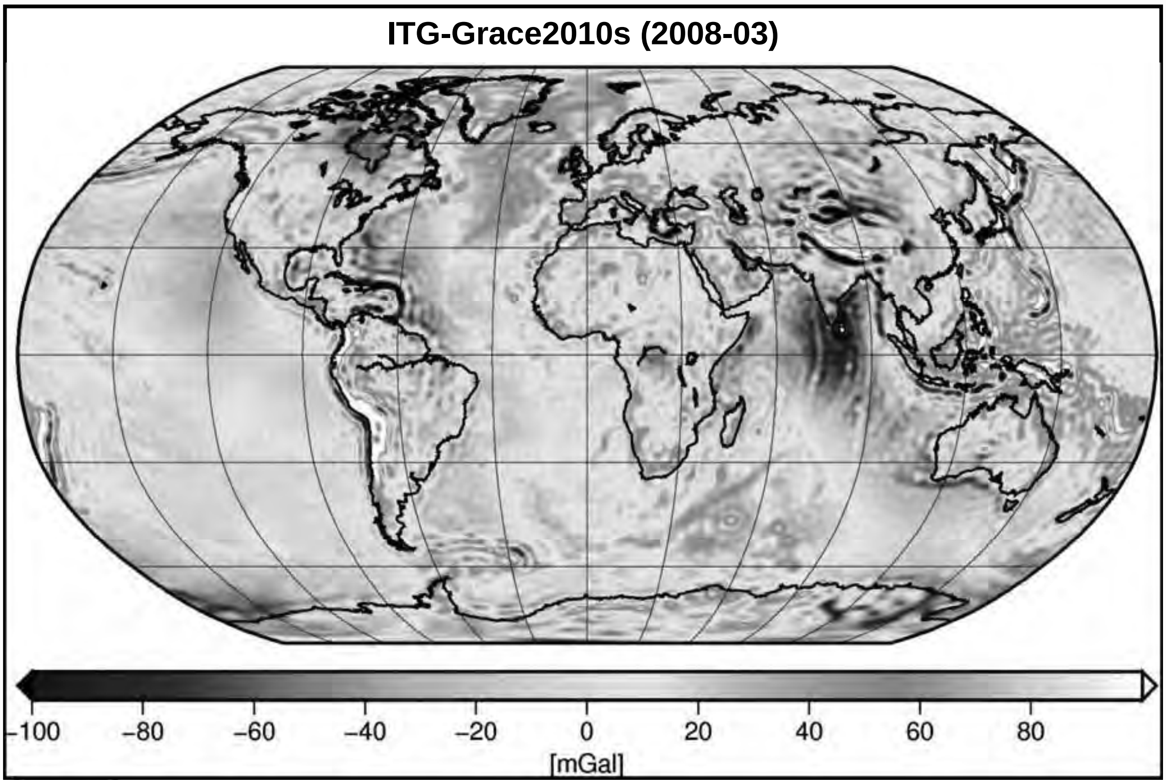

37

DFG SPP 1257

Gravity disturbances

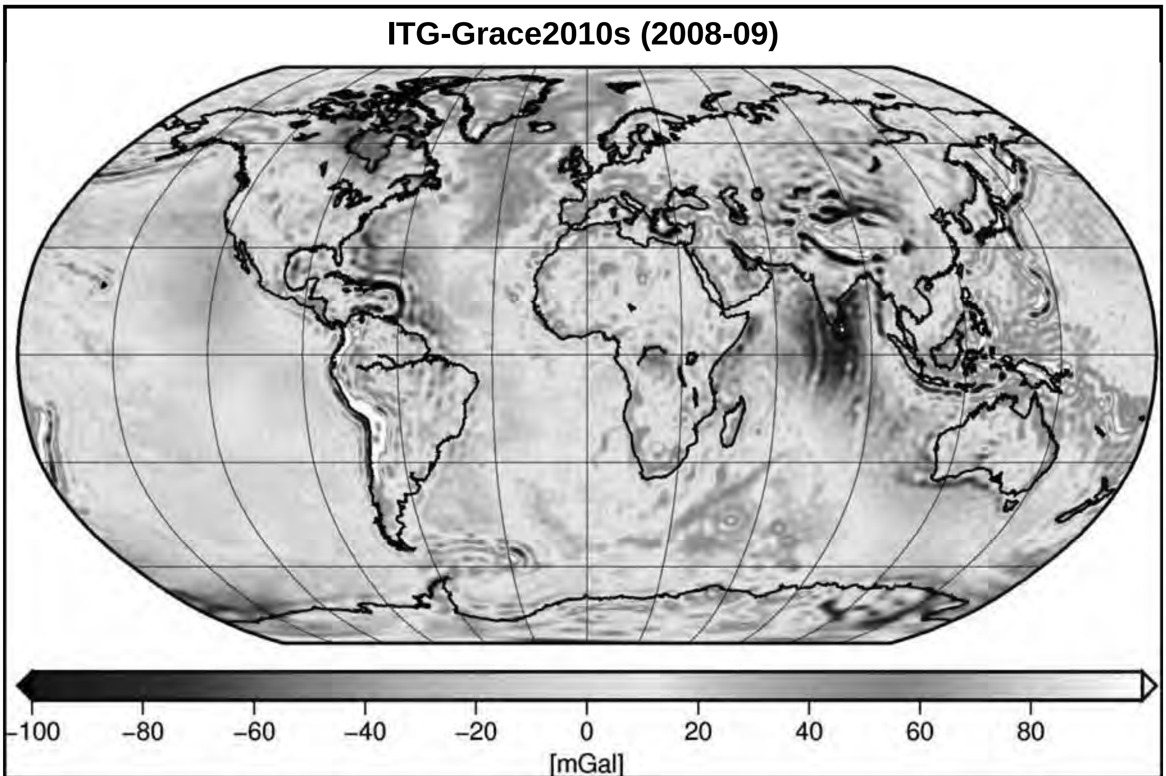

38

DFG SPP 1257

Gravity disturbances

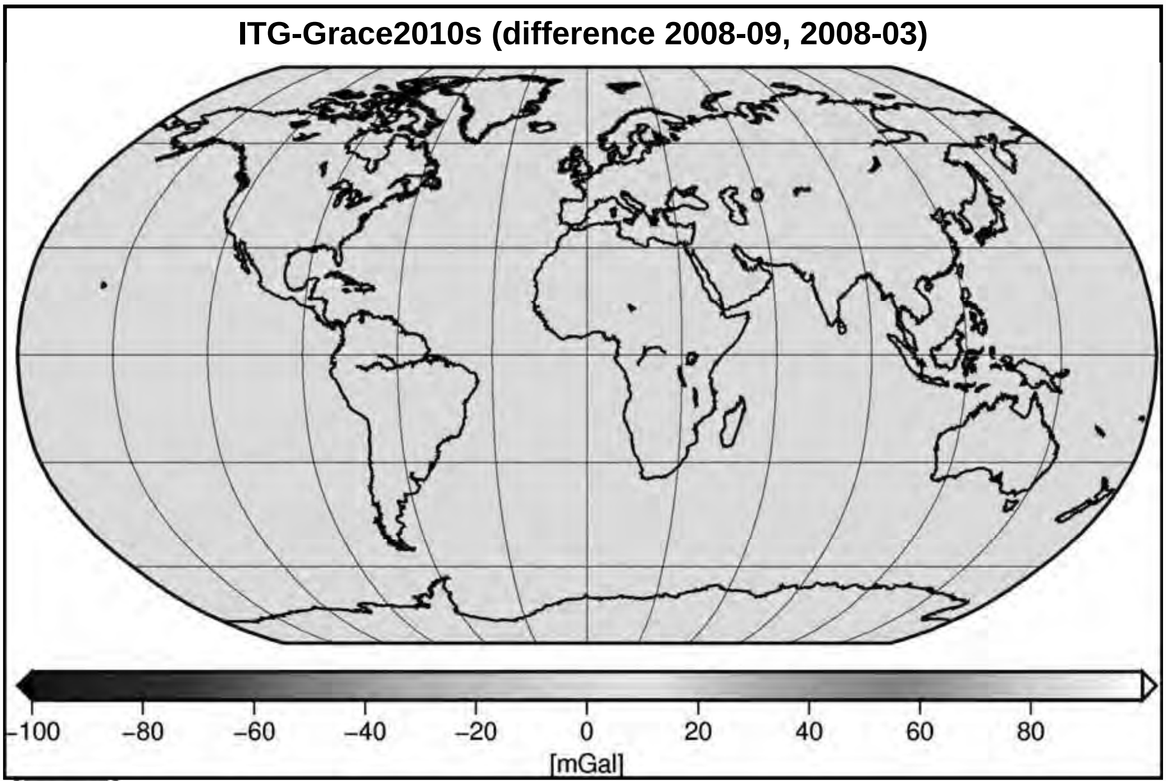

DFG SPP 1257

39

Gravity disturbances

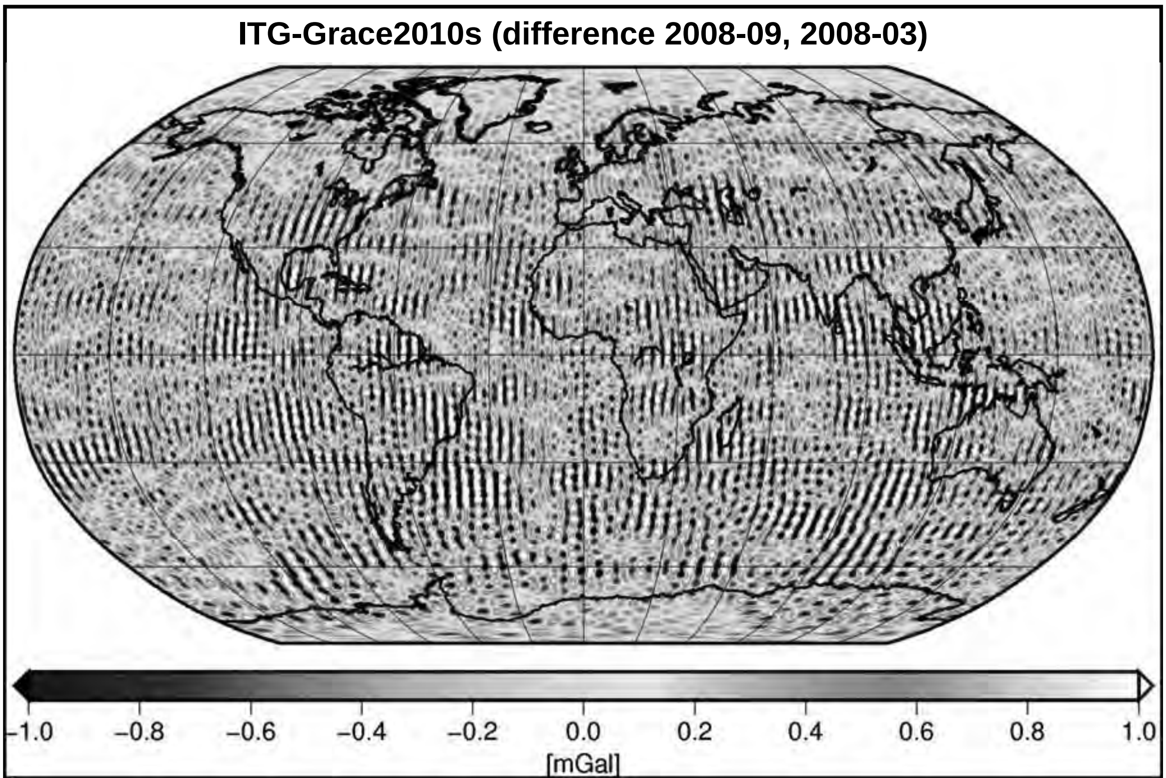

DFG SPP 1257

40

Gravity disturbances

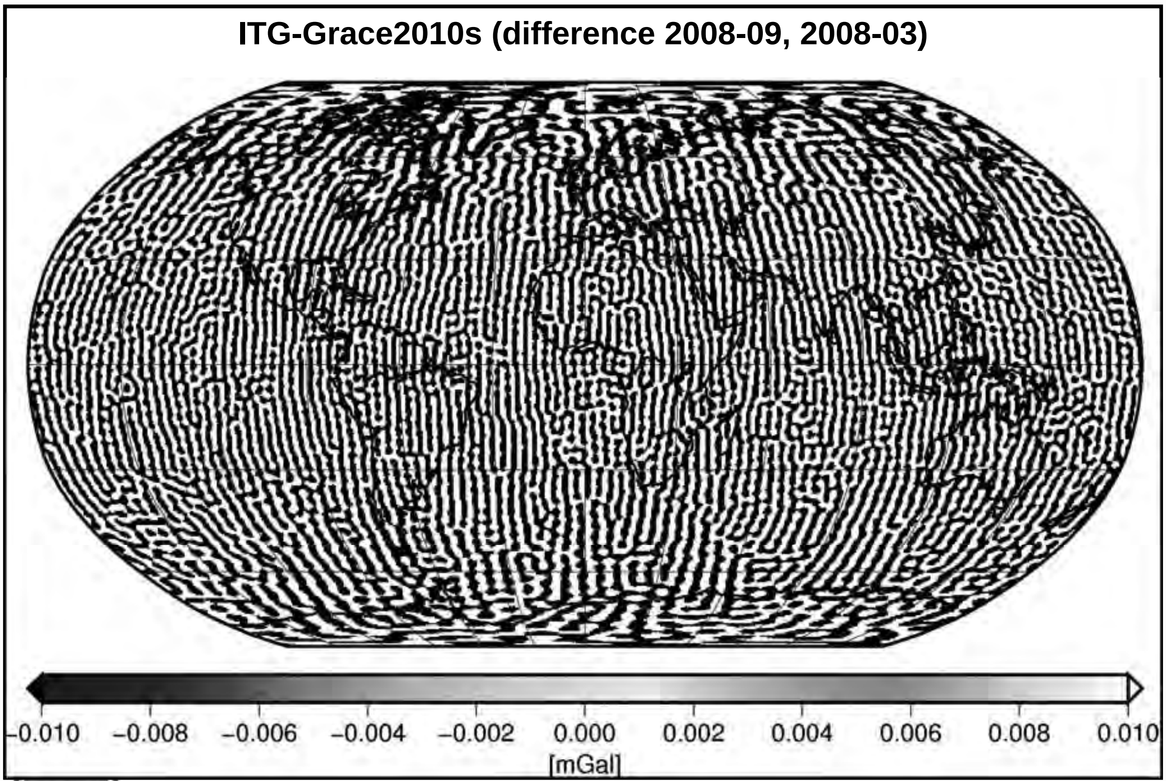

41

DFG SPP 1257

Gravity disturbances

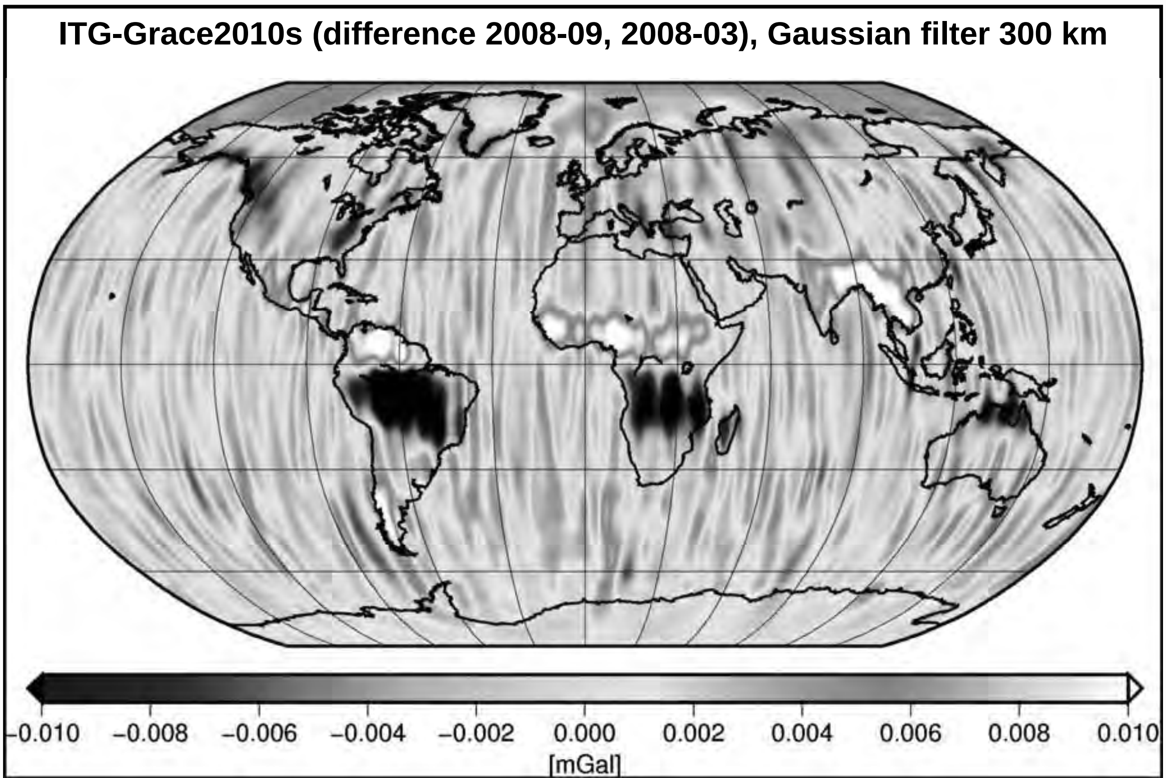

42

DFG SPP 1257

Gravity disturbances

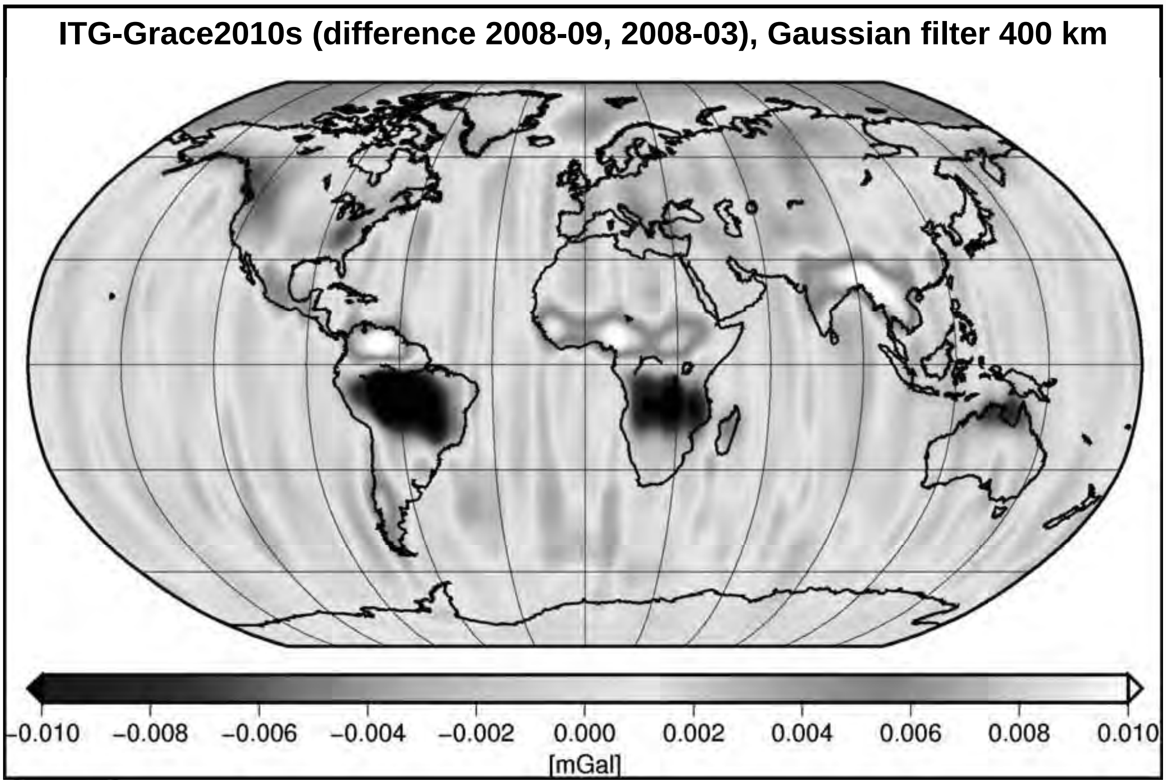

43

DFG SPP 1257

Gravity disturbances

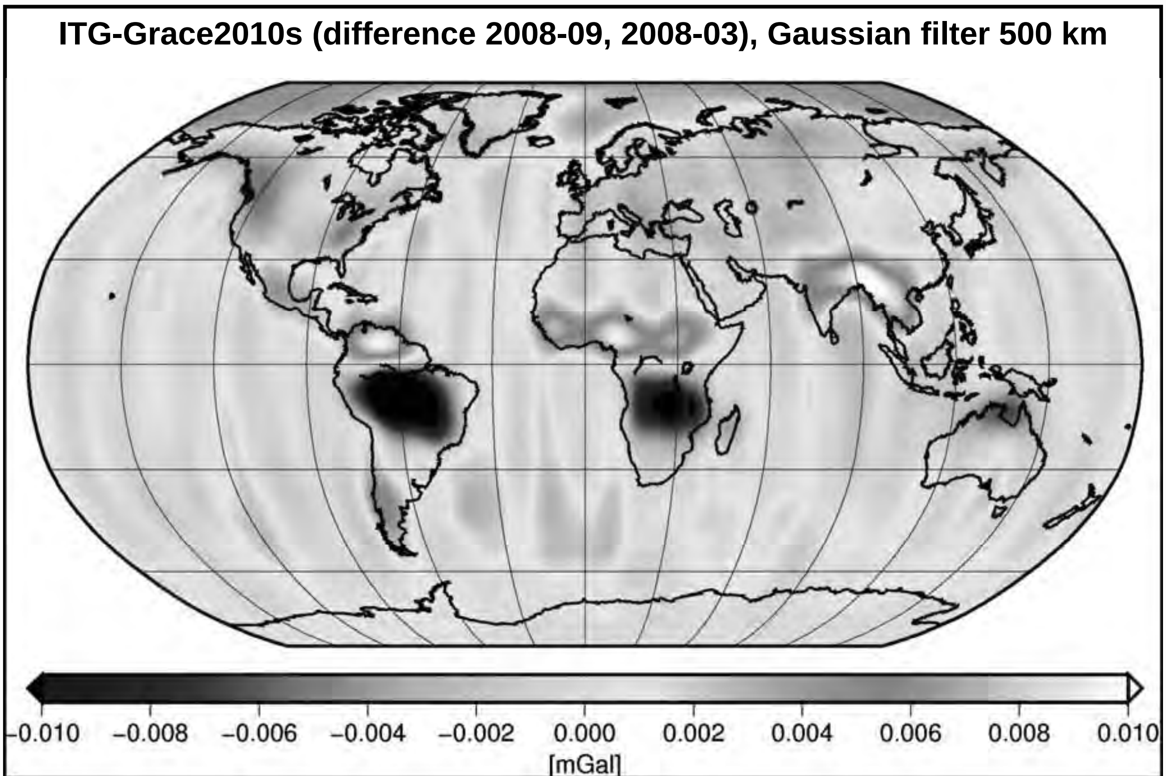

44

DFG SPP 1257

Gravity field

Sphere

$$g = \frac{GM}{R^2} \approx 10\frac{m}{s^2} \qquad C_{00} = 1$$

Flattening

$$g = \pm 0.03\frac{m}{s^2} \qquad C_{20} = -0.0004842$$

Normal field (Geodetic Reference System, GRS80)

Static part

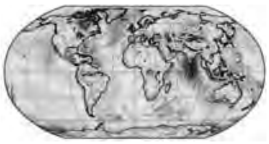

$$\delta g \approx 0.001\frac{m}{s^2} = 100\,\mathrm{mGal}$$

Spherical approximations + ellipsoidal corrections

Time variable part

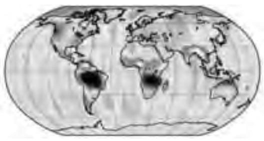

$$\Delta\delta g \approx 0.0000001\frac{m}{s^2} = 0.01\,\mathrm{mGal}$$

Spherical approximations

Gravity field functionals

Disturbing potential

$$T = V - U$$

Normal potential

$$T(\lambda,\vartheta,r) = \frac{GM}{R}\sum_{n=0}^{\infty}\left(\frac{R}{r}\right)^{n+1}\sum_{m=-n}^{n} a_{nm}Y_{nm}(\lambda,\vartheta)$$

gravity

$$g = \|\nabla V\|$$

Geoid heights

$$V(\mathbf{r}) \approx V(\mathbf{r}_0) + \|\nabla V\| dr$$

$$N = dr = \frac{T}{\|\nabla V\|} = \frac{T}{g}$$

Geoid heights changes

$$\Delta N = \frac{\Delta T}{g}$$

Spherical approx

$$g \approx \frac{GM}{R^2}$$

$$\Delta N(\lambda,\vartheta) = R\sum_{n=0}^{\infty}\sum_{m=-n}^{n}\Delta a_{nm}Y_{nm}(\lambda,\vartheta)$$

Gravity field functionals

Disturbing potential $T = V - U$	$T(\lambda,\vartheta,r) = \frac{GM}{R}\sum_{n=0}^{\infty}\left(\frac{R}{r}\right)^{n+1}\sum_{m=-n}^{n} a_{nm} Y_{nm}(\lambda,\vartheta)$
Gravity disturbances $\delta g = \lVert\nabla T\rVert \approx -\frac{\partial T}{\partial r}$	$\delta g(\lambda,\vartheta,r) = \frac{GM}{R}\sum_{n=0}^{\infty}\frac{n+1}{r}\left(\frac{R}{r}\right)^{n+1}\sum_{m=-n}^{n} a_{nm} Y_{nm}(\lambda,\vartheta)$
Gravity anomlies $\Delta g = \lVert g(r_P) - \gamma(r_Q)\rVert \approx -\frac{\partial T}{\partial r} - 2\frac{T}{r}$	$\Delta g(\lambda,\vartheta,r) = \frac{GM}{R}\sum_{n=0}^{\infty}\frac{n-1}{r}\left(\frac{R}{r}\right)^{n+1}\sum_{m=-n}^{n} a_{nm} Y_{nm}(\lambda,\vartheta)$
Surface density changes $\Delta\sigma \approx -\frac{1}{4\pi RG}\left(2\frac{\partial \Delta T}{\partial r} + \frac{\Delta T}{r}\right)\Big\|_{r=R}$	$\Delta\sigma(\lambda,\vartheta) = \frac{M}{4\pi R^2}\sum_{n=0}^{\infty}(2n+1)\sum_{m=-n}^{n}\Delta a_{nm} Y_{nm}(\lambda,\vartheta)$
$\rho_e = \frac{M}{4/3\pi R^3}$	Total water storage changes $\Delta TWS(\lambda,\vartheta) = \frac{\rho_e R}{3}\sum_{n=0}^{\infty}\frac{2n+1}{1+k_n}\sum_{m=-n}^{n}\Delta a_{nm} Y_{nm}(\lambda,\vartheta)$

47

Degree variances

48

DFG SPP 1257

Degree variances

Variance/Variablility of geoid heights:

$$\sigma^2(N) = \frac{1}{4\pi}\iint_\Omega N^2(\lambda,\vartheta)d\Omega$$

Variance of gravity disturbances:

$$\sigma^2(\delta g) = \frac{1}{4\pi}\iint_\Omega \delta g^2(\lambda,\vartheta)d\Omega$$

In terms of spherical harmonics:

$$\sigma^2(N) = R^2\sum_{n=0}^{\infty}\sum_{m=0}^{n}\left(C_{nm}^2 + S_{nm}^2\right)$$

In terms of spherical harmonics:

$$\sigma^2(\delta g) = \left(\frac{GM}{R^2}\right)^2\sum_{n=0}^{\infty}(n+1)^2\sum_{m=0}^{n}\left(C_{nm}^2 + S_{nm}^2\right)$$

Degree variances:

$$\sigma_n^2 = \sum_{m=0}^{n}\left(C_{nm}^2 + S_{nm}^2\right)$$

Degree variances

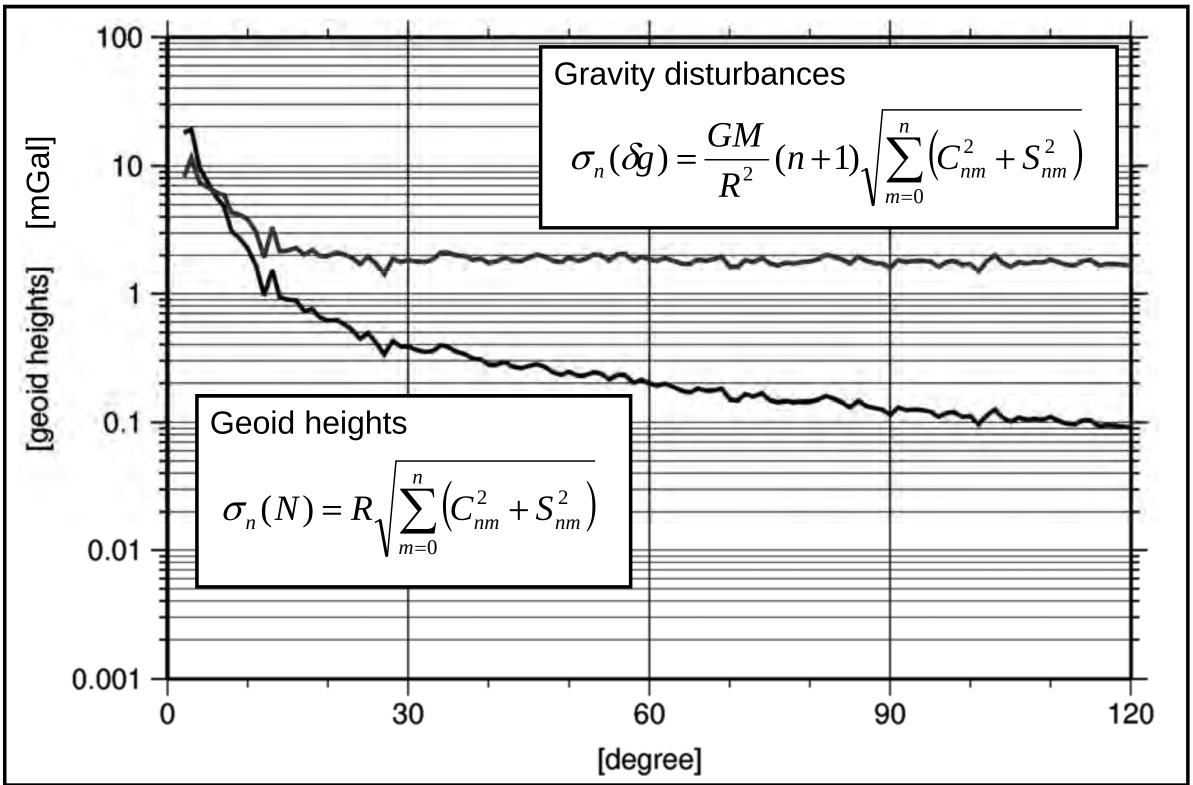

Degree

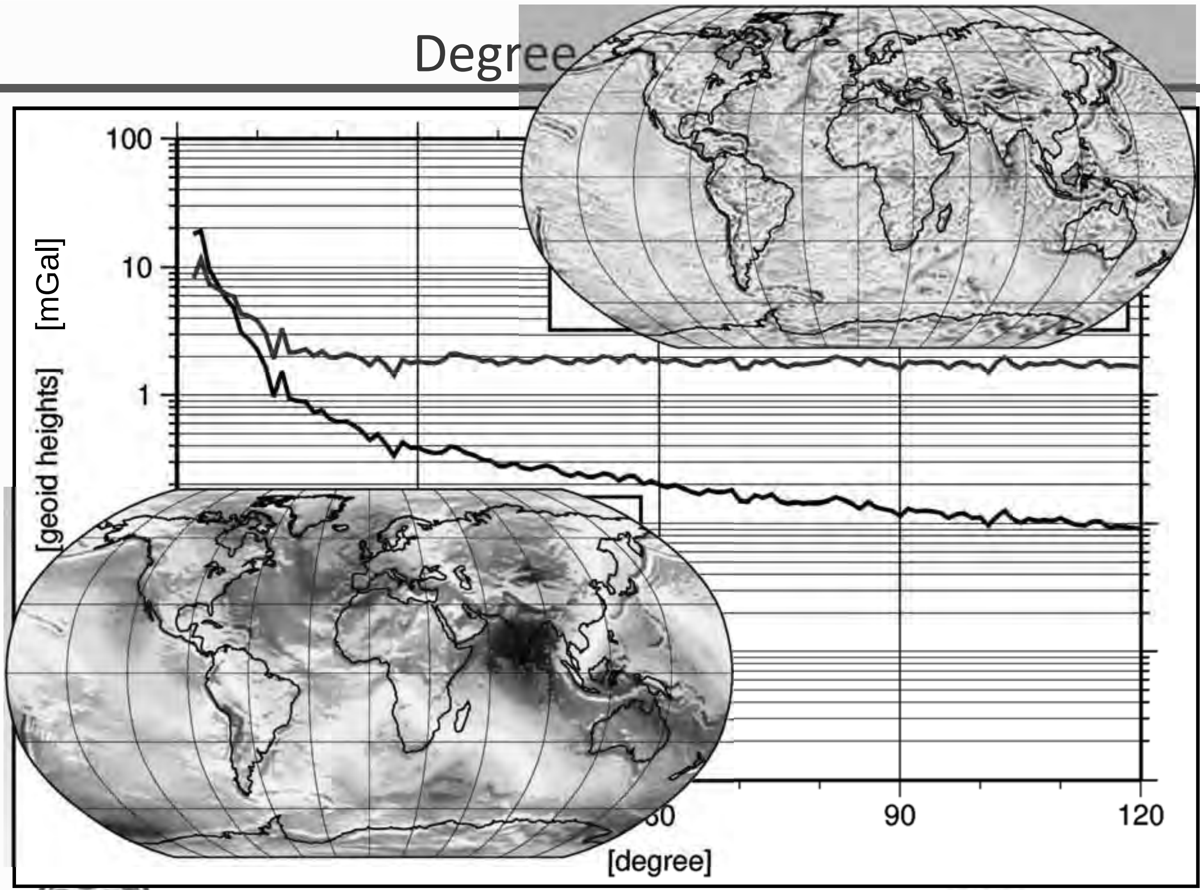

Upward continuation

Upward continuation

Gravitational potential:

$$V(\lambda,\vartheta,r)=\frac{GM}{R}\sum_{n=0}^{\infty}\left(\frac{R}{r}\right)^{n+1}\sum_{m=-n}^{n}a_{nm}Y_{nm}(\lambda,\vartheta)$$

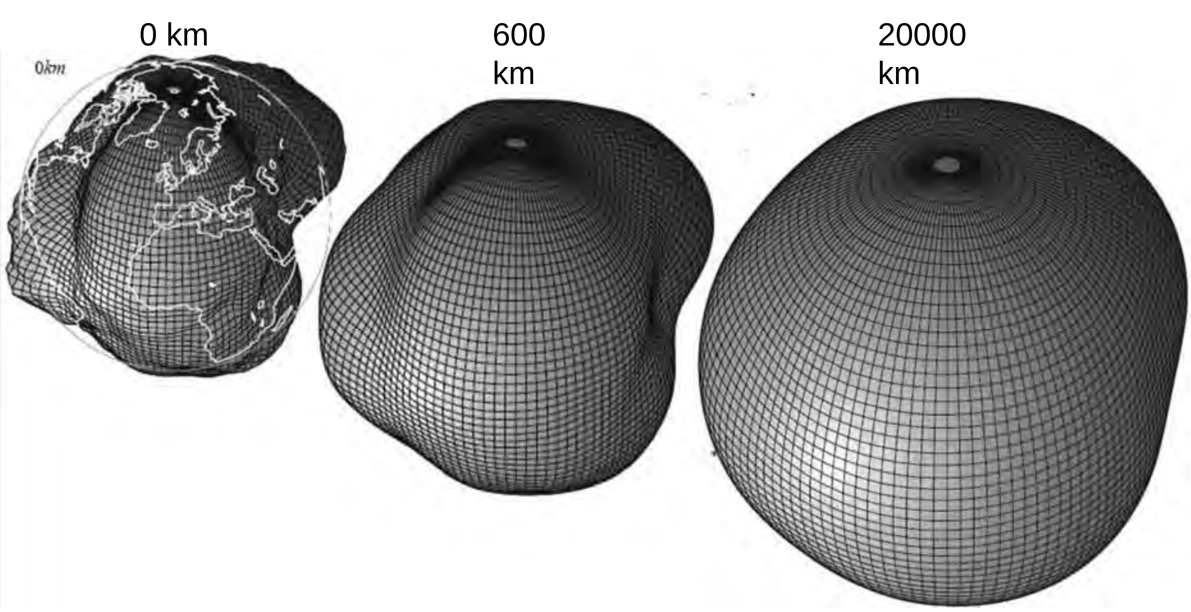

53

Upward continuation

Gravitational potential:

$$V(\lambda,\vartheta,r)=\frac{GM}{R}\sum_{n=0}^{\infty}\left(\frac{R}{r}\right)^{n+1}\sum_{m=-n}^{n}a_{nm}Y_{nm}(\lambda,\vartheta)$$

GRACE:

$$R = 6378\ km$$
$$r = R + 450\ km$$

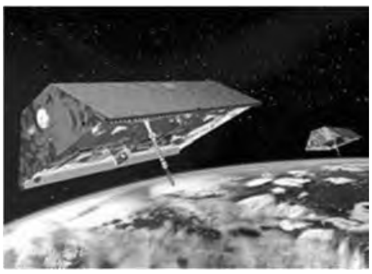

Damping factors

$$\left(\frac{R}{r}\right)^{n+1} = 0{,}934095 \quad \text{für } n=0$$

$$\left(\frac{R}{r}\right)^{n+1} = 0.815029 \quad \text{für } n=2$$ (10.000 km)

$$\left(\frac{R}{r}\right)^{n+1} = 0.000261 \quad \text{für } n=120$$ (160 km)

$$\left(\frac{R}{r}\right)^{n+1} = 0.000004 \quad \text{für } n=180$$ (110 km)

54

Degree variances

Satellite height (450 km):

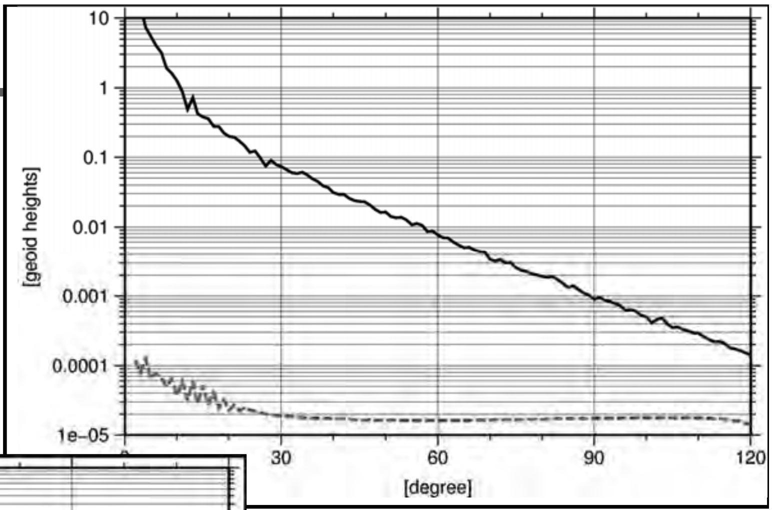

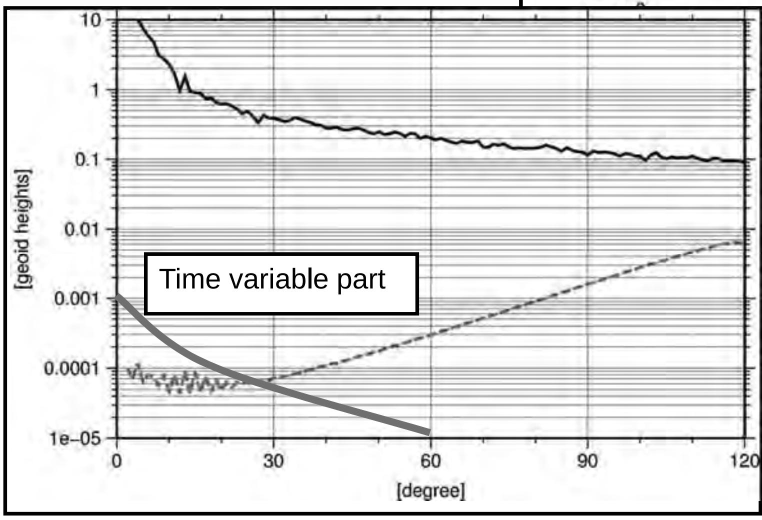

: Earth surface (0 km)

DFG SPP 1257

Lecture: Satellite Altimetry
a 1.5 hour crash course

Wolfgang Bosch

Summer School „Global Water Cycle“
12.-16. September 2011
Mayschoss

DFG SPP 1257

1

What you shall learn:

Altimetry:	**how does it work?**
Missions:	**which, when, what properties ?**
Resources:	**Where to get what data (& doc's) ?**
Data:	**organisation, content, format**
Tools:	**read, extract, decode data**
Sampling:	**spatio-temporal resolution; aliasing**
Gridding:	**brute force and sophisticated → SSHs**
XO-Analysis:	**taking advantage of redundancy**
Time series:	**analysis and interpretation**
PCA:	**identify dominant SSH variability**
DOT:	**the geodetic way to surface circulation**

DFG SPP 1257

2

What you get

A memory stick with
- Slides of this (all) lessons
- Additional infos (glossary & abbreviations)
- Altimetry data (GDR-like and stacked)
- Portable version of Qtoctave (a Matlab clone with GUI)
- scripts for your exercises

3

Altimetry: how does it work?

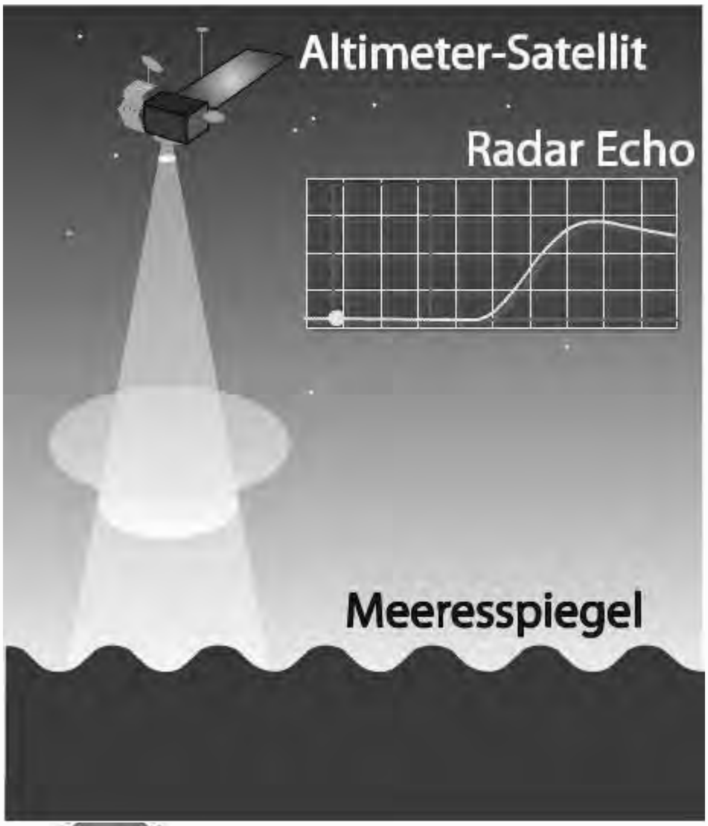

- **Most Altimeter Systems are realized by radar technology**
- **ICESat was carrying „GLAS“, a Geoscience Laser Altimeter**

4

Typical Characteristics (Radar):

Carrier frequency	13.5 GHz
Pulse duration	12.5 nsec
Pulse travel time	5 msec
Pulse repetition	1000Hz
Averaging	0,05 sec
Satellite height	800km
Radius of „footprint“	2-11 km
Ground velocity	6,7 km/sec

Altimetry: how does it work?

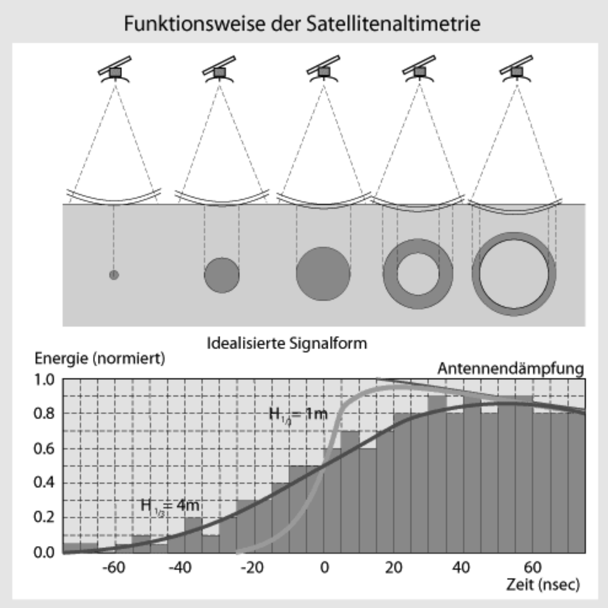

Return signal & Analysis

← Footprint development

← Idealized echo (ocean surface)

(waveforms)

round trip travel time (half power point) → height above sea level
slope of leading edge → significant wave height
energy balance → backscatter coefficient → wind speed

Missions: which, when, what properties ?

Mission (repeat cycle[days]/ground track separation at equator [km])

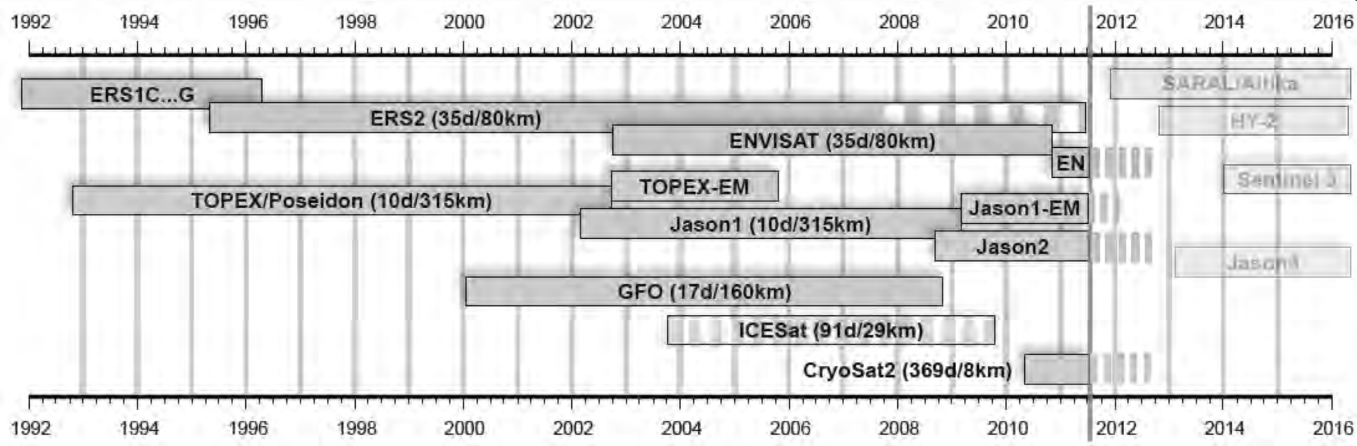

ERS1 was operated with different repeat cycles (3,35,169 days/?, 80, 16 km)

ERS2: tape recorder failed late 2007 ; since then data limited to direct downloads

Orbits of TOPEX-EM, Jason1-EM and EN were shifted to double/improve spatial resolution

ICESat: only episodic operations due to failure/problems of Laser

Topex/Poseidon

- Most sucessfull altimeter mission ever
- about 13 years operation
- 9,9516 repeat cycle
- Ground track distance 311km
- Precise orbits through Laser, DORIS and GPS
- First two frequency altimeter sensor
- Continuous calibration
- Latitude coverage ±66.0°

- Follow-on mission: Jason1

7

ENVISAT

- Operated by ESA
- Largest and most complex environmental satellite
- In operation since March 2002
- 35 day repeat cycle
- Ground track distance 80km
- Latitude range ± 81.5°
- Two frequency altimeter sensor
- Automatic tracking mode switching allows observation over lakes, rivers, ice, and land

8

CryoSat-2

Objectives
- **thickness of land ice and sea ice**
- **melting of the polar ice**
- **Sea level rise**

Launch Apr. 2010

Orbit
- **Inclination I = 92°**
- **Mean height 717 km**
- **Repeat cycle 369 days (30 d sub cycle)**
- **7.5 km track separation**

Measurement modes
- **Ku-band only, no radiometer**
- **LRM pulse limited**
- **Delay Doppler**
- **Interferometric SAR mode**

9

DFG SPP 1257

SARAL/Altika

- **Indian Space Research Organization (ISRO)**
  - ✓**CNES: Altimeter**
  - ✓**Alti-Ka**
  - ✓**Ka-band 0.84 cm (*viz 2.2 cm at Ku-band*)**
  - ✓**Bandwidth (480 MHz) => 0.31 ρ (*viz 0.47*)**
  - ✓**Otherwise "conventional" RA**
  - ✓**PRF ~ 4 kHz (*viz 2 kHz at Ku-band*)**
  - ✓**Full waveform mode**
- **P/L includes dual-frequency radiometer**
- **Sun-synchronous, 35-day repeat cycle**
- **Navigation and control: DEM and DORIS**
- **Launch late 2010**

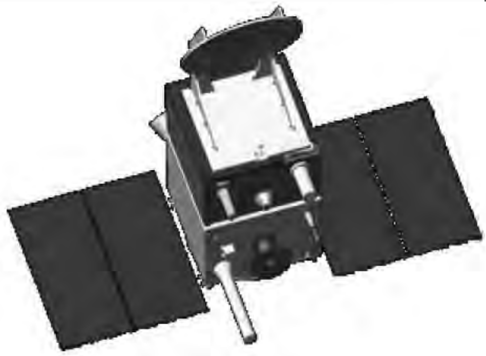

Coastal relevance?
- Smaller (along-track) footprint than Ku-band RAs
- Longer repeat orbit
- Better SSH precision
- Soon to be operational

10

DFG SPP 1257

HY-2A (China)

Coastal relevance?
- Non-repeat orbit
- Soon to be operational

Note: this figure, usually claimed to be HY-2A, most likely is for its predecessor, HY-1

- Chinese Academy of Sciences
- Ku- and C-band (conventional RAs)
- Payload also includes Scatterometer, 2-frequency radiometer, microwave imager
- Sun-synchronous orbit, 963 km, 99.3° inclination
- Repeat: 14 days (2 years) & 168 days (1 year) w/ 5-day sub-cycle
- Launch September 2010

11

DFG SPP 1257

Sentinel-3 (ESA)

- European mission
- 7-year design lifetime (12 year reserves)
- Sun-synchronous, 27-day repeat cycle, inclination 98.65°
- Ku/C Radar Altimeter (SRAL)
- SAR (DDA) & conventional RA modes
  - ✓ DEM, multi-mode tracker, full-waveform subsets
- Dual Frequency Radiometer
- Payload includes Ocean and Land Color Instrument (OLCI), Sea and Land Surface temperature (SLST)
- Launch ~ 2012

Coastal relevance?
- Longer-repeat orbit
- SAR (DDA) mode
- Full waveform mode
- Operational w/in a few years

12

DFG SPP 1257

Altimetry Missions – Main Characteristics

Mission	Geosat [1]	ERS-1	TOPEX/Poseidon [2]	ERS-2	GFO [3]	Jason-1 [4]	EnviSat [5]	ICESat	CryoSat
	Pulsewidth-limited altimeter systems							New technologies	
Operated by …	NOAA	ESA	CNES/NASA	ESA	US-NAVY	CNES/NASA	ESA	NASA	ESA
Launch (month/year)	03/85	07/91	09/92	04/95	02/98	01/02	03/02	01/03	05/05
Acquisition until (month/year)	09/89	03/96	degraded but ongoing	degraded but ongoing	ongoing	ongoing	ongoing	ongoing	-
Mean height (km)	785.5	785.0	1336.0	781.4	784.5	1336.0	799.8	600	717
Inclination (°)	108.0	98.5	66.0	98.54	108.04	66.0	98.54	94.	92.
Latitude coverage (°)	±72.0	±81.5	±66.0	±81.46	±72.0	±66.0	±81,45	±86.0	±88.0
Repeat cycle (days)	17.05 [1]	3/35/168	9.9156	35	17	9.9156	35	183	369
Track separation (km)	165 [1]	933/80/16	316	80	165	316	80	15	7.5
Frequencies (GHz) /wavelengths	13.5	13.5	5.3 + 13.6	13.5	13.5	5.3 + 13.575	3.2 + 13.575	Laser 1064+532nm	SIRAL [6] 13.8
Altimeter noise (cm)	7	5	2	3	3.5	1.5	2	10 (ice)	0.7 [7]
Radiometer/Frequencies	no	yes/2	yes/2	yes/3	yes/2	yes/3	yes/2	no	no

1) Geosat had two different mission phases, a 'geodetic mission' (GM) with a non-repeat, drifting orbit, and an 'exact repeat mission' (ERM) with the orbit characteristics given in the table
2) After the tandem configuration with Jason-1 (up to 08/2002) the TOPEX/Poseidon orbit was shifted by half the track separation to double the spatial resolution of both missions.
3) GFO continues to observe the same ground tracks as monitored by Geosat ERM (exact repeat mission)
4) Jason-1 continues to observe the same ground tracks as monitored by TOPEX/Poseidon until 08/2002
5) EnviSat continues to observes the same ground tracks as ERS-2
6) SIRAL = Synthetic Aperture Interferometric Radar Altimeter
7) A□

Missions: which, when, what properties ?

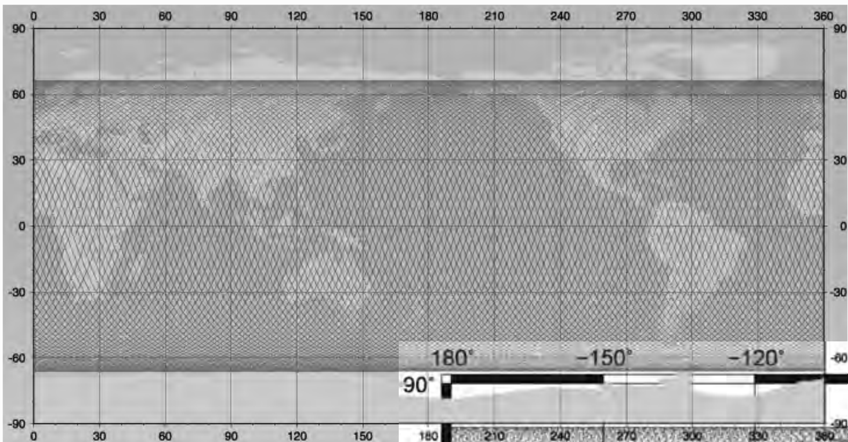

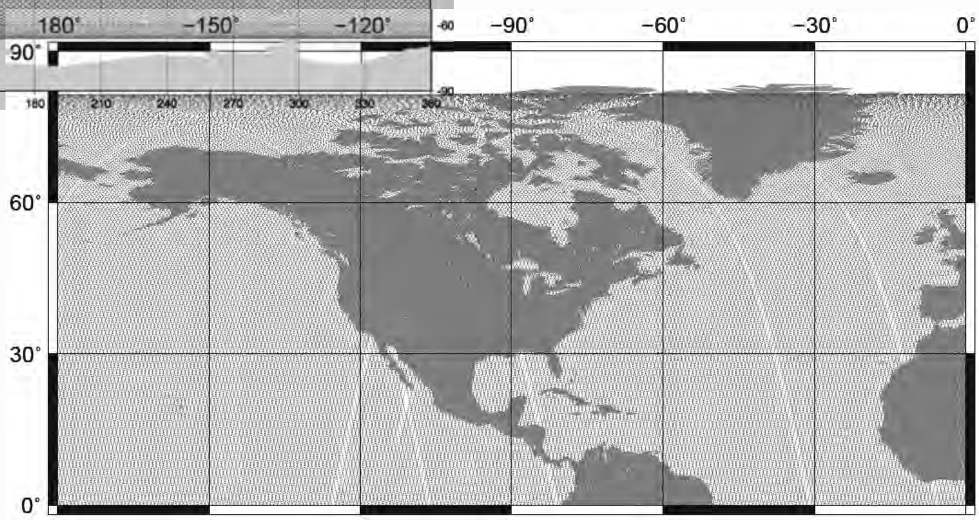

Ground track pattern of TOPEX (10 day repeat, 311km spacing), ENVISAT (35 day repeat, 80 km spacing)

Polar Ground Track Pattern

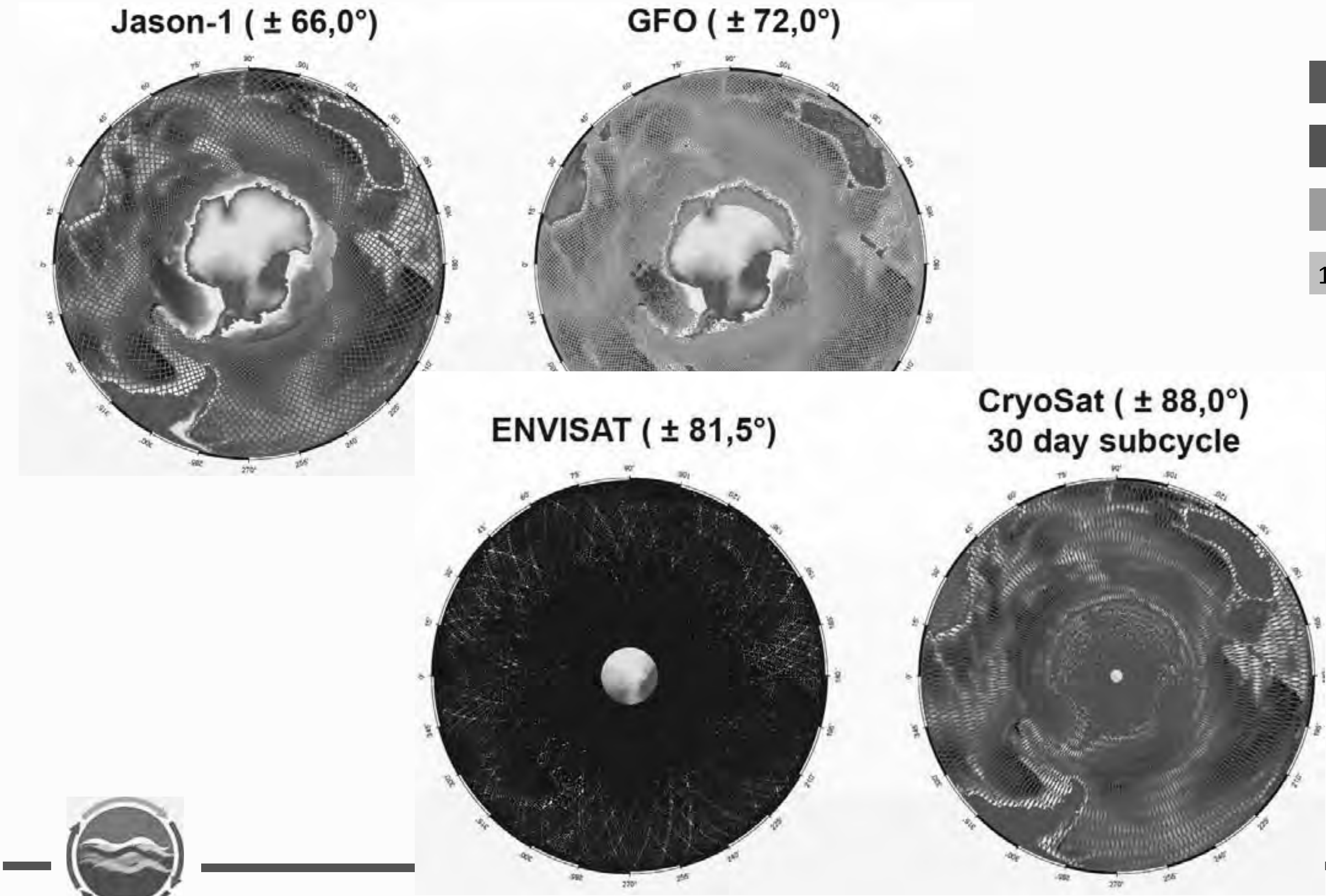

15

Orbit configuration - Rationale

- The energy limits of the radar system require satellite heights between 500 and 1500 km
- High orbits are less affected by air drag (TOPEX/Poseidon and Jason1 are at 1336km height others at ~800km heights)
- Small excentricities shall provide everywhere same precision
- Inclination determines the latitudal coverage

- Repeatibility is choosen to get reliable time series over the same ground track
- Short repeatibility and high spatial resolution exclude each other (due to orbit dynamics)

16

Where to get what data?

Mission	Cycle [days]	Provider	Access	Medium	Volume [GByte]
Geosat	GM & ERM(17)	NOAA	Free	CD-ROM	~ 6.5
ERS-1	3,35,168	ESA	Accepted proposal [1)]	DVD, ftp	~ 30.0
TOPEX/Poseidon	9,9516	CNES/JPL	Free	CD-ROM DVD, ftp	~ 80.0
ERS-2	35	ESA	Accepted proposal [1)]	DVD, ftp	~ 55.0
GFO	17	NOAA	Free	DVD, ftp	~ 35.0
Jason1	9,9516	CNES/JPL	Free	DVD, ftp	~ 20.0
ENVISAT	35	ESA	Accepted proposal [1)]	DVD, ftp	~ 1200

1) Free access for scientific purpose if there is a project proposal accepted by ESA, see http://eopi.esa.int/esa/esa/

Documents for altimeter mission data

T/P: [AVISO User Handbook - Merged TOPEX/Poseidon Products (GDR-M) (*http://www-aviso.cnes.fr/HTML/information/publication/hdbk/gdrm/hdbk_gdrm.pdf*)], AVI-NT-02-101-CN, Ed. 3.0, July 1996 (pdf, ?MB)

T/P: [NASA TOPEX/Poseidon User Handbook (*ftp://podaac.jpl.nasa.gov/pub/sea_surface_height/topex_poseidon/mgdrb/doc/uhmgdrb/html/usr_toc.htm*)] July 1997 (Robert Benada) (html)

Jason-1: [AVISO and PODAAC User Handbook - IGDR and GDR Jason-1 Products (*http://www.aviso.oceanobs.com/documents/donnees/produits/handbook_jason.pdf*)], SMM-MU-M5-OP-13184-CN, Ed. 2.0, April 2003 (pdf,3.53MB)

ERS1/2: [Altimeter & Microwave Radiometer ERS Products - User Manual (*ftp://ftp.ifremer.fr/pub/ifremer/cersat/manuels/muta01.pdf*)], C2-MUT-A-01-IF, Ed. 2.3, July 2001 (pdf, 2.99 MB)

ERS1-Version5: [Altimeter & Microwave Radiometer ERS Products - User Manual (*ftp://ftp.ifremer.fr/pub/ifremer/cersat/manuels/muta0112.ps*)], C2-MUT-a-01-IF, Ed. 1.2, July 1995 (PS, 9.14 MB)

ENVISAT: [ENVISAT RA2/MWR Product Handbook (*http://envisat.esa.int/pub/ESA_DOC/ENVISAT/RA2/ra2.ProductHandbook.1_2e.pdf.zip*)], Ed. 1.2, September 2004 (zipped pdf) see also [html-Version (*http://envisat.esa.int/dataproducts/ra2/CNTR.htm*)]

GFO: [GFO GDR User Handbook (*http://ibis.grdl.noaa.gov/SAT/gfo/gdr_hbk.htm*)], June 2002

Providers of value-added altimeter data (non-exclusive list!)

AVISO Archiving, Validation and Interpretation of Satellite Oceanographic data http://www.aviso.oceanobs.com

Provides access to

- **GDR and IGDR mission data of Topex/Poseidon, Jason-1 (on behalf of CNES; binary format)**
- **CorSSH and SLA for most of the repeat missions (User handbook: DT CorSSH and DT SLA Product Handbook, CLS-DOS-NT-05.097) in a) gridded form or b) along-track in i) near real time or ii) delay time mode in netcdf-format**
- **Special products like Mean sea surface models (MSS) of (absolute) dynamic ocean topography (ADT or DOT)**
- **Wind & wave data (wind speed and significant wave height)**
- **Auxilary data**

Access free but subscription required

Providers of value-added altimeter data (non-exclusive list!)

CTOH (Centre of Topography of the Oceans and the Hydrosphere http://ctoh.legos.obs-mip.fr **)**

Provides (for scientific users):

- **alongtrack GDR data with up-to-date corrections (for Topex/Poseidon, Jason-1, Jason-2, GFO, ENVISAT).**
- **coastal alongtrack GDR data with specific Xtrack processing**
- **global surface currents (Geostrophic and Ekman) from 1999-2008**

Close cooperation with

- **Hydroweb (for lake and river levels) and**
- **OSCAR (for ice products)**

Providers of value-added altimeter data (non-exclusive list!)

PO.DACC Physical Oceanography DAAC
(http://podaac.jpl.nasa.gov/ JPL)

- **TOPEX/Poseidon and Jason-1 mission data: GDR, IGDR, OGDR (binary coded; on behalf of NASA)**
- **TOPEX and Jason-1 Sea Surface Height Anomalies (ASCII header followed by binary data records)**
- **TOPEX and Jason-1 along-track gridded sea surface heights (ASCII header with binary coded data)**
- **Historical data sets from GEOS-3 and Geosat**

Providers of value-added altimeter data (non-exclusive list!)

RADS Radar Altimeter Data Base System
http://rads.tudelft.nl/rads/rads.shtml

- **An altimeter data base establishing harmonized, validated and cross-calibrated sea level data, developed and maintained by DEOS (Earth Oriented Space Research of the Delft Technical University)**
- **For GEOSAT, ERS-1, TOPEX, Poseidon, ERS-2, GFO, Jason-1 ENVISAT, Jason-2**
- **Most recent orbits, geophysical corrections and models are applied**
- **User can extract data with user defined options.**

Providers of value-added altimeter data (non-exclusive list!)

ESA/CNES Basic Radar Altimeter Toolbox (BRAT)
http://earth.eo.esa.int/brat/html/data/toolbox_en.htm

23

Software Toolbox (v2.1.1, June 25, 2010)

- **read all altimetry mission data for ERS-1/2, Topex/Poseidon, GFO, Jason-1, Envisat, Jason-2 and Cryosat, (from SGDR to gridded merged data)**
- **do some processing and computations**
- **visualise the results**

Includes

- **A tutorial on altimetry and a mission overview**
- **Description of applications**

Providers of value-added altimeter data (non-exclusive list!)

DGFI OpenADB Open Altimeter Data Base
(http://openadb.dgfi.badw.de , experimental)

24

Similar intention like RADS (DEOS):

- **altimeter data base with easy update capability for individual record parameter.**
- **Data extracts with number and sequence of record parameters defined by users.**

Two data structures:

- **MVA for along track data, and**
- **BINS for time series analysis (similar to NASA's along-track gridded products)**

Data: organisation, content, format

- „Level2" or „Geophysical Data Records" (GDR)
  Includes: precise orbit, range measurement, instrument status and health and all environmental and geophysical corrections

- Altimeter mission data is sequentially ordered and structured according to the following hierarchy:
  Mission -- 1:n -- cycles -- 1:n -- passes

- Passes: duration during which the subsatellite track moves with either
  - increasing latitude "ascending pass„ or
  - decreasing latitude "descending pass„

- Why this partitioning?
  - best suited for follow-on analysis of the data (repeat-pass and crossover)

Data: organisation, content, format

- There is NO standard format ! Every mission has it's own format

The only (initial) convention is:

- Altimeter mission data is binary coded with parameter values stored as scaled integers, 4, 2, or 1 Byte in length
  e.g. latitude 126.2346° is resolved with 10^{-6} degree; Thus scaled latitude is 126234600 and then stored as 4 Byte integer

Advantage:

- Compact storage
- Protection against accidental editing

Disadvantage:

- Can be read only by decoding software

Data: organisation, content, format
(Tools to read binary coded data)

- **Mission specific interface programs (usually in C and Fortran) provided by mission data providers – to be adapted by user requirements**

- **Binread: a generic C-program to decode and extract binary coded data. Requires a ‚record map‘, describing sequence and coding of record parameters**

- **Matlab/octave functions : readrecmap.m & bin2dat.m to decode and load binary coded data. Requires a ‚record map‘, describing sequence and coding of record parameters**

- **How does a ‚record map‘ look like ?**

Data: organisation, content, format
(What is a record map ?)

- **Record map: ASCII-file defining sequence and coding of record parameters of binary coded data**
- **Geosat.rmp**

```
000  34   78      geosat.rmp    <>
001  +4   s        0            2147483647  isec     UTC seconds since epoch (1.1.1985)
002  +4   -6.s     0            1000000     msec     UTC microseconds for parameter 1
003   4   -6.deg  -72100000     72100000    glat     geodetic latitude (GRS80)
004  +4   -6.deg   0            360000000   glon     longitude
005  +4   -3.m     700000000    900000000   hsat     orbit (above GRS80 ellipsodi)
006   2   -2.m    -32766        32766       ssh      Sea surface height (above GRS80
ellipsoid)
007  +2   -2.m     0            32766       stdh     sigma ssh
008   2   -2.m    -15000        15000       geoid    geoid height (above GRS80 ellipsoid)
009   2   -2.m    -32766        32766       dsh1     H(1)
010   2   -2.m    -32766        32766       dsh2     H(2)
011   2   -2.m    -32766        32766       dsh3     H(3)
012   2   -2.m    -32766        32766       dsh4     H(4)
013   2   -2.m    -32766        32766       dsh5     H(5)
014   2   -2.m    -32766        32766       dsh6     H(6)
015   2   -2.m    -32766        32766       dsh7     H(7)
016   2   -2.m    -32766        32766       dsh8     H(8)
017   2   -2.m    -32766        32766       dsh9     H(9)
018   2   -2.m    -32766        32766       dsh10    H(10)
019   2   -2.m     0            2000        swh      Significant Wave Height
020  +2   -2.m     0            2000        stdswh   sigma SWH
021  +2   -2.db    0            6400        sigm0    sigma NAUGHT
022   2   -2.db    0            6400        agc      Automatic Gain Control
023  +2   -2.db    0            6400        stdagc   sigma AGC
024  +2   -        0            32766       iflag    FLAGS
025   2   m        0            50000       hoff     H and H(i) offset
026   2   -3.m    -1000         1000        etide    solid Earth tide Cartwright/Taylor)
027   2   -3.m    -10000        10000       otide    ocean tide (Schwiderski 1980)
028   2   -3.m    -1000         0           tropw    wet troposphere (FNOC)
029   2   -3.m    -1000         0           trop2    wet troposphere (SMMR)
030   2   -3.m    -3000         -2000       tropd    dry troposphere (FNOC)
031   2   -3.m    -500          0           iono     ionosphere (GPS)
032   2   -3.m    -1000         0           trop3    WET (TOVS/SSMI)
033   2   -3.m    -3000         -2000       trope    DRY (ECMWF)
034   2   -2.deg   0            200         satt     satellite attitude
```

Data: organisation, content, format

Format more and more applied in altimetry: netcdf

- **Self-explained freely available machine-independent format for binary storage of multi-dimensional data**
- **Developed by Unidata**
- **See http://www.unidata.ucar.edu/software/netcdf**
- **libraries for C/C++ and Fortran with interfaces to MATLAB, Objective-C, Perl, Python, R, Ruby, Tcl/Tk**

- **Basic programs:** ncgen, ncdump, and nccopy
- **Matlab Interface:** netcdf.m
- **Java Browser:** ncbrowse

Binary coded data of Jason1
prepared for an exercise to estimate ocean topography

Record map:

000	9	34	ssgh.rmp	
001	+4	-6.deg	glon.00	longitude of satellite footprint
002	4	-6.deg	glat.00	geodetic latitude of satellite footprint
003	4	-5.d	jday.00	julian day epoch 2000.0
004	4	-3.m	ssh.03	sea surface heights (unfiltered)
005	4	-3.m	geoh.15	geoid heights ITG-Grace03s (satellite-only, unfiltered)
006	4	-3.m	geoh.00	geoid heights EGM2008 (high resolution, unfiltered)
007	4	-3.m	sshs.08	smoothed sea surface (Gauss filter length D = 97 km)
008	4	-3.m	geohs.08	smoothed geoid heights (GOCO02S; Gauss filter length D = 97 km)
009	2	-3.m	dot.18	dynamic ocean topography (DOT); DGFI-version

…/data/altimetry/jason1

L 101
  L 101_001ssgh.00
  L …
  L 101_254ssgh.00
L 102

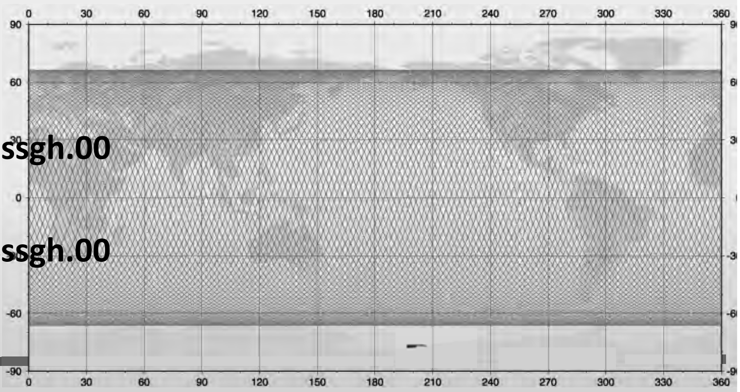

Sample code to decode binary data by means of matlab/octave functions readrecmap.m and bin2dat.m

```
pfad = ‘D: ??? \data\altimetry\jason1';    %% path to jason1 (to be adapted)
cycle = '101'                              %% one particular cycle
recmap = 'ssgh.rmp'                        %% record-map file binary coded data
format short

recmapfile = fullfile (pfad,recmap)         %% path to recordmap file
[byte,exps] = readrecmap (recmapfile)      %% read and get record structure

binfile = fullfile (pfad,cycle,'101_127ssgh.00') %% path to a particular binfile
[data,nrec] = bin2dat (binfile,byte,exps); %% decode all records of binfile

lonlatssh = [data(:,1), data(:,2), data(:,4)]; %% select lon, lat, & ssh param.

format long g
lonlatssh(1:5,:)                           %% output first 5 records
lonlatssh(nrec-4:nrec,:)                   %% output last 5 records
```


Sample output: decoding binary data by means of readrecmap.m and bin2dat.m

```
>>>recmapfile = C:\Users\bosch\DATEN\data\jason1\ssgh.rmp
byte =
        4  4  4  4  4  4  4  4  2
exps =
        -6  -6  -5  -3  -3  -3  -3  -3  -3
binfile = C:\Users\bosch\DATEN\data\jason1\101\101_127ssgh.00
ans =
        76.993642       -56.703619      28.708
        77.06203        -56.666922      28.747
        77.130277       -56.630182      27.248
        77.198383       -56.593399      28.363
        77.266349       -56.556575      27.591
ans =
        157.558032      59.643155       14.887
        157.639667      59.675656       14.876
        157.721467      59.7081         14.801
        157.967869      59.805092       14.635
        158.050337      59.837309       14.55
```

From data to sea surface heights

Necessary Information:

- **Satellite position by precise orbit determination xyz→ ellipsoidal coordinates**
- **altimeter range** corrected for instrumental-, media-, and target-corrections
- **SSH = hsat – range**

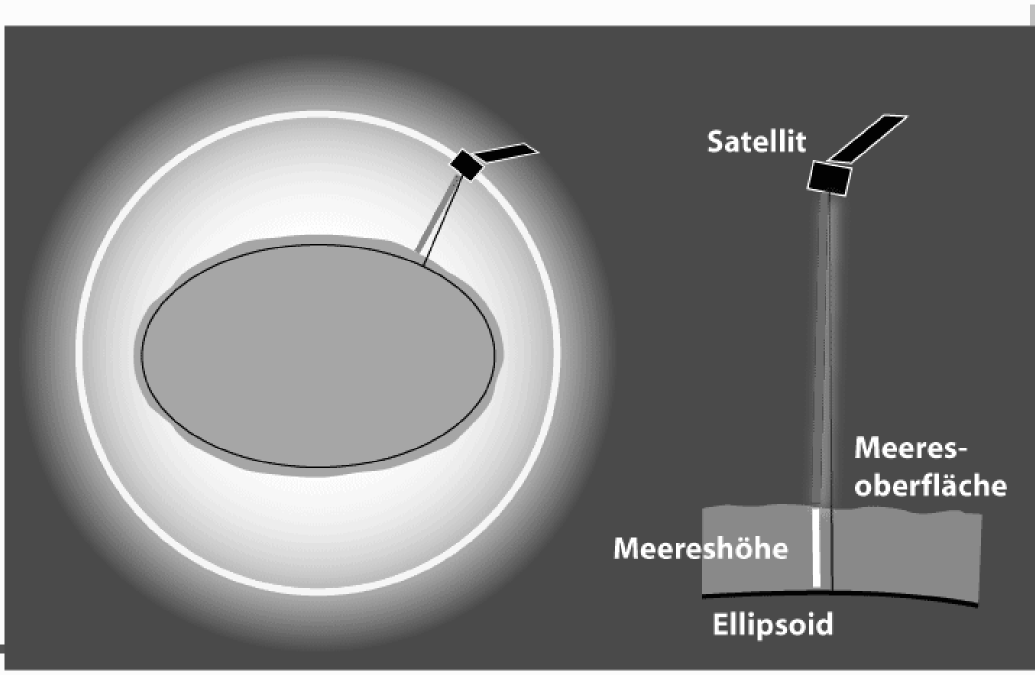

Necessary (critical) corrections [order of magnitude]

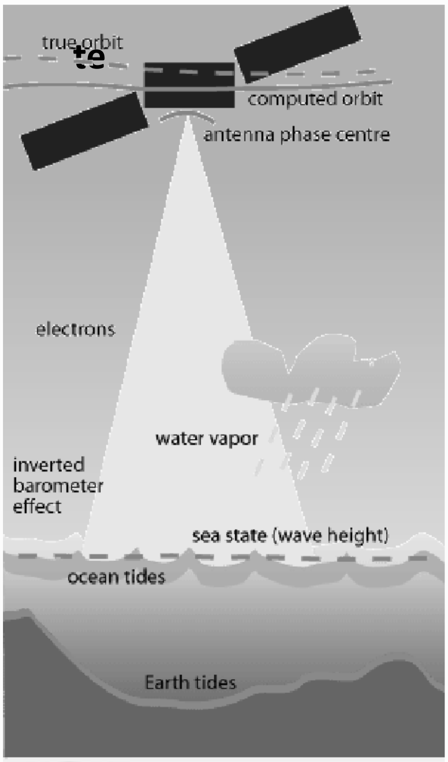

orbit error (radial component) [< 1 dm]

instrumental effects
- **electronic time delay**
- **clock (oscillator) drift**
- **offset antenna phase centre**
- **centre of gravity**
- **time tagging of observations**
- **doppler shift error**

atmospheric refraction (signal delay) due to
- **Ionosphere [~3-5cm]**
- **troposphere, dry component [~2.3m !!]**
- **troposphere, wet component [~3-45cm]**

target (ocean surface)
- **ocean tides [up to few m] , loading effects[~10%]**
- **Earth tides [~3dm], pole tide [~1cm]**
- **electromagnetic bias (sea state) [~5% of SWH]**
- **inverted barometer effect [up to 3 dm]**

Wet troposphere correction – why is it critical?

Facts:

- **Most modern altimeter systems carry an on board radiometers.**
- **Radiometer observe brightness temperature (BT) at different channels**
- **The total water vapor content can be estimated by an empirical linear combination of BTs of different channels**

35

Problems:

- **The radiometer beamwidth causes a footprint radius of about 50 km**
- **The emissivity of ocean and land surfaces are very different**
- **BT observations become unreliable as soon as the satellite aproaches the coast**

Strategy:

- **Take water vapor content from Met.-Services (ECMWF, NCEP, …)**
- **Account for mixed land/ocean footprint (S.Brown algorithm)**
- **Estimate water vapor content from GPS observations**

MSL: Global map of time averaged sea surface heights

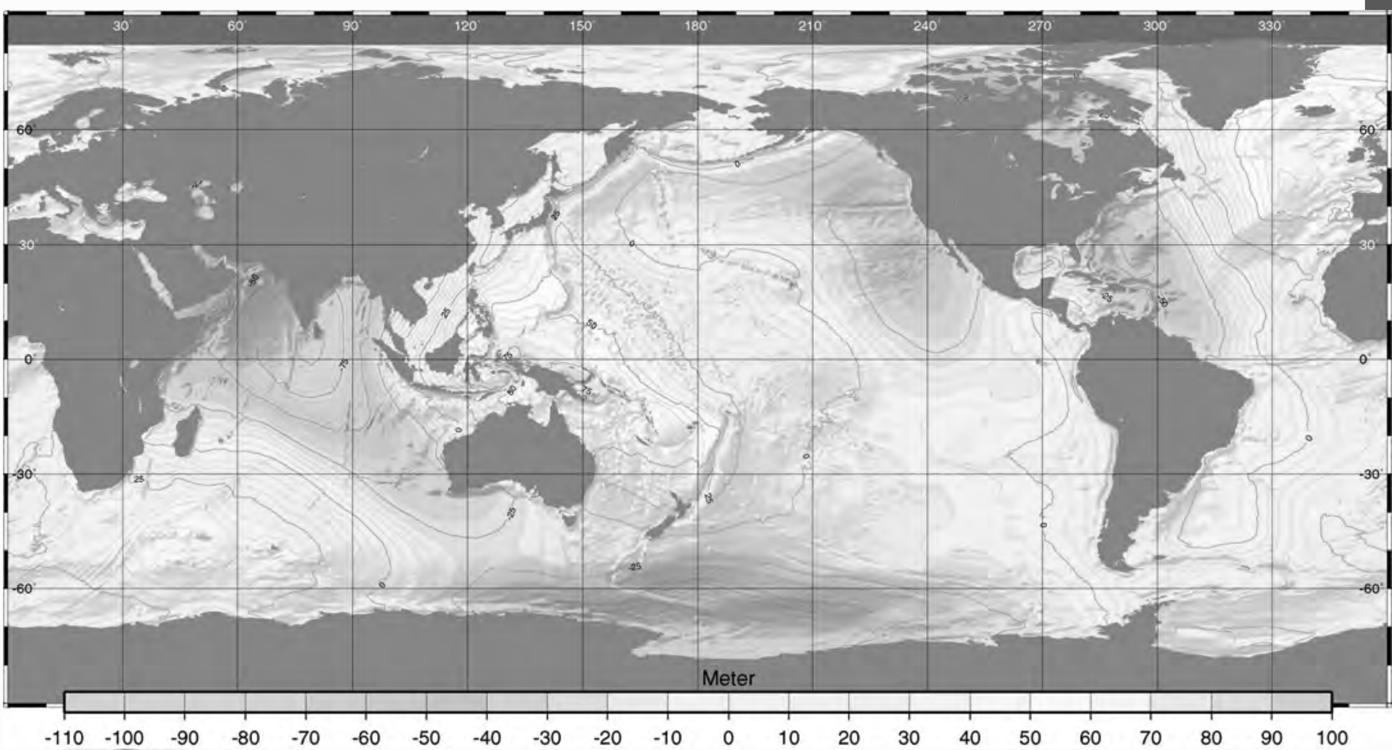

6

Focus of MSL to the West Pacific

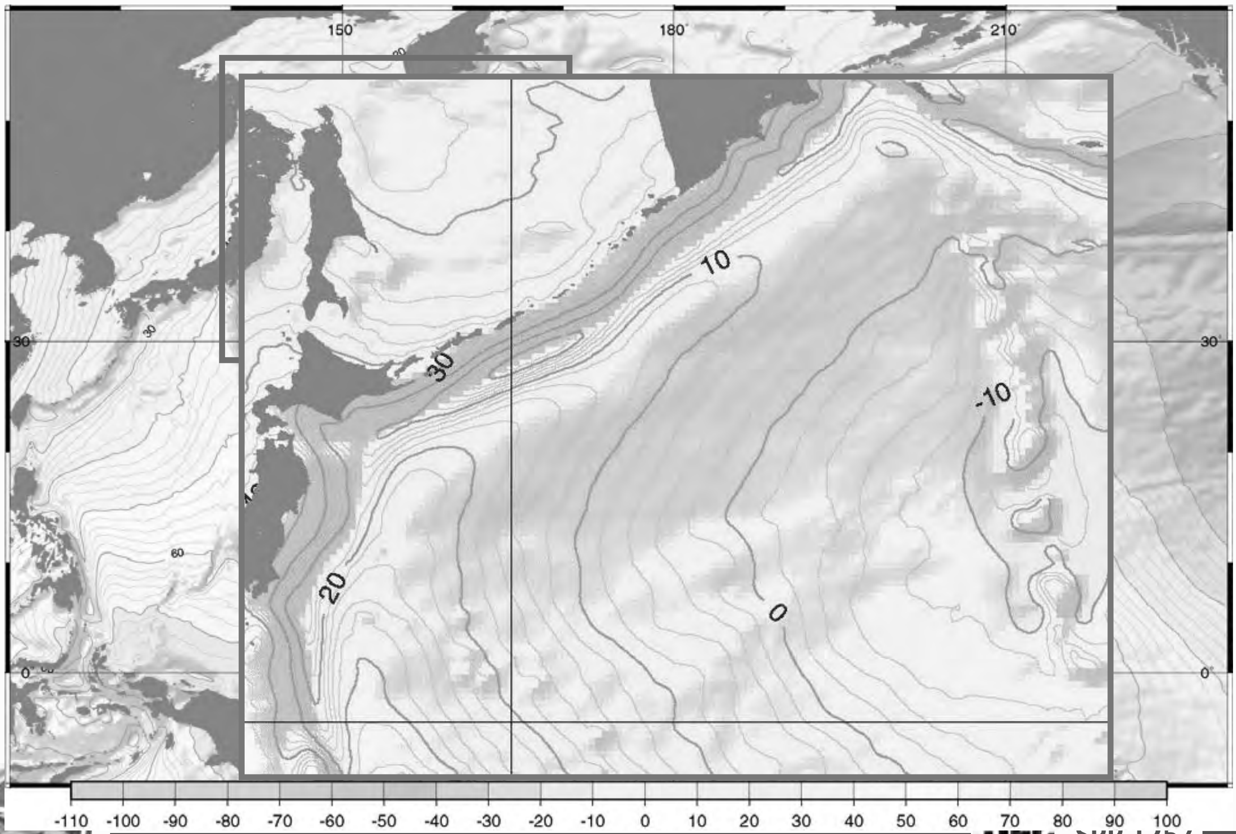

Mean Sea level is (to first order) in balance with gravity

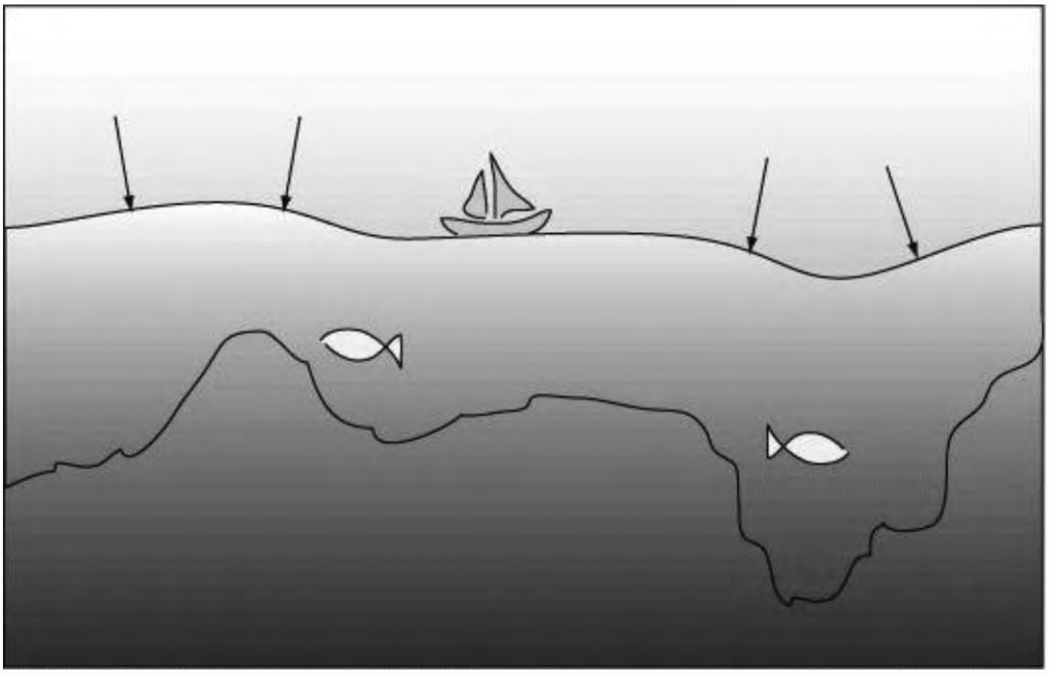

Least Squares Harmonic Analysis

39

- **Estimating periodic oscillations of sea surface heights or sea level anomalies**

$$h_q(\Delta t_k) + v_{qk} = c_q + d_q \cdot \Delta t_k + \sum_{p=1}^{2} A_{pq} \cdot \cos(\omega_p \cdot \Delta t_k - \Phi_{pq})$$

$$\omega_p = \frac{2\pi}{T_p} \qquad T_1 = 365.25,\ T_2 = 182{,}625$$

where

Δt_k	**times of observation, relative to a reference epoch**
h_{qk}	**observed sea surface height at point q and time t_k**
v_{qk}	**sea surface height residual**
c_q	**mean value of ssh at point q (solve-for parameter)**
d_q	**drift term at q (solve-for parameter)**
A_{pq}	**Amplituds of the p-th period at point q (solve-for parameter)**
Φ_{pq}	**Phases of the p-th period at point q (solve-for parameter)**
ω_p	**angular velocity for the p-th period $\omega_p = 2\pi/T_k$, e.g. T_1=365 days**

DFG SPP 1257

Time series of Topex SLA
for period 01/1993 – 07/2002 (Cycle 011 – 365)

40

…/data/altimetry/topex

L	**011sla.xyz**
L	**012sla.xyz**
L	**…**
L	**364sla.xyz**
L	**365sla.xyz**

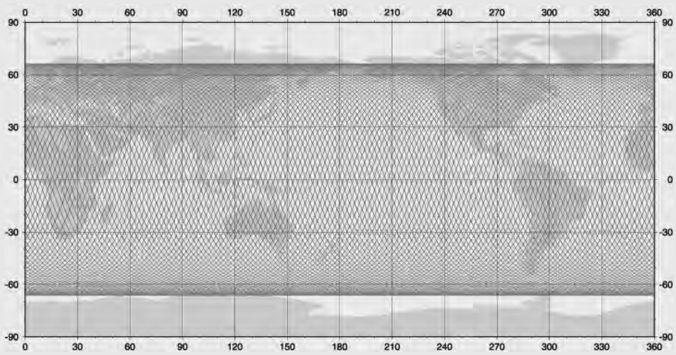

The files *nnn*.sla.xyz give sea level anomalies SLA

SLA = instantaneous sea level w.r.t a long term mean sea level MSL [in this case CLS01])

for a sequence of 10-day TOPEX cycles *nnn* = 011..365 (period 01/1993 – 07/2002)

The SLA were gridded from TOPEX ground tracks to a grid (which was adapted to the output of an ocean model and) whose grid nodes are defined bylon = linspace (1.75, 359.875, 192); lat = linspace (-65.625, 65.625, 71); Grid nodes over land are not listed. Every file contains exactly the same sequence and number grid nodes.

DFG SPP 1257

Code snippet for harmonic analysis of gridded SLA data

41

```
pfad = 'C:\Users\bosch\DATEN\data\topex' ; %% pfad is to be adapted to stick
pattern = '.sla.xyz';
ftfile = 'fileliste';                        %% list of sla files with their epochs

df = dir( fullfile (pfad,['*' pattern '*']) ); %% get a handle to all sla files
nf = length(df);                               %% the number of sla files
R = [];
for i =1:nf
   slafile = fullfile (pfad, df(i).name)       %% a single sla file
   sla = load (slafile);
   R = [R sla(:,3)];                        %% concatenate sla to an (n x q) matrix R
end
[n q]= size(R)

data = dlmread (fullfile (pfad, ftfile)) %% get file list with associated epochs
dtimes = data(:,2)
cs = [ones(q,1) dtimes]; %% initialize Jacobi matrix for mean and drift
for k=1:1
    w = 2*pi/365.25;
    cs = [cs, cos(w*dtimes), sin(w*dtimes)];   %% Jacobi matrix
end
X = ((cs'*cs) \ (cs'*R'))' %% least squares estimate of mean, drift, cos, and
sin-term
```


Annual sea level variability

42

Annual signal explains about 22% of observed sea level anomalies

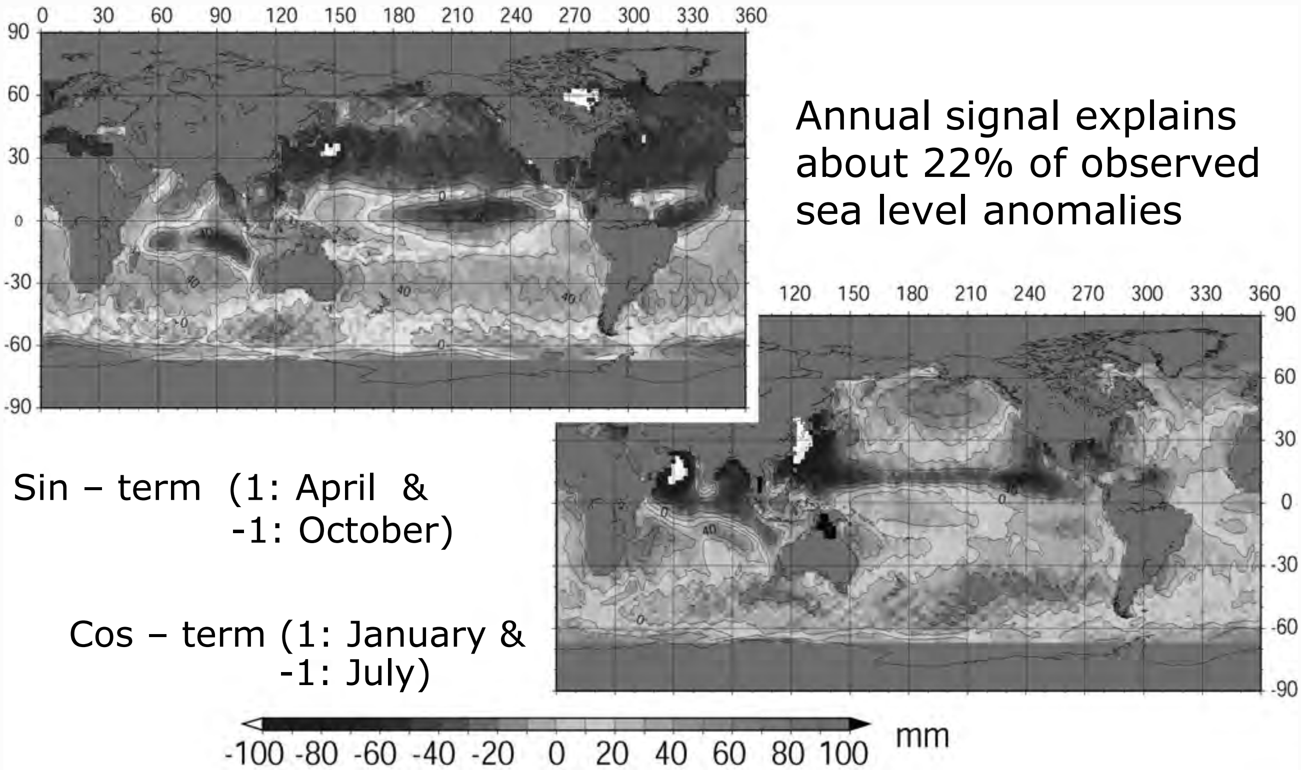

Sin – term (1: April & -1: October)

Cos – term (1: January & -1: July)

Secular sea level change for the decade 08/1992 – 08/2002

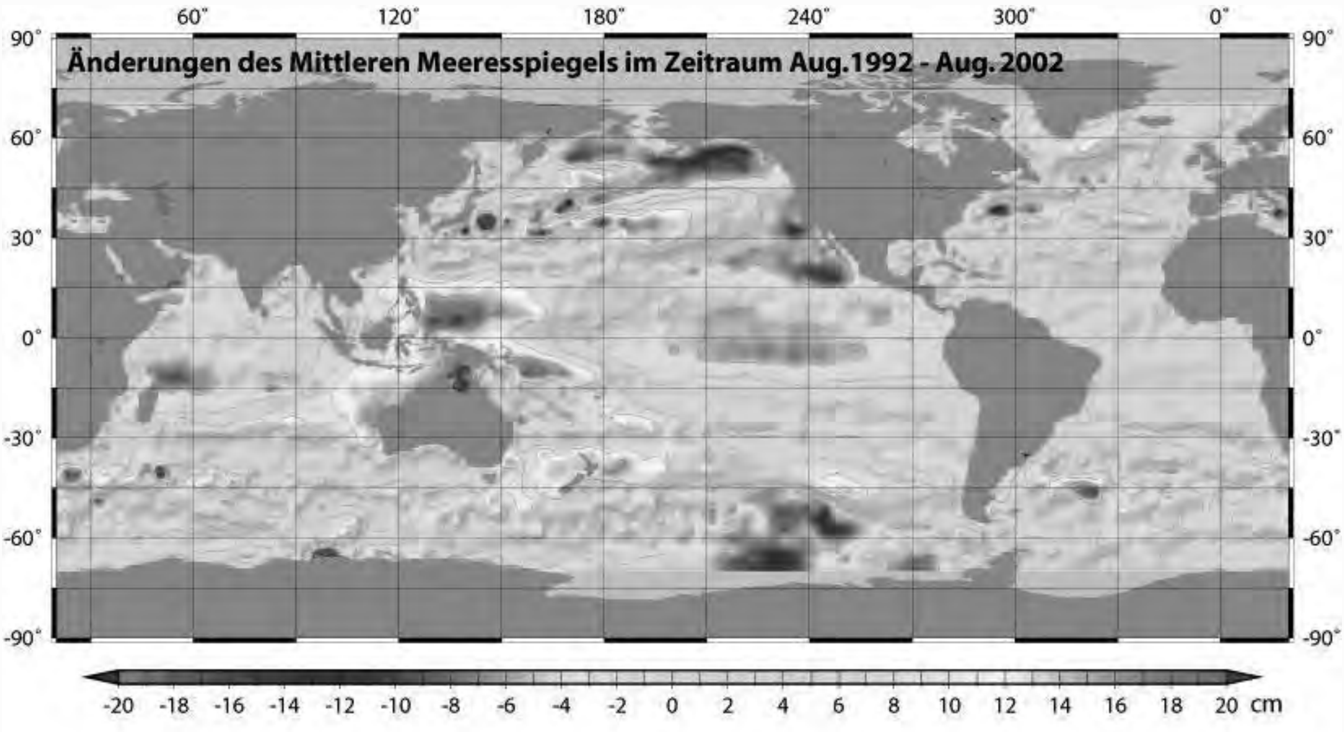

43

DFG SPP 1257

The sampling problem

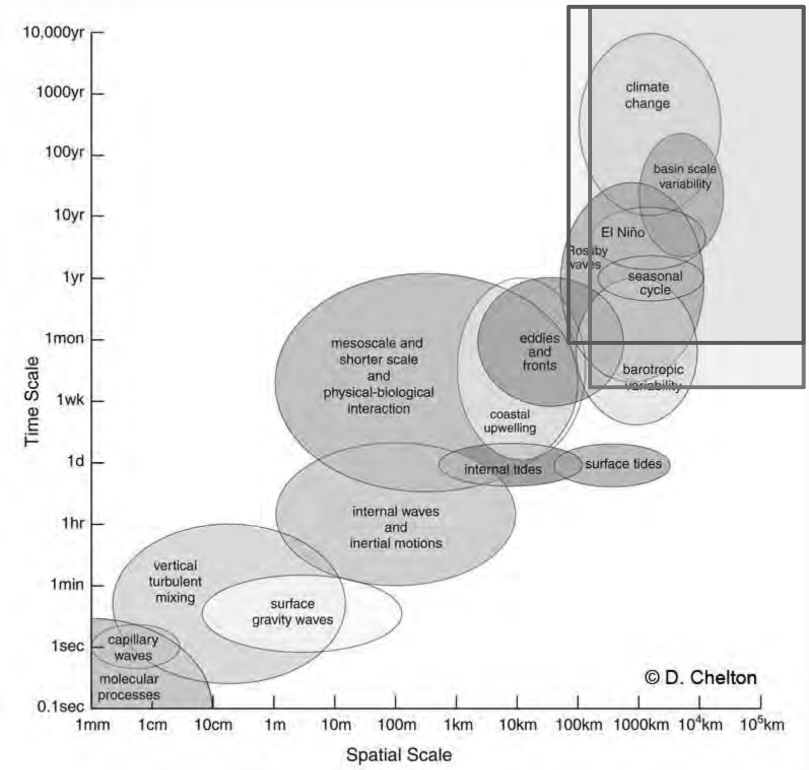

Space and time scales of ocean processes (© D. Chelton)

Visible by single altimeter satellites:

Envisat

Topex/Poseidon

44

DFG SPP 1257

The alias problem

Whenever high-frequency signals are sampled with rather long period, then the high frequency signal appears with a period which is even much longer than the sampling period.

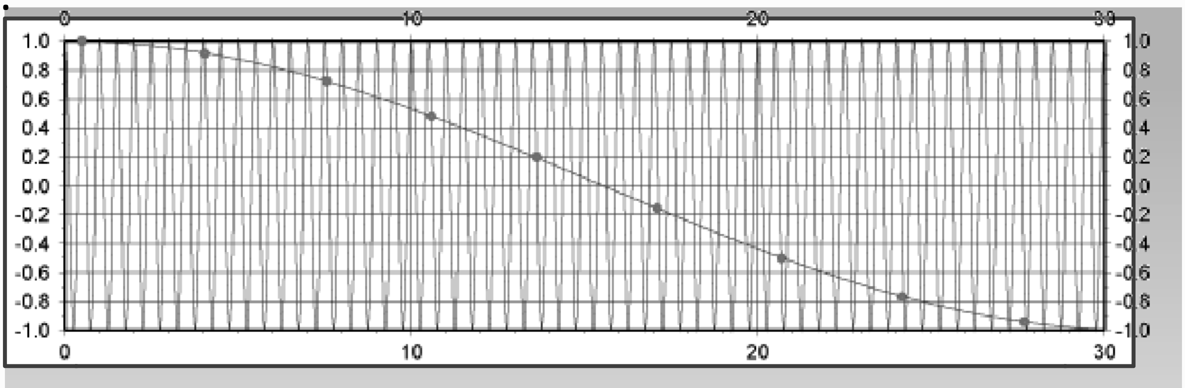

E.g.: **M2 tide is a semi-diurnal sea level change**
if sampled by Topex (every 9.9156 days) it maps into a 62.1 day alias period

45

DFG SPP 1257

Alias and rayleigh periods [days] for Topex/poseidon

	M_2	S_2	N_2	K_2	K_1	O_1	P_1	Q_1	S_{sa}	S_a
M_2	62	1084	245	220	97	173	206	594	94	75
S_2		59	316	183	89	206	173	384	87	70
N_2			50	116	69	594	112	173	68	57
K_2				87	173	97	3355	349	165	114
K_1					173	62	183	116	3355	329
O_1						46	94	134	61	52
P_1							89	316	173	118
Q_1								69	112	86
S_{sa}									183	365
S_a										365

46

DFG SPP 1257

Alias and rayleigh periods [days] for ERS-2/ENVISAT

47

	M_2	S_2	N_2	K_2	K_1	O_1	P_1	Q_1	S_{sa}	S_a
M_2	95	95	3169	196	128	365	128	328	196	128
S_2		∞	97	183	365	75	365	130	183	365
N_2			97	209	133	328	133	365	209	133
K_2				183	365	127	365	487	∞	365
K_1					365	95	∞	209	365	∞
O_1						75	95	173	128	95
P_1							365	209	365	∞
Q_1								133	487	209
S_{sa}									183	365
S_a										365

Space-time sampling by multi-mission altimetry

48

- **Topex/Jason1 & Topex-EM**
  10 day repeat;
  ~2.8° (1.4°) eq. track distance
- **GFO**
  17 day repeat;
  ~1.6° eq. track distance
- **ERS1/2 & Envisat**
  35 day repeat;
  ~0.8° eq. track distance
- **ERS-1 & Geosat geodetic phases**
  (not shown)

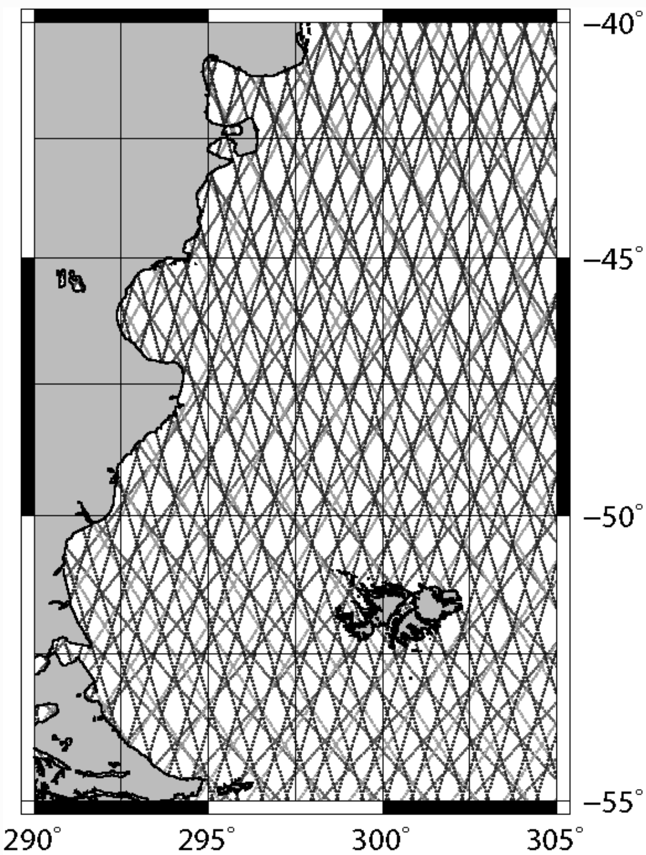

Multi-mission altimetry: Eddy tracking (compared to ARGO floats)

49

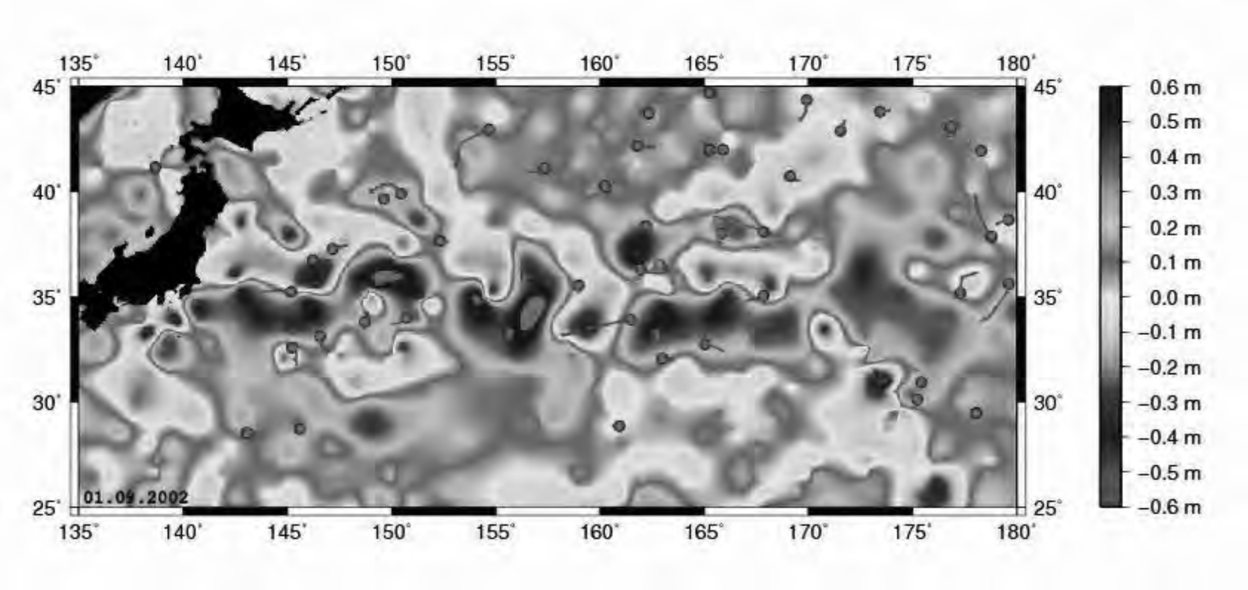

Identifying aperiodic sea level variation

50

Principal Component Analysis (PCA)
or
Empirical Orthogonal Functions (EOF) Analysis

What is it for?

- **For a given multi-variate random time series PCA identifies those spatial pattern (eigenvectors, EOF's) and their temporal evolution (principal components, PC) that explain – in decreasing order – the most dominant contributions to the signal variance.**

"Mode": A single eigenvector (EOF) and the associated PC's

- **The first mode explains the most dominant part of the signal**
- **The second mode explains the second largest signal contribution**
- **Allows to control the degree of approximation**
- **PCA is the most economic representation of a multivariate time series**

Sea level anomalies as multi-variate time series

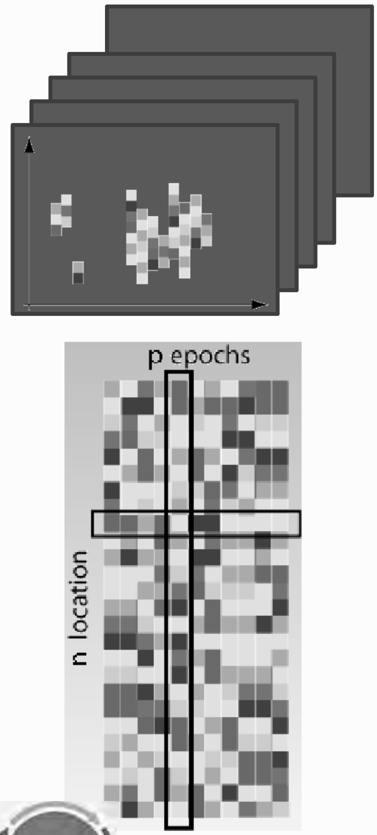

Observed:

Sea level anomalies at *n* locations for q epochs

Asumption:

Data is centered: temporal mean subtracted 51

Re-arranged:

Residual matrix Y with size (nxq)

Eigenvalue analysis of the (nxn) signal covariance C = Y·Y'

C is a positive-semidefinit quadratic form, , such that $\lambda_j \geq 0$

Code snippet for PCA of gridded SLA data

```
pfad = 'D:\data\altimetry\topex' ;       %% path is to be adapted to stick
pattern = '.sla.xyz';
ftfile = 'fileliste';                    %% list of sla files with their epochs

%%      >>> Insert code from previous code snippets <<<

[n q]= size(R)                           %% R-matrix as in previous snippet
data = dlmread (fullfile (pfad, ftfile)) %% get file list with associated epochs
dtimes = data(:,2)

rmean = mean(R')' ;             %% find mean values w.r.t time
R = R - rmean*ones(1,q);        %% perform residuals w.r.t. mean values

[u,s,v] = svd (R,xy);           %% perform singular value decomposition
lambdas = diag(s(1:q,1:q)^2);   %% eigen values are singular values squared
evs = [ xy(:,1:2), u(:,1:q)]    %% eigen vectors (=spatial pattern)
A = (u(:,1:q))'*R               %% Principle components (= temporal coeffcients)
pcs = [dtimes', A']

                                %% plotting not included
```

52

Pacific sea level variability 10/1992 – 01/2000

El-Niño pattern

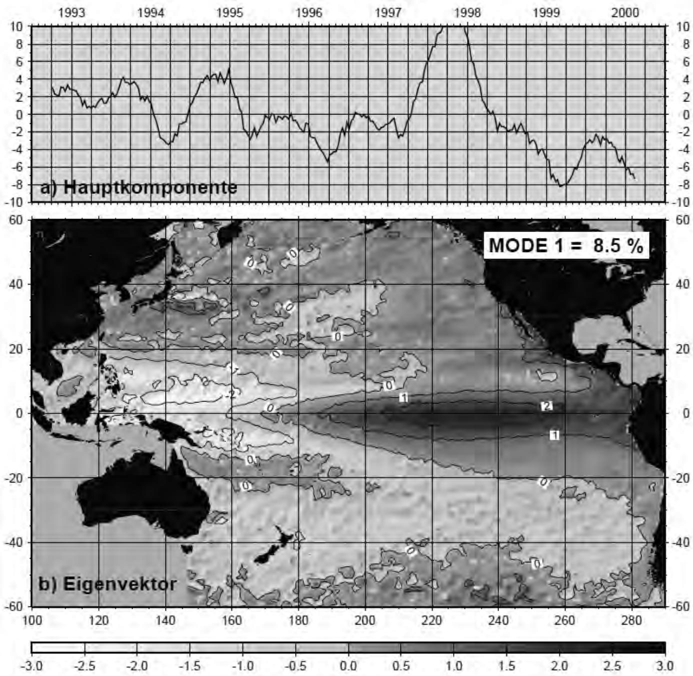

annual signal

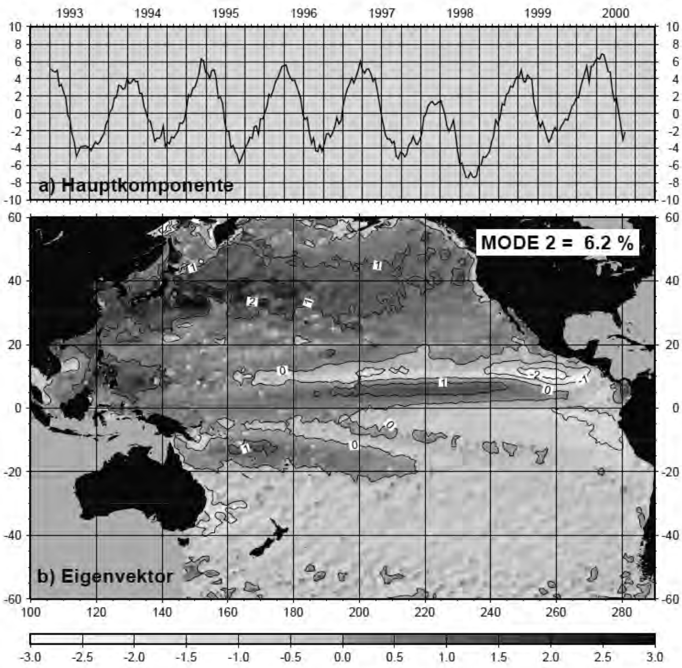

Pacific sea level variability 10/1992 – 01/2000

Here: seasonal signal (annual + semi-annual period) removed

El-Niño pattern

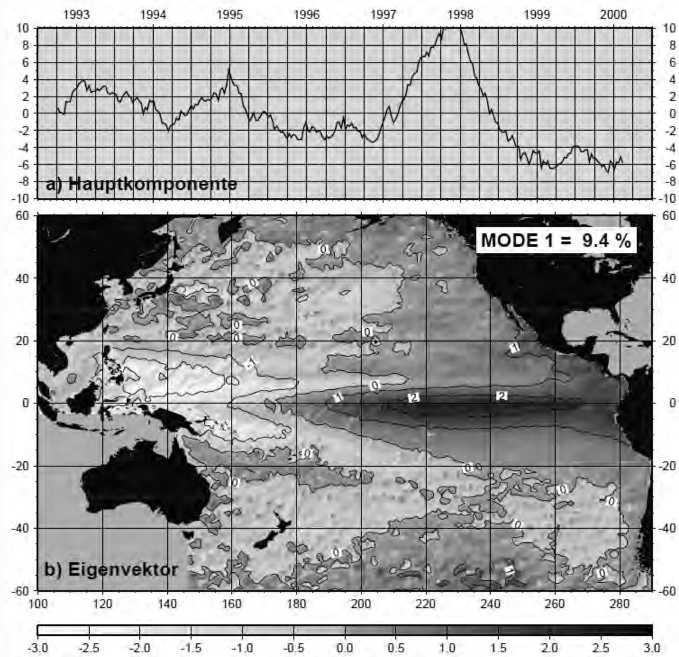

La Niña pattern

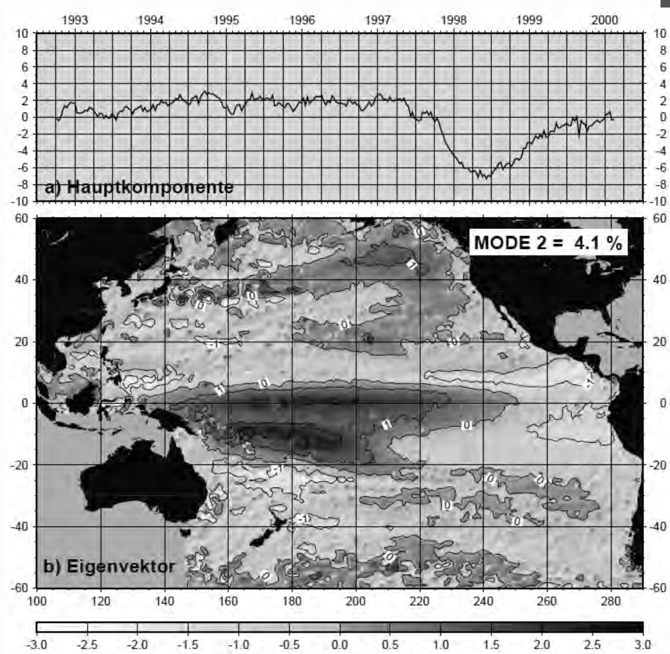

4

PCA – a tool to identify data problems

Mode 6 with a high frequency of the principle components and a track-related spatial pattern!

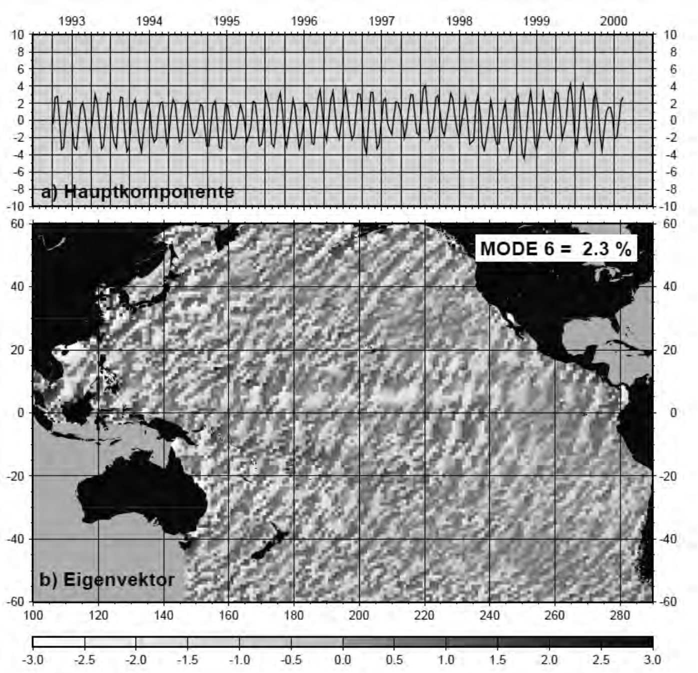

Fourier-Analysis of PCs shows: Period = 62 days

„Alias period“ if M2 (12hours) is sampled by TOPEX every 9.9156 days

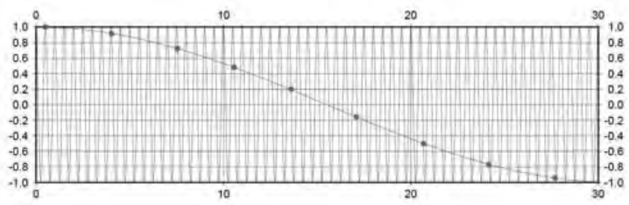

Obviously a significant error of the tide model applied to correct SSH

55

Dynamic Ocean Topography (DOT)

Hydrodynamic processes (density differences, wind pressure) cause the sea level to deviate from a geopotential surface (geoid). This deviation is called Dynamic Ocean Topography (DOT). It has a magnitude of only ±1–2 metres.

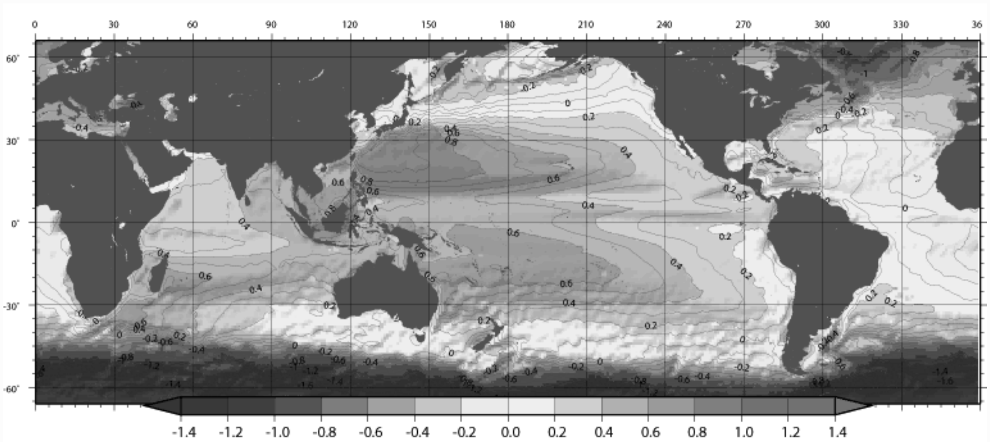

There are two independent ways to assess the DOT

a) model the hydrodynamic processes

b) estimate the difference between sea level and geoid: DOT = SSH - N

56

DOT: The geodetic way

Equation $\boxed{DOT = SSH - N}$ **not as simple as it seems!**

Geoid heights *N*
- are defined everywhere
- Relative smooth spherical harmonics)

Sea surface heights *SSH*
- observed on ocean profiles only
- High along-track resolution (e.g. 7km sampling)

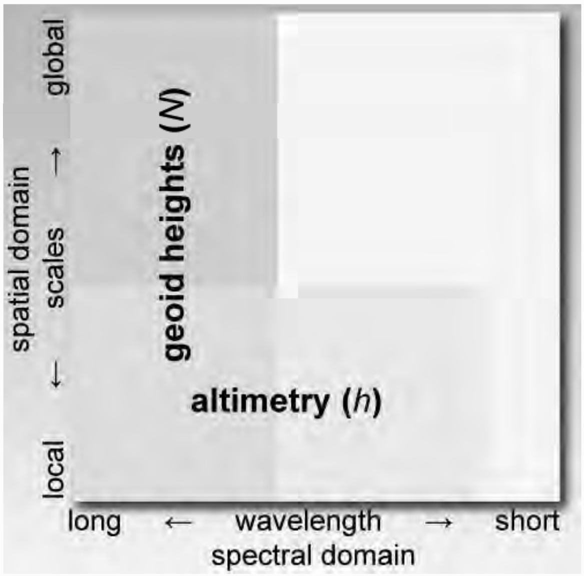

Strategies to perform DOT = SSH – N with consistent filtering

Global approach
- **rationale: filtering and performing differences is easy in the spectral domain. Geoid is already defined in terms of spherial harmonics. Thus SSH are expanded into spherical harmonics.**
- **Problem: SSH over land undefined! How to handle this? Fill land area with geoid. Step function at the coast remains and must be smoothed.**

Profile approach
- **Rationale: stay as long as possible on the altimeter ground tracks to maintain the high resolution and avoid undesirable gridding of SSH**
- **Problem: Systematic differences if SSH is filtered along track (1-D) and the geoid is filtered spectrally (2-D) – can be accounted for by a „filter correction“**

Data profiles of Jason1 (binary coded)
prepared for an exercise to estimate ocean topography

59

Record map:

000	**9**	**34**	**ssgh.rmp**	
001	**+4**	**-6.deg**	**glon.00**	**longitude of satellite footprint**
002	**4**	**-6.deg**	**glat.00**	**geodetic latitude of satellite footprint**
003	**4**	**-5.d**	**jday.00**	**julian day epoch 2000.0**
004	**4**	**-3.m**	**ssh.03**	**sea surface heights (unfiltered)**
005	**4**	**-3.m**	**geoh.15**	**geoid heights ITG-Grace03s (satellite-only, unfiltered)**
006	**4**	**-3.m**	**geoh.00**	**geoid heights EGM2008 (high resolution, unfiltered)**
007	**4**	**-3.m**	**sshs.08**	**smoothed sea surface (Gauss filter length D = 97 km)**
008	**4**	**-3.m**	**geohs.08**	**smoothed geoid heights (GOCO02S; Gauss filter length D = 97 km)**
009	**2**	**-3.m**	**dot.18**	**dynamic ocean topography (DOT); DGFI-version**

…/data/altimetry/jason1

```
        L    101
             L    101_001ssgh.00
             L    …
             L    101_254ssgh.00
        L    102
```

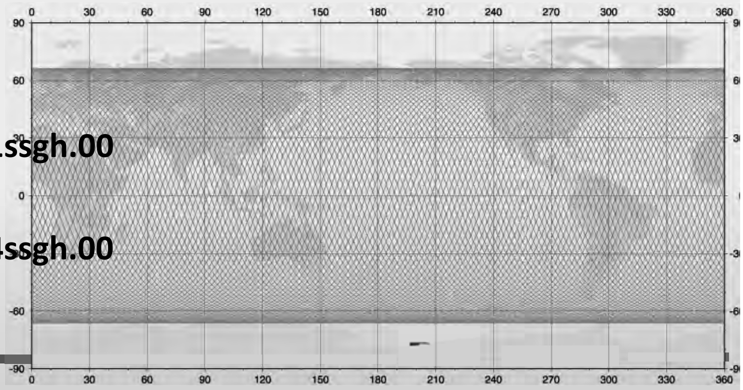

Code snippet to estimate DOT on individual profiles

60

```
pfad = 'D: ??? \data\altimetry\jason1';    %% path to jason1 (to be adapted)
cycle = '101'                              %% one particular cycle
recmap = 'ssgh.rmp'                        %% record-map file binary coded data

recmapfile = fullfile (pfad,recmap)         %% path to recordmap file
[byte,exps] = readrecmap (recmapfile)      %% read and get record structure

df = dir(fullfile(pfad,cycle));    %% list of files in the cycle directory
xyz = [];
for i = 1:length(df)                       %% loop to run through all pass-files
   binfile = fullfile(pfad,cycle,df(i).name)  %% construct full path to binfile
   [data,nrec] = bin2dat (binfile,byte,exps); %% decode all data of a pass
   xyz = [xyz; data] ;    %%  concatenate all data from all passes to xyz
End                       %%  xyz available as dgfi_data.mat for ocean Exercise

%% uncomment only one of the following lines (according to record map ssgh.rmp)
% DOT = xyz(:,4) - xyz(:,5);     %% DOT = SSH - N (unfiltered with ITG03S-geoid)
DOT = xyz(:,7) - xyz(:,8);       %% DOT = SSH - N (filtered with GOCO02S)
% DOT = xyz(:,9);                %% DOT (with filter correction); DGFI version
%%                       gridding (not shown here)
```

DFG SPP 1257

10-day DOT snapshot (Jason1 and Topex)

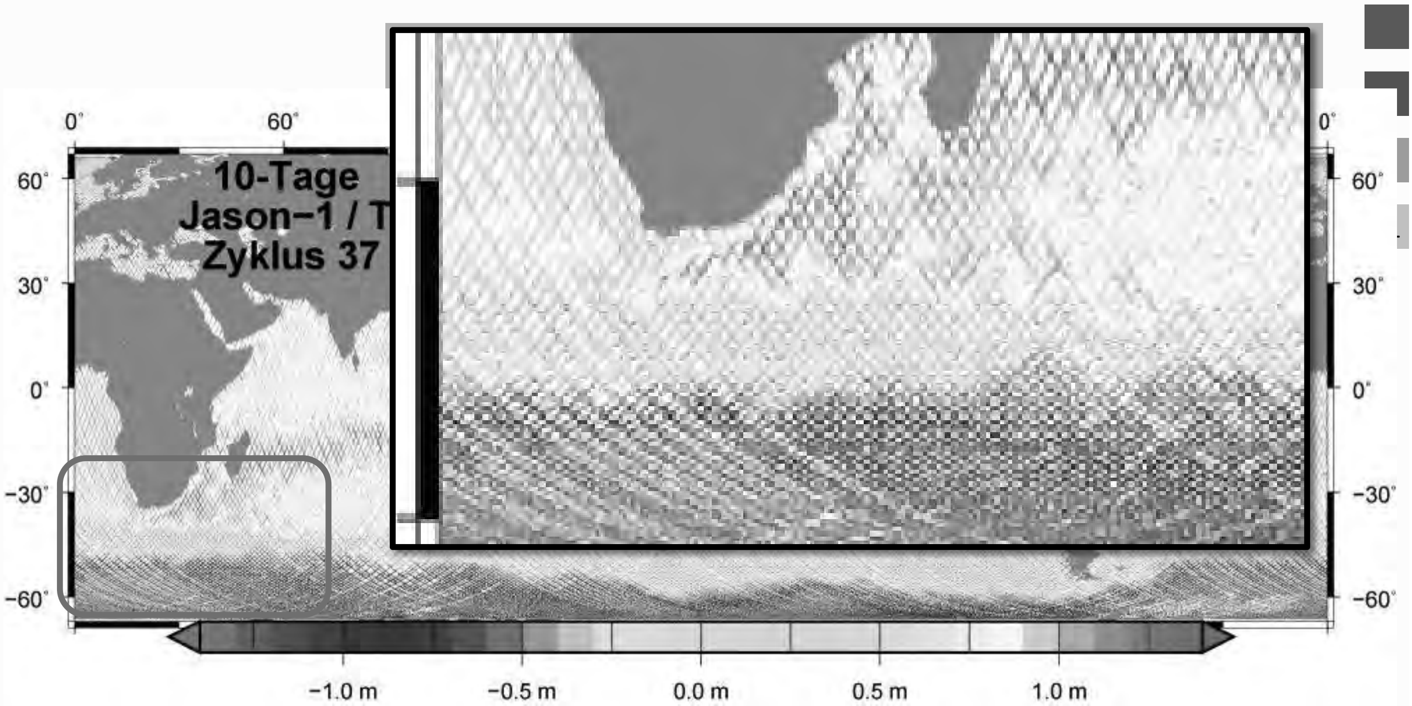

Mean GOCE DOTs (D=121km/L=120) compared with external estimates

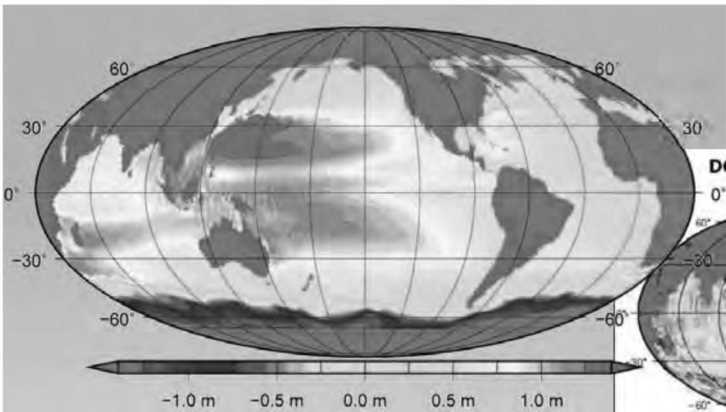

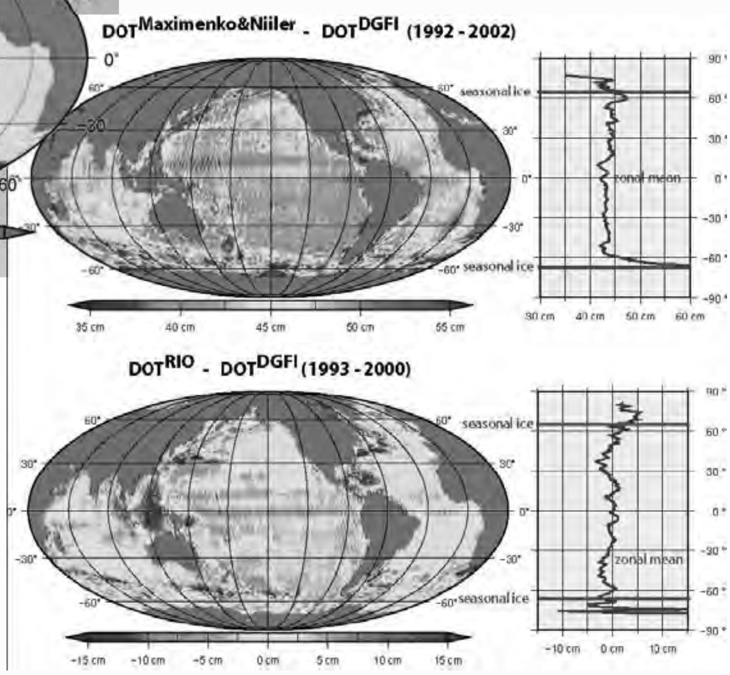

62

DOT evolution South Atlantic / Agulhas Stream

Multi-mission altimetry – GOCO02S geoid (Filter with D = 70km)

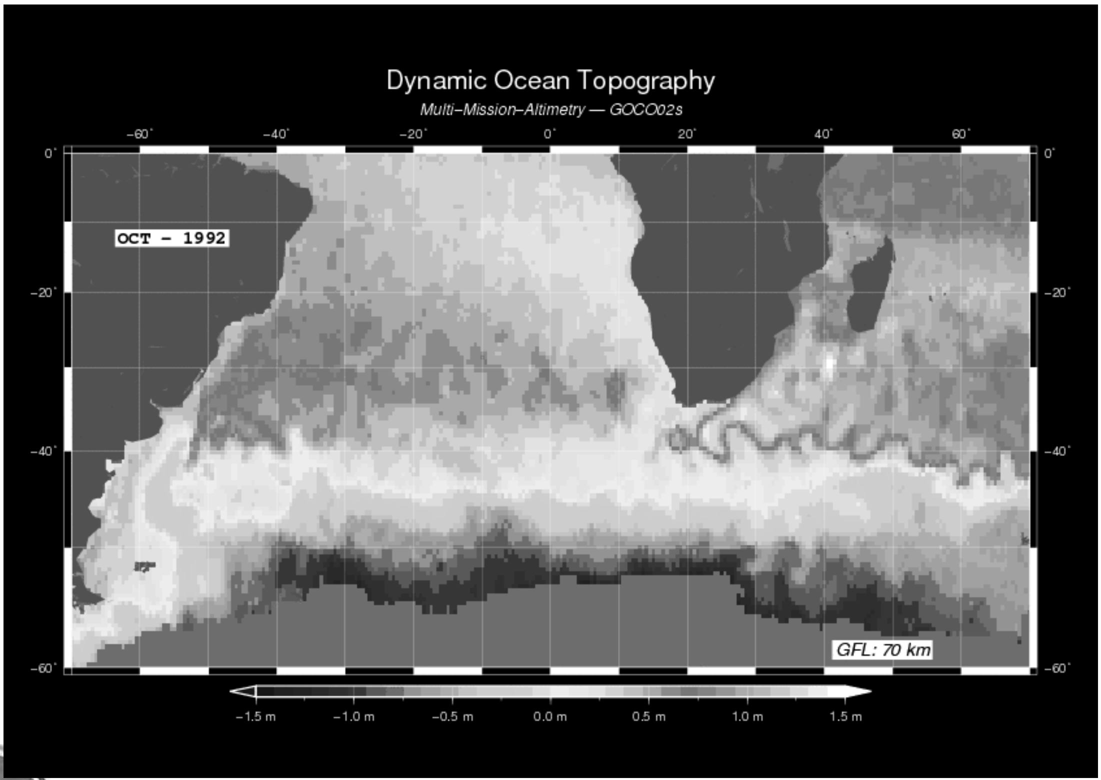

63

DFG SPP 1257

Geostrophic velocities for South Atlantic / Agulhas Stream

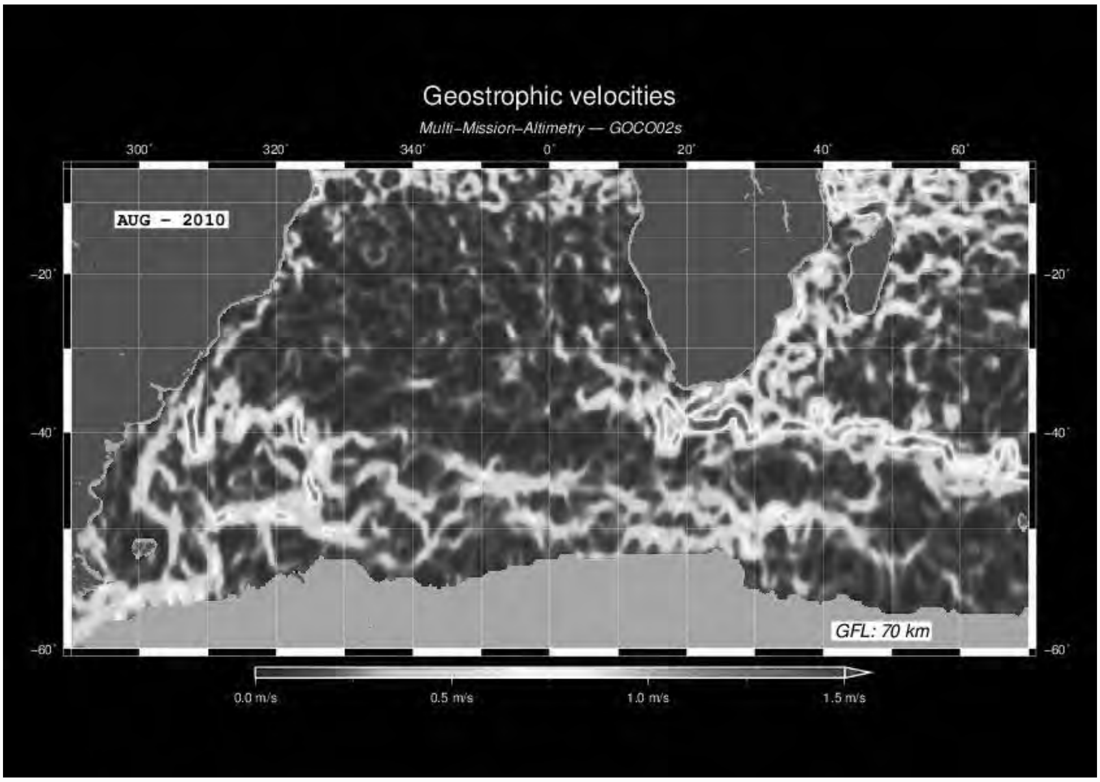

64

DFG SPP 1257

Acronyms

SLA	**Sea level anomaly**
DOT	**Dynamic Ocean Topography**
SSH	**Sea surface height**
GDR	**Geophysical data record**
SWH	**significant waveheight**
MWR	**Microwave radiometer**
GLAS	**Geoscience Laser Altimeter (on ICESat)**
PRF	**Pulse repetition frequency**

Lecture: Analysis Tools

Jürgen Kusche

Summer School „Global Water Cycle“
12.-16. September 2011
Mayschoss

Analysis Tools

Why this lecture?

By now (see lecture by T. Mayer-Gürr and F. Flechtner) it has become clear that GRACE solutions (say SH coefficients converted to TWS, total water storage) require some post-processing by the user, beyond projecting the coefficients into space domain

- to suppress correlated noise, remove ‚stripes‘ ($\rightarrow$ filtering)
- to extract the dominating ‚modes‘ of temporal variability ($\rightarrow$ PCA, …)

Being in general use, these analysis tools always remove signal content together with ‚noise‘. For any comparison of GRACE data with geophysical modelling, it is imperative therefore that the same tool is applied to both. For getting ‚absolute‘ amplitudes, rates, etc., it is imperative to consider the ‚bias‘ of an analysis technique.

Analysis Tools

This lecture will deal with both filtering techniques for data on the sphere and with PCA-related techniques.

While the first is often considered an obscure magic conceived by geodesists, the second is in general use in the atmosphere/ocean communities. See textbooks by Preisendorfer, Joliffe, von Storch & Zwiers…

Note: If you download GRACE gridded products from GRACE Tellus website, GFZ ICGEM or others, some filtering has been applied already.

Analysis Chain: Filtering

GRACE data	Geophysical model
GRACE SHC $\bar{C}_{nm}$ $\bar{S}_{n\|m\|}$	SHA geophysical model $\rightarrow$ SHC
↓	↓ Globally defined?
Treatment degree 1 & 2, temporal anomalies wrt epoch t, restore AOD	Temporal alignement, possibly remove deg. 1 consistent to GRACE
↓	↓
Filtering (in spectral domain)	Filtering (in spectral domain)
↓	↓ Multiplication in spectral domain
Mapping to space domain or basin averaging	Mapping to space domain or basin averaging
↓	↓
OR Filtering (in space domain)	OR Filtering (in space domain)
	Convolution on the sphere

Analysis Chain: Filtering - quite often

GRACE SHC $\bar{C}_{nm}$ $\bar{S}_{n|m|}$

Treatment degree 1 & 2, temporal anomalies wrt epoch t, restore AOD

Filtering (in spectral domain)

Mapping to space domain or basin averaging

Geophysical model

Temporal alignement, possibly remove deg. 1 consistent to GRACE

Filtering (in spectral domain)

Mapping to space domain or basin averaging

Filtering (in space domain)

5

Analysis Tools: PCA

Filtering (in spectral domain)

Mapping to space domain or basin averaging

Filtering (in spectral domain)

Mapping to space domain or basin averaging

Computation of EOFs

from GRACE or model

Project gridded data onto EOFs: PCs for GRACE and model

Comparison

Truncated (filtered) reconstruction

6

Analysis Chain: PCA - also possible…

GRACE SHC $\bar{C}_{nm}$ $\bar{S}_{n|m|}$

↓

Treatment degree 1 & 2, temporal anomalies wrt epoch t, restore AOD

SHA geophysical model → SHC

↓

Temporal alignement, possibly remove deg. 1 consistent to GRACE

↓

PCA & truncated reconstruction (in spectral domain)

↓

Mapping to space domain or basin averaging

7

Part I: Filtering techniques and their application to GRACE data

Filtering

- Attempts to suppress ‚noise' in data (here: SH coefficients)
- Requires that we have an a-priori knowledge of expected ‚noise' (→ characterize spectral behaviour of noise)
- Filters take this into account either implicitly (‚deterministic filters' or explicitly ‚stochastic filters')
- Also regularizing or ‚constraining' GRACE normal equations corresponds to some kind of filtering (Kusche 2007, Klees et al 2008, Swenson & Wahr 2011)

Data sets e.g.

- GRACE-derived SH coefficients or maps of geoid, gravity anomalies,TWS
- SH coefficients or maps of TWS and other data from model output

8

What is the purpose of filtering a GRACE solution?

Unfiltered GRACE solution

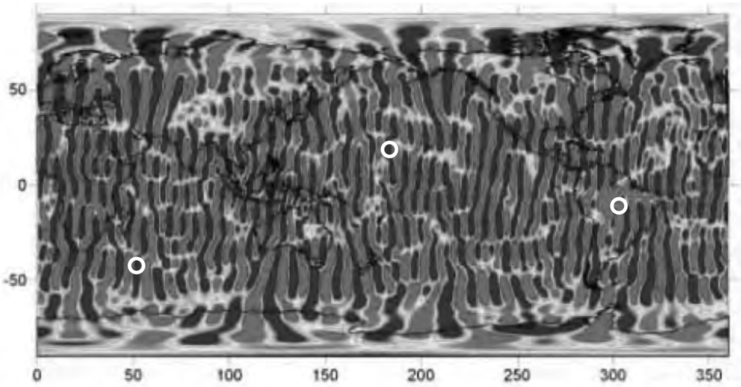

What is the purpose of filtering a GRACE solution?

Boxcar-filtered GRACE solution: Remove stripes by averaging, convolution

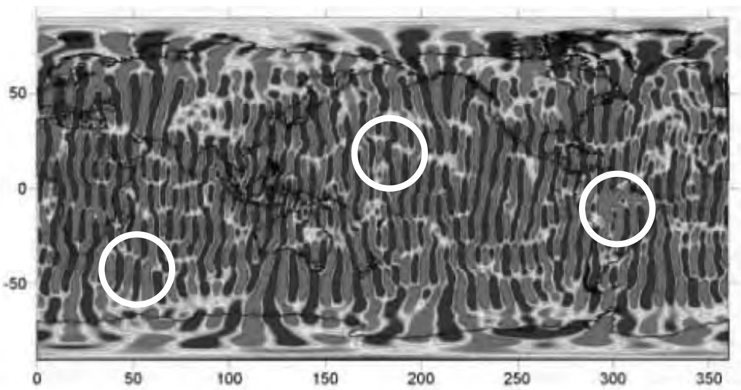

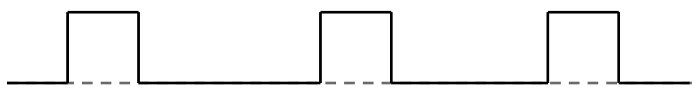

What is the purpose of filtering a GRACE solution?

Boxcar-filtered GRACE solution: Remove stripes by averaging, convolution

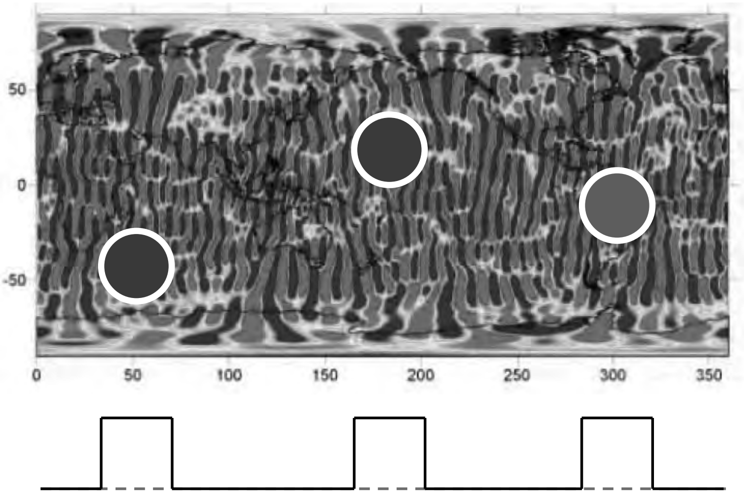

What is the purpose of filtering a GRACE solution?

Boxcar-filtered GRACE solution: Remove stripes by averaging, convolution

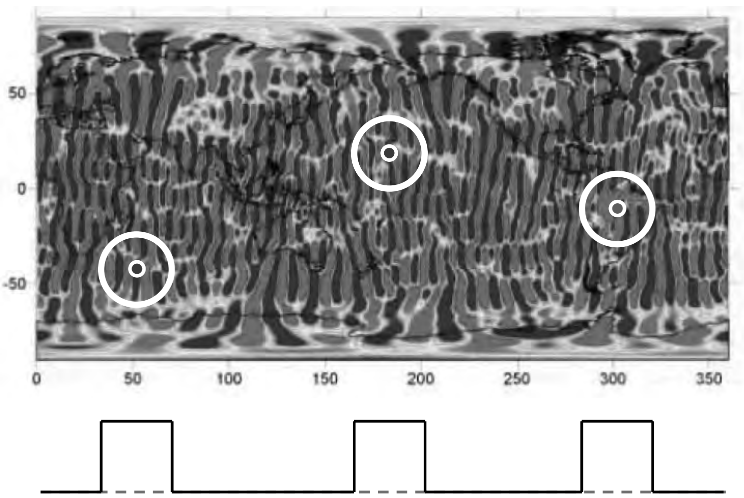

What is the purpose of filtering a GRACE solution?

Gaussian-filtered GRACE solution: convolution with a smooth kernel

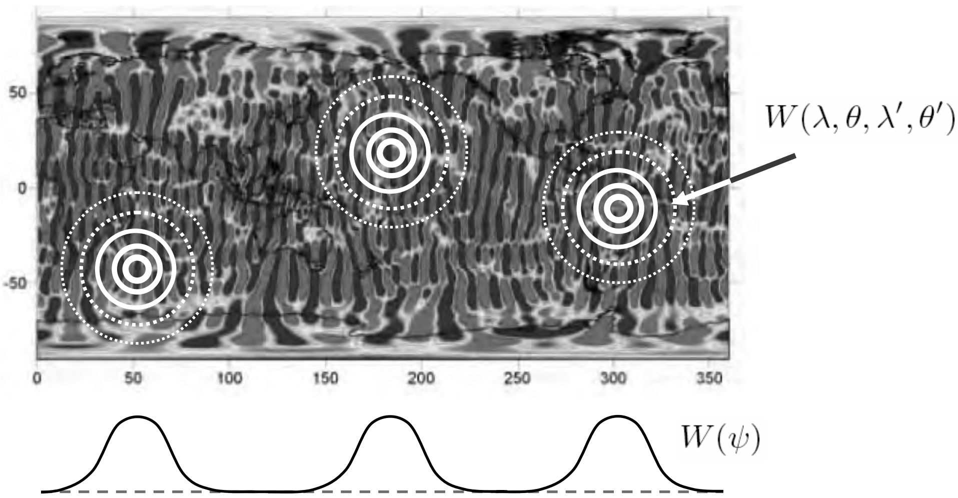

Filtering a GRACE solution in spatial and in spectral domain

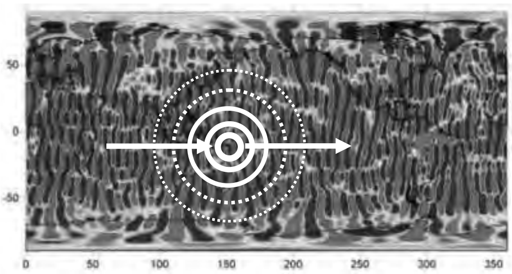

$$F_W(\lambda, \theta) = \int_\Omega W(\lambda, \theta, \lambda', \theta') F(\lambda', \theta') d\omega$$

$$\bar{f}^W_{nm} = \sum_{n'=0}^{\infty} \sum_{m'=-n'}^{n'} \bar{w}^{n'm'}_{nm} \bar{f}_{n'm'}$$

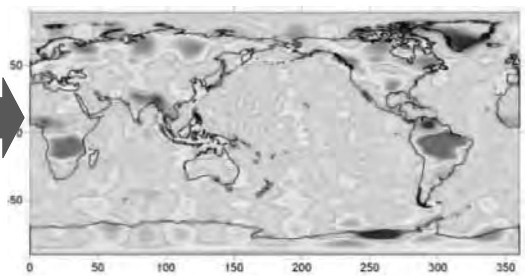

$$V(r,\theta,\lambda,t) = \frac{GM}{r} + \frac{GM}{r}\sum_{n=2}^{\bar{n}}\left(\frac{R}{r}\right)^n \sum_{m=0}^{n} P_{nm}(\cos\theta)\left(\bar{C}_{nm}(t)\cos m\lambda + \bar{S}_{nm}(t)\sin m\lambda\right)$$

$$\bar{v}_{nm} = \bar{C}_{nm} \quad \text{for } m \geq 0$$

$$\bar{v}_{nm} = \bar{S}_{n|m|} \quad \text{for } m < 0$$

Notations I use

- Positive and negative order
- Fully normalized
- All factors are put into the coefficients

Potential $\rightarrow$ Surface Mass

$$F = \sum_{n=0}^{\bar{n}}\sum_{m=-n}^{n} \bar{f}_{nm}\bar{Y}_{nm}(\lambda,\theta) \qquad \bar{f}_{nm}(t) = R\frac{\rho_e}{3}\frac{2n+1}{1+k'_n}\left(\bar{v}_{nm}(t) - \bar{v}_{nm}\right)$$

Part I: Filtering techniques and their application to GRACE data

Isotropic filters

$$F_W(\lambda,\theta) = \sum_{n=0}^{\infty}\sum_{m=-n}^{n} \bar{f}^W_{nm}\bar{Y}(\lambda,\theta)$$

$$\bar{f}^W_{nm} = \sum_{n'=0}^{\infty}\sum_{m'=-n'}^{n'} \bar{w}^{n'm'}_{nm}\bar{f}_{n'm'}$$

$$\bar{w}^{n'm'}_{nm} = \delta^{n'm'}_{nm} w_n$$

$$F_W(\lambda,\theta) = \sum_{n=0}^{\infty}\sum_{m=-n}^{n} w_n\bar{f}_{nm}\bar{Y}(\lambda,\theta)$$

17

Isotropic filters: Gaussian filter (Wahr et al., JGR 1998)

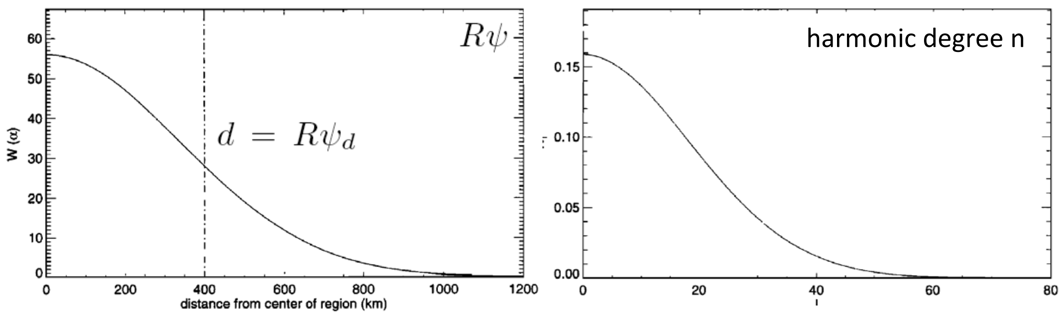

$$W_d(\psi) = 2b\frac{e^{-b(1-\cos\psi)}}{1-e^{-2b}} = \sum_{n=0}^{\infty}(2n+1)w_n^{(d)}P_n(\cos\psi)$$

$$w_{n+1}^{(d)} = -\frac{2n+1}{b}w_n^{(d)} + w_{n-1}^{(d)}$$

18

Destriping filters

$$F_W(\lambda,\theta) = \sum_{n=0}^{\infty}\sum_{m=-n}^{n} \bar{f}_{nm}^{W}\bar{Y}(\lambda,\theta)$$

$$\bar{f}_{nm}^{W} = \sum_{n'=0}^{\infty}\sum_{m'=-n'}^{n'} \bar{w}_{nm}^{n'm'}\bar{f}_{n'm'}$$

$$\bar{w}_{nm}^{n'm'} = \delta_{nm}^{n'm'}w_n$$

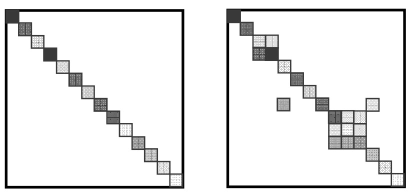

Isotropic Non-isotropic

19

Destriping filters

$$W(\lambda,\theta,\lambda',\theta') = \sum_{n=0}^{\infty}\sum_{m=-n}^{n}\sum_{n'=0}^{\infty}\sum_{m'=-n'}^{n} \bar{w}_{nm}^{n'm'}\bar{Y}_{nm}(\lambda,\theta)\bar{Y}_{n'm'}(\lambda',\theta')$$

Swenson & Wahr
GRL, 2006

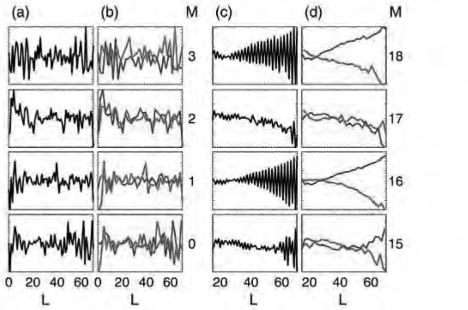

Figure 2. Stokes coefficients (C_{lm}), converted to mass, plotted as functions of degree for orders m = 0–3 and m = 15–18. (a) and (c) Coefficients plotted for every degree; (b) and (d) coefficients plotted separately for even and odd degrees.

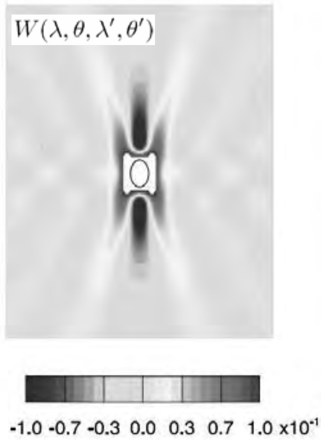

Part I: Filtering techniques and their application to GRACE data

20

Destriping filters

$$W(\lambda,\theta,\lambda',\theta') = \sum_{n=0}^{\infty}\sum_{m=-n}^{n}\sum_{n'=0}^{\infty}\sum_{m'=-n'}^{n} \bar{w}_{nm}^{n'm'}\bar{Y}_{nm}(\lambda,\theta)\bar{Y}_{n'm'}(\lambda',\theta')$$

Kusche 2007, J Geodesy

$$\mathbf{W}_{(\alpha)} = \mathbf{L}_\alpha \mathbf{N} = (\mathbf{N} + \alpha\mathbf{M})^{-1}\mathbf{N}$$

$$\mathbf{C_f} = E\{\mathbf{ff}^T\}$$

$$\mathbf{C_{\hat{f}}} = E\{\hat{\mathbf{f}}\hat{\mathbf{f}}^T\}$$

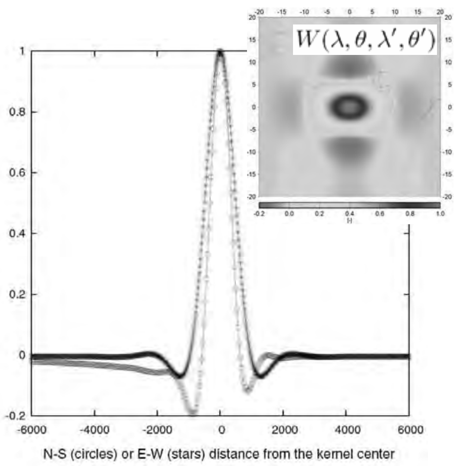

Part I: Filtering techniques and their application to GRACE data

Destriping filters and WRMS reduction
(Kusche et al., J Geodesy 2009)

GRACE TWS WRMS [cm], 3 filters

	GRACE WRMS		
	DDK1	DDK2	DDK3
Global	3.87	4.77	6.46
Continents	5.89	7.03	8.58
Ocean	2.66	3.44	5.33
Amazon	14.34	16.47	17.66
Sahara	1.75	2.56	4.82

stronger ⟵ filtering ⟶ less

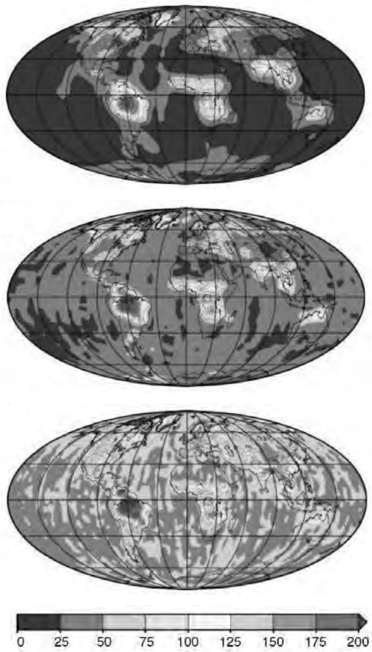

21

Part I: Filtering techniques and their application to GRACE data

Basin averaging

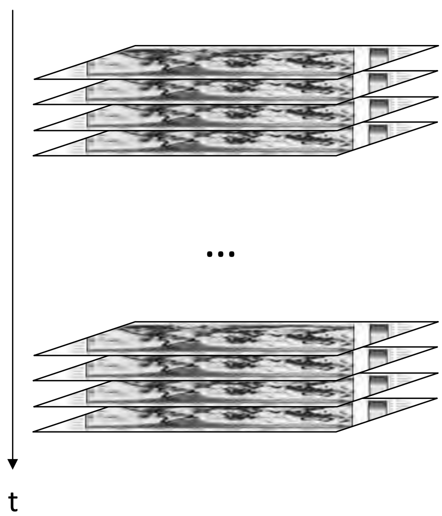

Ocean mass

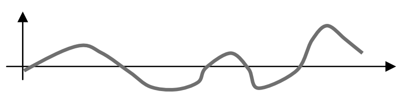

22

Basin averaging

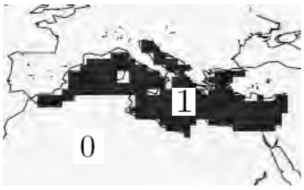

$$\bar{F}_O = \frac{1}{\bar{O}}\int_O F d\omega = \frac{1}{\bar{O}}\int_\Omega OF d\omega \quad \text{(spatial domain)}$$

$$O = O(\lambda,\theta) = \begin{cases} 1 & (\lambda,\theta) \in O \\ 0 & (\lambda,\theta) \notin O \end{cases}$$

$$\bar{O} = \int_\Omega O\bar{Y}_{00} d\omega = 4\pi\ \bar{O}_{00}$$

$$\bar{F}_O = \frac{1}{\bar{O}_{00}} \sum_{n=0}^{\infty}\sum_{m=-n}^{n} \bar{O}_{nm}\bar{f}_{nm} \quad \text{(spectral domain)}$$

Basin averaging

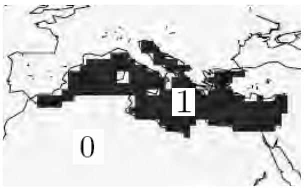

$$\bar{F}_O = \frac{1}{\bar{O}}\int_O F d\omega = \frac{1}{\bar{O}}\int_\Omega OF d\omega$$

$$\bar{F}_O = \frac{1}{\bar{O}_{00}} \sum_{n=0}^{\infty}\sum_{m=-n}^{n} \bar{O}_{nm}\bar{f}_{nm} \quad \text{(spectral domain)}$$

$$O = \sum_{n=0}^{\infty}\sum_{m=-n}^{n} \bar{O}_{nm}\bar{Y}_{nm}(\lambda,\theta)$$

Note: Equality requires

- the integral is discretized at an error small enough
- the SH truncation degree is big enough OR BOTH F and O are band-limited

Smoothed basin averaging and bias

$$O_W(\lambda,\theta)=\sum_{n=0}^{\infty}\sum_{m=-n}^{n}\bar{O}_{nm}^{W}\bar{Y}_{nm}(\lambda,\theta)$$

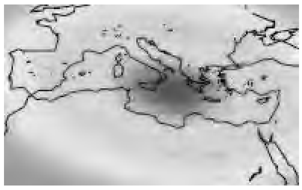

$$\bar{F}_{O_W}=\frac{1}{\bar{O}_{00}^{W}}\sum_{n=0}^{\infty}\sum_{m=-n}^{n}w_n\bar{O}_{nm}\bar{f}_{nm}$$

$$\beta_{O,W,F}=\frac{\bar{F}_{O_W}}{\bar{F}_O}=\frac{1}{w_0}\frac{\sum_{n=0}^{\infty}\sum_{m=-n}^{n}w_n\bar{O}_{nm}\bar{f}_{nm}}{\sum_{n=0}^{\infty}\sum_{m=-n}^{n}\bar{O}_{nm}\bar{f}_{nm}}$$

Part I: Filtering techniques and their application to GRACE data

Leakage problem and filter bias: basin averaging, what happens?

Model

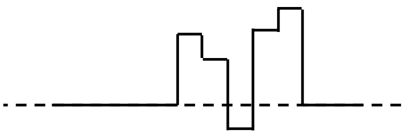

GRACE (truncated SH)

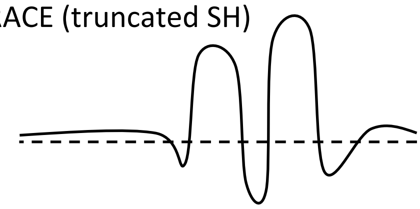

Part I: Filtering techniques and their application to GRACE data

Leakage problem and filter bias: basin averaging, what happens?

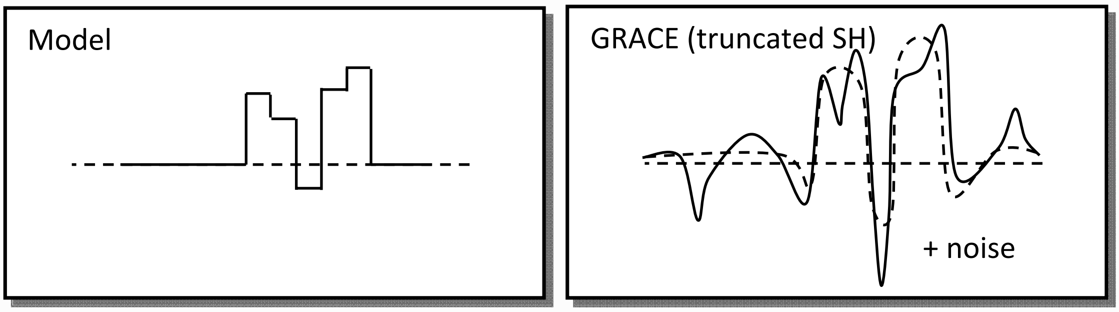

27

Part I: Filtering techniques and their application to GRACE data

Leakage problem and filter bias: basin averaging, what happens?

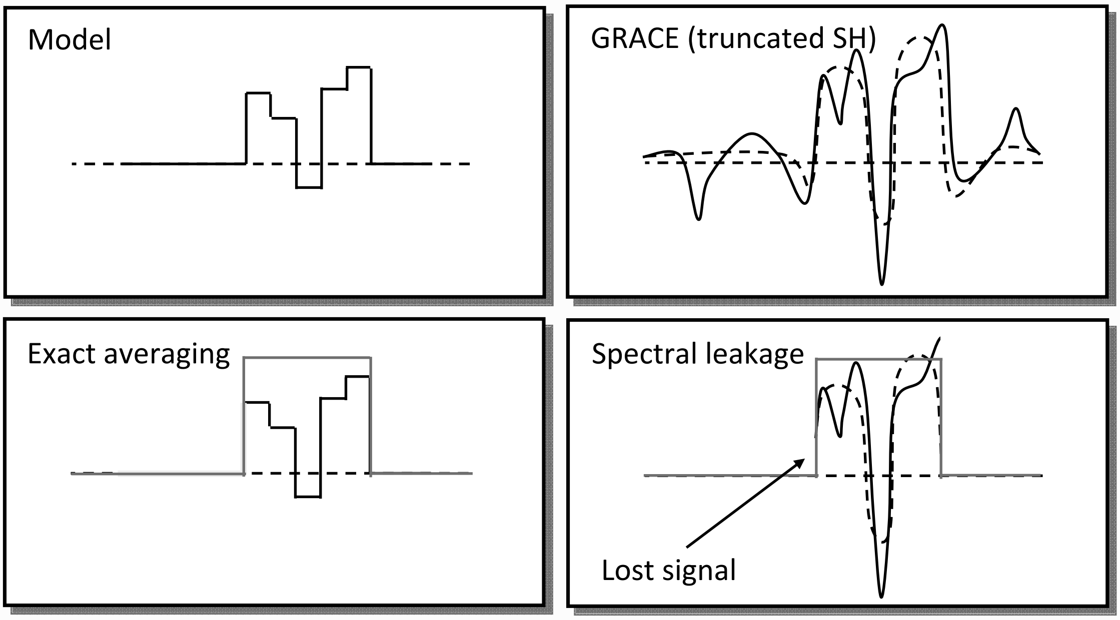

28

Part I: Filtering techniques and their application to GRACE data

Leakage problem and filter bias: basin averaging, what happens?

Model

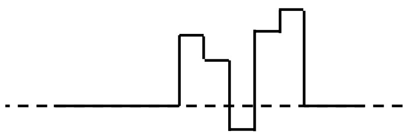

GRACE (truncated SH)

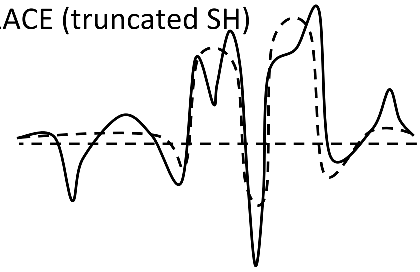

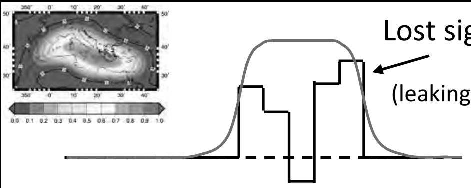

Bias can be computed from model

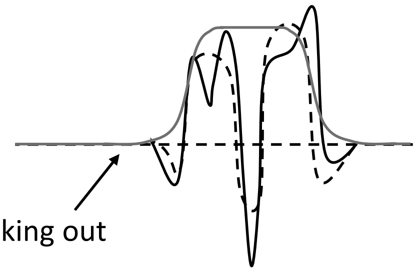

29

Jürgen Kusche

DFG SPP 1257

Part I: Filtering techniques and their application to GRACE data

Leakage problem and filter bias: basin averaging, what happens?

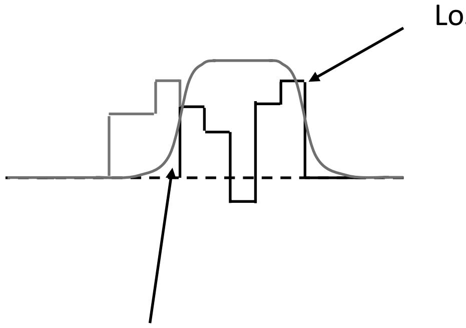

30

Jürgen Kusche

DFG SPP 1257

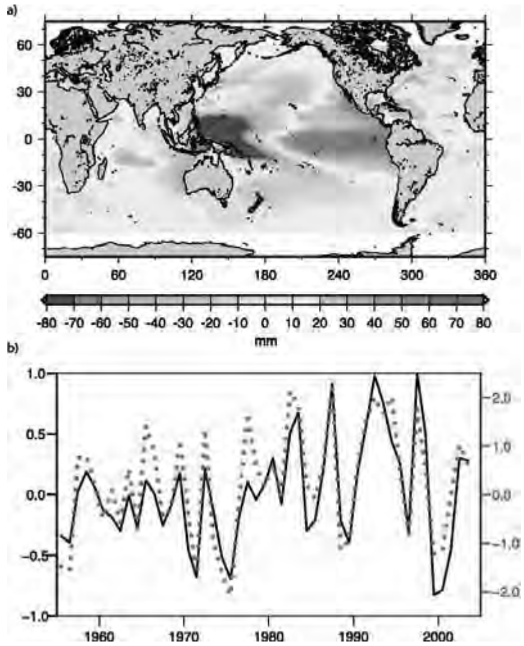

Empirical orthogonal function analysis

Principle components

Related concepts

(Fig.: SST, from IPPC 4AR)

Part II: Principle component analysis and related ideas

PCA

- attempts to find a relatively small number of independent modes in a data set that convey as much as possible information without redundancy
- can be used to explore the structure of the data variability in an objective way, i.e. without assumptions on periodic behaviour etc.
- and EOF analysis are the same.

Data sets e.g.

- GRACE-derived maps of TWS, TWS and other maps from model output
- Sea level anomalies
- Other related spatial fields (SST, SLP, …)

What does PCA do?

PCA uses a set of orthogonal functions (EOFs) to represent a spatio-temporal data field in the following way

epochs (time)

PCs (expansion coefficients)

$$\mathbf{y}_i = \begin{pmatrix} y_{1;i} \\ y_{2;i} \\ \vdots \\ y_{n;i} \end{pmatrix} \quad i = 1 \dots p \quad = \sum_{j=1}^{n} d_{j;i} \mathbf{e}_j = \mathbf{E}\mathbf{d}_i$$

grid points

EOFs (new basis)

EOF e_j =e (λ, θ) show spatial patterns of the major factors (‚modes') that account for temporal variations.

PC $d_{j;i}$ = d(t) tells how the amplitude of EOF varies with time.

Part II: Principle component analysis and related ideas

How do we obtain the PCs?

Practical: WGHM and GRACE

$$\mathbf{y}_i = \sum_{j=1}^{n} d_{j;i} \mathbf{e}_j = \mathbf{E}\mathbf{d}_i \qquad \mathbf{Y} = (\mathbf{y}_1, \mathbf{y}_2, \dots, \mathbf{y}_p) = \mathbf{E}\mathbf{D}$$

Lets assume the EOFs are orthogonal (why are they called EOF, after all) and normalized.

$$\mathbf{d}_i = (\mathbf{E}^T\mathbf{E})^{-1}\mathbf{E}^T\mathbf{y}_i = \mathbf{E}^T\mathbf{y}_i \qquad d_{j;i} = \mathbf{e}_j^T\mathbf{y}_i$$

The PCs are found as an orthogonal projection of the data onto the new basis functions (the EOFs). We can try to reconstruct the original data using only the ‚major' EOFs

$$\bar{\mathbf{y}}_i = \sum_{j=1}^{\bar{n}} d_{j;i} \mathbf{e}_j$$

Jürgen Kusche

DFG SPP 1257

Part II: Principle component analysis and related ideas

What do we get from PCA?

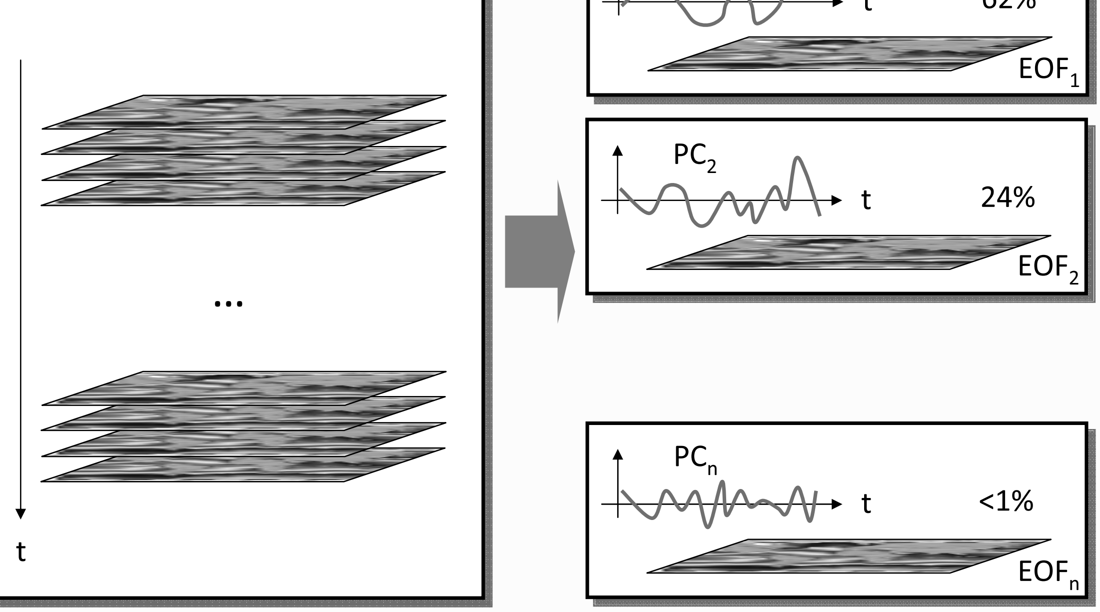

Part II: Principle component analysis and related ideas

Example (I)

GRACE TWS 400km Gaussian filtered (note: EOF $\times$ PC has unit of data)

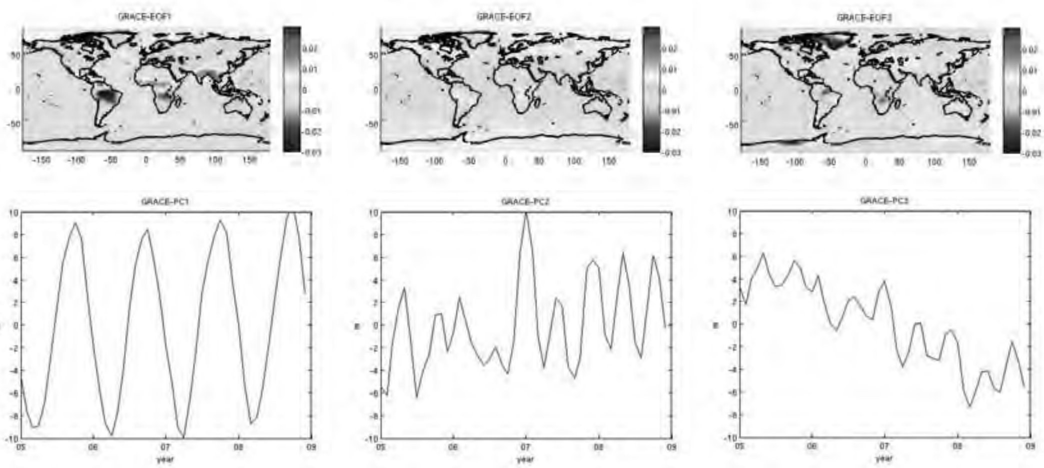

How do we choose the EOFs?

Total variance

$$d_{j;i} = \mathbf{e}_j^T \mathbf{y}_i$$

$$\Delta^2 = \operatorname{trace}\left(\mathbf{E}\mathbf{D}\mathbf{D}^T\mathbf{E}^T\right) = \operatorname{trace}\left(\mathbf{D}^T\mathbf{D}^T\right) = \sum_{j=1}^{n}\sum_{i=1}^{p} d_{j;i}^2$$

Then, the maximum variance is concentrated in a single EOF if

$\mathbf{Y}\mathbf{e} \quad \rightarrow$ max. variance

I.e., maximize $\frac{1}{p}(\mathbf{Y}\mathbf{e})^T(\mathbf{Y}\mathbf{e}) = \frac{1}{p}\mathbf{e}^T\mathbf{C}\mathbf{e}$ subject to $\mathbf{e}^T\mathbf{e} = 1$

Or, solve an eigenvalue problem

$$\mathbf{C}\mathbf{e} = \lambda\mathbf{e}$$

How do we choose the EOFs?
The EOFs are found as the eigenvectors of the data covariance matrix.

$$\mathbf{C} = \frac{1}{p}\mathbf{Y}\mathbf{Y}^T = \frac{1}{p}\begin{pmatrix} \sum_{i=1}^{p} y_{1;i}^2 & \sum_{i=1}^{p} y_{1;i}y_{2;i} & \ldots \sum_{i=1}^{p} y_{1;i}y_{n;i} \\ \sum_{i=1}^{p} y_{2;i}y_{1;i} & \sum_{i=1}^{p} y_{2;i}^2 & \ldots \sum_{i=1}^{p} y_{2;i}y_{n;i} \\ \vdots & \vdots & \vdots \\ \sum_{i=1}^{p} y_{n;i}y_{1;i} & \sum_{i=1}^{p} y_{n;i}y_{2;i} & \ldots \sum_{i=1}^{p} y_{n;i}^2 \end{pmatrix}$$

$$\mathbf{C} = \mathbf{E}\mathbf{\Lambda}\mathbf{E}^T$$

Some remarks (I)

– The covariance as above is temporal, i.e. it considers auto- and covariances of time series per grid point (for n grid points)

(we‘ll come back to this point)

Representing data in an eigenvector basis

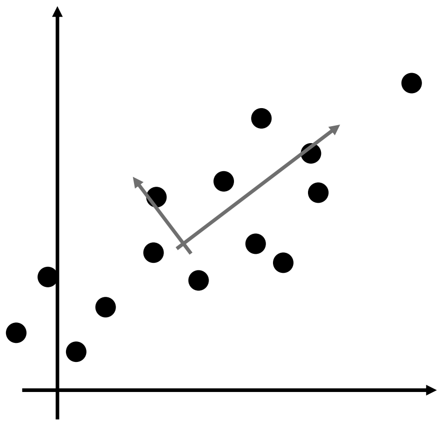

Part II: Principle component analysis and related ideas

The EOFs are found as the eigenvectors of the data covariance matrix.

Some remarks (II)

- It is an <u>empirical</u> realization. Should we know the true covariance, we might better use this one instead of the empirical one
- All data has been considered as (perfectly) centered
- Eigenvectors require normalization and a further convention for uniqueness, e.g.

$$\mathbf{e}_j^T \mathbf{e}_j = 1$$

$$e_{1;j} > 0$$

Jürgen Kusche

DFG SPP 1257

Part II: Principle component analysis and related ideas

The EOFs are found as the eigenvectors of the data covariance matrix.

Some remarks (III)

- Alternatively, we could use SVD applied to the data matrix
- Each EOF explains a fraction of the total variance, given by the ratio of the EV vs. TV (total variance)

$$\Delta^2 = \frac{1}{p}\sum_{j=1}^{n}\left(\sum_{i=1}^{p} y_{j;i}^2\right) = \mathrm{trace}(\mathbf{C})$$

$$\eta_j = \frac{\lambda_j}{\Delta^2}$$

Practical

- It is common to choose the number of EOFs as to ‚explain" 90% (or …) of the TV

41

Part II: Principle component analysis and related ideas

Example

GRACE global analysis (left: EV, right: cumulative percentage of TV)

(courtesy E. Forootan)

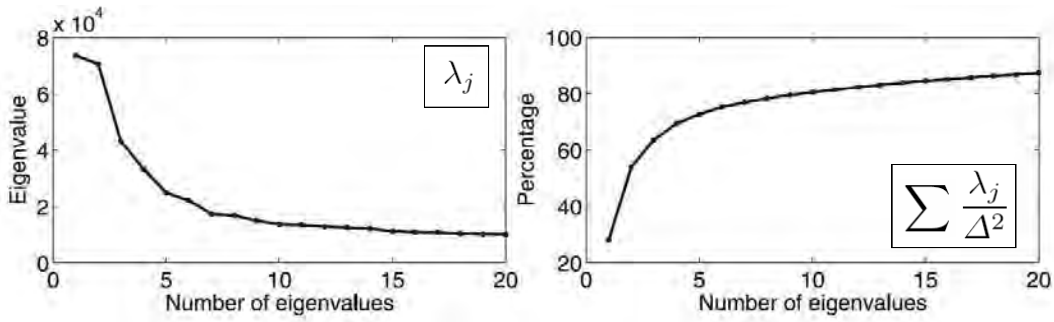

42

The EOFs are found as the eigenvectors of the data covariance matrix.

Some remarks (IV)

Practical

- Instead of computing the temporal data covariance, we may compute the spatial covariance (spatial variance and covariances for the p epochs)

$$\mathbf{C}' = \frac{1}{n}\mathbf{Y}^T\mathbf{Y} = \frac{1}{n}\begin{pmatrix} \sum_{j=1}^n y_{j;1}^2 & \sum_{j=1}^n y_{j;1}y_{j;2} & \cdots \sum_{j=1}^n y_{j;1}y_{j;p} \\ \sum_{j=1}^n y_{j;2}y_{j;1} & \sum_{j=1}^n y_{j;2}^2 & \cdots \sum_{j=1}^n y_{j;2}y_{j;p} \\ \vdots & \vdots & \vdots \\ \sum_{j=1}^n y_{j;p}y_{j;1} & \sum_{j=1}^n y_{j;p}y_{j;2} & \cdots \sum_{j=1}^n y_{j;p}^2 \end{pmatrix}$$

- Requires less memory for p < n
- Temporal and spatial covariance matrices share the same p EVs
- k-th EOF (spatial) ~ k-th PC (temporal) and vice versa

43

Part II: Principle component analysis and related ideas

Some remarks (V)

- Linear transformations of the data lead to new eigenvectors and –values

$$\mathbf{z}_i = \mathbf{A}\mathbf{y}_i, \qquad i = 1 \ldots p$$

$$\lambda_i^z \in [\min(\mu_i)\cdot\min(\lambda_i), \underset{\substack{\uparrow \\ \mathbf{A}^T\mathbf{A}}}{\max(\mu_i)}\cdot\max(\lambda_i)]$$

Therefore:

Practical

- EOFs and PCs computed on a regional grid look different from EOFs/PCs computed on a global grid
- GRACE: EOFs of geoid change look different from EOF of TWS change
- PCA applied to GRACE SH coefficients (EOF filter of Schrama & Wouters) looks different from PCA applied to grids.

44

45

Example (I) revisited

Annual signals out of phase

Semi-annual (modulation of annual)

Trend (decrease)+ annual

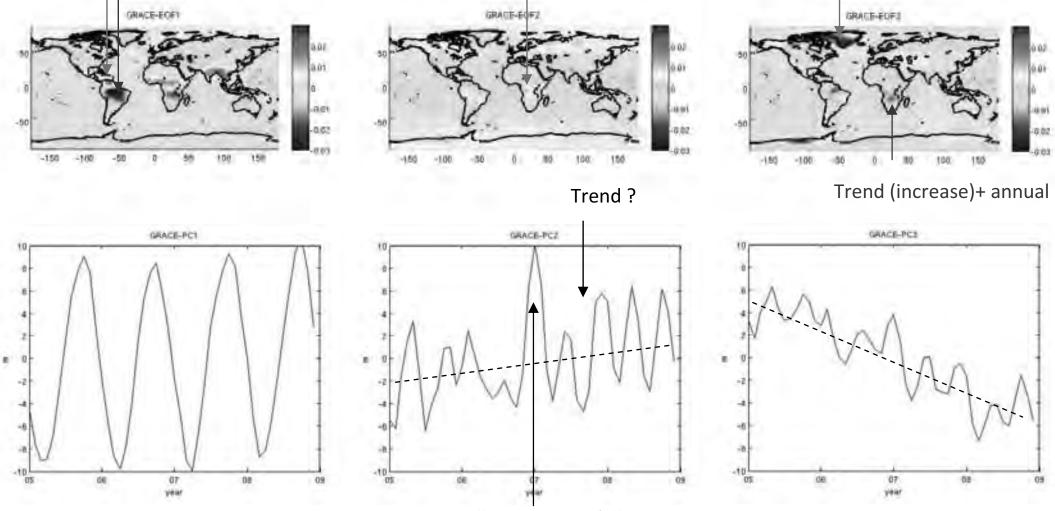

2007: unusually strong rainfall in Congo

Part II: Principle component analysis and related ideas

46

Example (I) revisited

Annual signals out of phase

Semi-annual (modulation of annual)

Trend (decrease)+ annual

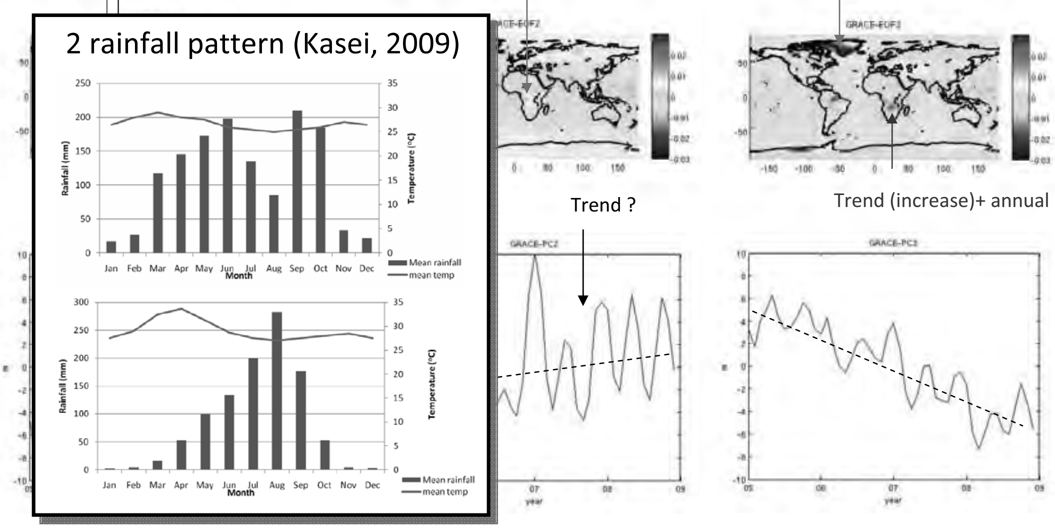

Examples (II)
Wouters & Schrama (GRL, 2007) Direct EOF filtering of GRACE SH coefficients

Top: Unfiltered/Gaussian, Middle: EOF filtered, Bottom: difference. Unit [cm]

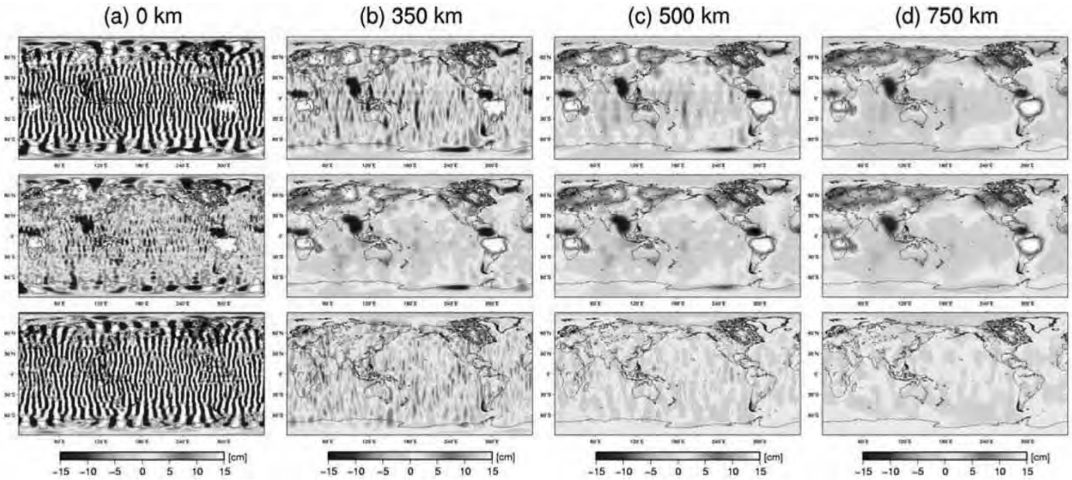

Part II: Principle component analysis and related ideas

How many modes (EOFs) should we retain? In other words, how many % of the data TV should we reconstruct?

North et al. 1982, Month. Weath. Rev.: Consider the spatio-temporal data as stochastic, i.e. perturbed by e.g. Gaussian noise. Then, the covariance

$$\mathbf{C} = \frac{1}{p}\mathbf{Y}\mathbf{Y}^T$$

and the eigenvalues / -vectors will be stochastic as well. In first order…

$$\delta\lambda_j = \sqrt{\frac{2}{n}}\lambda_j + \cdots \quad \delta\mathbf{e}_j = \frac{\delta\lambda_j}{\lambda_k - \lambda_j}\mathbf{e}_k + \cdots$$

If the sampling error in the eigenvalue is comparable to the spacing of the eigenvalues, then the sampling error of the EOF will be comparable to the nearby EOF.

And then it is time to truncate.

Jürgen Kusche
DFG SPP 1257

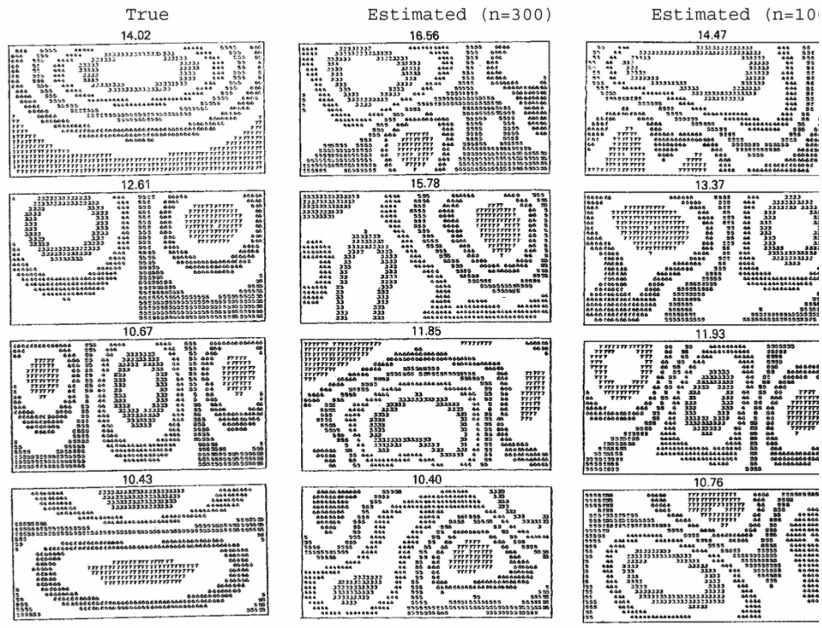

Figure 13.2: *North et al.'s [296] illustration of North's Rule-of-Thumb [13.3.5]. From [296].*
Left: The first four true eigenvalues and EOFs.
Middle: Corresponding estimates obtained from a random sample of size $n = 300$.
Right: As middle column, except $n = 1000$.

North et al (Mon. Wea. Rev.1982), reprinted in Von Storch & Zwiers 1999

Comparing two (or multiple) data sets (e.g. GRACE TWS and hydrology TWS, altimetric sea level and model steric sea level)

1. If you trust all data are ‚consistent', i.e. they show the same physics apart from sampling errors

$$\mathbf{X} = \left(\mathbf{Y}^{(1)}, \mathbf{Y}^{(2)}, \ldots, \mathbf{Y}^{(m)}\right)$$

$$\mathbf{C} = \frac{1}{pM}\mathbf{X}\mathbf{X}^T$$

Practical

2. If not, use the <u>same</u> basis for comparing. Compute EOFs from the above or from <u>one</u> of the data sets, project data on these and compare PCs

$$\mathbf{d}_i^{(m)} = \mathbf{E}^T \mathbf{y}_i^{(m)} \qquad \text{or} \qquad \mathbf{d}_i^{(m)} = \mathbf{E}^{(m^*)^T} \mathbf{y}_i^{(m)}$$

Related concepts: (Orthogonal) EOF rotation

$$\mathbf{y}_i = \sum_{j=1}^{n} d_{j;i}\mathbf{e}_j = \mathbf{E}\mathbf{d}_i$$

$$\Big\downarrow \; \mathbf{V}^T\mathbf{V} = \mathbf{I}$$

$$\mathbf{F} = \mathbf{E}\mathbf{V}^T \longrightarrow \mathbf{F}^T\mathbf{F} = \mathbf{V}\mathbf{E}^T\mathbf{E}\mathbf{V}^T = \mathbf{I}$$

$$\mathbf{y}_i = \mathbf{F}^T\mathbf{r}_i$$

$$\Big\downarrow$$

$$\mathbf{r}_i = \mathbf{V}\mathbf{d}_i = \mathbf{F}^T\mathbf{y}_i \longrightarrow \mathbf{C}_\mathbf{r} = \mathbf{V}\mathbf{\Lambda}\mathbf{V}^T$$

REOFs are still orthogonal - RPCs are correlated now.

How can we use this degree of freedom?

Part II: Principle component analysis and related ideas

Related concepts: REOF, how can we use this degree of freedom? I.e. how do we find the rotation matrix?

E.g. VARIMAX, maximize the variance of the square of the REOFs (i.e. the spreading of the total variability of the modes)

$$\mathcal{F}(\mathbf{V}) = \sum_{i=1}^{\bar{n}} \left(\sum_{j=1}^{n} f_{j;i}^4 - \frac{\gamma}{n} \left(\sum_{j=1}^{n} f_{j;i}^2 \right)^2 \right) \qquad \mathbf{F} = \mathbf{E}\mathbf{V}^T$$

E.g. ICA, minimize 3th / 4th statistical moments of the REOFs to maximize the independence of the RPCs

Part II: Principle component analysis and related ideas

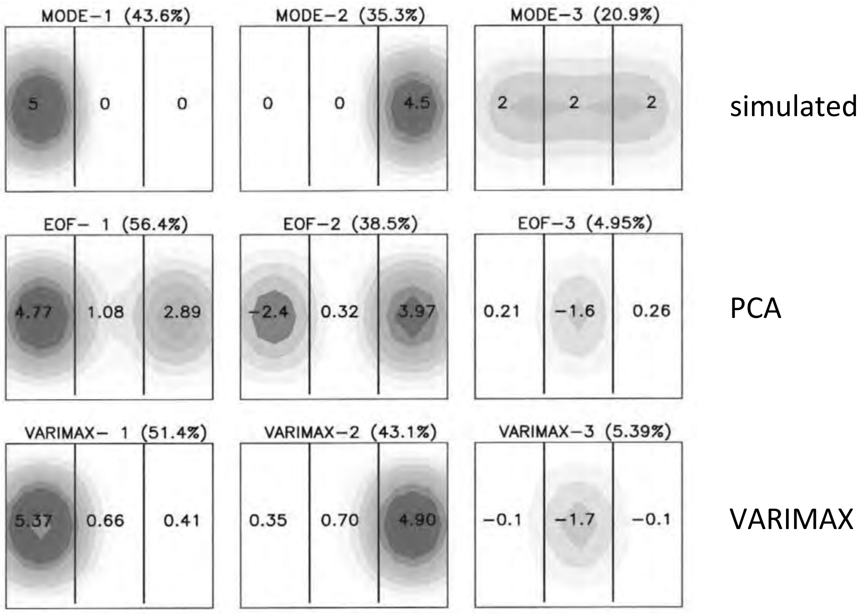

Dommenget & Latif (J Clim 2001)

53

Jürgen Kusche

DFG SPP 1257

Take-home message

Filtering is a necessary tool for interpreting GRACE data correctly.

- What we have discussed here are the options that the user of Level-2 data products has. Some filtering has been applied in the Level-1 processing as well. There is simply no point in using ‚unfiltered' data.

PCA is a useful tool for interpreting GRACE and other geophysical data and model outputs. It is either applied as a kind of filtering (see above) or as a tool to explore the major directions of data variability.

- It is easy to construct counterexamples where PCA fails to isolate physical modes!
- „PCA may help you to find the needle in the haystack. But once you found it, you should be able to recognize it as a needle" [v. Storch]. I.e. you should be able to assign some physics to it, otherwise it might be just an artefact.

54

Jürgen Kusche

DFG SPP 1257

The global climate system and the water cycle

Andreas Hense

Sommerschule ”Globaler Wasserkreislauf” 13. September 2011

Meteorologisches Institut Universität Bonn

universitätbonn
RHEINISCHE FRIEDRICH-WILHELMS-UNIVERSITÄT

Climate System as the bio-geophysical/chemical Earth system

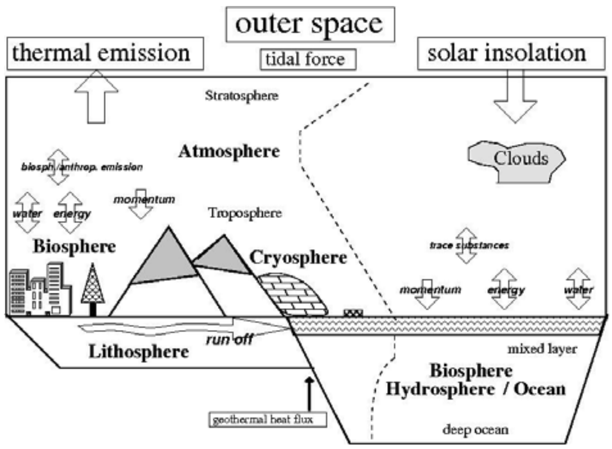

The division is based on

- the media (Gases, water in liquid /solid phase, biological material poreous solids)
- the time scales e.g. defined by the impulse response function / correlation function of typical fluctuation
- the couplings between the subsystems.

	Atmosphere:	Ocean:	Lithosphere
mass M:	1	16	0.5
heat capacity $M \cdot c_p$:	1	68	0.5

Interacting cycles

- Energy cycle; basic mathematical description is through the First Law of Thermodynamics
- Hydrological cycle; basic mathematical description is through the conservation law of water mass, continuity equation
- angular momentum cycle; basic mathematical description is through the conservation law of angular momentum (modified Newton's law, Navier Stokes equations in a rotating frame of reference)

- trace elements and trace particles; basic mathematical description is mass conservation (continuity equation) and the law of mass action from chemistry e.g. for C,N, S (bio-geochemical cycles)
- the (non-reactive) bulk mass of each subsystem, mathematical description by mass conservation, continuity equation

Application of classical hydro-thermodynamics with phase changes of water and possibly reactive cycles, liquid/solid water and trace particles distinguished by particle size and shape

Boundary conditions

- **solar insolation** as external and variable parameter of the energy cycle
- **Land-Ocean distribution** e.g. influences the hydrological cycle
- **orography on land and in the ocean, land-ocean distribution und Earth rotation velocity and the Moon by its ephemerides** are relevant external parameter of the angular momentum cycle in atmosphere and ocean
- solar insolation influences bio-geochemical cycles e.g ozone or through photosynthesis

Two definitions of the climate / Earth system which are complementary

- e.g. the energy cycle: First law $de = \delta q + \delta a$ in its variants for the subsystems
- the exchange of energy, momentum and mass across the boundaries between the subsystems: the interface between two systems can not store a property therefore fluxes of energy, momentum and mass directed to or away from the boundary have to sum to zero: budget conditions

Further ordering is necessary to keep the problem tractable ...

climatology, scales in space and time, statistics and statistical physics

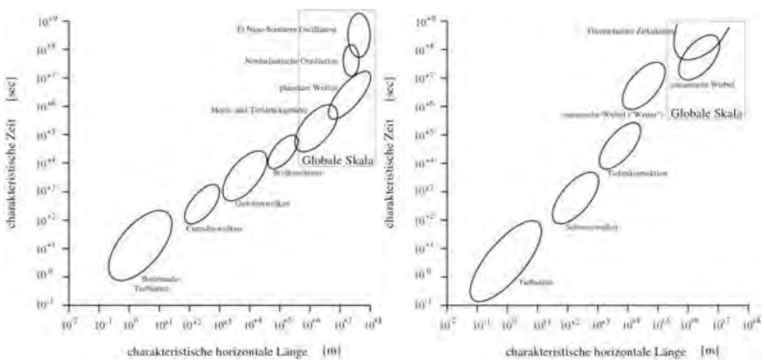

Spatial and temporal scales

- climate dynamics are realized on vastly different space and time scales
- for analysis one has to select a-priori specific scales
  - *urban climate*
  - *regional* or **mesoscale climate**
  - **global climate**

The problem of high dimensionality

- total volume of the global climate system: spherical shell of depth $h \sim 100$km
- smallest unit volume $V_0 \sim 1\text{mm}^3 = 10^{-9}\text{m}^3$ "Kolmogorov" micro-scale
- within each unit volume there are $n_i \sim \mathcal{O}(100)$ variables like T, p, ρ_i, u, v, etc

$$\begin{aligned} V &\sim 4\pi h R_{Earth}^2 \\ &\sim 4\pi 10^5 (6.37^2 10^{12}) \\ &\sim 5 \quad 10^{19} m^3 \\ \frac{V}{V_0} &\sim 5 \quad 10^{28} \\ \frac{V n_i}{V_0} &\sim 10^{31} \end{aligned}$$

There are about 10^{31} degree-of-freedom to be treated

- arrange all degrees-of-freedom in a state vector $\vec{Y}$
- the classical statistical physics argument: detailed computations are not possible
- the climate state vector is a random variable $\vec{Y}$
- define a probability density $p(y)$for a specific climate state

$$\mathrm{Prob}(\vec{Y} \in \mathrm{Sphere}(\vec{y}, d\vec{y})) = p(\vec{y})d\vec{y}$$

Nonlinearities

- probabilistic descriptions not only for high dimensional systems
- but also for nonlinear, dissipative, lowdimensional systems (z.B. $dim(\vec{x}) = 3$), Eckman and Ruelle, 1985
- Lorenz (1963): butterfly effect (actually a sea gull effect)
- minimal differences in initial conditions magnify exponentially
- dissipation counteracts and keep the phase space trajectories on the attractor
- two initially indistinguishable states evolve into two randomly selected states on the attractor
- positive Lyapunov exponents

yet another interpretation

a system far from thermodynamical equilibrium

- differential solar insolation, high at the equator, low at polar latitudes (black body radiation at $\sim$ 6000 K)
- differential loss of radiative energy by thermal emissions at $\sim$ 250-280K, higher in low latitudes than at higher latitudes
- continously externally driven system
- continously generating entropy
- the climate system state probability $p(y)$ (climate-pdf) can not computed from first principles

- climatology now is the description of the climate-pdf and its dynamics (similar as in statistical physics of non-equilibrium systems)
- direct computation e.g. by a master equation or even only a Fokker-Planck equation prohibitive due to the high dimensional problem
- climate modelling can offer a first solution if the climate model is low dimensional ($< 20 - 100$)
- only reasonable solution: estimate properties of the climate pdf from data
- unfortunately reality provides only one realisation / one sample, single case probability, non-ergodic
- climate modelling can offer a second solution: Monte Carlo simulations

climate modelling

climate system: a system of coupled cycles

- energy cycle based on the First Law
- water cycle based on the conservation of water mass
- angular momentum cycle based on angular momentum conservation/Newton's law
- trace substances cycles based on mass conservation and law of mass action
- and inert mass conservation in each subsystem

Total energy equation in the atmosphere, valid on scales $L_x > 20$ km, $T > 1$h under hydrostatic assumption

$$\frac{\partial}{\partial t}(c_p T + Lq + \frac{v_H^2}{2}) + \nabla_H(\vec{v}_H(c_p T + Lq + \Phi + \frac{v_H^2}{2}))+$$
$$+\frac{\partial}{\partial p}(\omega(c_p T + Lq + \Phi + \frac{v_H^2}{2})) =$$
$$g\frac{\partial}{\partial p}(Q + \underbrace{H + LE}_{\text{turbulent and convective subscale fluxes}}) \quad (1)$$

- turbulent : Kolomogorov-Prandtl like threedimensional turbulence
- convective: thunderstorm related turbulence

Total energy equation (atmosphere), vertical average

$$\int \left(\frac{\partial}{\partial t}(c_p T + Lq + \frac{v_H^2}{2})\right)\frac{dp}{g} + \int \left(\nabla_H\left(\vec{v}_H(c_p T + Lq + \Phi + \frac{v_H^2}{2})\right)\right)\frac{dp}{g}$$
$$= \left(Q(p=0) - (Q + H + LE)(p_b)\right)$$

if $\omega(p_b) = 0$ on the resolved scales (no atmospheric mass transport into/out off the surface of the solid Earth or ocean

The atmospheric water budget

- total water concentration q_T in the atmosphere
- sum of water vapour concentration q, liquid water q_ℓ and frozen water q_I
- mass weighted verical average gives the total water substance in an atmospheric column $m_T = \int \rho q_T dz$ with the budget equation

$$\frac{d}{dt}m_T = \frac{\partial}{\partial t}m_T + \vec{\nabla}_h(\vec{v}_h m_T) = E - P$$

- m_T is called precipitable water experessed as height of a liquid water column
- E Evapo-Transpiration mass flux of water (MKS unit $\mathrm{kgm^{-2}sec^{-1}}$)
- P precipitation mass flux of water

Oceanic water budget

- ocean water is a solution of salt in freshwater
- salt concentration s and freshwater concentration $1 - s$
- budget equation for the vertical integral of the salt concentration $S = \int s dz$

$$\frac{d}{dt}(\int \rho_w (1 - s) dz) = -\rho_w \frac{d}{dt} S = P - E$$

- water sources of the atmosphere are salt source for the ocean

Energy budget equation time averaged and vertically averaged in atmosphere and ocean

$$\frac{\partial}{\partial t} e + \vec{\nabla}_h \vec{H}_e = \bar{Q}(p = 0)$$

energy and water budget equation vertically averaged for the atmosphere

$$\frac{\partial}{\partial t} e_A + \vec{\nabla}_h \vec{H}_{e,A} = \bar{Q}(p = 0) - (\bar{Q} + \bar{H} + L\bar{E})$$

$$\frac{\partial}{\partial t} m_T + \vec{\nabla}_h \vec{H}_m = \bar{E} - \bar{P}$$

energy and water budget equation vertically averaged for the ocean

$$\frac{\partial}{\partial t} e_O + \vec{\nabla}_h \vec{H}_{e,O} = \bar{Q} + \bar{H} + L\bar{E}$$

$$\frac{\partial}{\partial t} S + \vec{\nabla}_h \vec{H}_S = \bar{E} - \bar{P}$$

boundary conditions along the coastlines

$$\vec{H}_{e,O}\vec{n}_o = Q_{e,O} \sim 0$$

$$\vec{H}_S\vec{n}_o = Q_S = \sum_k Q_{S,K}\delta(\vec{r} - \vec{r}_k)$$

prognostic modelling is not possible: the system of equations is not closed

- transports $\vec{H}$ can not be calculated
- without considering the angular momentum budget in atmosphere and ocean
- mean $\bar{\vec{v}}_h$ and random fluctiations $\vec{v}'$ can not be calculated

but an inverse calculation is possible

- take Q, H, E, P and $\vec{H}$ from observations
- incomplete data
- spoiled by observational and sampling errors

under stationary conditions $\frac{\partial}{\partial t} e = 0, \frac{\partial}{\partial t} m_T = 0$ the budget equations can be reduced to

$$\vec{\nabla}_h \vec{H} = R$$

if observations and its errors can be characterized by

- transports $\vec{H}_{obs}$ with white Gaussian errors $\vec{\epsilon}_H$
- energy sinks/sources R_{obs} with white Gaussian errors ϵ_R

find $\vec{H}$ and R such that

$$\mathcal{J} = \frac{1}{2}\int\left((\vec{H}-\vec{H}_{obs})^T(\Sigma_H)^{-1}(\vec{H}-\vec{H}_{obs}) + \frac{(R-R_{obs})^2}{\sigma_R^2}\right)d\Omega + \int\left(\lambda(\vec{\nabla}\vec{H}-R)\right)d\Omega \overset{!}{=} \text{Minimum}$$

a variational problem with the Euler-Lagrange system of equations

$$\begin{aligned}\vec{\nabla}H - R &= 0\\ \Sigma_H^{-1}(\vec{H}-\vec{H}_o) - \vec{\nabla}\lambda &= 0\\ \frac{1}{\sigma_R^2}(R-R_o) - \lambda &= 0\end{aligned}$$

leading to an elliptical problem in λ

$$\vec{\nabla}(\Sigma_H\vec{\nabla}\lambda) - \sigma_R^2\lambda = (\vec{\nabla}H_o - R_o)$$

Top-of-the-atmosphere radiation budget (solar)

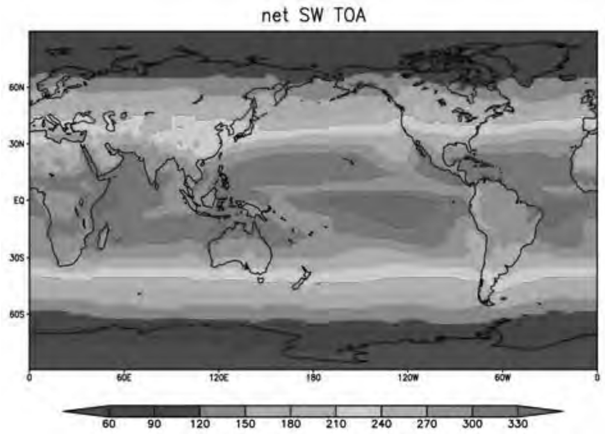

Top-of-the-atmosphere radiation budget(IR)

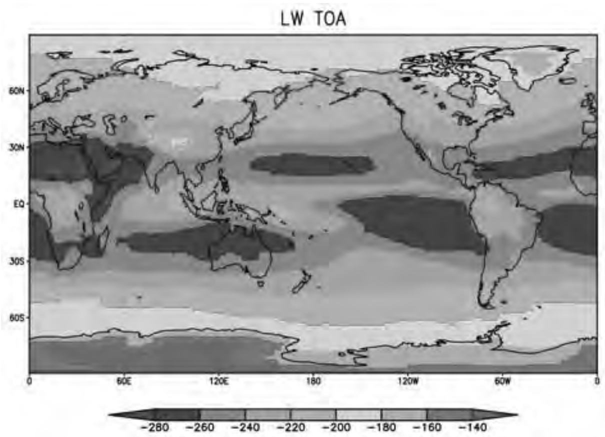

Top-of-the-atmosphere radiation budget (Net)

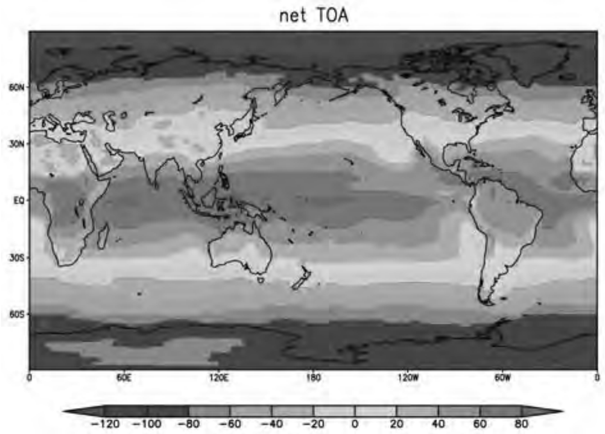

atmospheric energy budget (Diploma thesis Chris Wosnitza, 2011)

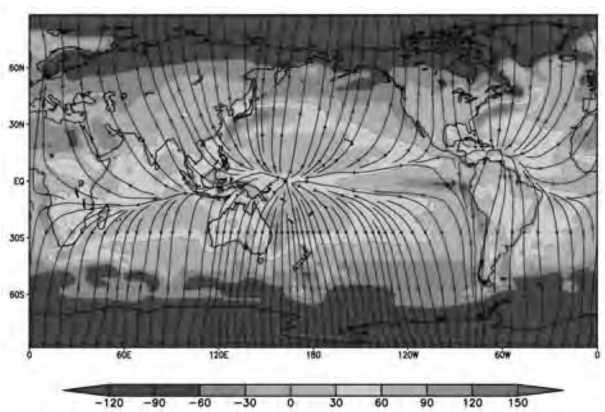

atmospheric water budget (Diploma thesis Chris Wosnitza, 2011)

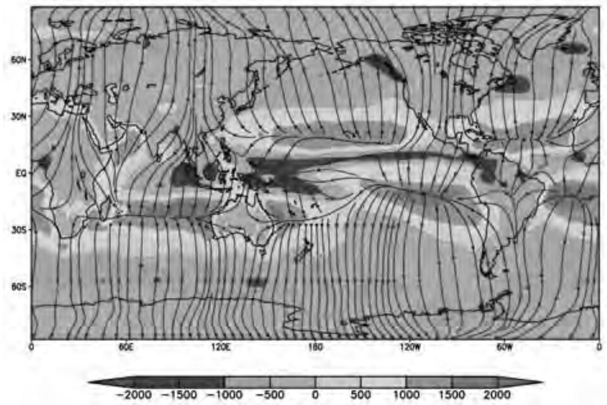

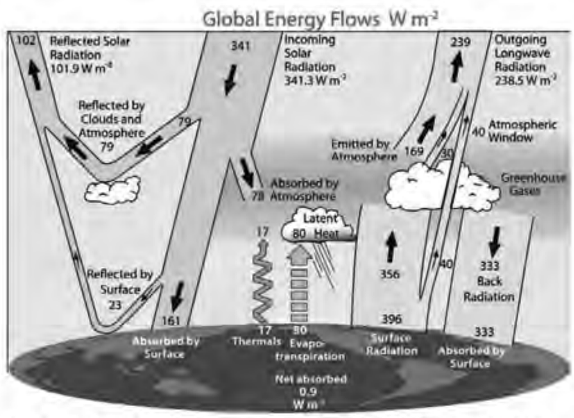

Fig. 1. The global annual mean Earth's energy budget for the Mar 2000 to May 2004 period (W m⁻²). The broad arrows indicate the schematic flow of energy in proportion to their importance.

in Wm^2 after Trenberth, Fasullo, Kiehl (2009) Earth global energy budget, Bull. Amerc. Meteorol. Soc, p.311-323

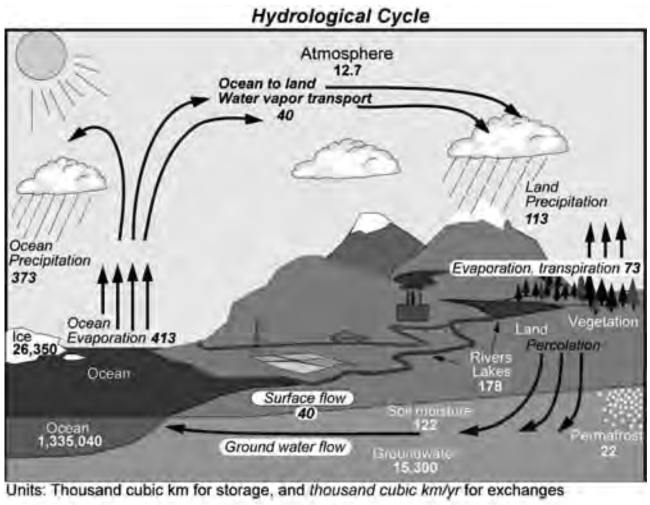

after Trenberth, Smith, Qian, Dai,Fasullo (2007) J. Hydrometeorology, 8, 758-769

Climate sensitivity: global mean temperature

- how large is the change ΔT of the global mean temperature if the CO_2 concentration are doubled?
- doubling CO_2 concentration will give a change in radiative forcing Q': $\Delta T = \lambda_0 Q'$
- feedbacks in the climate system will enhance the pure temperature change $\Delta T = \lambda_0(Q' + C\Delta T)$
- $\lambda_0 \sim 0.3 - 0.31 \mathrm{K}(\mathrm{W/m^2})^{-1}$
- equilibrium with ocean

$$\Delta T = \frac{\lambda_0}{1-f} Q'$$

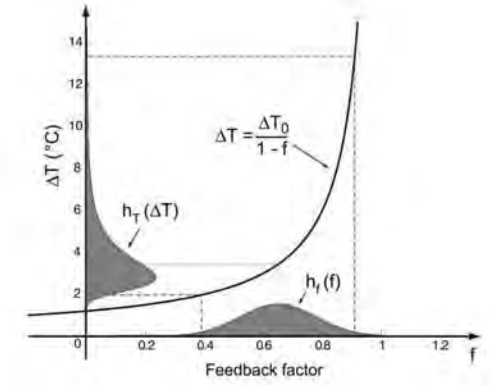

(after Roe and Baker (2007), Science, 318, 629ff)

Sensitivity of global mean water content ”precipitable water”:

$$W = \int_\lambda \int_\varphi \left(\int_0^\infty \rho q dz \right) a^2 d \sin\varphi d\lambda$$

$$\int_\lambda \int_\varphi \left(\int_0^{p_0} q \frac{dp}{g} \right) a^2 d \sin\varphi d\lambda$$

relative change

$$\frac{1}{W}\frac{dW}{dQ'} = \frac{1}{W}\frac{dW}{dT} \qquad \underbrace{\frac{dT}{dQ'}}_{\text{climate sensitivity}}$$

$$\frac{1}{W}\frac{dW}{dT} = \frac{1}{W}\frac{d}{dT}\int q\frac{dp}{g}$$
$$= \frac{1}{W}\frac{d}{dT}\int (r\frac{R_l e_s(T)}{R_w p}\frac{dp}{g}$$
$$\frac{1}{W}\int (r\frac{R_l}{R_w p}\frac{Le_s}{R_w T^2}\frac{dp}{g}$$
$$\sim \frac{L}{R_w T_R^2} \sim 0.065 - 0.075\mathrm{K}^{-1}$$

famous **Clausius-Clapeyron** constraint

Not correct for global mean precipitation:

$$\frac{d}{dt}W = E - P \sim 0$$

recycling time of atmospheric water $\sim$ 10 days
Instead consider atmospheric energy budget (equilibrium with ocean)

$$Q_c' + \frac{1-f}{\lambda_0}\Delta T = H' + LE' = LE'(1+\beta)$$

- Q'_c loss of energy by infrared radiation due to an increased CO_2 concentration
- $\frac{1-f}{\lambda_0}\Delta T$ gain of energy by absorption of radiative energy Q' from the surface
- β Bowen ratio $\frac{H'}{LE'}$
- water balance $E' \sim P'$

$$\frac{Q'_c}{L(1+\beta)} + \frac{1-f}{\lambda_0 L(1+\beta)}\Delta T = P'$$

Precipitation sensitivity: $\frac{1-f}{\lambda_0 L(1+\beta)} \sim 37\mathrm{mm}(\mathrm{yrK})^{-1}$
or about 3.7 % per K if $P \sim 1000\mathrm{mm}(\mathrm{yr})^{-1}$

The Basics
The Energy and Water cycles

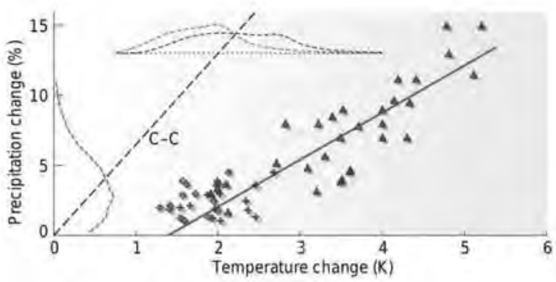

(after Allen and Ingram (2002), Nature, 419, 224)

Andreas Hense The global climate system and the water cycle

Lecture: Hydrological Models

Andreas Güntner

Summer School „Global Water Cycle“
12.-16. September 2011
Mayschoss

What is a hydrological model ?

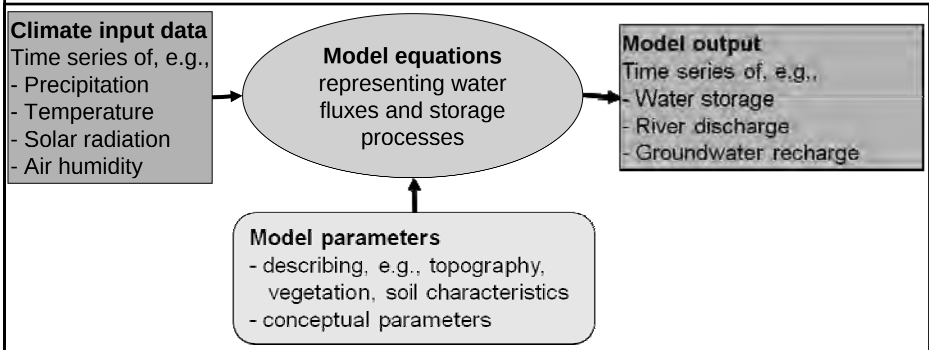

Storage variations in the continental water cycle

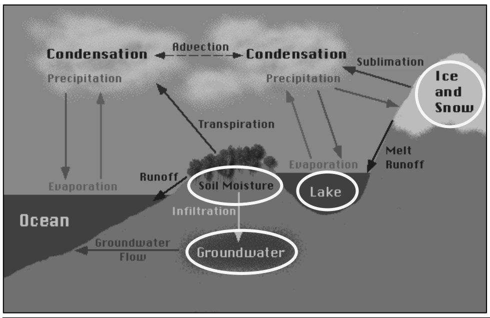

Several storage components:

- **Snow and ice**
- **Groundwater**
- **Soil moisture**
- **Surface water storage**

GRACE

$\boxed{\Delta S} = P - E - R$

Hydrological models

Continental water balance equation

P:	Precipitation
E:	Evaporation
R:	Runoff
ΔS:	Water storage change

Detailed physically-based models

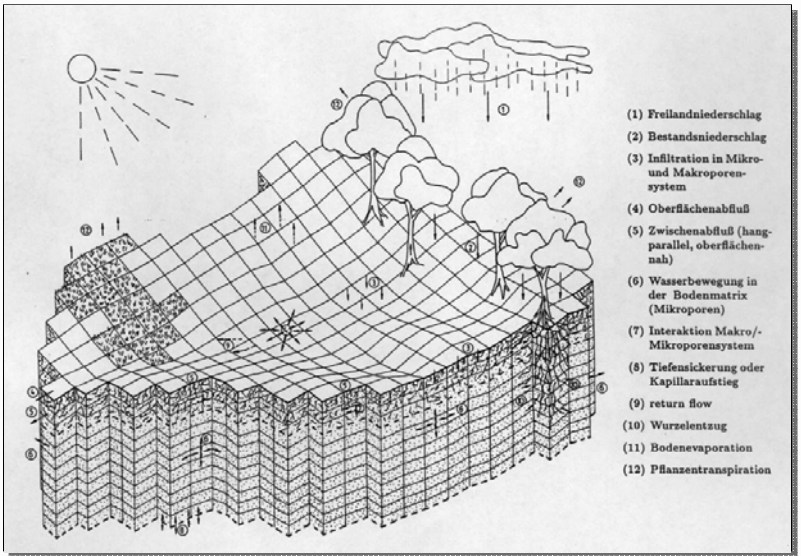

Detailed physically-based models

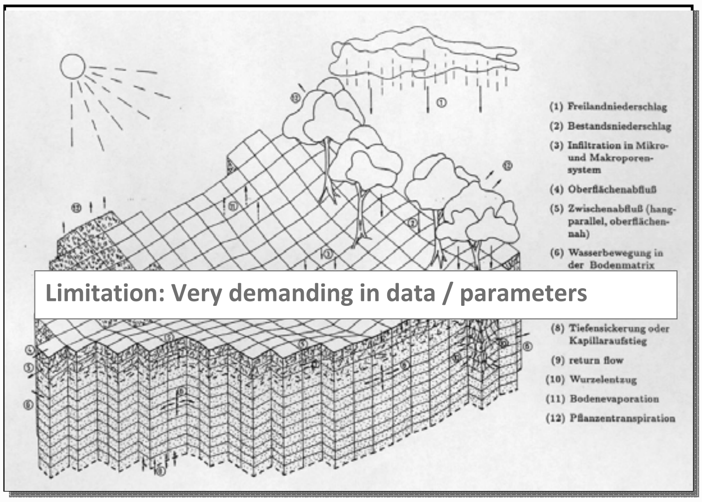

Limitation: Very demanding in data / parameters

5

For example:
Differential equation for unsaturated flow in a porous medium (Richards equation):

Soil water content

Hydraulic conductivity

$$\frac{\partial}{\partial x}\left(k_{xx}(\theta)\cdot\frac{\partial\psi}{\partial x}\right)+\frac{\partial}{\partial y}\left(k_{yy}(\theta)\cdot\frac{\partial\psi}{\partial y}\right)+\frac{\partial}{\partial z}\left(k_{zz}(\theta)\cdot\frac{\partial\psi}{\partial x}+1\right)=\frac{\partial\theta}{\partial t}-S$$

Gradient of soil water

Limitations of detailed physically-based models

Example: Soil water fluxes

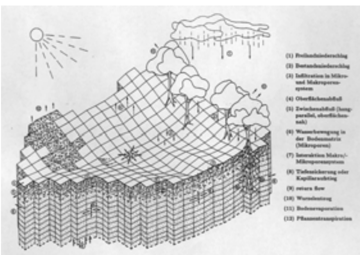

$$\frac{\partial}{\partial z}\left(k(\theta)\cdot\frac{\partial\psi}{\partial z}+1\right)=\frac{\partial\theta}{\partial t}-S$$

Richards equation assumes a **homogeneous porous medium**

$\neq$

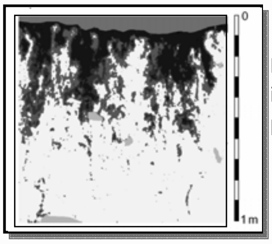

Real-world infiltration pattern in a soil

6

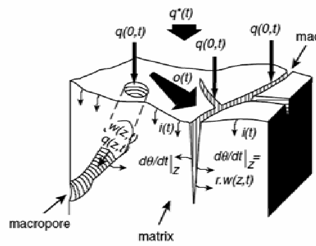

Physically-based model with macropores

Conceptual models

Linear storage (bucket approach)

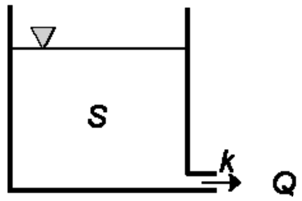

$$Q = k \cdot S$$

Q	Outflow (runoff)
k	Storage coefficient
S	Actual storage volume

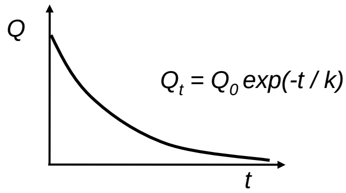

Conceptual models

Example: Soil and ground water fluxes

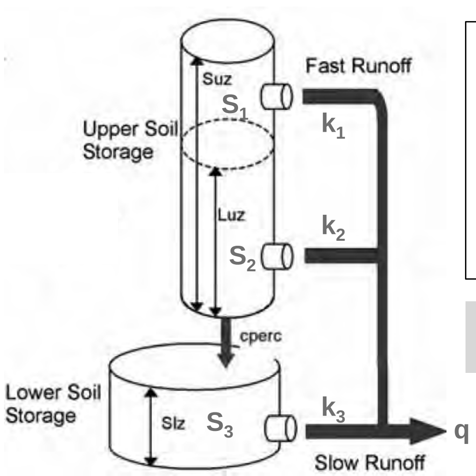

Linear storage approach used in many large-scale models

$$Q = k \cdot S$$

Q	Outflow (runoff)
k	Storage coefficient
S	Actual storage volume

k may be estimated/calibrated from observed discharge time series

Conceptual models

Example: Soil and ground water fluxes

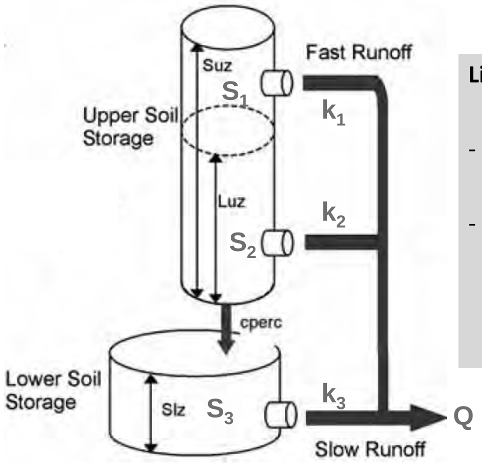

Limitations:

- Model cannot be transferred to other areas
- Model can usually only be applied to situations for which it has been calibrated (poor for extremes, inter-annual variations, trends)

Conceptual models

Runoff generation by a non-linear response function at the 0.5° scale

$$Q = P_{eff} \cdot \left(\frac{S}{S_{\max}} \right)^b$$

Q	Runoff
P_{eff}	Effective precipitation
S	Actual soil water content
S_{max}	Maximum soil water storage
b	Calibration parameter

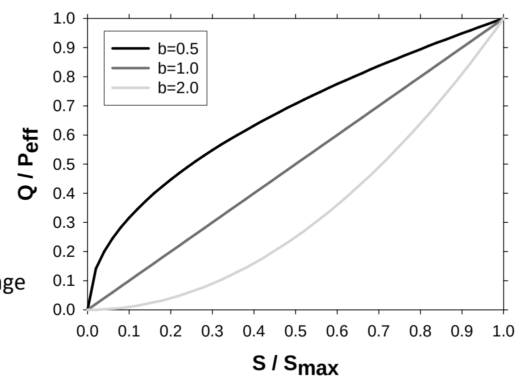

This equation is used in the WaterGAP global hydrology model (WGHM), for example.

Water storage – spatial variability

Tarrawarra catchment (Victoria, Australia) (Western & Grayson, 2001)

Water storage – spatial variability

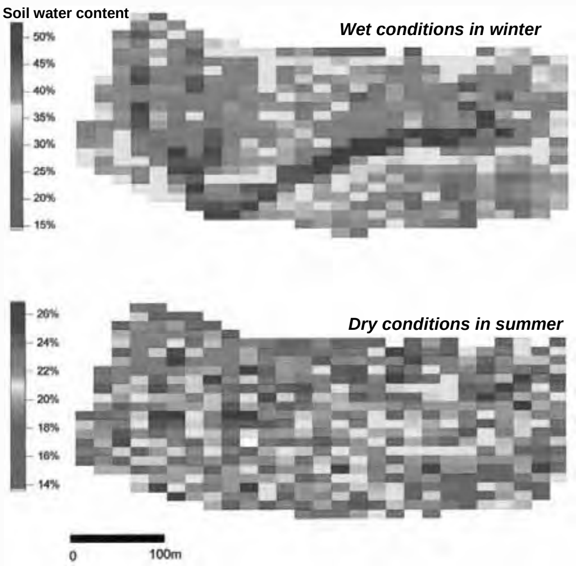

Tarrawarra catchment (Victoria, Australia) (Western & Grayson, 2001)

Representing spatial variability

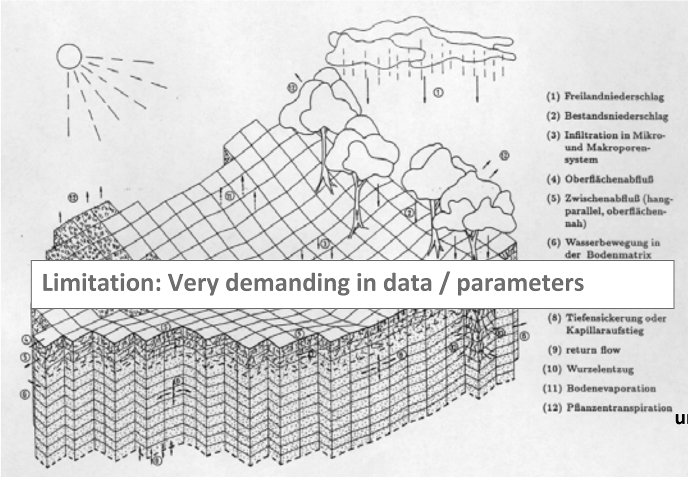

Limitation: Very demanding in data / parameters

For example: Differential equation for unsaturated flow in a porous medium (Richards equation):

$$\frac{\partial}{\partial x}\left(k_{xx}(\theta)\cdot\frac{\partial\psi}{\partial x}\right)+\frac{\partial}{\partial y}\left(k_{yy}(\theta)\cdot\frac{\partial\psi}{\partial y}\right)+\frac{\partial}{\partial z}\left(k_{zz}(\theta)\cdot\frac{\partial\psi}{\partial x}+1\right)=\frac{\partial\theta}{\partial t}-S$$

13

DFG SPP 1257

Representing spatial variability

Variations of parameter values within a grid cell

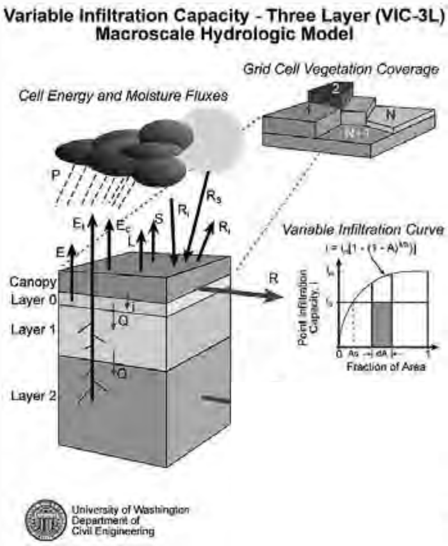

Mosaic approach

Distribution function

(Beispiel: VIC-Modell)

14

DFG SPP 1257

Large-scale models of continental hydrology

Land Surface Models

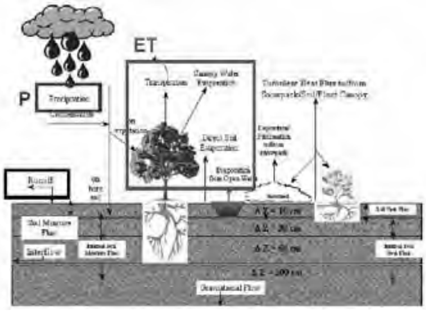

- Land surface description in climate models
- Water balance
- Energy balance
- (Carbon fluxes)
- Vertical water fluxes, several soil layers
- High temporal resolution (minutes-hours)

Global hydrological models

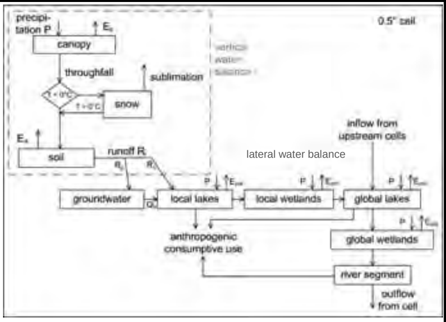

- Water balance for grid cells / river basins
- Lateral water fluxes
- Routing in river network
- (Water use / consumption)
- Daily – monthly temporal resolution
- Conceptual process representation

15

SPP 1257

Large-scale models of continental hydrology

Land Surface Models

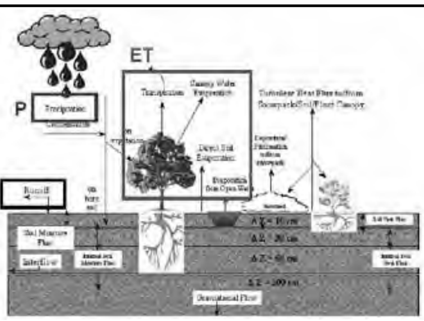

- Land surface description in climate models
- Water balance
- Energy balance
- (Carbon fluxes)
- Vertical water fluxes, several soil layers
- High temporal resolution (minutes-hours)

Global hydrological models

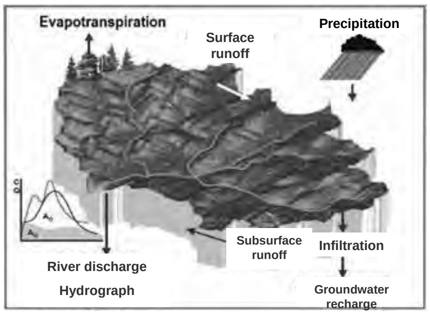

- Water balance for grid cells / river basins
- Lateral water fluxes
- Routing in river network
- (Water use / consumption)
- Daily – monthly temporal resolution
- Conceptual process representation

16

SPP 1257

Large-scale models of continental hydrology

WaterMIP (Water Model Intercomparison Project)

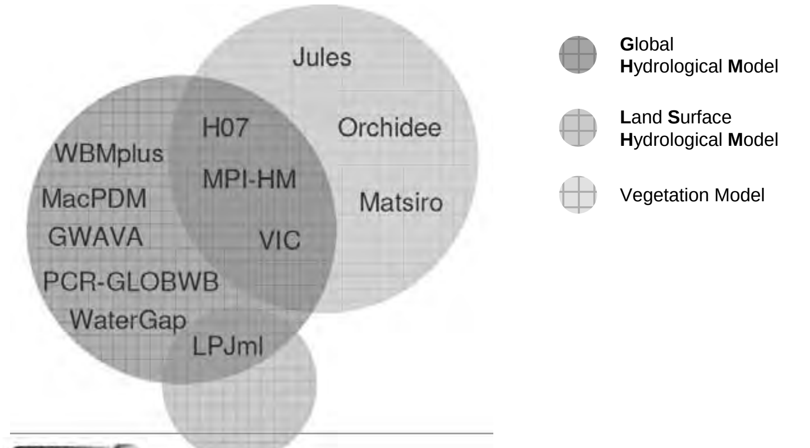

Haddeland et al. 2011, J. Hydrometeor.
Harding et al. 2011, J. Hydrometeor.

Large-scale models of continental hydrology

WaterMIP (Water Model Intercomparison Project)

Model name[1]	Model time step	Meteorological forcing variables[2]	Energy balance	Evapotranspiration scheme[3]	Runoff scheme[4]	Snow scheme	Reference(s)
GWAVA	Daily	P, T, W, Q, LWn, SW, SP	No	Penman-Monteith	Saturation excess / Beta function	Degree day	Meigh et al. (1999)
H08	6 h	R, S, T, W, Q, LW, SW, SP	Yes	Bulk formula	Saturation excess / Beta function	Energy balance	Hanasaki et al (2008a)
HTESSEL	1 h	R, S, T, W, Q, LW, SW, SP	Yes	Penman-Monteith	Infiltration excess / Darcy	Energy balance	Balsamo et al (2009)
JULES	1 h	R, S, T, W, Q, LW, SW, SP	Yes	Penman-Monteith	Infiltration excess / Darcy	Energy balance	Cox et al. (1999), Essery et al. (2003)
LPJmL	Daily	P, T, LWn, SW	No	Priestley-Taylor	Saturation excess	Degree day	Bondeau et al. (2007), Rost et al. (2008)
MacPDM	Daily	P, T, W, Q, LWn, SW	No	Penman-Monteith	Saturation excess / Beta function	Degree day	Arnell (1999); Gosling and Arnell (2010)
MATSIRO	1 h	R, S, T, W, Q, LW, SW, SP	Yes	Bulk formula	Infiltration and saturation excess / Groundwater	Energy balance	Takata et al (2003), Koirala (2010)
MPI-HM	Daily	P, T	No	Thornthwaite	Saturation excess / Beta function	Degree day	Hagemann and Gates (2003), Hagemann and Dümenil (1998)
Orchidee	15 min	R, S, T, W, Q, SW, LW, SP	Yes	Bulk formula	Saturation excess	Energy balance	De Rosnay and Polcher (1998)
VIC	Daily/ 3h	P, Tmax, Tmin, W, Q, LW, SW, SP	Snow season	Penman-Monteith	Saturation excess / Beta function	Energy balance	Liang et al (1994)
WaterGAP	Daily	P, T, LWn, SW	No	Priestley-Taylor	Beta function	Degree day	Alcamo et al (2003)

Haddeland et al. 2011, J. Hydrometeor.

Column 3: R: Rainfall rate, S: Snowfall rate, P: Precipitation, T: Mean daily air temperature, Tmax: Maximum daily air temperature, Tmin: Minimum daily air temperature, W: Wind speed, Q: Specific humidity, LW: Longwave radiation flux (downward), LWn: Longwave radiation flux (net), SW: Shortwave radiation flux (downward), SP: Surface pressure

Large-scale models of continental hydrology

WaterMIP (Water Model Intercomparison Project)

Global simulation results (mean annual values 1985-1999)

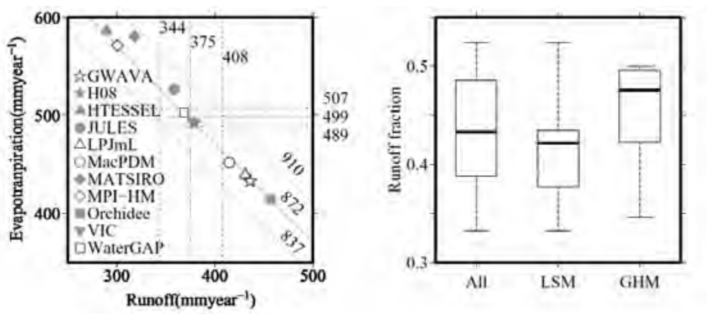

LSM: Land Surface Model

GHM: Global Hydrological Model

Haddeland, I., et al. (2011):
Multi-model estimate of the global terrestrial water balance: Setup and first results. J. Hydrometeor., in print.

Structure of large-scale hydrological models

Total continental water storage ≈ GRACE

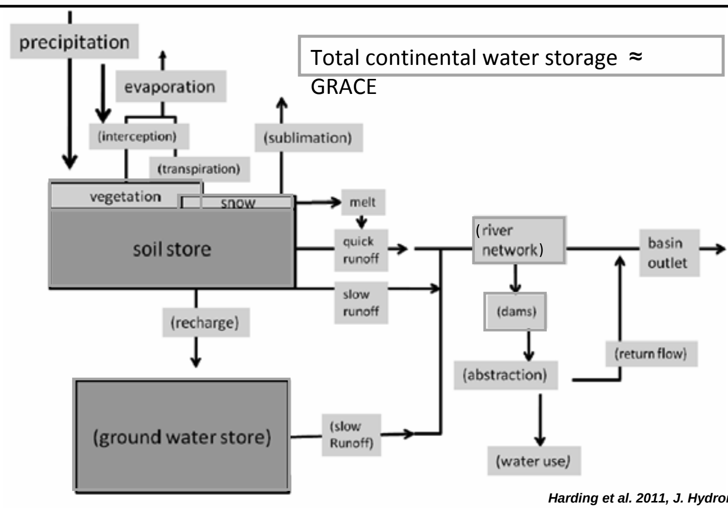

Harding et al. 2011, J. Hydrometeor.

Processes and storages in brackets are not represented in all models

Large-scale models of continental hydrology

1) WaterGAP Global Hydrology model (WGHM)

Total continental water storage change ΔS :

$\Delta S = \Delta S_{canopy} + \Delta S_{snow} + \Delta S_{soil} + \Delta S_{groundwater} + \Delta S_{rivers} + \Delta S_{lakes/reservoirs} + \Delta S_{wetlands}$

Soil depth = root zone

2) Land Dynamics (LaD) World

$\Delta S = \Delta S_{snow} + \Delta S_{soil} + \Delta S_{groundwater}$

Soil depth = root zone

3) Global Land Data Assimilation System (GLDAS)

$\Delta S = \Delta S_{canopy} + \Delta S_{snow} + \Delta S_{soil}$

Soil depth		
	GLDAS-CLM	= 3.43m
	GLDAS-Mosaic	= 3.50m
	GLDAS-Noah	= 2.00m
	GLDAS-VIC	= 1.90m

Large-scale models of continental hydrology

Variations of continental water storage

RMS variability of monthly values around annual mean for 2004
(in mm w.eq.)

LaD

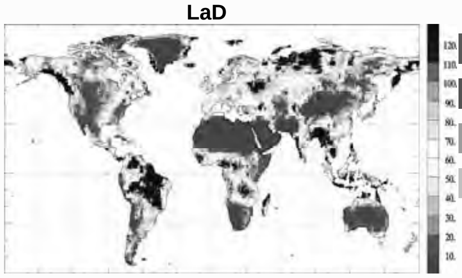

WGHM

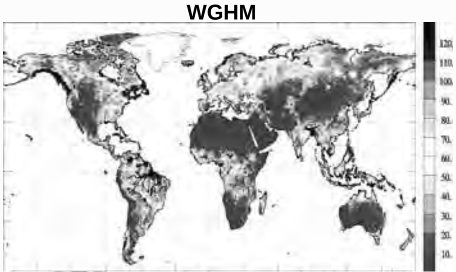

GLDAS-Noah

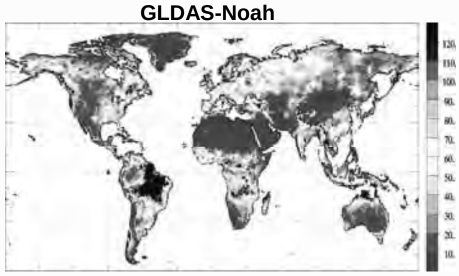

Variations of continental water storage

Mean monthly water storage in different storage compartments
(WGHM simulation results)

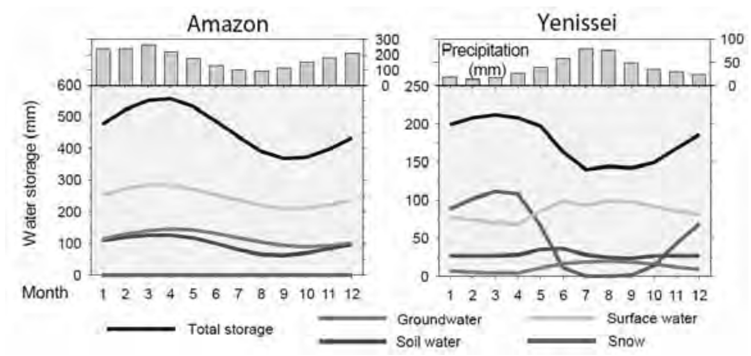

23

DFG SPP 1257

Variations of continental water storage

Köppen climate zones

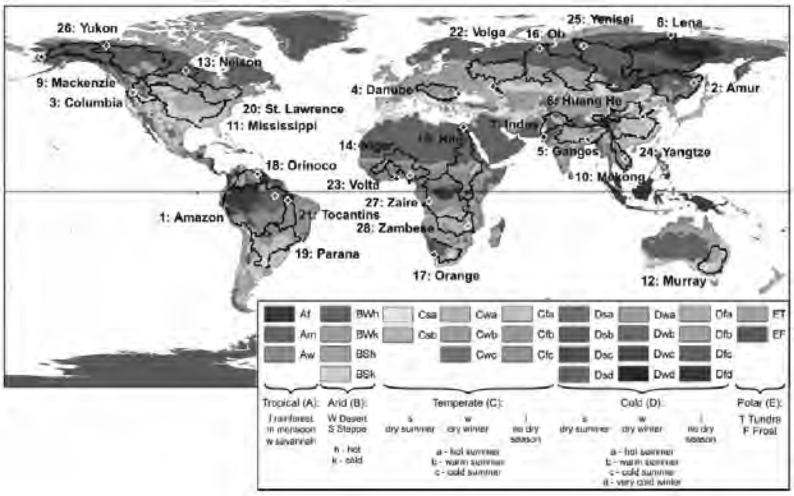

24

DFG SPP 1257

Variations of continental water storage

Month of maximum water storage (based on WGHM simulation)

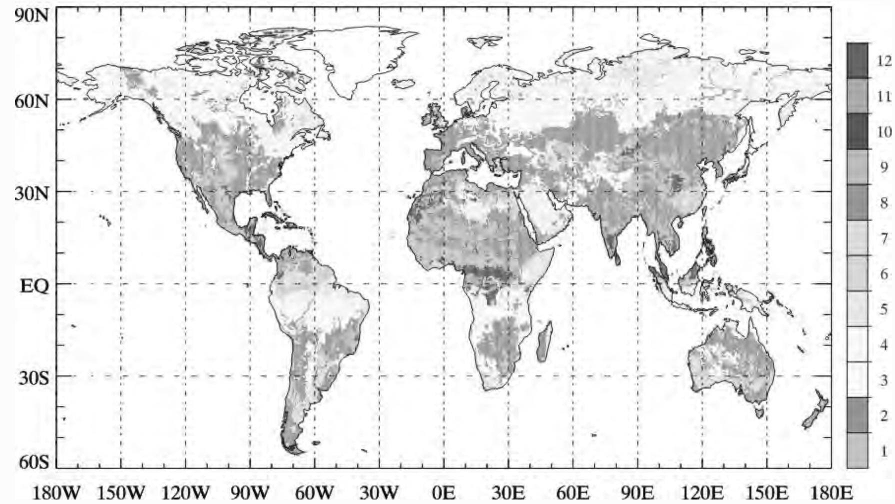

Güntner et al. 2007, WRR

Water storage variations at the river basin scale

Basin-average water storage – GRACE filter effects

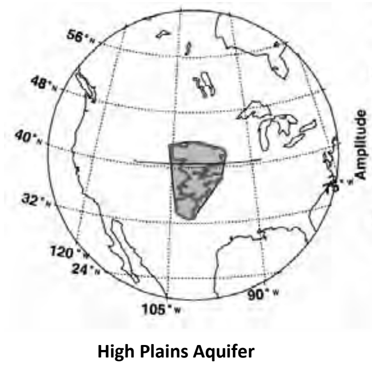

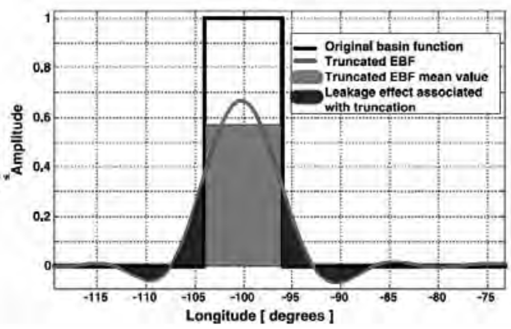

High Plains Aquifer

EBF: Effective basin function

(here: simple truncation at Lmax=60)

Longuevergne et al. 2010, WRR

Water storage variations at the river basin scale

Basin-average water storage – GRACE filter effects

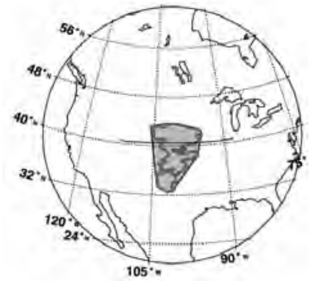

High Plains Aquifer

Effective basin function

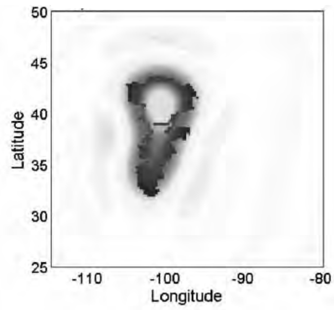

Swenson & Wahr (2002) filter

Longuevergne et al. 2010, WRR

DFG SPP 1257

Water storage variations at the river basin scale

GRACE filter-induced bias in basin-average water storage

	Bias of seasonal amplitude (mm)						Bias of seasonal phase (days)					
Filter type	**I**	**II**	**III**	**IV**	**V**	**VI**	**I**	**II**	**III**	**IV**	**V**	**VI**
Amazon	-18	-2	-6	-18	-47	1	-2	0	0	-1	-2	0
Amur	-3	0	-4	-3	-9	-1	-29	7	8	-40	-64	-7
Danube	-3	-15	-1	-1	-17	-2	5	1	4	2	9	3
Ganges	-27	-19	-22	-43	-49	-6	-3	-1	-2	1	-3	-2
Indus	-2	-7	-7	2	7	-5	-94	-41	-67	-91	-117	-29
Lena	-3	-1	-7	6	-8	0	1	1	6	-9	-5	3
Mackenzie	5	-1	-3	-9	-1	2	0	-1	-1	4	1	1
Mississippi	-1	0	-1	-7	-7	0	2	-1	1	17	1	-1
Nelson	1	-4	1	-5	-4	1	-3	2	1	6	-14	4
Niger	-8	-9	-15	2	-23	2	1	-1	-2	-1	2	0
Nile	-4	-4	-1	-17	-9	0	-4	-7	-4	8	-5	-5
Ob	-3	-1	-7	-2	-24	1	0	0	-1	2	5	0
Orange	3	7	5	4	5	-1	21	-167	-171	11	20	-119
Parana	-10	-31	-29	-16	-20	-11	2	9	8	7	3	4
St. Lawrence	-17	-16	-16	-47	-42	-2	6	-1	4	4	6	1
Tocantins	-42	-145	-27	-45	-89	-22	-4	2	-3	-4	-6	-4
Volga	-12	-7	-9	-10	-33	-2	1	0	2	4	4	1
Yangtse	2	-4	-1	-11	-5	0	-8	2	-3	1	-9	0
Yenisei	0	0	1	7	-15	2	-1	0	-2	-2	-2	-1
Yukon	4	3	-7	6	-8	17	-1	-3	-3	-3	-1	-2
Zaire	-1	-1	0	4	-8	1	-5	-2	-3	-19	-5	-5
Zambezi	-17	-22	-25	-21	-38	-2	2	2	2	1	2	1

Werth et al. 2009, Geophys. J. Int.

Filter type
I: Gaussian filter (500km)
II: Swenson & Wahr (2002) maximum allowed satellite error
III: Swenson & Wahr (2002) min. satellite and leakage error
IV: Seo et al. (2006) dynamic filter
V: Swenson & Wahr (2006) decorrelation filter
VI: Kusche (2007) decorrelation filter

DFG SPP 1257

Water storage variations at the river basin scale

GRACE filter-induced bias in basin-average water storage

Filter type	Bias of seasonal amplitude (mm) I	II	III	IV	V	VI	Bias of seasonal phase (days) I	II	III	IV	V	VI
Amazon	-18	-2	-6	-18	-47	1	-2	0	0	-1	-2	0
Amur	-3	0	-4	-3	-9	-1	-29	7	8	-40	-64	-7
Danube	-3	-15	-1	-1	-17	-2	5	1	4	2	9	3
Ganges	-27	-19	-22	-43	-49	-6	-3	-1	-2	1	-3	-2
Indus	-2	-7	-7	2	7	-5	-94	-41	-67	-91	-117	-29
Lena	-3	-1	-7	6	-8	0	1	1	6	-9	-5	3
Mackenzie	5	-1	-3	-9	-1	2	0	-1	-1	4	1	1
Mississippi	-1	0	-1	-7	-7	0	2	-1	1	17	1	-1
Nelson	1	-4	1	-5	-4	1	-3	2	1	6	-14	4
Niger	-8	-9	-15	2	-23	2	1	-1	-2	-1	2	0
Nile	-4	-4	-1	-17	-9	0	-4	-7	-4	8	-5	-5
Ob	-3	-1	-7	-2	-24	1	0	0	-1	2	5	0
Orange	3	7	5	4	5	-1	21	-167	-171	11	20	-119
Parana	-10	-31	-29	-16	-20	-11	2	9	8	7	3	4
St. Lawrence	-17	-16	-16	-47	-42	-2	6	-1	4	4	6	1
Tocantins	-42	-145	-27	-45	-89	-22	-4	2	-3	-4	-6	-4
Volga	-12	-7	-9	-10	-33	-2	1	0	2	4	4	1
Yangtse	2	-4	-1	-11	-5	0	-8	2	-3	1	-9	0
Yenisei	0	0	1	7	-15	2	-1	0	-2	-2	-2	-1
Yukon	4	3	-7	6	-8	17	-1	-3	-3	-3	-1	-2
Zaire	-1	-1	0	4	-8	1	-5	-2	-3	-19	-5	-5
Zambezi	-17	-22	-25	-21	-38	-2	2	2	2	1	2	1

Werth et al. 2009, Geophys. J. Int.

➡ **Consistent filtering of GRACE and hydrological model data needed before comparing or merging**

DFG SPP 1257

29

Water storage variations at the river basin scale

Flow chart for estimating basin-scale water storage variations from GRACE level 2 spherical harmonic products

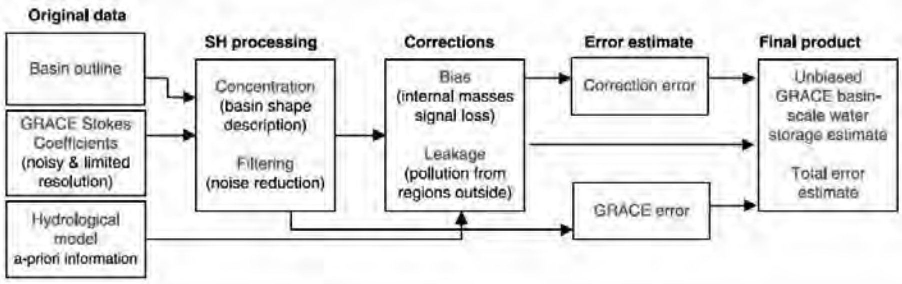

Longuevergne et al. 2010, WRR

➡

DFG SPP 1257

30

What is a hydrological model ?

Climate input data
Time series of, e.g.,
- Precipitation
- Temperature
- Solar radiation
- Air humidity

Model equations
representing water fluxes and storage processes

Model output
Time series of, e.g.,
- Water storage
- River discharge
- Groundwater recharge

Model parameters
- describing, e.g., topography, vegetation, soil characteristics
- conceptual parameters

31

DFG SPP 1257

Large-scale models of continental hydrology: parameters

Vegetation parameters (partly time-variable)
- Leaf area index
- Albedo
- Interception storage capacity
- Stomata resistence
- Aerodynamisc roughness
- Canopy hight
- Root depth
- …

Soil parameters
- Porosity
- Field capacity
- Hydraulic conductivity
- Soil depth
- Capillary head as function of water content
- Heat transport and storage
- …

Snow parameters, e.g., density, water and energy storage and transport parameters

Other hydrological / hydraulic parameters
- Slope gradient
- River cross section geometry
- Lake /reservoir storage capacity …..

32

DFG SPP 1257

Conceptual models

Example: Soil and ground water fluxes

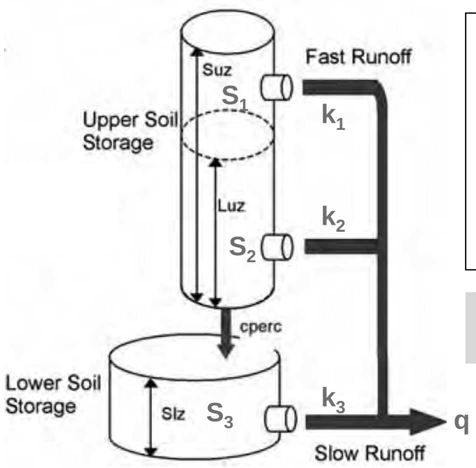

Linear storage approach used in many large-scale models

$$Q = k \cdot S$$

Q	Outflow (runoff)
k	Storage coefficient
S	Actual storage volume

k may be estimated/calibrated from observed discharge time series

33

What is a hydrological model ?

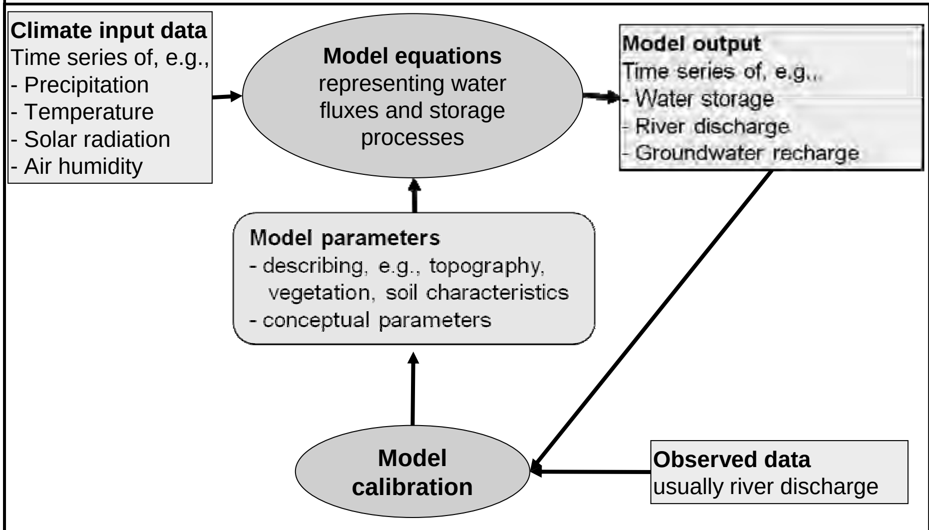

34

Calibration of hydrological models

35

Water balance of a river basin :

Traditional calibration variable

$$P = E + Q + \Delta S$$

Model input

Simulated in the model based on meteorological input data

P: Precipitation

E: Evapotranspiration

Q: Runoff (measured time series of river discharge)

ΔS: Water storage change

DFG SPP 1257

Calibration of hydrological models

36

River discharge simulations for the Danube basin (Hainburg, Austria, basin area 104 000 km²)

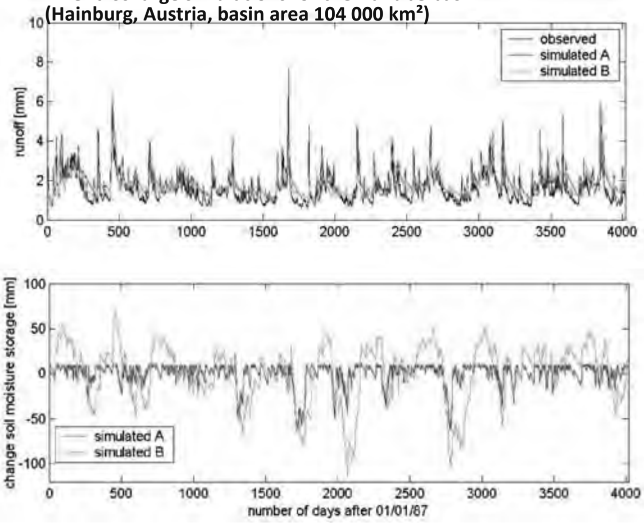

Simulated basin-average soil moisture for the two model versions

(Data from Merz & Blöschl, TU Wien)

DFG SPP 1257

Multi-criterial calibration of hydrological models

37

Water balance of a river basin :

$$P = E + Q + \Delta S$$

Traditional calibration variable (Q)

Additional calibration variable (ΔS)

P: Precipitation
E: Evapotranspiration
Q: Runoff (**measured time series of river discharge**)
ΔS: Water storage change (**basin-average values from GRACE**)

Multi-criterial calibration of hydrological models

38

Example: Amazon basin

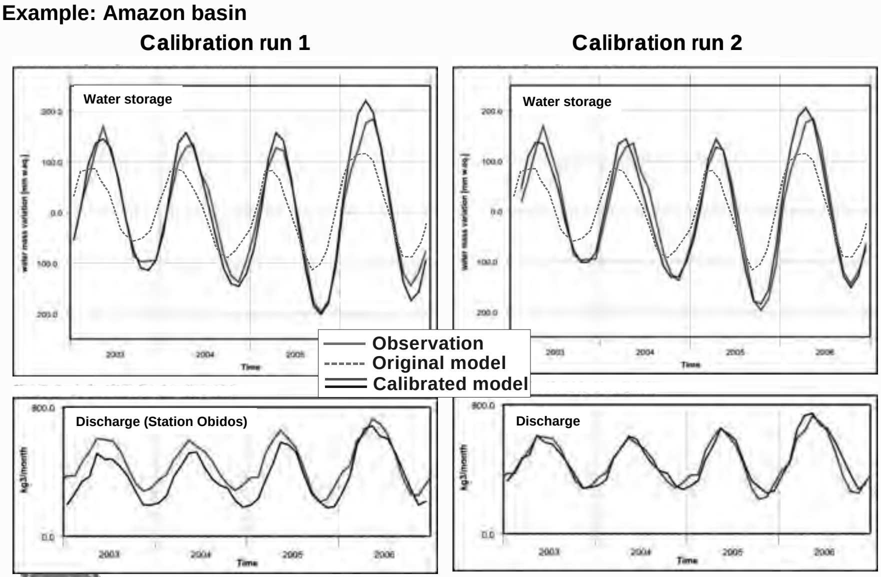

Multi-criterial calibration of hydrological models

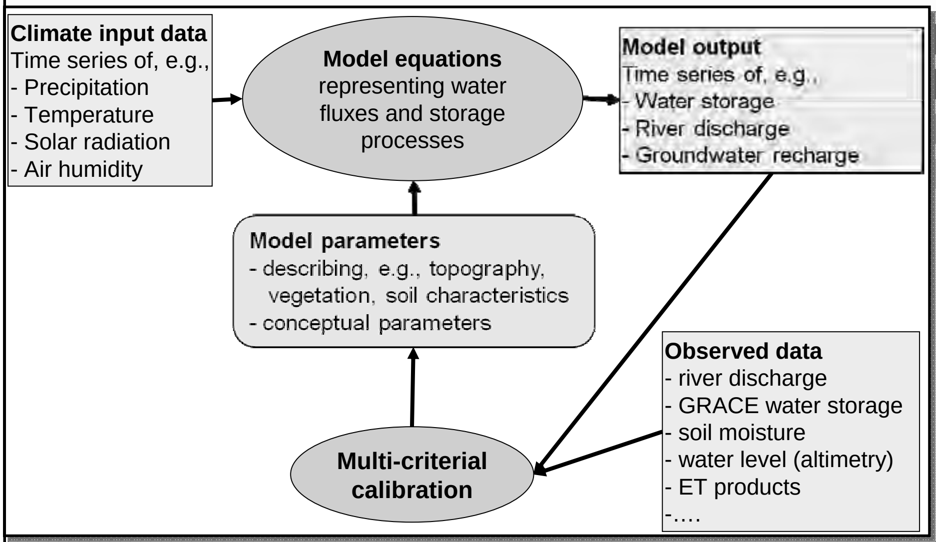

39

Integration of GRACE data into large-scale hydrological models

Water storage variations from GRACE are not routinely incorporated into hydrological models so far.

Only few examples:

- Zaitchik et al. (2008): Data assimilation, Kalman filter (Mississippi, CLSM)
- Werth et al. (2009, 2010): Multi-objective calibration (large basins worldwide, WGHM)
- Lo et al. (2010): Multi-objective calibration (Illinois, CLM)
- Milzow et al. (2011): Multi-objective calibration (Okavango, SWAT)

40

Availability of model output

Simulation results of global hydrological models usually are available on request from the modellers only.

Only few free download sites:

- GLDAS (Mosaic, CLM, Noah, VIC)
http://disc.sci.gsfc.nasa.gov/services/grads-gds/gldas

Lessons learned

- Large uncertainties / differences in simulation results of global hydrological models
→ try to use multi-model ensembles
- Preserve consistency when comparing / combining GRACE data and hydrological model data:
→ GRACE sees total water storage variations – a model should represent all storage compartments
→ do the same signal processing (filtering) for GRACE and model data
→ or: correct for filter effects (bias, leakage) in final GRACE-based basin water storage variations
- Comprehensive improvement of models by using various observation data (satellite-based) as multiple constraints

Lecture: Surface loading

Volker Klemann, GFZ

Summer School „Global Water Cycle"
12.-16. September 2011
Mayschoß

Motto

- Interaction between surface processes and solid earth

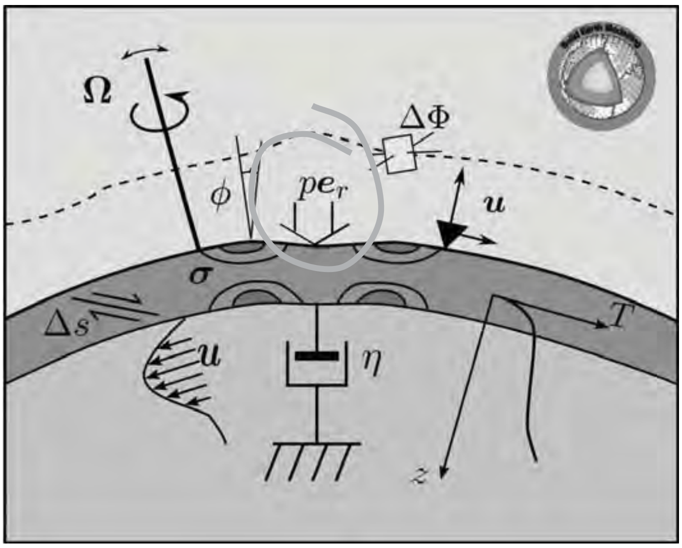

Overview

1. Mathematical prerequisites

   Surface load – loading processes – separation of signals – solid earth response – Representation by spherical harmonics– spheroidal/toroidal motion

2. The sea-level equation (SLE)

   Geoid – sea level – ocean function – moving coast line – coupling of surface and solid-earth processes – solution of SLE – features of solution

3. Reference systems

   Position and orientation in space

4. Glacial-isostatic adjustment

   The process – field equations – solution

1. Mathematical prerequisites

- Concept of a surface load
- Processes acting as a surface load
- Separation of signals
- Solid earth response
  - Excursion to physical meaning of Legendre degrees 0 and 1
  - Toroidal motion

1. Concept of surface load

Surface mass density at earth surface, a, is defined as

$$\sigma(a,\Omega) := \int_{r_0} \rho_\sigma(r,\Omega)\,dr \,.$$

$\Omega = (\theta, \phi)$ is the coordinate pair,

r_0 is the considered radial range,

ρ_σ is the density distribution of the load.

1.2 Processes acting as a surface load

- Hydrological water storage
- Mass redistribution inside the ocean
- Glacial melting
- (Atmosphere)

GFZ Helmholtz Centre POTSDAM

1.3 Separation of signals

- Spatial distribution
  - Masking
  - Spectral analysis
  - EOF ?
- Temporal behavior
  - Spectral analysis (annual signal)
  - Separation of linear trend
  - EOF ?

7

DFG SPP 1257

GFZ Helmholtz Centre POTSDAM

Temporal variations of geoid from GRACE

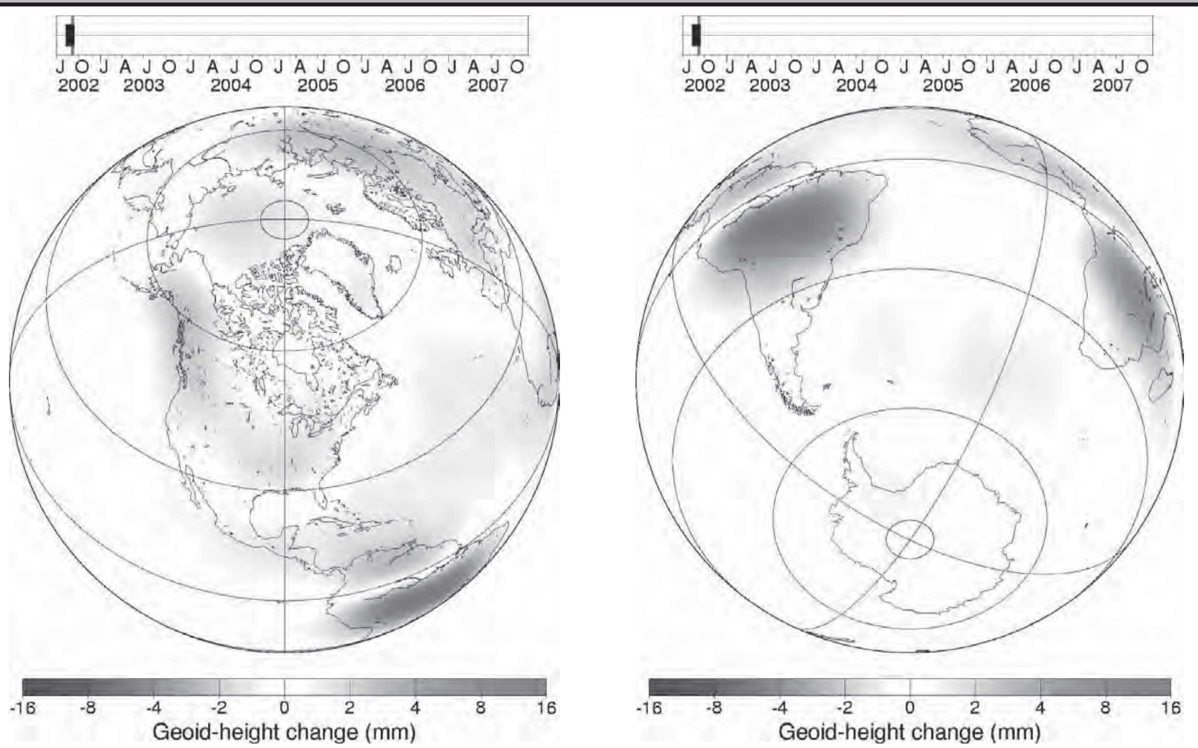

8

courtesy of I. Sasgen

DFG SPP 1257

1.4 Solid earth response

- Representation of fields
- Linear response
- Relation between load and displacements expressed by load-Love numbers

Spectral representation of field quantities

Displacement

$$u(r,\Omega) = \sum_{lm} \Big[U_{lm}(r)\, S_{lm}^{(-1)}(\Omega) + V_{lm}(r)\, S_{lm}^{(+1)}(\Omega) + W_{lm}(r)\, S_{lm}^{(0)}(\Omega) \Big]$$

Potential perturbation

$$\varphi_1(r,\Omega) = \sum_{lm} \Phi_{lm}(r)\, Y_{lm}(\Omega)$$

1.4.2 Toroidal motion

$$u_{\text{toro}}(r,\Omega) = \sum W_{jm}(r)\, Sjm^{(0)}(\Omega)$$

where

$$S^{(0)}_{jm} = (e_r \times \nabla_\Omega)\, Y_{jm}$$

Motion is not excited as long as

1. the earth structure is spherical symmetric
2. the loading is only acting in vertical direction

Convolution integral

Surface mass density

$$\sigma(\Omega) = \sum \Sigma_{lm}\, Y_{lm}(\Omega)\,.$$

Spherical symmetry of Earth structure

$$\Rightarrow \quad \varphi(\Omega) = a^2 \int_{\Omega_0} g_\varphi(\gamma)\, \sigma(\Omega')\, d\Omega\,, \quad \gamma = |\Omega - \Omega'|,$$

with Green's function,

$$g_\varphi(\gamma) = \sum_l G^\varphi_l\, P_l(\cos\gamma)\,,$$

$$\Rightarrow \quad \varphi(\Omega) = 4\pi a^2 \sum G^\varphi_l\, \Sigma_{lm} Y_{lm}(\Omega)\,.$$

Green's functions – Load Love numbers

Displacement of reference potential and surface:

$$g_e(\gamma) := a/M_e \sum_l (1 + k_l)\, P_l(\cos\gamma)\ ,$$

$$g_u(\gamma) := a/M_e \sum_l h_l\, P_l(\cos\gamma)$$

where h_l and k_l are the load Love numbers.

$$e(\Omega) = \frac{3}{\bar{\rho}} \sum \frac{1 + k_l}{2l + 1} \Sigma_{lm}\, Y_{lm}(\Omega)$$

$$u(\Omega) = \frac{3}{\bar{\rho}} \sum \frac{h_l}{2l + 1} \Sigma_{lm}\, Y_{lm}(\Omega)$$

GFZ
Helmholtz Centre
POTSDAM

Characteristics of Love numbers

- Response of solid earth
  - Spherical symmetric (average crust, no difference between continent and ocean)
  - Elastic, compressible
  - The effect of self gravitation is considered

see GIA section

- h, k, l describe vertical, potential and horizontal displacement.
- 2 process
  - load Love numbers (response to surface pressure)
  - tidal love numbers (response to tidal forcing)
- They are valid for instantaneous processes
- Anelasticity is not considered

Load Love numbers

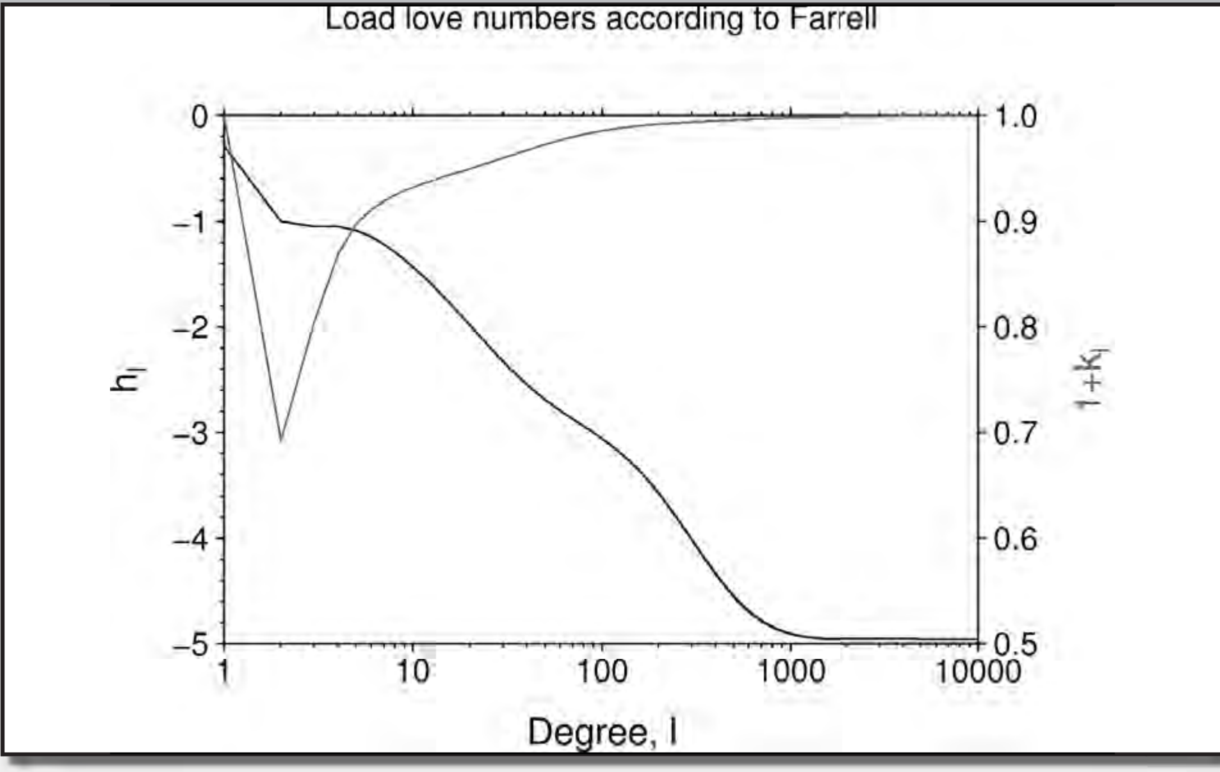

1.4.1 Legendre degrees 0 and 1

$$\int_\Omega Y_{lm}\, d\Omega = \sqrt{4\pi}\,\delta_{l0}\,\delta_{m0}\,,$$

$$\int_\Omega \sigma d\Omega = 0 \quad \Rightarrow \quad [U, E]_{00} = 0$$

$$\int_\Omega S^{(\lambda)}_{jm}\, d\Omega = \sqrt{\frac{4\pi}{3}}\,\delta_{j\,1}\,(2\,\delta_{\lambda\,1} + \delta_{\lambda\,-1})\,e_m$$

$$u_{\mathrm{CF}} := \frac{1}{A}\int_{\partial V} u\, dS \propto [U, V]_{1m}\Sigma_{1m}$$

$$u_{\mathrm{CM}} := \frac{1}{M}\left(\int_V \rho u\, dV + \int_{\partial V} \sigma r\, dS\right) \propto \Phi_{1m}\,\Sigma_{1m}$$

How is the water distributed in the loaded bath-tub if the ice is melting?

$$m_{\text{load}}(\Omega) = m_{\text{ice}}(\Omega) + m_{\text{oce}}(\Omega) = 0\,.$$

1. Definition of geoid
   Physicist – Geodesist
2. Definition of sea level variation
   Static equilibrium surface – deforming earth
3. Ocean function
   Where can water be filled into?
4. Moving coastlines
   A bathtub with slopes
5. Coupling
   Loading effect of redistributed water
6. Formulation of SLE
   Integral equation
7. Features of its solution

GFZ Helmholtz Centre Potsdam

2.7 Features of solution

19

– Ice load
– Conservation of mass
– Gravitational attraction
– Deformation
– Change of geoid
– Melting of ice

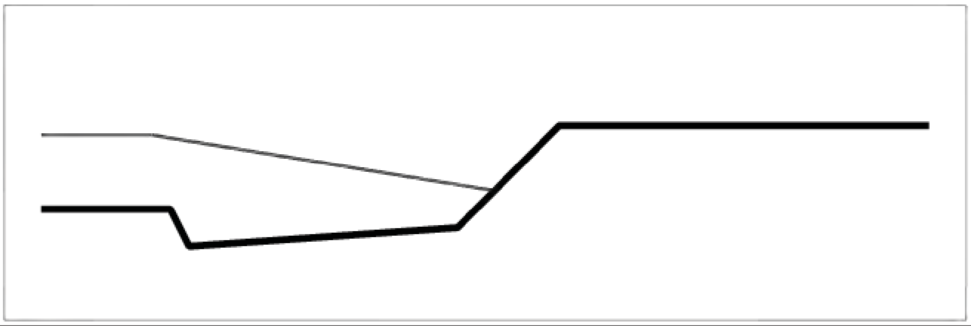

DFG SPP 1257

GFZ Helmholtz Centre Potsdam

2.1 The concept of geoid

20

The geoid is that equipotential surface which would coincide exactly with the mean ocean surface of the Earth, if the oceans were in equilibrium, at rest (relative to the rotating Earth), and extended through the continents (such as with very narrow canals).

According to C.F. Gauss, who first described it, it is the "mathematical figure of the Earth", a smooth but highly irregular surface that corresponds not to the actual surface of the Earth's crust, but to a surface which can only be known through extensive gravitational measurements and calculations.

Wikipedia

DFG SPP 1257

Geodesists view?

The reference geoid is defined by a specific potential value (IERS-2010 convention)

$$W_0 = 62636856.0\,\mathrm{m}^2\,\mathrm{s}^{-2} \pm 0.5\,\mathrm{m}^2\,\mathrm{s}^{-2}$$

So, the geoid corresponds to the equipotential surface, W_0??

$$\Rightarrow \quad e(\Omega) = \varphi_1(\Omega)/g_0$$

We call this quantity potential displacement.

21

DFG SPP 1257

2.2 Definitions of sea level

The geoid is defined as

$$n(\Omega, t) := e(\Omega, t) + h_{\mathrm{wl}}(t)$$

with h_{wl} the distance between the reference-potential height and the potential height which the current sea level is following.

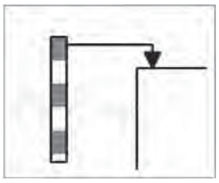

Then, relative sea level:

$$h_{\mathrm{RSL}}(\Omega, t) := [n - u](\Omega, t) - [n - u](\Omega, t_0) \,,$$

altimetric sea level:

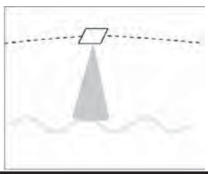

$$h_{\mathrm{alt}}(\Omega, t) := n(\Omega, t) - n(\Omega, t_0)$$

22

DFG SPP 1257

Definitions of datum

- Surface displacement, h_{surf}, is measured by GPS is measured in a specific reference system.
- Altimetric sea level, h_{alt}, is measured in a specific reference system.
- Relative sea level: Sea level change at a tide gauge
- The relative sea level is the difference, $h_{alt} - h_{surf}$, only if the reference systems, +, are defined in the same way.

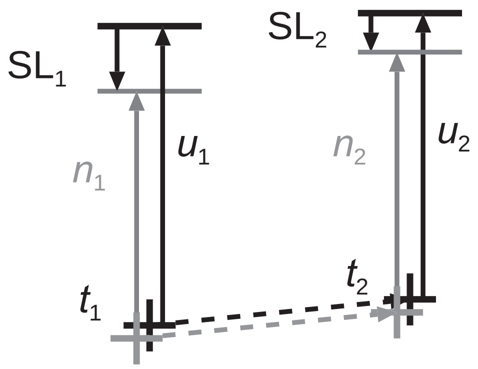

$$h_{surf} = u_2 - u_1$$

$$h_{alt} = n_2 - n_1$$

$$h_{RSL} = SL_2 - SL_1$$

$$= h_{alt} - h_{surf} \ ?$$

2.3 The ocean function

$$O(\Omega, t) := \begin{cases} 0 & \text{if} \quad T(\Omega, t) > 0 \\ 1 & \text{if} \quad T(\Omega, t) \leq 0 \end{cases}$$

with time-dependent topography

$$T(\Omega, t) = T_0 - h_{RSL}(\Omega, t)$$

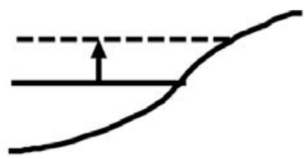

2.4 Moving coastlines

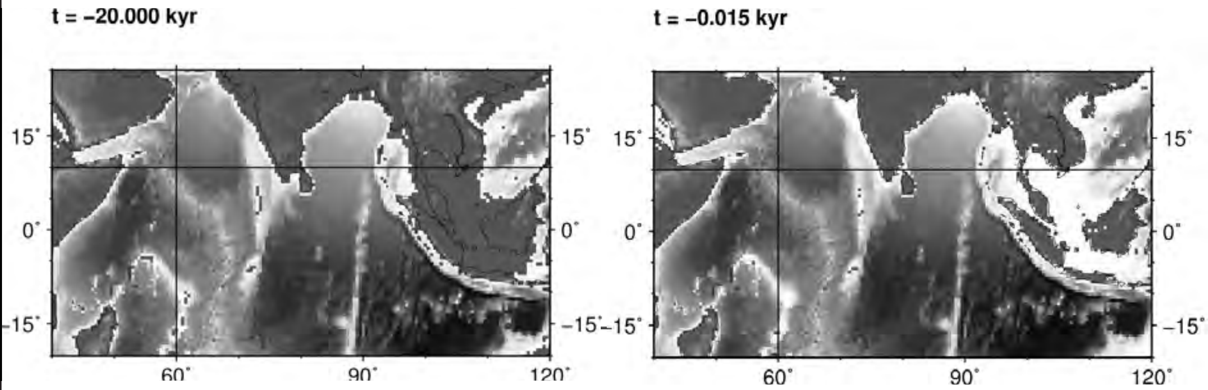

During last glacial maximum large continental-shelf areas were above sea level.

2.6 The sea-level equation of Farrell and Clark (1976)

We assume that all perturbations vanish at $t = 0$.

$$h_{\mathrm{rsl}}(\Omega, t) = [h_{\mathrm{wl}}(t) + e(\Omega, t) - u(\Omega, t)]\,O(\Omega, t)\,,$$

with

$$h_{\mathrm{wl}}(t) = \frac{-m_{\mathrm{ice}}(t)}{\rho_{\mathrm{oce}} A_{\mathrm{oce}}(t)} - \frac{1}{A^{\mathrm{oce}}(t)} \int_{\Omega} [e(\Omega, t) - u(\Omega, t)]\,O(\Omega, t)\,d\Omega$$

and

$$A_{\mathrm{oce}}(t) = \int_{\Omega} O(\Omega, t)\,d\Omega$$

GFZ Helmholtz Centre POTSDAM

Iterative procedure

At each time, t:

$$
\begin{aligned}
(e-u)_i(\Omega) &= g_{e-u} * \left[m_{\rm ice}(\Omega) + h^{\rm rsl}_{i-1}(\Omega)\,\rho_w\,O(\Omega)\right], \\
h^{\rm rsl}_i(\Omega) &= h^{\rm wl}_i + (e-u)_i(\Omega)\,O(\Omega), \\
h^{\rm wl}_i &= -\frac{\int_\Omega m_{\rm ice}(\Omega)}{\rho_w A_o} - \frac{1}{A_o}\int (e-u)_i(\Omega)\,O(\Omega)\,d\Omega, \\
h^{\rm rsl}_0 &= -\frac{\int m_{\rm ice}(\Omega)}{\rho_w A_o}.
\end{aligned}
$$

27

DFG SPP 1257

GFZ Helmholtz Centre POTSDAM

3. Reference systems

- Reference frame

  A set of axes within which to measure the position, orientation, and other properties of an object or a process
- Geodetic data (more than one datum)

  are used in geodesy to translate positions indicated on their products to their real position on earth
- 3 coordinates for orientation
- 3 coordinates for position

28

DFG SPP 1257

3.1 Orientation

1. no surface net rotation (NF) $\int_{\partial B} e_r \times u \, dS = 0$
2. conservation of total momentum (NM)
$$\int_B \rho e_r \times u \, dV + \int_{\partial B} e_r \times \sigma \, dS = 0$$
3. no lithosphere net rotation (NL) $\int_{B_L} \rho e_r \times u \, dV = 0$
4. no internal rotation (NE) $\int_B \rho e_r \times u \, dV = 0$
5. no mantle rotation (NMa) $\int_{B_M} \rho e_r \times u \, dV = 0$

29

3.2 Position

1. centre of mass (CM) $\int_B \rho r \, dV + \int_{\partial B} \sigma r \, dS = 0$
2. centre of figure (CF) $\int_{\partial B} u \, dS = 0$
3. centre of deformation (CD) $\int_B u \, dV = 0$
4. centre of internal masses (CE) $\int_B \rho r \, dV = 0$

30

CM and CF motion due to GIA

- Surface loading
  - CM towards load
  - GC in opposite direction
- Viscoelastic compensation
  - downward displacement
  - CM away from load
  - CF away from load
- After deglaciation
  - CM first away from load area than moves towards load centre
  - CF towards load area

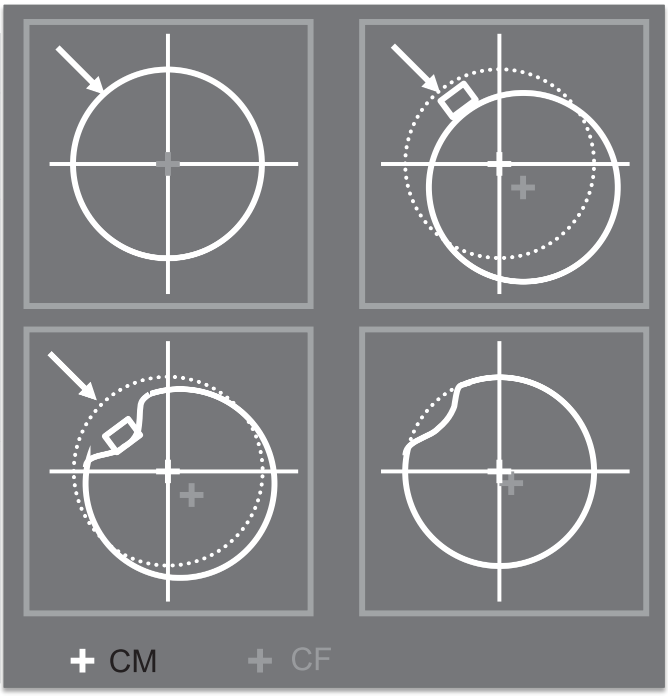

GIA contribution to present-day processes

- Prediction of GIA component for present-day dynamics and its environmental impact

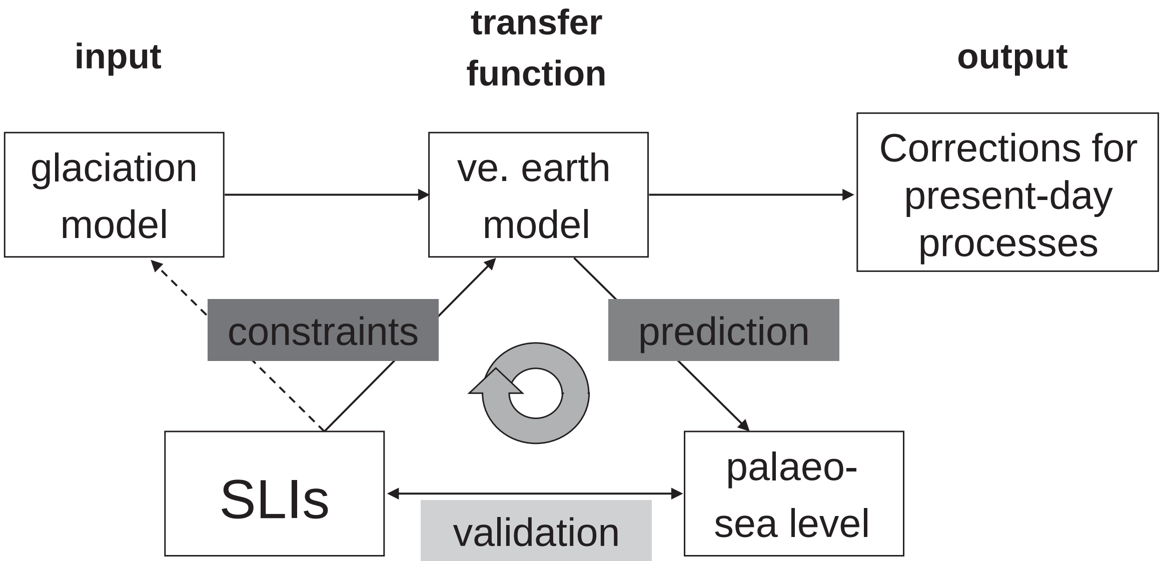

GFZ Helmholtz Centre Potsdam

RSL change from SLIs

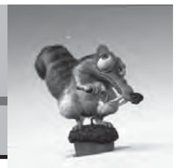

- Land uplift – representation by fossil samples (SLI) deposited subsequently

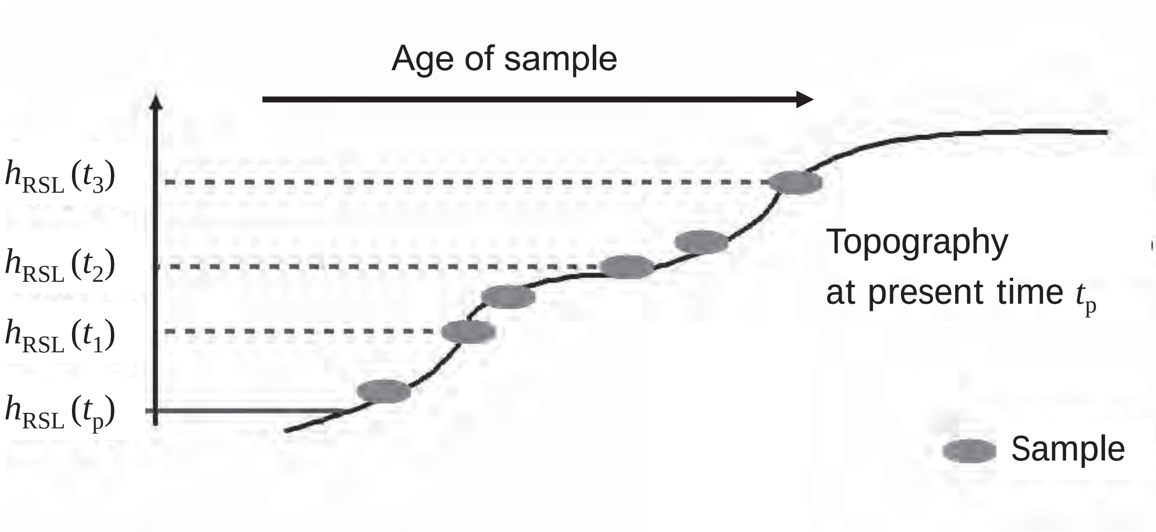

33

DFG SPP 1257

GFZ Helmholtz Centre Potsdam

4. Glacial Isostatic Adjustment (GIA)

- GIA describes the kinematic and dynamic response of the earth's interior to surface loading related to the glacial periods
  - Reconfiguration inside the solid earth
  - Coupling to ice/ocean mass redistribution
- Mathematical formulation
  - Continuum mechanical field equations describing
    - the momentum of a visco-elastic material filling a planet
    - the gravitational perturbation due to reconfiguration
    - Excitation by surface and body forces

34

DFG SPP 1257

Features of GIA modelling

- PREM structure for shear modulus and density
- Viscosities: $\eta_{UM} = 0.6 \times 10^{20}$ Pa s,
  $\eta_{LM} = 1 \times 10^{22}$ Pa s
- Elastic lithosphere of variable thickness
  Predefined ice history (e.g. ICE5G)

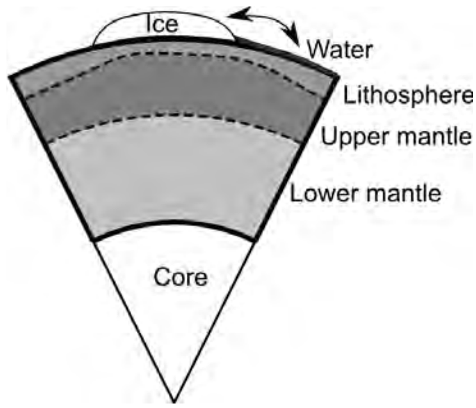

- S-FE formulation (Martinec, GJI, 2000)
  - incompressible
  - Compressibility Tanaka et al. (2011)
  - self-gravitating
  - rotating
  - hydrostatically pre-stressed
- Uniqueness conditions
  - centre of mass
  - no surface net-rotation

Main aspects of process

- Loading force = flexure of lithosphere + buoyancy
- Elasticity
- gravity
- Fluid dynamics

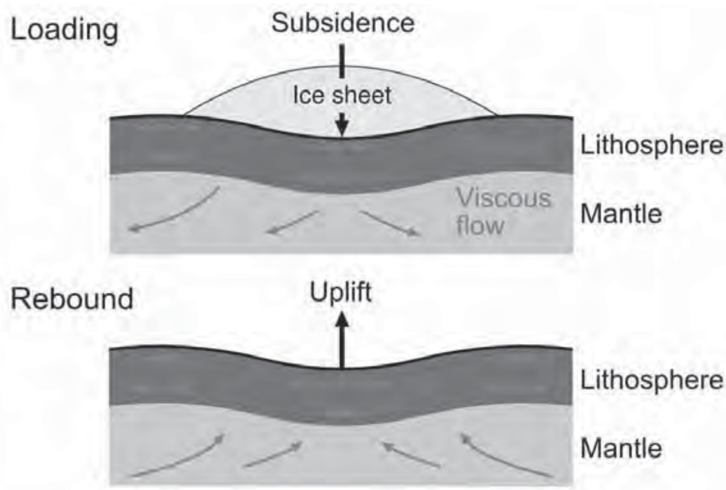

Flow field at surface

1D earth structure

- standard viscosity model with

  η_{UM} = 6 x 10^{20} Pa s
  η_{LM} = 1 x 10^{22} Pa s
- ICE3G history
- fixed coastlines

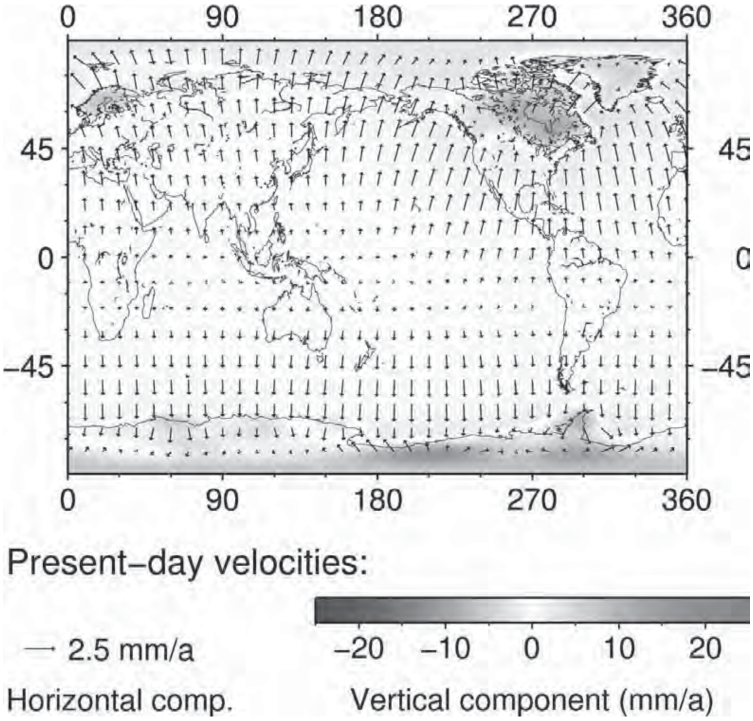

Flow field in earth's mantle

Mid Ocean Ridge
(**MOR**)
Ice sheets:
Laurentide (LIS)
Greenland (GIS)
Fennoscandia (FIS)

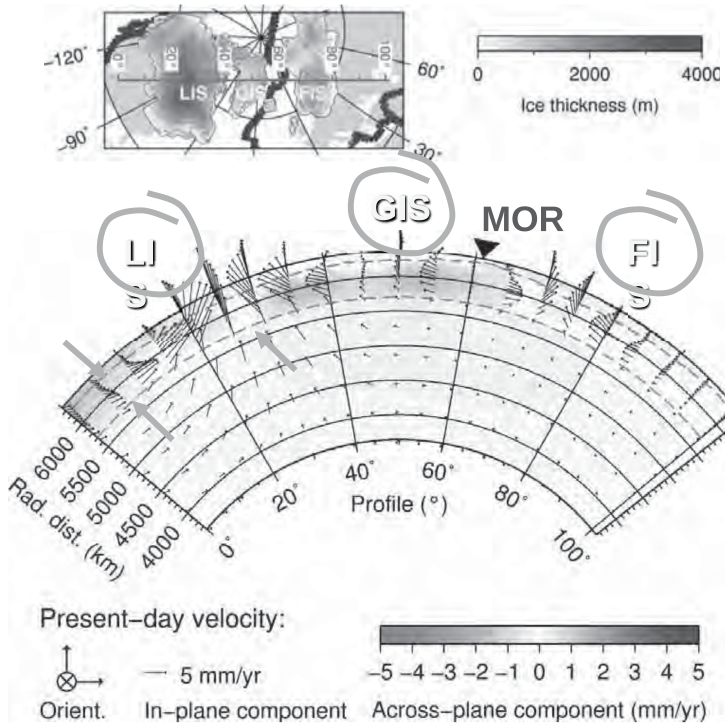

Last glacial cycle

- Glaciated regions on northern hemisphere:
  - North America, Greenland
  - Fennoscandia
- on southern hemisphere
  - Antarctica

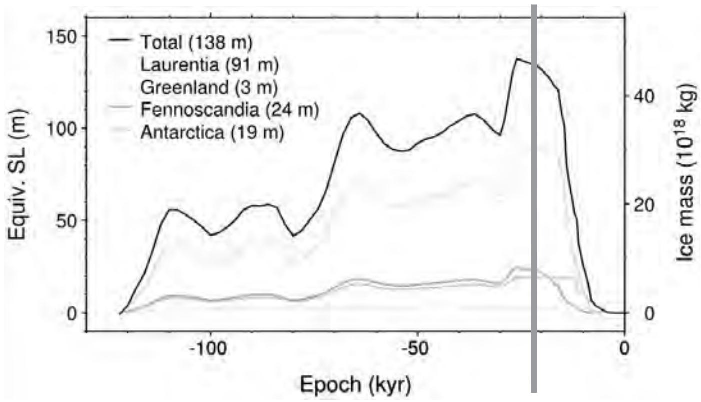

21 kyr b.p.

Ice thickness (m)

2.7 Features of solution

- Ice load
- Conservation of mass
- Gravitational attraction
- Deformation
- Change of geoid
- Melting of ice
- Conservation of mass + change of geoid
- Uplift

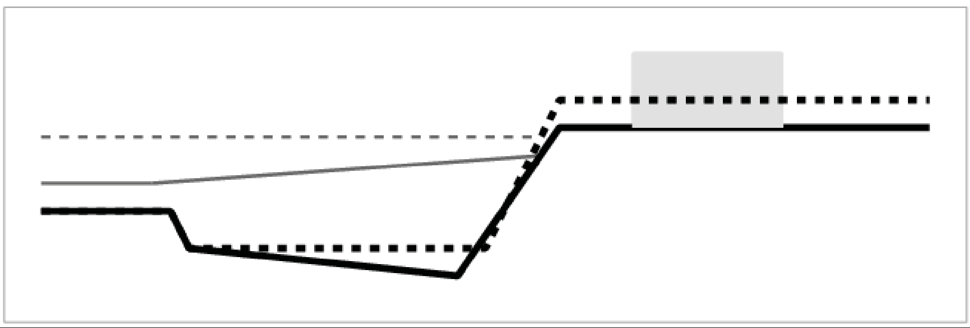

Interplay of solid earth, ocean and ice sheets

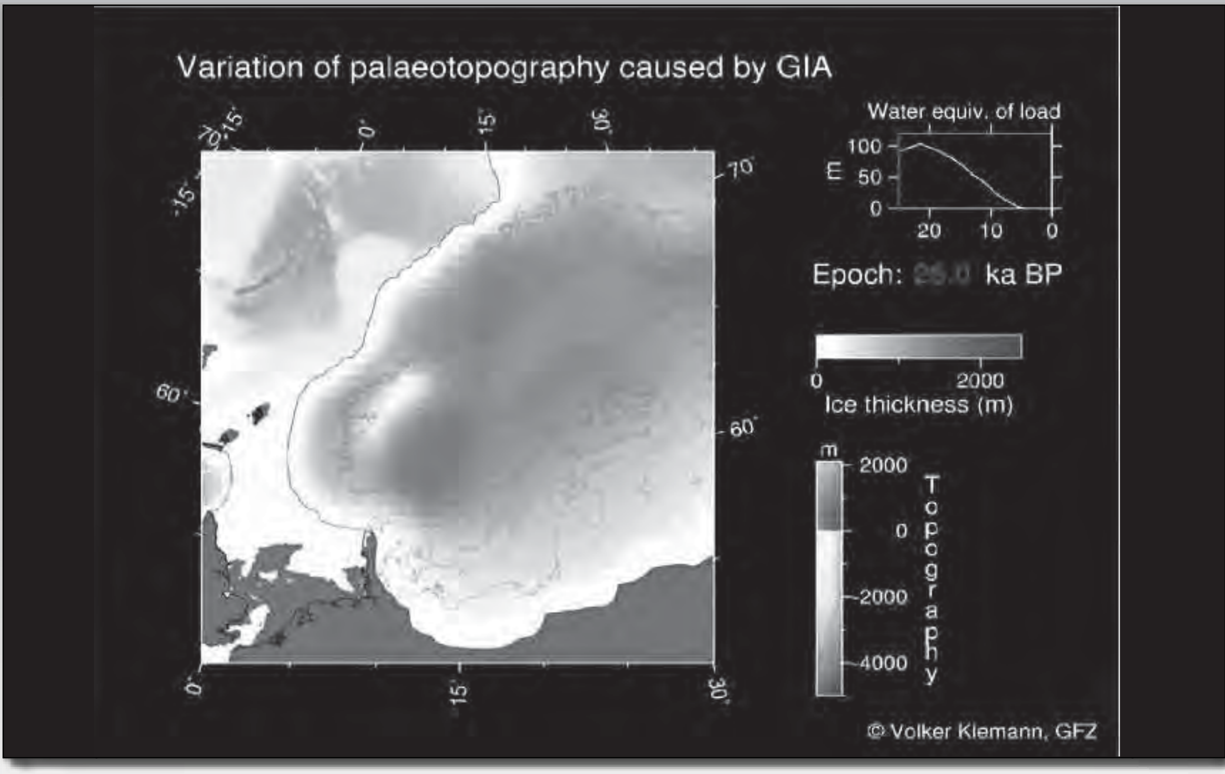

4.1 Field equations describing the solid earth response

Lagrange' formulation of equation of motion – Potential equation – Constitutive equation – Continuity equation

$$\nabla \cdot \tau - \rho_0 \nabla \varphi_1 + \boxed{\nabla \cdot (\rho_0 u)\, \varphi_0} - \boxed{\nabla (\rho_0 u \cdot \nabla \varphi_0)} = \boxed{0}$$

$$\boxed{\nabla^2 \varphi_1 + 4 \pi G \nabla \cdot (\rho_0 u) = 0}$$

$$\boxed{\dot{\tau} = \dot{\tau}^E - \frac{\mu}{\eta} (\tau - \Pi I), \quad \tau^E = \Pi I + \mu (\nabla u + \nabla u^T)}$$

$$\boxed{\nabla \cdot u = 0}$$

inside the earth, B: Displacement, u – Stress, τ – Pressure, Π – Potential, φ_1. — Material parameters: Density, ρ_0 – Shear modulus, μ – Viscosity, η

GFZ Helmholtz Centre POTSDAM

Boundary conditions

Loading of surface mass – free slip – continuity of gravitational potential – potential of surface mass

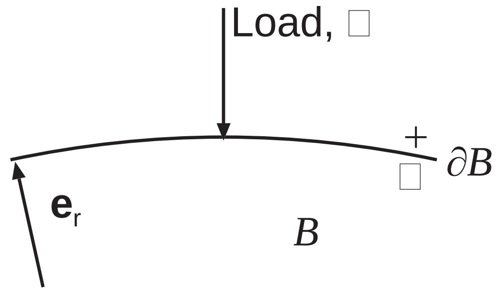

$$
\begin{aligned}
e_r \cdot \tau^- \cdot e_r &= -g_0(a)\,\sigma \\
\tau^- \cdot e_r - (e_r \cdot \tau^- \cdot e_r)\, e_r &= 0 \\
[\varphi_1]_-^+ &= 0 \\
[\nabla \varphi_1]_-^+ \cdot e_r + 4\pi G \rho^- \,(u^- \cdot e_r) &= 4\pi G \sigma
\end{aligned}
$$

43

DFG SPP 1257

GFZ Helmholtz Centre POTSDAM

Green's function for the viscoelastic case

Convolution in space and time

$$
\varphi(\Omega, t) = \int_{-\infty}^{t} \int_{\Omega_0} g_\varphi(\gamma, t - t')\, \sigma(\Omega', t')\, d\Omega'\, dt'
$$

Features of g_φ

- fading memory
- objectivity
- ...

44

DFG SPP 1257

Maxwell rheology

- Linear transition from elastic to viscous material behavior

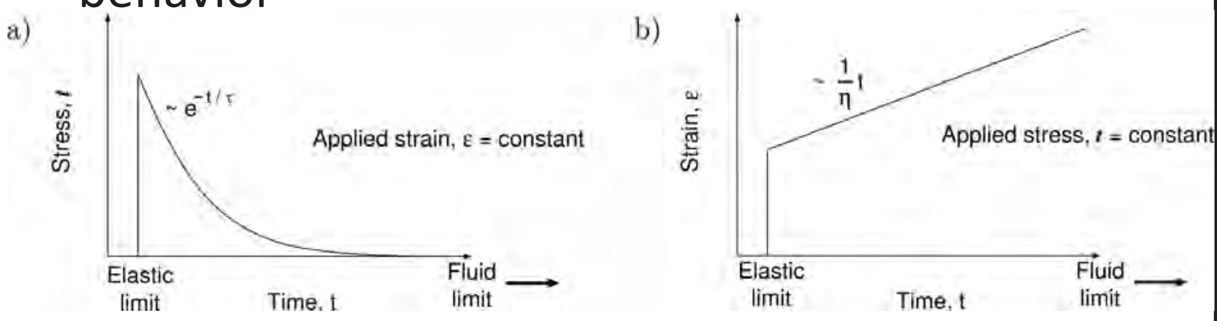

$$\dot{\tau} + \frac{\mu_0}{\eta}\tau = 2\mu\dot{\epsilon}^d$$

$$\tau(s) = \mu(s)\,\epsilon^d(s)$$

$$\mu(s) = \frac{2\mu_0 s}{s + \mu_0/\eta}$$

45

Normal mode approach

- Peltier, 1974, Rev. Geophys. Space Phys.
  - Representation of fields in spatial domain by series expended in spherical harmonics for lateral directions
  - Replacement of relaxation function by complex shear modulus (in contrast to the free oscillation problem, a Laplace transformation is applied.)
  - Representation of solution by set of eigen modes, which are determined by the roots of the secular determinant (Inverse Laplace transformation - Bromwhich path – Residue theorem)

46

Solution of radial part

$$\frac{\partial}{\partial r} \mathrm{Y} = \mathrm{A\,Y}$$

The formal solution is

$$\mathrm{Y}(r) = e^{\mathrm{A}\,r}\,\mathrm{C}$$

Being Y the solution at r:

$$\mathrm{Y}(r) =: \mathrm{L}(r)\,\mathrm{C}$$

with L the fundamental matrix of A.

Transformation to time domain

$$\mu(s) = \frac{\mu_0}{1 + (s\,\tau)^{-1}}$$

s-dependent solution has to be transformed into spatial domain.

$$f(t) = \frac{1}{2\,\pi\,i} \int_{\gamma - i\,\infty}^{\gamma + i\,\infty} f(s)\,e^{st}\,ds$$

Closing Bromwich path, we can replace the integral by the residues of $f(s)$.

$$f(t) = \sum_{j=1}^{M} \mathrm{Res}\,\{\, f(s)\,e^{st}\,\}\,|_{s=s_j}$$

$$\mathrm{Res}\left\{ \frac{p(s_j)}{q(s_j)} \right\} = \frac{p(s)}{d/ds\,q(s)}|_{s=s_j}$$

...

$$\mathbf{s}(a,t) = \mathbf{K}(t) = \mathbf{K}_e\delta(t) + \sum_{j=1}^{M} \mathbf{K}_j(a)\,e^{s_j\,t}$$

Meaning of relaxation modes

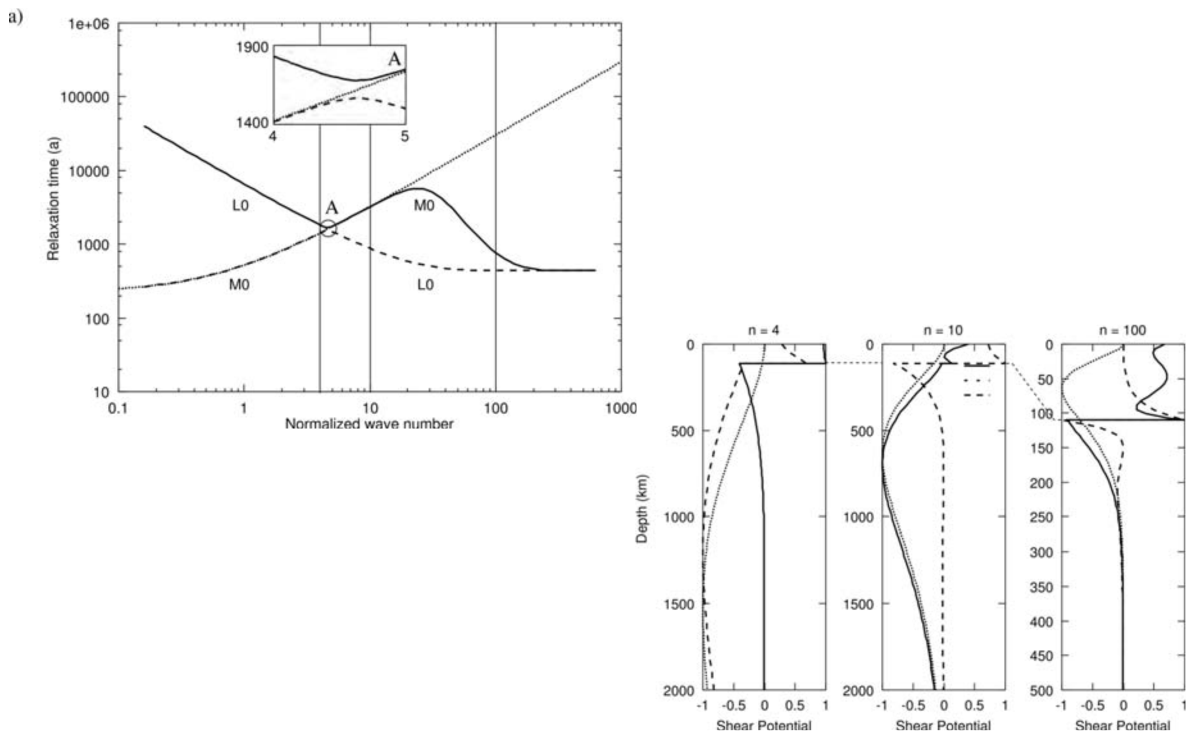

Geocenter motion

$$u_{gc} := u_{cf} - u_{cm}$$

or in components

$$u_{gc}^{x} = -\frac{1}{2}\sqrt{\frac{2}{\pi}}\,\mathrm{Re}\{U_{11} + 2V_{11} + 3F_{11}/g_0\}$$

$$u_{gc}^{y} = \frac{1}{2}\sqrt{\frac{2}{\pi}}\,\mathrm{Im}\{U_{11} + 2V_{11} + 3F_{11}/g_0\}$$

$$u_{gc}^{z} = \frac{1}{2}\sqrt{\frac{1}{\pi}}\,(U_{10} + 2V_{10} + 3F_{10}/g_0)$$

GC, CM and CF motion

$$\int_V \rho \, \boldsymbol{u} \, dV = 0$$

- Evolution of motions in the CE realization during last glacial cycle
  - CF is delayed and opposite to CM
  - amplitude of GC is largest during LGM and reaches 70 m
  - after deglaciation CM is negligible and GC is dominated by the delayed CF

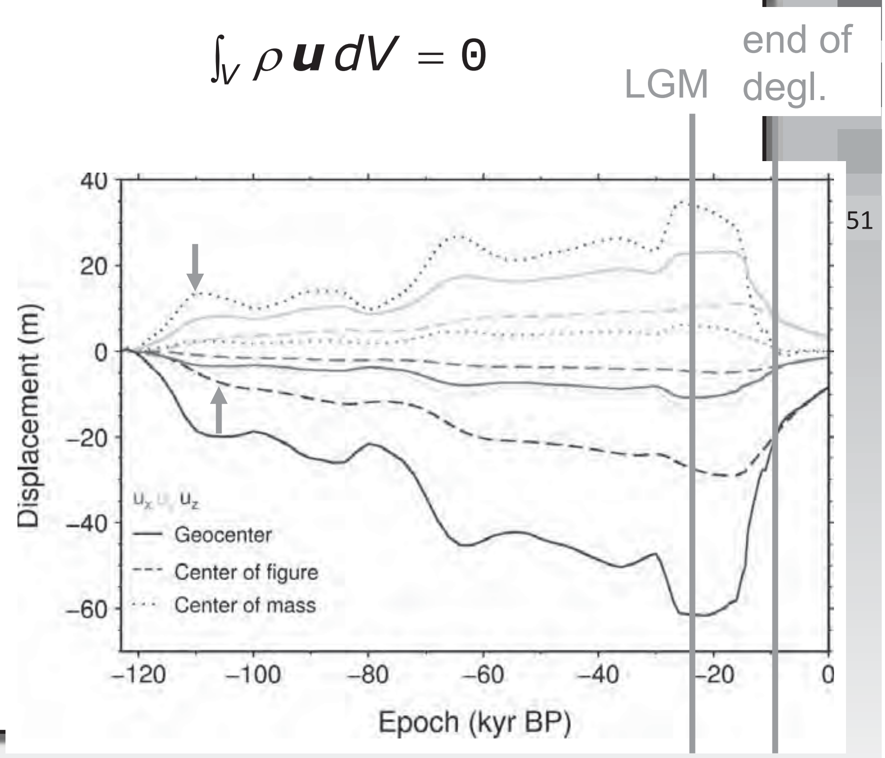

Influence of lower-mantle viscosity on GC motion

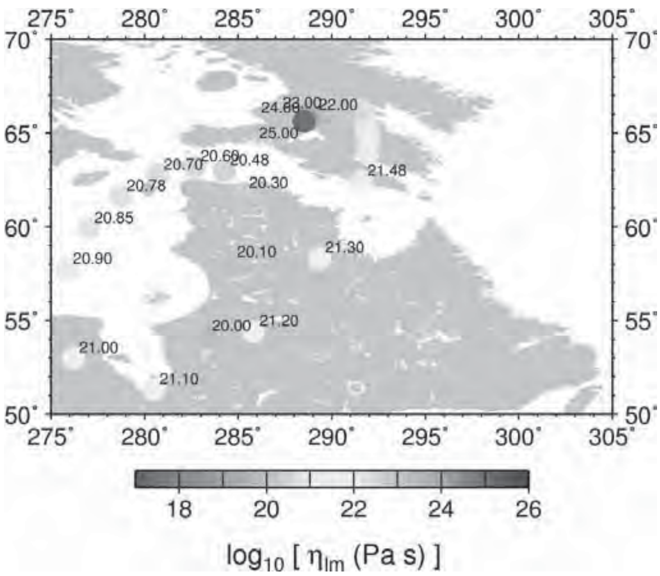

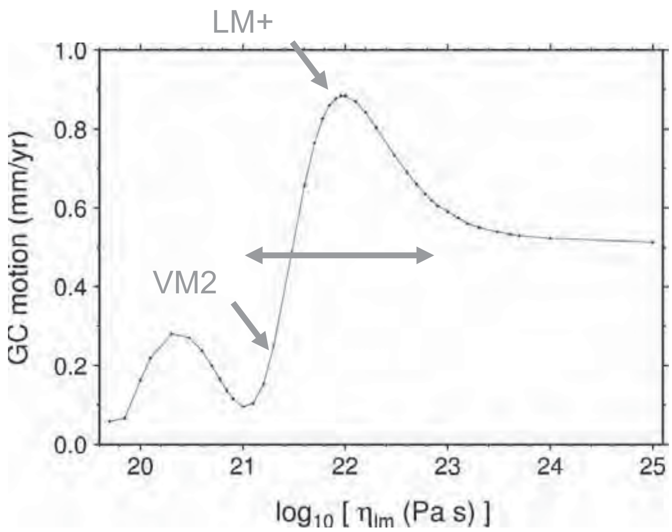

- Variation in direction of GC motion ~ 2000 km
- Velocity of motion varies by almost one magnitude
- largest sensitivity between 10^{21} and 10^{23} Pa s

Spectral—finite element method

$$\delta\mathcal{E}\left(\boldsymbol{u}^{i+1},\,\phi_1^{i+1},\,\Pi^{i+1},\,\delta\boldsymbol{u}\,,\delta\phi_1,\delta\Pi\right)\;=\;\delta\mathcal{F}\left(\delta\boldsymbol{u},\,\delta\phi_1\right)$$

- Weak formulation
- Spectral parameterization in horizontal direction
- Radial FE for each spectral component
- Explicit time scheme
- Elastic part on left-hand side
- Viscous part and boundary conditions on right-hand side

spectral
representation

finite elements

Laterally variable
and non-linear
rheology

GFZ
Helmholtz Centre
POTSDAM

4.2 Solution of field equations

- Advanced modelling with spectral—finite elements
  - Solution directly in the time domain
  - Lateral variations in viscoelastic parameters are possible
  - Dynamic coupling to other processes is more easy to establish
  - Consideration of non-linear viscoelasticity

Elastic thickness of Lithosphere

- Depth defined by characteristic isotherm (1100 ° C)
- Mosaic
  - Continental lithosphere from thermal data (Artemieva, Tectonophysics, 2003)
  - Oceanic lithosphere from ocean floor ages (Müller et al., JGR, 1997)
  - Plate boundaries from Bird (G³, 2003)

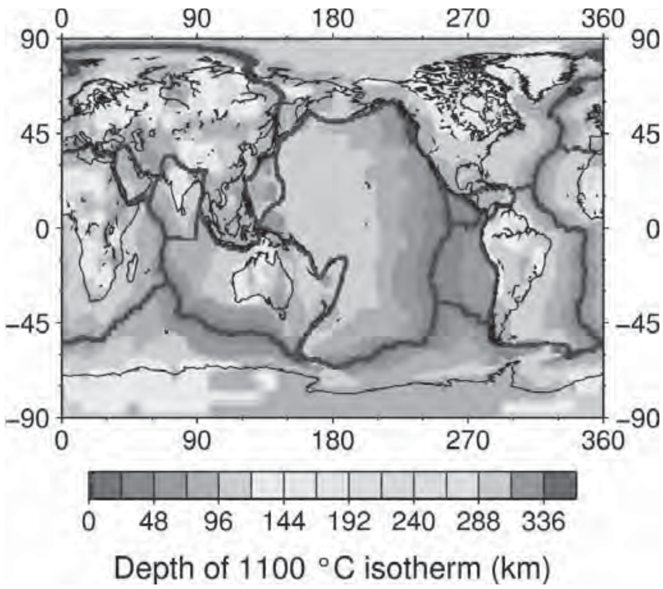

Induced horizontal motions

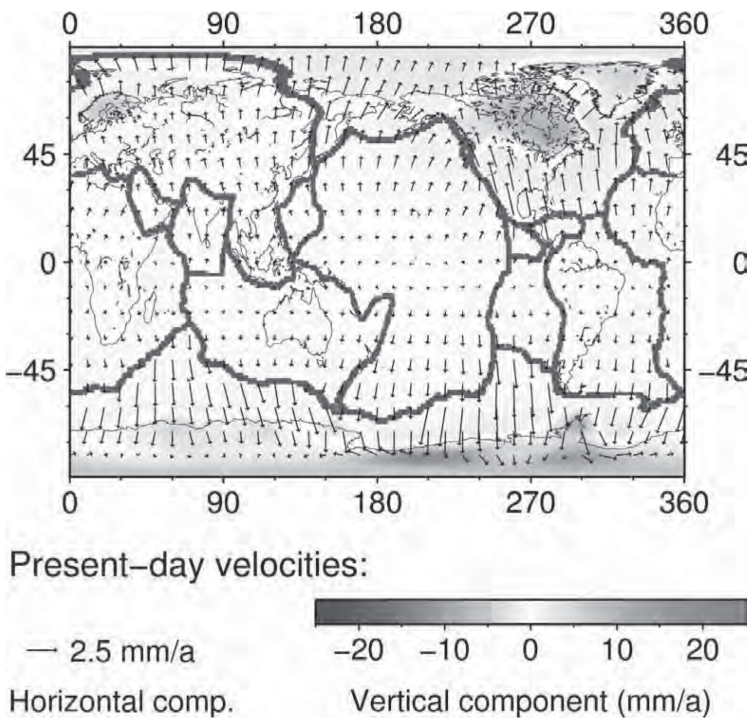

(Klemann, et al, 2008, JGdyn)

Divergence and vorticity

57

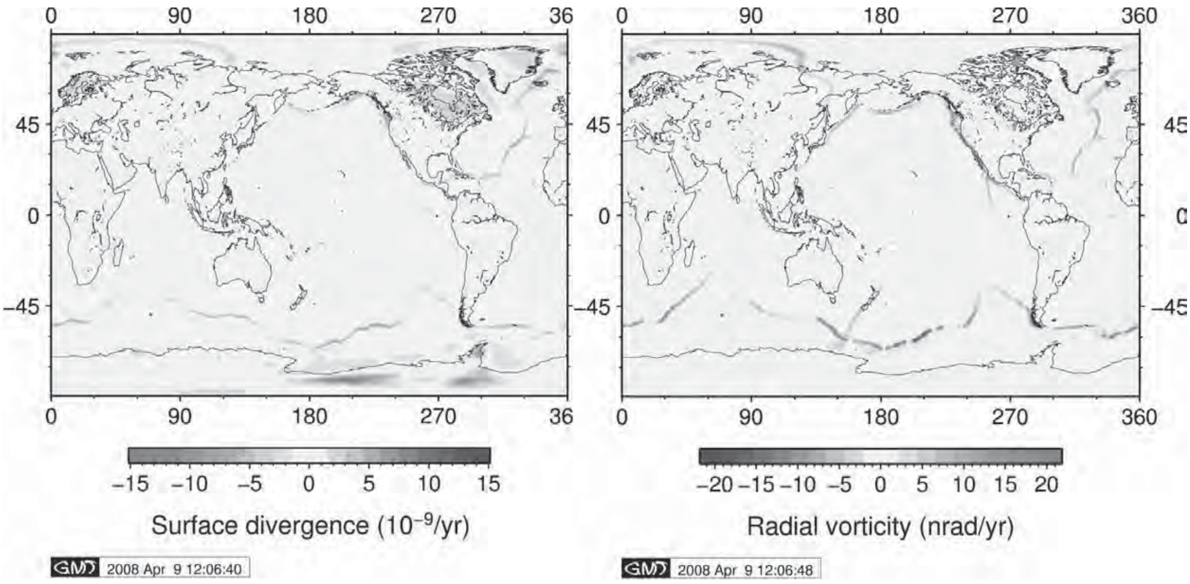

Klemann, et al., 2008, JGdyn

Degree variances of surface motion

Influence of plates

– Equipartitioning of spheroidal and toroidal component of GIA induced horizontal motions for $j > 3$
– Equipartitioning appears in plate motions driven by convective flow (e.g. Čadek & Ricard, EPSL, 1992)
– Toroidal motion vanishes for $j = 1$ due to uniqueness condition of no surface net-rotation

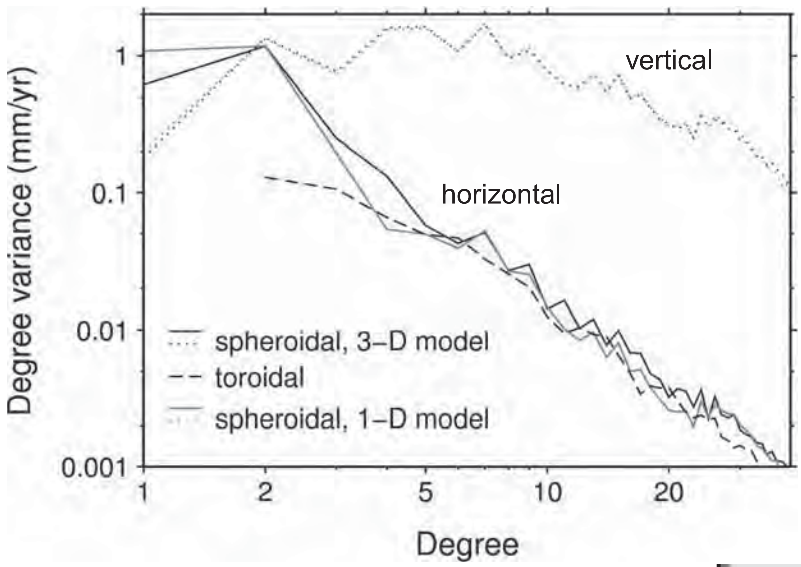

Klemann et al. 2008, J. Geodyn.

Solid earth – ice coupling

- Polythermal ice model
  - forced by atmosphere
    - air temperature
    - precipitation
  - forced by ocean
    - sea level
    - grounding line
  - forced by solid earth
    - heat flow
  - response to loading
    - viscoelastic earth
- Dynamic coupling
  - $h_{ICE} = t_{ICE} - u$
  - flow inside ice sheet

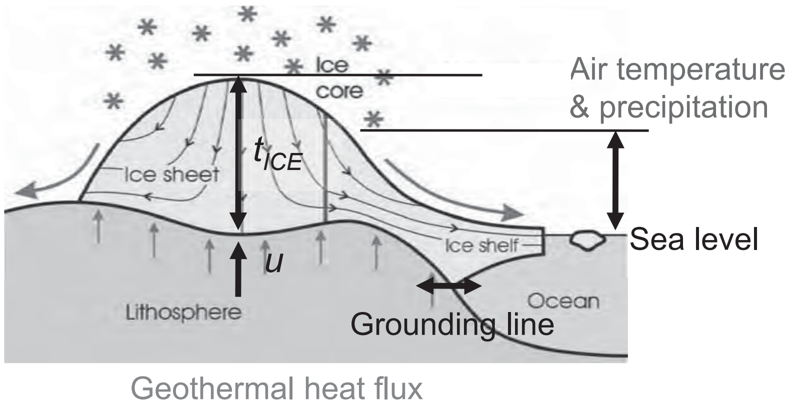

Summary

- Love numbers
  - Elastic response of the earth's interior to surface processes
  - Spherical symmetry
  - Gravitational consistent
- Sea level equation
  - Mandatory to describe static redistribution of water inside the ocean for a loading process
- Glacial isostatic adjustment
  - Most important secular process for geodetic observables
  - Earth interior is usually represented by a simplified structure

Practical: Ice and loading

Volker Klemann, Andreas Groh

Summer School „Global Water Cycle“
12.-16. September 2011
Mayschoss

GFZ
Helmholtz Centre
POTSDAM

Main tasks

- Convolution
- Analysis
- Synthesis

First exercise

Solution of sea-level equation (**sle_pt.m**)

1. Definition of global parameters.
2. Definition of Input files. The LLN, the topography and the ice-height changes are provided.
3. Read in of LLN and definition of the Green's function needed for the SLE
4. Determination of ocean function: read in of topography – define 1/0 grid
5. Initialise iteration procedure: initialise working grid – dermine ocean surface – read in of load and transfer to surface-mass density – synthesise – initialise sea level
6. Iterate sea-level equation: convolution – determine and add new equivalent sea level

6. Iterative procedure

At each time, t:

$$(e-u)_i(\Omega) = g_{e-u} * [m_{\mathrm{ice}}(\Omega) + h^{\mathrm{rsl}}_{i-1}(\Omega)\,\rho_w\,O(\Omega)\,],$$

$$h^{\mathrm{rsl}}_i(\Omega) = h^{\mathrm{wl}}_i + (e-u)_i(\Omega)\,O(\Omega)\,,$$

$$h^{\mathrm{wl}}_i = -\frac{\int_\Omega m_{\mathrm{ice}}(\Omega)}{\rho_w A_o} - \frac{1}{A_o}\int (e-u)_i(\Omega)\,O(\Omega)\,d\Omega\,,$$

$$h^{\mathrm{rsl}}_0 = -\frac{\int m_{\mathrm{ice}}(\Omega)}{\rho_w A_o}\,.$$

First exercise

Your task:

– Program the convolution
– Run the code
– Discuss the convergence of the solution
– **Keep the solution for the second exercise**

- Analysis of present day fields (**compare_pt.m**)
- 1. i/o
- 2. i/o
- 3. i/o
- 4. Determination of ocean function: read in of topography – define 1/0 grid
- 5. Read in of GRACE stokes trend coefficients and conversion into geoid trend coefficients
- 6. Read in of GIA equipotential surface trend coefficients
- 7. Read in of the relative sea-level change from the last iteration of Exercise 1 and the ice
- height changes
- 8. Combination of the later and transformation into spherical harmonic coefficients
- 9. Perform the convolution in order to derive present-day geoid changes
- 10. Combination of GIA and present-day geoid changes and comparison to GRACE results

Solutions

- On the next slides the solutions of the practicals are presented.

Rsl 0

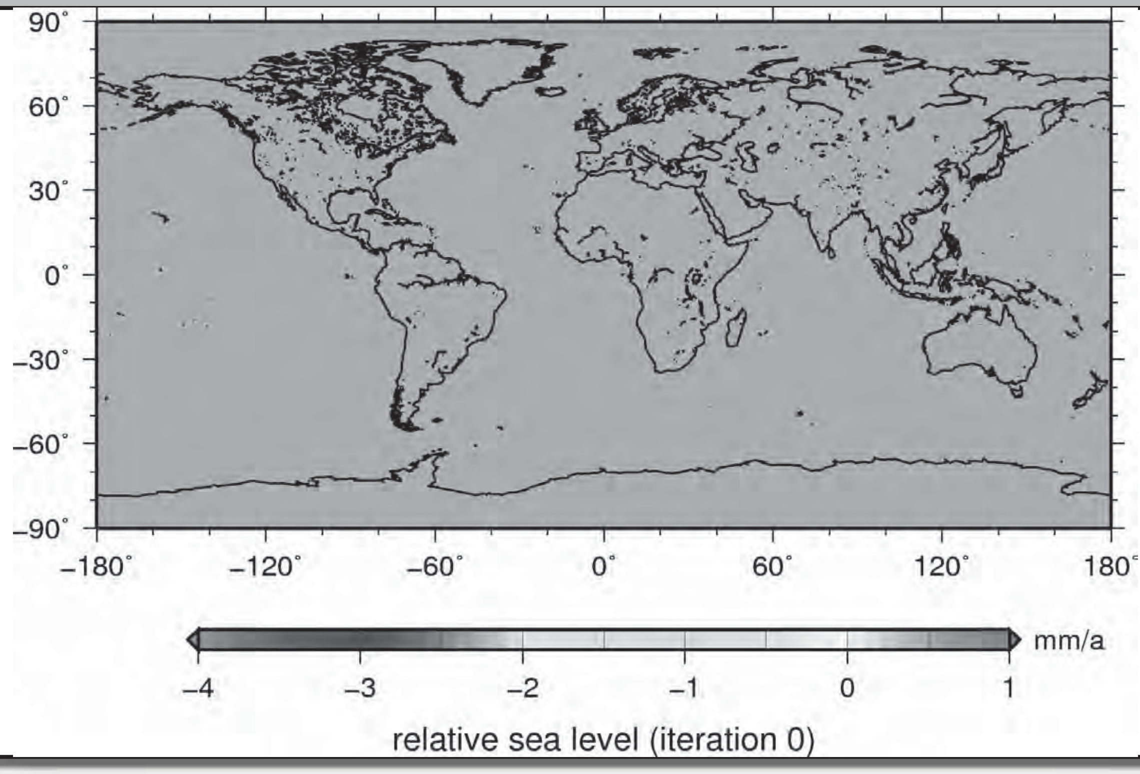

rsl1

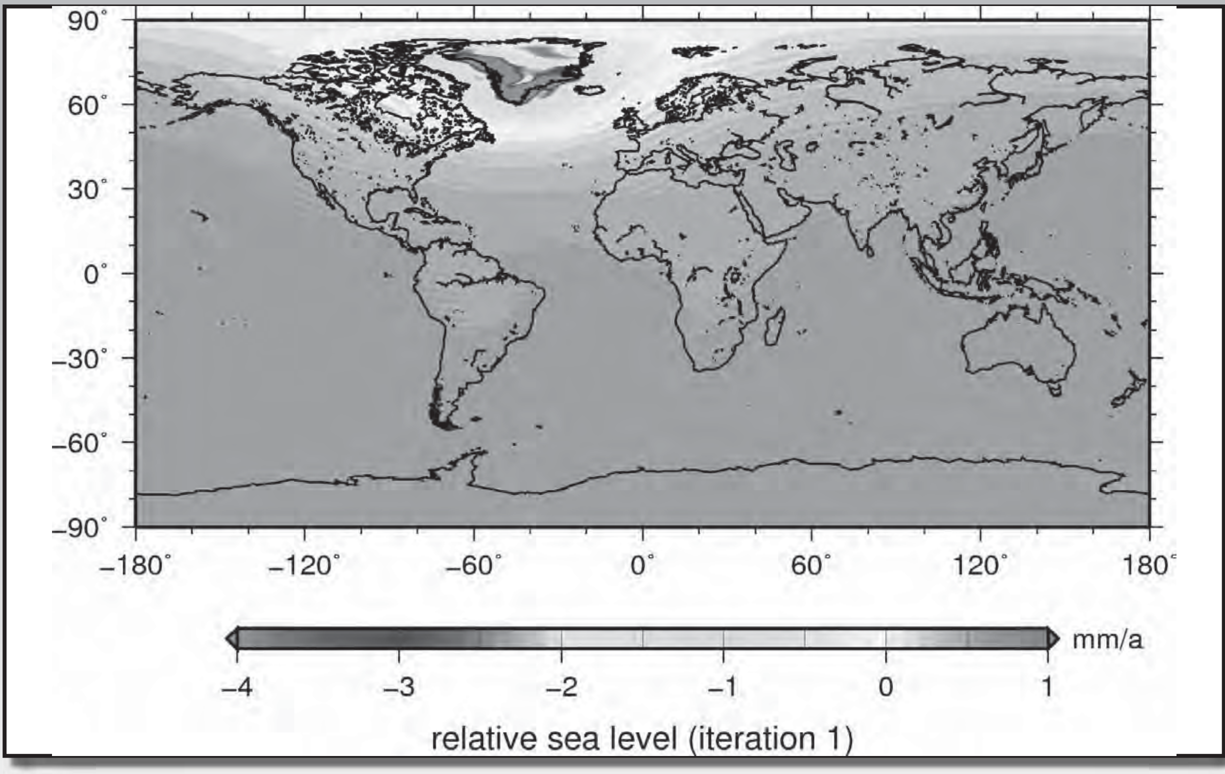

69

DFG SPP 1257

rsl2

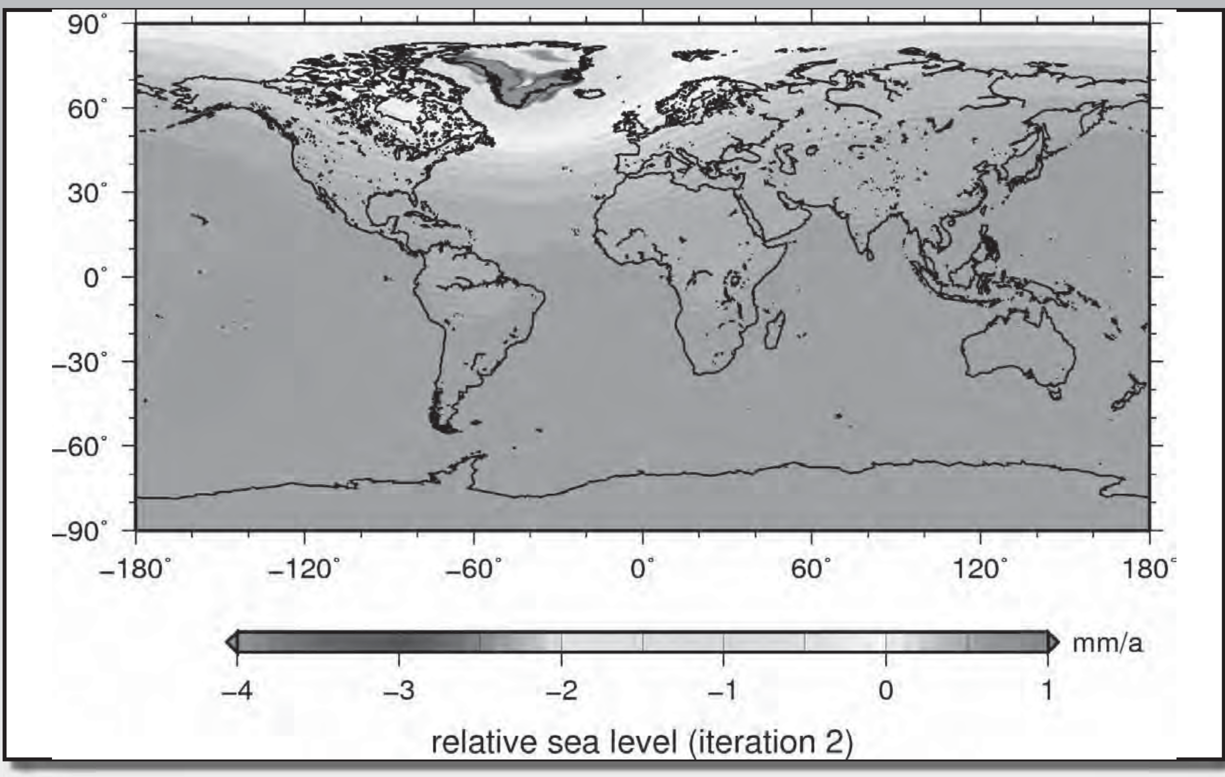

70

DFG SPP 1257

GFZ Helmholtz Centre POTSDAM

rsl3

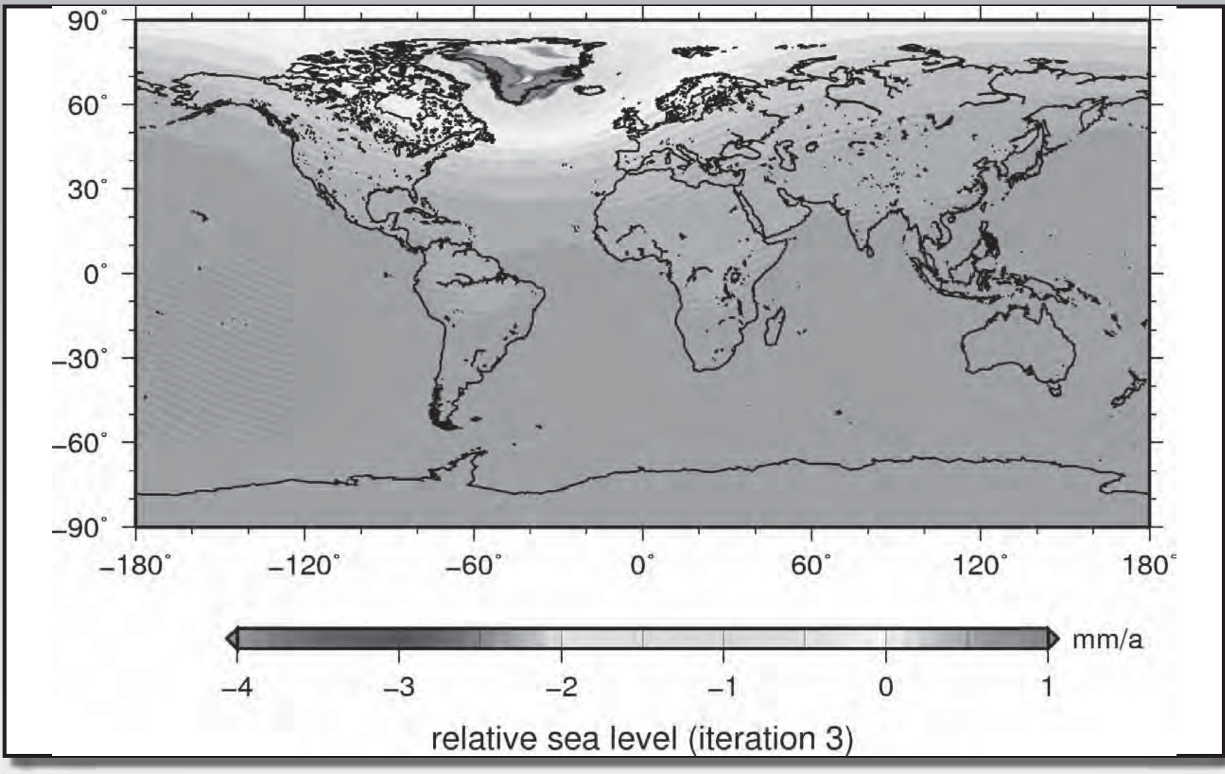

71

DFG SPP 1257

GFZ Helmholtz Centre POTSDAM

Rsl 2 - 1

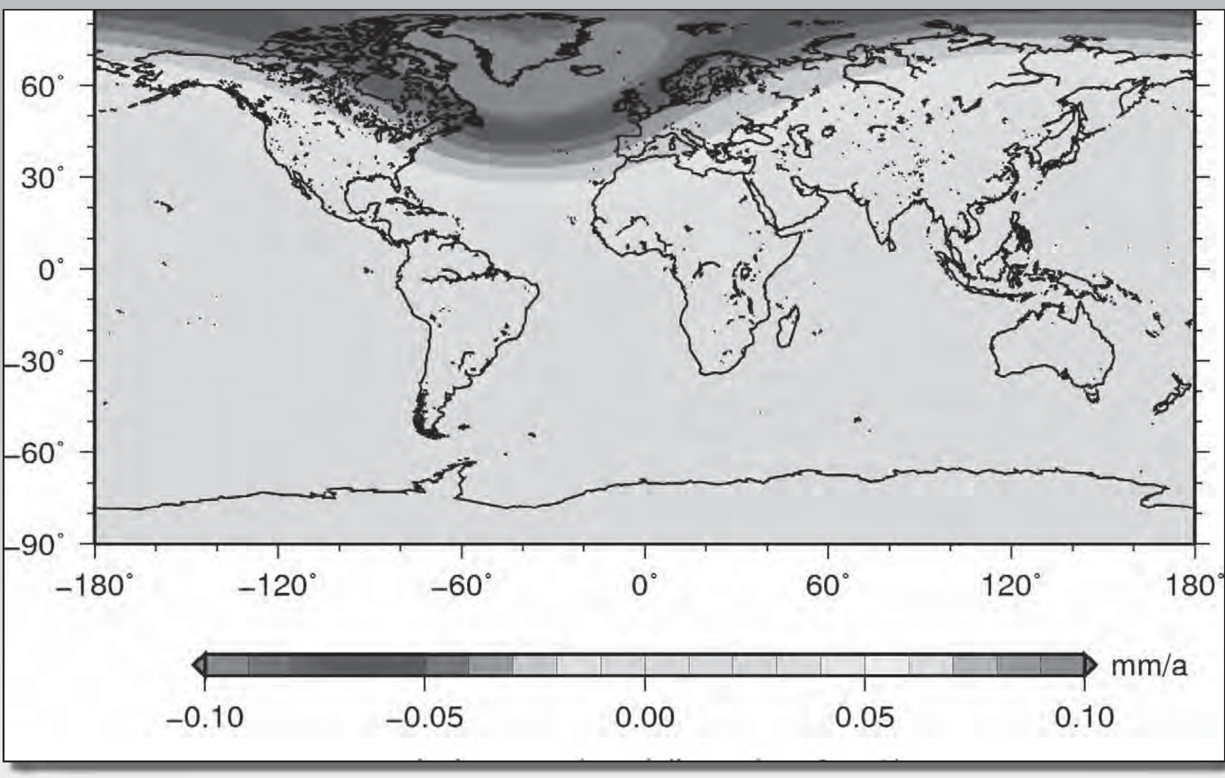

72

DFG SPP 1257

GFZ
Helmholtz Centre
POTSDAM

Rsl 3 -2

73

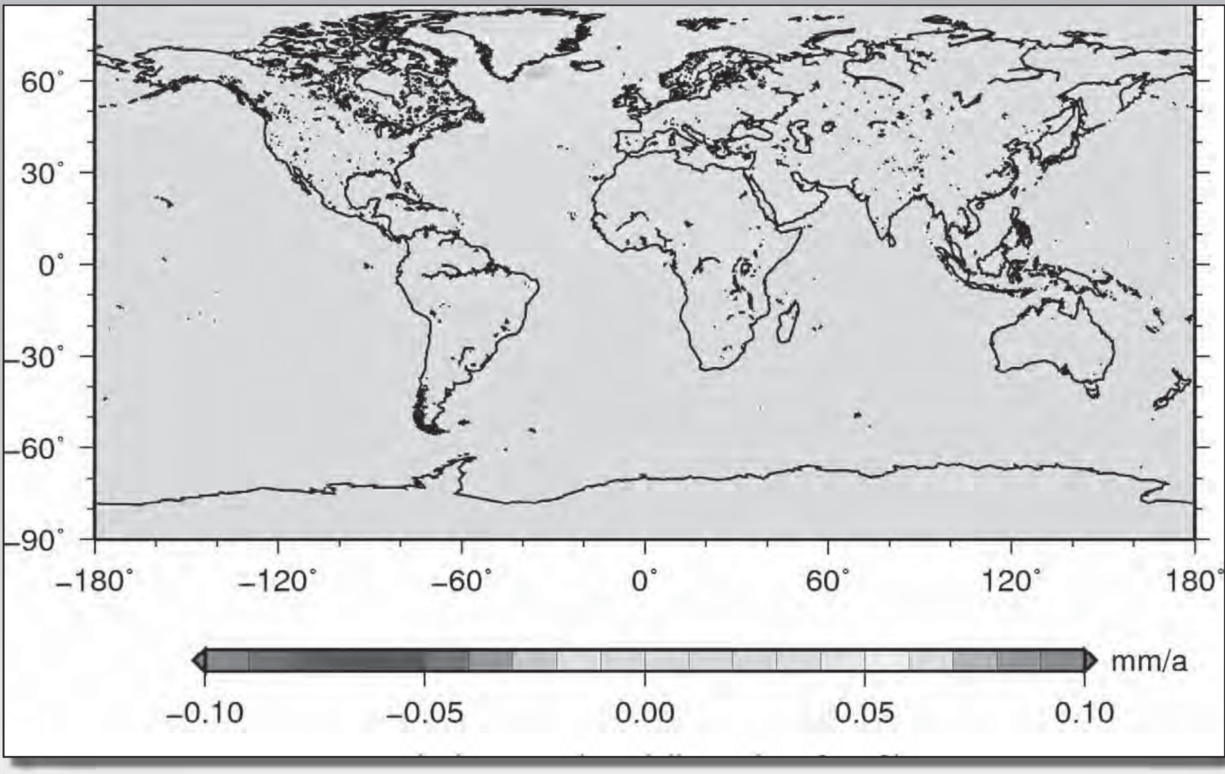

DFG SPP 1257

GFZ
Helmholtz Centre
POTSDAM

grace

74

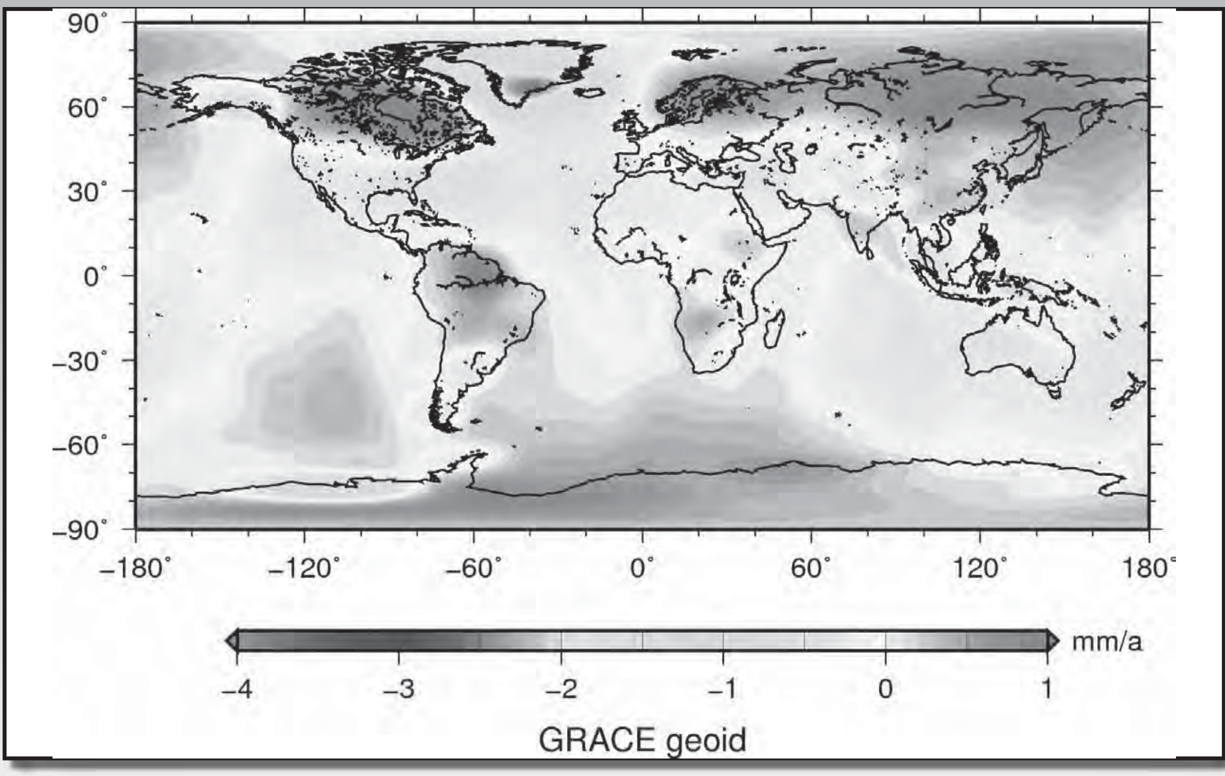

DFG SPP 1257

ela

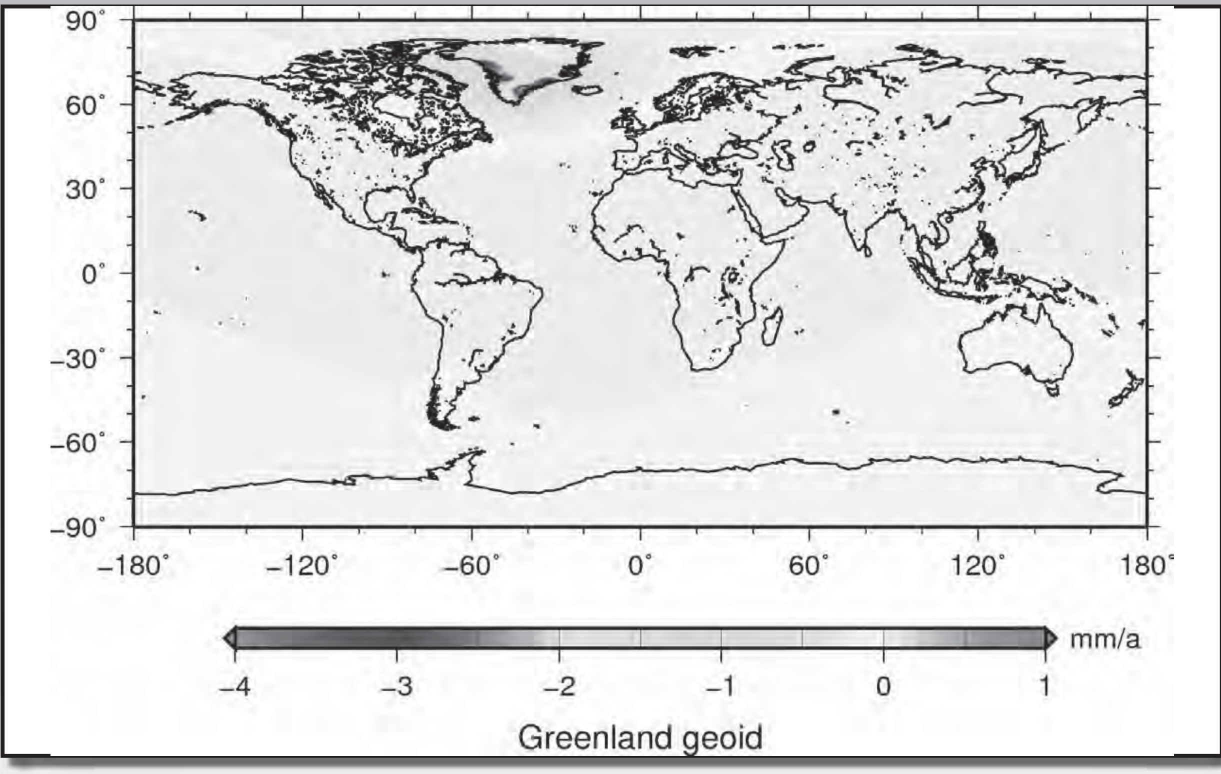

75

DFG SPP 1257

gia

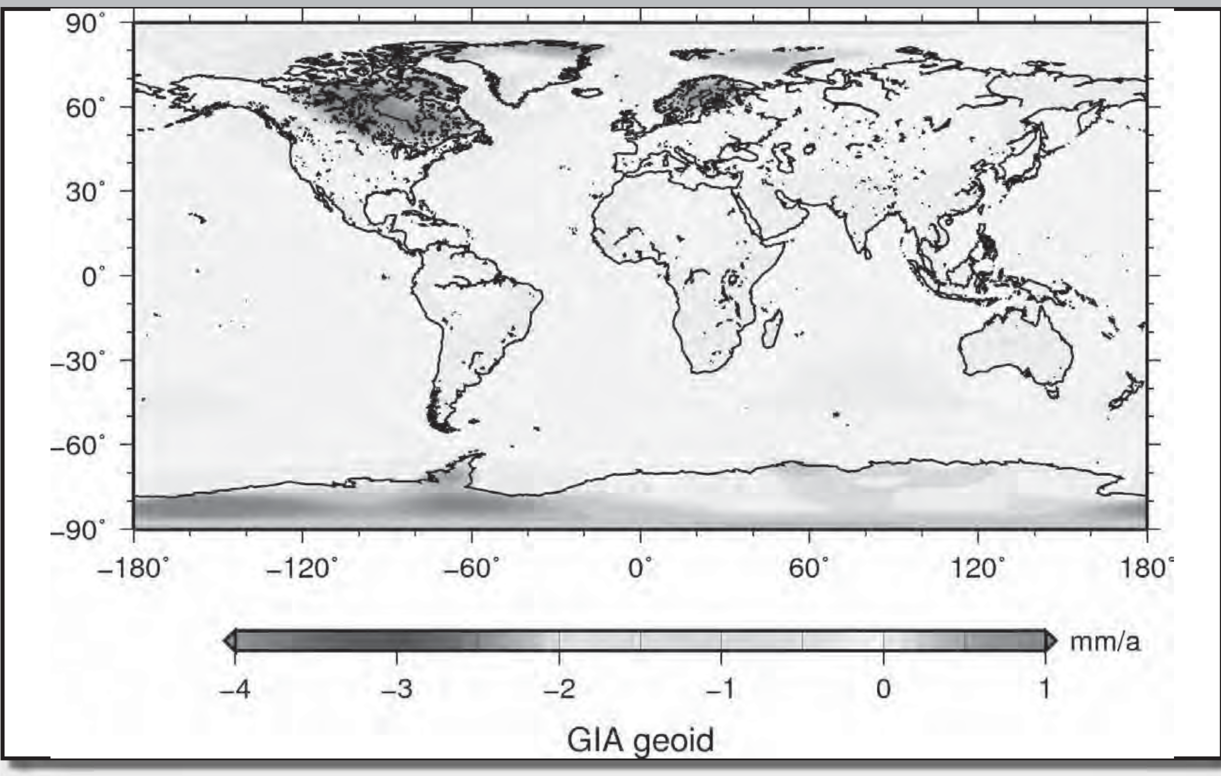

76

DFG SPP 1257

Gia + Greenland

77

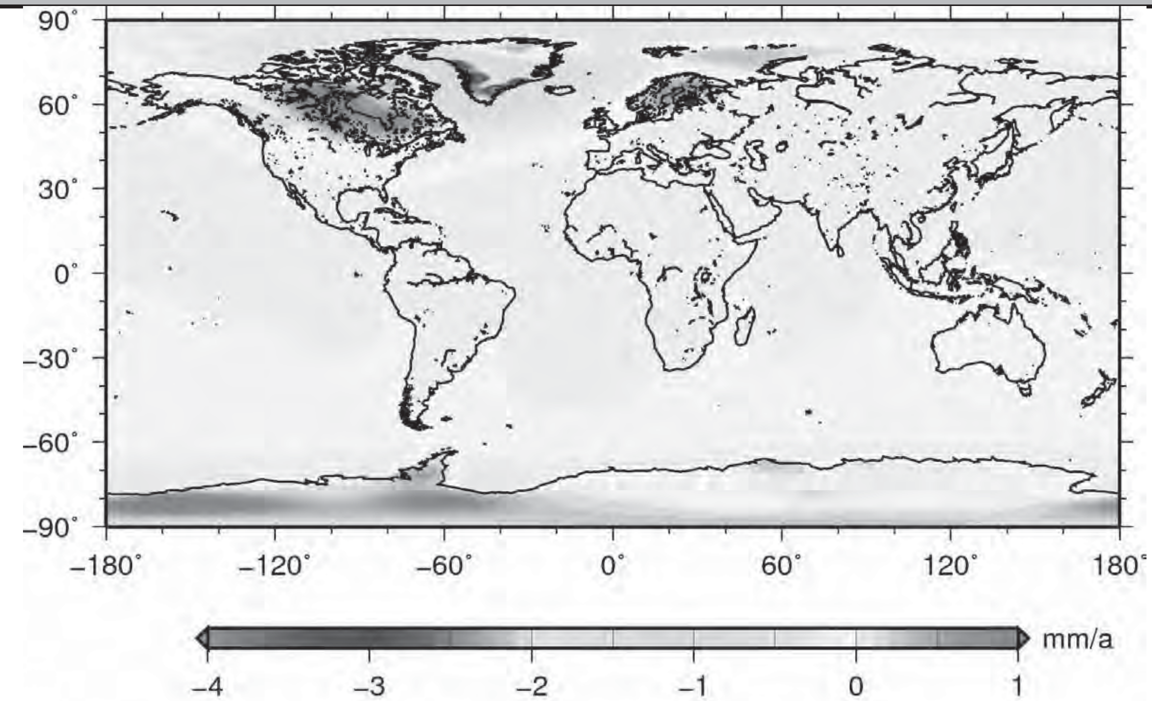

GIA + Greenland geoid

GFZ
Helmholtz Centre
POTSDAM

Gia+greenland-grace

78

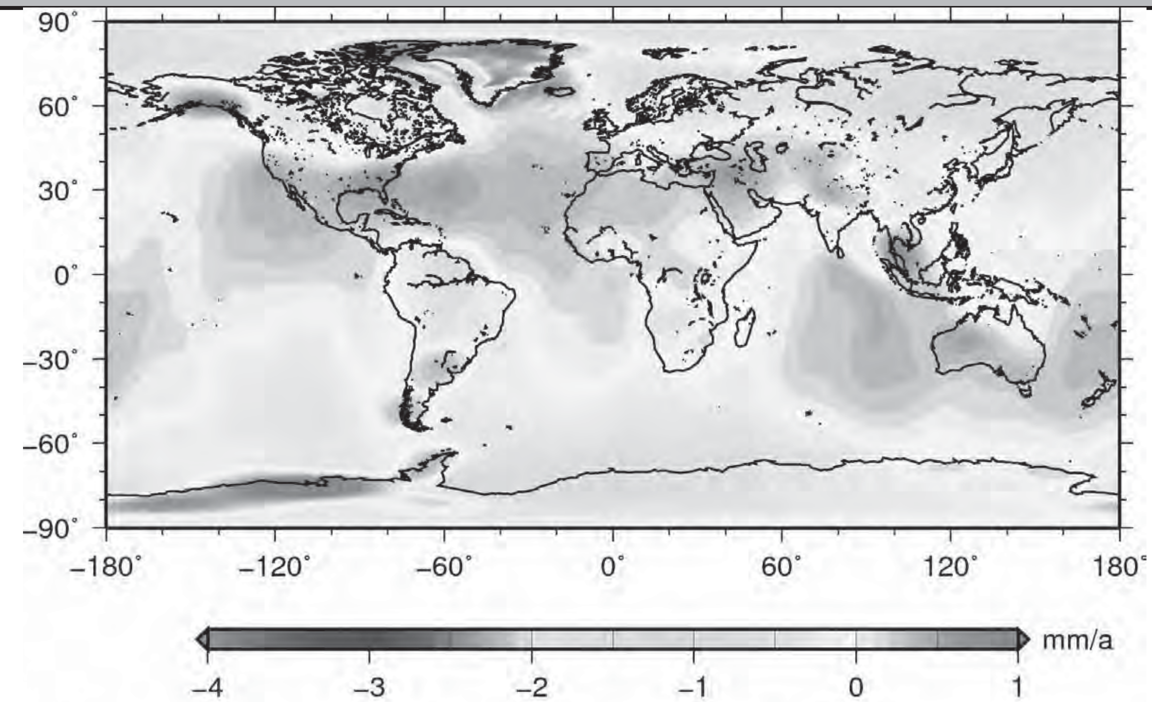

(GIA + Greenland) – GRACE geoid

DFG SPP 1257

Gia+Greenland - GRACE

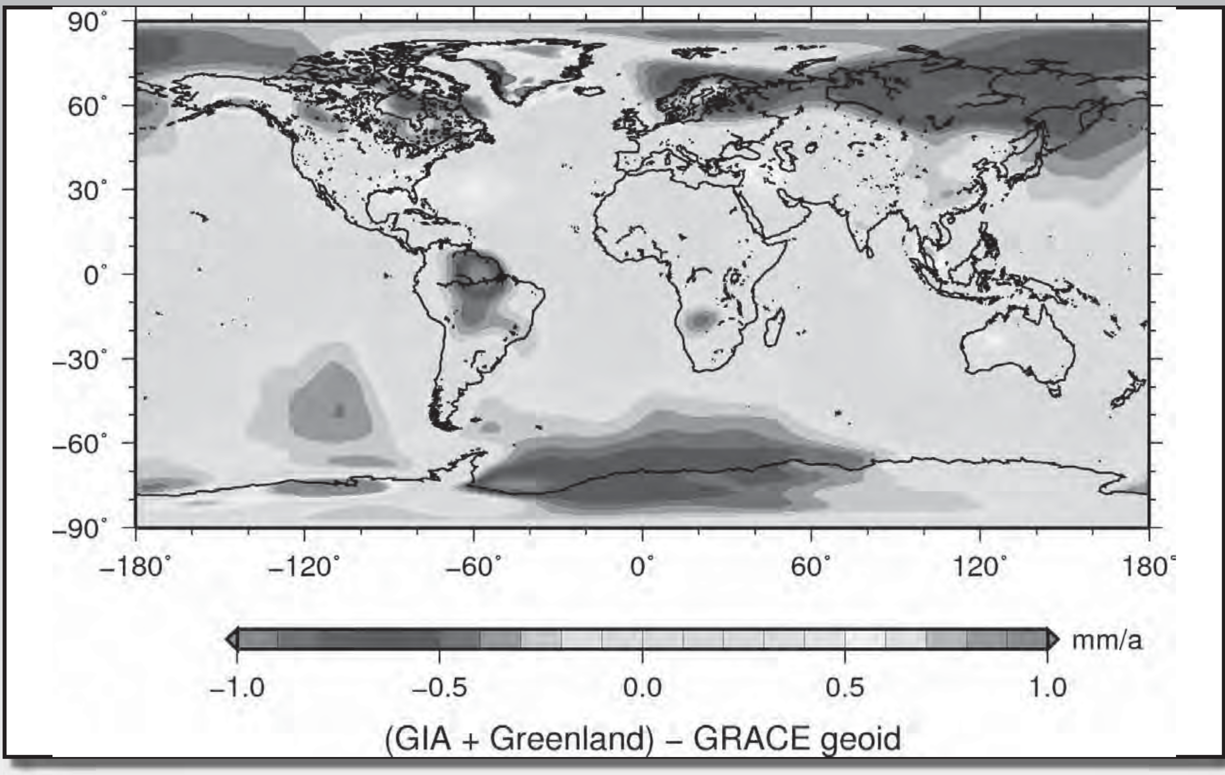

79

DFG SPP 1257

Ocean function

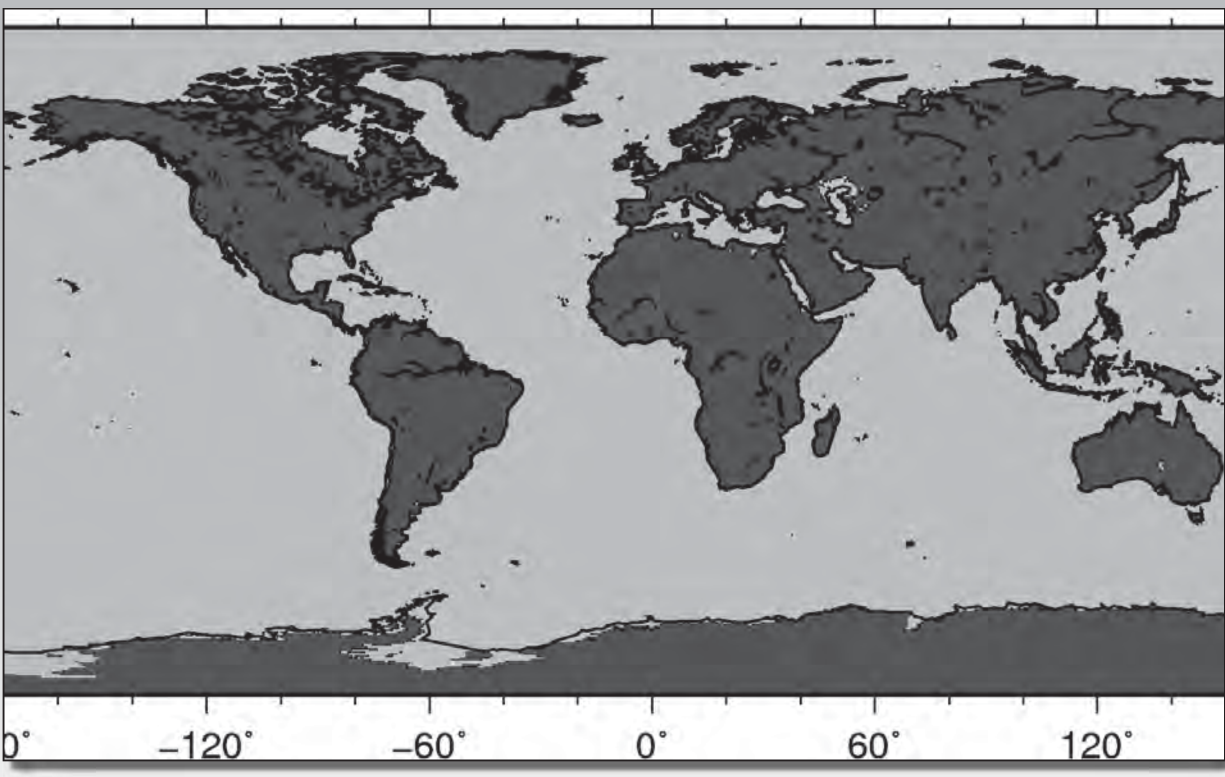

80

DFG SPP 1257

Lecture: Ocean Dynamics

Martin Losch, Henryk Dobslaw

Summer School „Global Water Cycle“
12.-16. September 2011
Mayschoss

DFG SPP 1257

1

Introduction:
Sea level variability at Bermuda

DFG SPP 1257

2

Bermuda Sea Level (Carl Wunsch, 1972)

- tide gauge at Biological Station (8 years)
- surface pressure
- local wind speed
- air temperature
- hydrographic data (bi-weekly)
- secondary tide gauge (~3 km away)

TABLE 4. Sea-Level Variance

Major Sources		Percentage of Total
M_2 tide	60	
All linear tides		70
Radiational tides		0.2
Overtides (including thermal tides S_3, S_4)		negligible
Atmospheric pressure	6	
Atmospheric pressure and winds		14
Dynamic height variations to 1500 db		3
Least count noise		0.2
Total		87

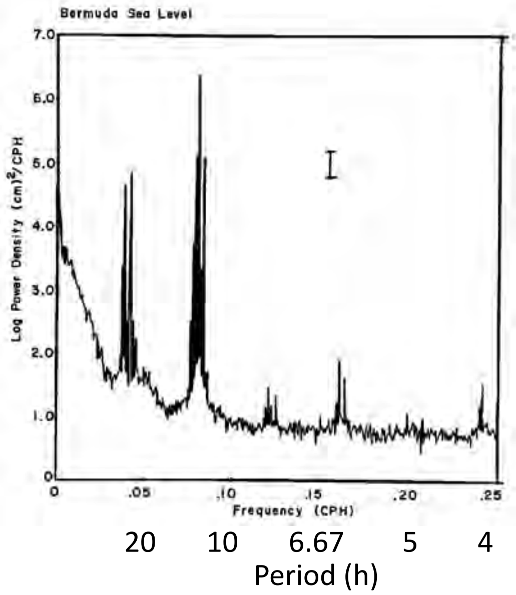

Wunsch (1972)

Bermuda Sea Level (Carl Wunsch, 1972)

- tide gauge at Biological Station (8 years)
- surface pressure
- local wind speed
- air temperature
- hydrographic data (bi-weekly)
- secondary tide gauge (~3 km away)

TABLE 4. Sea-Level Variance

Major Sources		Percentage of Total
M_2 tide	60	
All linear tides		70
Radiational tides		0.2
Overtides (including thermal tides S_3, S_4)		negligible
Atmospheric pressure	6	
Atmospheric pressure and winds		14
Dynamic height variations to 1500 db		3
Least count noise		0.2
Total		87

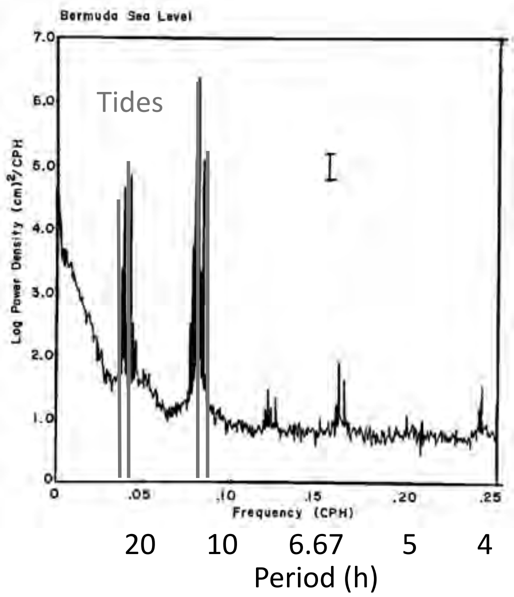

Wunsch (1972)

Bermuda Sea Level (Carl Wunsch, 1972)

- tide gauge at Biological Station (8 years)
- surface pressure
- local wind speed
- air temperature
- hydrographic data (bi-weekly)
- secondary tide gauge (~3 km away)

TABLE 4. Sea-Level Variance

Major Sources		Percentage of Total
M_2 tide	60	
All linear tides		70
Radiational tides		0.2
Overtides (including thermal tides S_3, S_4)		negligible
Atmospheric pressure	6	
Atmospheric pressure and winds		14
Dynamic height variations to 1500 db		3
Least count noise		0.2
Total		87

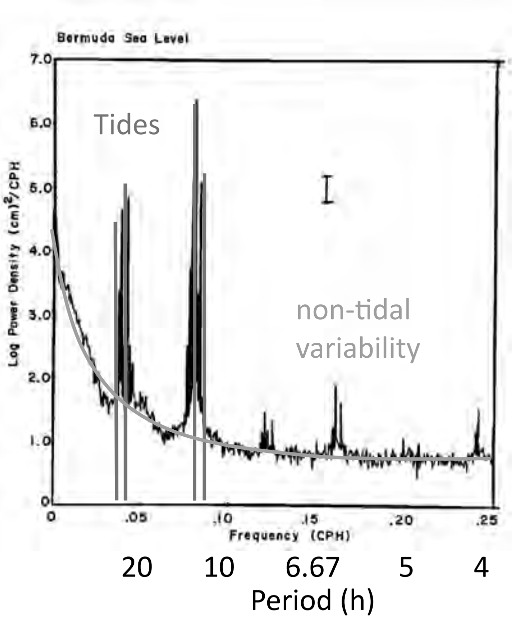

Wunsch (1972)

Objective of Oceanography

- Describe three-dimensional ocean circulation and associated transports of energie (heat) and matter (salt, nutrients, etc.)
- Methods are in principle:
  - observations
  - mathematical and numerical modelling
  - combination of observations and models

Content

1. Properties of Sea Water
2. Ocean Dynamics: equations of motion, common approximations and consequences
3. Non-Tidal short-term variability: effects of pressure, effects of wind, recent models, consideration for GRACE
4. Ocean Tides: tidal potential, Laplace's Tidal Equations, classes of solutions to LTE, recent models, semi-empirical models from GRACE & altimetry
5. De-aliasing

Properties of Sea Water

Properties of Sea Water

Constitutents of sea water: fresh water, minerals/salt (order 35 g/kg)
observable properties:

- temperature: (degree celsius) in-situ (-> potential and conservative temperature)
- salinity: (practical salinity scale), do not use “psu” (practical salinity unit) as “unit”
- density: function of temperature, salinity, pressure (depth), so-called equation of state (EOS). Most recent official EOS is TEOS10 (McDougall et al. 2010).
    - flow is driven by horizontal density gradients
    - flow it predominantly along isopycnals -> potential density, neutral density

- sea water is compressible, water column can expand and contract; bottom pressure changes through mass changes (mass flux at surface, lateral mass flux), but not through expansion/contraction due to warming/cooling

7

Properties of Sea Water: Temperature

- in-situ temperature
- potential temperature: (temperature of a water parcel after being lifted adiabatically to a reference level, usually the surface)
- conservative temperature

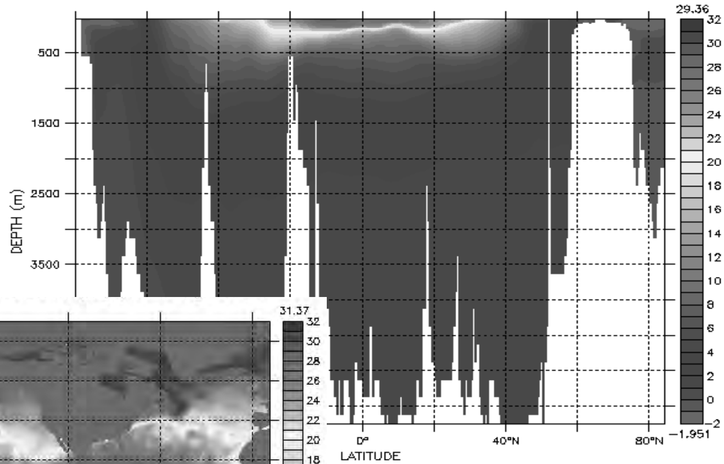

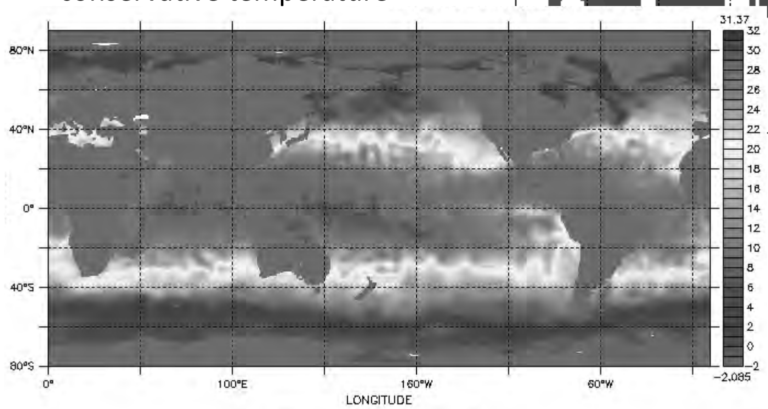

- TEOS10 (McDougall et al 2010) uses concept of conservative temperature (potential enthalphy)

8

ICDC, WOCE data

Properties of Sea Water: Salinity

- practical salinity scale (pss), not a “unit”
- absolute salinity (SA): g of dissolved minerals per kg sea water

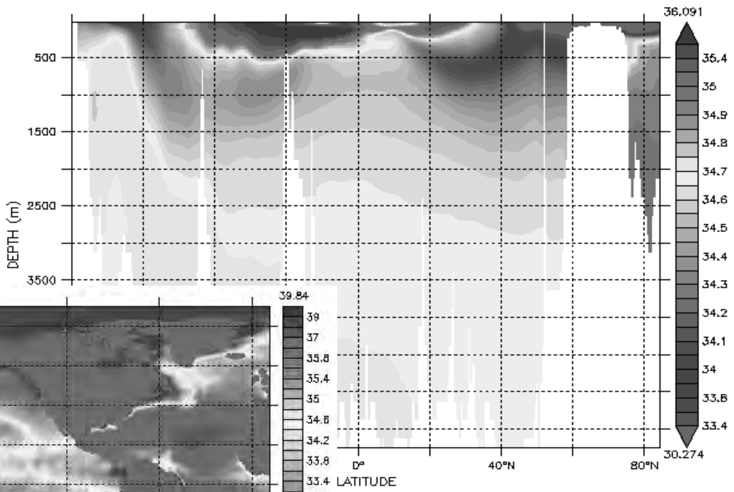

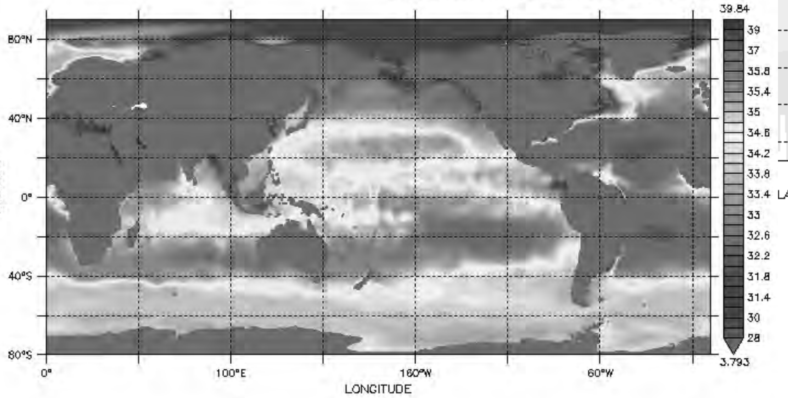

ICDC, WOCE data

Properties of Sea Water: Density = *R(S,T,p)*

In-situ density, potential density (density of a water parcel after lifting adiabatically to a reference level (e.g. surface)), neutral density. Convention: $\sigma = \rho - 1000$ kg/m^3

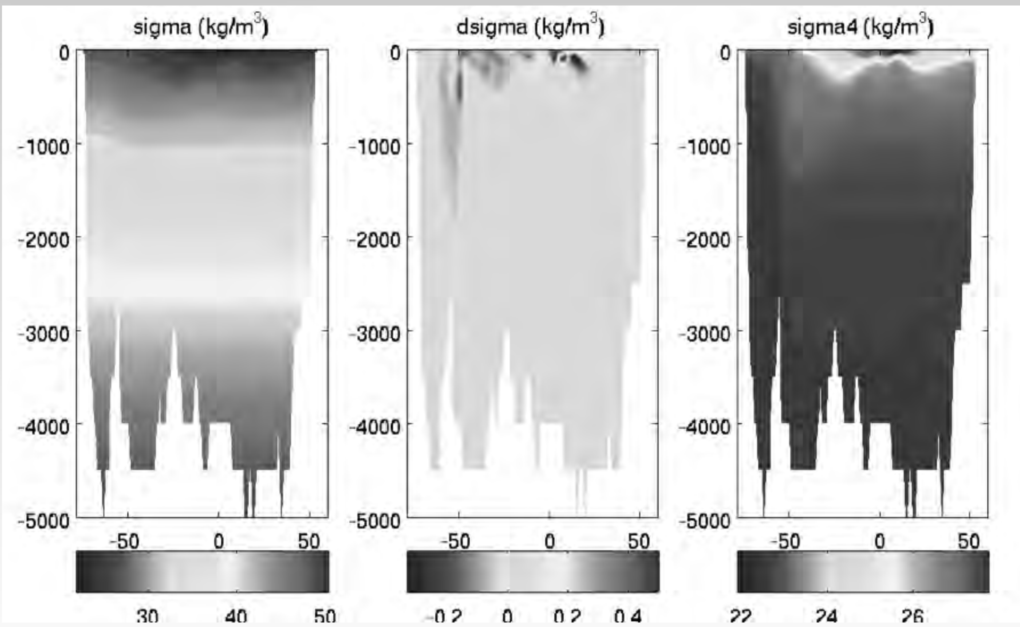

data source: Levitus (1994)

Properties of Sea Water: Density

TABLE 2.1 *Values of density* in situ *for fresh and sea water* ($kg\,m^{-3}$)
(International Equation of State 1980)

Sea pressure	Approx. depth	Fresh water S = 0 temperature		Average sea water S = 35 temperature		Red Sea (winter) S = 40 temperature
10^2 kPa	m	0°	30°C	0°	30°C	18°C
0	0	999.8	995.7	1028.1	1021.7	1029.1
10	100	1000.4	996.1	1028.6	1022.2	1029.6
100	1000	1004.9	(1000.0)	1032.8	(1026.0)	1033.4
400	4000	(1019.3)	(1012.7)	1046.4	(1038.1)	1045.8
1000	10 000	(1045.3)	(1035.9)	1071.0	(1060.4)	(1068.7)

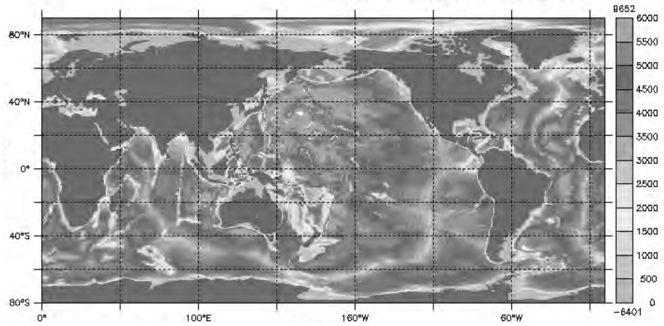

bathymetry [m]

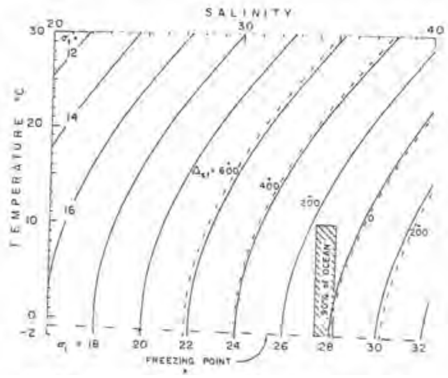

Pond & Pickard (1980)

Properties of Sea Water

Mechanical and thermal properties of sea water at salinity 35 g kg^{-1} and atmospheric pressure (unless otherwise stated)

Property	0 °C	20 °C
Dynamic viscosity	1.88×10^{-3} Pa s	1.08×10^{-3} Pa s
Kinematic viscosity, ν	$1.83 \times 10^{-6}\ m^2\ s^{-1}$	$1.05 \times 10^{-6}\ m^2\ s^{-1}$
Thermal conductivity	$0.563\ W\ m^{-1}\ K^{-1}$	$0.596\ W\ m^{-1}\ K^{-1}$
Thermal diffusivity, κ	$1.37 \times 10^{-7}\ m^2\ s^{-1}$	$1.46 \times 10^{-7}\ m^2\ s^{-1}$
Prandtl number, ν/κ	13.4	7.2
Specific heat capacity, C_p	$3985\ J\ kg^{-1}\ K^{-1}$	$3993\ J\ kg^{-1}\ K^{-1}$
Thermal expansion coefficient		
Pressure = 0.1 MN m^{-2}	$52 \times 10^{-6}\ K^{-1}$	$250 \times 10^{-6}\ K^{-1}$
Pressure = 100 MN m^{-2}	$244 \times 10^{-6}\ K^{-1}$	$325 \times 10^{-6}\ K^{-1}$
Ratio of specific heat capacities, C_p/C_V	1.000 4	1.010 6
Velocity of sound*	1449 m s^{-1}	1522 m s^{-1}
Compressibility	$4.65 \times 10^{-10}\ Pa^{-1}$	$4.28 \times 10^{-10}\ Pa^{-1}$
Freezing point		− 1.910 °C
Boiling point		100.56 °C

Kaye & Laby (2011)

Ocean dynamics

Equations of motion (I)

7 state variables:
3D velocity (u,v,w), pot.temperature (Θ), salinity (S), pressure (p), density (ρ)
require 7 equations
1.-3. Newtons 2. law -> momentum equations (3 components)

$$a = \frac{F}{m} \quad \Leftrightarrow \quad a = \frac{\tilde{F}}{\rho} = \mathcal{F}$$

$$\frac{D\mathbf{v}}{Dt} + f(\mathbf{k} \times \mathbf{v}) \quad = \quad -\frac{1}{\rho}\nabla p - g\mathbf{k} + \mathcal{F}$$

4. mass conservation -> continuity equation

$$\frac{1}{\rho}\frac{D\rho}{Dt} + \nabla \cdot \mathbf{v} = 0$$

Equations of motion (II)

5. equation of state

$$\rho = R(S,T,p) \approx \rho_r[1-\alpha(T-T_r)+\beta(S-S_r)]$$

6. conservation of energy -> equation for potential (conservative) temperature

$$\frac{De}{Dt} = Q_e, \quad e = \rho\, c_p \theta, \quad \Rightarrow \frac{D\theta}{Dt} = \frac{Q_e}{\rho\, c_p}$$

7. conservation of salt -> equation for salinity

$$\frac{DS}{Dt} = Q_S \propto (E-P-R)$$

Important simplifications and approximations follow:
hydrostatic balance, geostrophic balance, Boussinesq approximation

15

DFG SPP 1257

hydrostatic balance

3rd component of momentum equation (vertical momentum)

$$\begin{aligned} \frac{Dw}{Dt} + [f(\mathbf{k}\times\mathbf{v})]_z &= -\frac{1}{\rho}\frac{\partial p}{\partial z} - g + \mathcal{F}_z \\ \Rightarrow \frac{\partial p}{\partial z} &= -g\,\rho \end{aligned}$$

$$\int_{-H}^{\eta} \frac{\partial p}{\partial z}\, dz = \int_{p(-H)}^{p(\eta)} dp = p(\eta) - p_b = -g\int_{-H}^{\eta} \rho\, dz$$

$$p_b = p(\eta) + g\int_{-H}^{\eta} \rho\, dz$$

η = dynamic topography, sea level

bottom pressure = atomspheric pressure + mass/area

$$p_b \approx p(\eta) + g\int_{-H}^{0} \rho\, dz + g\int_{0}^{\eta} \rho_0\, dz = p(\eta) + g\int_{-H}^{0} \rho\, dz + g\rho_0\eta$$

16

DFG SPP 1257

hydrostatic balance

3rd component of momentum equation (vertical momentum)

$$
\begin{aligned}
\frac{Dw}{Dt} + [f(\mathbf{k}\times\mathbf{v})]_z &= -\frac{1}{\rho}\frac{\partial p}{\partial z} - g + \mathcal{F}_z \\
\Rightarrow \frac{\partial p}{\partial z} &= -g\,\rho \\
\int_{-H}^{\eta} \frac{\partial p}{\partial z}\,dz = \int_{p(-H)}^{p(\eta)} dp = p(\eta) - p_b &= -g\int_{-H}^{\eta} \rho\,dz \\
p_b &= p(\eta) + g\int_{-H}^{\eta} \rho\,dz
\end{aligned}
$$

η = dynamic topography, sea level

bottom pressure = atomspheric pressure + mass/area

$$
p_b \approx p(\eta) + g\int_{-H}^{0} \rho\,dz + g\int_{0}^{\eta} \rho_0\,dz = p(\eta) + g\int_{-H}^{0} \rho\,dz + g\rho_0\eta
$$

geostrophic balance

Geostrophy:
Balance between pressure gradient force and Coriolis force

1st and 2nd component of momentum equation (horizontal momentum)

$$
\begin{aligned}
\frac{Du}{Dt} - fv &= -\frac{1}{\rho}\frac{\partial p}{\partial x} + \mathcal{F}_x \quad \Rightarrow \quad fv = +\frac{1}{\rho}\frac{\partial p}{\partial x} \\
\frac{Dv}{Dt} + fu &= -\frac{1}{\rho}\frac{\partial p}{\partial y} + \mathcal{F}_y \quad \Rightarrow \quad fu = -\frac{1}{\rho}\frac{\partial p}{\partial y}
\end{aligned}
$$

∂/∂z and replacing the hydrostatic pressure gives the so-called thermal or geostrophic wind equations: level-of-no-motion problem

$$
\begin{aligned}
f\frac{\partial v}{\partial z} &= +\frac{1}{\rho}\frac{\partial^2 p}{\partial z\partial x} \quad \Rightarrow \quad \frac{\partial v}{\partial z} = -\frac{g}{\rho f}\frac{\partial \rho}{\partial x} \\
f\frac{\partial u}{\partial z} &= -\frac{1}{\rho}\frac{\partial^2 p}{\partial z\partial y} \quad \Rightarrow \quad \frac{\partial u}{\partial z} = +\frac{g}{\rho f}\frac{\partial \rho}{\partial y} \\
\Rightarrow v(z) &= v_0 - \int_{z_0}^{z} \frac{g}{\rho f}\frac{\partial \rho}{\partial x}\,dz'
\end{aligned}
$$

geostrophic balance

Geostrophy:
Balance between pressure gradient force and Coriolis force

1st and 2nd component of momentum equation (horizontal momentum)

$$\frac{Du}{Dt} - fv = -\frac{1}{\rho}\frac{\partial p}{\partial x} + \mathcal{F}_x \quad \Rightarrow \quad fv = +\frac{1}{\rho}\frac{\partial p}{\partial x}$$

$$\frac{Dv}{Dt} + fu = -\frac{1}{\rho}\frac{\partial p}{\partial y} + \mathcal{F}_y \quad \Rightarrow \quad fu = -\frac{1}{\rho}\frac{\partial p}{\partial y}$$

∂/∂z and replacing the hydrostatic pressure gives the so-called thermal or geostrophic wind equations: level-of-no-motion problem

$$f\frac{\partial v}{\partial z} = +\frac{1}{\rho}\frac{\partial^2 p}{\partial z \partial x} \quad \Rightarrow \quad \frac{\partial v}{\partial z} = -\frac{g}{\rho f}\frac{\partial \rho}{\partial x}$$

$$f\frac{\partial u}{\partial z} = -\frac{1}{\rho}\frac{\partial^2 p}{\partial z \partial y} \quad \Rightarrow \quad \frac{\partial u}{\partial z} = +\frac{g}{\rho f}\frac{\partial \rho}{\partial y}$$

$$\Rightarrow v(z) = v_0 - \int_{z_0}^{z} \frac{g}{\rho f}\frac{\partial \rho}{\partial x}\, dz'$$

17

DFG SPP 1257

geostrophic balance

Geostrophy:
Balance between pressure gradient force and Coriolis force

1st and 2nd component of momentum equation (horizontal momentum)

$$\frac{Du}{Dt} - fv = -\frac{1}{\rho}\frac{\partial p}{\partial x} + \mathcal{F}_x \quad \Rightarrow \quad fv = +\frac{1}{\rho}\frac{\partial p}{\partial x}$$

$$\frac{Dv}{Dt} + fu = -\frac{1}{\rho}\frac{\partial p}{\partial y} + \mathcal{F}_y \quad \Rightarrow \quad fu = -\frac{1}{\rho}\frac{\partial p}{\partial y}$$

∂/∂z and replacing the hydrostatic pressure gives the so-called thermal or geostrophic wind equations: level-of-no-motion problem

$$f\frac{\partial v}{\partial z} = +\frac{1}{\rho}\frac{\partial^2 p}{\partial z \partial x} \quad \Rightarrow \quad \boxed{\frac{\partial v}{\partial z} = -\frac{g}{\rho f}\frac{\partial \rho}{\partial x}}$$

$$f\frac{\partial u}{\partial z} = -\frac{1}{\rho}\frac{\partial^2 p}{\partial z \partial y} \quad \Rightarrow \quad \boxed{\frac{\partial u}{\partial z} = +\frac{g}{\rho f}\frac{\partial \rho}{\partial y}}$$

$$\Rightarrow v(z) = v_0 - \int_{z_0}^{z} \frac{g}{\rho f}\frac{\partial \rho}{\partial x}\, dz'$$

17

DFG SPP 1257

alternative to thermal wind: dynamic method

classical method for infering horizontal velocity normal to “hydrographic sections” (equivalent to thermal wind), see e.g. Gill (1980)

geopotential height: $\Phi = g\,z$

insert in hydrostatic balance:

$$-\rho\, g\, dz = -\rho\, d\Phi = dp \Leftrightarrow d\Phi = -\frac{dp}{\rho} = -v_s\, dp$$

$$\Rightarrow \qquad fv = \frac{1}{\rho}\frac{\partial p}{\partial x} = -\frac{\partial \Phi}{\partial x}$$

$$-fu = \frac{1}{\rho}\frac{\partial p}{\partial x} = -\frac{\partial \Phi}{\partial x}$$

geopot. height anomaly: $-\,\Phi'(p) = \int_p^0 \left(\frac{1}{\rho(S,T,p')} - \frac{1}{\rho(35,0,p')}\right) dp'$

$$\Rightarrow \qquad f\left\{v(p) - v(0)\right\} = -\frac{\partial \Phi'(p)}{\partial x} \Rightarrow f\left\{v(p_1) - v(p_2)\right\} = -\frac{\partial}{\partial x}\left\{\Phi'(p_1) - \Phi'(p_2)\right\}$$

$$-f\left\{u(p) - u(0)\right\} = -\frac{\partial \Phi'(p)}{\partial y} \Rightarrow f\left\{u(p_1) - u(p_2)\right\} = -\frac{\partial}{\partial y}\left\{\Phi'(p_1) - \Phi'(p_2)\right\}$$

18

DFG SPP 1257

alternative to thermal wind: dynamic method

classical method for infering horizontal velocity normal to “hydrographic sections” (equivalent to thermal wind), see e.g. Gill (1980)

geopotential height: $\Phi = g\,z$

insert in hydrostatic balance:

$$-\rho\, g\, dz = -\rho\, d\Phi = dp \Leftrightarrow d\Phi = -\frac{dp}{\rho} = -v_s\, dp$$

$$\Rightarrow \qquad fv = \frac{1}{\rho}\frac{\partial p}{\partial x} = -\frac{\partial \Phi}{\partial x}$$

$$-fu = \frac{1}{\rho}\frac{\partial p}{\partial x} = -\frac{\partial \Phi}{\partial x}$$

geopot. height anomaly: $-\,\Phi'(p) = \int_p^0 \left(\frac{1}{\rho(S,T,p')} - \frac{1}{\rho(35,0,p')}\right) dp'$

$$\Rightarrow \qquad f\left\{v(p) - v(0)\right\} = -\frac{\partial \Phi'(p)}{\partial x} \Rightarrow \boxed{f\left\{v(p_1) - v(p_2)\right\} = -\frac{\partial}{\partial x}\left\{\Phi'(p_1) - \Phi'(p_2)\right\}}$$

$$-f\left\{u(p) - u(0)\right\} = -\frac{\partial \Phi'(p)}{\partial y} \Rightarrow \boxed{f\left\{u(p_1) - u(p_2)\right\} = -\frac{\partial}{\partial y}\left\{\Phi'(p_1) - \Phi'(p_2)\right\}}$$

18

DFG SPP 1257

geostrophic balance and surface elevation

19

1st and 2nd component of momentum equation (horizontal momentum)

$$\frac{Du}{Dt} - fv = -\frac{1}{\rho}\frac{\partial p}{\partial x} + \mathcal{F}_x \quad \Rightarrow \quad fv = +\frac{1}{\rho}\frac{\partial p}{\partial x}$$
$$\frac{Dv}{Dt} + fu = -\frac{1}{\rho}\frac{\partial p}{\partial y} + \mathcal{F}_y \quad \Rightarrow \quad fu = -\frac{1}{\rho}\frac{\partial p}{\partial y}$$

integrating the hydrostatic pressure again gives:

$$\begin{aligned} \int_0^\eta \frac{\partial p}{\partial z}\,dz = \int_{p(0)}^{p(\eta)} dp &= -\int_0^\eta g\rho\,dz \\ p(\eta) - p(0) &= -g\rho\eta \\ \Rightarrow u &= -\frac{g}{f}\frac{\partial \eta}{\partial y} \\ v &= +\frac{g}{f}\frac{\partial \eta}{\partial x} \end{aligned}$$

η = dynamic topography, sea level

DFG SPP 1257

geostrophic balance and surface elevation

19

1st and 2nd component of momentum equation (horizontal momentum)

$$\frac{Du}{Dt} - fv = -\frac{1}{\rho}\frac{\partial p}{\partial x} + \mathcal{F}_x \quad \Rightarrow \quad fv = +\frac{1}{\rho}\frac{\partial p}{\partial x}$$
$$\frac{Dv}{Dt} + fu = -\frac{1}{\rho}\frac{\partial p}{\partial y} + \mathcal{F}_y \quad \Rightarrow \quad fu = -\frac{1}{\rho}\frac{\partial p}{\partial y}$$

integrating the hydrostatic pressure again gives:

$$\begin{aligned} \int_0^\eta \frac{\partial p}{\partial z}\,dz = \int_{p(0)}^{p(\eta)} dp &= -\int_0^\eta g\rho\,dz \\ p(\eta) - p(0) &= -g\rho\eta \\ \Rightarrow u &= -\frac{g}{f}\frac{\partial \eta}{\partial y} \\ v &= +\frac{g}{f}\frac{\partial \eta}{\partial x} \end{aligned}$$

η = dynamic topography, sea level

DFG SPP 1257

geostrophic balance and surface elevation

19

1st and 2nd component of momentum equation (horizontal momentum)

$$\frac{Du}{Dt} - fv = -\frac{1}{\rho}\frac{\partial p}{\partial x} + \mathcal{F}_x \quad \Rightarrow \quad fv = +\frac{1}{\rho}\frac{\partial p}{\partial x}$$
$$\frac{Dv}{Dt} + fu = -\frac{1}{\rho}\frac{\partial p}{\partial y} + \mathcal{F}_y \quad \Rightarrow \quad fu = -\frac{1}{\rho}\frac{\partial p}{\partial y}$$

integrating the hydrostatic pressure again gives:

$$\begin{aligned} \int_0^\eta \frac{\partial p}{\partial z}\,dz = \int_{p(0)}^{p(\eta)} dp &= -\int_0^\eta g\rho\,dz \\ p(\eta) - p(0) &= -g\rho\eta \end{aligned}$$
$$\boxed{\begin{aligned} \Rightarrow u &= -\frac{g}{f}\frac{\partial \eta}{\partial y} \\ v &= +\frac{g}{f}\frac{\partial \eta}{\partial x} \end{aligned}}$$

η = dynamic topography, sea level

DFG SPP 1257

geostrophic balance and surface elevation

19

1st and 2nd component of momentum equation (horizontal momentum)

$$\frac{Du}{Dt} - fv = -\frac{1}{\rho}\frac{\partial p}{\partial x} + \mathcal{F}_x \quad \Rightarrow \quad fv = +\frac{1}{\rho}\frac{\partial p}{\partial x}$$
$$\frac{Dv}{Dt} + fu = -\frac{1}{\rho}\frac{\partial p}{\partial y} + \mathcal{F}_y \quad \Rightarrow \quad fu = -\frac{1}{\rho}\frac{\partial p}{\partial y}$$

integrating the hydrostatic pressure again gives:

$$\begin{aligned} \int_0^\eta \frac{\partial p}{\partial z}\,dz = \int_{p(0)}^{p(\eta)} dp &= -\int_0^\eta g\rho\,dz \\ p(\eta) - p(0) &= -g\rho\eta \\ \Rightarrow u &= -\frac{g}{f}\frac{\partial \eta}{\partial y} \\ v &= +\frac{g}{f}\frac{\partial \eta}{\partial x} \end{aligned}$$

η = dynamic topography, sea level

DFG SPP 1257

geostrophic balance and surface elevation

1st and 2nd component of momentum equation (horizontal momentum)

$$\frac{Du}{Dt} - fv = -\frac{1}{\rho}\frac{\partial p}{\partial x} + \mathcal{F}_x \quad \Rightarrow \quad fv = +\frac{1}{\rho}\frac{\partial p}{\partial x}$$

$$\frac{Dv}{Dt} + fu = -\frac{1}{\rho}\frac{\partial p}{\partial y} + \mathcal{F}_y \quad \Rightarrow \quad fu = -\frac{1}{\rho}\frac{\partial p}{\partial y}$$

integrating the hydrostatic pressure again gives:

$$\int_0^\eta \frac{\partial p}{\partial z}\,dz = \int_{p(0)}^{p(\eta)} dp = -\int_0^\eta g\rho\,dz$$

Inverted Barometer $\quad p(\eta) - p(0) = -g\rho\eta$

$$\Rightarrow u = -\frac{g}{f}\frac{\partial \eta}{\partial y}$$

$$v = +\frac{g}{f}\frac{\partial \eta}{\partial x}$$

η = dynamic topography, sea level

19

DFG SPP 1257

Boussinesq Approximation

According to Spiegel and Veronis (1960):

1. The fluctuations in density which appear with the advent of motion result principally from thermal (as opposed to pressure) effects.
2. In the equations for the rate of change of momentum and mass, density variations may be neglected except when they are coupled to the gravitational acceleration in the buoyancy force.

$$1.\quad \frac{1}{\rho}\frac{D\rho}{Dt} + \nabla\cdot\mathbf{v} = 0 \Rightarrow \nabla\cdot\mathbf{v} = 0$$

mass balance becomes volume balance

$$2.\quad \frac{D\mathbf{v}}{Dt} + f(\mathbf{k}\times\mathbf{v}) = -\frac{1}{\rho_0}\nabla p - g\mathbf{k} + \mathcal{F}$$

20

DFG SPP 1257

Consequences of the Boussinesq Approximation

Integrating the continuity equation vertically gives:

$$
\begin{aligned}
\int_{-H}^{\eta}\left(\frac{1}{\rho}\frac{D\rho}{Dt}+\nabla\cdot\mathbf{v}\right)dz &= Q_{\mathbf{FW}}\\
\int_{-H}^{\eta}\nabla_h\cdot\mathbf{u}\,dz+\int_{-H}^{\eta}\frac{\partial w}{\partial z}\,dz &= Q_{\mathbf{FW}}-\int_{-H}^{\eta}\frac{1}{\rho}\frac{D\rho}{Dt}\,dz\\
\int_{-H}^{\eta}\frac{\partial w}{\partial z}\,dz = w(\eta)-w(-H) &= Q_{\mathbf{FW}}-\nabla_h\cdot\int_{-H}^{\eta}\mathbf{u}\,dz-\int_{-H}^{\eta}\frac{1}{\rho}\frac{D\rho}{Dt}\,dz\\
w(\eta)=\frac{d\eta}{dt} &= Q_{\mathbf{FW}}-\nabla_h\cdot\int_{-H}^{\eta}\mathbf{u}\,dz+w(-H)-\int_{-H}^{\eta}\frac{1}{\rho}\frac{D\rho}{Dt}\,dz\\
\frac{d\eta}{dt} &= Q_{\mathbf{FW}}-\nabla_h\cdot\int_{-H}^{\eta}\mathbf{u}\,dz+w(-H)\\
&\quad+\int_{-H}^{\eta}\frac{\rho_r}{\rho}\frac{D(\alpha T)}{Dt}\,dz-\int_{-H}^{\eta}\frac{\rho_r}{\rho}\frac{D(\beta S)}{Dt}\,dz\\
\text{horizontal integral:}\quad\frac{\partial\overline{\eta}}{\partial t} &= \overline{Q_{\mathbf{FW}}}+\int_{-H}^{\eta}\overline{\frac{\rho_r}{\rho}\frac{D(\alpha T)}{Dt}}\,dz-\int_{-H}^{\eta}\overline{\frac{\rho_r}{\rho}\frac{D(\beta S)}{Dt}}\,dz
\end{aligned}
$$

21

DFG SPP 1257

Consequences of the Boussinesq Approximation

Integrating the continuity equation vertically gives:

$$
\begin{aligned}
\int_{-H}^{\eta}\left(\frac{1}{\rho}\frac{D\rho}{Dt}+\nabla\cdot\mathbf{v}\right)dz &= Q_{\mathbf{FW}}\\
\int_{-H}^{\eta}\nabla_h\cdot\mathbf{u}\,dz+\int_{-H}^{\eta}\frac{\partial w}{\partial z}\,dz &= Q_{\mathbf{FW}}-\int_{-H}^{\eta}\frac{1}{\rho}\frac{D\rho}{Dt}\,dz\\
\int_{-H}^{\eta}\frac{\partial w}{\partial z}\,dz = w(\eta)-w(-H) &= Q_{\mathbf{FW}}-\nabla_h\cdot\int_{-H}^{\eta}\mathbf{u}\,dz-\int_{-H}^{\eta}\frac{1}{\rho}\frac{D\rho}{Dt}\,dz\\
w(\eta)=\frac{d\eta}{dt} &= Q_{\mathbf{FW}}-\nabla_h\cdot\int_{-H}^{\eta}\mathbf{u}\,dz+w(-H)-\int_{-H}^{\eta}\frac{1}{\rho}\frac{D\rho}{Dt}\,dz\\
\frac{d\eta}{dt} &= Q_{\mathbf{FW}}-\nabla_h\cdot\int_{-H}^{\eta}\mathbf{u}\,dz+w(-H)\\
&\quad+\int_{-H}^{\eta}\frac{\rho_r}{\rho}\frac{D(\alpha T)}{Dt}\,dz-\int_{-H}^{\eta}\frac{\rho_r}{\rho}\frac{D(\beta S)}{Dt}\,dz\\
\text{horizontal integral:}\quad\frac{\partial\overline{\eta}}{\partial t} &= \overline{Q_{\mathbf{FW}}}+\int_{-H}^{\eta}\overline{\frac{\rho_r}{\rho}\frac{D(\alpha T)}{Dt}}\,dz-\int_{-H}^{\eta}\overline{\frac{\rho_r}{\rho}\frac{D(\beta S)}{Dt}}\,dz
\end{aligned}
$$

21

DFG SPP 1257

Consequences of the Boussinesq Approximation

21

Integrating the continuity equation vertically gives:

$$
\begin{aligned}
\int_{-H}^{\eta} \left(\frac{1}{\rho}\frac{D\rho}{Dt} + \nabla\cdot\mathbf{v} \right) dz &= Q_{\mathbf{FW}} \\
\int_{-H}^{\eta} \nabla_h \cdot \mathbf{u}\, dz + \int_{-H}^{\eta} \frac{\partial w}{\partial z}\, dz &= Q_{\mathbf{FW}} - \int_{-H}^{\eta} \frac{1}{\rho}\frac{D\rho}{Dt}\, dz \\
\int_{-H}^{\eta} \frac{\partial w}{\partial z}\, dz = w(\eta) - w(-H) &= Q_{\mathbf{FW}} - \nabla_h \cdot \int_{-H}^{\eta} \mathbf{u}\, dz - \int_{-H}^{\eta} \frac{1}{\rho}\frac{D\rho}{Dt}\, dz \\
w(\eta) = \frac{d\eta}{dt} &= Q_{\mathbf{FW}} - \nabla_h \cdot \int_{-H}^{\eta} \mathbf{u}\, dz + w(-H) - \int_{-H}^{\eta} \frac{1}{\rho}\frac{D\rho}{Dt}\, dz \\
\frac{d\eta}{dt} &= Q_{\mathbf{FW}} - \nabla_h \cdot \int_{-H}^{\eta} \mathbf{u}\, dz + w(-H) \\
&\quad + \int_{-H}^{\eta} \frac{\rho_r}{\rho} \frac{D(\alpha T)}{Dt}\, dz - \int_{-H}^{\eta} \frac{\rho_r}{\rho} \frac{D(\beta S)}{Dt}\, dz \\
\text{horizontal integral:} \quad \frac{\partial \overline{\eta}}{\partial t} &= \overline{Q_{\mathbf{FW}}} + \overline{\int_{-H}^{\eta} \frac{\rho_r}{\rho} \frac{D(\alpha T)}{Dt}\, dz} - \overline{\int_{-H}^{\eta} \frac{\rho_r}{\rho} \frac{D(\beta S)}{Dt}\, dz}
\end{aligned}
$$

Consequences of the Boussinesq Approximation

21

Integrating the continuity equation vertically gives:

$$
\begin{aligned}
\int_{-H}^{\eta} \left(\frac{1}{\rho}\frac{D\rho}{Dt} + \nabla\cdot\mathbf{v} \right) dz &= Q_{\mathbf{FW}} \\
\int_{-H}^{\eta} \nabla_h \cdot \mathbf{u}\, dz + \int_{-H}^{\eta} \frac{\partial w}{\partial z}\, dz &= Q_{\mathbf{FW}} - \int_{-H}^{\eta} \frac{1}{\rho}\frac{D\rho}{Dt}\, dz \\
\int_{-H}^{\eta} \frac{\partial w}{\partial z}\, dz = w(\eta) - w(-H) &= Q_{\mathbf{FW}} - \nabla_h \cdot \int_{-H}^{\eta} \mathbf{u}\, dz - \int_{-H}^{\eta} \frac{1}{\rho}\frac{D\rho}{Dt}\, dz \\
w(\eta) = \frac{d\eta}{dt} &= Q_{\mathbf{FW}} - \nabla_h \cdot \int_{-H}^{\eta} \mathbf{u}\, dz + w(-H) - \int_{-H}^{\eta} \frac{1}{\rho}\frac{D\rho}{Dt}\, dz \\
\frac{d\eta}{dt} &= Q_{\mathbf{FW}} - \nabla_h \cdot \int_{-H}^{\eta} \mathbf{u}\, dz + w(-H) \\
&\quad + \int_{-H}^{\eta} \frac{\rho_r}{\rho} \frac{D(\alpha T)}{Dt}\, dz - \int_{-H}^{\eta} \frac{\rho_r}{\rho} \frac{D(\beta S)}{Dt}\, dz \\
\text{horizontal integral:} \quad \frac{\partial \overline{\eta}}{\partial t} &= \overline{Q_{\mathbf{FW}}} + \overline{\int_{-H}^{\eta} \frac{\rho_r}{\rho} \frac{D(\alpha T)}{Dt}\, dz} - \overline{\int_{-H}^{\eta} \frac{\rho_r}{\rho} \frac{D(\beta S)}{Dt}\, dz}
\end{aligned}
$$

Consequences of the Boussinesq Approximation

21

Integrating the continuity equation vertically gives:

$$\begin{aligned}
\int_{-H}^{\eta}\left(\frac{1}{\rho}\frac{D\rho}{Dt}+\nabla\cdot\mathbf{v}\right)dz &= Q_{\mathbf{FW}}\\
\int_{-H}^{\eta}\nabla_h\cdot\mathbf{u}\,dz+\int_{-H}^{\eta}\frac{\partial w}{\partial z}\,dz &= Q_{\mathbf{FW}}-\int_{-H}^{\eta}\frac{1}{\rho}\frac{D\rho}{Dt}\,dz\\
\int_{-H}^{\eta}\frac{\partial w}{\partial z}\,dz = w(\eta)-w(-H) &= Q_{\mathbf{FW}}-\nabla_h\cdot\int_{-H}^{\eta}\mathbf{u}\,dz-\int_{-H}^{\eta}\frac{1}{\rho}\frac{D\rho}{Dt}\,dz\\
w(\eta)=\frac{d\eta}{dt} &= Q_{\mathbf{FW}}-\nabla_h\cdot\int_{-H}^{\eta}\mathbf{u}\,dz+w(-H)-\int_{-H}^{\eta}\frac{1}{\rho}\frac{D\rho}{Dt}\,dz\\
\frac{d\eta}{dt} &= Q_{\mathbf{FW}}-\nabla_h\cdot\int_{-H}^{\eta}\mathbf{u}\,dz+w(-H)\\
&\quad+\int_{-H}^{\eta}\frac{\rho_r}{\rho}\frac{D(\alpha T)}{Dt}\,dz-\int_{-H}^{\eta}\frac{\rho_r}{\rho}\frac{D(\beta S)}{Dt}\,dz\\
\text{horizontal integral:}\quad\frac{\partial\overline{\eta}}{\partial t} &= \overline{Q_{\mathbf{FW}}}+\int_{-H}^{\eta}\overline{\frac{\rho_r}{\rho}\frac{D(\alpha T)}{Dt}}\,dz-\int_{-H}^{\eta}\overline{\frac{\rho_r}{\rho}\frac{D(\beta S)}{Dt}}\,dz
\end{aligned}$$

DFG SPP 1257

Consequences of the Boussinesq Approximation

21

Integrating the continuity equation vertically gives:

$$\begin{aligned}
\int_{-H}^{\eta}\left(\frac{1}{\rho}\frac{D\rho}{Dt}+\nabla\cdot\mathbf{v}\right)dz &= Q_{\mathbf{FW}}\\
\int_{-H}^{\eta}\nabla_h\cdot\mathbf{u}\,dz+\int_{-H}^{\eta}\frac{\partial w}{\partial z}\,dz &= Q_{\mathbf{FW}}-\int_{-H}^{\eta}\frac{1}{\rho}\frac{D\rho}{Dt}\,dz\\
\int_{-H}^{\eta}\frac{\partial w}{\partial z}\,dz = w(\eta)-w(-H) &= Q_{\mathbf{FW}}-\nabla_h\cdot\int_{-H}^{\eta}\mathbf{u}\,dz-\int_{-H}^{\eta}\frac{1}{\rho}\frac{D\rho}{Dt}\,dz\\
w(\eta)=\frac{d\eta}{dt} &= Q_{\mathbf{FW}}-\nabla_h\cdot\int_{-H}^{\eta}\mathbf{u}\,dz+w(-H)-\int_{-H}^{\eta}\frac{1}{\rho}\frac{D\rho}{Dt}\,dz\\
\frac{d\eta}{dt} &= Q_{\mathbf{FW}}-\nabla_h\cdot\int_{-H}^{\eta}\mathbf{u}\,dz+w(-H)\\
&\quad+\int_{-H}^{\eta}\frac{\rho_r}{\rho}\frac{D(\alpha T)}{Dt}\,dz-\int_{-H}^{\eta}\frac{\rho_r}{\rho}\frac{D(\beta S)}{Dt}\,dz\\
\text{horizontal integral:}\quad\frac{\partial\overline{\eta}}{\partial t} &= \overline{Q_{\mathbf{FW}}}+\int_{-H}^{\eta}\overline{\frac{\rho_r}{\rho}\frac{D(\alpha T)}{Dt}}\,dz-\int_{-H}^{\eta}\overline{\frac{\rho_r}{\rho}\frac{D(\beta S)}{Dt}}\,dz
\end{aligned}$$

DFG SPP 1257

Consequences of the Boussinesq Approximation

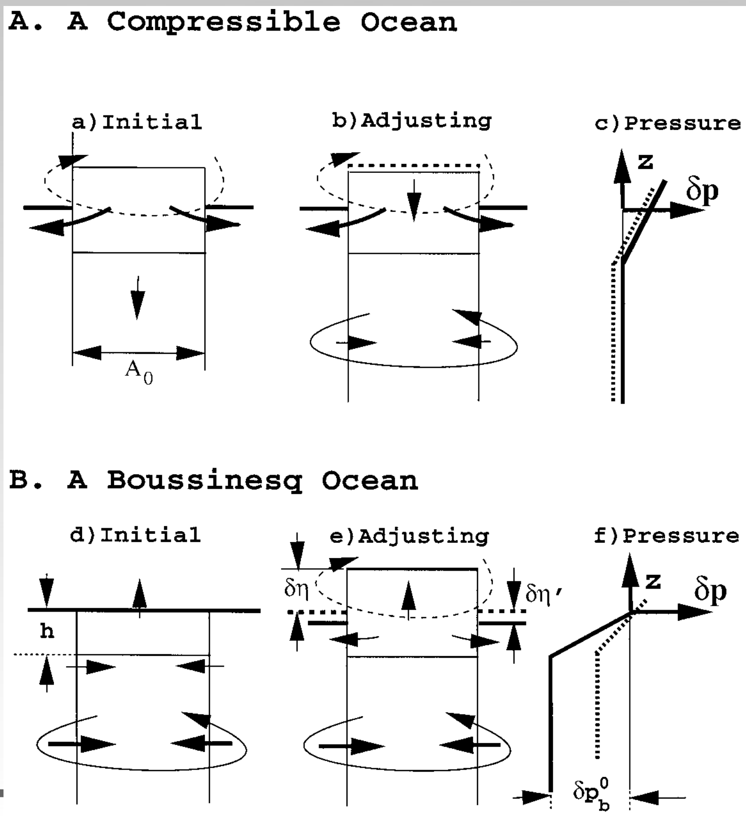

FIG. 1. Sketch of geostrophic adjustment in response to surface heating.

example of Boussinesq effect: geostrophic adjustment after surface heating,
Huang and Jin (2002)

Surface wind forcing

surface winds exert stress (τ) on ocean surface and drive a thin (order 100 m) surface layer with a lot of turbulence -> turbulent stress divergence ∂σ/∂z

$\rho_0 f($

w ... $_E\, dz$

... $\frac{\tau}{\rho_0 f}$

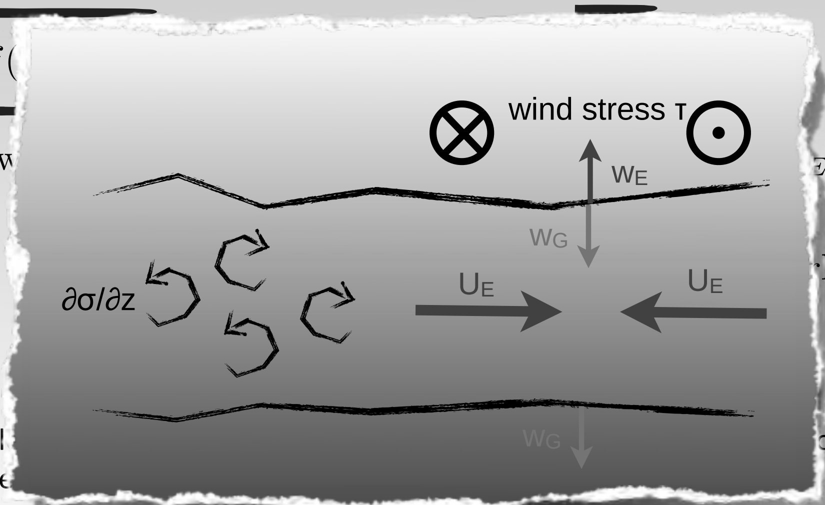

...on,

correlations between OBP and WSC, but note assumption of stationarity: d/dt = 0 => only long/seasonal timescales can be considered, e.g. Gill and Niiler, 1973 (DSR).

Surface wind forcing

surface winds exert stress (τ) on ocean surface and drive a thin (order 100 m) surface layer with a lot of turbulence -> turbulent stress divergence ∂σ/∂z

$$\boxed{\rho_0 f(\mathbf{k}\times\mathbf{u}_E)} + \boxed{\rho_0 f(\mathbf{k}\times\mathbf{u}_G) = -\nabla_h p} + \boxed{\frac{\partial\sigma}{\partial z}},$$

$$\text{with}\quad \nabla_h\mathbf{u}_E + \frac{\partial w_E}{\partial z} = 0 \Rightarrow w_E(0) = -\nabla_h\int_{-h_m}^{0}\mathbf{u}_E\,dz$$

$$\nabla_h\int_{-h_m}^{0}\mathbf{u}_E\,dz = -\nabla_h\left(\mathbf{k}\times\frac{\tau}{\rho_0 f}\right) = \mathrm{curl}\frac{\tau}{\rho_0 f}$$

$$w_G(0) + w_E(0) \stackrel{!}{=} 0 \Rightarrow w_G(0) = \mathrm{curl}\frac{\tau}{\rho_0 f}$$

leads to Ekman transport, Ekman pumping and mass redistribution, e.g. Song and Zlotnicki, 2008, Chambers and Willis, 2008 find correlations between OBP and WSC, but note assumption of stationarity: d/dt = 0 => only long/seasonal timescales can be considered, e.g. Gill and Niiler, 1973 (DSR).

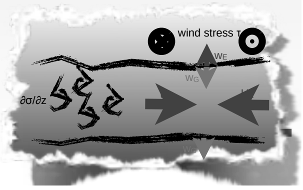

23

Short-term Non-Tidal Variability: The ocean‘s response to atmospheric forcing

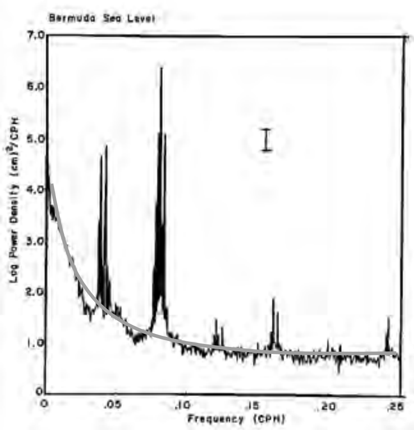

24

DFG SPP 1257

Wind Stress: time variations

Theory for seasonal ocean variability by Gill and Niiler (Deep Sea Res., 1973):

- adjustment of density field slow wrt. seasonal time-scales
- bottom pressure changes related to changes in wind stress curl

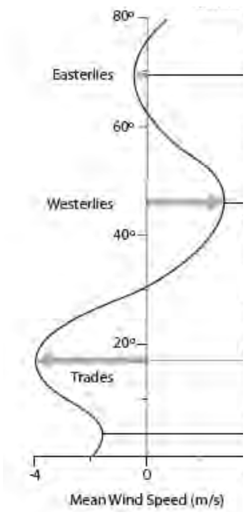

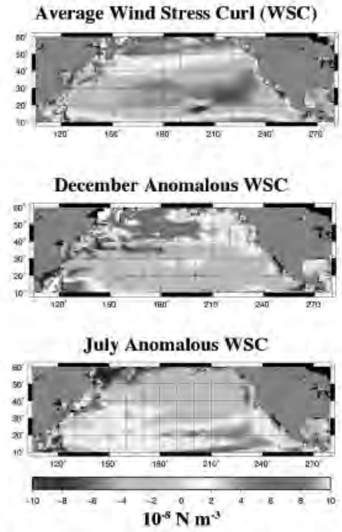

CCMP winds & OMCT bottom pressure (1992 – 2008)

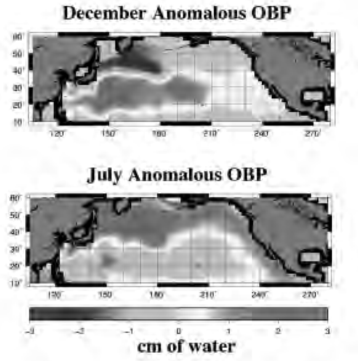

Chambers (OSD, 2011)

Atmospheric Pressure Forcing

IB assumption:

ocean is assumed to react iso-statically to changes in surface pressure

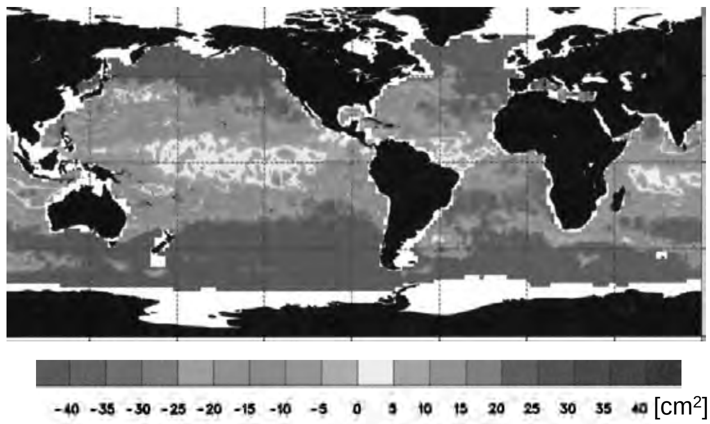

$$\eta(t) = -\frac{p'_a(t)}{\rho_0 g}$$

$$p'_a(t) = p_a(t) - \int\int_{Ocean} p_a(\theta, \lambda, t)\, d\theta\, d\lambda$$

IB assumption is justified away from the tropics and on time-scales longer than a few days

Wunsch and Stammer (1997)

Atmospheric Tides and the Ocean's Response

- daily varying solar insolation is absorbed by water vapor and ozone
- causes variations in temperature, winds, and consequently surface pressure

short periods:
daily, twice-daily

ocean response deviates substantially from IB assumption

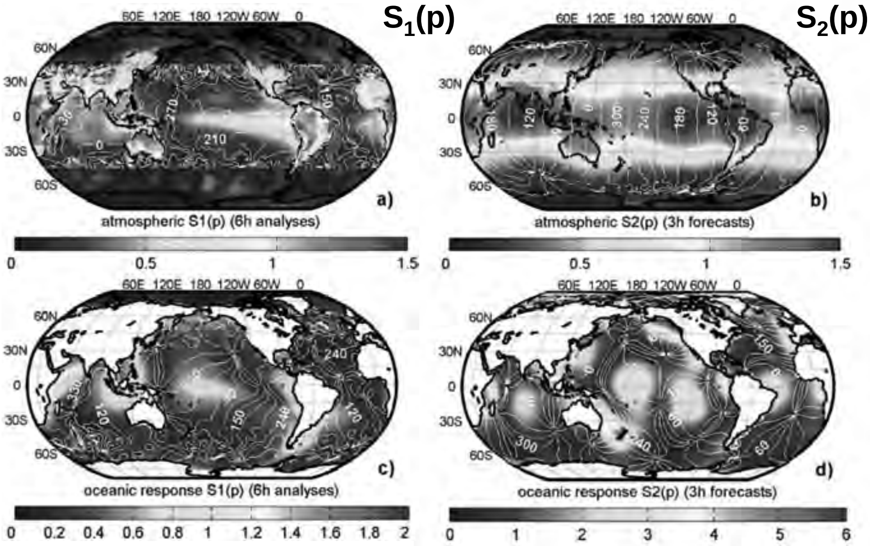

Dobslaw and Thomas (2005)

Freshwater Fluxes

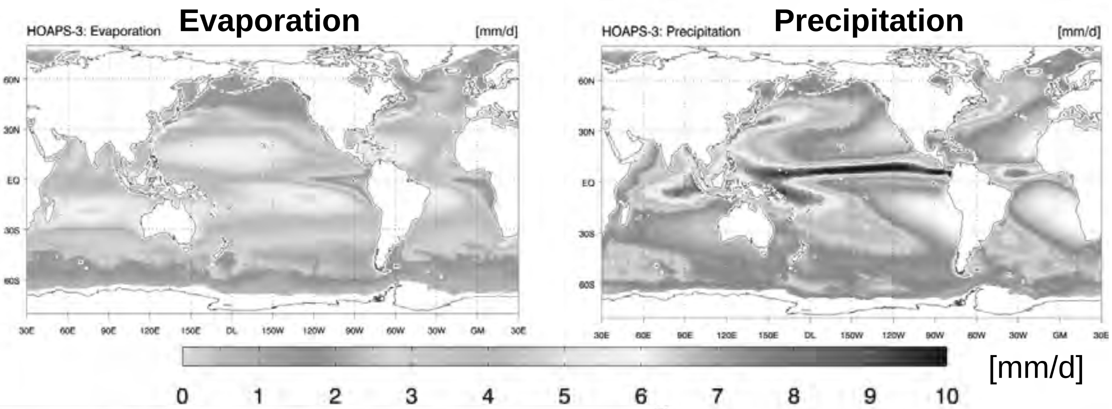

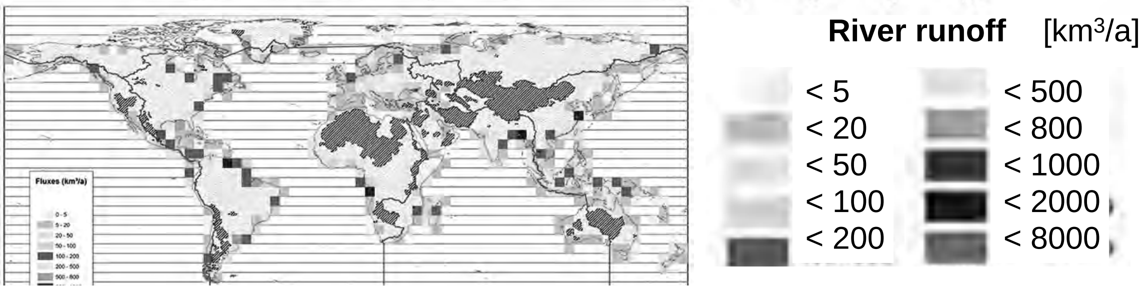

GRDC; HOAPS, MPI-M & Uni HH

Freshwater Fluxes: variations in total ocean mass

variations in total ocean mass are predominantly seasonal:

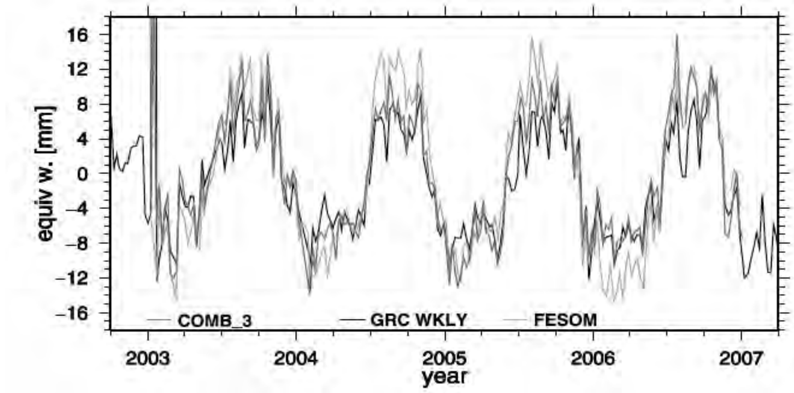

Rietbroek et al. (2008)

29

DFG SPP 1257

Freshwater Fluxes: variations in total ocean mass

variations in total ocean mass are predominantly seasonal:

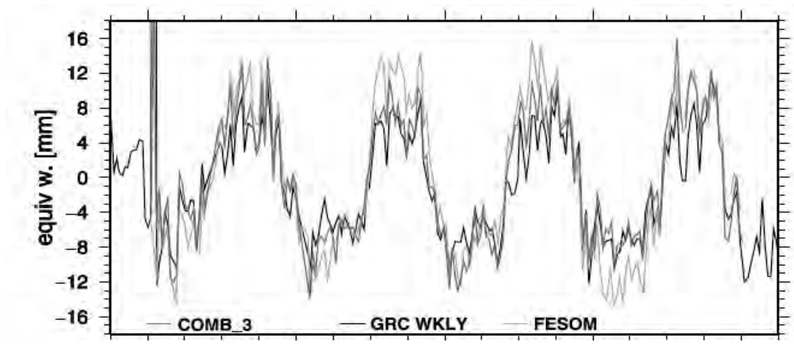

Rietbroek et al. (2008)

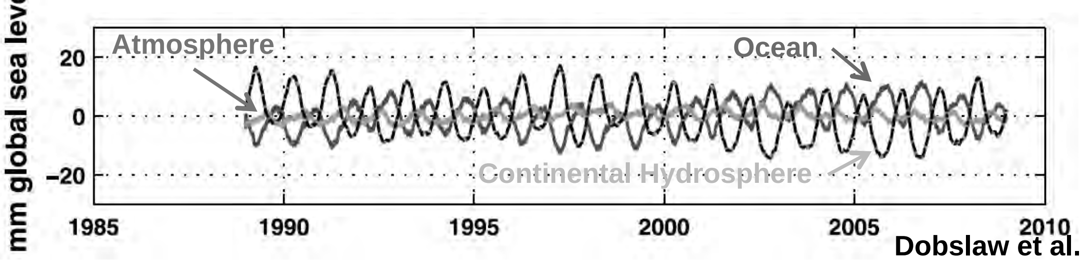

Dobslaw et al. (2010)

29

DFG SPP 1257

Ocean Tides

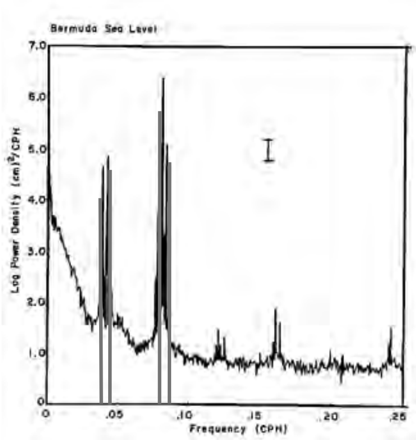

30

Tide Generating Potential

gravitational potential V excerted by the moon:

$$V = \frac{GM}{\rho} = \frac{GM}{R}\frac{1}{\sqrt{1+(a/R)^2 - 2(a/R)cos\alpha}}$$

$$V = \frac{GM}{R}\sum_{n=0}^{\infty}\left(\frac{a}{R}\right)^n P_n(cos\alpha)$$

tidal potential Γ:

$$\Gamma = V - \frac{GM}{R} - \frac{GM}{R^2}a\cos\alpha$$

$$\Gamma = \frac{GM}{R}\sum_{n=2}^{\infty}\left(\frac{a}{R}\right)^n P_n(\cos\alpha)$$

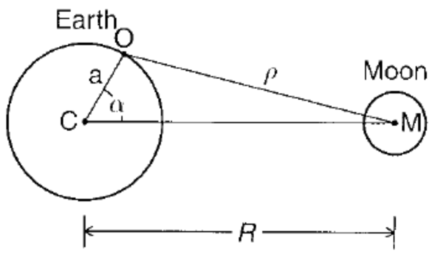

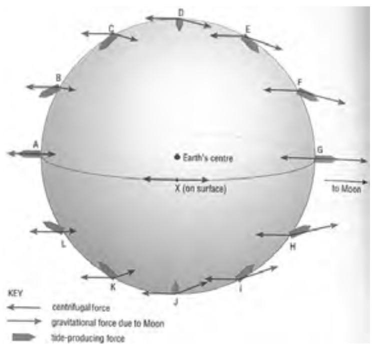

31

Agnew (2009)

Tide Generating Potential

consider degree 2 only:

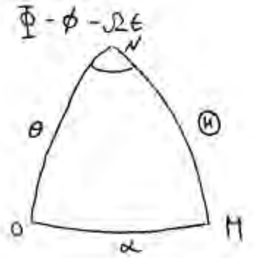

$$\Gamma = \frac{GM}{R}\left(\frac{a}{R}\right)^2 \frac{1}{2}(3\cos^2\alpha - 1)$$

express solid angle α in equatorial coordinates of O and M:

$$\Gamma = \frac{3GM}{2R}\left(\frac{a}{R}\right)^2 \quad [\quad \cos^2\theta\cos^2\Theta + \frac{1}{2}\sin^2\theta\sin^2\Theta - \frac{1}{3} \qquad \text{long-period}$$
$$+ \quad \frac{1}{2}\sin 2\theta \sin 2\Theta \cos(\Phi - \phi - \Omega t) \qquad \text{diurnal}$$
$$+ \quad \frac{1}{2}\sin^2\theta\sin^2\Theta\cos 2(\Phi - \phi - \Omega t) \quad] \qquad \text{semi-diurnal}$$

time dependency remains in R, Θ, Φ

Agnew (2009)

32

DFG SPP 1257

Ephemerides of Moon and Sun

Nutation Series based on Delauney Arguments:

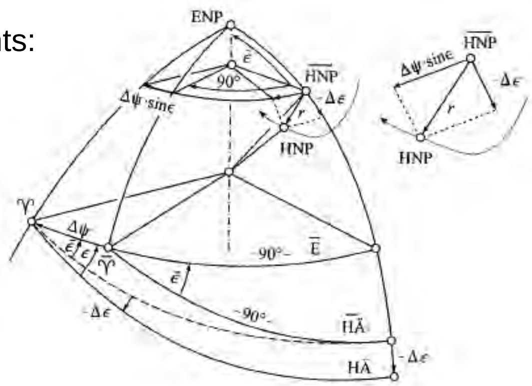

$$\Delta\psi = \sum_{i=1}^{106} \Delta\psi_i = \sum_{i=1}^{106}\left(a_{0i} + a_{1i}\cdot(T - T_0)\right)\cdot \sin L\,;$$

$$\Delta\epsilon = \sum_{i=1}^{106} \Delta\epsilon_i = \sum_{i=1}^{106}\left(b_{0i} + b_{1i}\cdot(T - T_0)\right)\cdot \cos L\,,$$

$$L = k_{1i}\cdot l + k_{2i}\cdot l' + k_{3i}\cdot F + k_{4i}\cdot D + k_{5i}\cdot \Omega$$

- l mean anomaly Moon (anomalistic month: 27d 13h 19min)
- l‘ mean anomaly Sun (anomalistic year: 365d 06h 14min)
- F difference between ascending node of the mean orbit and mean longitude of the moon (draconitic month: 27d 05h 06min)
- D mean elongation of the moon wrt. the sun (synodic month: 29d 12h 44min)
- Ω longitude of the ascending node of the mean orbit (18.6 years)

Schödlbauer (2000)

33

DFG SPP 1257

Harmonic Expansion of the Tidal Potential

TABLE 1. Expansion of the Tidal Argument

Tide	Period (hours)	Period (days)	l	l'	F	D	Ω	γ	Phase (degrees)
Semidiurnal									
S_2	12.00		0	0	−2	2	−2	2	0
M_2	12.42		0	0	−2	0	−2	2	0
N_2	12.66		−1	0	−2	0	−2	2	0
Diurnal									
K_1	23.93		0	0	0	0	0	1	+90.0
P_1	24.07		0	0	−2	2	−2	1	−90.0
O_1	25.82		0	0	−2	0	−2	1	−90.0
Long Period									
Mf'		13.63	0	0	2	0	1	0	0
Mf		13.66	0	0	2	0	2	0	0
Mm		27.55	1	0	0	0	0	0	0
Ssa		182.62	0	0	2	−2	2	0	0

Gross (1993), IERS Conv. (2003)

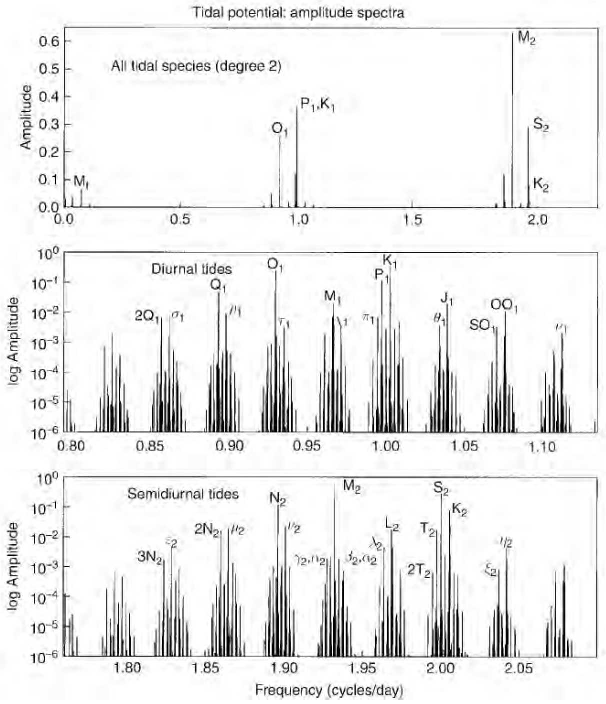

Agnew (2009)

Equations of Ocean Tidal Dynamics

Laplace Tidal Equations (LTE):

$$\frac{\partial \boldsymbol{v}}{\partial t} + \boldsymbol{f} \times \boldsymbol{v} = -g\nabla(\eta - \eta_{EQ} - \eta_{SAL}) - \mathcal{F}$$

$$\eta_{EQ} = \frac{(1 + k_2 - h_2)\Gamma}{g}$$

$$\eta_{SAL} = \frac{3\rho_0}{2\rho_e} \sum_n \frac{1}{2n+1}(1 + k'_n - h'_n)\eta_n$$

more general formulations include non-linear terms
and stratification (see, e.g. Zahel, 1986)

analytical solutions only available for simplified geometries: hemispheric ocean, rectangular channel, etc.

Ray (1998)

Equations of Ocean Tidal Dynamics

Laplace Tidal Equations (LTE):

$$\frac{\partial \boldsymbol{v}}{\partial t} + \boldsymbol{f} \times \boldsymbol{v} = -g\nabla(\eta - \eta_{EQ} - \eta_{SAL}) - \mathcal{F}$$

$$\eta_{EQ} = \frac{(1 + k_2 - h_2)\Gamma}{g}$$

$$\eta_{SAL} = \frac{3\rho_0}{2\rho_e} \sum_n \frac{1}{2n+1}(1 + k'_n - h'_n)\eta_n$$

more general formulations include non-linear terms
and stratification (see, e.g. Zahel, 1986)

analytical solutions only available for simplified geometries: hemispheric ocean, rectangular channel, etc.

Ray (1998)

Ocean Normal Modes

numerical solutions of LTE depend on the resonance characteristics of the ocean basins:

(a) gravitational modes

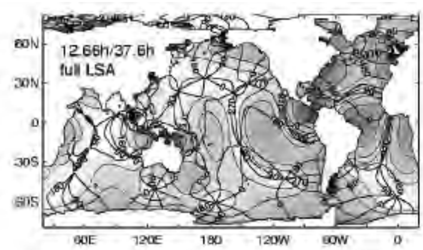

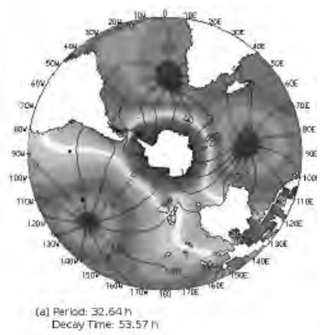

(b1) planetary vorticity modes

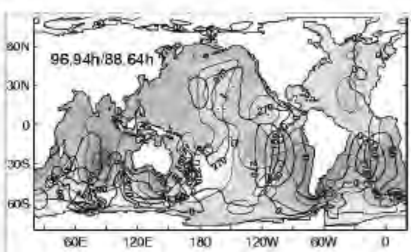

(b2) topographic vorticity modes

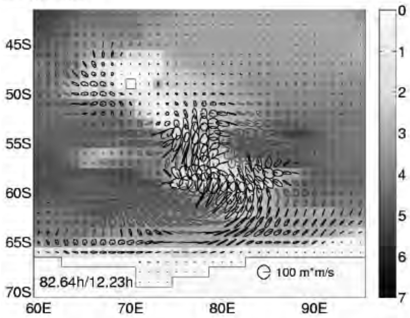

Malte Müller (2008)

Tide Models: (a) (semi-)empirical models: EOT08ag

analysis of residual tidal signals in T/P and GRACE

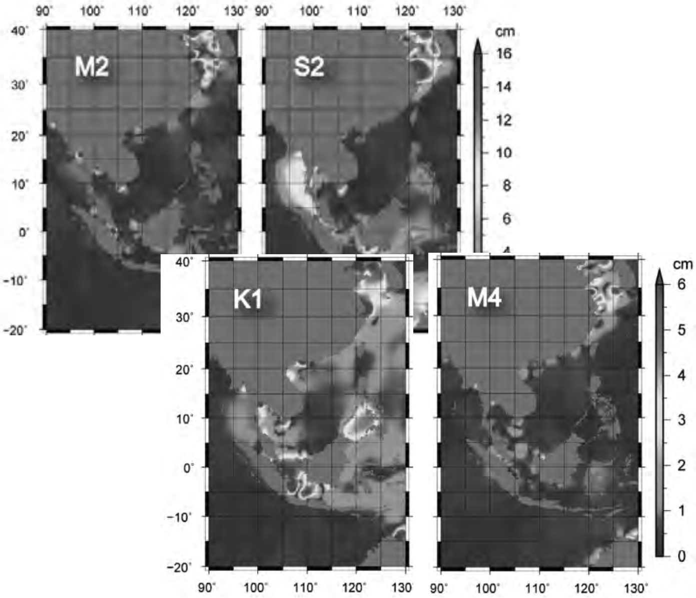

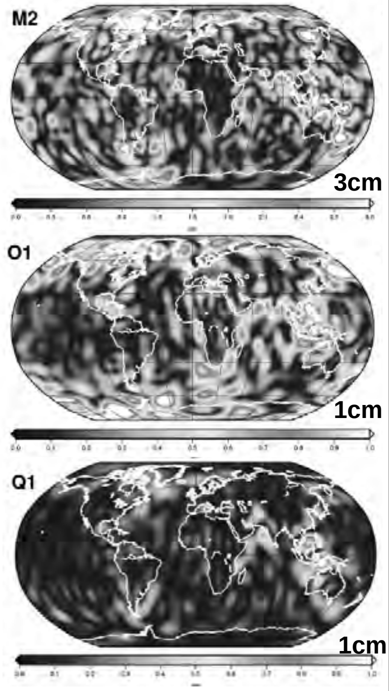

Bosch et al. (2009), Mayer-Gürr et al. (accepted)

Tide Models: (b) hydrodynamic w/o assimilation: TiME

- finite difference scheme
- 5‘ spatial resolution (2-10 km)
- time-stepping model
- forced by complete luni-solar tidal potential (Thomas, 2002)

impact of bathymetry

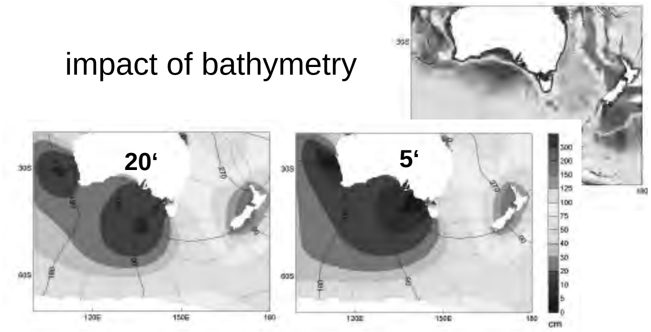

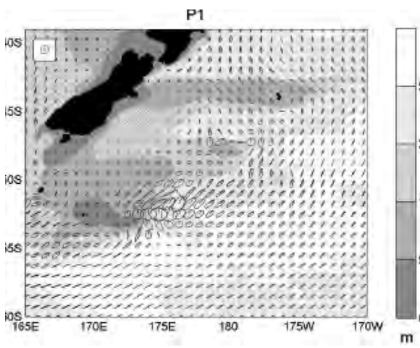

transport ellipses (5‘)

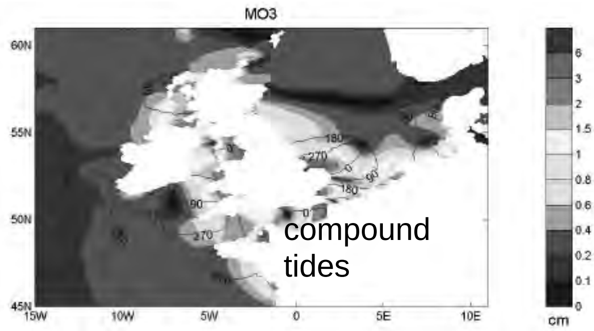

Philipp Weis (2006), Weis et al. (2008)

Tide Models: (c) hydrodynamic with assimilation: FES2004

finite element model

assimilates T/P altimetry by means of representer method (Bennet, 1990)

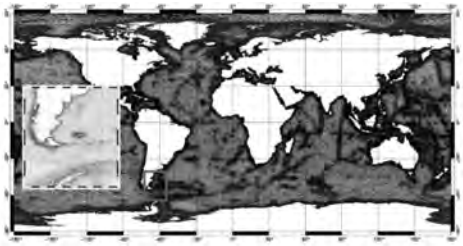

K1 (<100 cm)

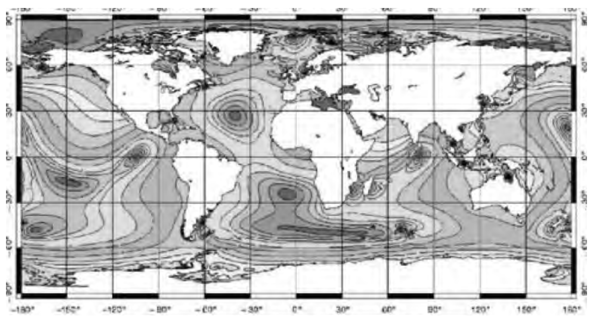

M2 (<120 cm)

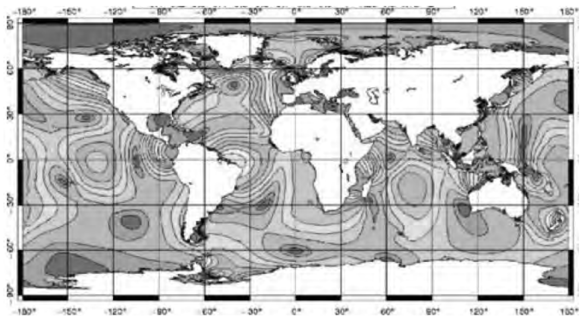

Lyard et al. (2006)

Summary on Short-Term Variability

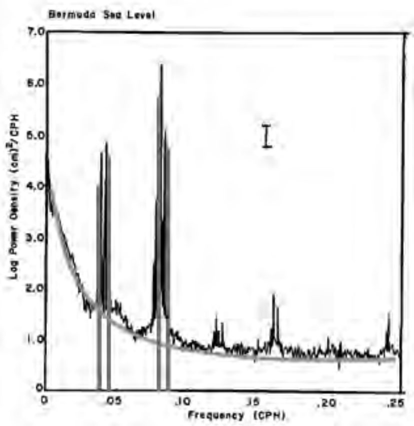

OMCT variability: bottom pressure (30 days low-pass)

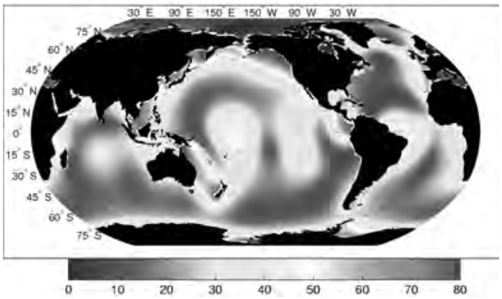

1. gravitational tides: ~ 80 hPa

41

Dobslaw (2007)

DFG SPP 1257

OMCT variability: bottom pressure (30 days low-pass)

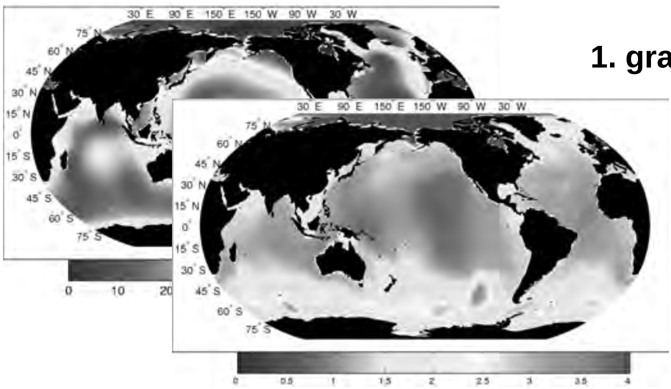

1. gravitational tides: ~ 80 hPa

2. atmospheric pressure: ~ 4 hPa

41

Dobslaw (2007)

DFG SPP 1257

OMCT variability: bottom pressure (30 days low-pass)

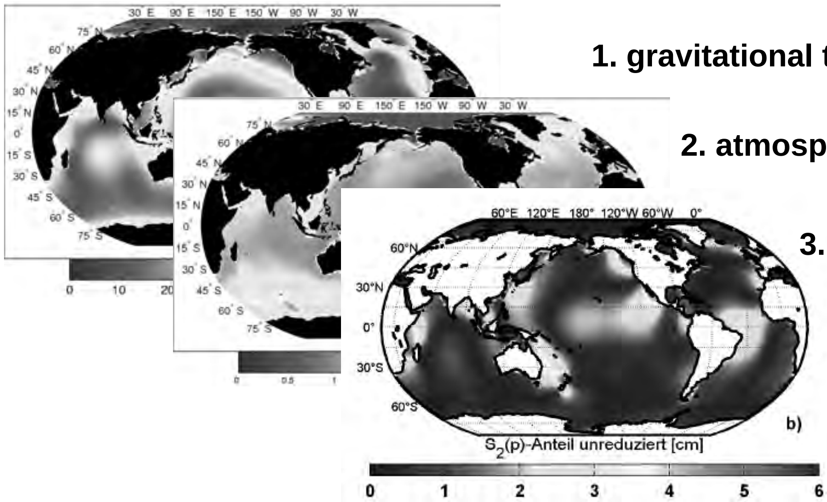

1. gravitational tides: ~ 80 hPa
2. atmospheric pressure: ~ 4 hPa
3. pressure tides: ~ 6 hPa

41

Dobslaw (2007)

DFG SPP 1257

OMCT variability: bottom pressure (30 days low-pass)

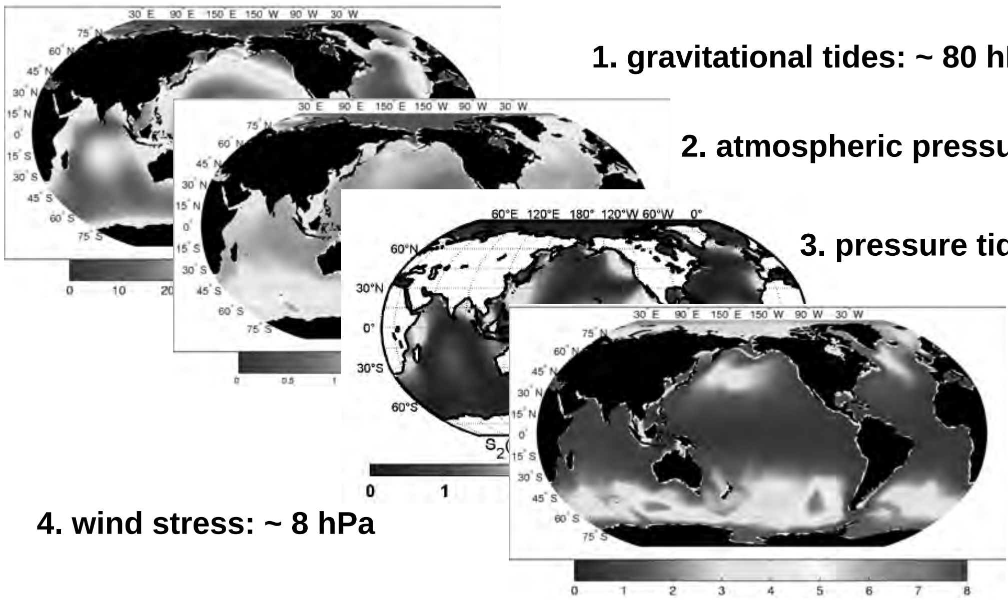

1. gravitational tides: ~ 80 hPa
2. atmospheric pressure: ~ 4 hPa
3. pressure tides: ~ 6 hPa
4. wind stress: ~ 8 hPa

41

Dobslaw (2007)

DFG SPP 1257

OMCT variability: bottom pressure (30 days low-pass)

1. gravitational tides: ~ 80 hPa

2. atmospheric pressure: ~ 4 hPa

3. pressure tides: ~ 6 hPa

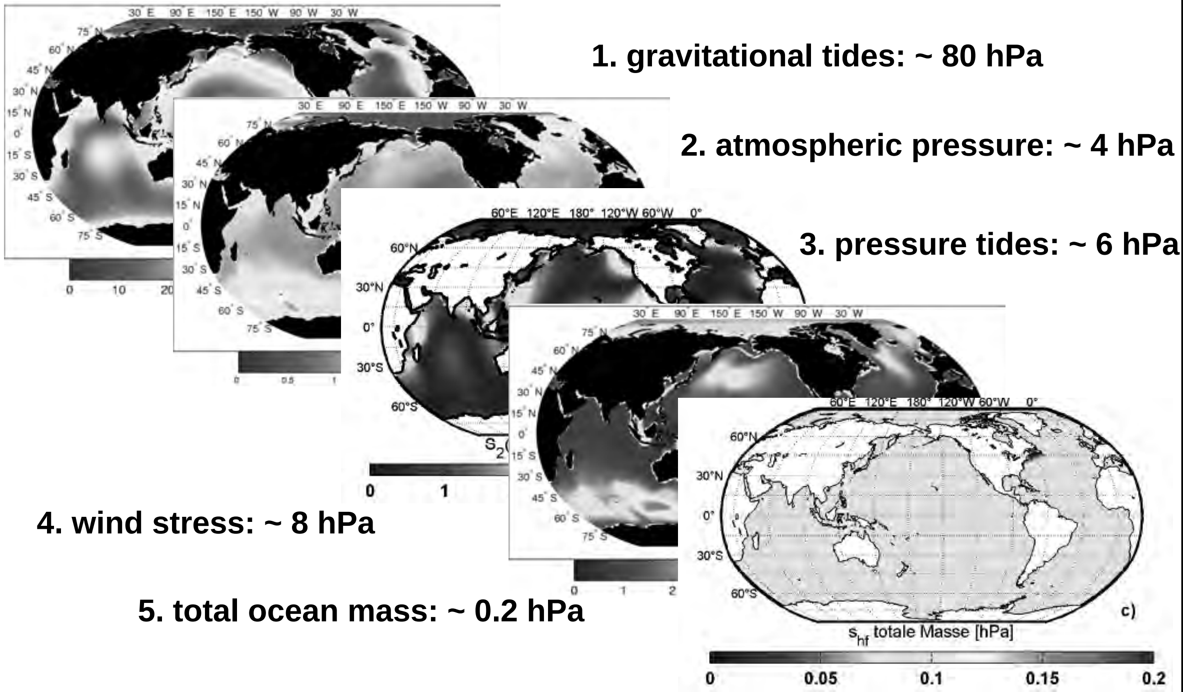

4. wind stress: ~ 8 hPa

5. total ocean mass: ~ 0.2 hPa

Dobslaw (2007)

DFG SPP 1257

41

OMCT variability: sea surface height (30 days low-pass)

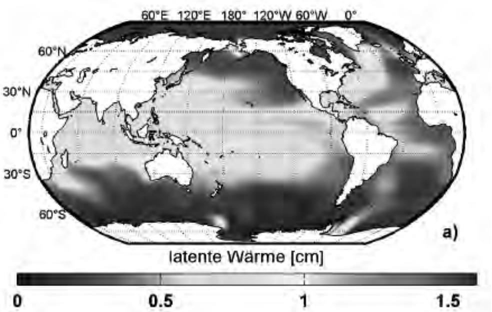

1. latent heat: ~ 1.5 cm

Dobslaw (2007)

DFG SPP 1257

42

OMCT variability: sea surface height (30 days low-pass)

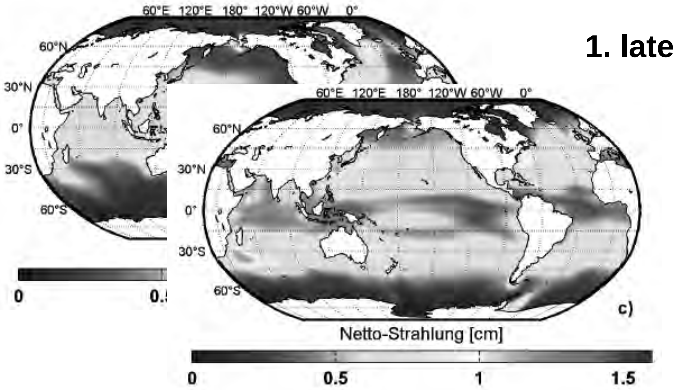

1. latent heat: ~ 1.5 cm

2. net radiation: ~ 1.5 cm

42

Dobslaw (2007)

DFG SPP 1257

OMCT variability: sea surface height (30 days low-pass)

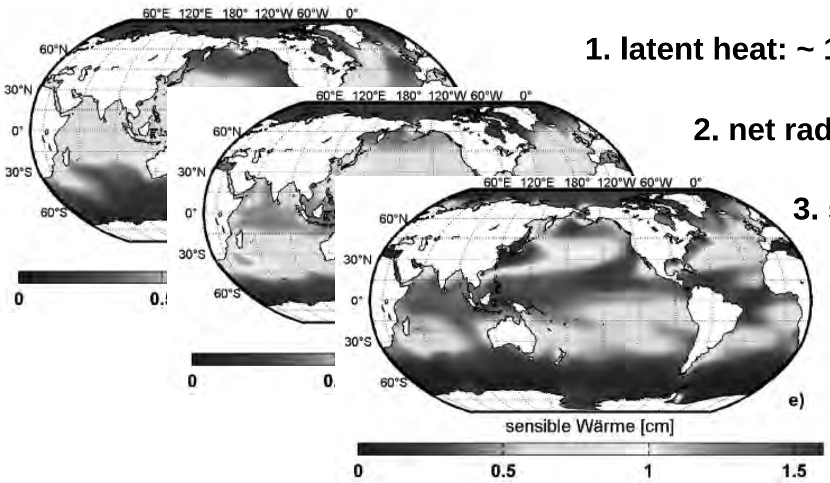

1. latent heat: ~ 1.5 cm

2. net radiation: ~ 1.5 cm

3. sensible heat: ~ 1.5 cm

42

Dobslaw (2007)

DFG SPP 1257

OMCT variability: sea surface height (30 days low-pass)

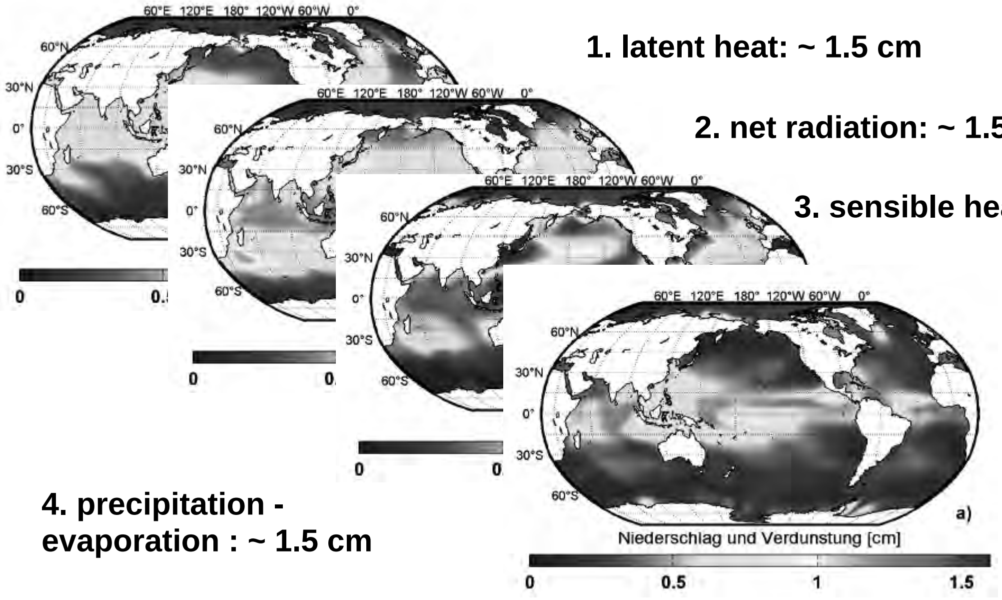

1. latent heat: ~ 1.5 cm

2. net radiation: ~ 1.5 cm

3. sensible heat: ~ 1.5 cm

4. precipitation - evaporation : ~ 1.5 cm

Dobslaw (2007)

OMCT variability: sea surface height (30 days low-pass)

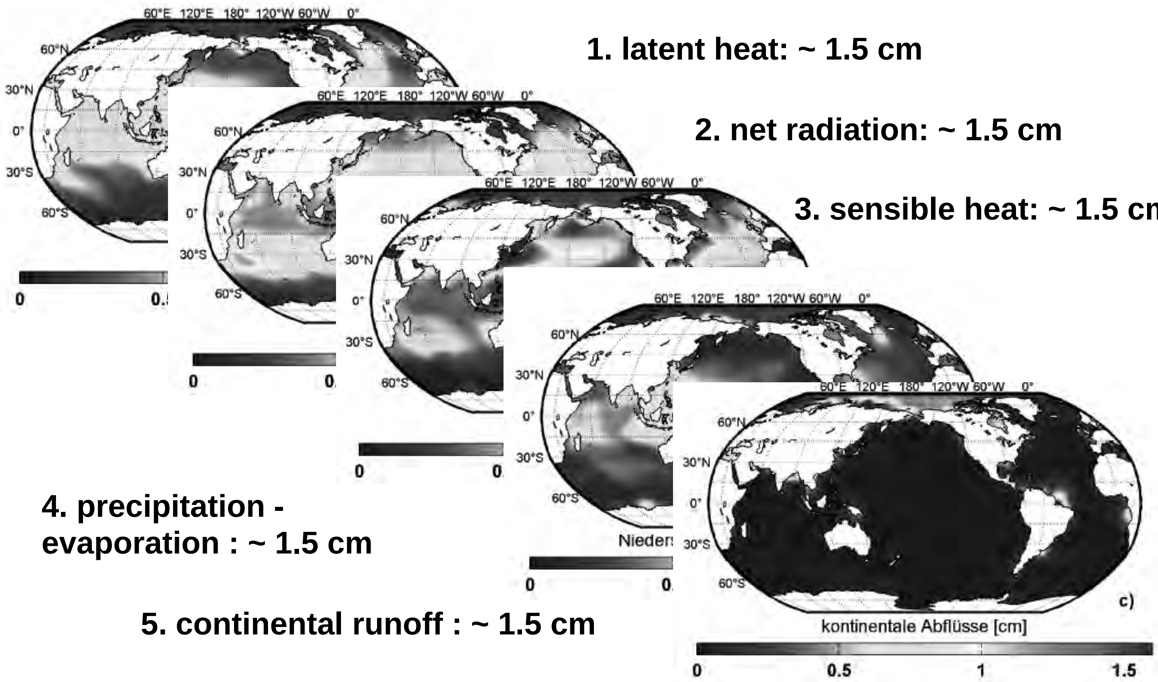

1. latent heat: ~ 1.5 cm

2. net radiation: ~ 1.5 cm

3. sensible heat: ~ 1.5 cm

4. precipitation - evaporation : ~ 1.5 cm

5. continental runoff : ~ 1.5 cm

Dobslaw (2007)

De-Aliasing

Sampling Characteristics of Satellite Missions: Aliasing

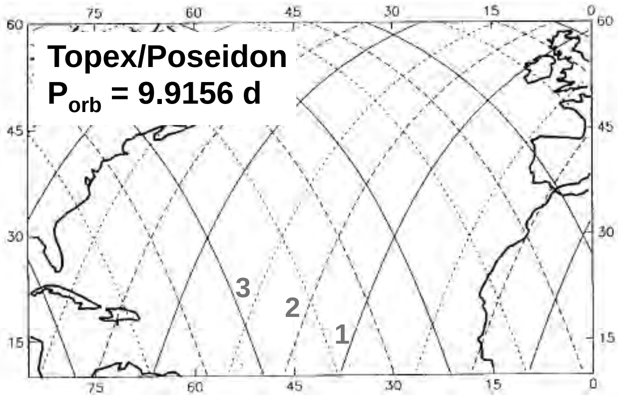

$$\Delta\phi_{tide} = \frac{2\pi P_{orb}}{T_{tide}}$$

$$T_{alias} = \frac{2\pi P_{orb}}{|\Delta\phi_{tide}|}$$

Tide	Period (hr)	T_{alias} (days)
M_2	12.420601	62.11
S_2	12.000000	58.74
N_2	12.658348	49.53
K_1	23.93447	173.19
O_1	25.819342	45.71
P_1	24.06589	88.89

…But what about variability without decent frequency characteristics?

Chelton et al. (2001)

De-aliasing for Satellite Altimetry: Mog2D/T-UGO

Predictions of non-tidal variability at high temporal resolution (3-6 h).

- finite element barotropic ocean model forced by 6 hourly ECMWF wind and surface pressure

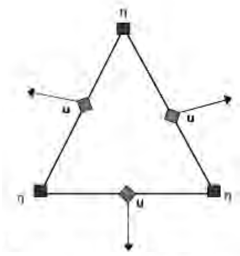

Dynamic Atmosphere Correction (DAC) for Satellite Altimetry (AVISO):

•Mog2D-G for high frequencies (< 20 days)

•low frequencies (>20 days): IB model, static response of the ocean to pressure, no consideration of wind effects

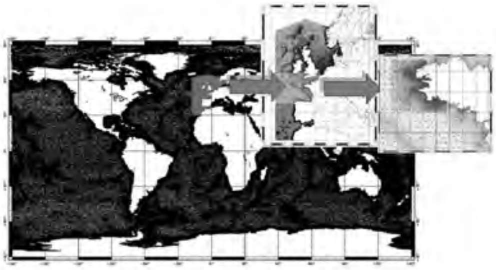

http://www.aviso.oceanobs.com

F. Lyard; P. Gegout et al. (2009)

De-aliasing for Satellite Gravimetry: OMCT

- 1.875° regular grid, 13 z-layers, 30 min
- forced by wind, pressure, freshwater, heat
- optional: tides, river runoff from LSDM, SAL

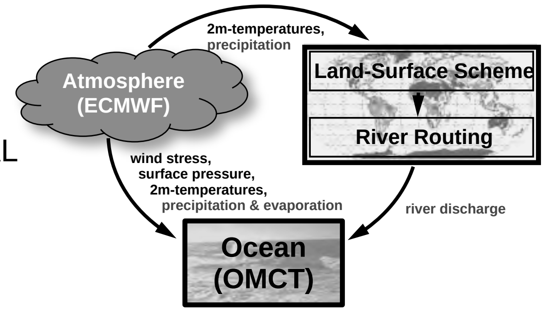

AOD1B RL04:

- no tides, no river runoff
- total ocean mass constant
- forcing from ECMWF 6h analyses

AOD1B RL05alpha:

- 1.0° regular grid, 20 z-layers, 20 min
- forcing as for RL04

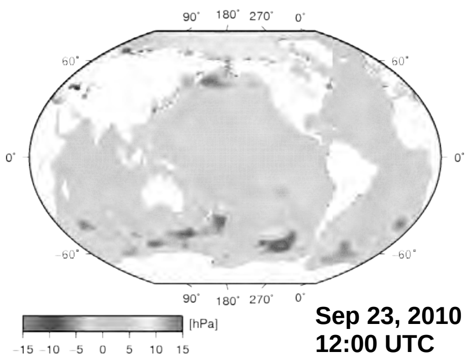

Sep 23, 2010
12:00 UTC

Dobslaw and Thomas (2007)

GRACE product philosophy: GSM and GAx

GAA: Atmosphere (3D)

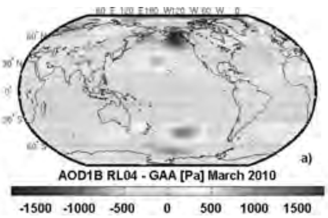

GAB: Ocean

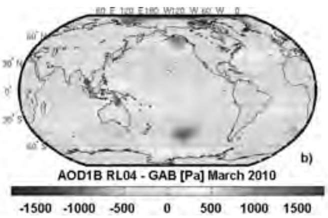

Atmosphere (3D) + Ocean
GAC= GAA+GAB

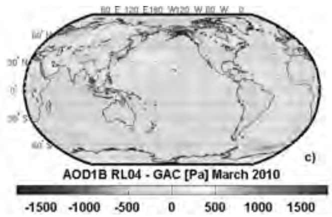

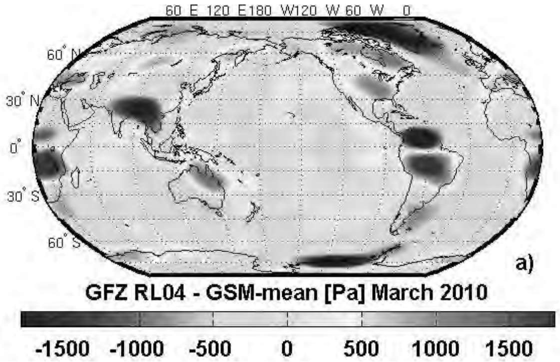

Ocean Bottom Pressure
GAD= GAB + atm. surface pressure @ wet points

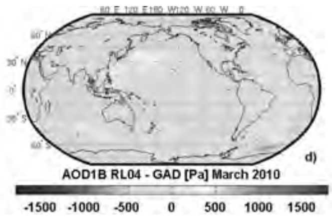

GSM: variability without Atmosphere and Ocean

Flechtner (2007)

GRACE product philosophy: GSM and GAx

GAA: Atmosphere (3D)

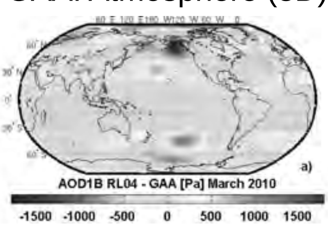

GAB: Ocean

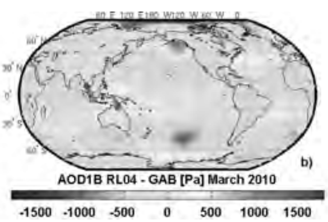

Atmosphere (3D) + Ocean
GAC= GAA+GAB

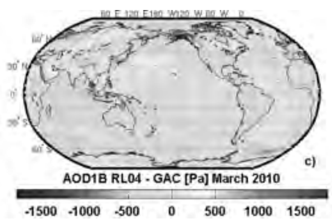

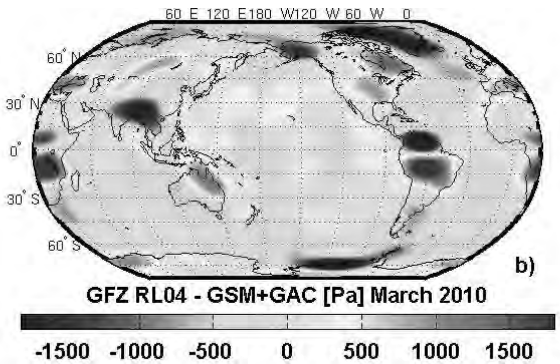

Ocean Bottom Pressure
GAD= GAB + atm. surface pressure @ wet points

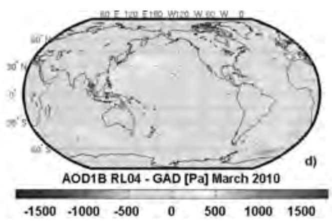

GSM+GAC: variability including Atm. and Ocean

Flechtner (2007)

GRACE product philosophy: GSM and GAx

GAA: Atmosphere (3D)

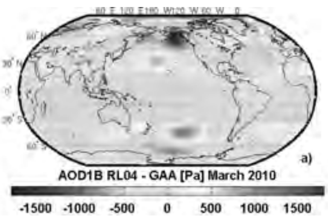

GAB: Ocean

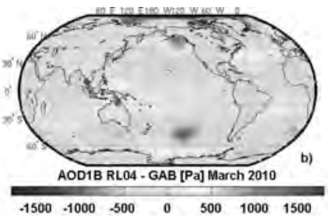

Atmosphere (3D) + Ocean
GAC= GAA+GAB

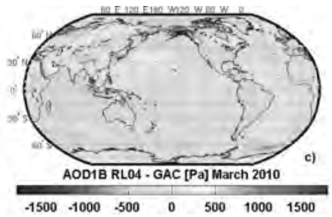

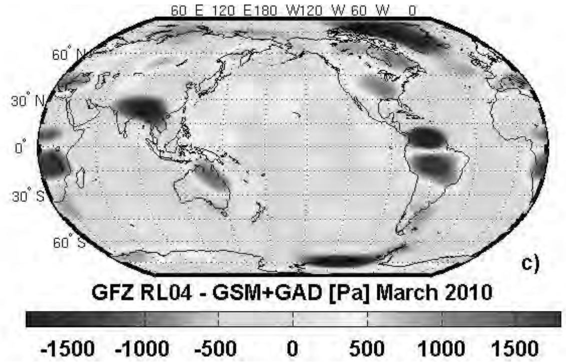

GSM+GAD: variability incl. ocean bottom pressure

Ocean Bottom Pressure
GAD= GAB + atm. surface pressure @ wet points

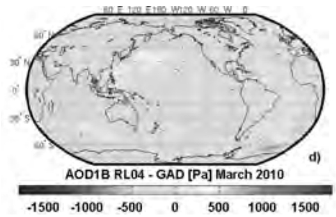

Flechtner (2007)

Beyond De-aliasing: Kalman Smoother Approach

- Kurtenbach et al. (2009): consideration of correlations between daily snap-shots of the gravity field
- auto-covariances have been derived empirically from numerical models of water storage variations
- extension of the approach to include atmosphere and ocean as well (AOD products applied only for sub-daily variability)

OBP variability ACC area: 10-30 days band pass

ITG-Kalman (daily)
CNES/GRGS (10 days)

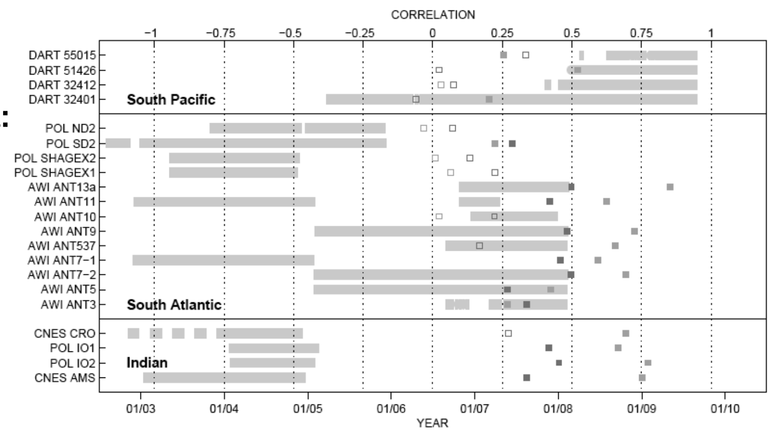

Bergmann et al., in prep.

Messages to take home….

- ocean dynamics are generally described by seven equations: (momentum, continuity, conservation equations for heat and salt)
- approximations are frequently applied in OGCMs: hydrostatic, Boussinesq -> be aware of their implications!
- sea-level (and bottom pressure) variability are dominated by ocean tides and non-tidal variability (red spectrum)
- selected geophysical signals are removed from observations before averaging: tides, atmospheric pressure effects, response to winds, etc. -> be aware of the way these signals have been removed!

49

DFG SPP 1257

Textbooks

- Stewart, R. H. (2008), Introduction to Physical Oceanography, available online, http://oceanworld.tamu.edu/home/course_book.htm, 345 pp.
- Pond, St., Pickard, G. L. (1983), Introductory Dynamical Oceanography, Pergamon Press, Oxford, 329 pp.
- Agnew (2009), Earth Tides, In: Herring, T. [ed.] Treatise in Geophysics – Geodesy, p.163-195, Elsevier, Amsterdam.
- Schödlbauer, A. (2000), Geodätische Astronomie, 634 pp., de Gruyter, Berlin.
- Gill, A.E. (1982), Atmosphere-Ocean Dynamics, 662 pp., Academic Press, San Diego
- Pedlosky, J. (1996), Ocean Circulation Theory, 453 pp. Springer, Berlin.
- Marshall, J., Plumb, R. A., (2008) Atmosphere, Ocean, and Climate Dynamics: An Introductory Text, 319 pp., Academic Press, San Diego.

50

DFG SPP 1257

Requirements for future satellite missions

Reiner Rummel
Institut für Astronomische und Physikalische Geodäsie
Technische Universität München
rummel@bv.tum.de

SPP1257 Sommerschule – Globaler Wasserkreislauf
Mayschoß/Ahrtal
12.-16. September 2011

contents

- future satellite gravimetry missions
- „connector“: spectral connection of earth interior to its exterior
- its derivation
- its interpretation
- its relationship to geophysical mass processes
- its use for simple estimates

next generation satellite gravimetry

Point of departure:
• a successful CHAMP, GRACE and GOCE

The generally agreed wish list:
• continuation of GRACE time series: discover changes
• higher spatial resolution (from 400km to 200km or even 100km)
• no striation → less filtering → better mass estimates
• no aliasing: from ocean tides, atmosphere and ocean
• higher accuracy: better mass estimates
• series of missions

next generation satellite gravimetry

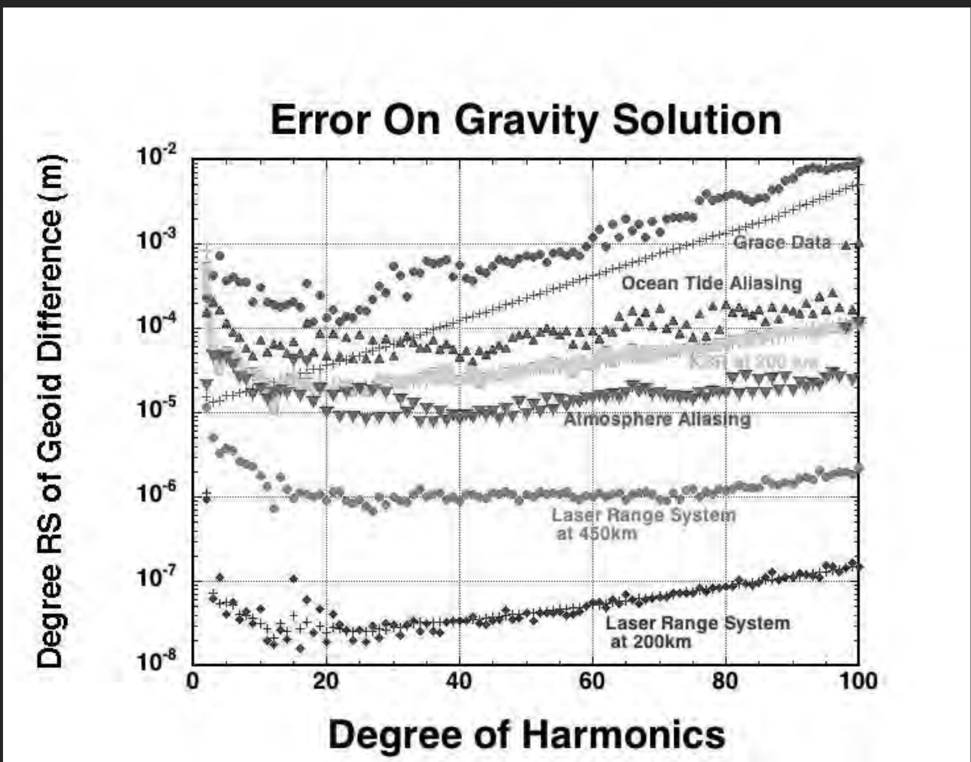

[Watkins M, JPL, 2007: workshop in Noordwijk]

next generation satellite gravimetry

Summary

Science Requirements (monthly time resolution)			Technical Requirements needed to reach science requirements (for satellite distance 200 km, height 373 km	
Spatial Resolution	Precision (EWH)	Precision (Geoid)	Laser Interferometer coloured noise with white noise level of:	Accelerometer coloured noise with white noise level of:
400 km	1 cm	0.1 mm	50 nm/√Hz	$1 \cdot 10^{-12}$ m/s²√Hz
	1 mm/y	0.01 mm/y		
200 km	10 cm	1 mm		
	1 cm/y	0.1 mm/y		

from: proposal e-motion to ESA, 2010

next generation satellite gravimetry

Summary

Mission Parameter	e.motion Proposal
Observation Concept	Satellite-to-Satellite Tracking in low-low mode: Observation is range (range-rate) between two low flying satellites.
Mission Duration	Nominal 7 years (plus possible extension).
Inclination	Polar or near-polar.
Repeat Cycle	Near monthly repeat cycle (with sub-cycle of about 10 days)
Orbit Height	373 km
Mission Configuration	Pendulum orbit with slightly rotated orbit planes (relative between the 2 satellites)

from: proposal e-motion to ESA, 2010

next generation satellite gravimetry

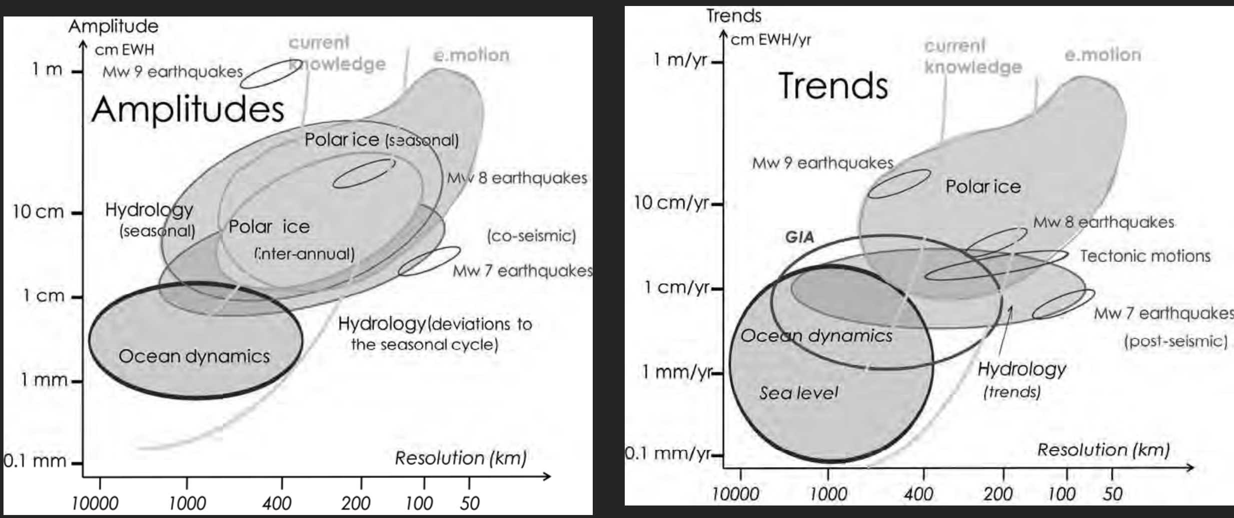

Signal amplitudes of mass variations in EWH as a function of spatial resolution, together with present-day and e-motion performance and resolution. Solid Earth mass variations are converted to EWH. Contributions from seasonal to inter-annual variations (left panel), and contributions from long-term trends (right panel).

from: proposal e-motion to ESA, 2010

next generation satellite gravimetry

Summary

Research objectives	Time scales	Expected signals (EWH,Geoid,g)	Precision, resolution
Continental water storage variations	weeks to decades	several dm EWH mm to cm EWH / y	1 cm EWH @ 400 km, 10 cm EWH @ 200 km 1mm EWH/y @ 400km
Ice sheets mass balance	months to decades	dm to m EWH dm EWH / y	1 cm EWH @ 400 km, 10 cm EWH @ 200 km 1mm EWH/y @ 400km
Oceanic mass variations	hours to decades	cm to dm EWH mm to cm EWH / y	5 mm EWH @ 500 km, 1 mm EWH / y
GIA	secular	2 mm geoid/y	0.01 mm geoid/y @ 400km
Earthquakes (Mw 7-8) Coseismic	instantaneous	0.1 to 1 mm geoid or 5 μGal	0.1 μGal @ 200 km or 0.1 mm geoid @ 400 km
Earthquakes (Mw 7-8) Post-seismic	to decades	0.01 to 0.1 mm geoid/y or 0.5 μGal/y	0.01 μGal/y @ 200 km or 0.01 mm/y geoid @ 400 km
Mantle convection & plate tectonics	decades to secular	0.05 mm geoid / yr	0.01 mm geoid /yr @ 400 km
Height reference, orbits, etc.	hours to decades	few cm geoid few mGal	1 mm geoid @ 200 km 1 μGal @ 200 km

1 cm EWH in a spherical cap of radius 2000 km (800 km, 400 km, 200 km, 100 km respectively) maps to a 0.5 mm amplitude geoid variation (0.3 mm, 0.15 mm, 0.08 mm, 0.04 mm resp.).

from: proposal e-motion to ESA, 2010

next generation satellite gravimetry

Flury J, R Rummel (eds.):
Future Satellite Gravimetry and
Earth Dynamics, Springer, 2005
Contributions by Flury J, Güntner A, Hughes Ch,
Legrand P, Riegger J, Rummel, R, Schrama EJO,
Sneeuw N, Vermeersen B, Woodworth Ph

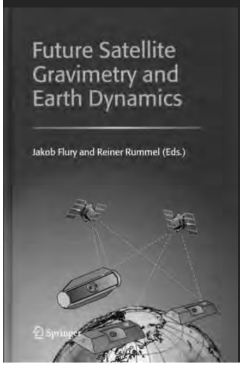

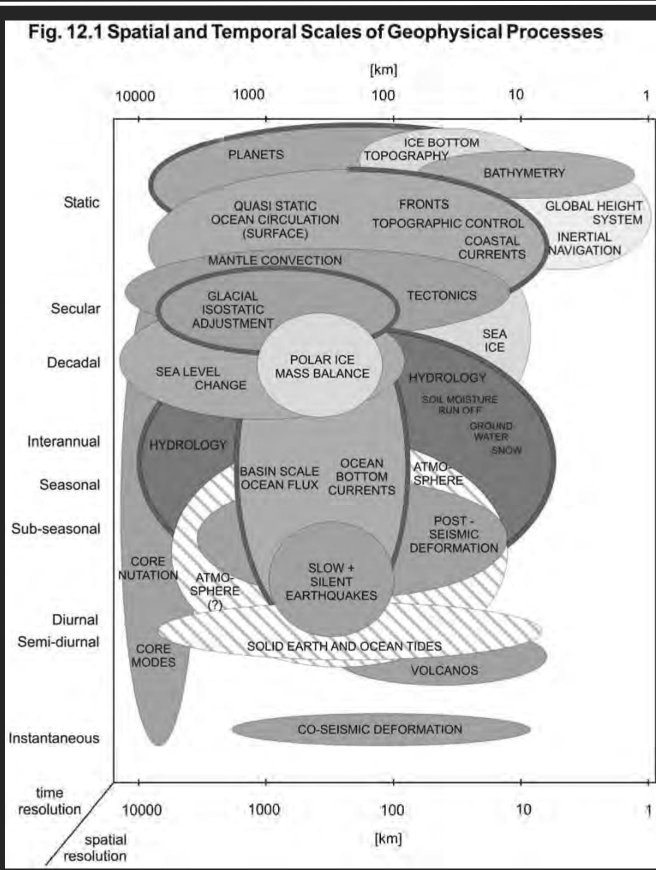

Fig. 12.1 Spatial and Temporal Scales of Geophysical Processes

next generation satellite gravimetry

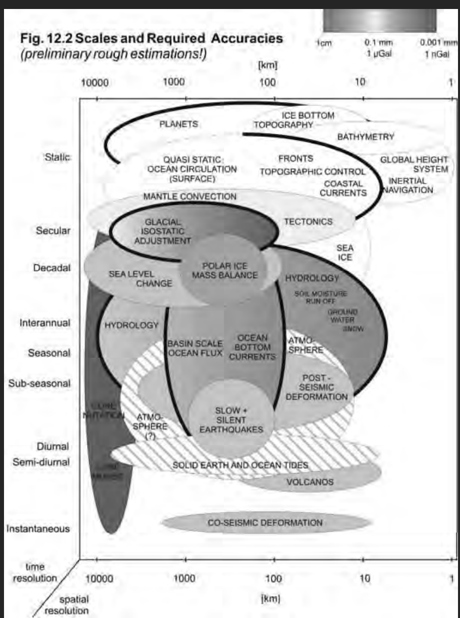

Fig. 12.2 Scales and Required Accuracies
(preliminary rough estimations!)

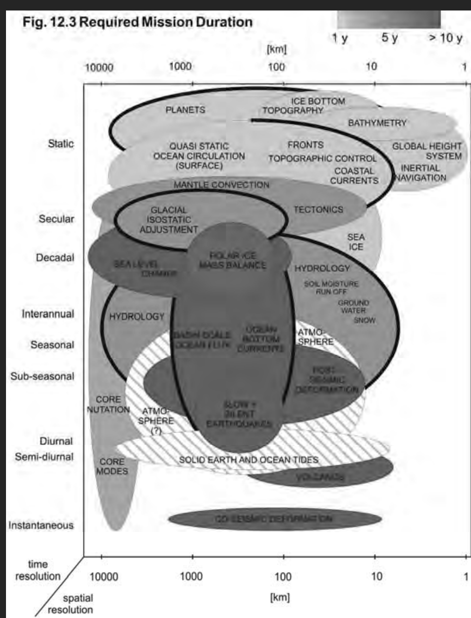

Fig. 12.3 Required Mission Duration

next generation satellite gravimetry

any proposal for a
next generation satellite gravimetry mission
will be based on a comprehensive end-to-end simulation,
using the actual requirements in earth sciences
(e.g. essential climate variables, ECVs)
and the heritage of CHAMP, GRACE and GOCE

thereby a key formula is

$$\begin{Bmatrix} \Delta\bar{C}_{nm} \\ \Delta\bar{S}_{nm} \end{Bmatrix} = \frac{3}{4\pi\bar{\rho}a}\frac{1+k_n}{2n+1}\iint_s \left[\int_r \Delta\rho\left(\theta_Q,\lambda_Q,r_Q\right)\left(\frac{r_Q}{a}\right)^{n+2} dr_Q\right]\bar{P}_{nm}(\cos\theta_Q)\begin{Bmatrix} \cos m\lambda_Q \\ \sin m\lambda_Q \end{Bmatrix} ds_Q$$

my lecture tries to be a summary of

Wahr, Molenaar & Bryan: Time variability of the Earth‘s gravity field: Hydrological and oceanic effects and their possible detection using GRACE, JGR, 1998

earth exterior

(residual) gravitational potential outside and on the earth surface:

$$\delta V_P = \frac{GM}{a}\sum_{n=0}^{n\max}\left(\frac{a}{r_P}\right)^{n+1}\sum_{m=0}^{n}(\Delta\bar{C}_{nm}\cos m\lambda_P + \Delta\bar{S}_{nm}\sin m\lambda)\bar{P}_{nm}(\cos\theta_P)$$

follows from

$$\begin{gathered} Lap\delta V = 0 \ for \ r_P > a \\ and \ boundary \ values \end{gathered}$$

example: (residual) geoid heights:

$$\delta N_P = a\sum_{n=0}^{n\max}\sum_{m=0}^{n}(\Delta\bar{C}_{nm}\cos m\lambda_P + \Delta\bar{S}_{nm}\sin m\lambda)\bar{P}_{nm}(\cos\theta)$$

Conclusion: no need to think about earth interior, densities, etc.

earth interior

the most important formula here:

$$\begin{Bmatrix} \Delta\bar{C}_{nm} \\ \Delta\bar{S}_{nm} \end{Bmatrix} = \frac{3}{4\pi a\bar{\rho}} \frac{1}{2n+1} \iint_s \left[\int_r \Delta\rho\left(\theta_Q, \lambda_Q, r_Q\right) \left(\frac{r_Q}{a}\right)^{n+2} dr_Q \right] \bar{P}_{nm}(\cos\theta_Q) \begin{Bmatrix} \cos m\lambda_Q \\ \sin m\lambda_Q \end{Bmatrix} ds_Q$$

Why?

- It delivers the $\Delta\bar{C}_{nm}$ *and* $\Delta\bar{S}_{nm}$
- It connects to densities
- It is the starting point of end-to-end simulations

But

- where does it come from,
- what do all terms mean and
- how can it be used for simple examples?

connection of earth exterior and interior

It is based on Newton‘s law of gravitation:

$$\delta V_P = G \iiint_\Sigma \frac{\Delta\rho_Q}{\ell_{PQ}} d\Sigma_Q$$

It connects the exterior („P“) with the interior („Q“).

The connector is:

$$1/\ell_{PQ}$$

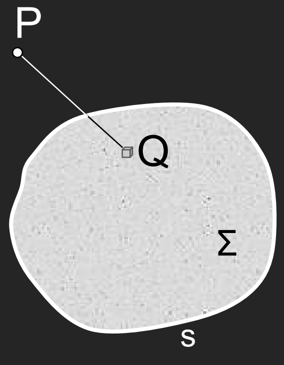

For integration P and Q have to be separated.

connection of earth exterior and interior

$$\delta V_P = G \iiint\limits_{\Sigma} \frac{\Delta\rho_Q}{\ell_{PQ}} d\Sigma_Q$$

(1) expansion of the reciprocal distance into Legendre polynomials

$$1/\ell_{PQ} = \frac{1}{r_P} \sum_{n=0}^{\infty} \left(\frac{r_Q}{r_P} \right)^n P_n \left(\cos \psi_{PQ} \right)$$

and $r_Q < r_P$

(2) addition theorem of Legendre functions:

$$P_n \left(\cos \psi_{PQ} \right) = \frac{1}{2n+1} \sum_{m=0}^{n} \left[\cos m\lambda_P \cdot \cos m\lambda_Q + \sin m\lambda_P \cdot \sin m\lambda_Q \right] \cdot \\ \cdot \bar{P}_{nm} \left(\cos \theta_P \right) \cdot \bar{P}_{nm} \left(\cos \theta_Q \right)$$

connection of earth exterior and interior

$$\delta V_P = \frac{GM}{a} \sum_{n=0}^{\infty} \left(\frac{a}{r_P} \right)^{n+1} \sum_{m=0}^{n} \left\{ \frac{1}{M(2n+1)} \int\limits_{\Sigma} \left(\frac{r_Q}{a} \right)^n \Delta\rho_Q \bar{P}_{nm}(\cos\theta_Q) \cos m\lambda_Q d\Sigma_Q \right\} \cos m\lambda_P \bar{P}_{nm}(\cos\theta_P) + \\ \left\{ \frac{1}{M(2n+1)} \int\limits_{\Sigma} \left(\frac{r_Q}{a} \right)^n \Delta\rho_Q \bar{P}_{nm}(\cos\theta_Q) \cos m\lambda_Q d\Sigma_Q \right\} \sin m\lambda_P \bar{P}_{nm}(\cos\theta_P)$$

Or divided into two parts:

$$\delta V_P = \frac{GM}{a} \sum_{n=0}^{n\max} \left(\frac{a}{r_P} \right)^{n+1} \sum_{m=0}^{n} (\Delta\bar{C}_{nm} \cos m\lambda_P + \Delta\bar{S}_{nm} \sin m\lambda) \bar{P}_{nm}(\cos\theta_P)$$

and with $\quad d\Sigma = r^2 dr ds = r^2 dr \sin\theta d\theta d\lambda$

and $\quad M = \bar{\rho} \cdot Volume = \bar{\rho} \cdot \frac{4}{3} \pi a^3$

$$\begin{Bmatrix} \Delta\bar{C}_{nm} \\ \Delta\bar{S}_{nm} \end{Bmatrix} = \frac{3}{4\pi\bar{\rho}a} \frac{1}{2n+1} \iint\limits_{s} \left[\int\limits_{r} \Delta\rho\left(\theta_Q, \lambda_Q, r_Q\right) \left(\frac{r_Q}{a} \right)^{n+2} dr_Q \right] \bar{P}_{nm}(\cos\theta_Q) \begin{Bmatrix} \cos m\lambda_Q \\ \sin m\lambda_Q \end{Bmatrix} ds_Q$$

connection of earth exterior and interior

$$\delta V_P = \frac{GM}{a}\sum_{n=0}^{\infty}\left(\frac{a}{r_P}\right)^{n+1}\sum_{m=0}^{n}\left\{\frac{1}{M(2n+1)}\int_{\Sigma}\left(\frac{r_Q}{a}\right)^{n}\Delta\rho_Q\bar{P}_{nm}(\cos\theta_Q)\cos m\lambda_Q d\Sigma_Q\right\}\cos m\lambda_P\bar{P}_{nm}(\cos\theta_P) + \left\{\frac{1}{M(2n+1)}\int_{\Sigma}\left(\frac{r_Q}{a}\right)^{n}\Delta\rho_Q\bar{P}_{nm}(\cos\theta_Q)\cos m\lambda_Q d\Sigma_Q\right\}\sin m\lambda_P\bar{P}_{nm}(\cos\theta_P)$$

Or divided into two parts:

$$\delta V_P = \frac{GM}{a}\sum_{n=0}^{n\max}\left(\frac{a}{r_P}\right)^{n+1}\sum_{m=0}^{n}(\Delta\bar{C}_{nm}\cos m\lambda_P + \Delta\bar{S}_{nm}\sin m\lambda)\bar{P}_{nm}(\cos\theta_P)$$

and with $d\Sigma = r^2 drds = r^2 dr\sin\theta d\theta d\lambda$

and $M = \bar{\rho}\cdot Volume = \bar{\rho}\cdot\frac{4}{3}\pi a^3$

$$\begin{Bmatrix}\Delta\bar{C}_{nm}\\ \Delta\bar{S}_{nm}\end{Bmatrix} = \frac{3}{4\pi\bar{\rho}a}\frac{1}{2n+1}\iint_s\left[\int_r\Delta\rho(\theta_Q,\lambda_Q,r_Q)\left(\frac{r_Q}{a}\right)^{n+2}dr_Q\right]\bar{P}_{nm}(\cos\theta_Q)\begin{Bmatrix}\cos m\lambda_Q\\ \sin m\lambda_Q\end{Bmatrix}ds_Q$$

connection of earth exterior and interior

$$\begin{Bmatrix}\Delta\bar{C}_{nm}\\ \Delta\bar{S}_{nm}\end{Bmatrix} = \frac{3}{4\pi\bar{\rho}a}\frac{1}{2n+1}\iint_s\left[\int_r\Delta\rho(\theta_Q,\lambda_Q,r_Q)\left(\frac{r_Q}{a}\right)^{n+2}dr_Q\right]\bar{P}_{nm}(\cos\theta_Q)\begin{Bmatrix}\cos m\lambda_Q\\ \sin m\lambda_Q\end{Bmatrix}ds_Q$$

Can be written as:

$$\begin{Bmatrix}\Delta\bar{C}_{nm}\\ \Delta\bar{S}_{nm}\end{Bmatrix} = \frac{3}{2n+1}\begin{Bmatrix}\Delta\bar{C}_{nm}^{\Delta\rho}\\ \Delta\bar{S}_{nm}^{\Delta\rho}\end{Bmatrix}$$

SH-potential coefficients versus SH-density coefficients

! on both sides dimensionless !

connection of earth exterior and interior

$$\begin{Bmatrix} \Delta\bar{C}_{nm} \\ \Delta\bar{S}_{nm} \end{Bmatrix} = \frac{3}{4\pi\bar{\rho}a}\frac{1}{2n+1}\iint_s \left[\int_r \Delta\rho\left(\theta_Q,\lambda_Q,r_Q\right)\left(\frac{r_Q}{a}\right)^{n+2} dr_Q \right] \bar{P}_{nm}(\cos\theta_Q) \begin{Bmatrix} \cos m\lambda_Q \\ \sin m\lambda_Q \end{Bmatrix} ds_Q$$

Can be written as:

$$\begin{Bmatrix} \Delta\bar{C}_{nm} \\ \Delta\bar{S}_{nm} \end{Bmatrix} = \frac{3}{2n+1} \begin{Bmatrix} \Delta\bar{C}_{nm}^{\Delta\rho} \\ \Delta\bar{S}_{nm}^{\Delta\rho} \end{Bmatrix}$$

SH-potential coefficients versus SH-density coefficients

! both dimensionless !

SH-pocket guide
of geodetic
gravity functionals
such as
gravity anomalies,
gravity gradients…

density distribution:
isostasy, GIA,
dynamic topography,
geophysical fluids
(ocean, hydrology,…)

interpretation

from a radial density distribution to a surface layer:

$$\begin{Bmatrix} \Delta\bar{C}_{nm} \\ \Delta\bar{S}_{nm} \end{Bmatrix} = \frac{3}{4\pi\bar{\rho}a}\frac{1}{2n+1}\iint_s \left[\int_r \Delta\rho\left(\theta_Q,\lambda_Q,r_Q\right)\left(\frac{r_Q}{a}\right)^{n+2} dr_Q \right] \bar{P}_{nm}(\cos\theta_Q) \begin{Bmatrix} \cos m\lambda_Q \\ \sin m\lambda_Q \end{Bmatrix} ds_Q$$

Replace integral by mass layer of constant (!) thickness Δr=h:

$$\int_r \Delta\rho\left(\theta_Q,\lambda_Q,r_Q\right)\left(\frac{r_Q}{a}\right)^{n+2} dr_Q \approx \Delta\rho(\theta,\lambda)\cdot h = \Delta\sigma(\theta,\lambda) = \rho_w \cdot h^{EWH}(\theta,\lambda)$$

It holds (for h < a):

$$\frac{1}{a^{n+2}}\int_{r=a}^{a+h} r^{n+2}dr = \frac{1}{a^{n+2}}\frac{1}{n+3}\left[(a+h)^{n+3} - a^{n+3}\right] = \frac{a}{n+3}\left[(1+\frac{h}{a})^{n+3} - 1\right]$$

$$= \frac{a}{n+3}\left[(n+3)\frac{h}{a} + \frac{(n+3)(n+4)}{2}\left(\frac{h}{a}\right)^2 + \ldots\right] \approx h$$

interpretation

from pressure to surface layer to equivalent water height

$$\left.\begin{matrix}\Delta\rho_{atm}(\theta,\lambda)\cdot h_{atm}\\ \Delta\rho_{w}(\theta,\lambda)\cdot h_{w}\\ \Delta\rho_{ice}(\theta,\lambda)\cdot h_{ice}\\ \Delta\rho_{rock}(\theta,\lambda)\cdot h_{rock}\end{matrix}\right\} = \Delta\sigma(\theta,\lambda) = \rho_w \cdot h^{EWH}(\theta,\lambda)$$

$$\left[{}^{kg}\!/_{m^3}\cdot m\right] = \left[{}^{kg}\!/_{m^2}\right] = \left[{}^{kg}\!/_{m^3}\cdot m\right]$$

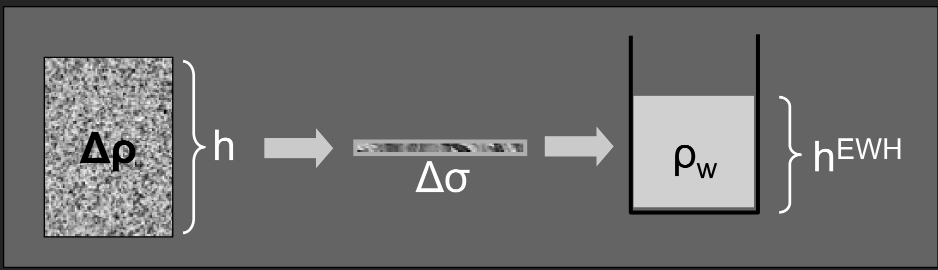

$$\bar{\rho} = 5517\ kg/m^3$$
$$\rho_w = 1000\ kg/m^3$$
$$\rho_{ocean} = 1027\ kg/m^3$$
$$\rho_{rock} = 2670\ kg/m^3$$

interpretation

$$\begin{Bmatrix}\Delta\bar{C}_{nm}\\ \Delta\bar{S}_{nm}\end{Bmatrix} = \frac{3}{4\pi\bar{\rho}a}\frac{1}{2n+1}\iint_s \left[\int_r \Delta\rho\left(\theta_Q,\lambda_Q,r_Q\right)\left(\frac{r_Q}{a}\right)^{n+2} dr_Q\right]\bar{P}_{nm}(\cos\theta_Q)\begin{Bmatrix}\cos m\lambda_Q\\ \sin m\lambda_Q\end{Bmatrix} ds_Q$$

$\Downarrow$

We can continue now to work with surface layers

$$\begin{Bmatrix}\Delta\bar{C}_{nm}\\ \Delta\bar{S}_{nm}\end{Bmatrix} = \frac{3}{2n+1}\frac{1}{4\pi}\iint_s \frac{\Delta\sigma(\theta,\lambda)}{\bar{\rho}a}\bar{P}_{nm}(\cos\theta_Q)\begin{Bmatrix}\cos m\lambda_Q\\ \sin m\lambda_Q\end{Bmatrix} ds_Q$$

or with equivalent water heights

$$\begin{Bmatrix}\Delta\bar{C}_{nm}\\ \Delta\bar{S}_{nm}\end{Bmatrix} = \frac{\rho_w}{\bar{\rho}}\frac{3}{2n+1}\frac{1}{4\pi}\iint_s \frac{h^{EWH}(\theta,\lambda)}{a}\bar{P}_{nm}(\cos\theta_Q)\begin{Bmatrix}\cos m\lambda_Q\\ \sin m\lambda_Q\end{Bmatrix} ds_Q$$

- dimensionless -

interpretation

load Love number k_n

The surface layer represents a load on the elastic earth body

$$\begin{Bmatrix} \Delta\bar{C}_{nm} \\ \Delta\bar{S}_{nm} \end{Bmatrix} = \frac{\rho_w}{\bar{\rho}} \frac{3\cdot(1+k_n)}{2n+1} \frac{1}{4\pi} \iint_s \frac{h^{EWH}(\theta,\lambda)}{a} \bar{P}_{nm}(\cos\theta_Q) \begin{Bmatrix} \cos m\lambda_Q \\ \sin m\lambda_Q \end{Bmatrix} ds_Q$$

We get the combined effect:

(1) the direct attraction of the surface layer and

(2) the secondary (negative) effect of deformation

Assumption: perfectly elastic earth i.e. Hooke's law

Literature:

Farrell WE: Deformation of the earth by surface loads, RevGeoph., 1972

Munk WH & GJF MacDonald: The rotation of the earth, ch.5.8, 1975

Chao BF: The geoid and earth rotation, in: Vanicek P & N Christou, 1994

Han D & J Wahr: the viscoelastic relaxation…GJI, 1995

interpretation

load Love number k_n

Table 1. Elastic Love Numbers k_l Computed by Dazhong Han as described by *Han and Wahr* [1995], for Earth Model PREM

l	k_l
0	+0.000
1	+0.027
2	-0.303
3	-0.194
4	-0.132
5	-0.104
6	-0.089
7	-0.081
8	-0.076
9	-0.072
10	-0.069
12	-0.064
15	-0.058
20	-0.051
30	-0.040
40	-0.033
50	-0.027
70	-0.020
100	-0.014
150	-0.010
200	-0.007

The $l = 1$ value assumes the origin of the coordinate system is the center of figure of the solid Earth's surface (see text).

for n>1:

all Love numbers

negative

Wahr, Molenaar & Bryan, JGR, 1998

interpretation

SH-degree n=0

- total mass of solid earth and its fluids remains constant (mass conservation)
- M in geodesy includes: solid earth, ice, oceans and atmosphere
- mass of single fluid components (atmosphere, ocean, ..) is not constant
- variable atmospheric and oceanic mass does not cause deformation of solid earth mass → $k_0=0$
- from Boussinesq approximation to mass conservation

interpretation

SH-degree n=1

$$\Delta\bar{C}_{10}, \Delta\bar{C}_{11} \textit{ and } \Delta\bar{S}_{11}$$

are proportional to the position of earth centre of mass (CoM) relative to centre of coordinate system

Case 1: origin of coordinate system: centre of mass

$$\Delta\bar{C}_{10} = \Delta\bar{C}_{11} = \Delta\bar{S}_{11} = 0$$

degree n=1 components need not to vanish, but their sum

The Love number is $k_{n=1}$= -1 in this case

Case 2: origin of c.s.: centre of figure of solid earth surface

degree n=1-coefficients define now the off-set between the CoM of solid earth plus deformation and the centre of the deformed figure

It holds now: $k_{n=1} = -(h_{n=1} + 2\ell_{n=1})/3 = +0.027$

just for completeness

the formula and its inverse

SH-analysis

$$\begin{Bmatrix} \Delta\bar{C}_{nm} \\ \Delta\bar{S}_{nm} \end{Bmatrix} = \frac{3\cdot(1+k_n)}{2n+1}\frac{1}{4\pi}\iint_s \frac{\Delta\sigma(\theta,\lambda)}{\bar{\rho}a}\bar{P}_{nm}(\cos\theta_Q)\begin{Bmatrix} \cos m\lambda_Q \\ \sin m\lambda_Q \end{Bmatrix} ds_Q$$

SH-synthesis

$$\Delta\sigma(\theta,\lambda) = a\cdot\bar{\rho}\sum_{n=0}^{n\max}\frac{2n+1}{3(1+k_n)}\sum_{m=0}^{n}\bar{P}_{nm}(\cos\theta)\{\Delta\bar{C}_{nm}\cos m\lambda + \Delta\bar{S}_{nm}\sin m\lambda\}$$

Chambers & Schröter, JoGeodynamics, 2011, accepted

$$\begin{Bmatrix} \Delta\bar{C}_{nm} \\ \Delta\bar{S}_{nm} \end{Bmatrix} = \frac{\rho_w}{\bar{\rho}}\frac{3\cdot(1+k_n)}{2n+1}\frac{1}{4\pi}\iint_s \frac{h^{EWH}(\theta,\lambda)}{a}\bar{P}_{nm}(\cos\theta_Q)\begin{Bmatrix} \cos m\lambda_Q \\ \sin m\lambda_Q \end{Bmatrix} ds_Q$$

$$h^{EWH}(\theta,\lambda) = a\cdot\frac{\bar{\rho}}{\rho_w}\sum_{n=0}^{n\max}\frac{2n+1}{3(1+k_n)}\sum_{m=0}^{n}\bar{P}_{nm}(\cos\theta)\{\Delta\bar{C}_{nm}\cos m\lambda + \Delta\bar{S}_{nm}\sin m\lambda\}$$

relationship to geophysical mass processes

TABLE 6.1 EARTH'S WATER

Estimates given in column 2 are in millions of cubic kilometers (MCkm), where a cubic kilometer is a billion cubic meters. LGM stands for the Last Glacial Maximum, 18,000 years ago. Equivalent depths (column 4) are obtained by dividing the volumes of water by the areas concerned. Rivers, streams, and the biosphere contain minute percentages of the total water, given in column 3 in parts per million (1 ppm = 0.0001%). Estimates of the amount of water underground are very uncertain. The entries correspond to layers from the surface down to 4,000 meters depth. Shallow fresh groundwater, from the surface down to 750 meters depth, amounts to about 4 MCkm, and has shorter residence time. Estimates for fresh and saline water in layers more than 4,000 meters deep, not included in the table, range from 50 to 320 MCkm.

Type of Water	Volume (MCkm)	Share of Total Water (% or ppm)	Equivalent Thickness or Depth (m)	Typical Renewal or Residence Time (years)
Total	1,422	100	2,800	4 Billion
Salt water (oceans, inland seas, salt lakes)	1,370	96.3	3,750	3,700
Of which, water from ice melt since LGM	40	2.8	120	
Present-day "permanent" snow/ice	29	2.0	2,000	From 30 years to 600,000
If it all melts	—	—	80	
Present-day permafrost	0.300	0.21	15	8,000
Soil moisture	0.066	0.005	0.8	1 month
Underground freshwater	10	0.7	65	From 50 years to five million
Underground saltwater	13	0.9	85	Very long
Freshwater lakes	0.12	0.008	75	10 to 1,000
Rivers and streams	0.002	1.4 ppm	13 mm !	18 days
Biosphere	0.001	0.7 ppm	2 mm !	Hours
Atmospheric water vapor and cloud water/ice	0.013	91 ppm	26 mm !	8 to 10 days

Kandel R: water from heaven, 2003

relationship to geophysical mass processes

from pressure to surface layer to equivalent water height

$$\left.\begin{array}{r}\Delta\rho_{atm}\cdot h_{atm}\\ \Delta\rho_{w}\cdot h_{w}\\ \Delta\rho_{ice}\cdot h_{ice}\\ \Delta\rho_{rock}\cdot h_{rock}\end{array}\right\}=\Delta\sigma(\theta,\lambda)=\rho_w\cdot h^{EWH}(\theta,\lambda)$$

$\bar{\rho}=5517\,kg/m^3$

$\rho_w=1000\,kg/m^3$

$\rho_{ocean}=1027\,kg/m^3$

$\rho_{rock}\,2670\,kg/m^3$

$$\Delta\sigma_{atm}=\frac{\Delta p_{atm}}{g}=\int\Delta\rho_{atm}dr$$

$$\Delta\sigma_{oce}=\rho_{oce}\Delta\varsigma_{forcing}$$

$$\Delta p_{OBP}=\left(\Delta p_{atm}+g\cdot\rho_{oce}\cdot\Delta\varsigma_{barometer}\right)+g\cdot\rho_{oce}\cdot\Delta\varsigma_{forcing}+g\cdot\int\Delta\rho_{oce}dr$$

relationship to geophysical mass processes

atmospheric pressure profiles provided by weather services 6-hourly on a global spherical 3D grid

atmosphere

continental processes:
- continental water storage
- ice sheet mass balance
- earthquakes (coseismic)
- earthquakes (post-seismic)
- volcano eruption
- mantle convection & plates

oceanic processes:
- assimilation into OCMs
- deep ocean currents
- separation of steric and non-steric part of sea level rise

glacial isostatic adjustment (GIA)

GIA-models depend on viscosity profile, ice loading history and polar wander

relationship to geophysical mass processes

Continental processes:

correct best possible for contributions from:

A) atmospheric mass changes
De-aliasing using data from ECMWF

continental processes:
- continental water storage
- ice sheet mass balance
- earthquakes (coseismic)
- earthquakes (post-seismic)
- volcano eruption
- mantle convection & plates

B) ocean contribution in coastal zones:
- tidal forcing,
- thermal and wind forcing,
- ocean part of global water cycle

C) glacial isostatic adjustment
modelling and where possible direct measurement

relationship to geophysical mass processes

pressure of total column: ocean plus atmosphere:

$$\Delta p_{OBP} = \left(\Delta p_{atm} + g \cdot \rho_{oce} \cdot \Delta\varsigma_{barometer}\right) + g \cdot \rho_{oce} \cdot \Delta\varsigma_{forcing} + g \cdot \int \Delta\rho_{oce}\, dr$$

atmosphere

remove: $\left(\Delta p_{atm} + g \cdot \rho_{oce} \cdot \Delta\varsigma_{barometer}\right)$

$\nabla_s\left(\Delta p_{OBP}\right)$

remove: $\Delta\varsigma_{barometer}$

oceanic processes:
- assimilation into OCMs
- deep ocean currents
- separation of steric and non-steric part of sea level rise

glacial isostatic adjustment (GIA)

Convenient test functions for load estimates

A) Circular Cylinder [H-M 1967, ch.3]: P located on symmetry axis on cylinder constant density ρ, radius s, height Δh (with Δh < s)

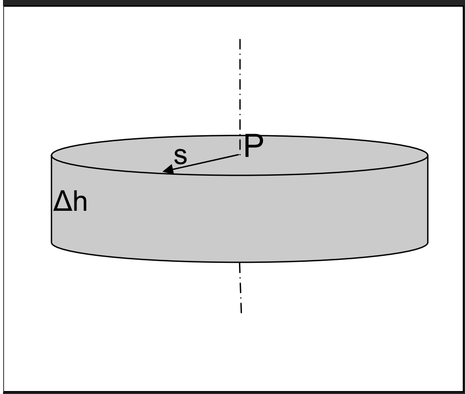

Effect on gravity potential in P:

$$\begin{aligned}\delta V &= \pi G \rho_w \left[-\Delta h^2 + \Delta h\sqrt{s^2+\Delta h^2} + \ln\frac{\Delta h + \sqrt{s^2+\Delta h^2}}{s} \right] \\ &= \pi G \rho_w \left[-\Delta h^2 + \Delta h \cdot s + \Delta h \cdot s \right] \\ &= 2\pi G \rho_w \Delta h \cdot s\end{aligned}$$

Effect on geoid in P:

$$\delta N = \frac{\delta V}{g} = \frac{2\pi G \rho_w \Delta h \cdot s}{(\frac{4}{3}\pi G \bar{\rho} R)} = \frac{3}{2}\frac{\rho_w}{\bar{\rho}}\frac{s}{R}\Delta h$$

Example with s=1000km:

$$\begin{aligned}&\delta N = 1.5 \cdot 0.18 \cdot 0.16 \cdot \Delta h = 0.042 \cdot \Delta h \\ &\textit{where } \rho_w / \bar{\rho} = 1000 / 5517 = 0.18\end{aligned}$$

Convenient test functions for load estimates

B) Spherical Density Layer [H-M 1967, ch.3-8]: P located on symmetry axis of spherical layer with constant surface density σ with radius opening angle Ψ

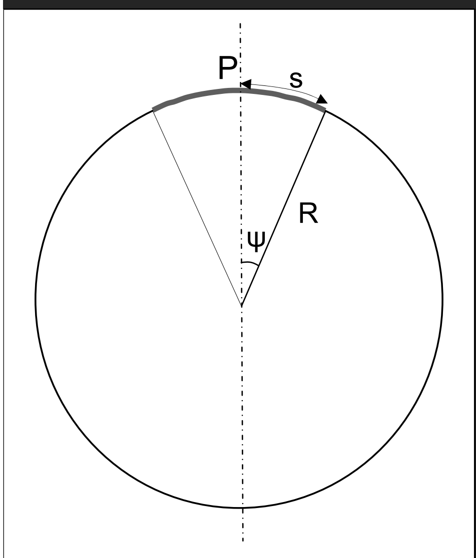

Effect on gravity potential:

$$\begin{aligned}\delta V &= GR^2\sigma \int_{\alpha=0}^{2\pi}\int_{\psi=0}^{\Psi} \frac{1}{\ell}\sin\psi \, d\psi \, d\alpha \\ &= 2\pi G R^2 \sigma \int_{\psi=0}^{\Psi} \frac{\sin\psi}{2R\sin\frac{\psi}{2}} d\psi \\ &= 4\pi G \sigma R \sin\tfrac{\Psi}{2}\end{aligned}$$

Effect on geoid:

$$\begin{aligned}\delta N &= \frac{\delta V}{g} = \frac{4\pi G \sigma R \sin\frac{\Psi}{2}}{\frac{4}{3}\pi G \bar{\rho} R} = 3\frac{\sigma}{\bar{\rho}}\sin\tfrac{\Psi}{2} \\ &\approx \frac{3}{2}\frac{\rho_w}{\bar{\rho}}\Delta h \frac{s}{R}\end{aligned}$$

application of basic formula to a mass layer

$$\begin{Bmatrix} \Delta\bar{C}_{nm} \\ \Delta\bar{S}_{nm} \end{Bmatrix} = \frac{\rho_w}{\bar{\rho}} \frac{3\cdot(1+k_n)}{2n+1} \frac{1}{4\pi} \iint_s \frac{h^{EWH}(\theta,\lambda)}{a} \bar{P}_{nm}(\cos\theta_Q) \begin{Bmatrix} \cos m\lambda_Q \\ \sin m\lambda_Q \end{Bmatrix} ds_Q$$

Example: mass change with the following properties

origin located at north pole

isotropic (not dependent on longitude)

thin layer of thickness h^{EWH}

This results in:

$$\Delta\bar{C}_n = \frac{\rho_w}{\bar{\rho}} \frac{3\cdot(1+k_n)}{2n+1} \frac{1}{2} \int_{\theta=0}^{\pi} \frac{h^{EWH}(\theta_Q)}{a} \bar{P}_n(\cos\theta_Q)\sin\theta d\theta_Q$$

application of basic formula to a mass layer

$$\Delta\bar{C}_n = \frac{\rho_w}{\bar{\rho}} \frac{3\cdot(1+k_n)}{2n+1} \frac{1}{2} \int_{\theta=0}^{\pi} \frac{h^{EWH}(\theta_Q)}{a} \bar{P}_n(\cos\theta_Q)\sin\theta d\theta_Q$$

Expansion of h^{EWH} into a Legendre series gives:

$$\frac{1}{2} \int_{\theta=0}^{\pi} \frac{h^{EWH}(\theta)}{a} \bar{P}_n(\cos\theta) d\theta = \frac{\sqrt{2n+1}}{2} \int_{\theta=0}^{\pi} \frac{h^{EWH}(\theta)}{a} P_n(\cos\theta) d\theta\sigma_n$$
$$= \sqrt{2n+1}\frac{h_n^{EWH}}{a} = \sqrt{2n+1}\Delta C_n^{EWH}$$

and therefore:

$$\Delta\bar{C}_{nm} = 0 \quad for\ m \neq 0 \ \ and \ \ \Delta\bar{S}_{nm} = 0 \quad and$$
$$\Delta\bar{C}_n = \frac{\rho_w}{\bar{\rho}} \frac{3\cdot(1+k_n)}{\sqrt{2n+1}} \frac{h_n^{EWH}}{a} = \frac{\rho_w}{\bar{\rho}} \frac{3\cdot(1+k_n)}{\sqrt{2n+1}} \Delta C_n^{EWH}$$

application of basic formula to a mass layer

Expansion into Legendre polynomials:

$$\int_{-1}^{+1} P_n(t)\,P_k(t)\,dt = \frac{2}{2n+1}\delta_{nk}$$

$$\overline{P}_n(t) = \sqrt{2n+1}\,P_n(t) \quad and \quad P_n(t) = \overline{P}_n(t)/\sqrt{2n+1}$$

$$\overline{f}_n = \frac{1}{2}\int f(t)\overline{P}_n(t)\,dt \quad and \quad f(t) = \sum \overline{f}_n \overline{P}_n(t)$$

$$f_n = \frac{2n+1}{2}\int f(t) P_n(t)\,dt \quad and \quad f(t) = \sum f_n P_n(t)$$

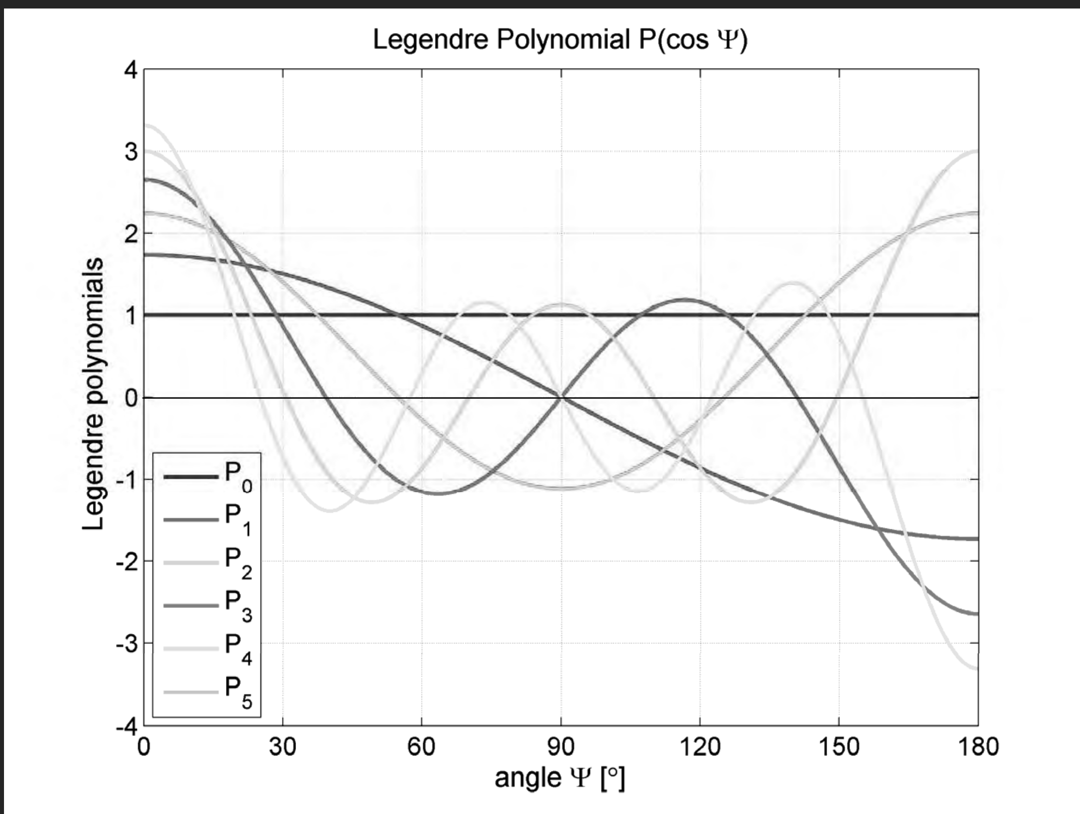

application of basic formula to a mass layer

$$\delta V_n = \frac{GM}{a}\left(\frac{a}{r}\right)^{n+1} \Delta\bar{C}_n \quad and \quad \delta N_n = a\Delta\bar{C}_n$$

$$\delta N_n = a \cdot \Delta\bar{C}_n = \frac{\rho_w}{\bar{\rho}} \frac{3\cdot(1+k_n)}{\sqrt{2n+1}} h_n^{EWH} = a \cdot \frac{\rho_w}{\bar{\rho}} \frac{3\cdot(1+k_n)}{\sqrt{2n+1}} \Delta C_n^{EWH}$$

convenient test functions for load estimates

C) Pellinen Function: spherical equivalent of a box function

$$B(\psi) = \begin{cases} \dfrac{1}{2\pi(1-\cos\Psi)} & and\ \psi \le \Psi \\ 0 & and\ \psi > \Psi \end{cases}$$

or as Legendre series

$$B(\psi) = \sum_{n=0}^{\infty} \frac{2n+1}{4\pi} \beta_n P_n(\cos\psi)$$

Expansion into Legendre polynomials:

$$\beta_n = 2\pi \int_{\psi=0}^{\pi} B(\psi) P_n(\cos\psi)\sin\psi\, d\psi = \frac{1}{1-\cos\Psi} \int_{\psi=0}^{\Psi} P_n(\cos\psi)\sin\psi\, d\psi$$
$$= \frac{1}{1-\cos\Psi} \frac{1}{2n+1} \left[P_{n-1}(\cos\Psi) - P_{n+1}(\cos\Psi)\right]$$

Or approximately (Sjöberg L,B.G.,1980):

$$\beta_n = \frac{2n-1}{n+1}\cos\Psi \cdot \beta_{n-1} - \frac{n-2}{n+1}\beta_{n-2} \quad with\ \beta_0 = 1\ and\ \beta_1 = \tfrac{1}{2}(1+\cos\Psi)$$

- Can be used as filter function, too -

convenient test functions for load estimates

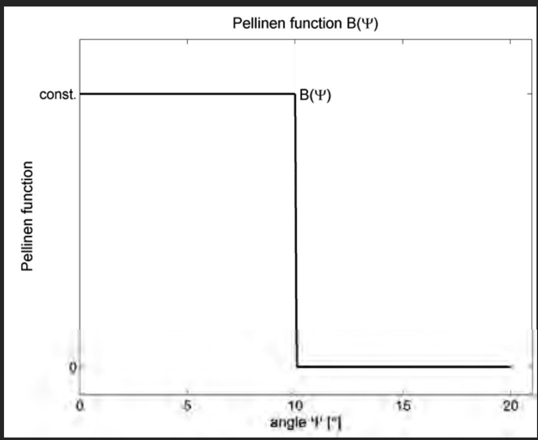

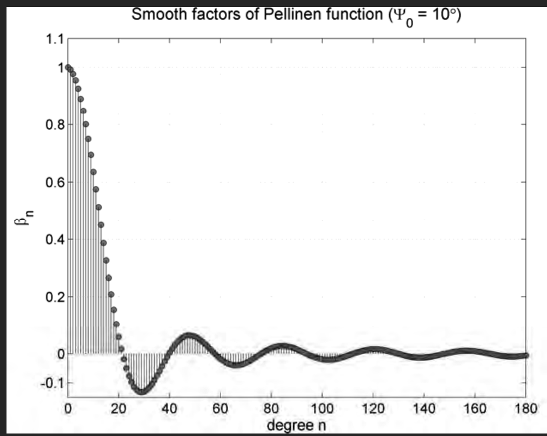

convenient test functions for load estimates

D) Jekeli Function: spherical equivalent of a Gauss function (Jekeli C, OSU327, 1981):

$$W(\psi) = \frac{b}{2\pi}\frac{\exp\left[-b\cdot(1-\cos\psi)\right]}{1-\exp(-2b)} \quad \textit{where } b = \frac{\ln(2)}{\left(1-\cos(s/R)\right)}$$

(It is s= full width (arc length on earth sphere) of half value and R = earth radius or Ψ=s/R)

Expansion of W(ψ) into Legendre polynomials:

$$W_n = \int_{\psi=0}^{\pi} W(\psi)P_n(\cos\psi)\sin\psi \, d\psi$$

Recursion formulae:

$$W_{n+1} = -\frac{2n+1}{b}W_n + W_{n-1} \quad \textit{where } W_0 = \frac{1}{2\pi} \textit{ and } W_1 = \frac{1}{2\pi}\left[\frac{1+\exp(-2b)}{1-\exp(-2b)} - \frac{1}{b}\right]$$

- Can be used as filter function, too; compare Wahr paper -

Convenient test functions for load estimates

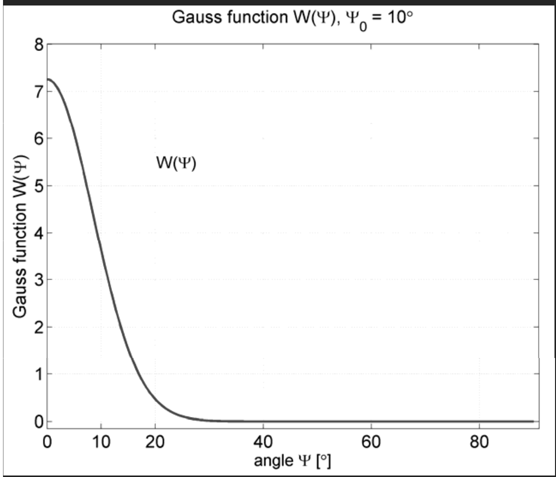

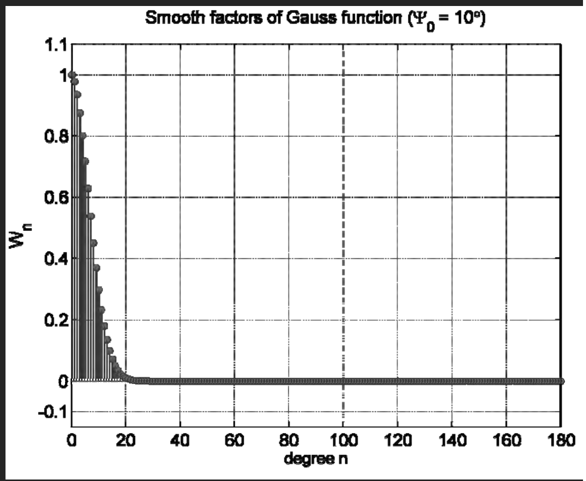

end

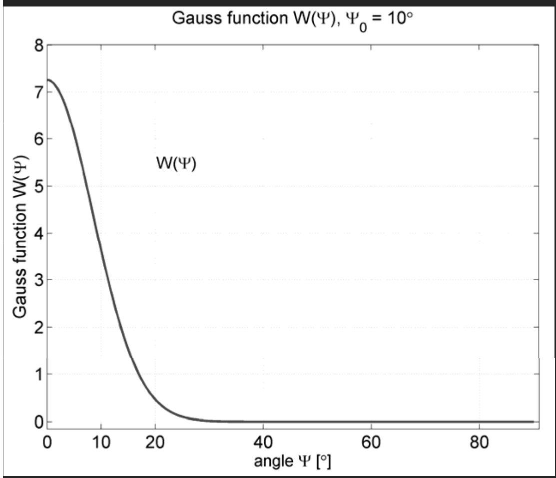
Gauss function W(Ψ), Ψ_0 = 10°
W(Ψ)
Gauss function W(Ψ)
angle Ψ [°]

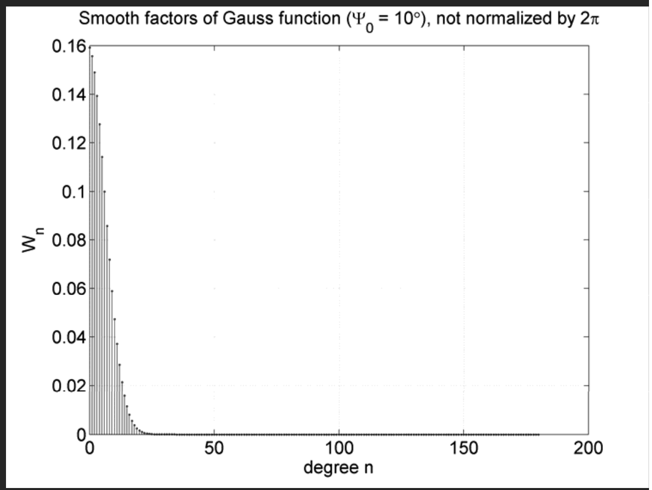
Smooth factors of Gauss function (Ψ_0 = 10°), not normalized by 2π
W_n
degree n

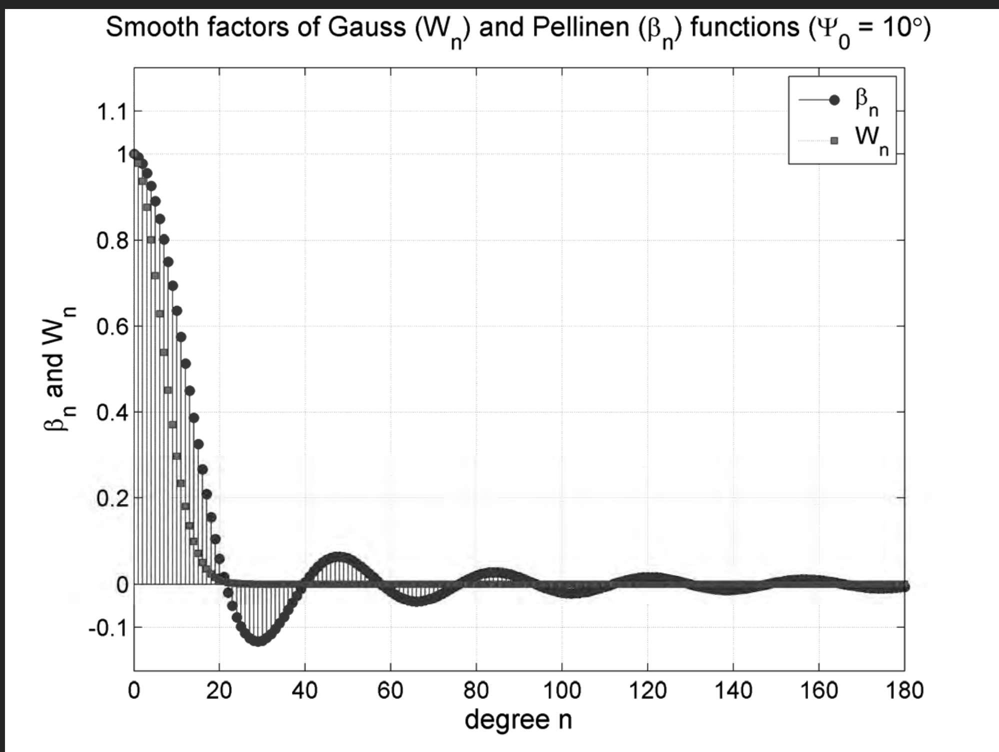
Smooth factors of Gauss (W_n) and Pellinen (β_n) functions (Ψ_0 = 10°)
β_n
W_n
β_n and W_n
degree n

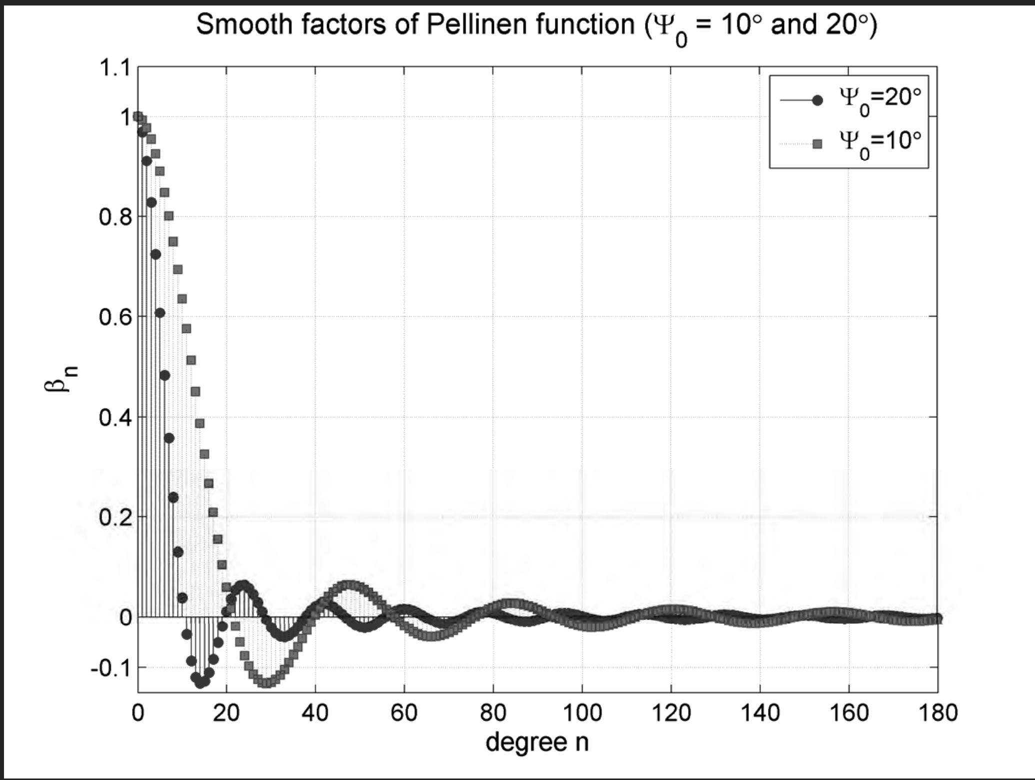

temporal gravity and mass exchange

gravity und oceanography:

geoid plus altimety =
dynamic ocean topography =
surface ocean circulation ⇨

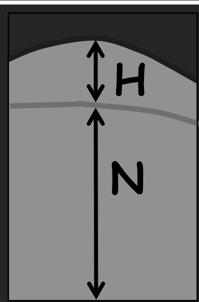

temporal gravity variation
and sea level change: ⇨
thermal expansion versus mass increase

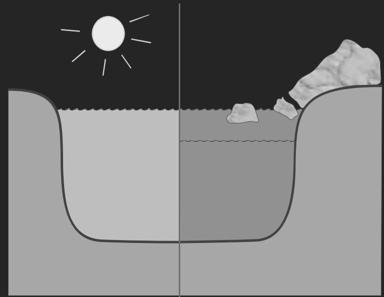

temporal gravity variation =
bottom pressure variation =
deep ocean circulation ⇨

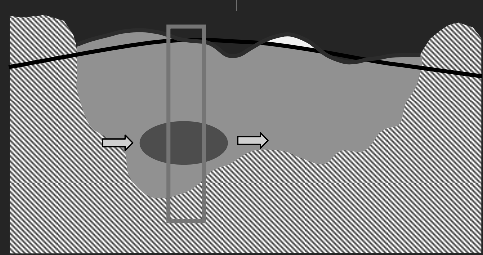

temporal gravity and mass exchange

from surface circulation to ocean velocity at depth
by measuring temperature and salinity profiles
(or vertical changes of pressure)

$$u = -\frac{1}{f\rho}\frac{\partial}{\partial y}\int_{\text{depth}}^{0} g(\varphi, z)\rho(z)\,dz - \frac{g}{f}\frac{\partial H}{\partial y}$$

$$v = -\frac{1}{f\rho}\frac{\partial}{\partial x}\int_{\text{depth}}^{0} g(\varphi, z)\rho(z)\,dz + \frac{g}{f}\frac{\partial H}{\partial x}$$

Lecture: Sea Level

Maik Thomas

Summer School „Global Water Cycle“
12.-16. September 2011
Mayschoss

Outline

What is sea level rise?

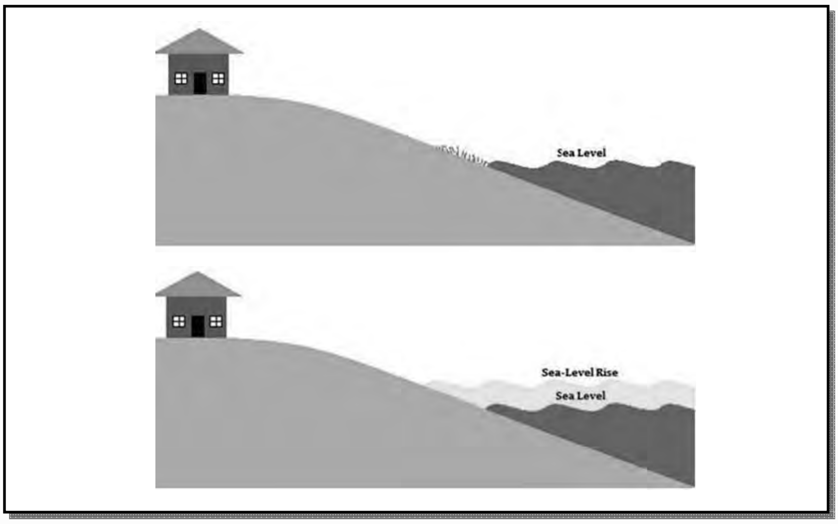

(C. Dziuba, NCDENR)

3

SPP 1257

Wikipedia‘s definitions

- **Sea level:**
  - the level of the ocean‘s surface
- **Mean sea level (MSL):**
  - average height of the ocean‘s surface
  - "still water level" - level of the sea with motions averaged out
  - measured in respect to land
    ↳ ΔMSL results from a real change in sea level or from a change in the height of the land on which the tide gauge operates
  - coincides with the geoid surface in a state of rest or absence of external forces
- **Local mean sea level (LMSL):**
  - time-averaged height of the sea with respect to a land benchmark
- **Relative sea level (RSL):**
  - distance between sea-surface and local moving datum
- **Eustatic SL changes** (as opposed to local change) result from changes in the volume of seawater or net changes in the volume of ocean basins

4

SPP 1257

Relative & eustatic sea level

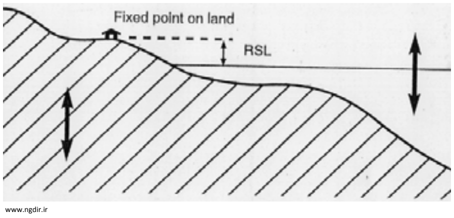

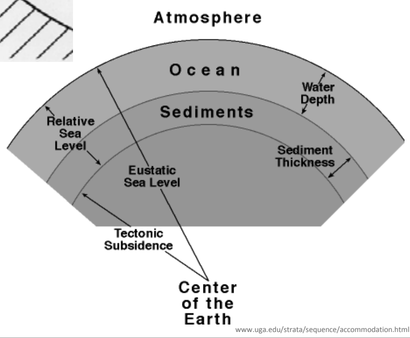

Sea level – an integral of changes in the Earth‘s heat budget

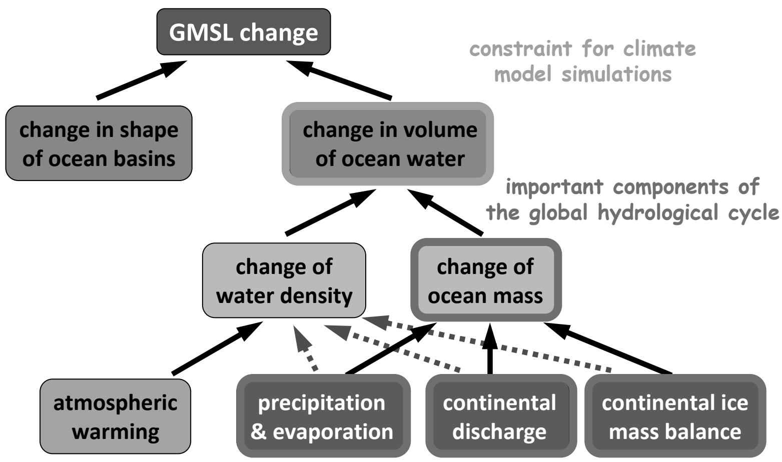

Outline

I. Introduction

II. Impacts of sea level changes

III. Recent sea level changes

IV. Paleo records & reconstructions

V. Causes of sea level variations:
   i) Loading
   ii) Mass changes & the global hydrological cycle
   iii) Volume changes & climate

VI. Projections

VII. Summary / Synthesis

7

SPP 1257

The Earth at night

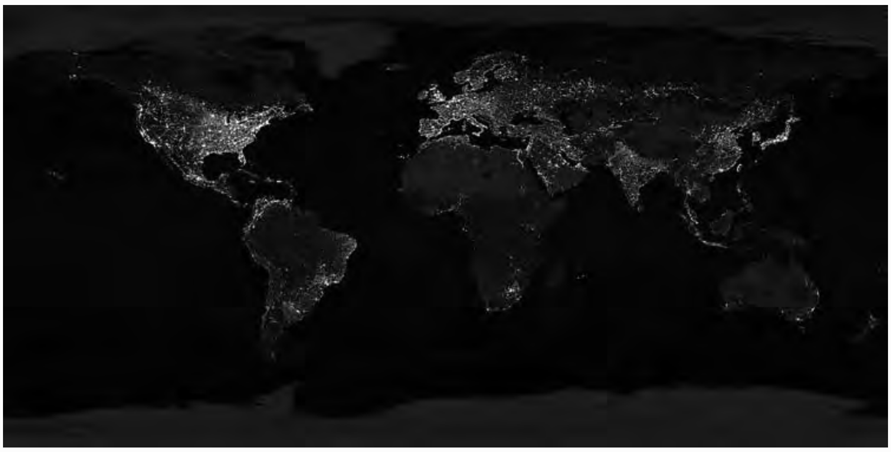

8

SPP 1257

Some numbers …

- MSL rise of 18 cm during the 20th century
- 1978 - 2000: 1565 km² of intertidal areas converted to open water
- by 2050 addtional 1300 km² land loss

- total sea level rise (1990 - 2100) acc. to IPCC AR4:
  - 18 – 59 cm (without increasing ice discharge)
  - 18 – 76 cm (with increasing ice discharge)
  - sea level rise > 1 m also *„physically plausible“*

- subsidence of …
  - megacities
    (subsidence of 2-5 m during the last century)
  - coasts including river deltas
    (9 Asian vulnerable deltas with a population of 250,000,000 people)

  ↳ threat to quality of and entry to drinking water

9

SPP 1257

Potential impact of a 5 m sea level rise …

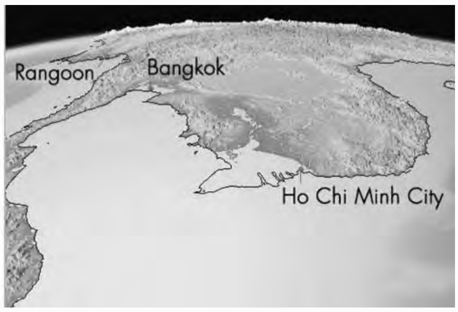

… in Florida and Southeast Asia

W. Haxby, Lamont Daherty Earth Observatory

10

SPP 1257

Subsiding coastal megacities

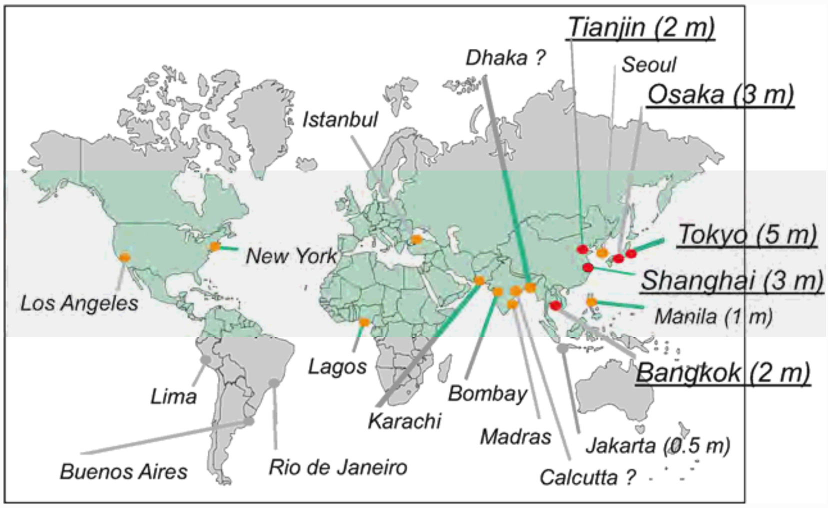

maximum subsidence during the 20th century

(Nicholls, 1995, GeoJournal)

Which cities will flood when?

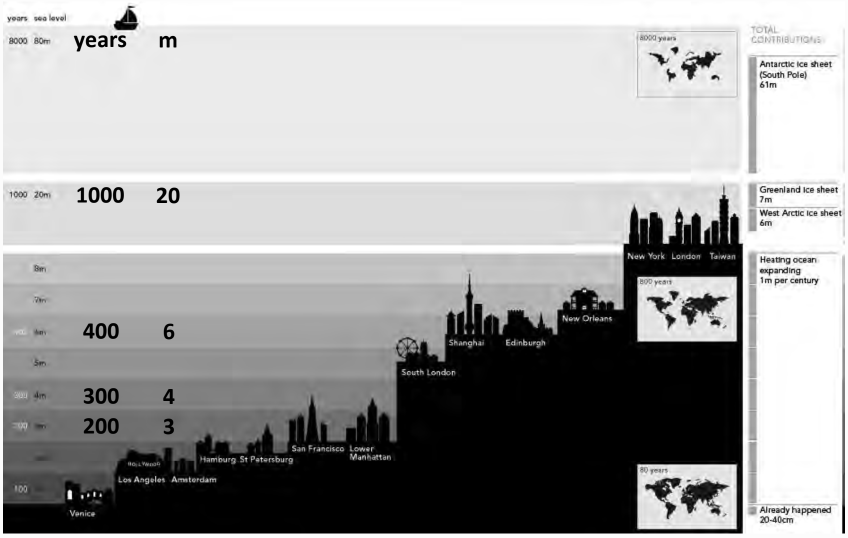

IPCC, NASA, NewScientist.com, Potsdam Institute, Sea Level Explorer

Threatened coastal areas

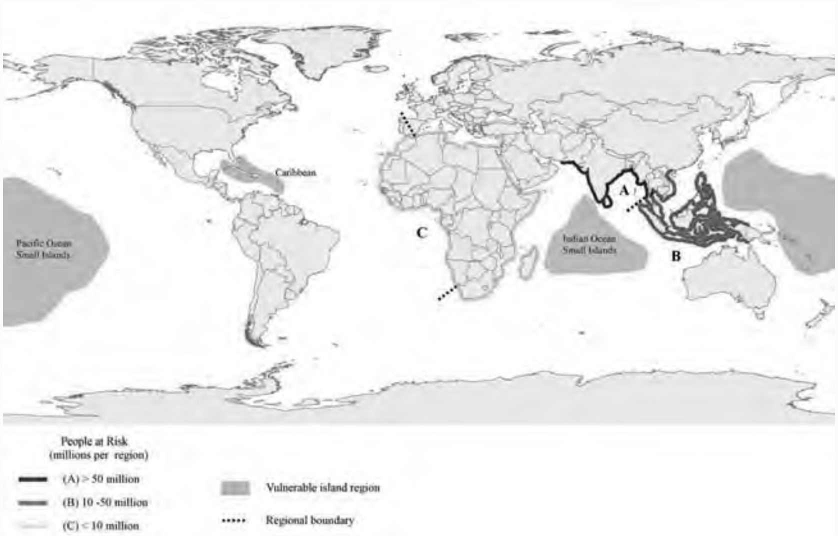

to 40 cm SLR by the 2080s

(Nicholls et al., 1999)

13

SPP 1257

Impacts of SLR

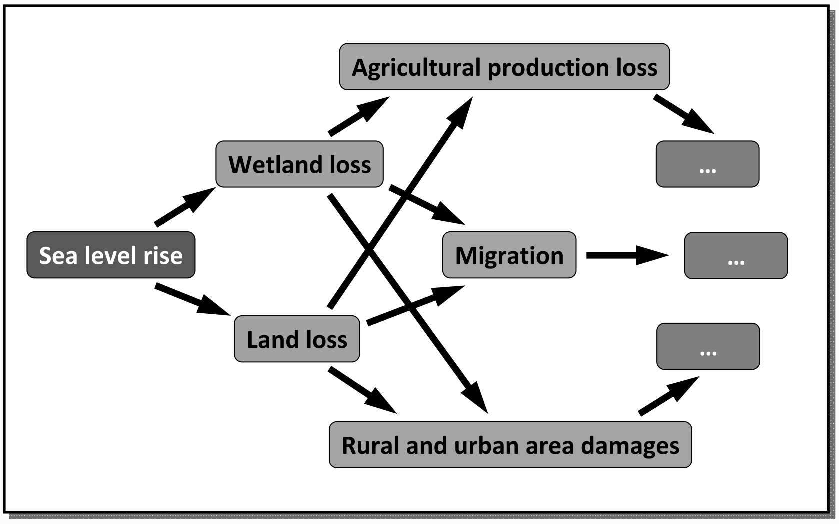

14

SPP 1257

Sea level rise – response strategies

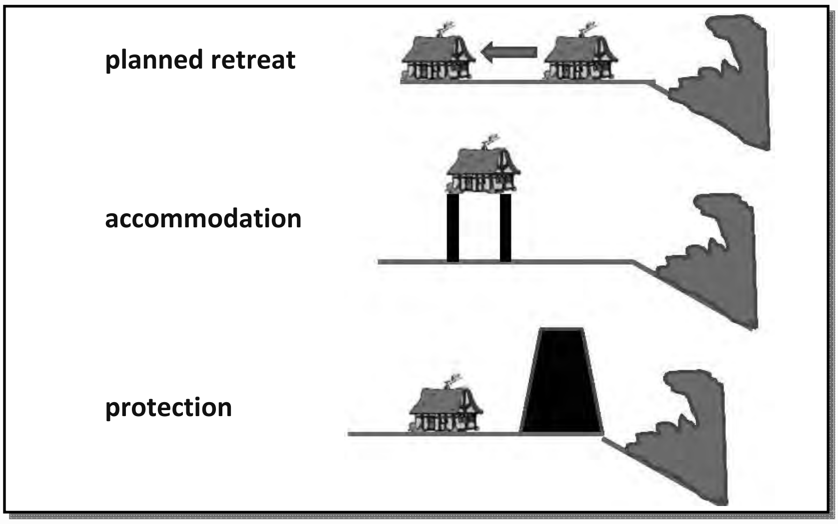

15

SPP 1257

Options for adaptation

NATURAL SYSTEM EFFECT		POSSIBLE ADAPTATION RESPONSES
1. Inundation, flood and storm damage	a. Surge b. Backwater effect	Dikes/surge barriers [P], Building codes/floodwise buildings [A], Land use planning/hazard delineation [A/R].
2. Wetland loss (and change)		Land use planning [A/R], Managed realignment/ forbid hard defences [R], Nourishment/sediment management [P].
3. Erosion (of 'soft' morphology)		Coast defences [P], Nourishment [P], Building setbacks [R].
4. Saltwater Intrusion	a. Surface Waters	Saltwater intrusion barriers [P], Change water abstraction [A/R].
	b. Ground-water	Freshwater injection [P], Change water abstraction [A/R].
5. Rising water tables/ impeded drainage		Upgrade drainage systems [P], Polders [P], Change land use [A], Land use planning/hazard delineation [A/R].

P – protection; A – accommodation; R - retreat

(Nicholls, 2010)

16

SPP 1257

Outline

I. Introduction
II. Impacts of sea level changes
III. Recent sea level changes
IV. Paleo records & reconstructions
V. Causes of sea level variations:
  i) Loading
  ii) Mass changes & the global hydrological cycle
  iii) Volume changes & climate
VI. Projections
VII. Summary / Synthesis

17

SPP 1257

Sea level observations

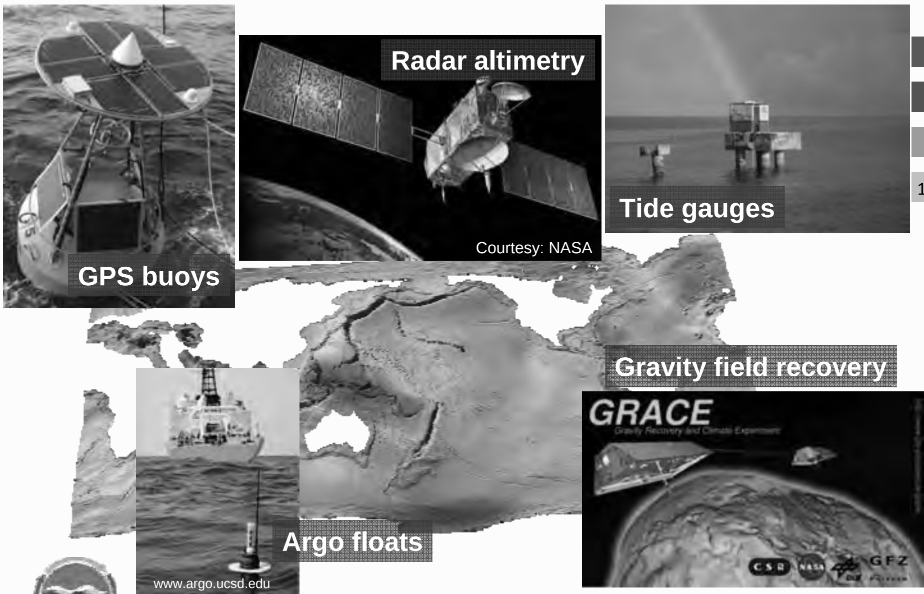

18

SPP 1257

Long-term records of relative sea level change

Distribution of PSMSL tide-gauge stations

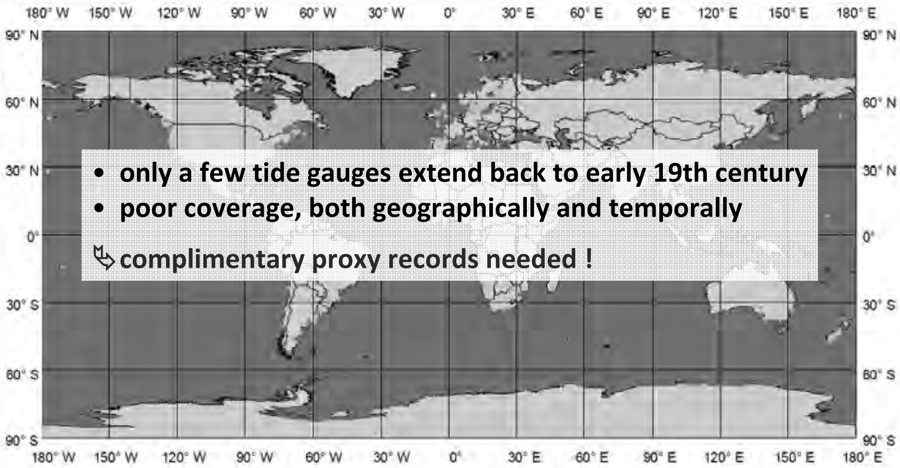

- **only a few tide gauges extend back to early 19th century**
- **poor coverage, both geographically and temporally**

↳ complimentary proxy records needed !

● Established before 1950 ● Established after 1950

SPP 1257

Permanent Service for Mean Sea Level, PSMSL: http://www.pol.ac.uk/psmsl/

19

Processes causing relative sea level change

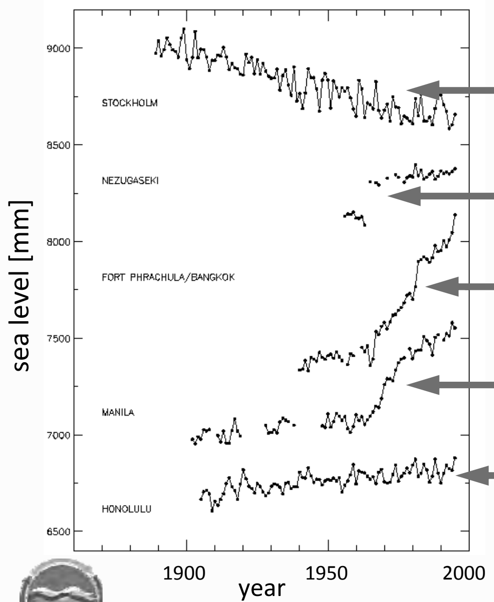

Stockholm, Sweden:
Subsidence due to land uplift

Nezugaseki, Japan:
Discontinuity due to earthquake (1964)

Bangkok, Thailand:
Rise due to ground water extraction

Manila, Philippines:
Rise due to high river discharges

Honolulu, Hawaii:
"Far field" signal, no significant tectonic signal;
secular trend ca. 1.5 mm/year

SPP 1257

20

Sea surface observations

satellite altimetry

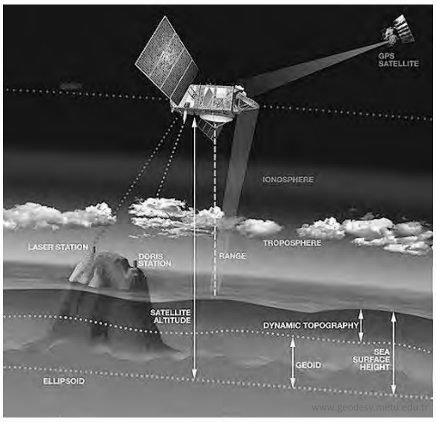

TOPEX/Poseidon (1995)

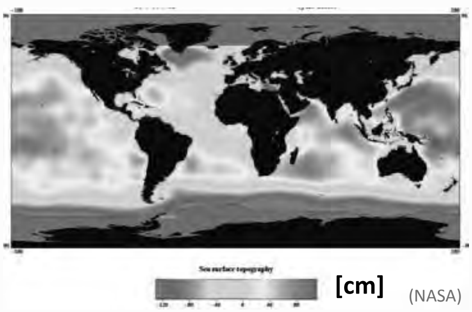

(NASA)

21

- ↳ determination of **dynamic topography**
- ↳ derivation of surface currents with **geostrophic method**

Sea level trend(s)

Radar altimetry since (1985) 1992

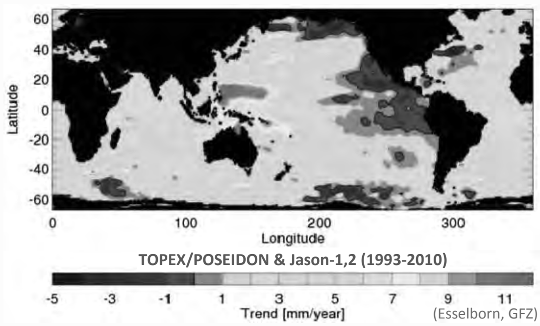

(Esselborn, GFZ)

mean global trend (60 S – 60 N): ca. 3 mm/year

depending on period, satellites
and correction models;
temporal coverage still below decades

Tide gauges for up to 150 years

Courtesy: G. Liebsch

pointwise measurements, offshore,
heterogeneous distribution,
difficult vertical control

22

Sea level trend(s)

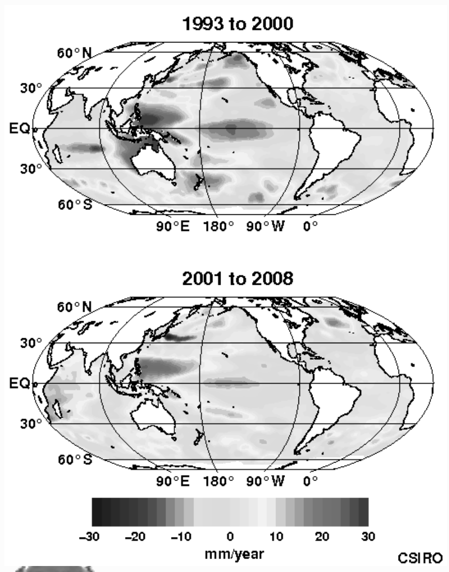

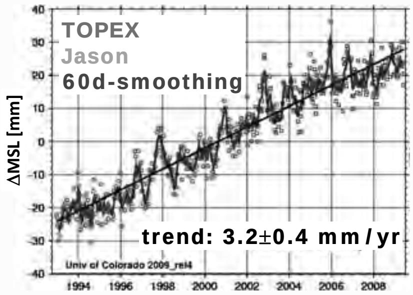

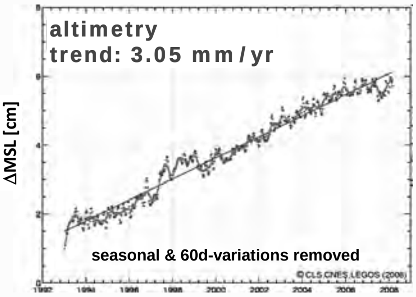

23

SPP 1257

Modern sea level change estimates

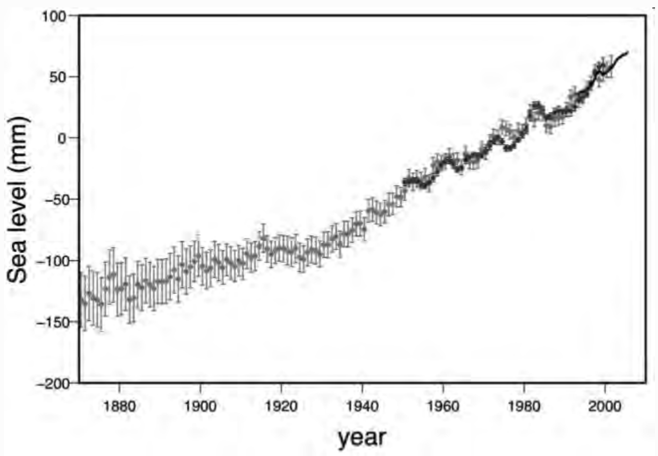

GMSL change since 1870 from three different studies (red, blue, black)

(IPCC AR4, 2007, Working Group 1, p. 410)

24

SPP 1257

Modern sea level change estimates

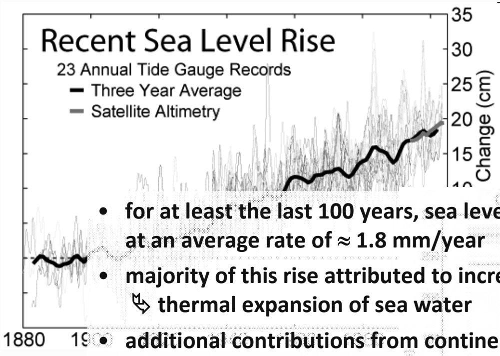

- measurements from 23 long tide gauge records in geologically stable environments
  ↳ rise of ≈ 20 cm/century or 2 mm/year

25

- for at least the last 100 years, sea level has been rising at an average rate of ≈ 1.8 mm/year
- majority of this rise attributed to increase in temperature of the sea
  ↳ thermal expansion of sea water
- additional contributions from continental discharge, e.g., melting snow and glaciers

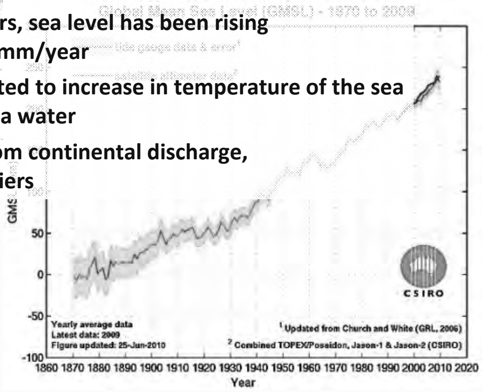

SPP 1257

Outline

26

SPP 1257

Sea level indicators

- **types:**
  - sedimentary (e.g., beachrock)
  - erosional (e.g., notches)
  - ecological (e.g., accretionary biotherms constructed by coralline algae)
  - microfossils (e.g., diatoms, testate amoebae, foraminifera)
  - archaeological (e.g., fish tanks)
  - …
- refer mostly to **ocean volume**
- refer, in general, to some **level within the tidal range**, not to MSL
- often just **indicative**, i.e., giving a limiting value only
- often affected by **age uncertainties**

↳ **combination of geological, biological, and archaeological proxy indicators to minimize error bars !**

27

Global sea level reconstructions during the last 500 Ma

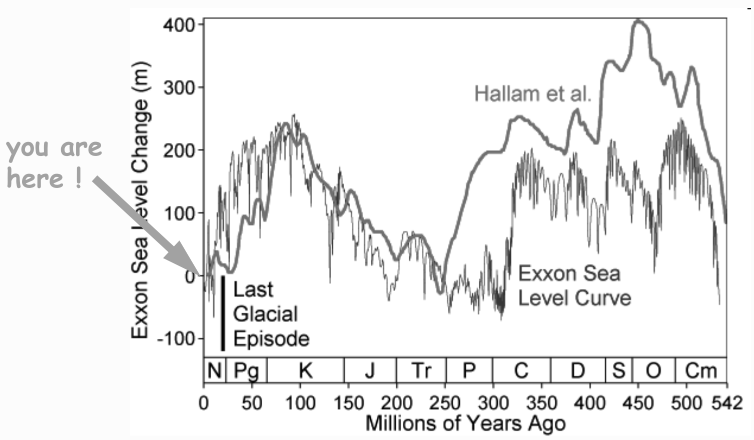

↳ **Over most of geologic history long-term average sea level has been significantly higher than today !**

Thomas M. Cronin (1999): Principles of Paleoclimatology

28

Global sea level reconstructions during the last 500 Ma

29

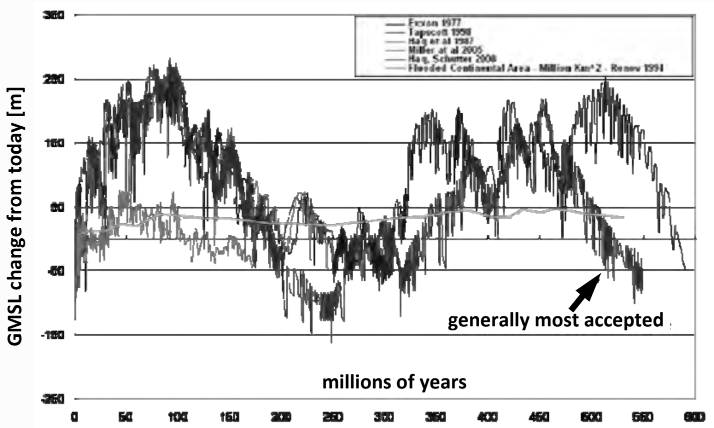

↳ **Sea levels were ≈ 265 m higher than today 100 million years ago.**

Global sea level reconstructions during the last 500 Ma

30

Main mechanisms:

(1) Sea level falls when glaciers build up on land.

***(2) Sea level falls when continental land masses are concentrated together*:**
collisions and mountain building squeeze Earth's landmasses together
↳ less continental shelf area affecting the average depth of the oceans
↳ ocean basins tend to be more mature and deeper

(3) Sea level rises when new ocean basins are opening:
new ocean basins generally form at only 2,500 m depth, while mature ocean basins tend to deepen to ≈ 6,000 m after 100 million years
↳ overall average depth of the ocean is lower when new oceans are forming
(e.g., during the Cretaceous when the Atlantic Ocean was opening up)

↳ **Sea levels were ≈ 265 m higher than today 100 million years ago.**

Global sea level reconstructions during the last 500 Ma

temperature, CO_2 and sea level

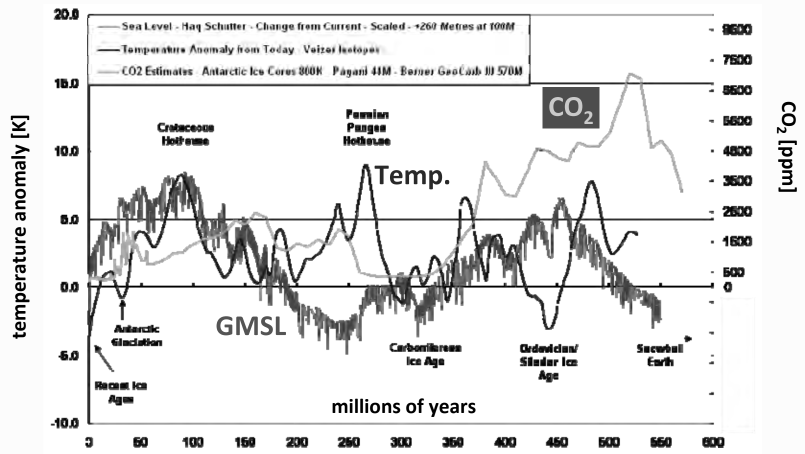

31

Sea level reconstructions (800 ky BP - present)

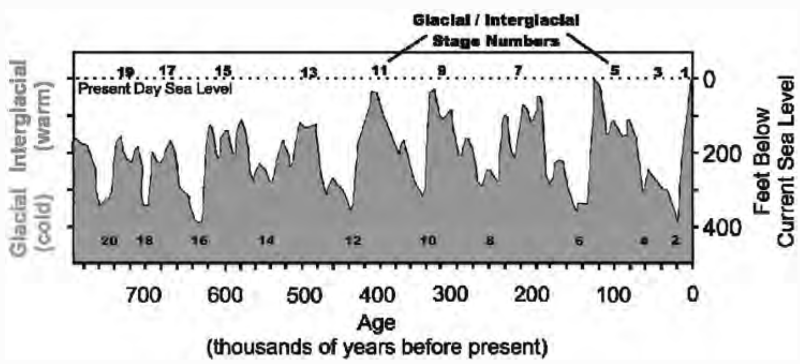

(DWR, 2006)

32

Post-glacial sea level rise

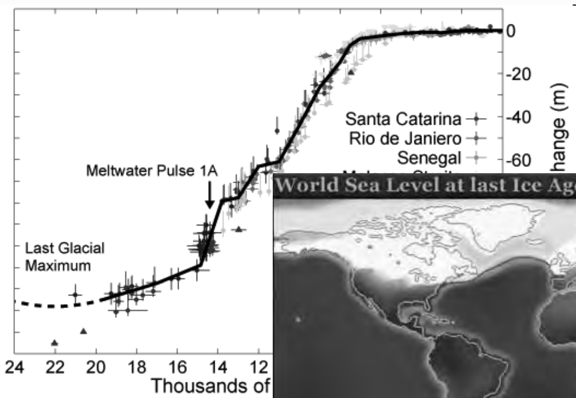

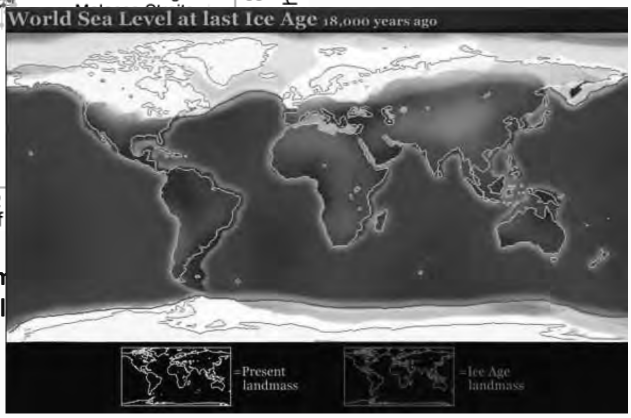

33

↳ **GMSL ≈ 120 m**
during Last Gl

Post-glacial sea level rise

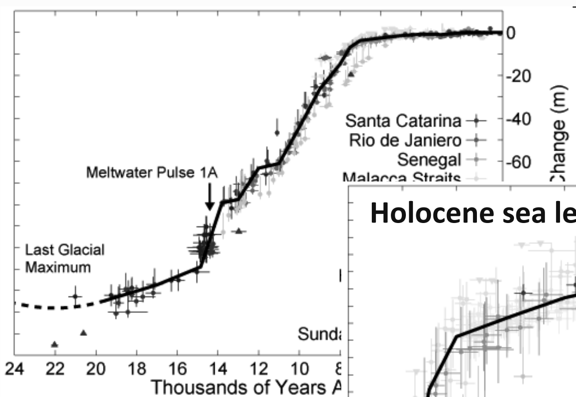

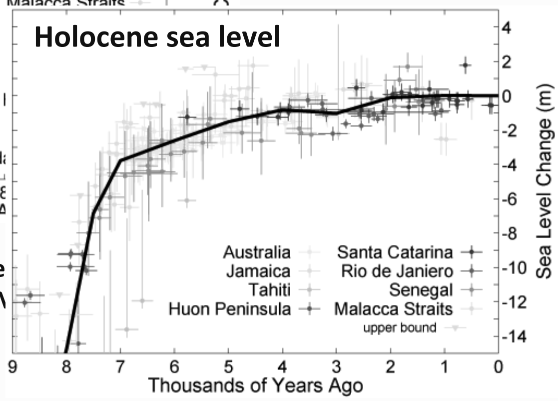

34

↳ **GMSL ≈ 120 m lowe**
during Last Glacial M

Outline

I. Introduction
II. Impacts of sea level changes
III. Recent sea level changes
IV. Paleo records & reconstructions
V. Causes of sea level variations:
  i) Loading
  ii) Mass changes & the global hydrological cycle
  iii) Volume changes & climate
VI. Projections
VII. Summary / Synthesis

Short-term and periodic SL changes

periodic SL changes		
diurnal & semidiurnal tides	12h … 24h	0.2m … 10m
long-period tides		
rotational variations (CW, …)	14 months	
meteorological & oceanographic fluctuations		
atmospheric pressure	hours … months	up to 1.3m
winds (storm surges)	1d … 5d	up to 5.0m
precipitation, evaporation	days … weeks	
sea surface topography	days … weeks	up to 1.0m
ENSO	6months every 5-10yr	up to 0.6m
seasonal variations		
river runoff/floods	2 months	1.0m
water density changes (T,S)	6 months	0.2m
seiches		
seiches (standing waves)	minutes … hours	up to 2.0m
earthquakes		
tsunamis	hours	up to 10m
abrupt change in land level	minutes	up to 10m

Long-term causes of SL change

long-term causes	*range of effect*	*vertical effect*
change in volume of ocean basins		
tectonics / sea floor spreading	eustatic	0.01mm/yr
marine sedimentation	eustatic	<0.01mm/yr
change in ocean mass		
melting / accumulation of cont. ice	eustatic	10mm/yr
climate changes during the 20th century		
Antarctica (increasing precipitation)	eustatic	-0.2 … 0.0mm/yr
Greenland (precipitation & runoff)	eustatic	0.0 … 0.1mm/yr
long-term adjustment to the end of the last ice age		
Greenland & Antarctica (20th cent.)	eustatic	0.0 … 0.5mm/yr
water release from Earth's interior	eustatic	
release/accum. of cont. reservoirs	eustatic	
uplift or subsidence of Earth's surface (isostasy)		
thermal-isostasy (interior T/ρ changes)	local	
glacio-isostasy (loading of ice)	local	10mm/yr
hydro-isostasy (loading of water)	local	
volcano-isostasy (magmatic extrusions)	local	
sediment-isostasy (deposition/ erosion)	local	<4mm/yr

37

1257

Long-term causes of SL change

long-term causes	*range of effect*	*vertical effect*
tectonic uplift / subsidence		
vertical and horizontal motions of crust (in response to fault motions)	local	1-3mm/yr
sediment compaction		
sediment compression (e.g., in deltas)	local	
loss of interstitial fluids (withdrawal of groundwater or oil)	local	<55mm/yr
earthquake-induced vibration	local	
departure from geoid		
shifts in hydrosphere, aestheno-sphere, core-mantle interface	local	
shifts in Earth's rotation, axis of spin, precession of equinox	eustatic	
external gravitational changes	eustatic	
evaporation and precipitation (if due to a long-term pattern)	local	

38

DFG SPP 1257

What causes the sea level to change?

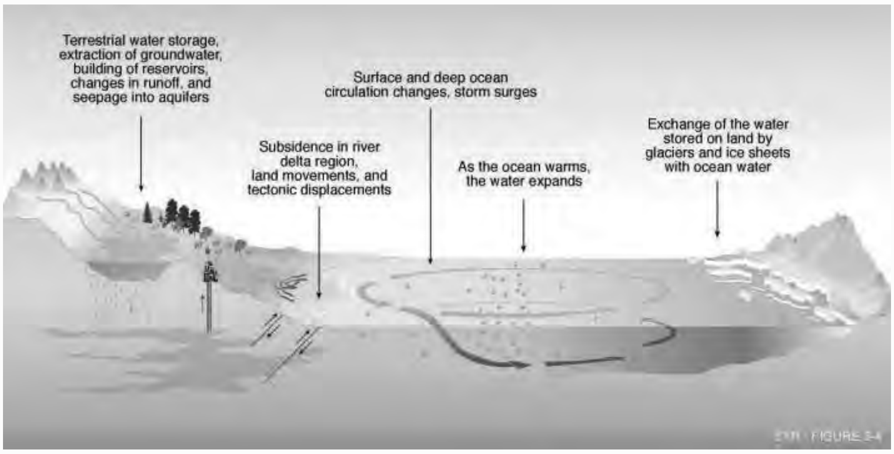

(IPCC, 2007)

39

SPP 1257

Causes of sea level change

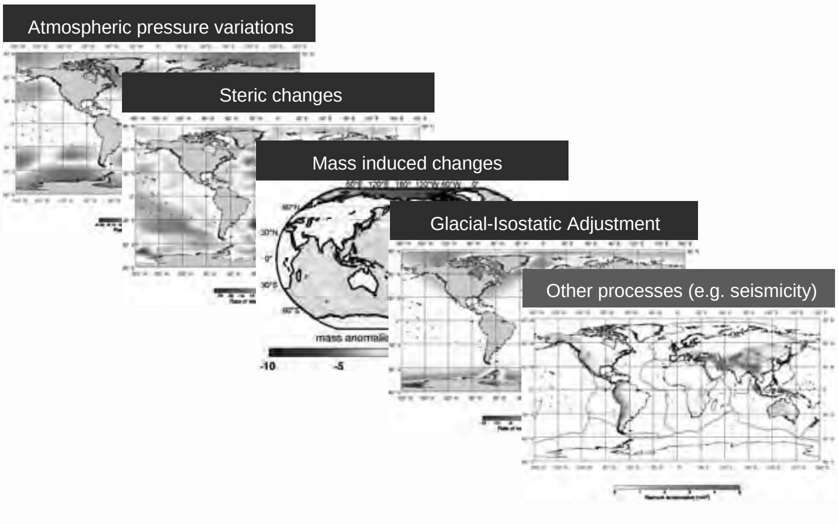

40

SPP 1257

Outline

41

Glacial isostatic adjustment (GIA)

42

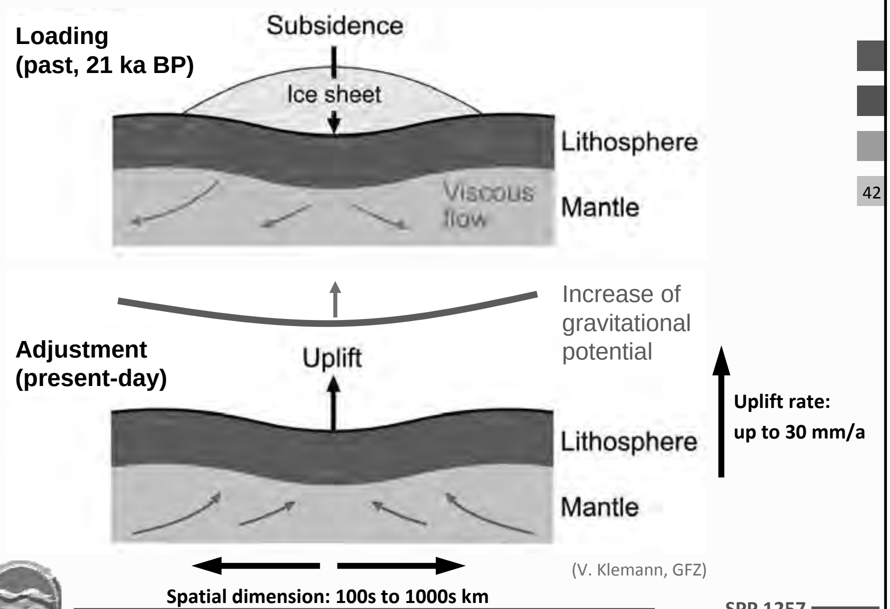

(V. Klemann, GFZ)

Prediction of GIA induced sea level variations

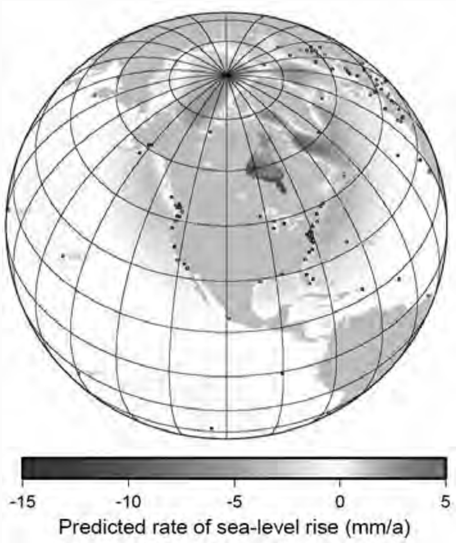

3-dim. visco-elastic model simulation with constraints from GPS data

43

(Hagedoorn, 2005)

SPP 1257

GIA correction at tide-gauge stations

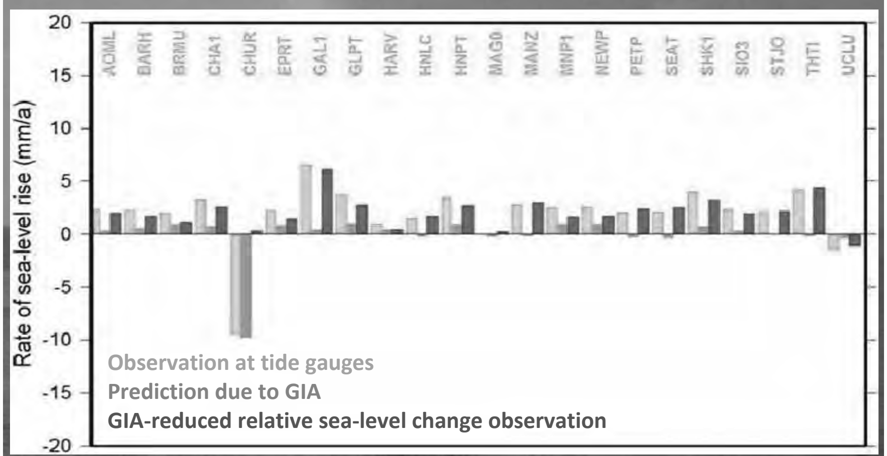

(Hagedoorn, 2005, updated)

44

SPP 1257

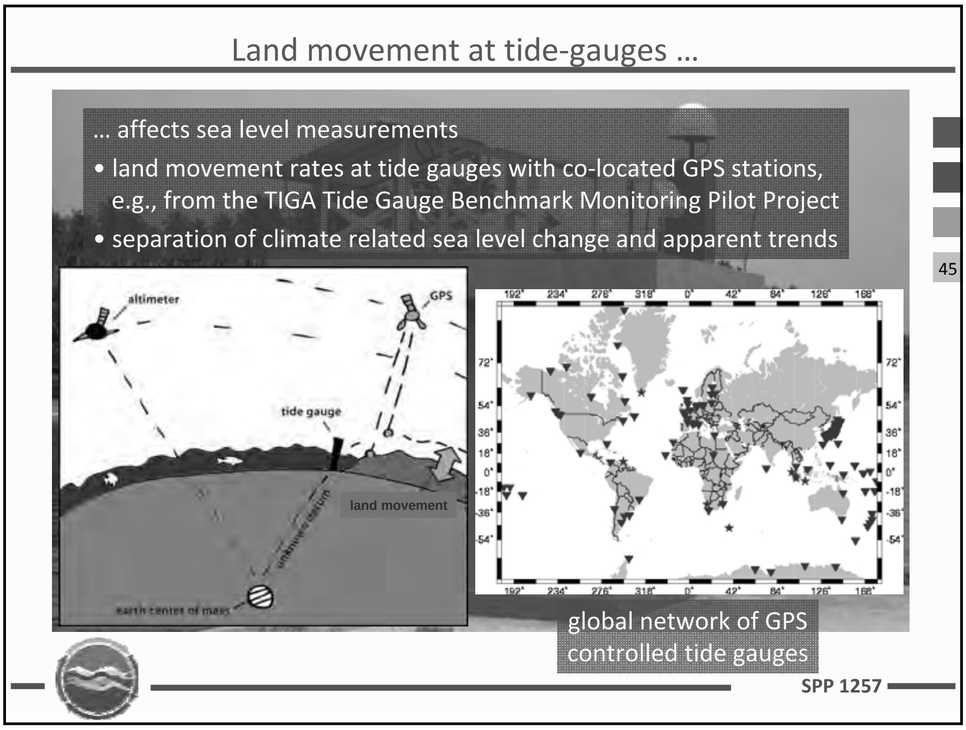
Land movement at tide-gauges …
… affects sea level measurements
• land movement rates at tide gauges with co-located GPS stations, e.g., from the TIGA Tide Gauge Benchmark Monitoring Pilot Project
• separation of climate related sea level change and apparent trends
45
altimeter
GPS
tide gauge
land movement
earth centre of mass
global network of GPS controlled tide gauges
SPP 1257

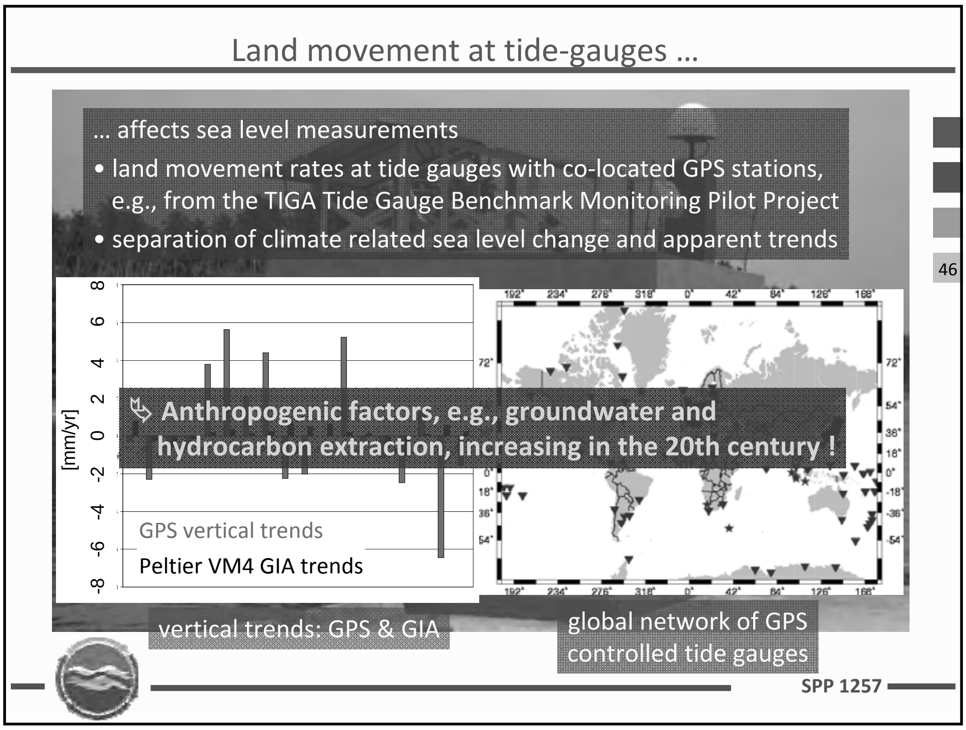
Land movement at tide-gauges …
… affects sea level measurements
• land movement rates at tide gauges with co-located GPS stations, e.g., from the TIGA Tide Gauge Benchmark Monitoring Pilot Project
• separation of climate related sea level change and apparent trends
46
[mm/yr]
8
6
4
2
0
-2
-4
-6
-8
Anthropogenic factors, e.g., groundwater and hydrocarbon extraction, increasing in the 20th century !
GPS vertical trends
Peltier VM4 GIA trends
vertical trends: GPS & GIA
global network of GPS controlled tide gauges
SPP 1257

Comparison of GIA & GPS vertical rates

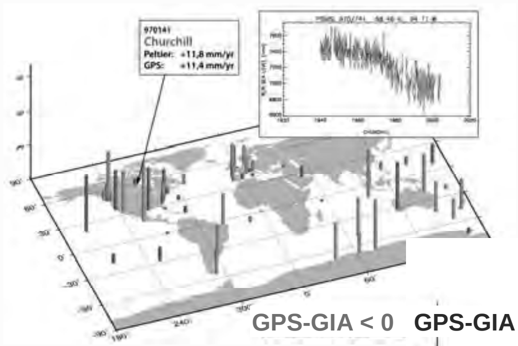

Good agreement in areas where GIA is dominant
(e.g. Churchill PSMSL 970/141)

47

GPS-GIA < 0 GPS-GIA > 0

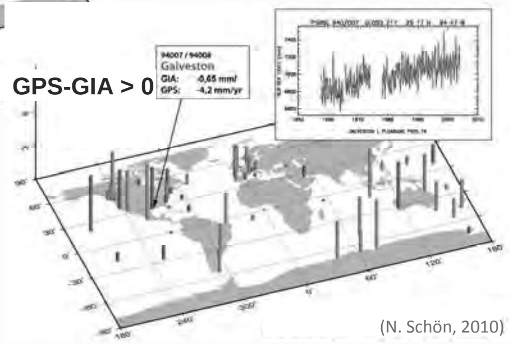

Large discrepancies in areas where land movement is mainly caused by anthropogenic effects or related to other geological processes
(e.g. Galveston PSMSL 940/007(8))

(N. Schön, 2010)

SPP 1257

Land movement: anthropogenic causes

Figure 2. 1926 photograph of a new fault scarp 0.5 miles north of the Goose Creek oil field. Fault offset at the surface is approximately 16 inches. From Galloway et al, 1999.

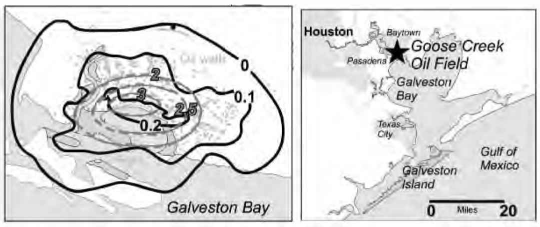

Figure 1. Measured subsidence between 1918 and 1926 around Goose Creek oilfield. Lines of equal subsidence (feet) for an 8-year period are shown in gray lines—for a 1-year period, in black lines. Modified from Galloway et al, 1999.

48

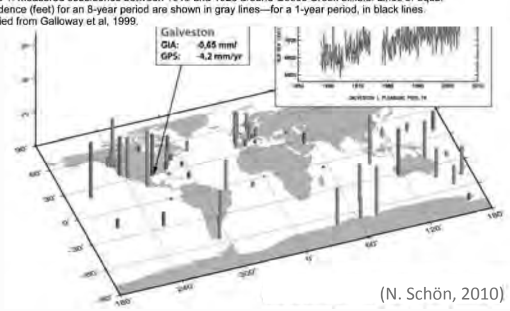

Subsidence at Galveston tide gauge caused by groundwater extraction related to oil drilling
(Source: Houston Geological Society)

(N. Schön, 2010)

SPP 1257

Sea level reconstructions

Combining GPS, tide gauges and radar altimetry for reconstruction of past sea level changes and variability

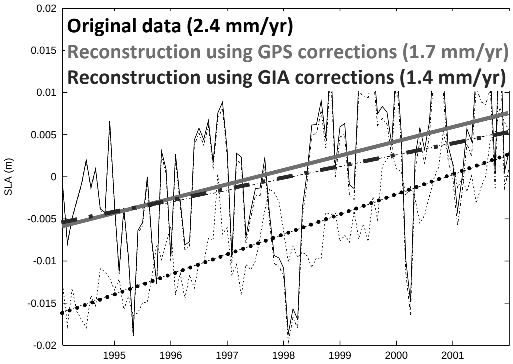

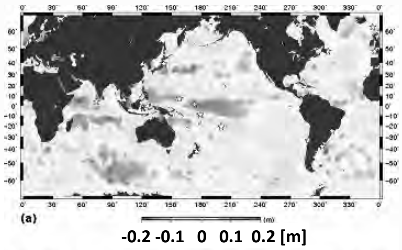

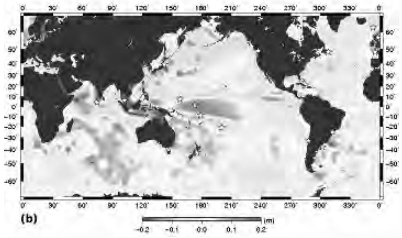

(a) TOPEX sea level anomalies 12/2001
(b) Reconstruction 12/2001 using 18 GPS corrected gauges (N. Schön, 2010)

SPP 1257

49

Outline

I. Introduction
II. Impacts of sea level changes
III. Recent sea level changes
IV. Paleo records & reconstructions
V. Causes of sea level variations:
- i) Loading
- **ii) Mass changes & the global hydrological cycle**
- iii) Volume changes & climate

VI. Projections
VII. Summary / Synthesis

SPP 1257

50

Global hydrological cycle

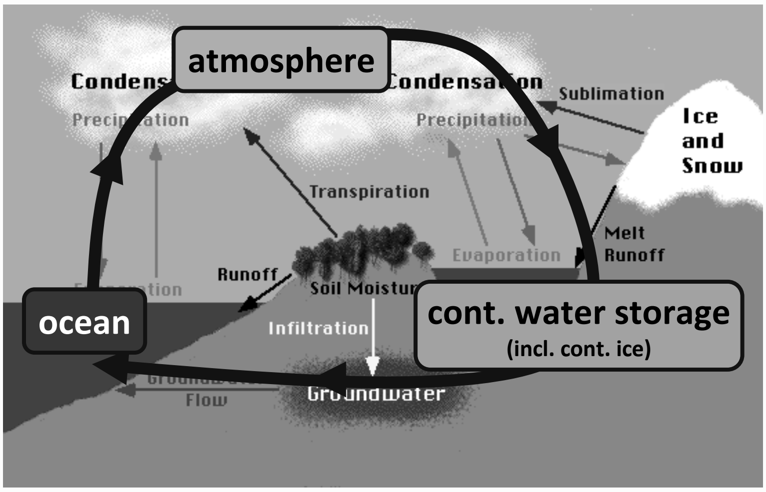

Pidwirny (2000)

SPP 1257

51

Variation of total ocean mass

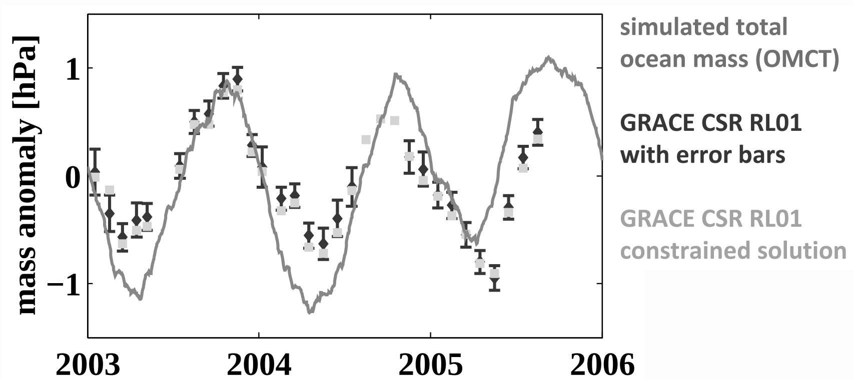

- total ocean mass from GRACE & ECMWF+HDM+OMCT
- cryospheric mass fluxes neglected
- linear trends removed

(Dobslaw & Thomas, 2007)

SPP 1257

52

Precipitation – evaporation [mm/month]

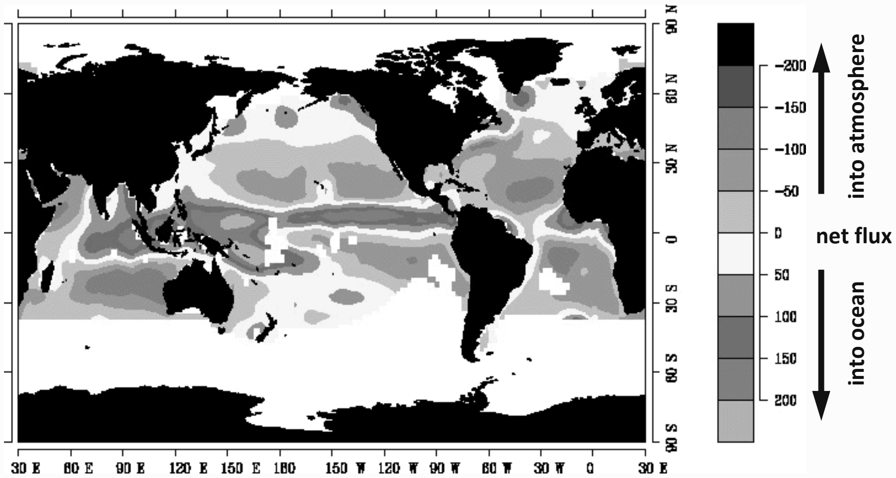

DKRZ (1999)

53

Terrestrial water storage anomalies

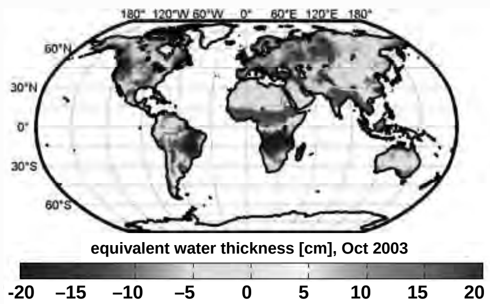

Monthly mean mass anomalies caused by continental hydrological processes as simulated with **LSDM**

54

Mass anomalies are related to recent precipitation events:

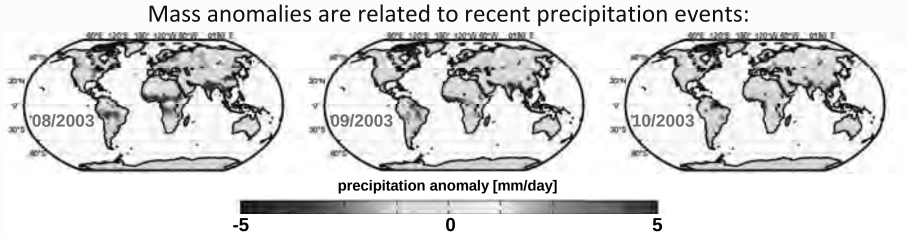

Terrestrial water storage anomalies

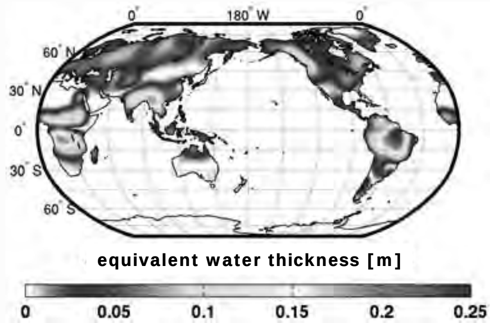

Mean annual amplitudes of hydro-logical mass anomalies as simulated with **LSDM (2002-2007, smoothed)**

55

Mean annual amplitudes of continental mass anomalies as observed by **GRACE (2002-2009)**

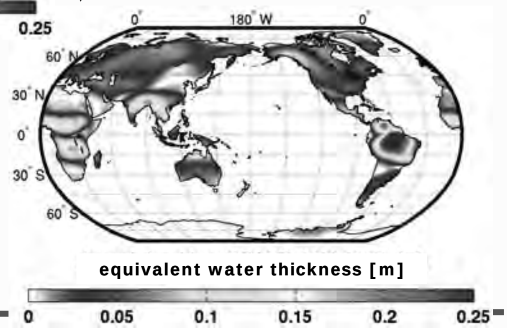

- currently:
  observation of hydrological mass redistributions
- future:
  removal of hydrological signals to assess secondary effects?

(Dill, GFZ)

Terrestrial water storage anomalies

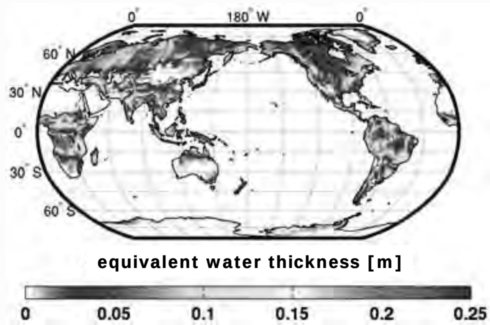

Mean annual amplitudes of hydro-logical mass anomalies as simulated with **LSDM (2002-2007, 0.5x0.5deg grid)**

56

Mean annual amplitudes of continental mass anomalies as observed by **GRACE (2002-2009)**

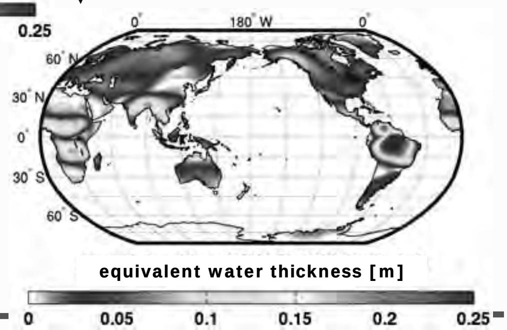

- currently:
  observation of hydrological mass redistributions
- future:
  removal of hydrological signals to assess secondary effects?

(Dill, GFZ)

Terrestrial water storage anomalies

Phase of mean annual hydrological mass signal as simulated with **LSDM**

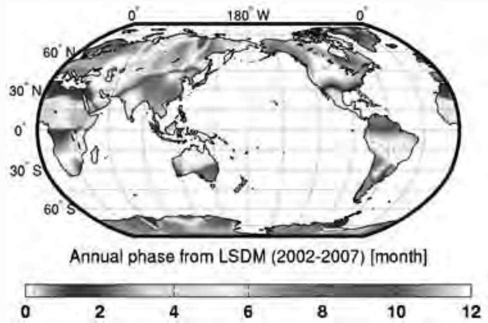

57

Phase of mean annual signal as observed by **GRACE**

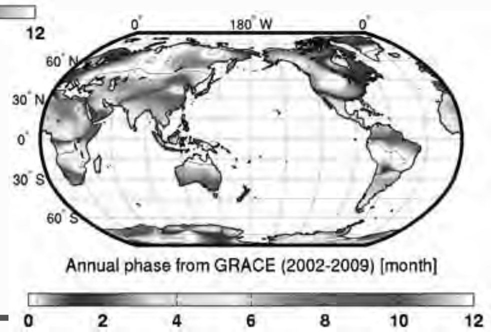

(Dill, GFZ)

Terrestrial water storage anomalies

Phase of mean annual hydrological mass signal as simulated with **LSDM**

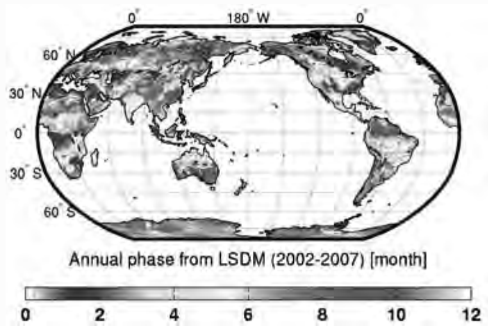

58

Phase of mean annual signal as observed by **GRACE**

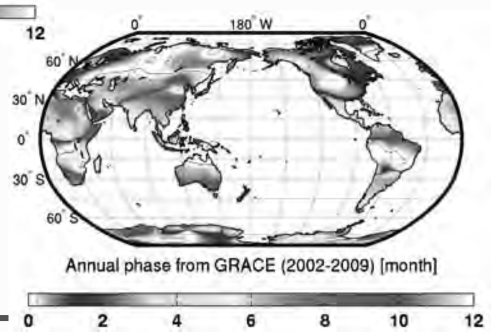

(Dill, GFZ)

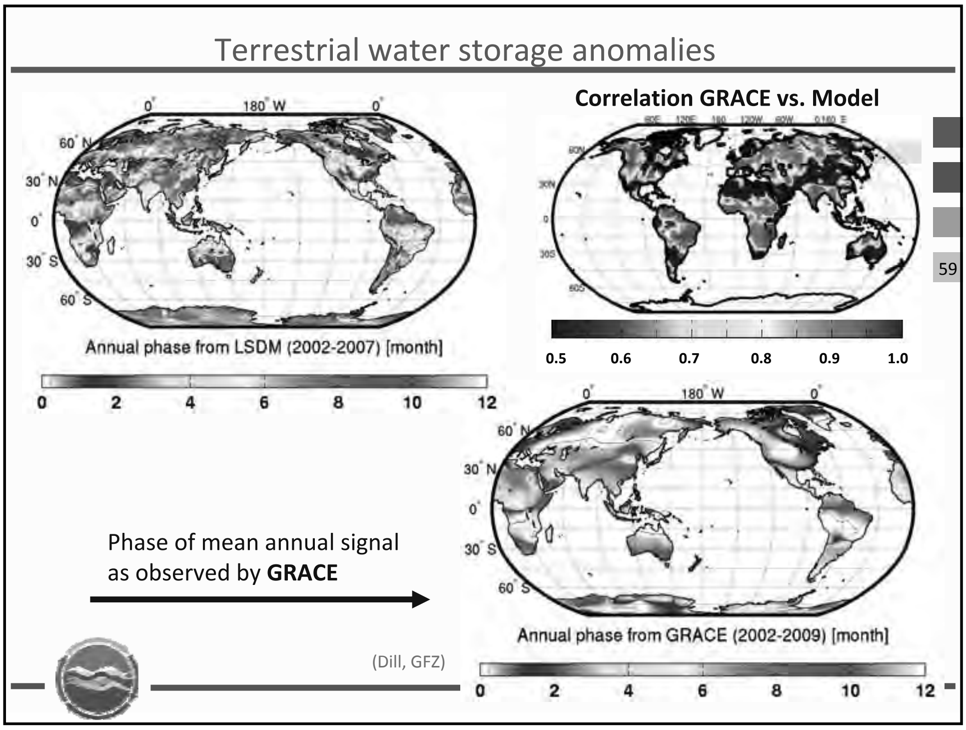
Terrestrial water storage anomalies
Correlation GRACE vs. Model
0.5 0.6 0.7 0.8 0.9 1.0
Annual phase from LSDM (2002-2007) [month]
0 2 4 6 8 10 12
Phase of mean annual signal
as observed by GRACE
Annual phase from GRACE (2002-2009) [month]
0 2 4 6 8 10 12
(Dill, GFZ)
59

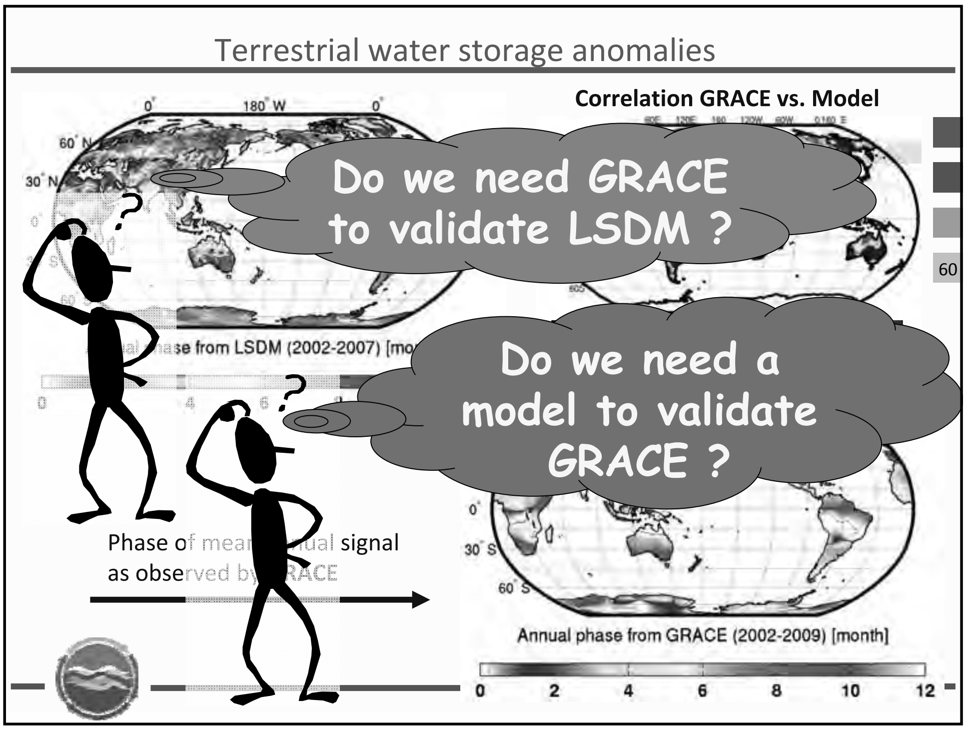
Terrestrial water storage anomalies
Correlation GRACE vs. Model
Do we need GRACE
to validate LSDM ?
Do we need a
model to validate
GRACE ?
Annual phase from GRACE (2002-2009) [month]
0 2 4 6 8 10 12
60

Variability of continental water masses

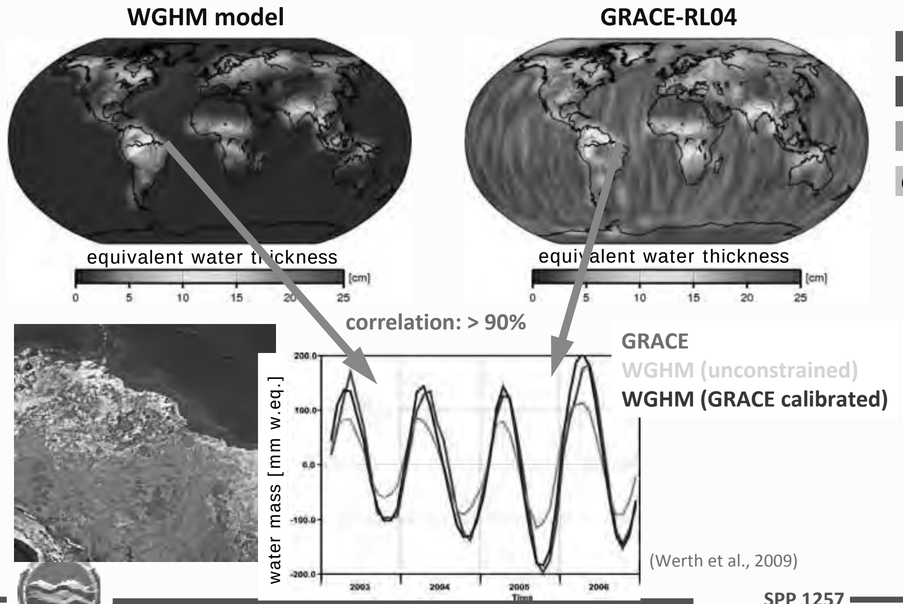

(Werth et al., 2009)

61

SPP 1257

Mass anomalies in the Arctic ocean due to continental freshwater fluxes

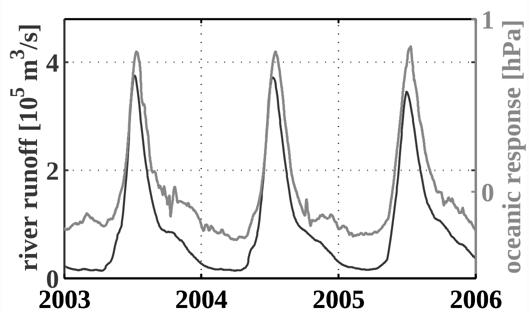

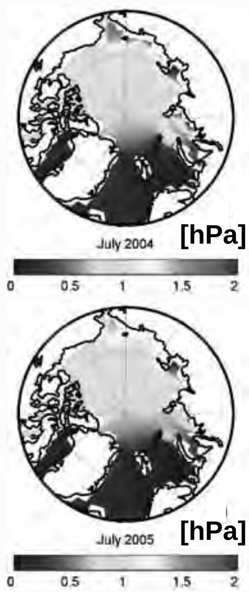

- dominant mass signal in July up to 2hPa
- probably detectable by GRACE

(Dobslaw & Thomas, 2007)

62

SPP 1257

Separation of mass change components

Model adjusted to GRACE data

Ice-mass change
➡ Sea-level contribution

GIA
➡ Earth's structure

63

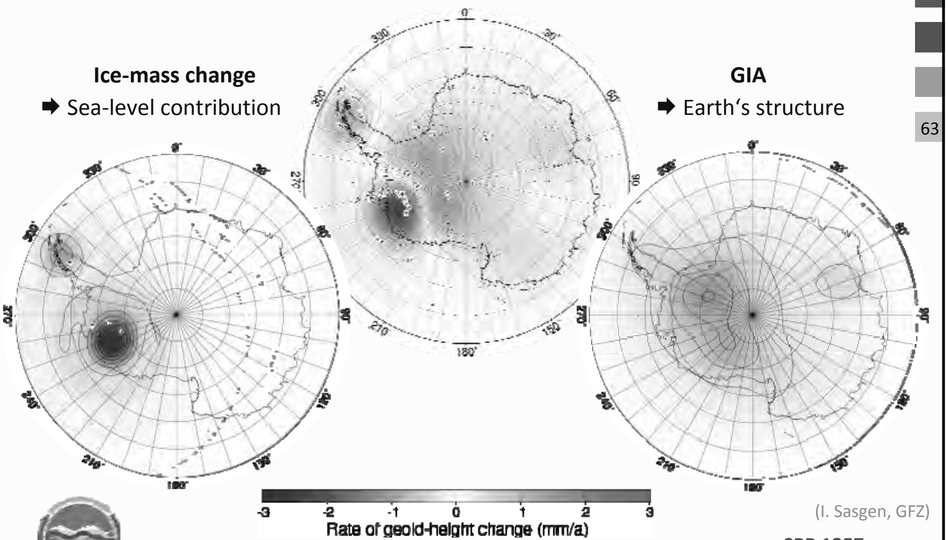

(I. Sasgen, GFZ)

SPP 1257

Ice-mass change: Rignot *et al.* 2008; GIA: Martinec (2000) and Huybrechts (2002)

Greenland ice mass change from 6yr GRACE

Spatial geoid height change

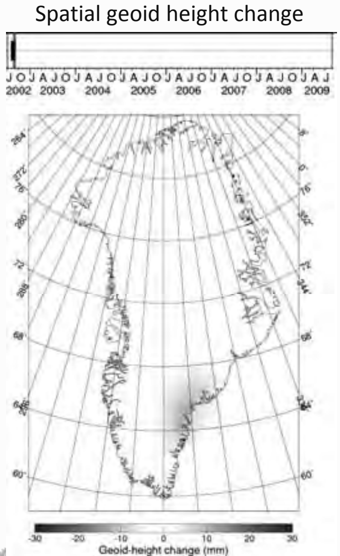

Ice mass change

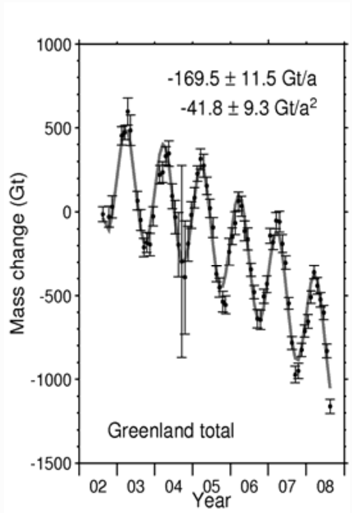

ca. 0.55mm contribution to global sea level change

64

GFZ RL04, August 2002 - August 2009, GIA corrected

(Sasgen *et al.*, GFZ)

SPP 1257

Greenland ice mass change from 6yr GRACE

Spatial geoid height change

Trend [mm/year]

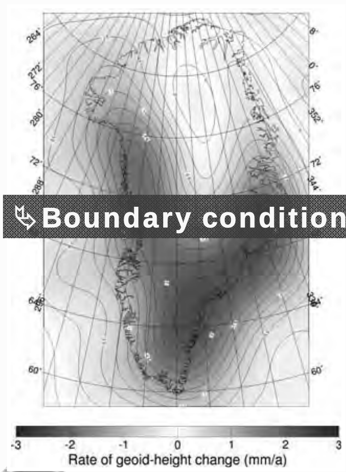

Ice mass change

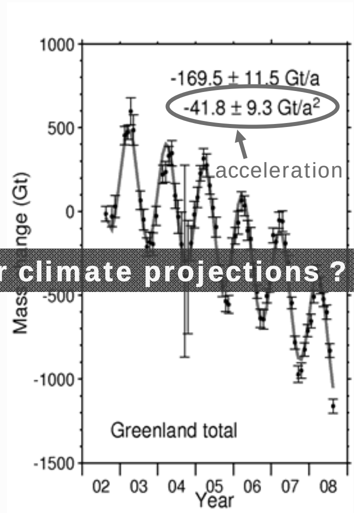

ca. 0.55mm contribution to global sea level change

65

↳ **Boundary conditions for climate projections ?**

GFZ RL04, August 2002 - August 2009, GIA corrected

(Sasgen *et al.*, GFZ)

Forward modelling of glaciation

Initialization phase (1958)

Observed heights of the ice sheet (Bamber et. al., 2001)

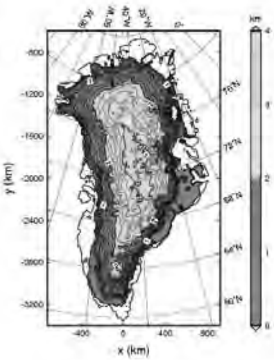

Height of the ice sheet after 250 kyr of palaeoclimatic simulation

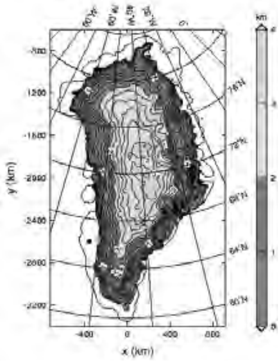

	Observed	Simulated
Volume (10^6 km^3)	2.9323	3.0251
Area (10^6 km^2)	1.6681	1.7969
Max. elevation (km)	3.2741	3.2826

(I. Rogozhina., GFZ)

Ocean mass variations

Annual changes in ocean mass from GRACE, GPS & ocean modelling

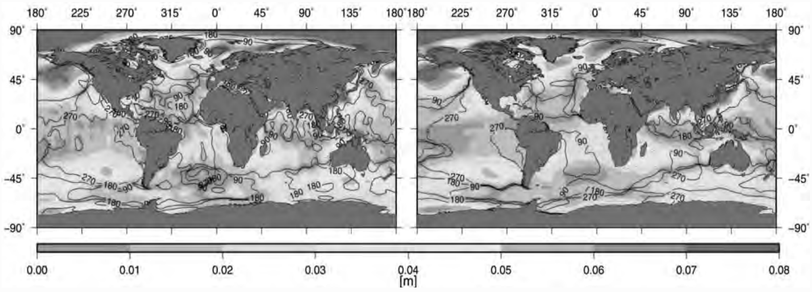

GRACE + GPS + FESOM **GPS + FESOM**

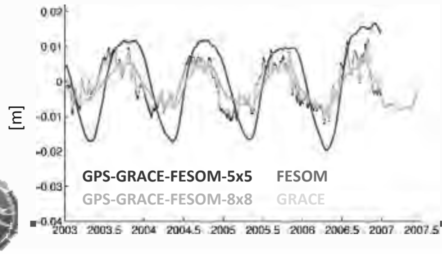

Mean sea level variations

Rietbroek et al., JGR (2009)

SPP 1257

67

Outline

I. Introduction

II. Impacts of sea level changes

III. Recent sea level changes

IV. Paleo records & reconstructions

V. Causes of sea level variations:

i) Loading

ii) Mass changes & the global hydrological cycle

iii) Volume changes & climate

VI. Projections

VII. Summary / Synthesis

SPP 1257

68

From sea surface heights to heat transports

total sea surface height anomalies

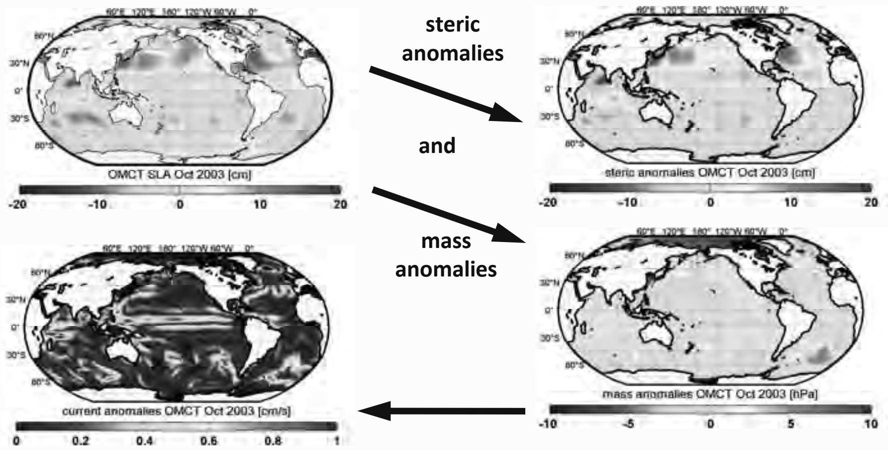

transformation to barotropic current anomalies associated with variations in oceanic heat transports

Temperature & salinity observations

ARGO float

www.poseidon.hcmr.gr

Distribution of ARGO floats (02/2011)

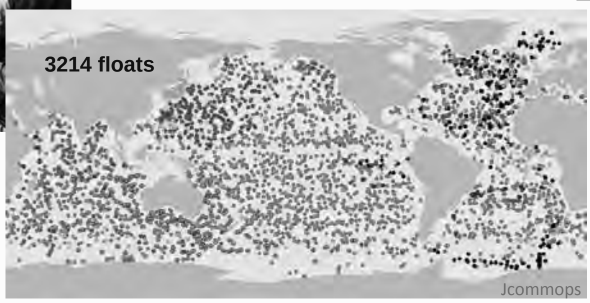

- **drifter with GNSS based positioning**
- **measurement of temperature & salinity up to ≈ 2000 m depth**

“GRACE = Altimetry - ARGO“

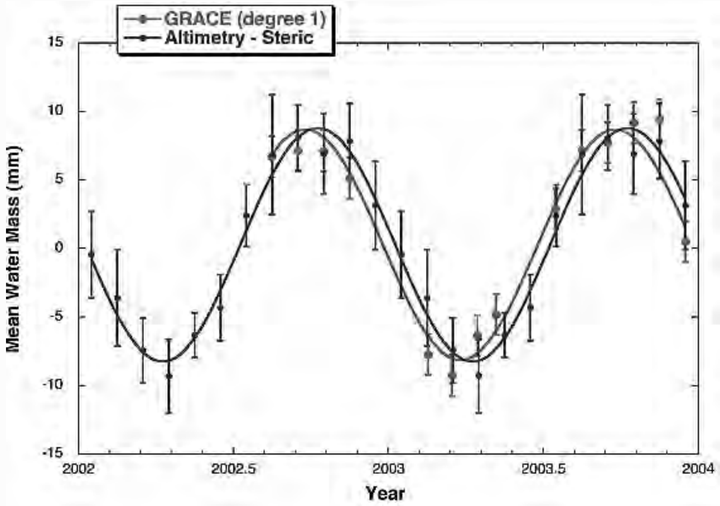

(Chambers et al., 2004, GRL)

71

Global mean surface temperature

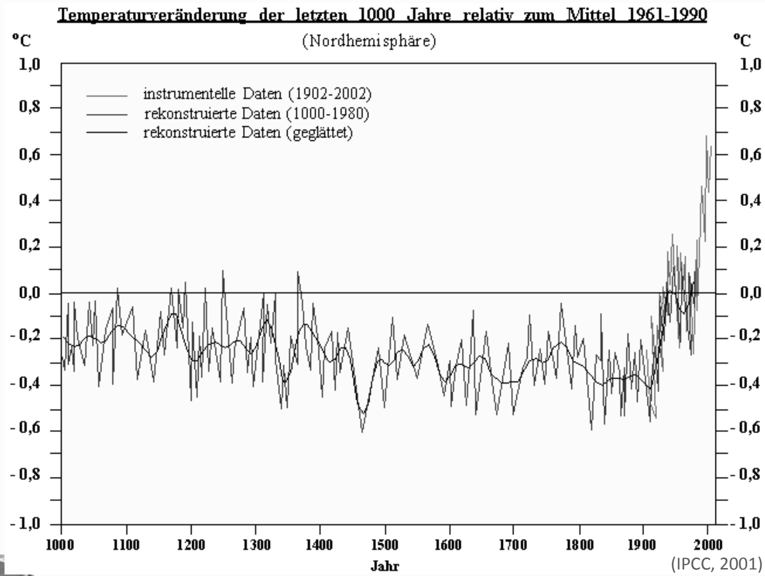

(IPCC, 2001)

72

Global mean surface temperature

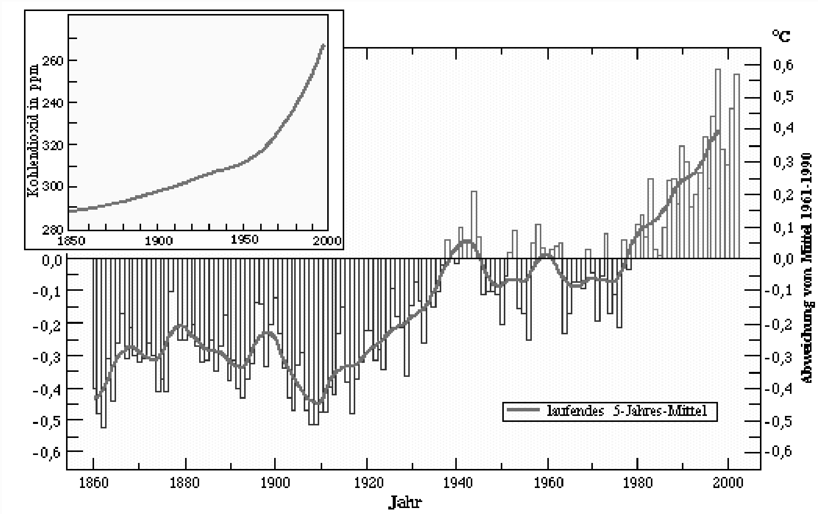

(IPCC, 2001)

SPP 1257

73

Change of surface temperatures

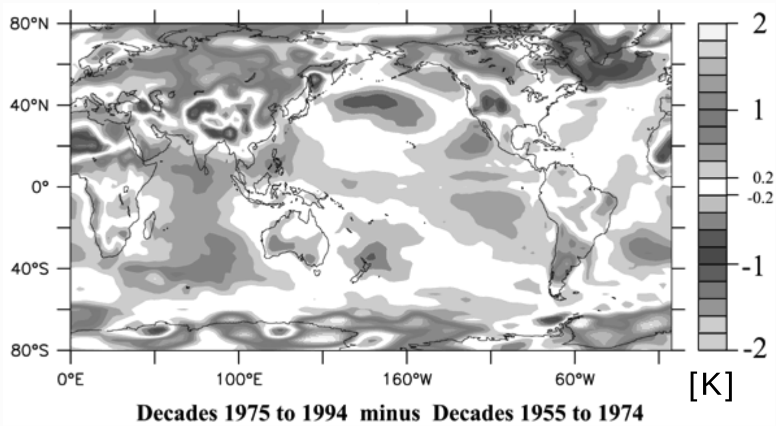

(NOAA)

SPP 1257

74

Mean surface heat fluxes

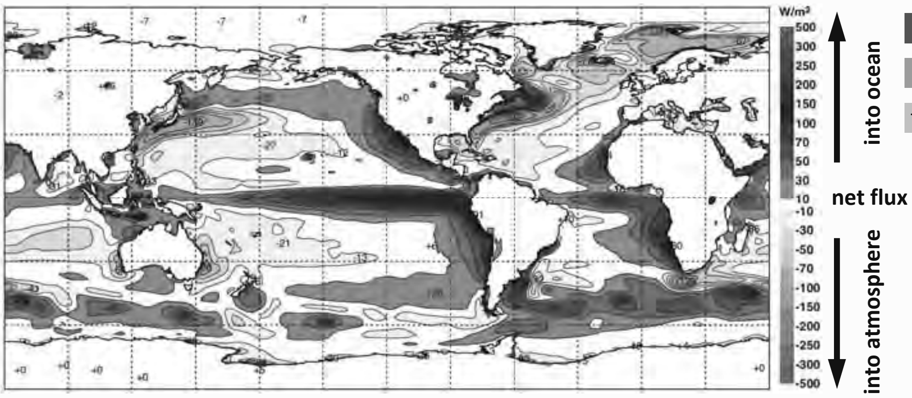

annual mean of net surface heat exchange [W/m²] from ERA-40 re-analyses

(Kallberg et al. 2005)

Oceanic heat content

heat content in [10^{22} J]

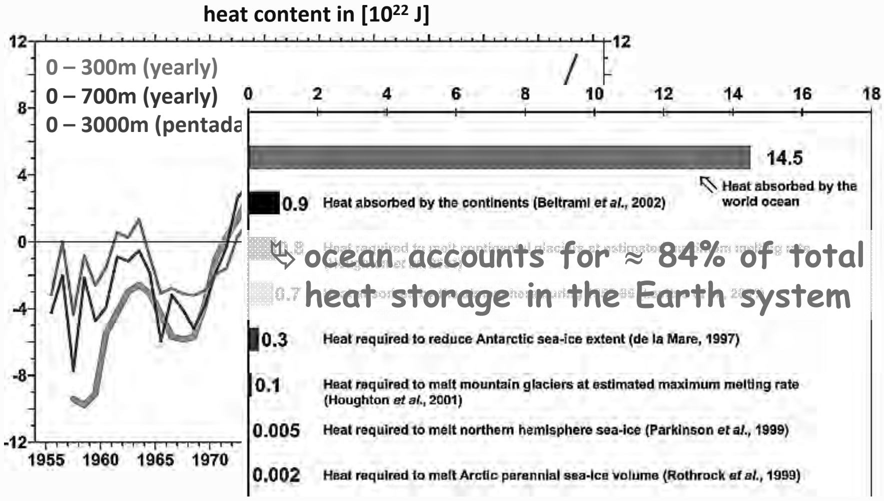

↳ ocean accounts for ≈ 84% of total heat storage in the Earth system

estimates of Earth's heat balance components [10^{22} J] (1955–1998)

(Levitus et al., 2005, GRL)

Thermosteric sea level anomalies [mm]

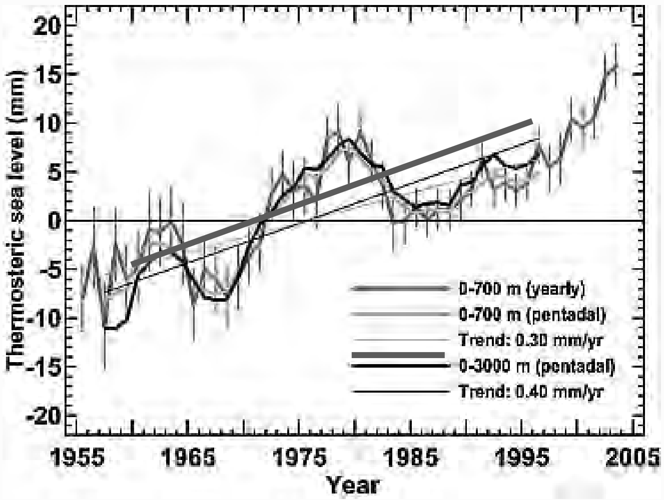

(Antonov et al., 2005, GRL)

Total vs. steric sea level variations ("trends" 2004 - 2007)

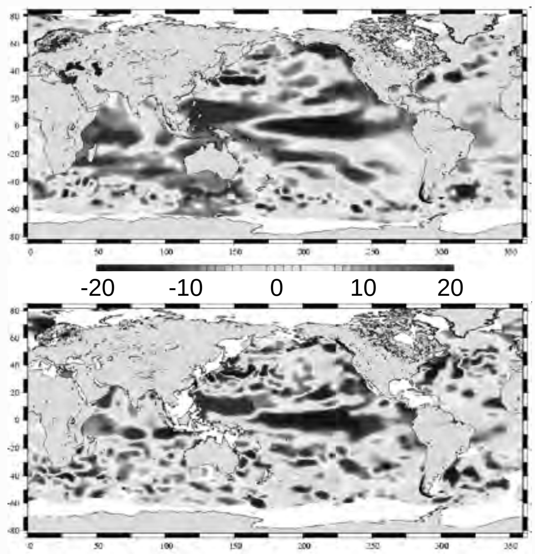

[mm/yr]

total sea level variations from altimetry

steric sea level variations from ARGO floats

(Cazenave et al., 2008)

Outline

I. Introduction

II. Impacts of sea level changes

III. Recent sea level changes

IV. Paleo records & reconstructions

V. Causes of sea level variations:
  - i) Loading
  - ii) Mass changes & the global hydrological cycle
  - iii) Volume changes & climate

VI. Projections

VII. Summary / Synthesis

79

SPP 1257

Climate projections (IPCC, 2007)

change of near-surface temperatures

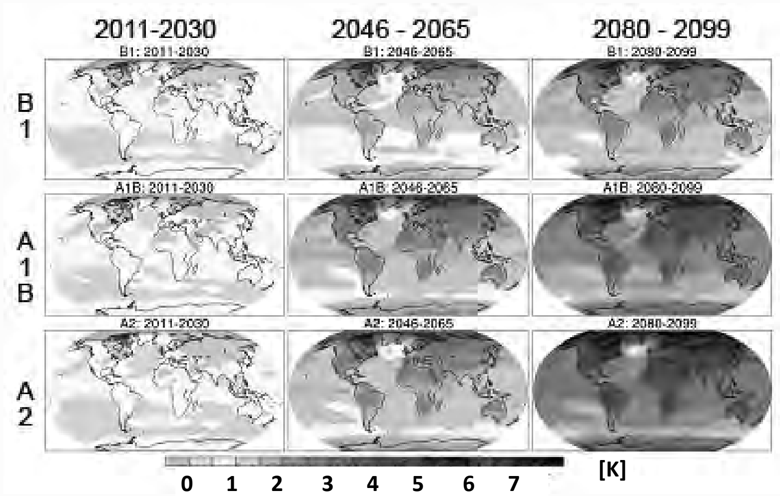

global environmental sustainability)

rapid economic growth (homogeneous world)

regionally oriented economic development (heterogeneous world)

80

SPP 1257

Sea level projections (IPCC, 2001)

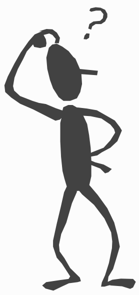

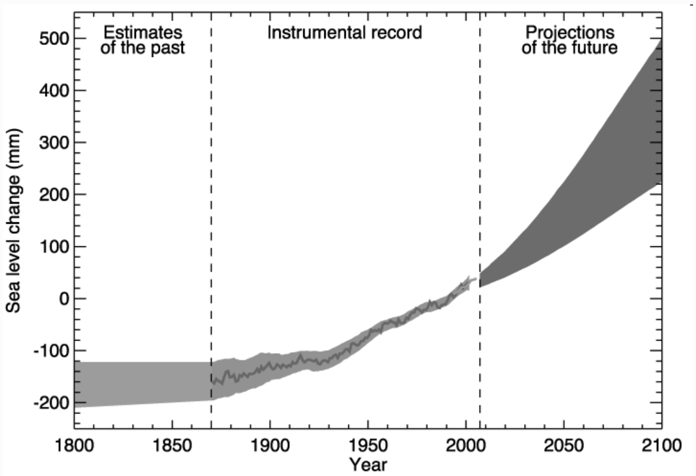

81

SPP 1257

Sea level projections (IPCC, 2001): Verification

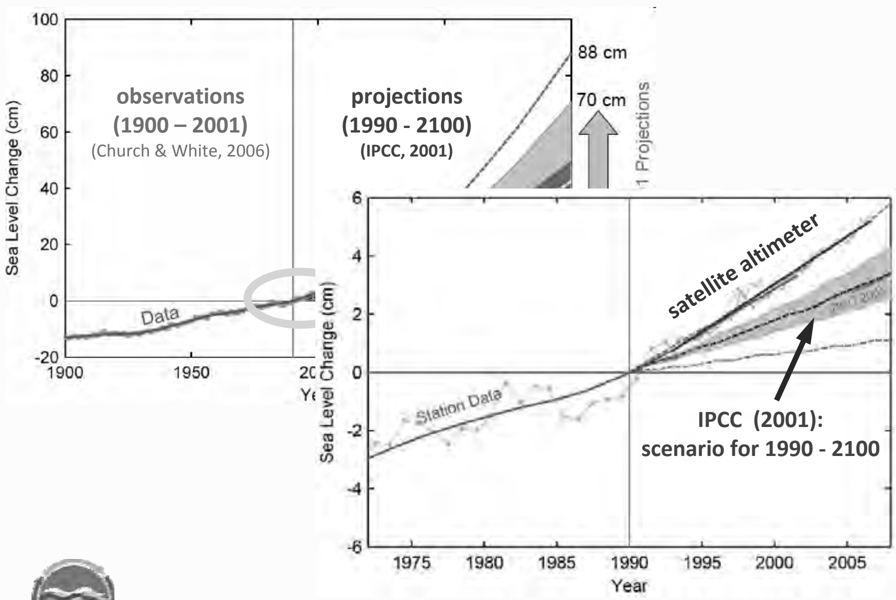

82

SPP 1257

(Church & White, 2006; Cazenave et al., 2008)

Sea level rise: predictions for 2100

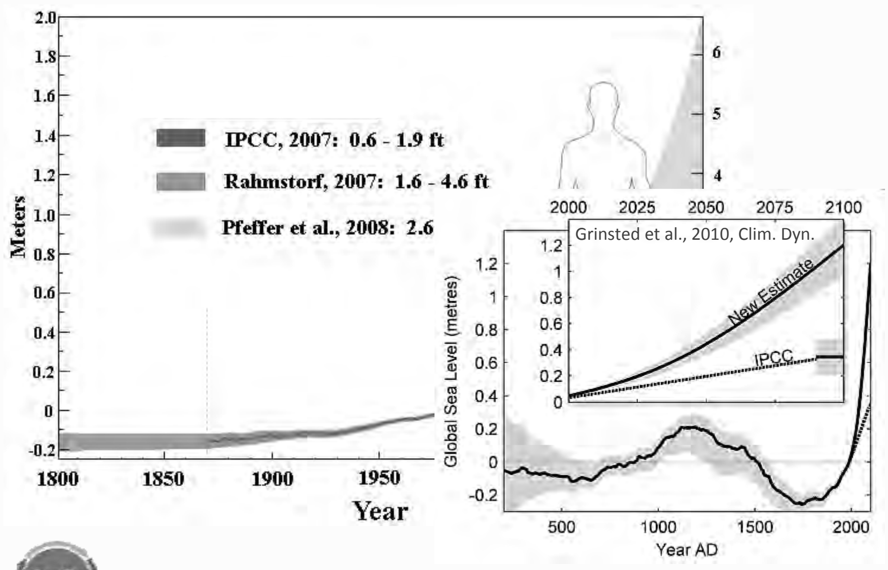

83

SPP 1257

Outline

84

SPP 1257

Contributions to sea level variations

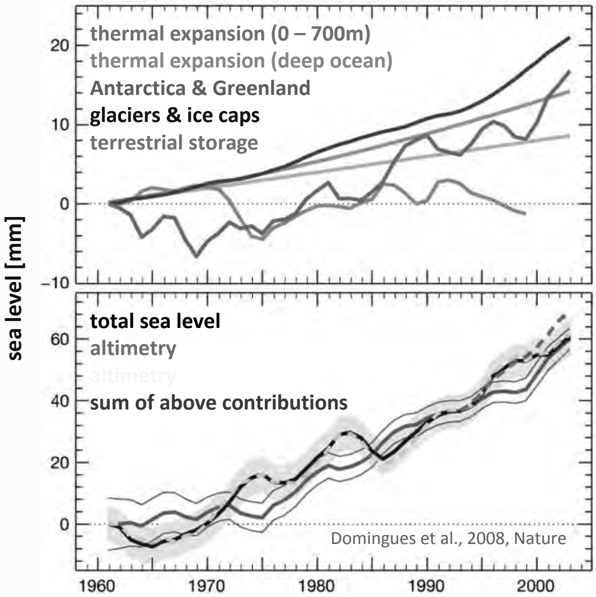

SPP 1257

85

Contributions to sea level trends (IPCC, 2007)

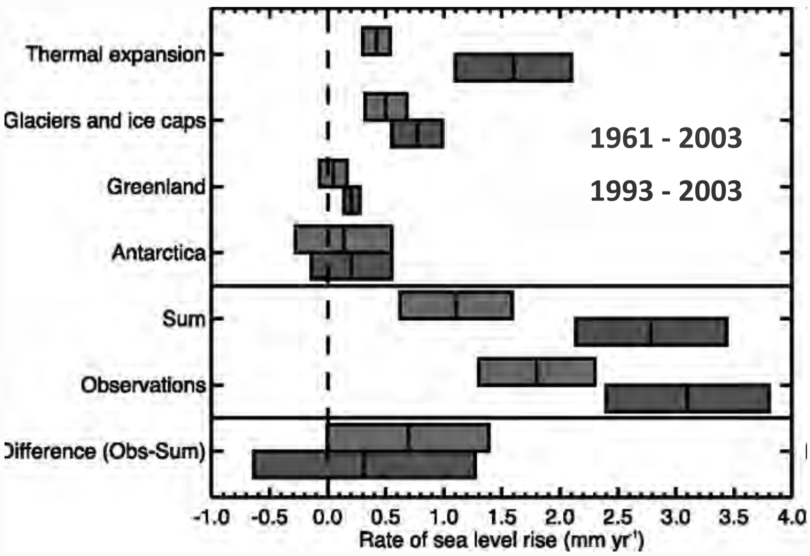

SPP 1257

86

Contributions to sea level trends (IPCC, 2007)

87

	Sea Level Rise [mm/yr]	
Source	**1961–2003**	**1993–2003**
Thermal Expansion	0.42 ± 0.12	1.6 ± 0.5
Glaciers and Ice Caps	0.50 ± 0.18	0.77 ± 0.22
Greenland Ice Sheet	0.05 ± 0.12	0.21 ± 0.07
Antarctic Ice Sheet	0.14 ± 0.41	0.21 ± 0.35
Sum	1.1 ± 0.5	2.8 ± 0.7
Observed	1.8 ± 0.5	3.1 ± 0.7
Difference (Observed –Sum)	0.7 ± 0.7	0.3 ± 1.0

SPP 1257

Future sea level rise

88

SPP 1257


Vielen Dank !

Summer School "Global Water Cycle"

12.-16. September 2011, Mayschoss

DFG Priority Programme SPP1257:
Mass transport and mass distribution in the Earth's system

Torsten Mayer-Guerr, Mail: mayer-guerr@tugraz.at
Frank Flechtner, Mail: flechtne@gfz-potsdam.de

Practical: Spherical Harmonics Synthesis

Purpose of the practical: The level-2 GRACE products are generally given as gravitational potential in terms of spherical harmonics. In this practical, different filtered gravity field functionals (e.g. total water storage, gravity disturbances) should be computed from these products as gridded data on the Earth's surface.

Directories: The required data sets can be found on the USB stick in the directory *practicals/data/pract1_sphericalHarmonics*. The provided matlab functions are located under *practicals/functions/pract1_sphericalHarmonics*.

Exercise 1: Spherical Harmonics Synthesis

- Load the potential coefficient files *ITG-Grace2010_2008-03.gfc* and *ITG-Grace2010_2008-09.gfc* using the function `readPotentialCoefficients`.
- Compute the difference between the coefficients of the monthly solutions.
- Filter the result with a gaussian filter ($R = 500\,\mathrm{km}$) using the filter coefficients computed by the function `filterCoefficientsGauss`.
- Compute gravity disturbance (in spherical approximation) on a $1^\circ \times 1^\circ$ geographical grid:

$$\delta g(\lambda, \theta) = \frac{GM}{R^2} \sum_{n=0}^{\infty} (n+1) \sum_{m=0}^{n} \bar{P}_{nm}(\cos\theta) \left(\bar{C}_{nm}\cos(m\lambda) + \bar{S}_{nm}\sin(m\lambda)\right) \tag{1}$$

  The Legendre functions $\bar{P}_{nm}$ can be computed by the function `legendreFunctions`.

- Visualize the result with `showGrid`.

Exercise 2 (optional): Spherical Harmonics Synthesis (different functionals)

- Transfer the computation of gravity disturbances into a function as defined at the end of this paper.

- Implement a function to compute geoid variations (in spherical approximation)

$$\Delta N(\lambda, \theta) = R \sum_{n=0}^{\infty} \sum_{m=0}^{n} \bar{P}_{nm}(\cos\theta) \left(\Delta\bar{C}_{nm}\cos(m\lambda) + \Delta\bar{S}_{nm}\sin(m\lambda)\right). \tag{2}$$

- Implement a function to compute total water storage change (common approximation)

$$\Delta TWS(\lambda, \theta) = \frac{\rho_e R}{3} \sum_{n=0}^{\infty} \frac{2n+1}{1+k'_n} \sum_{m=0}^{n} \bar{P}_{nm}(\cos\theta) \left(\Delta\bar{C}_{nm}\cos(m\lambda) + \Delta\bar{S}_{nm}\sin(m\lambda)\right), \tag{3}$$

  with the mean density of the Earth $\rho_e = 5540\,\mathrm{kg/m^3}$. The load love numbers k'_n are given in the file *loadLove.mat*.

Matlab functions:

function [cnm, snm, GM, R]=readPotentialCoefficients(filename)	
Read potential coefficients from file.	
Input	• `filename`: file of potential coefficients in ICGEM format (*.gfc).
Output	• `cnm,snm`: matricies containing the potential coefficients. The dimensions are $(n+1)\times(n+1)$ with n = maxDegree. The lower triangular matrix elements $cnm(n+1, m+1)$ and $snm(n+1, m+1)$ contain the potential coefficients of degree n and order m. • `GM`: Earth gravity constant. • `R`: Earth reference radius.

function Pnm = legendreFunctions(theta, maxDegree)	
Calculation of all Legendre Functions (4π-normalized) up to given degree and order at a specific co-latitude.	
Input	• `theta`: co-latitude in radians. • `maxDegree`: maximum degree and order to compute.
Output	• `Pnm`: matrix containing the 4π-normalized Legendre functions. The dimension is $(n+1)\times(n+1)$ with n = maxDegree. The lower triangular matrix element $Pnm(n+1, m+1)$ contains the Legendre function of degree n and order m.

function wn = filterCoefficientsGaussian(radius, maxDegree)	
Filter coefficients in the spectral domain of a Gaussian filter.	
Input	• `radius`: half-with radius parameter in km. • `maxDegree`: maximum degree to compute.
Output	• `wn`: $(n+1)\times 1$ vector with n = maxDegree. The vector element $wn(n+1)$ contains the filter coefficient of degree n.

function showGrid(lambda, theta, grid, title)	
Plot gridded data on Earth's surface. To plot the coast lines, the file *coast.dat* must be in the working directory.	
Input	• `lambda`: $p\times 1$ vector containing the longitudes (in radians). • `theta`: $q\times 1$ vector containing the co-latitudes (in radians). • `dg`: $q\times p$ matrix containing the gridded values. • `title`: the title text of the figure.
Output	•

Matlab to implement in this exercise:

function dg = gravityDisturbance(lambda, theta, cnm, snm, GM, R)	
Calculate gravity disturbances as gridded data defined by the vectors `lambda` and `theta`.	
Input	• `lambda`: $p \times 1$ vector containing the longitudes (in radians). • `theta`: $q \times 1$ vector containing the co-latitudes (in radians). • `cnm,snm`: matricies containing the potential coefficients • `GM`: Earth gravity constant. • `R`: Earth reference radius.
Output	• `dg`: $q \times p$ matrix containing the gridded gravity anomalies.

function dN = geoid(lambda, theta, cnm, snm, GM, R)	
Calculate geoid changes as gridded data defined by the vectors `lambda` and `theta` in spherical approximation	
Input	• `lambda`: $p \times 1$ vector containing the longitudes (in radians). • `theta`: $q \times 1$ vector containing the co-latitudes (in radians). • `cnm,snm`: matricies containing the potential coefficients • `GM`: Earth gravity constant. • `R`: Earth reference radius.
Output	• `dN`: $q \times p$ matrix containing the gridded geoid variations.

function tws = totalWaterStorage(lambda, theta, cnm, snm, GM, R)	
Calculate total water storage changes as gridded data defined by the vectors `lambda` and `theta` in spherical approximation. The file *loadLove.mat* must be in the working directory.	
Input	• `lambda`: $p \times 1$ vector containing the longitudes (in radians). • `theta`: $q \times 1$ vector containing the co-latitudes (in radians). • `cnm,snm`: matricies containing the potential coefficients • `GM`: Earth gravity constant. • `R`: Earth reference radius.
Output	• `tws`: $q \times p$ matrix containing the total water storage.

Summer School "Global Water Cycle"

12.-16. September 2011, Mayschoss

DFG Priority Programme SPP1257:
Mass transport and mass distribution in the Earth's system

Annette Eicker, Mail: eicker@geod.uni-bonn.de

Practical: Analysis Tools

Purpose of the practical: In the practical "Analysis Tools" the method of "Principal Component Analysis" (PCA) will be applied to time series of GRACE data and to hydrological model output provided by the WaterGAP Hydrology Model (WGHM). PCA is used to extract individual dominant *modes* of the data variability, while simultaneously suppressing those modes connected with low variability and therefore reducing the dimension of data efficiently. The given time-space data field (e.g. monthly data given on a geographical grid) is separated into spatial structures called *empirical orthogonal functions* (EOF) and their amplitudes in time, called *principle components* (PCs).

Additional material: Lecture Notes "Analysis Tools" by Jürgen Kusche, Annette Eicker and Ehsan Forootan

Directories: The Data sets needed for this practical can be found on the USB stick in the directories *practicals/data/generic* and *practicals/data/pract2_analysisTools*. The provided matlab functions can be found in the directory *practicals/functions/pract2_analysisTools*.

Exercise 1: Calculation and visualization of EOFs and PCs

- Load the files *wghm_filtered.mat* and *grace_filtered.mat*. Each file contains a monthly time series of filtered gridded values (Gauss filter with 400km radius, years 2005-2008) on a $1° \times 1°$ geographical grid stored in the data matrix $\mathbf{Y}$. The data sets are centered, i.e. they have zero mean. The gridded values of one month are sorted into one column of the matrix. Thus $\mathbf{Y}$ has the dimensions $n \times p$ with n = number of grid points and p = number of points in time. Furthermore, the files each contain two vectors with the dimensions $n \times 1$, containing the longitude values of the grid points (`lon`) and the latitude values of the grid points (`lat`).

- Calculate the spatial patterns (EOFs) from the WGHM data set using the function `calculateEOF`. These patterns serve as basis functions for further calculations.

- Visualize the spatial patterns for the first three modes using the function `showEOF`.

- Calculate the temporal evolution (PCs) of the above calculated basis functions both from the GRACE and the WGHM data using the function `calculatePC`.

- Visualize the temporal evolution for the first three modes, both for GRACE and WGHM using the function `showPC`.

- Compare the results for GRACE and WGHM.

Exercise 2: Understanding compression properties of PCA

- Visualize the eigenvalues calculated in Exercise 1. You can use the function `showEigenvalues` for an easy visualization.
- How many modes are needed to reconstruct 80% and 95% of the WGHM variability? Calculate the fraction of the signal variability reconstructed by $\bar{p}$ modes according to

$$var_{\bar{p}} = \frac{\sum_{j=1}^{\bar{p}} \lambda_j}{\Delta^2} \qquad \text{with the total variance} \qquad \Delta^2 = \sum_{j=1}^{p} \lambda_j. \tag{1}$$

- From a given matrix $\mathbf{E}$ containing the EOFs in its columns and a matrix $\mathbf{D}$ containing the PCs in its rows, the signal matrix $\mathbf{Y}$ can be reconstructed by

$$\mathbf{Y} = \mathbf{ED}. \tag{2}$$

  Use the calculated PCA from the global WGHM time series to reconstruct 80% and 95% of the variability.
- Plot the reconstructed signal (80%, 95%) and the original signal and the difference between both using the function `showData` for one arbitrary month (e.g. 2005-05).

Exercise 3 (optional): Understanding domain dependence of PCA

- Use the global WGHM time series.
- Cut out the data in the Amazon region and in the Orinoco region. You can use the function `inpolygon` provided by matlab. The boundary polygons for the two regions are provided by the files `amazon.mat` and `orinoco.mat`. Each file contains a matrix with two columns, the first column consisting of the longitude values of the polygon points, the second column containing the latitude values.
- Visualize only the first EOF and PC. Here you can use the function `showEOFlocal`.
- How many modes would be necessary to reconstruct 95% of the signal?
- Compare the two regional results and the global results (from Exercise 1 and 2) and discuss.

Matlab functions:

function [eigenvalues, E] = calculateEOF(Y)	
Calculation of EOFs from a given data matrix $\mathbf{Y}$. The function calculates the p eigenvectors (=EOFs) corresponding to the p non-zero eigenvalues of the covariance matrix $\mathbf{C} = \mathbf{Y}\mathbf{Y}^T$. To reduce the computation effort, the eigenvalue problem is in a first step solved for the smaller matrix $\mathbf{C}' = \mathbf{Y}^T\mathbf{Y}$, which has the same eigenvalues. The eigenvectors of the larger matrix can then be calculated from the eigenvectors of the smaller matrix. The eigenvalues are stored in the vector `eigenvalues` sorted according to their magnitude, the eigenvectors are returned in the matrix $\mathbf{E}$.	
Input	• `Y`: matrix containing the time series of gridded data sets. The dimension is $n \times p$ with $n =$ number of grid points and $p =$ number of points in time.
Output	• `eigenvalues`: $p \times 1$ vector containing the p non-zero eigenvalues of the covariance matrix $\mathbf{C}$, sorted according to decreasing size • `E`: $n \times p$ matrix containing in its columns the eigenvectors (EOFs) of the covariance matrix $\mathbf{C}$. EOFs are sorted according to size of corresponding eigenvalue.

function [D] = calculatePC(E, Y)	
Calculation of principle components (PCs) by projecting the original data onto the basis of the EOFs. The PCs are stored in the rows of the matrix $\mathbf{D}$	
Input	• `Y`: matrix containing the time series of gridded data sets. The dimension is $n \times p$ with $n =$ number of grid points and $p =$ number of points in time • `E`: $n \times p$ matrix containing in its columns the eigenvectors (EOFs) of the covariance matrix $\mathbf{C}$. EOFs are sorted according to size of corresponding eigenvalues.
Output	• `D`: $p \times p$ matrix containing the principle components in its rows.

Functions for visualization:

function showEigenvalues (Eigenvalues)	
Visualization of the evolution of the eigenvalues	
Input	• `Eigenvalues`: vector of eigenvalues
Output	• Plot of the eigenvalues

function showEOF (EOF,longitude,latitude,i,titleString)	
Visualization of the spatial pattern of one specific EOF with the index i.	
Input	• `EOF`: $n \times 1$ vector containing the gridded values of the one EOF to be plotted. E.g. one column of the matrix $\mathbf{E}$. • `longitude`: $n \times 1$ vector containing the longitude values of the grid points • `latitude`: $n \times 1$ vector containing the latitude values of the grid points • `i`: index of the EOF to be visualized (EOFs are sorted according to size of eigenvalue), needed for title of the plot • `titleString`: a string describing the data source (e.g. "WGHM"), used for the title of the plot.
Output	• Plot of the spatial pattern

function showEOFlocal (EOF,longitude,latitude,border, i,titleString)	
Visualization of the spatial pattern of one specific EOF with the index i on a spatial domain limited by the polygon `border`. The dimension n refers to the number of grid points within the polygon.	
Input	• `EOF`: $n \times 1$ vector containing the gridded values of the one EOF to be plotted. E.g. one column of the matrix $\mathbf{E}$. • `longitude`: $n \times 1$ vector containing the longitude values of the grid points • `latitude`: $n \times 1$ vector containing the latitude values of the grid points • `border`: matrix which contains the polygon around the regional area (e.g. Amazon). The first column consists of the longitude values of the polygon points, the second column contains the latitude values. • `i`: number of the EOF to be visualized (EOFs are sorted according to size of eigenvalue), needed for title of the plot • `titleString`: A string describing the data source (e.g. "WGHM"), used for the title of the plot.
Output	• Plot of the spatial pattern for a regional area

function showPC (PC,i,titleString)	
Visualization of the principle component with the index i.	
Input	• `PCs`: $1 \times p$ vector containing the principle component which shall be visualized. E.g. the i-th row of the matrix $\mathbf{D}$. • `i`: number of the PC to be visualized (sorted according to the size of the eigenvalues), needed for title of the plot • `titleString`: A string describing the data source (e.g. "WGHM" or "GRACE"), used for the title of the plot.
Output	• Plot of the principle component.

function showData(data,longitude,latitude)	
Visualization of (global) gridded data sets. All gridded values are given in a column vector **data**. The longitude and latitude values corresponding to the grid values are given in the vectors **longitude** and **latitude**	
Input	• `data`: $n \times 1$ vector containing the data values, e.g. one column of the data matrix $\mathbf{Y}$. • `longitude`: $n \times 1$ vector containing the longitude values of the grid points • `latitude`: $n \times 1$ vector containing the latitude values of the grid points
Output	• 2D-plot of the gridded values

Practical: Analysis Tools

1

Annette Eicker

Summer School „Global Water Cycle“
12.-16. September 2011
Mayschoss

DFG SPP 1257

Solutions

Download solutions to practical exercises:

ftp://skylab.itg.uni-bonn.de/summerschoolDownload/solutions/

2

DFG SPP 1257

Practical: Analysis Tools

3

Goal:
Understanding the method of Principal Component Analysis (PCA)

Application of PCA to gridded data sets of **GRACE** solutions and hydrological model output (**WGHM**), both given as equivalent water height, zero mean

Monthly solutions, time span: 01/2005 – 12/2008, Gauß filter: 400km

SPP 1257

Part II: Principle component analysis and related ideas

4

What do we get from PCA?

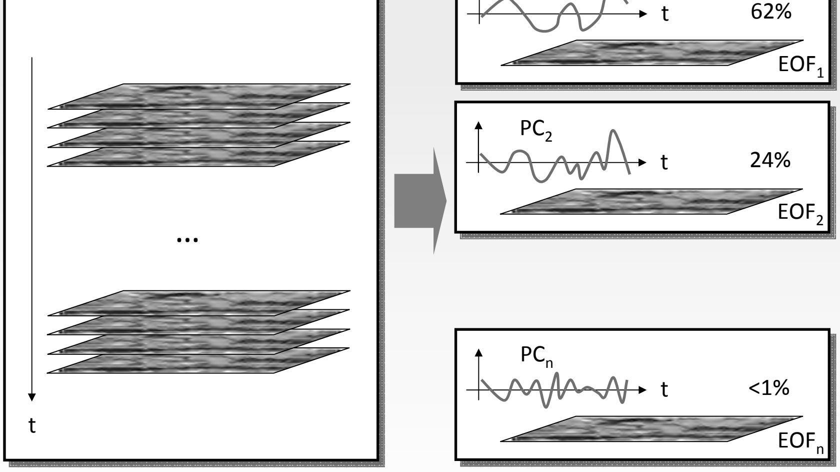

SPP 1257

Data matrix

Time series provided as data matrix:

time series for one location

$$\mathbf{Y} = (\mathbf{y}_1, \mathbf{y}_2, \ldots, \mathbf{y}_p) = \begin{pmatrix} y_{1;1} & y_{1;2} & \cdots & y_{1;p} \\ y_{2;1} & y_{2;2} & \cdots & y_{2;p} \\ \vdots & \vdots & & \vdots \\ y_{n;1} & y_{n;2} & \cdots & y_{n;p} \end{pmatrix}_{n \times p}$$

Ygrace, Ywghm

\# points in time
e.g. 48 months

\# locations
e.g. 64.000 grid points

gridded data for one point in time,
e.g. one monthly solution

⇨ ***grace_filtered.mat, wghm_filtered.mat***

DFG SPP 1257

5

Eigenvalue decomposition

Calculation of the temporal covariance matrix:

$$\mathbf{C} = \frac{1}{p}\mathbf{Y}\mathbf{Y}^T = \frac{1}{p}\begin{pmatrix} \sum_{i=1}^p y_{1;i}^2 & \sum_{i=1}^p y_{1;i}y_{2;i} & \cdots \sum_{i=1}^p y_{1;i}y_{n;i} \\ \sum_{i=1}^p y_{2;i}y_{1;i} & \sum_{i=1}^p y_{2;i}^2 & \cdots \sum_{i=1}^p y_{2;i}y_{n;i} \\ \vdots & \vdots & \vdots \\ \sum_{i=1}^p y_{n;i}y_{1;i} & \sum_{i=1}^p y_{n;i}y_{2;i} & \cdots \sum_{i=1}^p y_{n;i}^2 \end{pmatrix}_{n \times n}$$

Eigenvalue decomposition of the covariance matrix:

eigenvalues

$$\mathbf{C} = \mathbf{E}\Lambda\mathbf{E}^T = \begin{pmatrix} \mathbf{e}_1 & \mathbf{e}_2 & \ldots & \mathbf{e}_n \end{pmatrix} \begin{pmatrix} \lambda_1 & 0 & \cdots & 0 \\ 0 & \lambda_2 & & \vdots \\ \vdots & & \ddots & 0 \\ 0 & \cdots & 0 & \lambda_n \end{pmatrix} \begin{pmatrix} \mathbf{e}_1^T \\ \mathbf{e}_2^T \\ \vdots \\ \mathbf{e}_n^T \end{pmatrix}$$

eigenvectors

DFG SPP 1257

6

Eigenvalue decomposition

Calculation of the spatial covariance matrix:

$$\mathbf{C}' = \frac{1}{n}\mathbf{Y}^T\mathbf{Y} = \frac{1}{n}\begin{pmatrix} \sum_{j=1}^{n} y_{j;1}^2 & \sum_{j=1}^{n} y_{j;1}y_{j;2} & \dots \sum_{j=1}^{n} y_{j;1}y_{j;p} \\ \sum_{j=1}^{n} y_{j;2}y_{j;1} & \sum_{j=1}^{n} y_{j;2}^2 & \dots \sum_{j=1}^{n} y_{j;2}y_{j;p} \\ \vdots & \vdots & \vdots \\ \sum_{j=1}^{n} y_{j;p}y_{j;1} & \sum_{j=1}^{n} y_{j;p}y_{j;2} & \dots \sum_{j=1}^{n} y_{j;p}^2 \end{pmatrix}_{p \times p}$$

7

The matrices **C** and **C**‘ have the same p non-zero eigenvalues.

The p corresponding eigenvectors $\mathbf{e}_i$ of C can be calculated from eigenvectors of C‘.

Matrix containing the EOFs: (normalized)

$$\mathbf{E} = \begin{pmatrix} \mathbf{e}_1 & \mathbf{e}_2 & \dots & \mathbf{e}_p \end{pmatrix}_{n \times p}$$

basis functions from WGHM

Sorted according to size of eigenvalues:

$$\lambda_1 > \lambda_2 > \dots > \lambda_p$$

⇨ ***function [eigenvalues, E] = calculateEOF(Y)***

DFG SPP 1257

Principle components

Eigenvectors (= EOFs) constitute a new orthogonal basis.
PCs are calculated by projecting the data onto the new basis:

$$\mathbf{D} = \mathbf{E}^T\mathbf{Y}$$

$$\mathbf{D} = \begin{pmatrix} \boxed{d_{1;1}} & d_{1;2} & \cdots & d_{1;p} \\ d_{2;1} & d_{2;2} & & \\ \vdots & & \ddots & \\ d_{p;1} & & & d_{p;p} \end{pmatrix}_{p \times p}$$

PC_j = temporal evolution of j-th EOF

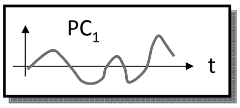

$\mathbf{d}_i$ scaling factors for in time i

8

⇨ ***function [D] = calculatePC(E,Y)***

Signal reconstruction:

$$\mathbf{Y} = \mathbf{ED}$$

DFG SPP 1257

Signal reconstruction

Signal reconstruction:

$$\mathbf{Y} = \mathbf{E}\mathbf{D}$$

Compression: using only the first $\overline{p}$ „major“ EOFs and PCs for the reconstruction as they contain most of the variability

9

Signal variability using $\overline{p}$ EOFs:

$$\mathrm{var} = \frac{\sum_{j=1}^{\overline{p}} \lambda_j}{\Delta^2} \quad \text{with} \quad \Delta^2 = \sum_{j=1}^{p} \lambda_j$$

(total variance)

Practical 2

Exercise 1: Calculation and visualization of EOFs and PCs

- calculate EOFs from WGHM
- calculate corresponding PCs from WGHM and GRACE

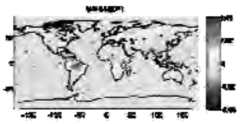

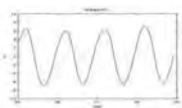

10

Exercise 2: Compression properties

- reconstruct 80% or 95% of the data

Exercise 3 (optional): Domain dependence

- repeat Exercise 1 & 2 for two individual river basins

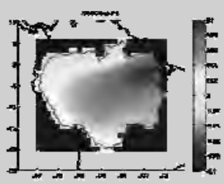

Results

11

DFG SPP 1257

Exercise 1

Calculation and visualization of EOFs and PCs

12

DFG SPP 1257

PCA: WGHM

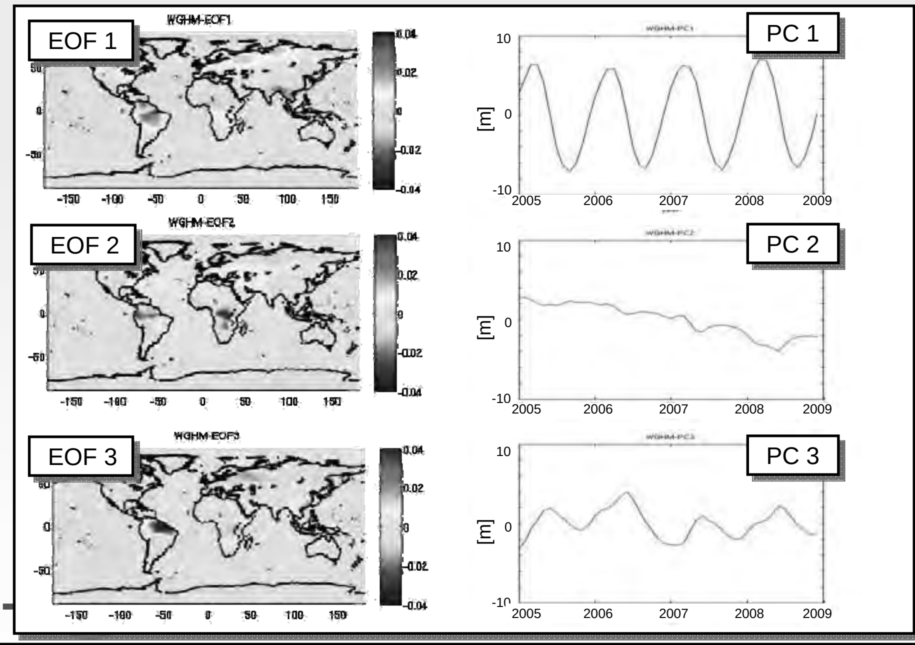

13

PCA: GRACE

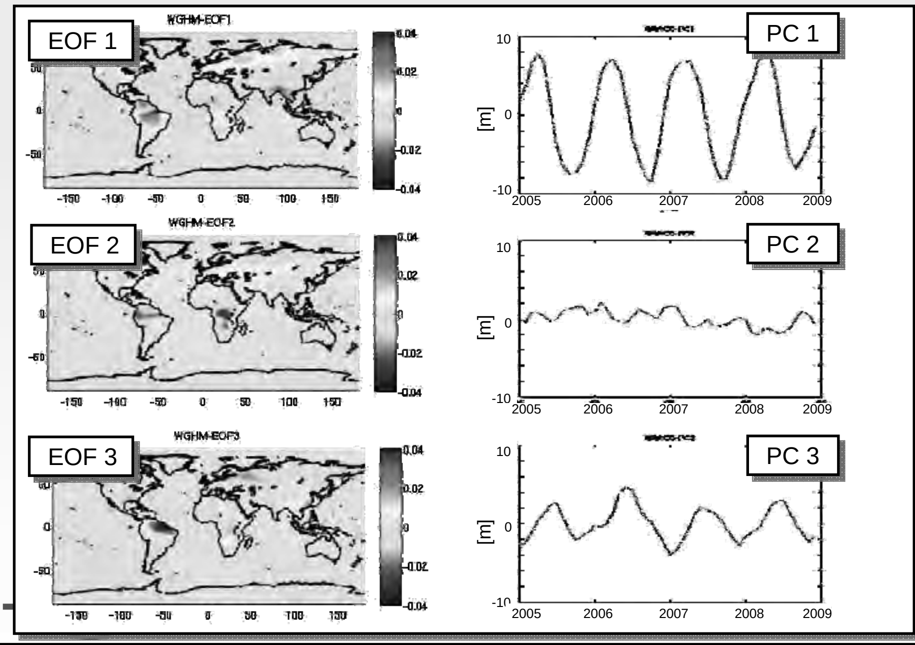

14

Exercise 2

Understanding compression properties of PCA

15

DFG SPP 1257

Eigenvalues

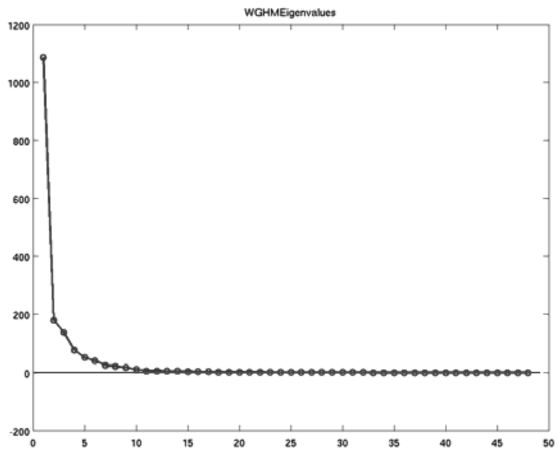

16

DFG SPP 1257

Signal reconstruction 2005-05

WGHM original data

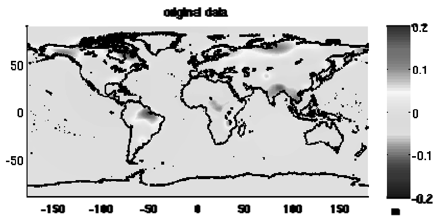

95% reconstruction

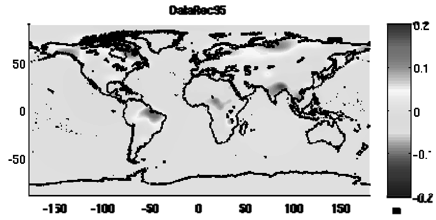

Differences

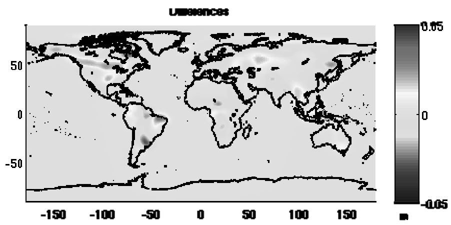

Original data: 48 monthly grids

8 EOFs needed to reconstruct 95%

3 EOFs needed to reconstruct 80%

17

Exercise 3

Understanding domain dependence of PCA

18

DFG SPP 1257

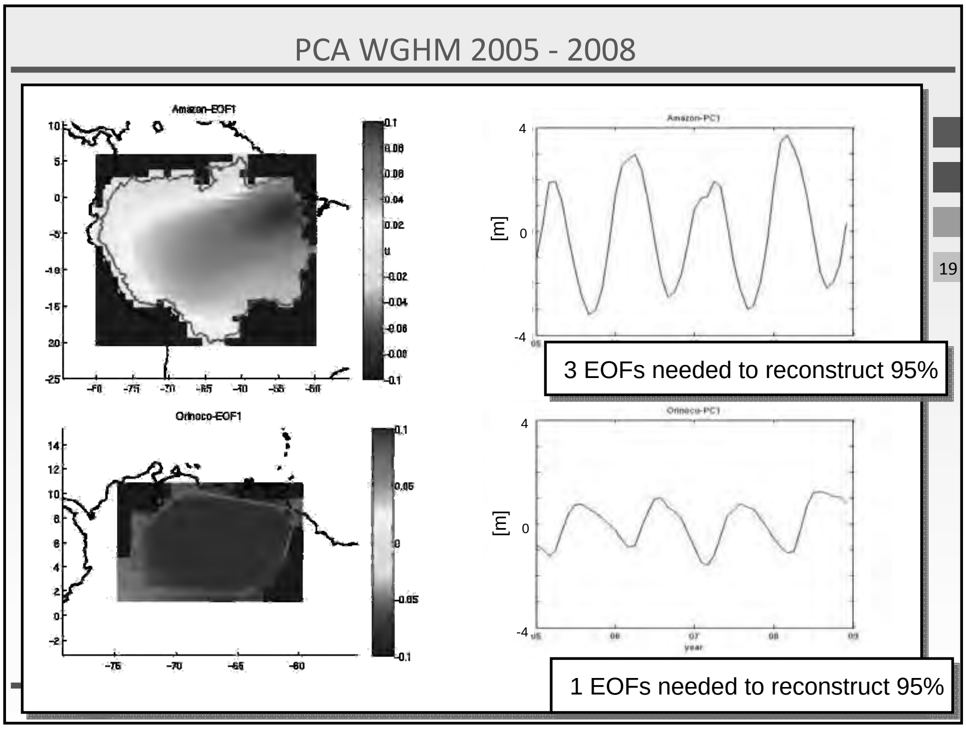
PCA WGHM 2005 - 2008
Amazon-EOF1
Orinoco-EOF1
Amazon-PC1
Orinoco-PC1
[m]
year
3 EOFs needed to reconstruct 95%
1 EOFs needed to reconstruct 95%
19

Summer School “Global Water Cycle”

12.-16. September 2011, Mayschoss

DFG Priority Programme SPP1257:
Mass transport and mass distribution in the Earth’s system

Volker Klemann, Mail: volkerk@gfz-potsdam.de
Andreas Groh, Mail: groh@ipg.geo.tu-dresden.de

Practical: Ice and Loading

Purpose of the practical: In the practical ’Ice and Loading’ the elastic response of the Earth and the ocean to a changing ice load will be investigated. For this purpose, ICESat-derived ice height changes over Greenland are provide and will be used as input for solving the ’sea-level equation’ iteratively. The inferred present-day changes of the Earth’s gravity field will be combined with GIA-induced viscous effects. This combined result and its comparison to the GRACE-derived geoid changes form the basis for concluding discussions.

Additional material: Lecture Notes ’Ice’ by Reinhard Dietrich and Lecture Notes ’Loading’ by Volker Klemann. Additional information can be found within this document.

Directories: The required data sets can be found on the USB stick in the directory *practicals/data/pract4_iceLoading*. The example scripts are located under *practicals/functions/pract4_iceLoading* and should be started from this directory. Utilised matlab functions can be found in the subdirectory *mtools*.

1 Exercise 1: Solving the sea-level equation for the elastic case

We want to calculate the adjustment of the sea level due to a loading process. Input is a load distribution, which is the spatial distribution of an ice-height change. Ice-mass changes are usually represented by a change in ice thickness or in equivalent water thickness. Here, `loadfile` contains ice-thickness changes. As discussed during the lecture, the sea-level equation (SLE) is an integral equation and will be solved here iteratively (Sec. 1.1, p. 2). The convolution integral is presented in Sec. 1.2, p. 3.

In the matlab script `sle_pt`, the i/o and iteration procedure is prepared.

Here, we give a small description of the steps to work through.

1. Definition of global parameters.
2. Definition of Input files. The LLN, the topography and the ice-height changes are provided.
3. Read in of LLN and definition of the Green's function needed for the SLE.
4. Determination of ocean function: read in of topography – define 1/0 grid.
5. Initialise iteration procedure: initialise working grid – dermine ocean surface – read in of load and transfer to surface-mass density – synthesise – initialise sea level.
6. iterate sea-level equation: convolution – determine and add new equivalent sea level.

The task of you will be to identify and program the convolution integral, and of course to discuss the results, which is how efficient the iteration is.

The output of each iteration is presented on the screen and will be stored in `../../data/pract4_iceLoading/output_data/rsl_XXX_YY.dat`, here XXX denotes the maximum degree and YY the number of iterations.

In `sle_pt.m`, the number of iteration steps is predefined. How can this be improved?

1.1 Iterative procedure

The steps of the iteration are represented below, where $*$ denotes the convolution of the appropriate Green's function.

$$
\begin{aligned}
(e-u)_i(\Omega) &= g_{e-u} * \left[m_{\text{load}}(\Omega) + s_{i-1}(\Omega)\,\rho_w\,\mathcal{O}(\Omega) \right] , \\
s_i(\Omega) &= s_i^{\text{esl}} + (e-u)_i(\Omega)\,\mathcal{O}(\Omega) , \\
s_i^{\text{esl}} &= -\frac{\int_\Omega m_{\text{load}}(\Omega)}{\rho_w\,A_o} - \frac{1}{A_o}\int (e-u)_i(\Omega)\,\mathcal{O}(\Omega)\,d\Omega \\
s_0 &= -\frac{\int m_{\text{load}}(\Omega)}{\rho_w\,A_o} ,
\end{aligned}
\qquad (1)
$$

Here, e is the displacement rate of the reference equipotential, u is the vertical displacement rate, m_{load} is the distribution of the load change, s_i represents the relative sea level, ρ_w is the density of sea water and $\mathcal{O}$ is the ocean function. $\Omega = (\theta, phi)$ represents the coordinates on the sphere. Furthermore, s_i^{esl} is the equivalent sea level due to mass conservation and deformation and A_o is the ocean surface. Alternatively the geoid, N, representing the actual averaged sea-level height, is defined as

$$n(\Omega) = s_i^{\text{esl}} + e(\Omega) \tag{2}$$

For the first approximation, s_0^{esl} only consists of the uniform sea-level change due to mass change of the load. Iteration steps $i \in \{1, ..., 3\}$ should be sufficient to reach convergence.

1.2 Convolution

The convolution in (1) can be replaced by multiplication in the spectral domain:

$$[g_\alpha * m](\Omega) = \sum_{l=0}^{\infty} \sum_{m=0}^{l} G_l^\alpha \, M_{l\,m} \, Y_{l\,m}(\Omega) \tag{3}$$

Here, g_α represents any Green's function, which are expressible for the elastic response to a surface load by combinations of load Love numbers (LLN), and M_{lm} is the spectral representation of the load, m. The most prominent Green's functions are for the potential displacement,

$$G_l^e = \frac{3}{\bar{\rho}} (1 + k_l) \frac{1}{2\,l + 1} \tag{4}$$

and for the vertical displacement

$$G_l^u = \frac{3}{\bar{\rho}} (h_l) \frac{1}{2\,l + 1} \tag{5}$$

from which the linear combination for the case of the relatve sea level follows

$$G_l^{e-u} = G_l^e - G_l^u \,. \tag{6}$$

In these equations, the mass of the Earth is replaced by its average density, $\bar{\rho}$.

2 Exercise 2: Comparison of GIA-induced and present-day geoid changes with GRACE

We want to combine the displacement of an equipotential surface, e, of the Earth's gravity field due to a changing ice and ocean load, discussed in Exercise 1 (Sec. 1, p. 2), with those induced by GIA. The replacement of the geoid by the potential displacement is valid, as long as we do not consider the degree 0 component, see lecture note 'Loading'. This combined result should be compared to the results derived from GRACE. All calculation will be performed in the spherical-harmonic domain. Just the graphical presentation of the results requires a transformation into the spatial domain.

In the matlab script `compare_pt`, the i/o and calculation procedure is prepared.

Here, we give a small description of the steps to work through.

1. Definition of global parameters.
2. Definition of Input files. The LLN and the topography are provided.
3. Read in of LLN and definition of the Green's function needed.
4. Determination of ocean function: read in of topography – define 1/0 grid.
5. Read in of GRACE stokes trend coefficients and conversion into geoid trend coefficients.
6. Read in of GIA equipotential surface trend coefficients.
7. Read in of the relative sea-level change from the last iteration of Exercise 1 and the ice height changes.
8. Combination of the later and transformation into spherical harmonic coefficients.
9. Perform the convolution in order to derive present-day geoid changes.
10. Combination of GIA and present-day geoid changes and comparison to GRACE results.

Again, your task will be to identify and program the convolution integral. Moreover, you should combine GIA and present-day effects in the spherical harmonic domain and compare them to the GRACE results. Therefore, plots in the space domain should be prepared.

How can the remaining differences, if there are any, be explained?

3 Matlab/ocatve functions:

Input

function [shc] = icgem2kff(fname [, nmax])	
Reads a file of spherical harmonic coefficients in ICGEM format and tranfers it to a 2d-array containing n, m, cnm, snm. Optionally the output can be reduced to a maximum degree, $n_{\max}$.	
Input	• `fname`: Input file in ICGEM format. • `[nmax]`: Optional maximum degree of coefficients to be read.
Output	• `n, m, cnm, snm`: 2d-arrays containing degree, order and the sphpotential coefficients. Dimension is $(n+1)(n+2)/2$ with n=`nmax` or maximum degree read in.

function [arr, [lon, lat]] = xyz2arr(fname, lonres, latres)	
Reads $lon, lat, value$ from a file and stores the $values$ in a 2d global array.	
Input	• `fname`: File containing a global regular grid in lon-lat convention. • `lonres`: Longitudinal grid sampling. • `latres`: Latitudinal grid sampling.
Output	• `arr`: 2d-array containing the grid values $[(90 : latres : -90) \times (0 : lonres : 360)]$. • `[lon, lat]`: 1d arrays containing longitude $[360/lonres + 1]$ and latitude $[180/latres + 1]$

function [n, h ,k ,l] = lln2arr(fname [, nmax])	
Reads load Love numbers from a file containing n, h, k, l and transfers them to arrays containing degrees n starting with 0 and corresponding h, k and l.	
Input	• `fname`: Input file containing the load Love numbers. • `nmax`: Optional maximum degree of numbers read in.
Output	• `n, h, k ,l`: 1d arrays containing degree and respective load Love numbers.

Output

kff2icgem(fname, shc, ,nmax, type, name)	
Writes a set of spherical harmonic coefficients (shc) to a file in ICGEM format.	
Input	• `fname`: File to which the coefficients are written (in ICGEM format). • `shc`: 2d-array holding n, m, cnm, snm. • `nmax`: Maximum degree of the coefficients that are written out. • `type`: Header information on the product type (one string without spaces). • `name`: Header information on the model name (one string without spaces).
Output	ASCII file.

function arr2xyz(fname, arr)	
Extracts $lon, lat, value$ from a global 2d-array and writes them to a file.	
Input	• `fname`: Name of the output file to which $lon, lat, value$ are written. • `arr`: 2d-array containing the grid values $[(90 : latres : -90) \times (0 : lonres : 360]$.
Output	ASCII file.

Analysis and Synthesis for Spherical harmonics representation

The two principle routines which are called from sle_pt.m are plm2xyz and xyz2plm which are listed below. These together with a number of further routines are provided by Frederik Simons, MIT, which can be downloaded from http://geoweb.princeton.edu/people/simons/software.html. The respective routines used in this practical can be found in *mtools/simons*.

function [r,lon,lat,Plm]=plm2xyz(lmcosi,degres,c11cmn,lmax,latmax,Plm)	
Inverse spherical harmonic transform. Compute a spatial field from spherical harmonic coefficients given as [l m Ccos Csin] (not necessarily starting from zero, but sorted), with degree resolution 'degres' [default: approximate Nyquist degree]. Using 4*pi-normalized real spherical harmonics.	
Input	• `lmcosi`: Matrix listing l,m,cosine and sine expansion coefficients e.g. those coming out of ADDMON • `degres`: Longitude/ latitude spacing, in degrees [default: Nyquist] OR "lat": a column vector with latitudes [degrees] OR [longitude-latitude-spacing], in degrees in combination with corner nodes in c11cmn • `c11cmn`: Corner nodes of lon/lat grid [default: 0 90 360 -90] OR "lon": a column vector with longitudes [degrees] • `lmax`: Maximum bandwidth expanded at a time [default: 720] • `latmax`: Maximum linear size of the latitude grid allowed [default: Inf] • `Plm`: The appropriate Legendre polynomials should you already have them
Output	• `r`: The field (matrix for a grid, vector for scattered points) • `lon,lat`: The grid (matrix) or evaluation points (vector), in degrees • `Plm`: The set of appropriate Legendre polynomials should you want them

function [lmcosi,dw]=xyz2plm(fthph,L,method,lat,lon,cnd)	
Forward real spherical harmonic transform in the 4pi normalized basis. Converts a spatially gridded field into spherical harmonics. For complete and regular spatial samplings [0 360 -90 90]. If regularly spaced and complete, do not specify lat,lon. If not regularly spaced, fthph, lon and lat are column vectors.	
Input	• `fthph` Function defined on colatitude theta and longitude phi • `L` Maximum degree of the expansion (Nyquist checked) • `method` 'gl' By Gauss-Legendre integration (fast, inaccurate) 'simpson' By Simpson integation (fast, inaccurate) 'irr' By inversion (irregular samplings) 'im' By inversion (fast, accurate, preferred) 'fib' By Riemann sum on a Fibonacci grid (not done yet) • `lat` If not [90,-90], give latitudes explicitly, in degrees • `lon` If not [0,360], give longitudes explicitly, in degrees • `cnd` Eigenvalue tolerance in the irregular case

Output	• `lmcosi` Matrix listing l,m,cosine and sine coefficients • `dw` Eigenvalue spectrum in the irregular case

Visualisation of fields

plot_grid(lon, lat, arr, label [,fname])	
Plots xyz-field `arr` to screen and optionally to an eps-file.	
Input	• `lon, lat`: 1d arrays containing longitude $[360/lonres + 1]$ and latitude $[180/latres + 1]$ • `arr`: 2d-array containing the grid values $[(90 : latres : -90) \times (0 : lonres : 360)]$. • `label`: Colorbar label. • `[fname]`: Name of the eps-file.
Output	N/A

4 Usage of matlab/octave functions

4.1 Input

`octave:1> [kff]=icgem2kff ("infile"[, nmax])`
reads in ICGEM file and tranfers it to `[kff]=[degree, order, cos, sin]` starting with degree=0.

`octave:2> [arr]=xyz2arr("infile", lonres, latres)`
reads in regular and global [lon, lat, value] list (resolution: lonres x latres) to global array.

`octave:3> [degree, h, k, l]=lln2arr("infile"[, nmax])`
reads in [degree, h, k, l] list and writes it to 1d-arrays `degree, h, k, l`.

4.2 Output

`octave:1> kff2icgem ("outfile", kff, nmax, type, name])`
writes `kff=[degree, order, cos, sin]` to an ASCII file in ICGEM format starting with degree=0. `Type` and `name` provide ICGEM format header information.

`octave:2> arr2xyz("outfile", arr)` writes global array, `arr` to `[lon, lat, value]` list.

4.3 SH synthesis

`octave:1> load -ascii ugeod.dat`
reads in a spectral array `[deg order cos sin]`.

`octave:2> [u,lon,lat,plm] = plm2xyz(ugeod, [0.351562 0.35122], [0 89.7367 360 -89.7367], 170)`
generates spatial field `u`, here for an equidistant grid approximateing a GL-grid of 2025×512 grid points.

`octave:3> help plm2xyz`
provides the information about the command.

4.4 SH analysis

`octave:1> [kff] = xyz2plm(arr, nmax,'im')`
transforms a regular global grid `arr` (as generated by `xyz2arr`) into spherical harmonic coefficients of maximum degree `nmax`, which are stored in `[kff]=[degree, order, cos, sin]` starting with degree=0.

`octave:2> help xyz2plm`
provides the information about the command.

4.5 Visualisation of fields

`octave:1> plot_grid(lon, lat, z, 'zlabel'[,'out.eps'])`

plots xyz-field `z` to screen and optionally to 'out.eps'. `lon, lat, z` are the 1d-longitude, -latitude arrays and the 2d-z array to be plotted, `'zlabel'` is the name of the annotation of the color bar and `'out.eps'` is the the optional ps file.

Summer School “Global Water Cycle”

12.-16. September 2011, Mayschoss

DFG Priority Programme SPP1257:
Mass transport and mass distribution in the Earth’s system

Martin Losch, Mail: Martin.Losch@awi.de
Henryk Dobslaw, Mail: dobslaw@gfz-potsdam.de
Wolfgang Bosch, Mail: bosch@dgfi.badw.de

Practical: Altimetry and Ocean Dyanmics

Purpose of the practical:

Information about the density distribution in the global ocean as provided by in-situ observations of temperature and salinity allows to derive the geostrophic shear field. Absolute geostrophic currents might be subsequently obtained by either assuming or observing the geostrophic velocities at a certain depth level. The dynamic ocean topography as derived from the difference between sea surface and geoid provides the required information to derive such currents along the surface.

- combine altimetry and geoid height to obtain dynamic topography field
- compute surface geostrophic velocities
- compute 3D-geostrophic velocity field in the ocean from hydrography and surface dynamic topography
- compare 3D-geostrophic velocity field with numerical ocean model

Input Data:

- geoid height field, unfiltered and filtered (`dgfi_alongtrack.mat`)
- sea surface height (SSH) from Jason 1 for five different cycles, unfiltered and filtered, along-track and gridded (`dgfi_alongtrack.mat`)
- multi-year mean dynamic topography (`dgfi_meandot.mat`)
- WOCE hydrographic atlas: in-situ temperature and salinity (`woce_climatology.mat`), additional information: http://icdc.zmaw.de/woce.html
- 3D velocity field and dynamic topography field from ECCO2 ocean general circulation model (`ecco2_data.mat`), additional information: http://ecco2.org/

Matlab Libraries and Functions:

- CSIRO Sea Water Library (`seawater_ver3_0`), additional information: http://www.cmar.csiro.au/datacentre/ext_docs/seawater.htm
- Gibbs-Sea Water Oceanographic Toolbox (`gsw_matlab_v3_0`), additional information: http://www.teos-10.org/software.htm

Exercise 1: Dynamic Topography

- load and plot gridded sea surface heights h and geoid heights N for cycle 101 (`dgfi_alongtrack.mat`)
- calculate and plot DOT η from unfiltered and filtered h, N, and compare
- derive surface geostrophic velocity field from grid spacing information and η
- optionally: project along-track data from another cycle onto the grid and compare η, $\mathbf{v}$ with previous results

Exercise 2: Geostrophic flow field

- load multi-year DOT η (`dgfi_meandot.mat`) and derive surface geostrophic velocities as in exercise 1
- load hydrographic climatology (T, S) (`woce_climatology.mat`)
- compute in-situ density $\sigma = \rho - 1000$, potential densities $\sigma_{0,2,4}$, neutral density γ_n (functions: `sw_dens` and `sw_pden`, alternatively corresponding functions from the GSW Toolbox) and compare
- compute geostrophic shear $\partial\mathbf{v}/\partial z$ from thermal wind ($-\frac{g}{\rho f}\mathbf{k}(\nabla \times \rho)$), and, optionally from "dynamic method" via geopotential height anomaly (functions: `sw_gpan.m` and `sw_gvel.m`, alternatively corresponding functions from the GSW Toolbox)
- compute absolute velocity relative to bottom and surface, use either $v_{\mathbf{ref}} = 0$ or $\frac{g}{f}\mathbf{k}(\nabla \times \eta)$, and compare

Exercise 3: Comparison to Numerical GCM Results

- load η and velocity fields of numerical GCM (`ecco2_data.mat`)
- compare to corresponding fields of Exercise 1 and 2

Jürgen Kusche, Annette Eicker and Ehsan Forootan

Analyis Tools for GRACE- and Related Data Sets

Theoretical Basis

Lecture Notes

Summerschool 'Global Hydrological Cycle', Mayschoss, Sept. 12-16, 2011

September 6, 2011

DFG Priority Program SPP1257
Mass Transport and Mass Distribution in the Earth System

Bonn University

These lecture notes were compiled on the occasion of the summerschool 'Global Hydrological Cycle', organized by DFG's priority program SPP1257 'Mass Transport and Mass Distribution in the System Earth' at September 12-16, 2011 in Mayschoss/Ahr. Our aim was to familiarize students with different background (geodesy, hydrology, oceanography, geophysics) with some mathematical concepts that are fundamental for analysing level-2 products (sets of spherical harmonic coefficients) from the GRACE mission and related geophysical data sets (model outputs in gridded form). The focus was on concepts, and technical proofs were avoided. Specific topics were filtering and basin averaging, and the application of the principal component analysis technique. Thanks for spotting typos go to Volker Klemann and Torsten Mayer-Gürr.

Jürgen Kusche, Annette Eicker and Ehsan Forootan

Bonn, September 6, 2011

Contents

1

Smoothing and Averaging of Functions on the Sphere

At the product level 2, GRACE data are condensed to monthly sets of fully normalized spherical harmonic coefficients. These coefficients are the outcome of a rather complex data processing scheme. For scientific analysis, users of GRACE data will have to perform a number of basic operations on the GRACE coefficients: transform dimensionless geopotential coefficients into gridded geoid heights or maps of surface density expressed through equivalent water heights, and average such maps over the surface of some hydrological catchment area or ocean basin. Moreover, one of the problems that users of the GRACE level-2 products face is the presence of increasing correlated noise ('stripes') at higher frequencies. Smoothing operators can be applied in either spatial or spectral domain in order to suppress the effect of noise in maps and area averages. The purpose of this chapter is to describe the mathematical concepts underying these procedures.

Notation

According to [2], we write the gravitational potential at a fixed location as a function of time as

$$
\begin{aligned}
V(r,\theta,\lambda,t) &= \frac{GM}{r} \\
&+ \frac{GM}{r}\sum_{n=2}^{\bar{n}}\left(\frac{R}{r}\right)^n \sum_{m=0}^{n} P_{nm}(\cos\theta)\left(\bar{C}_{nm}(t)\cos m\lambda + \bar{S}_{nm}(t)\sin m\lambda\right)
\end{aligned}
$$

with $\theta = \frac{\pi}{2} - \phi$, $GM = \mu$ (in [2]), and fully normalized spherical harmonic coefficients $\bar{C}_{nm}$ and $\bar{S}_{nm}$. The other quantities will be explained later.

In the following, we will refer to either temporal variations in the geoid or in total water storage (TWS), the spherical harmonic coefficients of which we will denote as $\bar{f}_{nm}$. These quantities are related to the gravitational potential via simple spectral relations, which are valid under certain assumptions ('spherical approximation', radial Earth model) that will be discussed elsewhere during the summer school. Under these assumptions, the geoid or TWS changes projected to the space domain read

$$F = \sum_{n=0}^{\infty} \sum_{m=-n}^{n} \bar{f}_{nm} \bar{Y}_{nm}(\lambda, \theta) \ .$$

Total water storage change from geopotential harmonics. In this case, the common approximation is

$$\bar{f}_{nm}(t) = R \frac{\rho_e}{3} \frac{2n+1}{1+k'_n} \left(\bar{v}_{nm}(t) - \bar{v}_{nm}\right)$$

with

$$\bar{v}_{nm} = \bar{C}_{nm} \quad \text{for } m \geq 0, \qquad \bar{v}_{nm} = \bar{S}_{n|m|} \quad \text{for } m < 0 \ ,$$

and $\bar{v}_{nm}$ either a suitable long-term mean of these (i.e. $\bar{v}_{nm} =< \bar{v}_{nm}(t) >_{t_A}^{t_B}$) or they refer to a reference epoch t_0.

In the above, TWS is expressed as a surface density (unit $\frac{\mathrm{kg}}{\mathrm{m}^2}$), the height of a water column is usually derived by scaling the above by a reference density of water, i.e. multiplication by $1/\rho_w$. Thus, ρ_w (if applied) is a reference quantity which has to be chosen as a convention (usually, $\rho_w = 1000 \frac{\mathrm{kg}}{\mathrm{m}^3}$ or $\rho_w = 1025 \frac{\mathrm{kg}}{\mathrm{m}^3}$. The average density of the Earth, ρ_e, is related to the Earth's mass M by $M = \frac{4\pi\rho_e}{3} R^3$ and follows therefore to $\rho_e = 5517 \frac{\mathrm{kg}}{\mathrm{m}^3}$. Finally, the k'_n are the elastic gravity load Love numbers and follow from 1D-models of the Earth's rheologic properties.

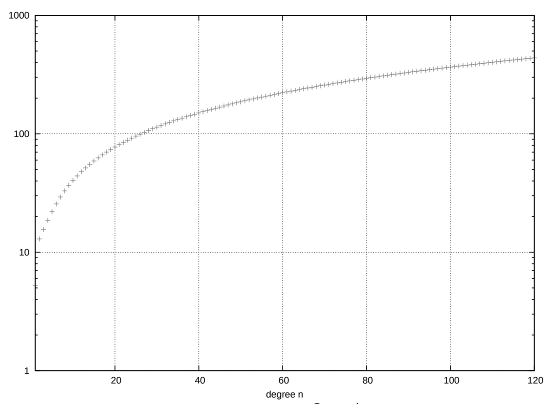

Fig. 1 Shown are the coefficients $\frac{\rho_e}{3\rho_w} \frac{2n+1}{1+k'_n}$. It is obvious that, when computing TWS harmonics from geopotential harmonics, errors in higher degrees will be amplified compared to those in low-degree coefficients

Geoid change from geopotential harmonics. In this case, the common approximation is

$$\bar{f}_{nm}(t) = R\ (\bar{v}_{nm}(t) - \bar{v}_{nm})$$

with the $\bar{v}_{nm}$ as defined above.

1.1 Area Averaging ('Windowing')

In many applications one is interested in averaging a field over a certain geographical area or region or basin. This is what we call area averaging or *windowing* here.

1.1.1 Exact Windowing

Let us start with a given field F defined on the sphere Ω,

$$F = F(\lambda, \theta) \tag{1.1}$$

expressed either in spatial domain or in spherical harmonic representation.

The area $O \subset \Omega$ can be mathematically expressed through its characteristic function

$$O = O(\lambda, \theta) = \begin{cases} 1 & (\lambda, \theta) \in O \\ 0 & (\lambda, \theta) \notin O \end{cases} \tag{1.2}$$

(1 inside the area, and 0 outside of it). Its area (size) $\bar{O}$ is

$$\bar{O} = \int_O d\omega = \int_\Omega O d\omega\ . \tag{1.3}$$

Windowing F over O means to derive an average

$$\bar{F}_O = \frac{1}{\bar{O}} \int_O F d\omega = \frac{1}{\bar{O}} \int_\Omega OF d\omega \tag{1.4}$$

of F over O.

Remark. If $F = F(\lambda, \theta, t)$ is a spatio-temporal field, the average $\bar{F}_O(t)$ will be a time-series.

Remark. Usually, a polygon $O(\lambda_i, \theta_i), i = 1 \ldots q$ will be used to characterize $O(\lambda, \theta)$.

Remark. In practical computations in the space domain, the integrals will be replaced by discrete sums, introducing a discretization error ϵ whose magnitude depends on the spatial grid resolution and the smoothness of both the function F and the region boundary of O. The discrete version of Eq. (1.4) can be cast as $\bar{F}_O = \mathbf{o}^T\mathbf{f}$ or $\bar{F}_O(t) = \mathbf{o}^T\mathbf{f}(t)$ if the field F is time-dependent.

Remark. If F is approximated by a spherical harmonic expansion before projecting onto a grid and evaluation of the discrete sum, an extra truncation error is introduced.

1.1.2 Exact Windowing in Spherical Harmonic Representation

Next, we consider both F and O expanded in 4π-normalized spherical harmonics $\bar{Y}_{nm}$.

$$F = \sum_{n=0}^{\infty} \sum_{m=-n}^{n} \bar{f}_{nm} \bar{Y}_{nm}(\lambda, \theta) \tag{1.5}$$

$$O = \sum_{n=0}^{\infty} \sum_{m=-n}^{n} \bar{O}_{nm} \bar{Y}_{nm}(\lambda, \theta) \tag{1.6}$$

(the overbar in $\bar{f}_{nm}$ etc. tells that coefficients are 4π-normalized). It is immediately clear that

$$\bar{O} = \int_{\Omega} O\bar{Y}_{00} d\omega = 4\pi\ \bar{O}_{00} \tag{1.7}$$

The exact average of F over O is then

$$\bar{F}_O = \frac{1}{\bar{O}_{00}} \sum_{n=0}^{\infty} \sum_{m=-n}^{n} \bar{O}_{nm} \bar{f}_{nm} \tag{1.8}$$

or, if $\bar{o}_{nm} = \frac{\bar{O}_{nm}}{\bar{O}_{00}}$ are the region's SH coefficients further normalized to $\bar{o}_{00} = 1$,

$$\bar{F}_O = \sum_{n=0}^{\infty} \sum_{m=-n}^{n} \bar{o}_{nm} \bar{f}_{nm} \tag{1.9}$$

Example. The first 4π-normalized coefficients of the *ocean function* are given in the table.

Table 1.1. Ocean function spherical harmonics

n m	$\bar{O}_{nm}$	$\bar{O}_{n\ -m}$
0 0	$0.701227 \cdot 10^{0}$	$0.000000 \cdot 10^{0}$
1 0	$-0.176689 \cdot 10^{0}$	$0.000000 \cdot 10^{0}$
1 1	$-0.115778 \cdot 10^{0}$	$-0.635533 \cdot 10^{-1}$
2 0	$0.618996 \cdot 10^{-2}$	$0.000000 \cdot 10^{0}$
2 1	$-0.450010 \cdot 10^{-1}$	$-0.717864 \cdot 10^{-1}$
2 2	$0.471078 \cdot 10^{-1}$	$0.464998 \cdot 10^{-2}$
3 0	$-0.355365 \cdot 10^{-2}$	$0.000000 \cdot 10^{0}$
3 1	$0.518058 \cdot 10^{-1}$	$-0.251440 \cdot 10^{-1}$
3 2	$0.691439 \cdot 10^{-1}$	$-0.992945 \cdot 10^{-1}$
3 3	$-0.135222 \cdot 10^{-1}$	$-0.947600 \cdot 10^{-1}$

Remark. In practical computations, the spherical harmonic summation will be evaluated up to finite degree $\bar{n}$, and a truncation error results. The exact average of F over O can be split into

$$\bar{F}_O = \frac{1}{\bar{O}_{00}} \sum_{n=0}^{\bar{n}} \sum_{m=-n}^{n} \bar{O}_{nm} \bar{f}_{nm} + \frac{1}{\bar{O}_{00}} \sum_{n=\bar{n}+1}^{\infty} \sum_{m=-n}^{n} \bar{O}_{nm} \bar{f}_{nm} \; . \tag{1.10}$$

This may be written as $\bar{F}_O = \mathbf{o}^T\mathbf{f} + \epsilon$. The second term is the truncation or omission error. It will vanish if either F or O is band-limited with degree $\bar{n}$, or if the high-degree components of F and O are orthogonal on the sphere in L_2-sense.

Remark. If F is truncated at degree $\bar{n}$, then projected into the space domain and the integral is evaluated over an exactly delineated area, the above mentioned truncation error will occur as well.

1.2 Smoothing of Spherical Harmonic Models

Smoothing or filtering a field is usually applied to suppress 'rough' or 'oscillatory' or 'noisy' components.

Consider F according to Eq. (1.1) and Eq. (1.5). A smoothed version is obtained by convolving F against a two-point kernel W with suitable properties. In the spatial domain,

$$F_W(\lambda, \theta) = \int_{\Omega} W(\lambda, \theta, \lambda', \theta') F(\lambda', \theta') d\omega \tag{1.11}$$

and in the spectral domain, in the rather general case of an arbitrarily shaped window function,

$$F_W(\lambda, \theta) = \sum_{n=0}^{\infty} \sum_{m=-n}^{n} \bar{f}^W_{nm} \bar{Y}(\lambda, \theta) \; , \qquad \bar{f}^W_{nm} = \sum_{n'=0}^{\infty} \sum_{m'=-n'}^{n'} \bar{w}^{n'm'}_{nm} \bar{f}_{n'm'} \; . \tag{1.12}$$

Thus, $W(\lambda, \theta, \lambda', \theta')$ describes the weighted contribution of F at point λ, θ to the windowed function F_W at point λ', θ'. In its discrete version in either spatial or spectral domain, smoothing will read $\mathbf{f}_W = \mathbf{W}\mathbf{f}$ (up to a truncation error, which we will omit in the sequel). The $\bar{f}^W_{nm}$ are the SH coefficients of the smoothed version of F. And the $\bar{w}^{n'm'}_{nm}$ are the 4π-normalized spherical harmonic coefficients of the two-point smoothing kernel

$$W(\lambda, \theta, \lambda', \theta') = \sum_{n=0}^{\infty} \sum_{m=-n}^{n} \sum_{n'=0}^{\infty} \sum_{m'=-n'}^{n} \bar{w}^{n'm'}_{nm} \bar{Y}_{nm}(\lambda, \theta) \bar{Y}_{n'm'}(\lambda', \theta') \; . \tag{1.13}$$

Or, $W(\lambda, \theta, \lambda', \theta') = \mathbf{y}^T(\lambda, \theta)\mathbf{W}\mathbf{y}(\lambda', \theta')$ with matrix $\mathbf{W}$ containing the elements $\bar{w}^{n'm'}_{nm}$. It is obvious that for fixed λ', θ' the $\bar{w}^{n'm'}_{nm} \bar{Y}_{n'm'}(\lambda', \theta')$ are the

4π-normalized spherical harmonic coefficients of $W(\lambda,\theta)$, and vice versa; for fixed λ,θ the $\bar{w}_{nm}^{n'm'}\bar{Y}_{nm}(\lambda,\theta)$ are the SH coefficients of $W(\lambda',\theta)$. Consequently, for a given two-point kernel W,

$$\bar{w}_{nm}^{n'm'} = \frac{1}{(4\pi)^2}\int_{\Omega}\int_{\Omega'} W(\lambda,\theta,\lambda',\theta')\bar{Y}_{nm}(\lambda,\theta)\bar{Y}_{n'm'}(\lambda',\theta')d\omega d\omega' \ . \tag{1.14}$$

This is the most general case of smoothing.

1.2.1 Isotropic Filters

Most filters that we encounter in the literature are isotropic, i.e. the smoothing kernel depends only on the spherical distance ψ between the two points λ,θ and λ',θ' and not on their relative orientation. A comprehensive review is [4]. For isotropic kernels, the SH coefficients of the kernel can be reduced to the Legendre coefficients of a zonal (z-symmetric) function w_n. Thus,

$$\begin{aligned} W(\psi) &= \sum_{n=0}^{\infty}(2n+1)w_n P_n(\cos\psi) \\ &= \sum_{n=0}^{\infty}\sum_{m=-n}^{n} w_n\bar{Y}_{nm}(\lambda,\theta)\bar{Y}_{nm}(\lambda',\theta') = W(\lambda,\theta,\lambda',\theta') \end{aligned} \tag{1.15}$$

(with $P_n(\cos\psi)$ being the unnormalized Legendre polynomials) or

$$\bar{w}_{nm}^{n'm'} = \delta_{nm}^{n'm'} w_n \ . \tag{1.16}$$

For isotropic filters, smoothing of F can be written as

$$F_W(\lambda,\theta) = \int_{\Omega} W(\psi)F(\lambda',\theta')d\omega \tag{1.17}$$

and in the spectral domain simply $\bar{f}_{nm}^{W} = w_n\bar{f}_{nm}$ and

$$F_W(\lambda,\theta) = \sum_{n=0}^{\infty}\sum_{m=-n}^{n} w_n\bar{f}_{nm}\bar{Y}(\lambda,\theta) \ . \tag{1.18}$$

Example. A first example is the *boxcar filter*, which simply truncates the function F at SH degree $\bar{n}$

$$W_{(\bar{n})}(\psi) = \sum_{n=0}^{\bar{n}}(2n+1)P_n(\cos\psi) \ , \qquad w_n^{(\bar{n})} = \begin{cases}1\\0\end{cases} \quad \text{for} \ \begin{cases}n\le\bar{n}\\ n>\bar{n}\end{cases}$$

Example. A second example is the *Gaussian filter*, popularized by [19], for which we know an analytic expression in the spatial domain ('bell-shaped') with

$$W_d(\psi) = 2b\frac{e^{-b(1-\cos\psi)}}{1-e^{-2b}} = \sum_{n=0}^{\infty}(2n+1)w_n^{(d)}P_n(\cos\psi)$$

with

$$b = \frac{\ln(2)}{1-\cos\frac{d}{R}} \ .$$

Here, $d = R\psi_d$ is the 'half-with' radius parameter where the kernel drops from 1 at $\psi = 0$ to $\frac{1}{2}$, which is commonly used to indicate the degree of smoothing. The Legendre coefficients of the Gaussian filter are found from recursion relations,

$$w_0^{(d)} = 1 \ , \qquad w_1^{(d)} = \left(\frac{1+e^{-2b}}{1-e^{-2b}} - \frac{1}{b}\right) \ , \qquad w_{n+1}^{(d)} = -\frac{2n+1}{b}w_n^{(d)} + w_{n-1}^{(d)} \ .$$

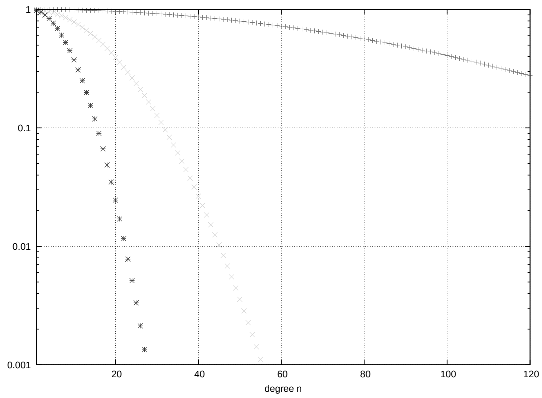

Fig. 2 Shown are the Legendre coefficients $w_n^{(d)}$ for d equalt to 100 km, 500 km and 1000 km.

1.2.2 Anisotropic Filters

Anisotropic filters can be characterized into symmetric (or diagonal) filters and non–symmetric filters ([14]). A further differentiation among non-symmetric filters is possible when thinking of the coefficients $\bar{w}_{nm}^{n'm'}$ as being ordered within matrix $\mathbf{W}$ (when we use a particular ordering scheme for the $\bar{f}_{nm}$, the same has to apply to the filter coefficients).

For *symmetric* filters, $\mathbf{W}$ is diagonal and

$$\bar{w}_{nm}^{n'm'} = \delta_{nm}^{n'm'} w_{nm} \ . \tag{1.19}$$

Thus the smoothing kernel has the shape

$$W(\lambda,\theta,\lambda',\theta') = \sum_{n=0}^{\infty}\sum_{m=-n}^{n} w_{nm}\bar{Y}_{nm}(\lambda,\theta)\bar{Y}_{nm}(\lambda',\theta') \ . \tag{1.20}$$

It is symmetric with respect to the points λ, θ and λ', θ'.

Example. Han's filter ([11]) is of this type. They chose a Gaussian filter with 'order-dependent' smoothing radius $d(m)$,

$$w_{nm} = w_n^{(d(m))} , \qquad d(m) = \frac{d_1 - d_0}{m_1} m + d_0$$

Example. The 'fan' ([21]) filter is simply a product of different Gaussian filters applied to order and degree,

$$w_{nm} = w_{nm}^{(d_1,d_2)} = w_n^{(d_1)} \cdot w_m^{(d_2)}$$

In the general case of Eq. (1.12), the filter is *non–symmetric* with respect to points λ, θ and λ', θ' and its matrix $\mathbf{W}$ is full.

Remark. Even if $\mathbf{W}$ is symmetric, the resulting filter would be *non–symmetric.*

Example. The DDK filter ([15], [16]). Here, the filter matrix is derived by regularization of a 'characteristic' normal equation system that involves a-priori information on the signal variance and the observation system from which we obtain the unfiltered coefficients,

$$\mathbf{W}_{(\alpha)} = \mathbf{L}_\alpha \mathbf{N} = (\mathbf{N} + \alpha \mathbf{M})^{-1} \mathbf{N}$$

or

$$\bar{w}_{nm}^{n'm'(\alpha)} = \sum_{n=0}^{\infty} \sum_{m=-n}^{n} L_{nm}^{n''m'(\alpha)'} N_{n''m''}^{n'm'}$$

with $\mathbf{M}$ being an approximation to $\mathbf{C_f} = E\{\mathbf{f}\mathbf{f}^T\}$, $\mathbf{N}$ being an approximation to $\mathbf{C_{\hat{f}}} = E\{\hat{\mathbf{f}}\hat{\mathbf{f}}^T\}$, and $L_{nm}^{n''m'(\alpha)'}$, $N_{n''m''}^{n'm'}$ the corresponding elements. In addition, α is a damping parameter. The DDK filters are non-symmetric. In [16] it was shown that the original $\mathbf{W}_{(\alpha)}$ of [15] can be safely replaced by a block-diagonal version of the matrix.

Example. The 'Swenson and Wahr' filter ([20]) is non-symmetric and it can also be represented by a block-diagonal $\mathbf{W}$. The idea of this filter is that an empirical model for the correlations between SH coefficients $\bar{f}_{nm}$ of the same order and parity is formulated and then used for decorrelation.

Example. EOF filtering means one applies PCA to a time series $\mathbf{f}_i$ of either gridded values of F or SH coefficients. A reconstruction with q modes provides

$$\mathbf{f}^{(q)} = \mathbf{E}\mathbf{I}^{(q)}\mathbf{E}^T\bar{\mathbf{f}} = \mathbf{W}^{(q)}\mathbf{f}$$

where $\mathbf{E}$ contains the EOFs of the time series and $\mathbf{I}^{(q)}$ is a diagonal matrix with unity in the first q entries and zero otherwise. EOF filtering corresponds to application of a non-symmetric filter as well.

1.3 Smoothed Area Averaging

Now let us come back to the windowing of a spherical harmonic model F, i.e. we wish to average F over the region O. Of course we can window a smoothed version F_W of F as well, if necessary.

Another view on the same operation is as follows: In place of Eq. (1.2), we may introduce a smoothed area function O_W,

$$O_W(\lambda, \theta) = \sum_{n=0}^{\infty} \sum_{m=-n}^{n} \bar{O}_{nm}^W \bar{Y}_{nm}(\lambda, \theta) = \frac{1}{4\pi} \int_\Omega W(\lambda, \theta, \lambda', \theta') O(\lambda', \theta') d\omega' \ , \tag{1.21}$$

and we will apply O_W to the original function F

$$\bar{F}_{O_W} = \frac{1}{\bar{O}_W} \int_\Omega O_W F d\omega \tag{1.22}$$

(note that $\bar{O}_W = \bar{O}$ if the filter is normalized, see below). In general, the smoothing kernel W is a two-point function on the sphere, cf. Eq. (1.3).

1.3.1 Spherical Harmonic Representation

In case of Eq. (1.15), i.e. W is isotropic, the smoothed area function can be written as

$$O_W(\lambda, \theta) = \sum_{n=0}^{\infty} \sum_{m=-n}^{n} \bar{O}_{nm}^W \bar{Y}_{nm}(\lambda, \theta) \tag{1.23}$$

with

$$\bar{O}_{nm}^W = \bar{w}_n \bar{O}_{nm} \ . \tag{1.24}$$

The smoothed area average is found in the spectral domain as

$$\bar{F}_{O_W} = \frac{1}{\bar{O}_{00}^W} \sum_{n=0}^{\infty} \sum_{m=-n}^{n} w_n \bar{O}_{nm} \bar{f}_{nm} \ . \tag{1.25}$$

The choice $w_0 = \bar{w}_{00}^{00} = 1$ ('filter normalization') guarantees that

$$\frac{1}{4\pi} \int_\Omega O_W d\omega = \bar{O}_{00}^W = \bar{O}_{00} = \frac{1}{4\pi} \int_\Omega O d\omega \ . \tag{1.26}$$

I.e. the 'area' of the smoothly varying window O_W equals to the area of O.

But, the smoothing kernel will inevitably 'leak' energy beyond the original region. I.e.

$$\frac{1}{4\pi} \int_\Omega O_W d\omega = \frac{1}{4\pi} \int_O O_W d\omega + \frac{1}{4\pi} \int_{\Omega/O} O_W d\omega \ . \tag{1.27}$$

The above can be transferred to the more general case of non-isotropic smoothing without any problem.

1.3.2 Amplitude Damping ('Bias')

For a given area O, windowing or smoothing will decrease the amplitude of the average $\bar{F}_W$ with respect to the original average $\bar{F}$. What causes this reduction is best understood by explicitly writing down the 'reduction factor' $\beta_{O,W,F}$, which we define as

$$\beta_{O,W,F} = \frac{\bar{F}_{O_W}}{\bar{F}_O} \tag{1.28}$$

and which is specific for a certain area O, a certain window kernel W, and an input function F. For an isotropic smoothing kernel,

$$\beta_{O,W,F} = \frac{\bar{O}}{\bar{O}_W} \frac{\int_\Omega O_W F d\omega}{\int_\Omega O F d\omega} = \frac{1}{w_0} \frac{\sum_{n=0}^{\infty} \sum_{m=-n}^{n} w_n \bar{O}_{nm} \bar{f}_{nm}}{\sum_{n=0}^{\infty} \sum_{m=-n}^{n} \bar{O}_{nm} \bar{f}_{nm}} \tag{1.29}$$

and for $w_0 = 1$

$$\beta_{O,W,F} = 1 - \frac{1}{\bar{O}_{00} \bar{F}_O} \sum_{n=1}^{\infty} \sum_{m=-n}^{n} (1 - w_n)\, \bar{O}_{nm} \bar{f}_{nm} \tag{1.30}$$

The reduction factor clearly depends on the basin shape, the filter coefficients, and the signal itself.

Example. For $w_0 = 1$ and $F = c$, where c is a constant (i.e. the signal is constant over the whole sphere), β is exactly one, i.e. no damping occurs at all.

Example. For $w_0 = 1$ and $F = c \cdot O(\lambda, \theta)$ (the signal is constant over the area O, and exactly zero outside), the damping factor becomes (considering $\int_\Omega O^2 d\omega = \int_\Omega O d\omega = \bar{O}_{00}$)

$$\beta_{O,W,c \cdot O} = 1 - \frac{1}{c \cdot \bar{O}_{00}} \sum_{n=1}^{\infty} \sum_{m=-n}^{n} (1 - w_n)\, \bar{O}_{nm}^2$$

Example. In ([15]), a 'standard damping factor' ('scaling bias') is defined for smoothing a constant signal over a spherical cap area, and numbers are provided for Gaussian and DDK filters of different degree of smoothing and at different geographical latitudes.

1.4 Filter Shape

1.4.1 Impulse Response

For comparing smoothing kernels in the spatial domain, it is helpful to map a kernel's impulse response. This can be best understood when we imagine an area O shrinks to a point on the sphere. By letting the basin function degrade to a Dirac function (we want to see the smoothing effect for a particular location λ', θ'), we obtain

$$O^{\delta}(\lambda,\theta) = \delta^{\lambda',\theta'}(\lambda,\theta) = \begin{cases} \infty & \text{for} \quad \lambda'=\lambda, \theta'=\theta \\ 0 & \quad \text{otherwise} \end{cases} \tag{1.31}$$

and

$$\bar{O}^{\delta}_{nm} = \frac{1}{4\pi}\int_{\Omega} \delta^{\lambda',\theta'}(\lambda'',\theta'')\bar{Y}_{nm}(\lambda'',\theta'')d\omega = \bar{Y}_{nm}(\lambda',\theta') \ . \tag{1.32}$$

Remark. Eq. (1.32) is very helpful in practical applications, since one only has to compute the $\bar{Y}_{nm}(\lambda',\theta')$. Or, with the spherical harmonic representation of the Dirac,

$$O^{\delta}(\lambda,\theta) = \sum_{n=0}^{\infty}\sum_{m=-n}^{n} \bar{Y}_{nm}(\lambda',\theta')\bar{Y}_{nm}(\lambda,\theta) \ . \tag{1.33}$$

Consequently, the impulse response of the most general non-isotropic two-point kernel W will be

$$O^{\delta}_{W}(\lambda,\theta) = \sum_{n=0}^{\infty}\sum_{m=-n}^{n}\sum_{n'=0}^{\infty}\sum_{m'=-n'}^{n'} \bar{w}^{n'm'}_{nm}\bar{Y}_{n'm'}(\lambda',\theta')\bar{Y}_{nm}(\lambda,\theta) \ . \tag{1.34}$$

And for an isotropic kernel

$$O^{\delta}_{W}(\lambda,\theta) = \sum_{n=0}^{\infty}\sum_{m=-n}^{n} w_n\bar{Y}_{nm}(\lambda',\theta')\bar{Y}_{nm}(\lambda,\theta) \ . \tag{1.35}$$

1.4.2 Localization

The localization of an isotropic smoothing kernel can be best measured by its 'half-with' radius, i.e. the distance $d = R\psi_d$ where the kernel drops from 1 at $\psi = 0$ to $\frac{1}{2}$

$$W(\psi_d) = \frac{1}{2} \ . \tag{1.36}$$

For non-isotropic kernels, measuring the localization is more difficult. Unlike with isotropic kernels, it will depend on the particular location λ', θ'. There, one might compute the half-with radius in two directions - North and East.

Following [17] and[1], [15] introduced the variance σ_W of the squared normalized window function $W(\lambda,\theta)$ at location λ', θ' as a single measure for its localization properties. The variance is the second centralized moment of a probability density function defined on the sphere; it is an integral measure for the spreading about the expectation and it is independent of introducing a particular coordinate system on the sphere.

We suppose with [1] that W^2 has been normaized,

$$\int_\Omega W^2(\lambda',\theta')d\omega = \sum_{n=0}^{\infty}\sum_{m=-n}^{n}\left(\bar{w}_{nm}^{n'm'}\bar{Y}_{n'm'}(\lambda',\theta')\right)^2 = 1\ . \tag{1.37}$$

The integration in the first term applies to λ, θ. Normalization is required in order to interprete W as a probability density function. The expectation in the space domain is introduced ([1]) via

$$\boldsymbol{\mu}_W = \int_\Omega \mathbf{e}\ W^2\ d\omega \tag{1.38}$$

where $\mathbf{e} = (\sin\theta\cos\lambda, \sin\theta\sin\lambda, \cos\theta)^T$ is the unit vector pointing from the origin to a location on Ω. If $W^2(\lambda,\theta)$ (for given λ',θ') is thought to represent a surface density distribution, $\boldsymbol{\mu}_W$ points to its center of mass (which is inside of Ω).

As the unit vector can be represented through the unnormalized degree-1 spherical harmonics

$$\mathbf{e} = (Y_{11}, Y_{1\ -1}, Y_{10})^T \tag{1.39}$$

we can write the components of $\boldsymbol{\mu}_W$ as

$$\mu_{W;x} = \int_\Omega W^2 Y_{11} d\omega = (W^2)_{11} \qquad \mu_{W;y} = (W^2)_{1\ -1} \qquad \mu_{W;z} = (W^2)_{10}\ . \tag{1.40}$$

The variance of $W(\lambda,\theta)$ is introduced in the usual fashion, i.e. as the expectation of $(\mathbf{e}-\boldsymbol{\mu}_W)^2$

$$\sigma_W^2 = \int_\Omega (\mathbf{e}-\boldsymbol{\mu}_W)^2 W^2 d\omega \tag{1.41}$$

Because of $(\mathbf{e}-\boldsymbol{\mu}_W)^2 = 1 + (\boldsymbol{\mu}_W)^2 - 2\mathbf{e}^T\boldsymbol{\mu}_W$ and $\int -2\mathbf{e}^T\boldsymbol{\mu}_W W^2 d\omega = -2(\boldsymbol{\mu}_W)^2$, the variance is simply

$$\sigma_W^2 = 1 - (\boldsymbol{\mu}_W)^2 = 1 - \sum_{m=-1}^{1}\left((W^2)_{1m}\right)^2\ . \tag{1.42}$$

and its computation requires only the computation of the degree–1 harmonics of W^2.

The degree–1 harmonics of W^2 may be computed directly, involving the *Clebsch-Gordon* coefficients, or simply by projecting the normalized W^2 onto a grid and subsequent spherical harmonic analysis.

2

Principal Component Analysis and Related Ideas

Products of geodetic observing systems (GRACE, altimetry) and geophysical modelling are most often represented in form of time series of spatial maps (total water storage, sea level anomalies,...). The user of these products will often find a few spatial pattern dominating the variability within these maps. Identifying these pattern can aid in physical interpretation, comparison of different data sets, and removing unnecessary small-scale signals or noise. Eigenspace techniques as the principal component method are among the most popular analysis techniques supporting these objectives. The purpose of this chapter is to describe the mathematical concepts behind the principle component analysis (PCA), to introduce some alternative formulations, and to make the reader aware of some of the many choices to be made by the analyst.

2.1 Principle Component Analysis

2.1.1 PCA as a Data Compression Method: Mode Extraction and Data Reconstruction

Sampling spatio-temporal fields can lead to huge amounts of data. For example, a field observed or modelled on a $1^\circ \times 1^\circ$ grid, with a time step of one day, provides already more than $23 \cdot 10^6$ data elements for one year of data. It is now a challenging task to reduce the dimensionality of the data vector and to identify the most important patterns explaining the variability of the system. The *Empirical Orthogonal Functions (EOF)* technique, also called *Principal Component Analysis (PCA)*, has become one of the most widely used methods. General references are [6] and [7]. In pattern analysis, PCA is also known as Karhunen-Loeve transform or Hotelling transform.

PCA has been used extensively to extract individual dominant *modes* of the data variability, while simultaneously suppressing those modes connected with low variability and therefore reducing the number of data efficiently. The physical interpretability of the obtained pattern (i.e. in terms of independent physical processes) is, however, a point of discussion as the obtained modes are by definition orthogonal in space and time and this is not necessarily so in reality.

Consider the $n \times 1$ data vector $\mathbf{y}$, given for p time epochs t_i,

$$\mathbf{y}_i = \begin{pmatrix} y_{1;i} \\ y_{2;i} \\ \vdots \\ y_{n;i} \end{pmatrix} \qquad i = 1 \dots p \; . \tag{2.1}$$

Typically, $\mathbf{y}_i$ contains the values of an observed or modelled field in n locations (the nodes of a two–dimensional grid or a set of discrete scattered observation sites; but the $\mathbf{y}_i$ could also contain n spherical harmonic coefficients), at time t_i. We will assume that the data are centered, i.e. the time average per node $\frac{1}{p}\sum_{i=1}^{p} y_{j;i}$ is already reduced from the observations $y_{j;i}$, or

$$\frac{1}{p}\sum_{i=1}^{p} y_{j;i} = 0 \tag{2.2}$$

Another way to look at eq. (2.1) is to decompose the data vector $\mathbf{y}_i = \mathbf{I}\mathbf{y}_i$ according to the individual locations,

$$\mathbf{y}_i = y_{1;i}\begin{pmatrix} 1 \\ 0 \\ \vdots \\ 0 \end{pmatrix} + y_{2;i}\begin{pmatrix} 0 \\ 1 \\ \vdots \\ 0 \end{pmatrix} + \dots + y_{n;i}\begin{pmatrix} 0 \\ 0 \\ \vdots \\ 1 \end{pmatrix} = y_{1;i}\mathbf{u}_1 + y_{2;i}\mathbf{u}_2 + \dots + y_{n;i}\mathbf{u}_n \; . \tag{2.3}$$

The basis vectors $\mathbf{u}_j$ are independent of time, orthogonal, normalized with respect to the standard scalar product $(\mathbf{a}, \mathbf{b}) = \mathbf{a}^T\mathbf{b}$, and they are each associated with an individual location. One may interprete the original observations $y_{j;i}$ as coordinates in an "observation space" with regard to the trivial unit basis $\mathbf{u}_j$, in an n-dimensional vector space. Clearly, this interpretation suggests that other bases and other coordinates might be useful as well. The following will lead to a different choice of basis.

We collect all $\mathbf{y}_i$ in the $n \times p$ data matrix $\mathbf{Y}$ (assuming in what follows that the data is complete in the sense that for every location j there exists a data value $y_{j;i}$ for any epoch t_i). With other words, we assume for every location in the set there exists an uninterrupted time series of observations. The data matrix is then

$$\mathbf{Y} = (\mathbf{y}_1, \mathbf{y}_2, \ldots, \mathbf{y}_p) = \begin{pmatrix} y_{1;1} & y_{1;2} & \cdots & y_{1;p} \\ y_{2;1} & y_{2;2} & \cdots & y_{2;p} \\ \vdots & \vdots & & \vdots \\ y_{n;1} & y_{n;2} & \cdots & y_{n;p} \end{pmatrix} . \tag{2.4}$$

Its rows contain the time series per location, whereas its columns contain the entire data from all locations per time epoch.

We might be weighting the data matrix, e.g taking the individual accuracy of the data at different locations into account, or according to the latitude of the nodes. In this case, the homogeneized data matrix becomes $\bar{\mathbf{Y}} = \mathbf{YG}$, where $\mathbf{GG}^T = \mathbf{P}$ is the weight matrix.

The $n \times n$ signal covariance matrix $\mathbf{C}$ contains the variances and covariances (i.e. second central moments) of the data viewed as time series per location. From the data samples $\mathbf{y}_i$, it can be estimated (empirically) as

$$\mathbf{C} = \frac{1}{p}\mathbf{YY}^T = \frac{1}{p} \begin{pmatrix} \sum_{i=1}^p y_{1;i}^2 & \sum_{i=1}^p y_{1;i}y_{2;i} & \cdots \sum_{i=1}^p y_{1;i}y_{n;i} \\ \sum_{i=1}^p y_{2;i}y_{1;i} & \sum_{i=1}^p y_{2;i}^2 & \cdots \sum_{i=1}^p y_{2;i}y_{n;i} \\ \vdots & \vdots & \vdots \\ \sum_{i=1}^p y_{n;i}y_{1;i} & \sum_{i=1}^p y_{n;i}y_{2;i} & \cdots \sum_{i=1}^p y_{n;i}^2 \end{pmatrix} , \tag{2.5}$$

or using the weighted matrix $\bar{\mathbf{Y}}$ instead. Note that the signal covariance matrix $\mathbf{C}' = \frac{1}{n}\mathbf{Y}^T\mathbf{Y}$, in contrast, contains the spatial variance and covariances of the data viewed as a function of position, for any t_i: there the sum extends over the n locations. Adding all the n individual variances from the time series provides what is often called the total variance,

$$\Delta^2 = \frac{1}{p}\sum_{j=1}^{n}\left(\sum_{i=1}^{p} y_{j;i}^2\right) = \mathrm{trace}(\mathbf{C}) . \tag{2.6}$$

An alternative way to decompose the data vector is given by the eigenvalue decomposition of the signal covariance matrix $\mathbf{C}$

$$\mathbf{C} = \mathbf{E}\boldsymbol{\Lambda}\mathbf{E}^T \tag{2.7}$$

where $\boldsymbol{\Lambda}$ is a diagonal matrix containing the n eigenvalues λ_i, and the columns of the orthogonal $n \times n$ matrix $\mathbf{E}$ contain the corresponding eigenvectors $\mathbf{e}_i$. The sum of all eigenvalues equals to the matrix trace, and therefore to the total variance

$$\sum_{j=1}^{n} \lambda_j = \Delta^2. \tag{2.8}$$

We assume the eigenvalues and eigenvectors are ordered according to the magnitude of the eigenvalues; i.e. λ_1 is the largest one. Then, one can state that each eigenvalue "explains" a fraction

$$\eta_j = \frac{\lambda_j}{\Delta^2} \tag{2.9}$$

of the total variance, with the first eigenvalue explaining the largest part and so on. The eigenvalues of $\mathbf{C} = \frac{1}{p}\mathbf{Y}\mathbf{Y}^T$ equal to $\frac{1}{\sqrt{p}}$ times the singular values of the data matrix $\mathbf{Y}$. The SVD of the data matrix can be written

$$\mathbf{Y} = \mathbf{E}\boldsymbol{\Delta}\bar{\mathbf{D}} \ , \tag{2.10}$$

where of course now

$$\lambda_j = \frac{1}{p}\Delta_j^2 \tag{2.11}$$

We will come back later to the $n \times n$ diagonal matrix $\boldsymbol{\Delta}$ and the $n \times p$ orthogonal matrix $\bar{\mathbf{D}}$.

Principle component analysis replaces the basis $\mathbf{u}_j$ by the eigenvectors $\mathbf{e}_j$ of $\mathbf{C}$ as the vector basis for representing the original observations $\mathbf{y}_i$. One has to adopt a convention about the scaling of the eigenvectors, and in what follows we will assume they are normalized,

$$\mathbf{e}_j^T\mathbf{e}_j = 1 \ , \tag{2.12}$$

and their first entry is positive

$$e_{1;j} > 0 \tag{2.13}$$

just as it was the case for the original basis $\mathbf{u}_j$. In the same way as the $\mathbf{u}_j$ can be associated with a discrete version of a delta function (they point exactly at the j-th data location with a value of one there, and zero values otherwise), the $\mathbf{e}_j$ can be viewed as discrete version of a function which describes common pattern in the entire data. They are called empirical orthogonal functions (EOFs) or simply 'modes'. The first EOF $\mathbf{e}_1$ contains thus the dominant pattern (that is, if λ_1 is distinctly larger than the other eigenvalues). If the original data is provided on two-dimensional gridded locations, it is common to visualize the corresponding EOFs on this grid. Then, the principal component representation of the $n \times 1$ data vactor at t_i, $i = 1, \ldots, p$ is

$$\mathbf{y}_i = d_{1;i}\mathbf{e}_1 + d_{2;i}\mathbf{e}_2 + \cdots + d_{n;i}\mathbf{e}_n = \sum_{j=1}^{n} d_{j;i}\mathbf{e}_j = \mathbf{E}\mathbf{d}_i \tag{2.14}$$

where the "principal components" (PCs) or PC scores $d_{j;i}$ are determined from projecting the original data onto the new basis

$$d_{j;i} = \mathbf{e}_j^T\mathbf{y}_i \ . \tag{2.15}$$

The $d_{j;i}$ can be viewed upon as time series, $i = 1 \ldots p$, wheras the index j points at the pattern $\mathbf{e}_j$ where the time series is associated with. Or,

$$\mathbf{d}_i = \mathbf{E}^T \mathbf{y}_i \ . \tag{2.16}$$

Since $\mathbf{E}^T\mathbf{E} = \mathbf{I}$, this can be written as $\mathbf{d}_i = (\mathbf{E}^T\mathbf{E})^{-1}\mathbf{E}^T\mathbf{y}_i$ as well. As the ordering is according to the magnitude of the eigenvalues, it is often sufficient to compute only a few, say $\bar{n}$, of the $d_{j;i}$. The reconstructed data will then still exhibit the largest part of the total variablity:

$$\bar{\mathbf{y}}_i = \sum_{j=1}^{\bar{n}} d_{j;i}\mathbf{e}_j \ . \tag{2.17}$$

By this construction, EOFs constitute (normalized) spatial patterns whose amplitude evolution is given by the corresponding PC. The EOF itself does not change in time.

Remark. In other words, PCA decomposes the original data into time-invariant ('standing') spatial pattern, which are scaled by the corresponding time-variable PC. Therefore, PCA is not suitable for discovering *propagating pattern* in the data, since those will be distributed over several standing modes in the analysis.

Remark. Since the data are assumed as centered, one may say that PCA makes use of the second central moments of the data (only) to decorrelate them.

Remark. From the point of view of estimation theory, Eq. (2.5) assumes that the data are perfectly centered. In practice, one will probably compute and remove the sample mean of the time series. Then, in Eq. (2.5), one might use $\frac{1}{p-1}$ in place of $\frac{1}{p}$ in order to unbiasedly estimate the second central moments. It does *not* matter for the computation of the EOFs and the PCs, since the EOFs will be normalized (Eq. 2.12) anyway and the PCs follow from the normalized EOFs and the data.

Remark. The reconstructed data, Eq. (2.17) can be expressed by

$$\bar{\mathbf{y}}_i = \mathbf{E}\mathbf{I}^{(\bar{n})}\mathbf{E}^T\mathbf{y}_i$$

where $\mathbf{I}^{(\bar{n})}$ is a diagonal matrix with unity in the first $\bar{n}$ entries and zero otherwise, I.e., decomposition and partial reconstruction can be viewed as a linear operation (in first order at least).

From Eq. (2.14), it is clear that the data matrix $\mathbf{Y}$ is referred to the EOFs by

$$\mathbf{Y} = \mathbf{E}\mathbf{D} \ , \tag{2.18}$$

where the rows of $\mathbf{D}$ now contain the PCs for all EOFs (e.g., the first row contains the temporal evolution of the first EOF), and the columns of $\mathbf{D}$ contain the PC vectors $\mathbf{d}_i$ (each vector contains the temporal amplitude of all EOFs for one particular epoch). With other words, we write

$$\mathbf{D} = (\mathbf{d}_1, \mathbf{d}_2, \ldots, \mathbf{d}_p) = \begin{pmatrix} d_{1;1} & d_{1;2} & \ldots & d_{1;p} \\ d_{2;1} & d_{2;2} & \ldots & d_{2;p} \\ \vdots & \vdots & & \vdots \\ d_{n;1} & d_{n;2} & \ldots & d_{n;p} \end{pmatrix} .$$

Then, for the total variance

$$\Delta^2 = \mathrm{trace}\left(\mathbf{E}\mathbf{D}\mathbf{D}^T\mathbf{E}^T\right) = \mathrm{trace}\left(\mathbf{D}^T\mathbf{D}^T\right) = \sum_{j=1}^{n}\sum_{i=1}^{p} d_{j;i}^2 \; . \tag{2.19}$$

The aim of PCA is to find a linear combination of the original data nodes that explains the maximum variability (variance) of the data. This means, we are searching for the mode $\mathbf{e}$ such that $\mathbf{Ye}$ has maximum variance. The variance of the centered time series $\mathbf{Ye}$ is

$$\frac{1}{p}(\mathbf{Ye})^T(\mathbf{Ye}) = \frac{1}{p}\mathbf{e}^T\mathbf{C}\mathbf{e} \; . \tag{2.20}$$

Usually we require $\mathbf{e}$ to be normalized. The task is then to maximize Eq. (2.20) subject to $\mathbf{e}^T\mathbf{e} = 1$. The solution to this problem is the eigenvalue problem $\mathbf{Ce} = \lambda\mathbf{e}$, with eigenvectors $\mathbf{e}_i$ and eigenvalues λ_i as introduced earlier.

However, the data vectors $\mathbf{y}_i$ will contain a random error, and such will the eigenvalues and eigenvectors derived from the data matrix. This has to be considered in particular if eigenvalues are close to each other.

2.1.2 Temporal PCA versus Spatial PCA

PCA as described above is sometimes called *temporal PCA*, since it departs from the correlations between time series of data (which are contained in the $n \times n$ covariance matrix $\mathbf{C}$). On the other hand, it is perfectly valid to consider, for the same data set, the spatial correlations and built the $p \times p$ spatial covariance matrix $\mathbf{C}' = \frac{1}{n}\mathbf{Y}^T\mathbf{Y}$, or

$$\mathbf{C}' = \frac{1}{n}\mathbf{Y}^T\mathbf{Y} = \frac{1}{n}\begin{pmatrix} \sum_{j=1}^n y_{j;1}^2 & \sum_{j=1}^n y_{j;1}y_{j;2} & \ldots \sum_{j=1}^n y_{j;1}y_{j;p} \\ \sum_{j=1}^n y_{j;2}y_{j;1} & \sum_{j=1}^n y_{j;2}^2 & \ldots \sum_{j=1}^n y_{j;2}y_{j;p} \\ \vdots & \vdots & \vdots \\ \sum_{j=1}^n y_{j;p}y_{j;1} & \sum_{j=1}^n y_{j;p}y_{j;2} & \ldots \sum_{j=1}^n y_{j;p}^2 \end{pmatrix} . \tag{2.21}$$

In fact, if $p << n$, storing $\mathbf{C}'$ requires much less memory space compared to storing $\mathbf{C}$.

PCA based upon $\mathbf{C}'$ is called spatial PCA. Of course, temporal and spatial PCA are closely related: $\mathbf{C}$ and $\mathbf{C}'$ are of different dimension but they share the same eigenvalues (apart from a factor that depends only on n and p).

An eigenvalue decomposition (and comparison with the decomposition of $\mathbf{C}$) reveals

$$\mathbf{C}' = \frac{p}{n}\,\bar{\mathbf{D}}^T\boldsymbol{\Lambda}\bar{\mathbf{D}} \tag{2.22}$$

where we have $\bar{\mathbf{D}} = \boldsymbol{\Delta}^{-1}\mathbf{E}^T\mathbf{Y} = \boldsymbol{\Delta}^{-1}\mathbf{D}$.

It is thus obvious that the k-th EOF of the spatial PCA (k-th column of $\bar{\mathbf{D}}^T$) corresponds to the k-th PCs of the temporal PCA. Alternatively, this can be seen as follows: From

$$\mathbf{C}\mathbf{e}_j = \lambda_j\mathbf{e}_j$$

follows

$$\frac{n}{np}\mathbf{Y}^T\mathbf{Y}\mathbf{Y}^T\mathbf{e}_j = \lambda_j\mathbf{Y}^T\mathbf{e}_j$$

and the eigenvectors of $\mathbf{C}'$ can be read off as $\mathbf{Y}^T\mathbf{e}_j$. Thus

$$\mathbf{E}' = \mathbf{Y}^T\mathbf{E} = \mathbf{D} = \boldsymbol{\Delta}\bar{\mathbf{D}}\ .$$

2.1.3 PCA of Linearly Transformed Data

It is interesting to consider the PCA of a set of linearly transformed $m \times 1$ data vectors

$$\mathbf{z}_i = \mathbf{A}\mathbf{y}_i, \qquad i = 1 \dots p \tag{2.23}$$

with $m \times n$ matrix $\mathbf{A}$. Again p is the number of time epochs. The number of data nodes m might be larger, equal or less than n.

Example. The original data might contain spherical harmonic coefficients of a field, and the transformed data contain gridded values. In this case $m > n$ is not uncommon. Matrix $\mathbf{A}$ contains the spherical harmonics for each given coefficient evaluated for each grid node.

Example. The original data contain values on a global grid of certain spacing. We ask in how far the EOFs and PCs on a local subgrid, i.e. for some region of the globe, will differ from those evaluated from the global data set. In this case, $m < n$ and the matrix $\mathbf{A}$ equals to the identity matrix, with its rows removed for all nodes that are not present in the local subgrid.

Obviously the transformed data matrix is $\mathbf{Z} = \mathbf{A}\mathbf{Y}$. Furthermore we have

$$\mathbf{C}_z = \frac{1}{p}\mathbf{Z}\mathbf{Z}^T = \frac{1}{p}\mathbf{A}\mathbf{Y}\mathbf{Y}^T\mathbf{A}^T = \mathbf{A}\mathbf{E}\boldsymbol{\Lambda}\mathbf{E}^T\mathbf{A}^T \tag{2.24}$$

where $\mathbf{E}$ and $\boldsymbol{\Lambda}$ contain the eigenvectors and eigenvalues of the original data covariance matrix. Obviously, the eigenvectors and eigenvalues of $\mathbf{C}_z$ will differ from those of $\mathbf{C}$, meaning that both the EOFs and the PCs of the transformed data will differ from those of the original data (unless in some special cases).

Let μ_i be the eigenvalues of $\mathbf{A}^T\mathbf{A}$. For the eigenvalues of $\mathbf{C}_z = \mathbf{A}\mathbf{C}\mathbf{A}^T$, which equal to the eigenvalues of $\mathbf{C}\mathbf{A}^T\mathbf{A}$, the following inclusion holds ([5])

$$\lambda_i^z \in [\min(\mu_i) \cdot \min(\lambda_i), \max(\mu_i) \cdot \max(\lambda_i)] \tag{2.25}$$

This illustrates clearly, how the spectrum of the transformed data is widened by the spectrum of $\mathbf{A}^T\mathbf{A}$.

2.1.4 PCA as a Data Whitening Method: Homogeneization

Obviously, one can interprete the PCs as a 'whitened' version of the original data. To make this clear, we will consider instead of

$$\mathbf{d}_i = \mathbf{E}^T \mathbf{y}_i \tag{2.26}$$

the homogeneized PCs $\bar{d}_{j;i} = \frac{1}{\sqrt{\lambda_i}} d_{j;i}$, or

$$\bar{\mathbf{d}}_i = \mathbf{\Lambda}^{-\frac{1}{2}} \mathbf{d}_i = \mathbf{\Lambda}^{-\frac{1}{2}} \mathbf{E}^T \mathbf{y}_i = \bar{\mathbf{E}}^T \mathbf{y}_i \ . \tag{2.27}$$

Here, we have introduced the column-by-column scaled matrix $\bar{\mathbf{E}} = \mathbf{E}\mathbf{\Lambda}^{-\frac{1}{2}}$.

Remark. It is clear by now that the homogeneized PCs $\bar{\mathbf{d}}_i$ are the column vectors of the SVD matrix $\bar{\mathbf{D}}$.

The scaled EOFs are not of unit length anymore, but still orthogonal,

$$\bar{\mathbf{E}}^T \bar{\mathbf{E}} = \mathbf{\Lambda}^{-1} \ . \tag{2.28}$$

The signal covariance matrix of the original data $\mathbf{y}_i$ is $\mathbf{C} = \mathbf{E}\mathbf{\Lambda}\mathbf{E}^T$, thus the covariance of the PCs will be

$$\mathbf{C}_{\mathbf{d}} = \mathbf{E}^T \mathbf{E}\mathbf{\Lambda}\mathbf{E}\mathbf{E}^T = \mathbf{\Lambda} \ , \tag{2.29}$$

or, for clarity,

$$\sum_{i=1}^{p} d_{j;i}^2 = \lambda_j \ .$$

And the signal covariance of the homogeneized PCs will be

$$\mathbf{C}_{\bar{\mathbf{d}}} = \mathbf{\Lambda}^{-\frac{1}{2}} \mathbf{E}^T \mathbf{E}\mathbf{\Lambda}\mathbf{E}\mathbf{E}^T \mathbf{\Lambda}^{-\frac{1}{2}} = \mathbf{I} \ . \tag{2.30}$$

From the last two expressions, it is obvious that the PCs and the homogeneized PCs are uncorrelated, with the latter ones also being of unit variance. Therefore, the (homogeneized) PCA is often viewed as a data whitening transformation. The homogeneized EOFs are directly obtained from applying the rescaling to the original eigenvectors

$$\bar{\mathbf{e}}_j = \frac{1}{\sqrt{\lambda_j}} \mathbf{e}_j \ , \tag{2.31}$$

of the data.

2.1.5 Number of Modes

In many applications of PCA, we will avoid to retain all n modes, but rather use a subset of $\bar{n}$ *dominant* ones. The reasoning can be different: We may want to compress the data, or we may want to get rid of those modes that supposedly contain noise. Or, PCA is just considered as a preprocessing and we will subsequently apply e.g. rotation on the dominant modes. Let $\bar{\mathcal{J}} = \{j_1, j_2, \ldots j_{\bar{n}}\}$ denote the index set of all modes to be retained, i.e.

$$\bar{\mathbf{y}}_i = \sum_{j \in \bar{\mathcal{J}}} d_{j;i} \mathbf{e}_j \ .$$

A rule that determines $\bar{\mathcal{J}}$ is called a *selection rule.*

It has been suggested by Eq. (2.9) that each eigenvalue of the data covariance explains a certain fraction of the total variance Δ^2, Eq. (2.6). This indicates that the strategy to choose a reasonable subset of modes could simply be

$$\bar{\mathcal{J}} = \{j | \sum_{j \in \bar{\mathcal{J}}} \eta_j > \epsilon\} \ .$$

This strategy is by far the most often followed one, with a typical threshold value of 0.9.

A selection rule (*North's rule*) that is often considered goes back to [18]. It is based on the perception that the data $\mathbf{y}_i$ represent independent realizations or samples of a random field with unknown stochastic moments. From these realizations, one will be able to reconstruct the *true* covariance $\mathbf{C}'$ only up to an error that depends on $\mathbf{C}'$ and the number n of data realizations. With other words, $\mathbf{C}$ as computed through Eq. (2.5) will be considered as a stochastic quantity being contaminated by an error whose covariance can be estimated from $\mathbf{C}$ and n. Therefore, the eigenvalues and eigenvectors of $\mathbf{C}$ have to be considered as stochastic as well. [18] proceed to show that 'typical' errors of neighbouring eigenvalues and eigenvectors will then be

$$\delta\lambda_j = \sqrt{\frac{2}{n}}\lambda_j + \cdots \qquad \delta\mathbf{e}_j = \frac{\delta\lambda_j}{\lambda_k - \lambda_j}\mathbf{e}_k + \cdots$$

'Neighbouring' means that λ_k is the eigenvalue numerically closest to λ_j. This selection rule says that if the 'typical' error of an eigenvalue is comparable to the difference of this eigenvalue to its neighbour, then the 'typical' error of the corresponding EOF will be of the size of the neighbouring EOF itself. One will then tend to disregard this mode in the reconstruction. Or,

$$\bar{\mathcal{J}} = \{j | \delta\lambda_j < |\lambda_k - \lambda_j| = \min_{i \neq j} |\lambda_i - \lambda_j|\} \ .$$

Several other selection rules have been proposed since then, based on different principles. More recently, Monte Carlo methods have been applied frequently to test the statistical significance of modes.

2.1.6 PCA as a Tool for Comparing Multiple Data Sets

We are often interested in comparing multiple data sets, e.g. satellite-derived vs. modelled, or different model output data sets. Several statistical algorithms allow to derive correlation measures, similarities and joint pattern and so on. Here, we will only focus on the application of the PCA as described before in such a situation.

Consider the $n \times 1$ vector $\mathbf{y}$, given for p time epochs t_i, and extracted from M different data sets, or

$$\mathbf{y}_i^{(m)} = \begin{pmatrix} y_{1;i}^{(m)} \\ y_{2;i}^{(m)} \\ \vdots \\ y_{n;i}^{(m)} \end{pmatrix} \qquad i = 1 \dots p \ , \qquad m = 1 \dots M \ , \tag{2.32}$$

which we may recast in a 'super data matrix'

$$\mathbf{X} = \left(\mathbf{Y}^{(1)}, \mathbf{Y}^{(2)}, \dots, \mathbf{Y}^{(m)} \right) \ . \tag{2.33}$$

If all data vectors are considered as equally good, bias-free (i.e. centered free of errors), and describing the same phenomena apart from unavoidable data/model errors, i.e. as independent realizations of the same data vector, one may simply compute the covariance matrix

$$\mathbf{C} = \frac{1}{pM} \mathbf{X}\mathbf{X}^T \tag{2.34}$$

and go on as described before.

If we suspect that different sensors or models see different phenomena, which is to say the data are not coming from the same p.d.f., one may of course apply PCA on each data set independently. This provides M covariance matrices $\mathbf{C}^{(m)}$. A comparison is then hampered by the fact that each data set will be represented in its own basis $\mathbf{e}_j^{(m)}$. To facilitate comparison, one may project all data sets onto the basis derived from $\mathbf{C}$ or from one of the data sets (maybe the one we trust most), say. from $\mathbf{C}^{(m^*)}$. This is, we compare the data sets on the level of principle componets with a joint basis,

$$\mathbf{d}_i^{(m)} = \mathbf{E}^T \mathbf{y}_i^{(m)} \tag{2.35}$$

or

$$\mathbf{d}_i^{(m)} = \mathbf{E}^{(m^*)^T} \mathbf{y}_i^{(m)} \ . \tag{2.36}$$

2.1.7 Rotation

Rotated EOF is a technique which attempts to overcome some common shortcomings of PCA. For example, the *mathematical* constraints (orthogonality of EOFs *and* uncorrelatedness of PCs) of PCA, in connection with the dependence of the computation doamin (see 'PCA of Linearly Transformed Data') may render the modes found in data difficult to interprete. *Physical modes* may not necessarily be orthogonal and thus leak into several different mathematical modes in PCA. REOF is a technique which sacrifies either orthogonality of the EOFs *or* uncorrelatedness of the PCs, while adding new optimization criteria that seek to find physically plausible modes.

Rotated homogeneized EOFs

An understanding of the idea of REOF starts with the observation that, viewed as a whitening transformation, PCA with the basis vectors $\bar{\mathbf{e}}_j$ is *not unique.* To see this, the data vectors $\mathbf{y}_i$, with covariance $\mathbf{C}$ are expressed by

$$\mathbf{y}_i = \mathbf{E}\mathbf{\Lambda}^{\frac{1}{2}}\bar{\mathbf{d}}_i \ . \tag{2.37}$$

It is possible to replace the $\bar{\mathbf{d}}_i$ by any set of $i = 1, \ldots, p$ *rotated* $n \times 1$ homogeneized PCs,

$$\bar{\mathbf{r}}_i = \mathbf{V}\bar{\mathbf{d}}_i \tag{2.38}$$

with $n \times n$ orthogonal matrix $\mathbf{V}$, i.e. $\mathbf{V}^T\mathbf{V} = \mathbf{I}$. Then,

$$\mathbf{C}_{\bar{\mathbf{r}}} = \mathbf{V}\mathbf{V}^T = \mathbf{I} \ . \tag{2.39}$$

We have

$$\bar{\mathbf{d}}_i = \mathbf{V}^T\bar{\mathbf{r}}_i \tag{2.40}$$

and

$$\mathbf{y}_i = \mathbf{E}\mathbf{\Lambda}^{\frac{1}{2}}\mathbf{V}^T\bar{\mathbf{r}}_i = \bar{\mathbf{E}}\mathbf{\Lambda}\mathbf{V}^T\bar{\mathbf{r}}_i \ . \tag{2.41}$$

It is obvious that the data covariance $\mathbf{C} = \mathbf{E}\mathbf{\Lambda}^{\frac{1}{2}}\mathbf{V}^T(\mathbf{E}\mathbf{\Lambda}^{\frac{1}{2}}\mathbf{V}^T)^T) = \mathbf{E}\mathbf{\Lambda}\mathbf{E}^T$ does not depend on $\mathbf{V}$. Hence, the transform $\mathbf{y}_i = \mathbf{E}\mathbf{\Lambda}^{\frac{1}{2}}\mathbf{V}^T\bar{\mathbf{r}}_i = \bar{\mathbf{E}}\mathbf{\Lambda}\mathbf{V}^T\bar{\mathbf{r}}_i$ with rescaled and rotated PCs whitens the data as good as the original homogeneized PCs. The rotated basis vectors (or rotated EOFs) are now the column vectors of $\bar{\mathbf{F}} = \mathbf{E}\mathbf{\Lambda}^{\frac{1}{2}}\mathbf{V}^T = \bar{\mathbf{E}}\mathbf{\Lambda}\mathbf{V}^T$.

We have seen in Eq. (2.40) that the rotated homogeneized PCs have diagonal and equal covariance, just as the original homogeneized PCs,

$$\mathbf{C}_{\bar{\mathbf{r}}} = \mathbf{C}_{\bar{\mathbf{d}}} = \mathbf{I} \ .$$

The PCs, viewed as time series per EOF, are uncorrelated and they do not loose this property when an arbitrary orthogonal rotation is applied to the EOFs. The rotated homogeneized EOFs, however, will not be orthogonal anymore,

$$\bar{\mathbf{F}}^T\bar{\mathbf{F}} = \mathbf{V}\mathbf{\Lambda}^{\frac{1}{2}}\mathbf{E}^T\mathbf{E}\mathbf{\Lambda}^{\frac{1}{2}}\mathbf{V}^T = \mathbf{V}\mathbf{\Lambda}\mathbf{V}^T \ . \tag{2.42}$$

Rotated EOFs

On the other hand, one can define rotated EOFs by straight application of an orthogonal matrix $\mathbf{V}$ to the EOFs $\mathbf{E}$,

$$\mathbf{F} = \mathbf{E}\mathbf{V}^T \tag{2.43}$$

i.e. without homogeneizing the PCs first. The data is then represented through rotated PCs,

$$\mathbf{y}_i = \mathbf{F}^T \mathbf{r}_i \ . \tag{2.44}$$

In this case, the rotated EOFs remain orthogonal, since

$$\mathbf{F}^T\mathbf{F} = \mathbf{V}\mathbf{E}^T\mathbf{E}\mathbf{V}^T = \mathbf{I} \ . \tag{2.45}$$

But now, the $i = 1, \ldots, p$ rotated PCs

$$\mathbf{r}_i = \mathbf{V}\mathbf{d}_i = \mathbf{F}^T\mathbf{y}_i \tag{2.46}$$

loose the property of being uncorrelated since

$$\mathbf{C}_\mathbf{r} = \mathbf{V}\mathbf{\Lambda}\mathbf{V}^T \ . \tag{2.47}$$

In summary, by rotation either the orthogonality of the EOFs or the uncorrelatedness of the PCs will be destroyed.

Rotation principles

So far, nothing has been said regarding the particular choice of an orthogonal matrix $\mathbf{V}$ in EOF and PC rotation. All orthogonal $\mathbf{V}$ are able to reproduce the data, whereas only for $\mathbf{V} = \mathbf{I}$ both orthogonality in space and time can be preserved. Which one (in space or time) we sacrify by rotation, depends upon application to homogeneized or original EOFs and PCs.

In REOF, one usually specifies an optimization criterion $\mathcal{F}(\mathbf{V})$ in terms of rotated EOFs or rotated PCs, to be met subject to the condition $\mathbf{V}\mathbf{V}^T = \mathbf{I}$. In other words, an orthogonal $n \times n$ matrix has $\frac{n(-1)}{2}$ degrees of freedom and these have to be chosen such as to optimize $\mathcal{F}(\mathbf{V})$.

When we have

$$\mathbf{F} = \mathbf{E}\mathbf{V}^T$$

with elements $f_{j;i}$ of the jth rotated EOF, the following family of VARIMAX criteria is in use

$$\mathcal{F}(\mathbf{V}) = \sum_{i=1}^{n} \left(\sum_{j=1}^{n} f_{j;i}^4 - \frac{\gamma}{n} \left(\sum_{j=1}^{n} f_{j;i}^2 \right)^2 \right) \ . \tag{2.48}$$

The quantity inside the summation is proportional to the variance of the square of the rotated EOFs $\mathbf{f}_j$ (for $\gamma = 1$). This variance will be big if some values $f_{j;i}$ are close to 1 and many are near 0. Consequently, it is often claimed that the varimax rotation attempts to 'simplify' the patterns by localizing the 'regions of action'.

In practice, one will rotate only the first $\bar{n}$ EOFs corresponding to the largest singular values, then the above reads

$$\mathcal{F}(\mathbf{V}) = \sum_{i=1}^{\bar{n}} \left(\sum_{j=1}^{n} f_{j;i}^4 - \frac{\gamma}{n} \left(\sum_{j=1}^{n} f_{j;i}^2 \right)^2 \right) . \tag{2.49}$$

2.2 Independent Component Analysis

We follow [12]. Consider orthogonal EOF rotation with homogeneized PCs, i.e

$$\bar{\mathbf{r}}_i = \mathbf{V}\bar{\mathbf{d}}_i \tag{2.50}$$

for $i = 1, \ldots p$ time steps. Collecting the $n \times 1$ vectors of homogeneized PCs in $n\times$ matrices $\bar{\mathbf{D}}$ and $\bar{\mathbf{R}}$, this is

$$\bar{\mathbf{R}} = \mathbf{V}\bar{\mathbf{D}} , \tag{2.51}$$

and the rotated EOFs will be

$$\bar{\mathbf{F}} = \mathbf{E}\mathbf{\Lambda}^{1/2}\mathbf{V} . \tag{2.52}$$

For any orthogonal $\mathbf{V}$ the rotated homogeneized PCs $\bar{\mathbf{r}}_i$ are uncorrelated and of unit variance, i.e. as a time series in i

$$\sum_{i=1}^{p} \bar{r}_{j;i}^2 = 1 \qquad j = 1 \ldots, n$$

$$\sum_{i=1}^{p} \bar{r}_{j;i}\bar{r}_{k;i} = 0 \qquad j \neq k$$

In [12] it is suggested to choose $\mathbf{V}$ such that the $\bar{\mathbf{r}}_i$ are close to being *independent.*

Independence is stronger than uncorrelatedness, and defining (and testing) it requires to involve higher moments of the pdf of the $\bar{r}_{j;i}$. Different criteria are in use in the literature on *Independent Component Analysis (ICA).*

The line of reasoning in [12] is as follows. If $\bar{r}_{j;i}$ and $\bar{r}_{k;i}$ are independent, then the time series of the squares $\bar{r}_{j;i}^2$, $\bar{r}_{j;i}^2$ should be uncorrelated (after centering), or

$$\sum_{i=1}^{p}\left(\bar{r}_{j;i}^2 - \frac{1}{p}\sum_{l=1}^{p}\bar{r}_{j;l}^2\right)\left(\bar{r}_{k;i}^2 - \frac{1}{p}\sum_{l=1}^{p}\bar{r}_{j;l}^2\right) = 0 \qquad j \neq k \ .$$

This can be written in matrix notation. Let $\odot$ denote the Hadamard matrix product, i.e.

$$\bar{\mathbf{R}} \odot \bar{\mathbf{R}} = \begin{pmatrix} r_{1;1}^2 & r_{1;2}^2 & \dots & r_{1;p}^2 \\ r_{2;1}^2 & r_{2;2}^2 & \dots & r_{2;p}^2 \\ \vdots & \vdots & & \vdots \\ r_{n;1}^2 & r_{n;2}^2 & \dots & r_{n;p}^2 \end{pmatrix}$$

and let $\mathbf{H} = \mathbf{H}^2$ be the $p \times p$ centering matrix (with $\mathbf{i} = (1, 1, \dots, 1)^T$)

$$\mathbf{H} = \mathbf{I} - \frac{1}{p}\mathbf{i}\mathbf{i}^T \ .$$

Then, for independent time series $\bar{r}_{j;i}$ the (empirical) covariance matrix of the centered squares

$$\mathbf{C}_{\mathbf{r}^2} = \frac{1}{p}\left((\bar{\mathbf{R}} \odot \bar{\mathbf{R}})\mathbf{H}\right)\left((\bar{\mathbf{R}} \odot \bar{\mathbf{R}})\mathbf{H}\right)^T = \frac{1}{p}(\bar{\mathbf{R}} \odot \bar{\mathbf{R}})\mathbf{H}(\bar{\mathbf{R}} \odot \bar{\mathbf{R}})^T \qquad (2.53)$$

must be diagonal.

In other words, an ICA approach can be constructed by defining an objective function $\mathcal{F}(\mathbf{V})$ that penalizes off-diagonal elements of $\mathbf{C}_{\mathbf{r}^2}$. ICA will then seek a rotation matrix $\mathbf{V}$ through optimization of $\mathcal{F}(\mathbf{V})$.

Remark. The above idea ([12]) makes use of fourth statistical moments, but other moments may be used for defining an objective function as well.

3

Appendix

3.1 Spherical Harmonics

Spherical harmonic series

It is common to represent real-valued phenomena on the sphere as spherical harmonic series

$$F(\lambda, \theta) = \sum_{n=0}^{\infty} \sum_{m=0}^{n} (C_{nm} \cos m\lambda + S_{nm} \sin m\lambda) \, P_{nm}(\cos\theta) \tag{3.1}$$

with longitude λ, colatitude θ, the spherical harmonic degree n and order m, where $n \geq m \geq 0$, the spherical harmonic coefficients C_{nm} and S_{nm}, and the associated Legendre functions of the first kind P_{nm}.

Legendre polynomials and associated Legendre functions

The associated Legendre functions of degree n and order m, $n \geq m \geq 0$, can be expressed through the m–th derivatives of the Legendre polynomials of degree n, $P_n = P_{n0}$, with respect to $t = \cos\theta$,

$$P_{nm}(t) = \left(1 - t^2\right)^{m/2} \frac{d^m P_n(t)}{dt^m} \ , \tag{3.2}$$

which may be written as

$$P_{nm}(\cos\theta) = \sin^m \theta \frac{d^m P_n(\cos\theta)}{d(\cos\theta)^m} \ . \tag{3.3}$$

They fulfill the differential equation

$$(1 - t^2)\frac{d^2 P_{nm}}{dt^2} - 2t\frac{dP_{nm}}{dt} + \left(n(n+1) - \frac{m^2}{1 - t^2}\right) P_{nm} = 0 \tag{3.4}$$

or

$$\frac{d}{d\theta}\left(\sin\theta\frac{dP_{nm}}{d\theta}\right)+\left(n(n+1)\sin\theta-\frac{m^2}{\sin\theta}\right)P_{nm}=0\ . \tag{3.5}$$

Note that sometimes (e.g. [3]) the associated Legendre functions are defined as $P_n^m=(-1)^m P_{nm}$. The Rodrigues formula expresses the Legendre polynomials P_n of degree n through the n–th derivatives of $(1-t^2)^n=\sin^{2n}\theta$,

$$P_n(t)=\frac{1}{2^n n!}\frac{d^n(t^2-1)^n}{dt^n} \tag{3.6}$$

they satisfy the differential equation

$$n(n+1)P_n-2t\frac{dP_n}{dt}+(1-t^2)\frac{d^2P_n}{dt^2}=0 \tag{3.7}$$

or

$$n(n+1)P_n+\frac{1}{\sin\theta}\frac{d}{d\theta}\left(\sin\theta\frac{dP_n}{d\theta}\right)=0\ . \tag{3.8}$$

An expansion of the Legendre polynomials and associated Legendre functions

Table 3.1. Legendre polynomials and associated Legendre functions

n	m	P_{nm}
0	0	1
1	0	$\cos\theta$
1	1	$\sin\theta$
2	0	$\frac{1}{2}(3\cos^2\theta-1)=\frac{1}{4}(3\cos 2\theta+1)$
2	1	$3\sin\theta\cos\theta=\frac{3}{2}\sin 2\theta$
2	2	$3\sin^2\theta$
3	0	$\frac{1}{2}(5\cos^3\theta-3\cos\theta)=\frac{1}{8}(5\cos 3\theta+3\cos\theta)$
3	1	$\sin\theta(\frac{15}{2}\cos^2\theta-\frac{3}{2})=\frac{3}{4}\sin\theta(5\cos 2\theta+3)$
3	2	$15\sin^2\theta\cos\theta=\frac{15}{2}\sin\theta\sin 2\theta$
3	3	$15\sin^3\theta$

into trigonometric series reads

$$P_{nm}(\cos\theta)=\sin^m\theta\sum_{q=0}^{\mathrm{int}(\frac{n-m}{2})}T_{nmq}\cos^{n-m-2q}\theta\ , \tag{3.9}$$

where $\mathrm{int}(x)$ means the integer part of x, and the coefficients T_{nmq} are given by ([10],[9])

$$T_{nmq}=\frac{(-1)^q(2n-2q)!}{2^n q!(n-q)!(n-m-2q)!}\ . \tag{3.10}$$

Relations (3.2) and (3.2) can be combined to

$$P_{nm}(t) = \frac{\left(1-t^2\right)^{m/2}}{2^n n!} \frac{d^{n+m}(t^2-1)^n}{dt^{n+m}} \ . \tag{3.11}$$

This is being used to define associate Legendre functions P_{nm} of negative order m; $0 > m \geq -n$. The relation between P_{nm} and $P_{n,-m}$ is ([8])

$$P_{n,-m}(t) = (-1)^m \frac{(n-m)!}{(n+m)!} P_{nm} \tag{3.12}$$

$$P_{nm}(t) = (-1)^m \frac{(n+m)!}{(n-m)!} P_{n,-m} \ . \tag{3.13}$$

Alternative notations for the real-valued spherical harmonic series

There are $2n+1$ spherical harmonics of degree n. Another way to write eq. (3.1) is

$$F(\lambda, \theta) = \sum_{n=0}^{\infty} \sum_{m=-n}^{n} f_{nm} Y_{nm}(\lambda, \theta) \tag{3.14}$$

with $f_{nm} = C_{nm}$ for $m \geq 0$, $f_{nm} = S_{n|m|}$ for $m < 0$, and

$$Y_{nm}(\lambda, \theta) = Y_{nm1}(\lambda, \theta) = \cos m\lambda \ P_{nm}(\cos\theta) \qquad m \geq 0 \tag{3.15}$$

$$Y_{nm}(\lambda, \theta) = Y_{n|m|2}(\lambda, \theta) = \sin |m|\lambda \ P_{n|m|}(\cos\theta) \qquad m < 0 \ . \tag{3.16}$$

Integration over the unit sphere

The spherical harmonics Y_{nm} are orthogonal on the unit sphere Ω. Integrating products of spherical harmonics Y_{nm} yields

$$\int_{\Omega} Y_{nm} Y_{n'm'} d\omega = 4\pi \frac{1}{\Pi_{nm}^2} \delta_{nn'} \delta_{mm'} \tag{3.17}$$

with

$$\Pi_{nm} = \sqrt{(2-\delta_{0m})(2n+1)\frac{(n-m)!}{(n+m)!}} \ , \tag{3.18}$$

in particular

$$\Pi_{n0} = \sqrt{(2n+1)} \ . \tag{3.19}$$

Consequently,

$$\int_{\Omega} Y_{nm} d\omega = 4\pi \delta_{n0} \delta_{m0} \ . \tag{3.20}$$

Integrals over various products of derivatives of spherical harmonics can be found in [13].

4π- or fully normalized spherical harmonics

It is common in geodesy to introduce 4π- or fully normalized associated Legendre functions

$$\bar{P}_{nm} = \Pi_{nm} P_{nm} \ . \tag{3.21}$$

The relation between the $\bar{P}_{nm}$ of positive order, $n \geq m \geq 0$ and those of negative order, $P_{n,-m}$, is

$$\begin{aligned} \bar{P}_{n,-m}(t) &= (-1)^m \bar{P}_{nm} & (3.22)\\ \bar{P}_{nm}(t) &= (-1)^m \bar{P}_{n,-m} \ . & (3.23) \end{aligned}$$

Using the $\bar{P}_{nm}$ of positive order, we introduce 4π- or fully normalized spherical harmonics

$$\bar{Y}_{nm} = \Pi_{nm} Y_{nm} \tag{3.24}$$

or

$$\begin{aligned} \bar{Y}_{nm}(\lambda,\theta) &= \cos m\lambda \ \bar{P}_{nm}(\cos\theta) \qquad m \geq 0 & (3.25)\\ \bar{Y}_{nm}(\lambda,\theta) &= \sin |m|\lambda \ \bar{P}_{n|m|}(\cos\theta) \qquad m < 0 \ . \end{aligned}$$

with spherical harmonic coefficients $\bar{C}_{nm} = \frac{1}{\Pi_{nm}} C_{nm}$, $\bar{S}_{nm} = \frac{1}{\Pi_{nm}} S_{nm}$, or $\bar{f}_{nm}$, $\bar{f}_{nm1}$, $\bar{f}_{nm2}$ accordingly. By definition, these fully normalized spherical harmonics fulfill

$$\int_{\Omega} \bar{Y}_{nm} \bar{Y}_{n'm'} d\omega = 4\pi \delta_{nn'} \delta_{mm'} \ . \tag{3.26}$$

The addition theorem relates fully (4π-) normalized spherical harmonics and the (un–normalized) Legendre polynomials

$$\frac{1}{2n+1} \sum_{m=-n}^{n} \bar{Y}_{nm}(\lambda,\theta) \bar{Y}_{nm}(\lambda',\theta') = P_n(\cos\psi) \ . \tag{3.27}$$

In particular,

$$\frac{1}{2n+1} \sum_{m=-n}^{n} \bar{Y}^2_{nm}(\lambda,\theta) = 1 \ . \tag{3.28}$$

Practical computation of the fully normalized spherical harmonics

In practice, the fully normalized associated Legendre functions $\bar{P}_{nm}(\cos\theta)$ are computed via recursion relations.

Example. One of the most often applied recursive algorithms for the normalized Legendre functions as a function of co-latitude θ is the following

$$
\begin{aligned}
c &= \cos\theta \\
s &= \sin\theta \\
\bar{P}_{00} &= 1 \\
\bar{P}_{11} &= \sqrt{3}\cdot s
\end{aligned}
$$

do $\quad n = 2, \bar{n}$

$$a_n = \sqrt{\frac{2n+1}{2n}}$$

$$\bar{P}_{nn} = a_n \cdot s \cdot \bar{P}_{n-1\,n-1}$$

end do

do $\quad n = 1, \bar{n}$

$$b_n = \sqrt{2n+1}$$

$$\bar{P}_{n\,n-1} = b_n \cdot c \cdot \bar{P}_{n-1\,n-1}$$

end do

do $\quad n = 2, \bar{n}$

do $\quad m = n, 0, -1$

$$c_n = \sqrt{\frac{(2n+1)}{(n-m)(n+m)}}$$

$$d_n = \sqrt{2n-1}$$

$$e_n = \sqrt{\frac{(n-m-1)(n+m-1)}{(2n-3)}}$$

$$\bar{P}_{nm} = c_n \cdot \left(d_n \cdot c \cdot \bar{P}_{n-1\,m} - e_n \cdot \bar{P}_{n-2\,m}\right)$$

end do

end do

Normalized complex spherical harmonics

Normalized complex spherical harmonics are introduced in different ways. Following e.g. [8] and using associated Legendre functions of positive and negative order, $n \geq m \geq -n$

$$
\begin{aligned}
\bar{\mathcal{Y}}_{nm} &= \frac{(-1)^m}{\sqrt{4\pi}} \Xi_{nm} \left(\cos m\lambda + i \sin m\lambda\right) P_{nm}(\cos\theta) \\
&= \frac{(-1)^m}{\sqrt{4\pi}} \Xi_{nm} \underbrace{e^{im\lambda} P_{nm}(\cos\theta)}_{\mathcal{Y}_{nm}}
\end{aligned}
\tag{3.29}
$$

where

$$\Xi_{nm} = \sqrt{(2n+1)\frac{(n-m)!}{(n+m)!}} = \frac{\Pi_{nm}}{\sqrt{2-\delta_{0m}}} \ . \tag{3.30}$$

Here

$$\bar{\mathcal{Y}}_{nm} = (-1)^m \bar{\mathcal{Y}}^*_{n,-m} \qquad \bar{\mathcal{Y}}^*_{nm} = (-1)^m \bar{\mathcal{Y}}_{n,-m} \tag{3.31}$$

follows from eq. (3.23) and

$$\begin{aligned}&\Xi_{nm} P_{nm}(\cos\theta)(\cos m\lambda + i \sin m\lambda)\\ &= (-1)^m \Xi_{n,-m} P_{n,-m}(\cos\theta)(\cos m\lambda - i\sin(-m\lambda)) \ .\end{aligned}$$

Consequently, in place of eq. (3.29) we could write

$$\begin{aligned}\bar{\mathcal{Y}}_{nm} &= \frac{(-1)^m}{\sqrt{4\pi}} \Xi_{nm} \left(\cos m\lambda + i \sin m\lambda\right) P_{nm}(\theta) \qquad m \geq 0 \\ &= (-1)^m \bar{\mathcal{Y}}^*_{n|m|} \qquad m < 0 \ .\end{aligned} \tag{3.32}$$

This is to relate complex spherical harmonics of negative order to associated Legendre functions of positive order. The $\bar{\mathcal{Y}}_{nm}$ are 1-normalized, thus

$$\int_\Omega \bar{\mathcal{Y}}_{nm} \bar{\mathcal{Y}}^*_{n'm'} d\omega = \delta_{nn'}\delta_{mm'} \ . \tag{3.33}$$

And,

$$\sum_{m=-n}^{n} \bar{\mathcal{Y}}_{nm}(\lambda,\theta)\bar{\mathcal{Y}}^*_{nm}(\lambda',\theta') \tag{3.34}$$

$$= \bar{\mathcal{Y}}_{n0}(\lambda,\theta)\bar{\mathcal{Y}}^*_{n0}(\lambda',\theta') + \sum_{m=1}^{n} \left(\bar{\mathcal{Y}}_{nm}(\lambda,\theta)\bar{\mathcal{Y}}^*_{nm}(\lambda',\theta') + \bar{\mathcal{Y}}^*_{nm}(\lambda,\theta)\bar{\mathcal{Y}}_{nm}(\lambda',\theta')\right)$$

$$= \frac{1}{4\pi} \sum_{m=-n}^{n} \bar{Y}_{nm}(\lambda,\theta)\bar{Y}_{nm}(\lambda',\theta') = \frac{2n+1}{4\pi} P_n(\cos\psi) \ . \tag{3.35}$$

The relation between the complex $\bar{\mathcal{Y}}_{nm}$ and the real-valued valued $\bar{Y}_{nm}$ is thus

$$\begin{aligned}\bar{\mathcal{Y}}_{nm} &= \frac{(-1)^m}{\sqrt{4\pi}} \frac{1}{\sqrt{2-\delta_{0m}}} (\bar{Y}_{nm} + i\bar{Y}_{n,-m}) \qquad m \geq 0 \\ \bar{\mathcal{Y}}_{nm} &= \frac{1}{\sqrt{4\pi}} \frac{1}{\sqrt{2}} (\bar{Y}_{n|m|} - i\bar{Y}_{n,-|m|}) \qquad m < 0 \ .\end{aligned}$$

Some integrals

Some useful integrals are expressed below, using both unnormalized and fully normalized spherical harmonic representation.

$$\frac{1}{4\pi}\int_\Omega F d\omega = f_{00} = \bar{f}_{00} \tag{3.36}$$

$$\frac{1}{4\pi}\int_\Omega F^2 d\omega = \sum_{n=0}^{\infty}\sum_{m=-n}^{n} \frac{f^2_{nm}}{\Pi^2_{nm}} = \sum_{n=0}^{\infty}\sum_{m=-n}^{n} \bar{f}^2_{nm} \tag{3.37}$$

$$\frac{1}{4\pi}\int_{\Omega} FG d\omega = \sum_{n=0}^{\infty}\sum_{m=-n}^{n} \frac{f_{nm}g_{nm}}{\Pi_{nm}^2} = \sum_{n=0}^{\infty}\sum_{m=-n}^{n} \bar{f}_{nm}\bar{g}_{nm} \tag{3.38}$$

$$\frac{1}{4\pi}\int_{\Omega} FY_{nm} d\omega = \frac{f_{nm}}{\Pi_{nm}^2} = \frac{\bar{f}_{nm}}{\Pi_{nm}} \tag{3.39}$$

$$\frac{1}{4\pi}\int_{\Omega} F\bar{Y}_{nm} d\omega = \frac{f_{nm}}{\Pi_{nm}} = \bar{f}_{nm} \tag{3.40}$$

$$\begin{aligned}\frac{1}{4\pi}\int_{\Omega} F\bar{\mathcal{Y}}_{nm} d\omega &= \frac{(-1)^m}{\sqrt{4\pi}}\frac{1}{\sqrt{2-\delta_{0m}}}\left(\bar{f}_{nm} + i\bar{f}_{n,-m}\right) \qquad m \geq 0 \\ &= \frac{(-1)^m}{\sqrt{4\pi}}\frac{1}{\sqrt{2}}\left(\bar{f}_{n|m|} + i\bar{f}_{n,-|m|}\right) \qquad m < 0\end{aligned} \tag{3.41}$$

3.2 Spherical Coordinates

We use spherical longitude λ, co-latitude $\theta = \frac{\pi}{2} - \phi$ and radius r. 'Geodetic' coordinates can all be easily transformed to spherical coordinates.

A vector field, when represented with respect to the local basis $\mathbf{e}_r$, $\mathbf{e}_\theta$, $\mathbf{e}_\lambda$, reads

$$\mathbf{f} = f_r\mathbf{e}_r + f_\theta\mathbf{e}_\theta + f_\lambda\mathbf{e}_\lambda \ . \tag{3.42}$$

The gradient and the Laplace operator applied to a 3D-function $F(\lambda,\theta,r)$ in spherical coordinates are

$$\boldsymbol{\nabla} F = \frac{\partial F}{\partial r}\mathbf{e}_r + \frac{1}{r}\frac{\partial F}{\partial \theta}\mathbf{e}_\theta + \frac{1}{r\sin\theta}\frac{\partial F}{\partial \lambda}\mathbf{e}_\lambda \ . \tag{3.43}$$

$$\begin{aligned}\Delta F = \boldsymbol{\nabla}\cdot\boldsymbol{\nabla} F &= \frac{1}{r^2}\frac{\partial}{\partial r}\left(r^2\frac{\partial F}{\partial r}\right) + \frac{1}{r^2}\left(\frac{1}{\sin\theta}\frac{\partial}{\partial\theta}\left(\sin\theta\frac{\partial F}{\partial\theta}\right)\right) \\ &+ \frac{1}{r^2\sin^2\theta}\frac{\partial^2 F}{\partial\lambda^2} \\ &= \frac{\partial^2 F}{\partial r^2} + \frac{2}{r}\frac{\partial F}{\partial r} + \frac{1}{r^2}\frac{\partial^2 F}{\partial\theta^2} + \frac{1}{r^2\tan\theta}\frac{\partial F}{\partial\theta} \\ &+ \frac{1}{r^2\sin^2\theta}\frac{\partial^2 F}{\partial\lambda^2}\end{aligned} \tag{3.44}$$

The gradient of the vector field can be written as a matrix, with entries

$$\boldsymbol{\nabla}\mathbf{f} = \begin{pmatrix} \frac{\partial f_r}{\partial r} & \frac{1}{r}\frac{\partial f_r}{\partial\theta} - \frac{f_\theta}{r} & \frac{1}{r\sin\theta}\frac{\partial f_r}{\partial\lambda} - \frac{f_\lambda}{r} \\ \frac{\partial f_\theta}{\partial r} & \frac{1}{r}\frac{\partial f_\theta}{\partial\theta} + \frac{f_r}{r} & \frac{1}{r\sin\theta}\frac{\partial f_\theta}{\partial\lambda} - \cot\theta\frac{f_\lambda}{r} \\ \frac{\partial f_\lambda}{\partial r} & \frac{1}{r}\frac{\partial f_\lambda}{\partial\theta} & \frac{1}{r\sin\theta}\frac{\partial f_\lambda}{\partial\lambda} + \cot\theta\frac{f_\theta}{r} + \frac{\partial f_r}{\partial r} \end{pmatrix} \tag{3.45}$$

The divergence of the vector field is

$$\begin{aligned}\nabla \cdot \mathbf{f} &= \frac{1}{r^2}\frac{\partial}{\partial r}\left(r^2 f_r\right) + \frac{1}{r\sin\theta}\frac{\partial}{\partial\theta}\left(\sin\theta f_\theta\right) + \frac{1}{r\sin\theta}\frac{\partial}{\partial\lambda}f_\lambda \\ &= \frac{2}{r}f_r + \frac{\partial}{\partial r}f_r + \frac{1}{r\sin\theta}\frac{\partial}{\partial\theta}\left(\sin\theta f_\theta\right) + \frac{1}{r\sin\theta}\frac{\partial}{\partial\lambda}f_\lambda\end{aligned} \tag{3.46}$$

For completeness, we note the strain tensor $\boldsymbol{\epsilon} = \frac{1}{2}(\nabla\mathbf{u} + (\nabla\mathbf{u})^{\mathbf{T}})$ and the (Cauchy) stress tensor in spherical coordinates:

$$\begin{aligned}\boldsymbol{\epsilon} = {} & \epsilon_{rr}\mathbf{e}_r{\mathbf{e}_r}^T + \epsilon_{\theta\theta}\mathbf{e}_\theta{\mathbf{e}_\theta}^T + \epsilon_{\lambda\lambda}\mathbf{e}_\lambda{\mathbf{e}_\lambda}^T \\ & + \epsilon_{r\theta}\left(\mathbf{e}_r{\mathbf{e}_\theta}^T + \mathbf{e}_\theta{\mathbf{e}_r}^T\right) + \epsilon_{r\lambda}\left(\mathbf{e}_r{\mathbf{e}_\lambda}^T + \mathbf{e}_\lambda{\mathbf{e}_r}^T\right) + \epsilon_{\theta\lambda}\left(\mathbf{e}_\theta{\mathbf{e}_\lambda}^T + \mathbf{e}_\lambda{\mathbf{e}_\theta}^T\right)\end{aligned} \tag{3.47}$$

in particular

$$\epsilon_{rr} = \frac{\partial u_r}{\partial r} \tag{3.48}$$

$$\epsilon_{\theta\theta} = \frac{1}{r}\frac{\partial u_\theta}{\partial\theta} + \frac{1}{r}u_r \tag{3.49}$$

$$\epsilon_{\lambda\lambda} = \frac{1}{r\sin\theta}\frac{\partial u_\lambda}{\partial\lambda} + \frac{1}{r}u_r + \frac{1}{r\tan\theta}u_\theta \tag{3.50}$$

$$\epsilon_{r\theta} = \frac{1}{2}\left(\frac{1}{r}\frac{\partial u_r}{\partial\theta} + \frac{\partial u_\theta}{\partial r} - \frac{1}{r}u_\lambda\right) \tag{3.51}$$

$$\epsilon_{r\lambda} = \frac{1}{2}\left(\frac{1}{r\sin\theta}\frac{\partial u_r}{\partial\lambda} + \frac{\partial u_\lambda}{\partial r} - \frac{1}{r}u_\lambda\right) \tag{3.52}$$

$$\epsilon_{\theta\lambda} = \frac{1}{2}\left(\frac{1}{r\sin\theta}\frac{\partial u_\theta}{\partial\lambda} + \frac{1}{r}\frac{\partial u_\lambda}{\partial\theta} + \frac{1}{r\tan\theta}u_\lambda\right) \tag{3.53}$$

and

$$\begin{aligned}\boldsymbol{\sigma} = {} & \sigma_{rr}\mathbf{e}_r{\mathbf{e}_r}^T + \sigma_{\theta\theta}\mathbf{e}_\theta{\mathbf{e}_\theta}^T + \sigma_{\lambda\lambda}\mathbf{e}_\lambda{\mathbf{e}_\lambda}^T \\ & + \sigma_{r\theta}\left(\mathbf{e}_r{\mathbf{e}_\theta}^T + \mathbf{e}_\theta{\mathbf{e}_r}^T\right) + \sigma_{r\lambda}\left(\mathbf{e}_r{\mathbf{e}_\lambda}^T + \mathbf{e}_\lambda{\mathbf{e}_r}^T\right) + \sigma_{\theta\lambda}\left(\mathbf{e}_\theta{\mathbf{e}_\lambda}^T + \mathbf{e}_\lambda{\mathbf{e}_\theta}^T\right) \ .\end{aligned} \tag{3.54}$$

References

1. Freeden W (1999) Multiscale modelling of spaceborne geodata, Teubner, Stuttgart
2. Bettadpur S (2007) Gravity Recovery and Climate Experiment: Level-2 Gravity Field Product User Handbook (Rev 2.3, February 20, 2007), GRACE 327-734
3. Press WH, Flannery BP, Teukolsky SA, Vetterling WT (1988) Numerical recipes in C, Cambridge University Press, Cambridge, NY
4. Jekeli C (1981) Alternative methods to smooth the Earth's gravity field, Rep. No, 327, Geodetic Science, Ohio State University
5. Hackbusch W (1993) Iterative solutions of large sparse systems of equations, Springer, New York
6. Jolliffe I (1986) Principal component analysis, Springer, New York
7. Preisendorfer R (1988) Principal component analysis in meteorology and oceanography, Elsevier, Amsterdam
8. Edmonds AR (1974) Angular momentum in quantum mechanics, Princeton University Press, Princeton, NJ
9. Heiskanen WA, Moritz H (1967) Physical geodesy, Freeman and Company, San Francisco
10. Kaula WM (1966) Theory of satellite geodesy, Blaisdell, Waltham, MA
11. Han S-C, Shum CK, Jekeli C, Kuo C-Y, Wilson CR, Seo K-W (2005) Non-isotropic filtering of GRACE temporal gravity for geophysical signal enhancement. Geophys J Int 163, 18-25
12. Hannachi A, Unkel S, Trendafilov NT, Jolliffe IT (2009) Independent component analysis of climate data: A new look at EOF rotation. Journal of Climate 22, 2797–2812
13. Higgins TP, Kopal Z (1968) Volume integrals of the products of spherical harmonics and their application to viscous dissipation phenomena in fluids, Astrophysics and space science 2:352-369
14. Klees R, Revtova E, Gunter B, Ditmar P, Oudman E, Winsemius H, Savenije H (2008) The design of an optimal filter for monthly GRACE gravity models, Geophys J I 175(2):417-432
15. Kusche J (2007) Approximate decorrelation and non-isotropic smoothing of time-variable GRACE-type gravity field models, J Geod (2007) 81:733749
16. Kusche J, Schmidt R, Petrovic S, Rietbroek R (2009) Decorrelated GRACE timevariable gravity solutions by GFZ, and their validation using a hydrological model, J Geod, 83:903-913

17. Narcowich F, Ward J (1996) Nonstationary wavelets on the m-sphere for scattered data, Appl Comp Harm Anal, 3:324-336
18. North G, Bell T, Cahalan R, Moeng F (1982) Sampling errors in the estimation of empirical orthogonal functions. Monthly Weather Review 110, 699–706
19. Wahr J, Molenaar M, Bryan F (1998) Time variability of the Earth's gravity field: Hydrological and oceanic effects and their possible detection using GRACE. J Geophys Res, 103, B12, 30205-30229
20. Swenson S, Wahr J (2006) Post-processing removal of correlated errors in GRACE data. Geophys. Res. Lett. 33, L08402
21. Zhang Z-Z, Chao BF, Hsu H, Lu Y (2009) An effective filtering for GRACE timevariable gravity: Fan filter. Geophys Res Lett, 36, L17311

Surface Loading

Volker Klemann
GFZ German Research Center for Geosciences Potsdam

Version of 06/09/2011

Contents

Part I

Surface loads

In this lecture I will present the basic concept of a load applied to the earth surface and its interaction with the earth's interior. Consider these notes as a draft.

1 Mathematical prerequisites

1.1 Definition of surface load

A mass at the surface of the earth is usually condensed to an infinitesimal layer at the reference height of the surface. Mass condensation results in representation of mass distribution as a surface mass density where the integral of density over the vertical reduces to a surface mass density measured in kg/m^2,

$$\sigma(a,\Omega) = \int_{r_0} \rho_\sigma(r,\Omega)dr\ . \tag{1}$$

There, ρ_σ is the density of the considered mass, $r_0 = [a \pm \delta r]$ is its height range, $\Omega = \theta, \varphi$ is the coordinate pair on the sphere. Furthermore, for a surface mass, the height range should not differ too much from the reference height to which it is condensed; usually it coincides with the earth radius, $a = 6.371 \times 10^6$ m. Furthermore the 3d character is of no importance as long as we are not to near to the load. With respect to solid earth problems, this is of course justified by the thin surface shell covering the earth's interior. In consequence, all redistribution of water, ice and vapor are considered as a surface mass. The total mass of the load is not considered but its conservation

$$\int_{\Omega_0} \sigma d\Omega = 0\ . \tag{2}$$

This is also stated in the title of the priority program, 'mass *distribution* and mass *transport* in the earth system'.

1.2 Processes inducing surface loading

The main processes responsible for mass transport at the surface are

- hydrological water cycle
- ocean currents
- glacial melting
- atmospheric water cycle

These processes are coupled by the transport of water between the subsystems. This motivates the focus of the SPP. Other material like CO_2 or sediments are not considered. The loading of these processes will all deform the solid earth but, due to their different scales in dimension, amplitude and duration, they are considered differently.

1.3 Separation of signals

In this lecture the focus is on the response of the solid earth to surface load variations, which is detectable in geodetic observables, like GNSS and gravity. These observables represent integral responses to all relevant processes which can be of internal and external origin. The usual task for the geoscientist before interpreting the signal is to separate the signals of different processes. The classical approach for field measurements in order to detect a specific signal was to choose an appropriate location. Signals determined from GRACE represent integrals over large spatial areas. Therefore this strategy is only in parts successful. One alternative strategy is to separate the signals due to their temporal behaviour. The most important signals in this respect are seasonal, interanual or secular. There, the seasonal signals are quite simple to isolate, whereas the separation of interanual and secular variaions is much more difficult. One of the most prominant secular signals is GIA proceeding on a time scale of kyr. It can be identified in gravity, surface displacement, rotational variations and in sea level. Other interanual signals which influence the mass redistribution are mostly of shorter time scales.

1.4 Solid earth response

One has of course to ask what is the response of the solid earth and how it is best modelled. Due to the mainly global scale of the considered loads, and the discussed response, we have to model the earth as a deformable sphere. With respect to the time scales involved for the ocean dynamics and atmosphere as for present day ice melting the earth is considered as an elastic body. But, the earth's mantle reacts only on short time scales like an elastic solid, with the duration of the process, also anelasticity has to be considered and for very long time scales (thousands of years) the earth's mantle behaves like a Newtonian fluid. Secular motions are therefore affected by both phenomena long-period mass redistributions at the surface and the visco-elastic response of the solid earth. The details will be discussed in Section 4, p. 14.

Basically for geodetic purpose, the response of the earth results in a displacement and a variation of the gravity potential considered at the earth's surface. The latter is described as the change of the reference potential. These fields are usually represented by spherical-harmonics decomposition, i.e.

$$\boldsymbol{u}(R,\Omega) \;=\; \sum_{lm} U_{lm}(R)\,\boldsymbol{S}^{-1}_{lm}(\Omega) + \sum_{lm} V_{lm}(R)\,\boldsymbol{S}^{+1}_{lm}(\Omega) + \sum_{lm} W_{lm}(R)\,\boldsymbol{S}^{0}_{lm}(\Omega) \quad (3)$$

and

$$\phi^{(1)}(R,\Omega) \;=\; \sum_{lm} \Phi_{lm}(R)\,Y_{lm}(\Omega) \quad (4)$$

Here, U, V and W are radial functions describing the spheroidal displacement in radial and horizontal direction and the toroidal displacement, resectively, and $\boldsymbol{S}^{(}_{lm}p)$ are the corresponding vector spherical harmonics.[1] The potential perturbation, $\phi^{(1)}$, is represented in the same way by scalar spherical harmonics Y_{lm}. In this formal representation the quantities are complex in order to keep a more compact representation. The relation to the real-valued 4π-normalized spherical harmonics you will find in the appendix to the lecture notes 'Analysis Tools'. The explicit conversion of coefficients is given in App. A, p. 21. The surface mass density is represented in the same way,

$$\sigma(\Omega) \;=\; \sum \Sigma_{lm}\,Y_{lm}(\Omega)\;. \quad (5)$$

If we assume a linearised theory we can expect a proportionality between excitation and response:

$$\{[U,V,W,\Phi]_{lm}\} \;=\; \mathbf{A}\{\Sigma_{lm}\} \quad (6)$$

If we assume a radially stratified Earth structure the relation between the load and the response only depends on the distance between load and observation, which means the field quantity describing the observation, ϕ, can be written as a convolution integral, g_ϕ,

$$\phi(\Omega) \;=\; a^2 \int_{\Omega_0} \sigma(\Omega')\,g_\phi(\gamma)\,d\Omega\;, \quad (7)$$

where $\gamma = (|\Omega - \Omega'|)$ is the distance between the two coordinate pairs on the sphere and g_ϕ is the Green's function for the considered scalar field quantity, ϕ. The depends only on γ allows the Green's functions to be represented by Legendre functions:

$$g_e(\gamma) \;:=\; a/M_e \sum_l (1+k_l)\,P_l(\cos\gamma)\;, \quad (8)$$

$$g_u(\gamma) \;:=\; a/M_e \sum_l h_l\,P_l(\cos\gamma) \quad (9)$$

[1] The representation of vector spherical harmonics is quite compact, for details see Martinec (2000). The full calculus is outlined in Varshalovich *et al.* (1988).

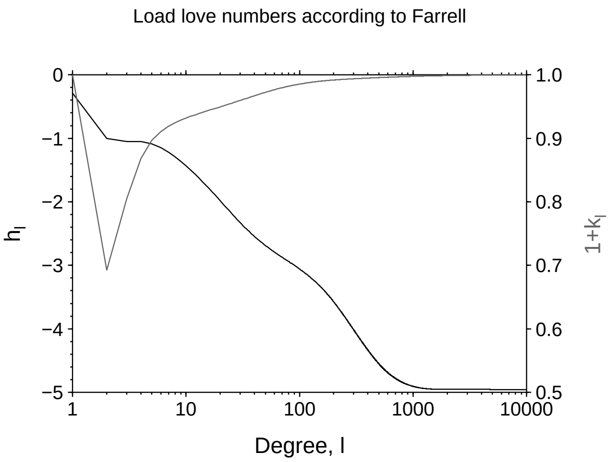

Figure 1: Vertical load Love numbers, h and k according to Farrell (1972).

Considering the load in (5), the displacements can be written then

$$e(\Omega) = \frac{3}{\bar{\rho}} \sum \frac{1+k_l}{2\,l+1} \Sigma_{lm}\, Y_{lm}(\Omega) \tag{10}$$

$$u(\Omega) = \frac{3}{\bar{\rho}} \sum \frac{h_l}{2\,l+1} \Sigma_{lm}\, Y_{lm}(\Omega) \tag{11}$$

where h_l and k_l are the load Love numbers. If we look at their functional behaviour Figure 1, two things are of interest. The degree 0 does not appear in this figure. This is not due to the logarithmic scale but also due to the fact that it does not appear in the usual listing of Love numbers, e.g. by Farrell (1972). Furthermore $k_1 = -1$, this motivates a small excursion.

1.4.1 Excursion to physical meaning of degree 0 and 1

The displacements fields represented by Legendre degree 0 and 1 have to be considered separately. This is due to the integral character of these fields. the surface integral over a scalar spherical harmonics results in

$$\int_\Omega Y_{lm}\, d\Omega = \sqrt{4\,\pi}\, \delta_{l0}\, \delta_{m0} \tag{12}$$

For the surface mass density, σ (5), it means a finite mass of the perturbation, which violates the principle of mass conservation (2). So, mass conservation implies that $\Sigma_{00} = 0$ and from the linearity of the problem, we can conlude that for the assumed model, there is neither a degree-0 component in displacement (11) nor a degree-0 component in the gravitational potential or displacement (10). From this point of view we don't have to care about a numerical value for degree 0.

For degree 1, the representation of vector spherical harmonics are of interest. There, the integral

$$\int_{\Omega} \boldsymbol{S}^{(\lambda)}_{jm}\, dS \;=\; \sqrt{\frac{4\,\pi}{3}}\,\delta_{j\,1}\,(2\,\delta_{\lambda\,1}\,+\delta_{\lambda\,-1})\,\boldsymbol{e}_m \tag{13}$$

shows only spheroidal components, $\lambda = \pm 1$, in degree $l = 1$. The $\boldsymbol{e}_m$ are the covariant spherical base vectors. Considering the average motion of the surface, (3)

$$\begin{aligned} \boldsymbol{u}_{\mathrm{CF}} &:= \frac{1}{A}\int_{\partial V} \boldsymbol{u}\, dS \\ &= \frac{1}{4\,\pi}\int_{\Omega_0} \sum_{jm} \left[U_{jm}\,\boldsymbol{S}^{(-1)}_{jm} \,+\, V_{jm}\,\boldsymbol{S}^{(1)}_{jm} \,+\, W_{jm}\,\boldsymbol{S}^{(0)}_{jm} \right] d\Omega\;, \end{aligned} \tag{14}$$

we get in fully normalised complex spherical harmonics (Klemann & Martinec, 2009)

$$\begin{aligned} u^x_{\mathrm{CF}} &= -\frac{1}{2}\sqrt{\frac{2}{3\,\pi}}\;\mathrm{Re}\{U_{11} + 2\,V_{11}\} \\ u^y_{\mathrm{CF}} &= \frac{1}{2}\sqrt{\frac{2}{3\,\pi}}\;\mathrm{Im}\{U_{11} + 2\,V_{11}\} \\ u^z_{\mathrm{CF}} &= \frac{1}{2}\sqrt{\frac{1}{3\,\pi}}(U_{10} + 2\,V_{10}) \end{aligned} \tag{15}$$

That means, that the center-of-figure motion is described by the degree-1 components of the displacement field. Similar, the degree-1 perturbation of the potential describes the center of mass motion and the difference is the so called geocenter motion, which is invariant of the chosen earth related reference frame.

Here, the representation by load-Love numbers, is given, where the surface-mass coefficients are the valid for the 4π-normalised real spherical harmonics, Stoke's coefficients, and $\boldsymbol{u}$ is in Cartesian coordinates pointing to ($\boldsymbol{e}_x = 0^{\circ}\mathrm{N}/0^{\circ}\mathrm{E}$), ($\boldsymbol{e}_y = 0^{\circ}\mathrm{N}/90^{\circ}\mathrm{E}$) and ($\boldsymbol{e}_z = 90^{\circ}\mathrm{N}$):

$$\boldsymbol{u}^{\mathrm{gc}} \;=\; \frac{1}{3\,\bar{\rho}}[\,h_1 + 2\,l_1 - 3\,(1+k_1)\,]\begin{pmatrix} \Sigma^C_{11} \\ \Sigma^S_{11} \\ \Sigma_{10} \end{pmatrix} \tag{16}$$

From Figure 1, we observe that $k_1 = -1$. Not shown is the value $l_1 = 0.113$ of Farrell. This relation allows a quick assessment about the order of the geocenter motion. The specific value of $k_1 = -1$ in Farrell, is due to the chosen reference frame in which the kinematics of the solid earth is described. In Farrell it is the so-called center of the solid earth. For details see Lavallée *et al.* (2006). Due to GGOS this quantity is of interest and its more precise determination also one of the tasks for the next years. With respect to GIA, there are a number of studies, e.g. Greff-Lefftz (2000); Argus (2007); Klemann & Martinec (2009). As stated above the center of mass motion is described by $1 + k_1$.

1.4.2 Toroidal motion

A further result is, that for a surface load that acts as an attracting mass and as a vertical loading pressure on a spherically symmetric earth, a toroidal motion will not be excited, i.e. spheroidal and toroidal motions are decoupled. This is the reason why only three love Numbers describe the deformational behaviour of the earth body in response to a load, h, l for spheroidal displacement and k for gravity. If we assume a laterally varying earth structure this condition is not fullfilled any more and we get a coupling between different degrees and a coupling to the toroidal part (Klemann *et al.*, 2008).

The extension to a time dependent love number which is demanded for viscoelastic behaviour will add a convolution in the time domain.

2 The sea-level equation

The sea-level equation describes the mass redistribution between ice and ocean in a gravitational consistent way. The ocean is considered to follow the geoid. The geoid is calculated from the surface mass redistribution. The surface mass redistribution is considered to deform the solid earth and so, changes the gravity potential. Surface displacement and displacement of gravity potential defines the placement of the ocean which again modifies the load. This complicates the set up of the problem.

2.1 The concept of geoid

The static response of the ocean means that the sea-level follows the geoid which is generated by the mass redistribution. The geoid is here considered in the classical definition:

> *The geoid is that equipotential surface which would coincide exactly with the mean ocean surface of the Earth, if the oceans were in equilibrium, at rest (relative to the rotating Earth), and extended through the continents (such as with very narrow canals). According to C.F. Gauss, who first described it, it is the "mathematical figure of the Earth", a smooth but highly irregular surface that corresponds not to the actual surface of the Earth's crust, but to a surface which can only be known through extensive gravitational measurements and calculations.*
>
> Wikipedia

This definition deviates from that given in e.g. the IERS convention (Petit & Luzum, 2010), where the geoid is defined by a potential value Groten (2004):

$$W_0 = 62636856.0\,\mathrm{m^2\,s^{-2}} \pm 0.5, \mathrm{m^2\,s^{-2}} \tag{17}$$

This difference can lead to misinterpretations in literature. Whereas it is convenient to calculate this shift by the Bruns' formula, it will not hold for Gauss definition if a process changes the global sea level. The classical Farrell & Clark (1976) paper for instance use Gauss' definition. So, a suggestion to the students, take care that you are using the terms correctly and your orrespondent does the same.

So, considering a change of the gravity potential due to a dynamic process, the displacement of the potential surface can be calculated from Bruns' formula,

$$e = \phi_1/g_0 \tag{18}$$

with g_0 the normal gravity. This displacement, e, should not be mixed with the geoid change, n, which also contains a change of the total mass of the ocean or a steric change (thermal expansion). If we represent n and e in spherical harmonics, they will differ in the degree 0 component, which is 0 only for e (25).

2.2 Definition of sea level

The sea level was defined uniquely as long the geodesist remained to stay at the shore line and measured its height variations using tide gauges. There it was clear, the sea level was measured relative to the land surface (shore line) at a specified epoch, the relative sea level. This concept also applies to geological or historical markers or indicators of former sea level. With satellite altimetry this view changed, where the sea-level is measured independent from the land surface.

The geoid from Gauss' definition is

$$n(\Omega, t) = e(\Omega, t) + h_{\mathrm{wl}}(t) \tag{19}$$

with h_{wl} the shift between the reference-potential height and the current potential the sea level is following.

This means from a modelling perspective where we can predict field quantities w.r.t. displacement, u, and geoid, n, in a specified reference frame,

$$h_{\mathrm{RSL}}(\Omega, t) = [n - u](\Omega, t) - [n - u](\Omega, t_0) \tag{20}$$

as the relative sea level and

$$h_{\mathrm{alt}}(\Omega, t) = n(\Omega, t) - n(\Omega, t_0) \tag{21}$$

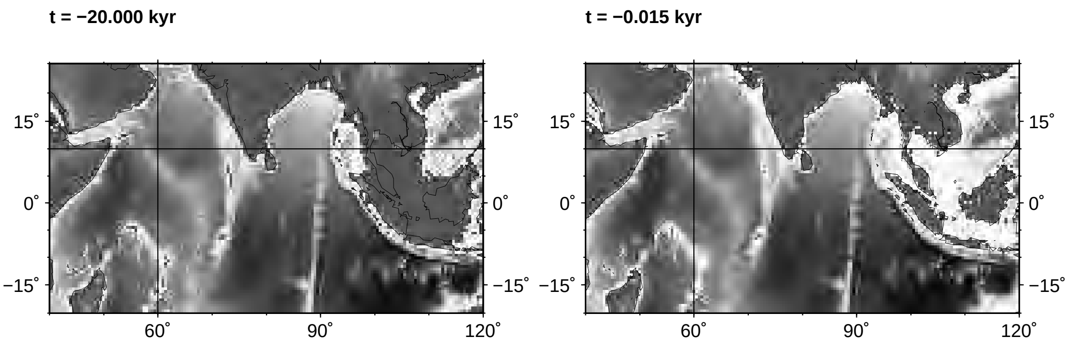

Figure 2: Change of shoreline at Sunda Strait from LGM to pt.

the altimetric sea level.

Here, one has to keep in mind that h_{alt} (21) is not invariant against the considered reference system. The same holds for the prediction of suface motion u. Also here, the translation of the whole network can differ between prediction and observation (Section 3, p. 12).

2.3 The ocean function

The ocean function is quite important. It defines the integration domain where the water level is affected by displacement and geoid. In this respect it is a masking function

$$\mathcal{O}(\Omega, t) \;=\; \begin{cases} 0 & \text{if} \quad T(\Omega, t) > 0 \\ 1 & \text{if} \quad T(\Omega, t) \leq 0 \end{cases} \tag{22}$$

If a deformation process is considered the topography, if defined relative to the mean sea level, may change. Considering an initial state where the topography is specified, $T_0 = T(t = 0)$, and the perturbation in relative sea level, $h_{\mathrm{RSL}}(t = 0) = 0$, the topography defined in the above sense is calculated by

$$T(\Omega, t) \;=\; T_0 - h_{\mathrm{RSL}}(\Omega, t) \tag{23}$$

This concept is quite important in GIA, where the sea-level not only changes vertically due to uplift but also the horizontal extension of the ocean, i.e. the ocean mask becomes a function of time. This motivates its name 'ocean function'. The currently applied theory is outlined in Kendall *et al.* (2005).

2.4 Moving coast lines

Figure 2 shows an example of how much the sea level varied during the last glacial cycle. At the last glacial maximum the global sea-level was approximately 130 m below its present height, therefore many continental shelves where dry areas. These regions wer unloaded during the LGM time range, which influences of course the dynamic response of the solid earth.

2.5 The coupling between sea-level variations and solid earth

As outlined in Section 1.4, p. 4, the earth responds to a surface load by deformation and so the earth's surface geometry and the gravity potential will change. The loading consists of the ice load on the continent and the ocean load due to mass redistribution.

$$m_{\mathrm{load}}(\Omega) = m_{\mathrm{ice}}(\Omega) + m_{\mathrm{oce}}(\Omega) . \tag{24}$$

The mass redistribution implies

$$\int_{\Omega_0} m_{\mathrm{load}}(\Omega)\, d\Omega = 0 \tag{25}$$

2.6 Solution of the sea-level equation

The sea-level equation is an integral equation (Farrell & Clark, 1976):

$$h_{\mathrm{RSL}}(\Omega, t) = [h_{\mathrm{wl}}(t) + e(\Omega, t) - u(\Omega, t)]\, \mathcal{O}(\Omega, t) , \tag{26}$$

where the homogeneous part describes the shift of the reference geoid

$$h_{\mathrm{wl}}(t) = \frac{-M_{\mathrm{ice}}(t)}{\rho_{\mathrm{oce}}\, A_{\mathrm{oce}}(t)} - \frac{1}{A^{\mathrm{oce}}(t)} \int_{\Omega} [e(\Omega, t) - u(\Omega, t)]\, \mathcal{O}(\Omega, t)\, d\Omega \tag{27}$$

and

$$A_{\mathrm{oce}}(t) = \int_{\Omega} \mathcal{O}(\Omega, t)\, d\Omega \tag{28}$$

It is important to note here, that also for the case of fixed coastlines the equivalent sea level has to be determined by iterations and is not known from the begining. Considering these aspects we end up with the following solution of the sea-level equation:

$$(e-u)_i(\Omega) = g_{e-u} * [m_{\mathrm{load}}(\Omega) + h^{\mathrm{rsl}}_{i-1}(\Omega)\, \rho_w\, \mathcal{O}(\Omega)] , \tag{29}$$

$$h^{\mathrm{rsl}}_i(\Omega) = h^{\mathrm{wl}}_i + (e-u)_i(\Omega)\, \mathcal{O}(\Omega) , \tag{30}$$

$$h^{\mathrm{wl}}_i = -\frac{\int_\Omega m_{\mathrm{load}}(\Omega)}{\rho_w\, A_o} - \frac{1}{A_o} \int (e-u)_i(\Omega)\, \mathcal{O}(\Omega)\, d\Omega \tag{31}$$

$$h^{\mathrm{rsl}}_0 = -\frac{\int m_{\mathrm{load}}(\Omega)}{\rho_w\, A_o} , \tag{32}$$

2.7 Features of its solution

The sea level does not respond uniformly on the melting of ice. Aspects are:

- The solid earth deforms due to changes in loading. Near the reducing load it will move upward.
- The ice load attracts the ocean due to its mass which means, if the ice is melting, the sea level will drop in the areas around the ice load.
- In the farfield the sea level rises due to the addtional amount of water.

3 Reference systems

A unique definition of a reference system is not possible. In fact, the earth is wobbeling around the sun and wobbeling itself, which makes it difficult for a person on the earth's surface to define the motion of a distributed range of points on the earth surface in an invariant reference frame. This is important in order to predict, from the set of motions by a functional relation i.e. physical process, the motion at other points of the surface. These reference frames are usually defined by the average motion of the set of points w.r.t. a fixed coordinate system at each epoch. In secular trends one important aspect is the stability of reference systems. But also from the numerical modelling point of view, a reference system has to be prescribed. Sometimes, this is implicitly assumed in the field equations, sometimes it has to be done explicitly. For a body in space we have to prescribe (or fix) 6 components: 3 describing the position and motion in space and 3 describing its orientation. For the latter, in geodesy usually no net rotation of the surface is assumed but other definitions are also possible:

1. no surface net rotation (NF) $\int_{\partial\mathcal{B}} \boldsymbol{e}_r \times \boldsymbol{u}\, dS = 0$
2. conservation of total momentum (NM) $\int_{\mathcal{B}} \rho\, \boldsymbol{e}_r \times \boldsymbol{u}\, dV + \int_{\partial\mathcal{B}} \boldsymbol{e}_r \times \boldsymbol{\sigma}\, dS = 0$
3. no lithosphere net rotation (NL) $\int_{\mathcal{B}_L} \rho\, \boldsymbol{e}_r \times \boldsymbol{u}\, dV = 0$
4. no internal rotation (NE) $\int_{\mathcal{B}} \rho\, \boldsymbol{e}_r \times \boldsymbol{u}\, dV = 0$
5. no mantle rotation (NMa) $\int_{\mathcal{B}_M} \rho\, \boldsymbol{e}_r \times \boldsymbol{u}\, dV = 0$

The position/motion in space is specified in IRTF2005 as the centre of mass, previously it was the centre of figure, the Love numbers are referenced to the center of internal masses. So, also here one has to be careful especially if discussing global processes, where derived motions can be depend on the considered reference frame:

1. centre of mass (CM) $\int_{\mathcal{B}} \rho\, \boldsymbol{r}\, dV + \int_{\partial\mathcal{B}} \sigma\, \boldsymbol{r}\, dS = 0$

2. centre of figure (CF) $\int_{\partial\mathcal{B}} \boldsymbol{u}\, dS = 0$
3. centre of deformation (CD) $\int_{\mathcal{B}} \boldsymbol{u}\, dV = 0$
4. centre of internal masses (CE) $\int_{\mathcal{B}} \rho\, \boldsymbol{r}\, dV = 0$

The advantage of CM is that it describes the center of satellite motions. The advantage of CF is its realisation for a network of GPS stations.

A definition which is invariant to the latter conventions is the geocenter motion

$$\boldsymbol{u}_{\mathrm{gc}} := \boldsymbol{u}^{\mathrm{CF}} - \boldsymbol{u}^{\mathrm{CM}} \tag{33}$$

This reduction to degree 1 of the displacement field can be explained by the definition of the centre of figure and centre of mass motion,

$$\boldsymbol{u}^{\mathrm{CF}} := \frac{1}{\Omega} \int_{\Omega} \boldsymbol{u}\, dS \tag{34}$$

The observed GC is dominated by a seasonal signal (e.g. Rietbroek *et al.*, 2011). At the moment, the accuracy of GC motion is not better than 1 mm/yr. the secular signal is about 1 mm/yr, i.e. 0.1 mm/yr is the demanded accuracy to analysis this kind of signal.

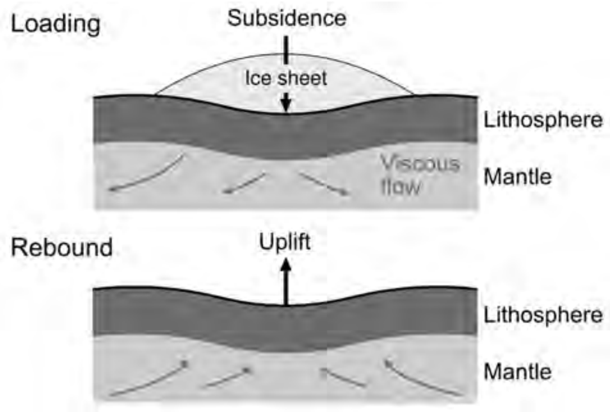

Figure 3: Retarded response of the viscoelastic earth to load-induced perturbations of its equilibrium configuration

4 Glacial isostatic adjustment

In literature there are two phrases commonly used to denote the process we will discuss during this course:

GIA glacial isostatic adjustment

PGR post glacial rebound

There, we can extract following competetive terms

glacial means related to glaciers and/or glacial cycle,

isostatic adjustment the movement to a new equilibrium state of forces,

post glacial means after end of the glaciation period,

rebound movement due to a disequilibrium.

Both definitions imply that there exists a static equilibrium state which is reached through time. The principle of this process is shown in Figure 3, where the arrows show the strain inside the lithosphere and the flow inside the mantle, respectively.

To understand the different meaning of the two expressions, we have to discuss what glacial stands for. As part of 'glaciology' it is related to the scientific discipline dealing with ice at the earth's surface and as part of glaciation it means the geological time intervals during which large parts of the earth's surface were covered by ice. Therefore, PGR describes the dynamic process after the last glaciation period and GIA means the response of the solid earth to any ice load redistribution.

Due to mass conservation, the ice-load variations have to be considered together with variations in sea level, which results in the modern definition of glacial isostatic adjustment: GIA describes the ongoing adjustment of the earth's interior to surface loading that is attributed to the changing mass distribution of ice **and** water.

The dimensions we have to deal with can be summarised as follows:

- extension of ice sheets $\mathcal{O}(1000\,\mathrm{km})$
- thickness of ice sheets $\mathcal{O}(1000\,\mathrm{m})$
- duration of process $\mathcal{O}(10,000\,\mathrm{yr})$
- termination of main glaciation 8,000 yr bp
- motion in previously glaviated regions of Scandinavia and Canada $\mathcal{O}(1\,\mathrm{cm/yr})$

So, we have to answer:

How deform glacial loads the earth? – 'Rebound' (germ.: Rückfederung, Erholung) implies already the understanding of the lithosphere as an elastic plate. This concept from plate tectonics can be used to describe the flexural behaviour of the lithosphere in response to loading.

Elastic plate is defined by technical mechanics as a thin plate, symmetric stress pattern, ... and its strength is simply the flexural rigidity. In geophysics, this fills already books (e.g. Watts, 2001).

The loads considered in GIA are glaciers or ice sheets which covered large areas of the continents on the northern hemisphere as additional masses. These ice sheets have to be carried by the lithosphere and the mantle below. On the time scale of glaciation process, the mantle does not react as an elastic body but as a viscous fluid. In consequence, we assume the lithosphere to be floating on the mantle, and we get the first physical principle which is the equilibrium of momentum:

Loading force = flexure of lithosphere + buoyancy (isostasy)

The process is slow, so we neglect the inertial forces. The buoyancy describes the fact, that the load deforms the lithosphere which is floating on the mantle.

$$D\,\frac{d^4 z}{dx^4} \;+\; \rho_m\, g\, z \;=\; \rho_{\mathrm{ice}}\, g\, h \tag{35}$$

where

$$D \;=\; \frac{E\,T_e^3}{12\,(1-\nu^2)} \tag{36}$$

This is, the flexure of a beam with flexural rigidity, D. The buoyancy of the underlaying material with density, ρ_m, is in equilbrium to the surface load. Of course, z is vertically down and x the horizontal of this 2d problem. From the equilibrium condition (35), it is evident that this equation describes the static state due to the fact that the mantle material is assumed to be an inviscid fluid.

The most important effect which makes this process such interesting is missing in both phrases (GIA and PGR), which is the *retarded response*, – the reason why still a vertical motion is observed. The mantle is not an ideal but a viscous fluid. Therefore, the adjustment or rebound due to the last glacial cycle is an ongoing process.

So, we have tp consider two physical phenomena, in order to describe the process:

- elastodynamics, which we need to describe mathematically the flexure of the lithosphere, and
- fluid dynamics to describe the viscous flow inside the mantle.

Both discicplines are part of the continuum mechanics and there, the two end members of the process:

strain $\propto$ stress: $\mu\,\boldsymbol{\epsilon} = \boldsymbol{\tau}$

strain rate (flow) $\propto$ stress: $\eta\,\dot{\boldsymbol{\epsilon}} = \boldsymbol{\tau}$

The third process which is present, is gravity, because buoyancy $\propto$ gravity: $\boldsymbol{b} = \nabla(\rho_m\,\boldsymbol{g}\cdot\boldsymbol{u})$

One interesting aspect to note is that the viscosity of the earth's interior can only be quantified by a dynamic process like GIA. Therefore, GIA is the discipline which gave the first estimates about the viscosity of the earth (e.g. Haskell, 1935), which is 10^{21} Pa s.

As stated above to consider the process of GIA we have to consider elastic as viscous behaviour at the same time, especially because although GIA is long time process it mainly describes a status of desiquilibrium. Therefore we are interested in a formulation of the rheology where elastic and viscous behaviour are described at the samte time. This is possible by viscoelasticity. The most elementary relation is the Maxwell body,

$$\dot{\boldsymbol{\epsilon}} = \dot{\boldsymbol{\tau}}/\mu + \boldsymbol{\tau}/\eta \tag{37}$$

This material law is considered generally in GIA. The main parameter to be investigated is the dynamic viscosity, η, whereas the shear modulus is considered from standard earth models like the Preliminary Reference Earth Model (PREM) from Dziewonski & Anderson (1981).

4.1 Field equations describing the solid earth response

The field equations here cited from Martinec (2000) describe the displacements of a viscoelastic, incompressible, non-rotating, self-gravitaing continuum in a spherical geometry. They consist of the equation of motion

$$\boldsymbol{\nabla}\cdot\boldsymbol{\tau} - \rho_0\,\boldsymbol{\nabla}\phi_1 + \boldsymbol{\nabla}\cdot(\rho_0\,\boldsymbol{u})\boldsymbol{\nabla}\phi_0 - \boldsymbol{\nabla}(\rho_0\,\boldsymbol{u}\cdot\boldsymbol{\nabla}\phi_0) = 0\,, \tag{38}$$

the potential equation

$$\nabla^2\phi_1 + 4\pi G\,\boldsymbol{\nabla}\cdot(\rho_0\boldsymbol{u}) = 0\,, \tag{39}$$

the constitutive equation of Mawxell viscoelasticity, here in 3d,

$$\dot{\boldsymbol{\tau}} = \dot{\boldsymbol{\tau}}^E - \frac{\mu}{\eta}(\boldsymbol{\tau} - \Pi\boldsymbol{I}) \qquad \boldsymbol{\tau}^E = \Pi\boldsymbol{I} + 2\,\mu\,\boldsymbol{\epsilon} \tag{40}$$

and the continuity equation, here formulated for the case of incompressibility.

$$\boldsymbol{\nabla}\cdot\boldsymbol{u} = 0\,. \tag{41}$$

These field equations have to be solved inside the solution domain, $\mathcal{B}$, for displacement $\boldsymbol{u}$, stress $\boldsymbol{\tau}$ and the potential ϕ_1. The material parameters considered, are the density, ρ, the shear modulus, μ, and the viscosity, η. The solution domain usually ranges inside a spherical shell from the surface to the core mantle boundary. The principles of this theory are outlined in Tromp & Mitrovica (1999).

The boundary conditions are at the surface the absence of any traction and free displacement and at the core-mantle boundary the conditions which describe the coupling to a homogeneous fluid sphere. The excitation is then represented by a surface load an internal load or a potential perturbation.

4.2 Solution of field equations

The classical method for solving the field equations is to transfer the time dependence which only appears in (40) into the spectral domain. This is done by Laplace transformation. Then the Laplace transformed equation of motion corresponds to the elastic problem, only that the shear modulus becomes a function of s. The horizontal dependence of the solutions are represented by scalar-, vector- and tensor-spherical harmonics, e.g. (3) and (4). The differential equation remains only with respect to radial distance, r. The system of equations can be represented for homogeneous layers by a first-order 6×6-differential system,

$$\frac{d}{dr}\mathbf{Y}_l(r) = \mathbf{A}_l(r)\,\mathbf{Y}_l(r) \tag{42}$$

which can be solved then for a stratified continuum by propagator matrices. As discussed in Section 1.4, p. 4 in the case of spherical symmetry, Y contains U, V representing the displacement the potential perturbation and respective terms of their first derivatives. The solution of this homogenous system of first order differential equations can be represented by its eigen modes, the so called relaxation time spectrum. For the specific form of A, which depends also on the Laplace parameter, s, the solution can be represented by $Y^S/\det\mathbf{M}(s)$. The determinant of the fundamental matrix $\mathbf{M}$ is unique for A and does not depend on the excitation represented by boundary conditions. The transformation back into the time domain, demands an inverse Laplace transformation. Here, the usual way is to apply the residue theorem, by identifying the roots of $\det \mathbf{M}(s)$, the eigenmodes of the system. Then, the solution is represented by the sum of the eigenmodes with an appropriate weighting. This method is based on Peltier (1974, 1976) and widely used (Sabadini & Vermeersen, 2004).

Martinec (2000) formulated the equations as an initial-value problem and the time dependence is solved directly in the time domain. This has a number of advantages: (1) the earth model can be coupled with a dynamic ice model. (2) It is possible to consider also lateral variations of viscous parameters in the earth structure. (3) In addition to a linear rheology also stress dependent rheologies can be considered.

5 Further reading

Arfken (1985): *Mathematical Methods for Physicists* – obvious what it is for.

Herring (2009): *Geodesy* – A nice new book about what I am not so familiar whith.

Karato (2008): *Deformation of Earth Materials: An Introduction to the Rheology of the Solid Earth* – My state of the art compenion discussing the rheological aspects of the earth's interior. It replaces the older standard by Ranalli (1987).

Kendall *et al.* (2005): *article* – Outline of the sea-level equation applied in GIA.

Petit & Luzum (2010): *IERS Conventions (2010)* – The earth from the geodetic perspective.

Sabadini & Vermeersen (2004): *Global Dynamics of the Earth* – The book about application of normal mode theory for a viscoelastic planet.

Varshalovich *et al.* (1988): *Quantum Theory of Angular Momentum* – If you really have to work with spherical harmonics.

Watts (2001): *Isostasy and Flexure of the Lithosphere* – For me, it is a standard when getting information about mechanical aspects of the lithosphere.

Whitehouse (2009): *Glacial isostatic adjustment and sea-level change: State of the art report* – A rather new summary about GIA and sea-level equation. Easily accessible from www.skb.se.

References

Arfken, G. (1985). *Mathematical Methods for Physicists*, 3 edn., Academic Press, Inc., San Diego, 985 p. 18

Argus, D. F. (2007). Defining the translational velocity of the reference frame of Earth, *Geophys. J. Int.*, **169**, 830–838, doi:10.1111/j.1365-246X.2007.03344.x. 7

Dziewonski, A. M. & Anderson, D. L. (1981). Preliminary reference earth model, *Phys. Earth Planet. Inter.*, **25**, 297–356. 16

Farrell, W. E. (1972). Deformation of the earth by surface loads, *Rev. Geophys.*, **10**, 761–797, doi:10.1029/RG010i003p00761. 6

Farrell, W. E. & Clark, J. A. (1976). On postglacial sea level, *Geophys. J. R. Astr. Soc.*, **46**, 647–667, doi:10.1111/j.1365-246X.1976.tb01252.x. 9, 11

Greff-Lefftz, M. (2000). Secular variation of the geocenter, *J. Geophys. Res.*, **105**, 25,685–25,692, doi:10.1029/2000JB900224. 7

Groten, E. (2004). Fundamental parameters and current (2004) best estimates of the parameters of common relevance to astronomy, geodesy, and geodynamics, *J. Geod.*, **77**, 724–731, doi:10.1007/s00190-003-0373-y. 9

Haskell, N. A. (1935). The motion of a viscous fluid under a surface load, *Physics*, **6**, 265–369. 16

Herring, T. (Ed.) (2009). *Geodesy*, *Treatise on Geophysics*, vol. 3, Elsevier, Amsterdam, 446 p. 18

Karato, S. (2008). *Deformation of Earth Materials: An Introduction to the Rheology of the Solid Earth*, Cambridge University Press, Cambridge, 463 p. 18

Kendall, R. A., Mitrovica, J. X. & Milne, G. A. (2005). On post-glacial sea level – II. numerical formulation and comparative results on spherically symmetric models, *Geophys. J. Int.*, **161**, 679–706, doi:10.1111/j.1365-246X.2005.02553.x. 10, 18

Klemann, V. & Martinec, Z. (2009). Contribution of glacial-isostatic adjustment to the geocenter motion, *Tectonophysics*, **online**, doi:10.1016/j.tecto.2009.08.031. 7

Klemann, V., Martinec, Z. & Ivins, E. R. (2008). Glacial isostasy and plate motions, *J. Geodyn.*, **46**, 95–103, doi:10.1016/j.jog.2008.04.005. 8

Lavallée, D. A., van Dam, T., Blewitt, G. & Clarke, P. J. (2006). Geocenter motions from GPS: A unified observation model, *J. Geophys. Res.*, **111**, B05,405, doi:10.1029/2005JB003,784, doi:10.1029/2005JB003784. 7

Martinec, Z. (2000). Spectral–finite element approach for three-dimensional viscoelastic relaxation in a spherical earth, *Geophys. J. Int.*, **142**, 117–141, doi:10.1046/j.1365-246x.2000.00138.x. 5, 16, 18

Pěč, K. & Martinec, Z. (1982). Expansion of geoid heights into spherical harmonic series, *Stud. Geophys. Geod.*, **26**, 115–119, doi:10.1007/BF01582304. 21

Peltier, W. R. (1974). The impulse response of a Maxwell earth, *Rev. Geophys. Space Phys.*, **12**, 649–669. 18

Peltier, W. R. (1976). Glacial–isostatic adjustment—II. The inverse problem, *Geophys. J. R. Astr. Soc.*, **46**, 669–705, doi:10.1111/j.1365-246X.1976.tb01253.x. 18

Petit, G. & Luzum, B. (2010). *"IERS Conventions (2010)"*, no. 36 in IERS Technical Note, Verlag des Bundesamts für Kartographie und Geodäsie, Frankfurt am Main, 179 p. 9, 18

Ranalli, G. (1987). *Rheology of the Earth, Deformation and Flow Processes in Geophysics and Geodynamics*, Allan & Unwin, Boston, 366 p. 18

Rietbroek, R., Brunnabend, S., Kusche, J. & Schröter, J. (2011). Resolving sea level contributions by identifying fingerprints in time-variable gravity and altimetry, *J. Geodyn.*, **In Press, Corrected Proof**, –, doi:10.1016/j.jog.2011.06.007. 13

Sabadini, R. & Vermeersen, B. (2004). *Global Dynamics of the Earth—Applications of Normal Mode Relaxation Theory to Solid-Earth Geophysics*, Kluwer Academic Publishers, Dordrecht, 329 p. 18

Tromp, J. & Mitrovica, J. X. (1999). Surface loading of a viscoelastic earth—I. general theory, *Geophys. J. Int.*, **137**, 847–855. 17

Varshalovich, D. A., Moskalev, A. N. & Khersonskii, V. K. (1988). *Quantum Theory of Angular Momentum*, World Scientific Publishing, Singapore, 514 p. 5, 18

Watts, A. B. (2001). *Isostasy and Flexure of the Lithosphere*, Cambridge University Press, Cambridge, 458 p. 15, 18

Whitehouse, P. (2009). *Glacial isostatic adjustment and sea-level change: State of the art report*, *Tech. Rep. TR-09-11*, Svensk Kärnbränslesäkerhet AB, Stockholm. 18

A Conversion of Stokes' coefficients

According to Pěč & Martinec (1982), the relation between coefficients related to real 4π-normalised spherical harmonics, Stokes' coefficients, and the fully normalized complex spherical harmonics are

$$\begin{aligned} A_{j0} &= \sqrt{4\,\pi}\,\bar{C}_{j0} \\ A_{jm} &= (-1)^m\,\sqrt{2\,\pi}\,(\bar{C}_{jm}\,-\,i\,\bar{S}_{jm})\,, \quad m>0 \\ A_{j\,-m} &= (-1)^m\,A_{jm}\,, \quad m>0 \end{aligned} \tag{43}$$

where $[C,S]_{jm}$ are the Stokes' coefficients and A_{jm} are the coefficients of complex spherical harmonics.

B Vector spherical harmonics

Based on the complex normalized spherical harmonics with Condon-Shortly phase, it is straight forward to define vector spherical harmonics.

$$\begin{aligned} \boldsymbol{S}_{jm}^{(-1)} &= Y_{jm}\,\boldsymbol{e}_r \\ \boldsymbol{S}_{jm}^{(1)} &= \boldsymbol{\nabla}_\Omega Y_{jm} \\ \boldsymbol{S}_{jm}^{(0)} &= (\boldsymbol{e}_r \times \boldsymbol{\nabla}_\Omega)\,Y_{jm} \end{aligned} \tag{44}$$

From these a number of integral relations can be derived. The most prominant in this respect is

$$\int_\Omega \boldsymbol{S}_{jm}^{(\lambda)}\,dS \;=\; \sqrt{\frac{4\,\pi}{3}}\,\delta_{j\,1}\,(2\,\delta_{\lambda\,1}\,+\delta_{\lambda\,-1})\,\boldsymbol{e}_m \tag{45}$$

which shows that the average motion of a surface is only expressed by spheroidal ($\lambda=\pm 1$) and degree-1 ($l=1$) components. The $\boldsymbol{e}_m$ are the covariant spherical base vectors.

In der Schriftenreihe des Instituts für Geodäsie und Geoinformation der Rheinischen Friedrich-Wilhelms-Universität Bonn sind erschienen:

Heft 30 2013	Annette Eicker / Jürgen Kusche (eds.) Lecture Notes from the Summer School of DFG SPP1257 Global Water Cycle
Heft 29 2012	Matthias Siemes Ein Beitrag zur koordinatengesteuerten Aussaat von Rübenpflanzen mittels Multi-Sensor-System und Filteransatz
Heft 28 2012	Jörg Schmittwilken Attributierte Grammatiken zur Rekonstruktion und Interpretation von Fassaden
Heft 27 2012	Markus Rembold Die Anerkennung und Feststellung von Grundstücksgrenzen Ein Beitrag zur Entwicklung des Liegenschaftskatasters im Lande Nordrhein-Westfalen in Vergangenheit, Gegenwart und Zukunft
Heft 26 2012	Lihua Li Separability of deformations and measurement noises of GPS time series with modified Kalman filter for landslide monitoring in real-time
Heft 25 2012	Benedikt Frielinghaus Ökonomisches Entscheidungstool zur Wohnbaulandentwicklung Wirtschaftlichkeitsanalysen potenzieller Wohnbauflächen auf der Ebene des Flächennutzungsplanes
Heft 24 2011	Enrico Kurtenbach Entwicklung eines Kalman-Filters zur Bestimmung kurzzeitiger Variationen des Erdschwerefeldes aus Daten der Satellitenmission GRACE
Heft 23 2011	Sarah Böckmann Robust determination of station positions and Earth orientation parameters by VLBI intra-technique combination
Heft 22 2011	20th Meeting of the European VLBI Group for Geodesy and Astronomy Proceedings
Heft 21 2011	Philipp Zeimetz Zur Entwicklung und Bewertung der absoluten GNSS-Antennenkalibrierung im HF-Labor
Heft 20 2011	Alessandra Roy Effects on the Geodetic-VLBI Observables Due to Polarization Leakage in the Receivers
Heft 19 2011	Dietmar Weigt Auswirkungen von Flughäfen insbesondere von Fluglärm auf den Immobilienmarkt am Beispiel des Marktsegments „individuelles Wohnen“
Heft 18 2011	Anno Löcher Möglichkeiten der Nutzung kinematischer Satellitenbahnen zur Bestimmung des Gravitationsfeldes der Erde
Heft 17 2010	Basem Elsaka Simulated Satellite Formation Flights for Detecting the Temporal Variations of the Earth’s Gravity Field
Heft 16 2010	2nd International Conference on Machine Control & Guidance Proceedings
Heft 15 2009	Alexandra Weitkamp Brachflächenrevitalisierung im Rahmen der Flächenkreislaufwirtschaft

Heft 14 2008	Akbar Shabanloui A New Approach for a Kinematic-Dynamic Determination of Low Satellite Orbits Based on GNSS Observations
Heft 13 2008	Frank Friesecke Stadtumbau im Konsens!? Zur Leistungsfähigkeit und Fortentwicklung des städtebaulichen Instrumentariums unter Schrumpfungsbedingungen
Heft 12 2008	Heinz Rütz Zur Kostenanalyse der privaten Umlegung als Teil der konsensualen integrierten Baulandentwicklung
Heft 11 2008	Gaby Alexandra Boele-Keimer Kommunales Kennzahlenmanagement am Beispiel von Vermessungs- und Katasterämtern in Nordrhein-Westfalen
Heft 10 2008	Annette Eicker Gravity Field Refinement by Radial Basis Functions
Heft 9 2008	Torsten Mayer-Gürr Gravitationsfeldbestimmung aus der Analyse kurzer Bahnbögen
Heft 8 2008	Boris Kargoll On the Theory and Application of Model Misspecification Tests
Heft 7 2008	Hamza Alkhatib On Monte Carlo Methods
Heft 6 2008	Klaus Borchard Annäherungen an Städtebau und Raumentwicklung
Heft 5 2008	Jens Jähnke Zur Teilmarktbildung beim Landerwerb der öffentlichen Hand
Heft 4 2008	Atef Abd-Elhakee Makhloof The Use of Topographic Isostatic Mass Information
Heft 3 2008	Markus Vennebusch Singular Value Decomposition and Cluster Analysis
Heft 2 2007	Christian Beder Grouping Uncertain Oriented Projective Geometric Entities
Heft 1 2007	Klaus Börger Geodäsie und Quantenphysik

Vertrieb: Rheinische Friedrich-Wilhelms-Universität Bonn
Institut für Geodäsie und Geoinformation
- Bibliothek -
Nußallee 17
53115 Bonn

Tel.: +49 (0)228 73-3566
Fax: +49 (0)228 73-2988

Internet: http://www.igg.uni-bonn.de

ISSN 1864-1113